https://ntrs.nasa.gov/search.jsp?R=19680026528 2018-12-31T22:35:35+00:00Z

General Disclaimer

One or more of the Following Statements may affect this Document

- This document has been reproduced from the best copy furnished by the organizational source. It is being released in the interest of making available as much information as possible.

- This document may contain data, which exceeds the sheet parameters. It was furnished in this condition by the organizational source and is the best copy available.

- This document may contain tone-on-tone or color graphs, charts and/or pictures, which have been reproduced in black and white.

- This document is paginated as submitted by the original source.

- Portions of this document are not fully legible due to the historical nature of some of the material. However, it is the best reproduction available from the original submission.

Produced by the NASA Center for Aerospace Information (CASI)

STUDY TO ESTABLISH CRITERIA FOR A SOLAR CELL ARRAY FOR USE AS A PRIMARY POWER SOURCE FOR A LUNAR-BASED WATER ELECTROLYSIS SYSTEM

Phase I Final Technical Report

09681-6002-R000

30 JUNE 1968

GPO PRICE $ _____

CFSTI PRICE(S) $ _____

Hard copy (HC) 3.00

Microfiche (MF) .65

ff 653 July 65

Contract No. NAS 8-21189
Period covered: 1 July 1967 to 30 June 1968

Prepared for
NATIONAL AERONAUTICS AND SPACE ADMINISTRATION
George C. Marshall Space Fligth Center
Huntsville, Alabama 35812

FACILITY FORM 602

N68-36000 (ACCESSION NUMBER)

(THRU)

549 (PAGES)

1 (CODE)

CR-61979 (NASA CR OR TMX OR AD NUMBER)

03 (CATEGORY)

TRW
SYSTEMS GROUP

09681-6002-R000

STUDY TO ESTABLISH CRITERIA FOR A SOLAR CELL ARRAY FOR USE AS A PRIMARY POWER SOURCE FOR A LUNAR-BASED WATER ELECTROLYSIS SYSTEM

PHASE I - FINAL TECHNICAL REPORT

Period Covered 1 July 1967 to 30 June 1968

J.E. Boretz
Project Manager

Approved:
A. Krausz, Manager
Electric Power Laboratory

Prepared for

National Aeronautics and Space Administration
George C. Marshall Space Flight Center
Huntsville, Alabama 35812

Contract No. NAS 8-21189
by
TRW SYSTEMS
One Space Park, Redondo Beach, California 90278

FOREWARD

This Phase I - Final Technical Report for the "Study to Establish Criteria for a Solar Cell Array for Use as a Primary Power Source for a Lunar-Based Water Electrolysis System" was prepared for the National Aeronautics and Space Administration, George C. Marshall Space Flight Center; Huntsville, Alabama, in partial fulfillment of Contract NAS8-21189. The report covers work performed from 1 July 1967, to 30 June 1968, and documents and summarizes the results of the Phase I portion of this contract effort. The work was conducted under the technical direction of the Astrionics Laboratory, Power Systems Branch of NASA/MSFC.

Distribution of this document is established by the Contracting Officer, Lawrence Garrison, or his authorized representative. Communications relative to this contract should be directed to the above Contract Specialist, Attention Code PR-SC, George C. Marshall Space Flight Center, Huntsville, Alabama 35812.

ACKNOWLEDGEMENTS

This study was conducted by the Electric Power Laboratory of TRW Systems Group, which is under the direction of Dr. A. Krausz. The Principal Investigator and Study Manager was J. E. Boretz.

Acknowledgement is expressed to the various Members of the Technical Staff named below for their valuable technical contributions to this effort:

W. G. Binckley	M. Koslover
R. Boring	J. B. Kendrick
W. Luft	G. Luckey
R. Fogle	C. E. Williamson
W. Scott	D. Wanous

E. Maiden

In addition, the technical direction, guidance, reviews, opinions and comments provided by J. Miller (COR Technical Representative) and other members of the NASA/MSFC Power Systems Branch of the Astronics Laboratory (R. Boehme, W. Goodhue, H. Wagner, A. J. Morgan, L. Crabtree), are also gratefully acknowledged.

CONTENTS

		Page
	FORWARD	ii
	ACKNOWLEDGEMENTS	iii
	ILLUSTRATIONS	ix
	TABLES	xxii
1.	INTRODUCTION	1-1
	1.1 General	1-1
	1.2 Study Objectives	1-1
	1.3 Study Approach	1-2
2.	SUMMARY	2-1
	2.1 Performance Considerations	2-1
	2.2 Mission Considerations	2-3
3.	CONCLUSIONS AND RECOMMENDATIONS	3-1
	3.1 Conclusions	3-1
	3.2 Recommendations	3-3
4.	MISSION AND SYSTEM REQUIREMENTS	4-1
	4.1 Mission Objectives	4-1
	4.2 Study Guidelines	4-2
	4.3 Energy Depot Requirements Analysis	4-4
	4.4 Electric Power System Definitions	4-7
	4.4.1 Lunar Exploration Primary Electric Power Systems (LEPEPS)	4-7
	4.4.2 Secondary Electrical Power Systems (SEPS)	4-12
	4.4.3 Alternate Modes of Reactant Supply and Power Requirements	4-13
	4.4.4 Lunar Surface Vehicle Auxiliary Power	4-15
	4.4.5 Surface Traverse Emergency Power	4-20
	4.5 Mining and Water Extraction Requirements	4-21
	4.6 Study Alternatives	4-23
	4.7 Operations Analysis	4-63
	4.7.1 Logistics and Stowage of Solar Array Power Systems	4-63
	4.7.2 Deployment of Solar Array Power Systems	4-78

Page

5. LUNAR SURFACE ENVIRONMENTAL MODEL 5-1
5.1 General Considerations 5-1
5.2 Lunar Thermal Model 5-2
5.3 Radiation Environment 5-8
5.4 Meteoroid Environment 5-13
5.5 Atmospheric Properties 5-20
5.6 Lunar Surface Properties 5-23
5.7 Impact on Solar Array 5-28
6. SOLAR ARRAY MATERIALS 6-1
6.1 Material Survey 6-1
7. SOLAR ARRAY DESIGN DATA 7-1
7.1 Structural 7-1
7.1.1 Comparison of Candidate Concepts from Industry 7-1
7.1.2 Concept Considerations 7-14
7.1.3 Candidate Structural Configurations 7-15
7.1.4 Lunar Surface Handling and Assembly . . . 7-17
7.2 Mechanical 7-18
7.2.1 Candidate Concepts 7-18
7.2.2 Concept Selections 7-21
7.3 Electrical 7-22
7.3.1 Solar Cells 7-22
7.3.2 Cover Slides 7-38
7.3.3 Circuit Interconnections 7-38
7.4 Weight 7-47
7.4.1 Structural 7-47
7.4.2 Electrical 7-49
7.4.3 Ancillary Components 7-51
8. SOLAR ARRAY PERFORMANCE CONSIDERATIONS . . 8-1
8.1 Introduction 8-1
8.1.1 Baseline Configurations 8-1
8.1.2 Concept Selection 8-5
8.2 Thermal Analysis 8-5
8.2.1 Thermal Model 8-7

Page

8.2.2 Oriented Arrays 8-15

8.2.3 Non-oriented Arrays 8-23

8.3 Performance Analysis 8-27

8.3.1 Efficiency and Voltage Variations with Lunar Phase 8-27

8.3.2 Power-to-Area Ratio for Various Mission Durations 8-44

9. SOLAR ARRAY CANDIDATE CONFIGURATIONS 9-1

9.1 Output Power Profile Comparisons 9-1

9.2 Candidate Array Considerations 9-2

9.3 Total Available Energy Comparisons 9-23

9.4 Reliability Considerations. 9-24

10. POWER SYSTEM SYNTHESIS AND DESIGN 10-1

10.1 Alternate Power Sources Survey 10-1

10.1.1 Primary Batteries 10-2

10.1.2 Secondary Batteries 10-5

10.1.3 Fuel Cells 10-8

10.1.4 Nuclear Static Sources 10-11

10.1.5 Nuclear Dynamic Sources 10-11

10.2 Requirements and Assumptions 10-18

10.2.1 General 10-18

10.2.2 Electrical Power Requirements 10-20

10.2.3 Environmental Requirements 10-22

10.2.4 Other Requirements 10-22

10.3 Candidate System Configurations 10-24

10.3.1 Basic Functional Power System Configurations 10-24

10.3.2 Candidate Configuration Selection 10-24

10.4 Power Conditioning and Distribution Data 10-30

10.4.1 Cabling 10-30

10.4.2 Voltage Regulators 10-34

10.4.3 DC-DC Converters 10-42

10.4.4 DC-AC Inverters 10-44

10.4.5 Correction Factors 10-44

Page

10.5 General System Considerations 10-51

10.5.1 Weight Tradeoff 10-51

10.5.2 Cost Tradeoff 10-56

10.5.3 Reliability 10-56

10.5.4 Volume and Shape 10-59

10.5.5 Thermal Control 10-60

10.5.6 Instrumentation 10-62

10.5.7 Fault Protection 10-62

10.5.8 Emergency Operation 10-64

10.5.9 Overall LEPEPS Criteria 10-64

10.6 Example of System Synthesis 10-65

10.6.1 Solar Array Type Considerations 10-65

10.6.2 Synthesis of Configuration Using Leanto Solar Array 10-68

10.6.3 Sensitivity to Changes in Parameters 10-77

10.6.4 Effects of Changes in Choice of Solar Array Type 10-85

10.6.5 Rationale for Power Distribution System Selection 10-85

11. PRELIMINARY DESIGN OF CANDIDATE POWER SYSTEM 11-1

11.1 Design Considerations 11-1

11.2 Design Requirements Document - Leanto Array Configuration 11-2

12. PROGRAM DEVELOPMENT PLAN 12-1

12.1 Program Considerations 12-1

12.2 Program Implementation Definition 12-2

12.3 Project Sequence and Baselines 12-3

12.4 Program Plan 12-11

12.4.1 Major Milestones 12-12

REFERENCES R-1

BIBLIOGRAPHY RB-1

APPENDIX A. . . . . A-i

APPENDIX B. . . . . B-i

APPENDIX C. . . . . C-i

APPENDIX D. . . . . D-i

Page

APPENDIX E. . . . . E-i
APPENDIX F. . . . . F-i
APPENDIX G. . . . . G-i

ILLUSTRATIONS

2.1	Comparison of Lunar Surface Power Systems	2-7
2.2	General Arrangement of Candidate Lunar Surface Power System (45 kw Leanto Solar Arrays)	2-10
2.3	2.5 Kw Power Level Flexible Substrate Leanto Solar Panel with Multifoil Insulation Skirting	2-11
2.4	2.5 Kw Power Level Rigid Substrate Leanto Solar Panel with Multifoil Insulation Skirting	2-12
2.5	2.5 Kw or 5 Kw Power Level Rigid Structure Oriented-Skirted Solar Panel with Multifoil Insulation Skirting (Concept 1)	2-13
2.6	2.5 Kw or 5 Kw Power Level Rigid Structure Oriented-Skirted Solar Panel with Multifoil Insulation Skirting (Concept 2)	2-14
4.1	Typical Power Profile for Energy Depot	4-7
4.2	Relative Effectiveness of Various Configurations	4-10
4.3	Final Solar Array Candidates (2.5 Kw Modules of Foldout Panels Shown)	4-11
4.4	Typical Lunar Surface Vehicles for Lunar Surface Exploration	4-16
4.5	Variation of p and Sin θ During Lunar Day	4-17
4.6	Tradeoffs with Solar Cells and Batteries on Lunar Surface Vehicles (MOLAB)	4-18
4.7	Total System Weights Vs. Time to Recharge Batteries	4-25
4.8	Comparison of Alternate System Weights	4-30
4.9	Comparison of Alternate Power System Weights	4-32
4.10	Power System Weights with Mining and Water Water Extraction	4-35
4.11	Typical Program V Power Load Profiles	4-37
4.12	Power Profile for Flat Solar Array	4-38
4.13	Power Profile for Leanto Array	4-39
4.14	Power Profiles for Oriented Arrays	4-40
4.15	Reactant Schedule for Program V - Comparison of Alternate Modes	4-44
4.16	Average Cost of Solar Arrays	4-49

ILLUSTRATIONS (Continued)

4.17	Power System Cost Nomograph	4-52
4.18	Cost Sensitivity to Input Values	4-54
4.19	Comparison of Lunar Surface Power Systems	4-59
4.20	Dimensions of Foldout Panels	4-64
4.21	Temperature Correction for Number of Panels	4-66
4.22	Typical Transport Trailers for 50 Kw Arrays	4-66
4.23	Roll Diameter and Number of Turns	4-67
4.24	Temperature Correction for Number of Turns and Diameter	4-68
4.25	Stowage and Unloading of Foldout Solar Array	4-70
4.26	Stowage Volume Available	4-71
4.27	Stowage and Unloading of Flexible Solar Array	4-72
4.28	Typical Assemblies of 2.5 Kw Flexible Silicon Cell Flat Arrays to Provide Various Power Levels	4-74
4.29	Typical Layout of Lunar Base with Leanto Solar Array	4-75
4.30	Roll-up Solar Array Packaging Detail	4-77
4.31	Surface Rubble to be Removed	4-83
4.32	Deployment of Flexible Solar Arrays	4-85
4.33	Deployment of Rigid Panel Arrays	4-86
4.34	Details of Deployment of Flexible Integrated Arrays	4-88
4.35	Deployment of 2.55 Kw Foldout Leanto	4-89
4.36	Structure for Flat Arrays of Rigid Panels	4-91
4.37	Typical Leanto Structures	4-92
4.38	Leanto Array Using Flexible Integrated Assembly	4-95
4.39	Deployment Time and Energy Required for Solar Arrays	4-99
5.1	Typical Temperature Variation of the Lunar Surface (Reference 5.4)	5-4
5.2	Theoretical Lunar Surface Temperature Variation for a Complete Lunation (Reference 5.1) at the Lunar Equator (where the lunar thermal inertia, $\gamma = (Kpc)^{-1/2}$)	5-5
5.3	Theoretical Lunar Surface Temperature Variation for a Complete Lunation on Lunar Central Meridian (Reference 5.1)	5-6

ILLUSTRATIONS (Continued)

5.4	Variation of Lunar Surface Temperature During a Complete Lunation (Reference 5.1)	5-7
5.5	Solar High Energy Particle Radiation Energy Level Versus Yearly Integrated Flux for 1 AU (Estimate Based on Reference 5.1)	5-10
5.6	The Probability, p, of the Occurrence of a Flare Whose Flux is Equal to or Greater Than N, and Whose Individual Particle Energies are Equal to or Greater Than 30 MEV (Reference 5.1)	5-11
5.7	Solar Radiation Pressure at 1 AU Versus Reflectivity	5-12
5.8	Cometary Micrometeoroid Flux and Secondary Ejecta Flux Vs. Particle Mass and Depth of Penetration into Aluminum	5-14
5.9	Particle Diameter Versus Mass for Typical Micrometeorite and Secondary Ejecta Particle Densities	5-15
5.10	Micrometeoroid Frequencies	5-16
5.11	Micrometeoroid and Secondary Ejecta Particle Penetration Depth for Thin Materials	5-17
5.12	Cumulative Frequency Distribution of Particles on the Lunar Surface Determined from Surveyor I Observation Photographs (Reference 5.5)	5-19
5.13	Solar Wind Data Vs. Distance from the Sun in AU	5-22
5.14	Estimated Depth of Penetration of Lunar Surface Vs. Static Load Based on Minimum Bearing Strength of the High Porosity Lunar Material	5-24
5.15	Cumulative Size-Frequency Distribution of Craters in Mare Cognitum (Based on Distribution of Craters Observed in Ranger VII Photographs (Reference 5.1)	5-25
5.16	Distribution of Size and Frequency of Post Maria Lunar Craters from Earth-Based and Ranger Photographs (Reference 5.1)	5-26
5.17	Percentage of Sunlight Portion (14.75 Days) of Lunar Day Available Due to Obstacles of Various Heights for Various Distances from the Obstacle	5-27
6.1	Estimate, Based on Laboratory Data, of the Ratio of Initial I_{sc} to Final I_{sc} for Silicon and CdS Solar Cells Versus Kinetic Energy of Cloud of Impinging Micrometeoroid Particles Weighing 10^{-8} to 10^{-12}	6-3

ILLUSTRATIONS (Continued)

7.1	Comparison of Industry Large Area Solar Array Concepts (Mass Density of Original Design and as Modified for Lunar Surface Application)	7-16
7.2	Typical Current-Voltage Characteristics for 2 and 10 ohm-cm Base Resistivity Silicon Solar Cells of Various Thicknesses	7-24
7.3	Current-Voltage Characteristics for Silicon Solar Cells Versus Equilibrium Temperature	7-25
7.4	Typical 10 Ohm-CM Single Crystal Silicon Solar Cell Current-Voltage Characteristic Curves for Lunar Noon and Terminator Conditions	7-26
7.5	Typical 10 Ohm-cm Single Crystal Silicon Solar Cell Current-Voltage Curves	7-27
7.6	Typical 10 Ohm-Cm Single Crystal Silicon Solar Cell Current-Voltage Curves	7-28
7.7	Current-Voltage Characteristics for Thin Film Cadmium Sulfide Solar Cells for Array Temperature Operating Range	7-29
7.8	Typical Cadmium Sulfide Thin Film Current-Voltage Curves	7-30
7.9	Typical Cadmium Sulfide Thin Film Current-Voltage Curves	7-31
7.10	Cell Open Circuit Voltage Versus Temperature for Silicon and CdS Thin Film Solar Cells	7-33
7.11	Power-to-Weight Ratio Versus Efficiency for Silicon and Thin Film Solar Cells	7-34
7.12	Cell Efficiency Versus Weight-Power Ratio	7-35
7.13	Cell Efficiency Versus Temperature Comparison for Silicon and Thin-Film Solar Cells	7-36
7.14	Silicon Cell and CdS Thin Film Cost Projections	7-37
7.15	Percent Power to Area Ratio Remaining After Ratiation Bombardment (Yearly) Versus Cover Thickness	7-40
7.16	Estimate, Based on Laboratory Data, of the Ratio of Initial I_{sc} to Final I_{sc} for Silicon and CdS Solar Cell Versus Kinetic Energy of Cloud of Impinging Micrometeoroid Particles Weighing 10^{-8} to 10^{-12} grams Whose Average Velocity is 2.65 km/sec (Reference 6.6)	7-41
7.17	Solar Array Voltage Versus Current for Various Power Output Levels at Normal Solar Insolance and Constant Temperature	7-42

ILLUSTRATIONS (Continued)

7.18	Solar Array Equivalent Cable Weight Versus Array Voltage	7-44
7.19	Solar Array Power Losses Versus Array Voltage	7-45
7.20	Comparison of Candidate Silicon Solar Cell Interconnect Material Thermal Expansion Coefficients with Single Crystal Silicon Cells	7-48
7.21	Estimated Depth of Penetration of the High Porosity Lunar Surface Versus Solar Array Static Load	7-52
8.1	Baseline Solar Array Configurations	8-2
8.2	Candidate Solar Array Configurations	8-6
8.3	Thermal Model for Temperature of Lunar Surface Solar Arrays	8-8
8.4	Flat Plat View Factors	8-9
8.5(a)	Typical Temperature Variation of the Lunar Surface	8-13
8.5(b)	Comparison of Shaded and Unshaded Lunar Surface Temperature (Lunar Equator)	
8.6	Average Solar Array Temperature Variation with Lunar Phase for Oriented Arrays (Non-insulated and Non-skirted)	8-16
8.7	Average Solar Array Temperature Variation with Lunar Phase for Oriented Arrays (Insulated and Non-skirted)	8-17
8.8	Oriented Solar Array Thermal Energy Inputs for Two Design Concepts	8-19
8.9	Oriented-Skirted (Non-insulated) Solar Array Temperature vs. Array Efficiency for Various Shaded Lunar Surface Temperatures at Lunar Noon	8-20
8.10	Schematic of Solar Thermal Energy Dissipation for a Silicon Cell Solar Array on the Lunar Surface	8-21
8.11	Assumed Lunar Surface Temperature Variation (Lunar Equator)	8-24
8.12	Thermal Sensitivity of a Non-insulated Silicon Cell Solar Array to Various Parameters at Lunar Noon	8-25
8.13	Thermal Sensitivity of a Non-insulated CdS Thin Film Solar Array to Various Parameters at Lunar Noon	8-26
8.14	Solar Array Temperature Variation with Lunar Phase for Non-oriented, Non-insulated Arrays	8-28
8.15	Silicon Cell Solar Array Equilibrium Temperature Versus Lunar Phase	8-29

ILLUSTRATIONS (Continued)

8.16	CdS Thin Film Solar Array Equilibrium Temperature Versus Lunar Phase	8-30
8.17	Flow Diagram Showing Sequence of Data Derivation for Lunar Array Performance Analysis	8-31
8.18	Factors Considered in Power-To-Area Ratio Computation for Lunar-Based Solar Arrays	8-32
8.19	Oriented Array (Non-Skirted and Non-Insulated) Efficiency Variation with Lunar Phase for Average Array Temperature (Using Single Crystal Silicon Cells)	8-34
8.20	Oriented (Non-Skirted, Non-Insulated) CdS Thin Film Array Efficiency Variation with Lunar Phase for Average Array Temperature	8-35
8.21	Oriented Arrays (Non-insulated) Open Circuit Voltage Variation with Lunar Day at Average Array Temperature	8-36
8.22	Oriented, Insulated Solar Array Efficiency Variation with Lunar Phase for Arrays with Multi-layer Insulation (Average)	8-37
8.23	Oriented, Insulated Solar Array Open Circuit Voltage Variation with Lunar Phase for Multi-insulated Arrays (Average)	8-38
8.24	Array Efficiency Variation with Lunar Phase for Non-oriented, Non-insulated arrays	8-40
8.25	Non-oriented Array (Non-insulated, Non-skirted) Open Circuit Voltage Variation with Lunar Phase at Average Array Temperatures	8-41
8.26	Silicon Cell Array (Non-Oriented) Efficiency and Open-Circuit Voltage Versus Lunar Phase	8-42
8.27	Non-Oriented, CdS Thin Film Array Efficiency and Open Circuit Voltage Variation with Lunar Base	8-43
8.28	Percent Change in Output Power for Electron-Bombarded and Proton-Bombarded Solar Cells	8-47
8.29	Silicon and CdS Thin Film Solar Cell Degradation Due to the Space Environment	8-48
8.30	Power-To-Area Ratio Sensitivity Curves (Silicon Cell Solar Arrays)	8-49
8.31	Power-To-Area Ratio Sensitivity Curves (CdS Thin Film Arrays)	8-50
8.32	Power-To-Area Ratio Versus Lunar Phase for Silicon Cell Solar Arrays (Oriented, Non-Insulated and Non-Skirted)	8-51

ILLUSTRATIONS (Continued)

8.33	Power-To-Area Ratio Versus Lunar Phase for CdS Thin Film Solar Arrays (Oriented, Non-Insulated, Non-Skirted)	8-52
8.34	Power-To-Area Ratio Versus Lunar Phase for Silicon Cell Solar Arrays (Non-Oriented, Non-Insulated, Non-Skirted)	8-53
8.35	Power-To-Area Ratio Versus Lunar Phase for CdS Solar Arrays (Non-Oriented, Non-Insulated, Non-Skirted)	8-54
8.36	Power-To-Area Ratio Versus Lunar Phase for Silicon Cell Solar Arrays (Non-oriented, Thermally Insulated)	8-55
8.37	Power-To-Area Ratio Versus Lunar Phase for CdS Thin Film Solar Arrays (Non-Oriented, Thermally Insulated)	8-56
8.38	Power-To-Area Ratio Versus Lunar Phase for Silicon Cell Solar Arrays (Non-Oriented, Non-Insulated, Skirted)	8-57
8.39	Power-To-Area Ratio Versus Lunar Phase for CdS Thin Film Solar Arrays (Non-Oriented, Non-Insulated, Skirted)	8-58
8.40	Power-To-Area Ratio for a Flat Silicon Cell Solar Array Configuration (Non-Insulated, Non-Oriented, Skirted)	8-60
8.41	Power-To-Area Ratio for a Flat CdS Thin Film Solar Array Configuration (Non-Insulated, Non-Oriented, Skirted)	8-61
8.42	Power-To-Area Ratio for a Leanto Silicon Cell Solar Array Configuration (Non-Insulated, Skirted	8-62
8.43	Power-To-Area Ratio for a Leanto CdS Thin Film Solar Array Configuration (Non-Insulated, Skirted	8-63
8.44	Power-To-Area Ratio for a Flat Silicon Cell Solar Array Configuration (Thermally Insulated, Non-Oriented)	8-64
8.45	Power-To-Area Ratio for a Flat CdS Thin Film Solar Array Configuration (Thermally Insulated, Non-Oriented)	8-65
8.46	Power-To-Area Ratio for a Leanto Silicon Cell Solar Array Configuration (Thermally Insulated, Non-Oriented)	8-66
8.47	Power-To-Area Ratio for a Leanto CdS Thin Film Solar Array Configuration (Thermally Insulated, Non-Oriented)	8-67

ILLUSTRATIONS (Continued)

8.48	Comparison of Performance for Leanto Solar Array Configuration as a Function of Lunar Surface Temperature (Constant Versus Varying)	8-68
8.49	Comparison of Performance Between 45° and 51° Leanto Solar Array Configuration at Constant -6°C Shaded Lunar Surface Temperature	8-68
8.50	Various "Hybrid" Solar Array Configuration	8-69
9.1	Silicon Cell Solar Array Gross Power Output Versus Lunar Phase for Constant Array Area (Non-Insulated)	9-3
9.2	Silicon Cell Solar Array Gross Power Output Versus Lunar Phase for Constant Array Weight (Non-Insulated)	9-4
9.3	Silicon Cell Solar Array Gross Power Output Versus Lunar Phase for Constant Array Cost (Non-Insulated)	9-5
9.4	CdS Thin Film Solar Array Gross Power Output Versus Lunar Phase for Constant Array Area (Non-Insulated)	9-6
9.5	CdS Thin Film Solar Array Gross Power Output Versus Lunar Phase for Constant Array Weight (Non-Insulated)	9-7
9.6	CdS Thin Film Solar Array Gross Power Output Versus Lunar Phase for Constant Array Cost (Non-Insulated)	9-8
9.7	Silicon Cell Solar Array Gross Power Output Versus Lunar Phase for Constant Array Area (Insulated)	9-9
9.8	Silicon Cell Solar Array Gross Power Output Versus Lunar Phase for Constant Array Weight (Insulated)	9-10
9.9	Silicon Cell Solar Array Gross Power Output Versus Lunar Phase for Constant Array Cost (Insulated)	9-11
9.10	CdS Thin Film Solar Array Gross Power Output Versus Lunar Phase for Constant Array Area (Insulated)	9-12
9.11	CdS Thin Film Solar Array Gross Power Output Versus Lunar Phase for Constant Array Weight (Insulated)	9-13
9.12	CdS Thin Film Solar Array Gross Power Output Versus Lunar Phase for Constant Array Cost (Insulated)	9-14

ILLUSTRATIONS (Continued)

9.13	Silicon Cell Solar Array (Leanto) Area Sensitivity to Shaded Lunar Surface Temperature	9-15
9.14	Silicon Cell Solar Array (Leanto) Weight Sensitivity to Shaded Lunar Surface Temperature	9-16
9.15	Silicon Cell Solar Array (Leanto) Cost Sensitivity to Shaded Lunar Surface Temperature	9-17
9.16	CdS Thin Film Solar Array (Leanto) Area Sensitivity to Shaded Lunar Surface Temperature	9-18
9.17	CdS Thin Film Solar Array (Leanto) Weight Sensitivity to Shaded Lunar Surface Temperature	9-19
9.18	CdS Thin Film Solar Array (Leanto) Cost Sensitivity to Shaded Lunar Surface Temperature	9-20
9.19	Comparison of Candidate Solar Arrays for Program V Mission	9-21
9.20	Candidate Solar Array Gross Output Power Profiles	9-22
9.21	Total Silicon Cell Solar Array Energy Output Versus Array Area and Fabrication Cost	9-24
9.22	Total Silicon Cell Solar Array Energy Output Versus Array Weight	9-25
9.23	Total CdS Thin Film Solar Array Energy Output Versus Array Area and Fabrication Cost	9-26
9.24	Total CdS Thin Film Solar Array Energy Output Versus Array Weight	9-27
9.25	Comparison of Silicon Cell Solar Array Configurations for Constant Total Energy Output	9-29
9.26	Shadow Time Versus Obstacle Height on Lunar Surface	9-30
9.27	Various Alternative High Voltage Solar Panel Configurations	9-32
9.28	Typical Current-Voltage Curves and their Probability of Occurrence for Configuration "P" (without shunt diodes) and for Various Numbers of Open-circuited Cells per Array	9-33
9.29	Allowable Power Loss Versus Reliability for 2.5 kw Silicon Cell Solar Array	9-39
9.30	Allowable Power Loss Versus Reliability for 2.5 kw CdS Thin Film Solar Array	9-40
9.31	Allowable Power Loss Versus Reliability for 2.5 kw Silicon Cell Array for Various Voltages	9-41
9.32	Allowable Power Loss Versus Reliability for 2.5 kw CdS Thin Film Solar Array for Various Voltages	9-42

ILLUSTRATIONS (Continued)

10.1	Projected Energy Density for Secondary Battery Cells (Reference 10.2)	10-6
10.2	Projected Life for Secondary Battery Cells (Reference 10.2	10-7
10.3	Two-Module Reactant Consumption Curves for AAP Earth Polar Orbital Mission	10-12
10.4	Two-Module Waste Heat Curves for AAP Earth Polar Orbital Mission (Reference 4)	10-12
10.5	Two Module Voltage/Power Characteristics for AAP Earth Polar Orbital Mission (Reference 10.4)	10-13
10.6	Fuel Cell Specific Fuel Consumption vs. % Rated Power (Reference 10.3)	10-14
10.7	Estimated Heat Rejection to Radiator for P and W Fuel Cells (Reference 12.12	10-15
10.8	Estimated Date of Development Technology Completion (Reference 10.1)	10-17
10.9	ERPS Power Profiles	10-21
10.10	Generalized System Concepts	10-25
10.11	Power System, Unregulated Bus Configuration	10-26
10.12	Functional Power System Configurations, Regulated Bus	10.27
10.13	Average Voltage Drop per 100 ft Versus Average Line Voltage	10-32
10.14	Power Loss per 100 ft Versus Line Voltage for Paralleled No. 20 AWG Wire	10-33
10.15	Parallel Arrays, Line Power Loss per 100 ft Distance for Insulated 3-Parallel Wire (No. 20 AWG)	10-35
10.16	Line Power Loss per 100 ft Distance for Insulated 6-Parallel Wire (No. 20 AWG)	10-36
10.17	Line Power Loss per 100 ft Distance for Insulated 12-Parallel Wire (No. 20 AWG)	10-37
10.18	Power Loss for Connecting Bus per 100 ft of length	10-38
10.19	Line Regulator, Redundant Efficiency Versus Power Output	10-40
10.20	Line Regulator (Redundant) Weight Versus Power Output	10-41
10.21	Block Diagram Unregulated DC-DC Converter	10-43
10.22	Converter (Redundant) Weight Versus Power Output	10-45

ILLUSTRATIONS (Continued)

10.23	Converter, Redundant Efficiency Versus Power Output	10-46
10.24	Regulator-Inverter (Redundant) Weight Versus Power Output	10-47
10.25	Load Power Conditioning Inverter (Redundant) Efficiency Versus Power Output	10-48
10.26	Weight and Efficiency Correction Factors for Converters, Regulator-Converters and Regulator-Inverter	10-49
10.27	Correction Factor for Power Loss and Voltage Drop	10-50
10.28	Schematic of Electric Power System for Lunar Base (45 Kw-Minimum Gross Power)	10-52
10.29	Standby Redundant System Reliability Model	10-58
10.30	Candidate Solar Array Configurations	10-66
10.31	Candidate Solar Array Gross Output Power Profiles	10-67
10.32	Block Diagram of Lunar Surface Power System (45 kw Leanto Configuration)	10-70
10.33	Breakdown of Leanto Lunar Power System Weight Vs. Array Voltage(Power Conditioning Shred-Out)	10-75
10.34	Required Array Power and System Efficiency Vs. Array Voltage	10-76
10.35	Breakdown of Leanto Lunar Power System Weight Versus Array Voltage	10-78
10.36	Total System Weight Ratio for Variable Line Temperature	10-80
10.37	Total System Weight Ratio for Variable Main Bus Length	10-81
10.38	Total System Weight Ratios for Variable Line Length	10-82
10.39	Total System Weight Ratio Versus Load Power	10-83
10.40	Percent Change in Total Power Systems Weight Ratio Vs. Array Voltage (ΔL_A = 100 ft)	10-84
10.41	Percent Change in Total Power System Weight Ratio Vs. Array Voltage (ΔL_B = 100 ft)	10-84
10.42	Comparison of Total Lunar Power System Weight for Various Array Configurations	10-86
12.1	Project Sequence and Baselines	12-4
12.2	Lunar Exploration Primary Electric Power System (LEPEPS) Program Development Plan	12-15

ILLUSTRATIONS (Continued)

A.1	Typical Power Profiles for LSV	A-3
A.2	Percent Power from Solar Array vs. Area (MOLAB)	A-6
A.3	System Weight vs. Stationary Time (MOLAB)	A-6
A.4	System Weight vs. Reactant Saved	A-7
A.5	Percent Energy vs. Stationary Time (MOLAB)	A-7
A.6	Percent Power from Solar Array vs. Area (Long Range Reconnaisance Vehicle)	A-8
A.8	System Weight vs. Reactant Saved	A-9
A.9	Percent Energy vs. Stationary Time (Long Range Reconnaisance Vehicle)	A-9
A.10	Percent Power from Solar Array vs. Area (LSSM)	A-10
A.11	System Weight vs. Stationary Time (LSSM)	A-10
A.12	System Weight vs. Reactant Saved	A-11
A.13	Percent Energy vs. Stationary Time (LSSM)	A-11
B.1	Block Diagram of Lunar Surface Power System (45 kw Leanto Configuration)	B-4
B.2	Schematic of Electric Power System for Lunar Base (45 kw-Minimum Gross Power)	B-5
B.3	Typical Maximum Solar Array Temperature Variations	B-17
B.4	Program V Power Profiles	B-18
E.1	Density of Typical Materials used in Aerospace Applications	E-2
E.2	Elastic Modulus of Typical Aerospace Materials	E-2
E.3	Modulus to Density Ratio of Various Metals	E-3
E.4	Ultimate Tensile Strength/Density Ratios of Various Structural Materials	E-3
E.5	Yield Strength vs. Temperature of Various Beryllium Products	E-4
E.6	Ultimate Tensile Strength vs. Temperature of Various Beryllium Products	E-4
E.7	Tension Modulus of Several Structural Metals at Various Temperatures (^{o}F)	E-4
E.8	Weight of Cylinders of Equal Length and Radius Which will Resist Equal Buckling Loads	E-4
E.9	Weight of Simple Cantilever Beams of Equal Length and Height Which will Deflect Equally with the Same Applied Load	E-4

ILLUSTRATIONS (Continued)

E.10	Specific Heat vs. Temperature	E-5
E.11	Mean Linear Coefficiency of Thermal Expansion Vs. Temperature	E-5
E.12	Thermal Conductivity vs. Temperature	E-6
F.1	Lunar Surface Power System (Configuration 1) (Full AC Distribution)	F-11
F.2	Lunar Surface Power System (Configuration 2) (Full DC Distribution)	F-12
F.3	Lunar Surface Power System (Configuration 3) (AC-DC Distribution)	F-13
F.4	Lunar Surface Power System (Configuration 4) (AC-DC Distribution)	F-14
F.5	Partial Shunt Solar Array Voltage Limiter	F-15
F.6	PWM Bucking Solar Array Voltage Limiter or Line Regulator	F-15
F.7	Block Diagram, PWI Converter	F-16
F.8	Pulse Width Modulated Bucking Regulator Block Diagram	F-17
F.9	Pulse Width Bucking Regulator, Saturated Conditions	F-17
F.10	Pulse Width Modulated Boost Regulator Block Diagram	F-18
F.11	Pulse Width Modulated Buck-Boost Regulator Block Diagram	F-18
F.12	Maximum Efficiency as a Function of Power Output	F-19
G.1	Solar Array Weight Versus Array Area as a Function of Array Specific Density	G-2
G.2	Solar Array Power Versus Array Area as a Function of Array Specific Power	G-3
G.3	Solar Array Power Versus Array Area as a Function of Array Specific Power	G-4

TABLES

1.1	Study Objectives	1-2
2.1	Total Mission Energy Requirements	2-5
2.2	Candidate Lunar Surface Power Systems	2-6
4.1	Specified Lunar Mission Programs	4-3
4.2	Block Diagram of Lunar Mission and Systems Analysis	4-5
4.3	Power and Reactant Requirements for Specified Missions	4-6
4.4	Comparison of Alternate System Weights (No mining, no solar arrays on LSV)	4-29
4.5	Solar Array Weights for Program V	4-42
4.6	Reactant Production/Consumption Rates for Program V	4-43
4.7	Comparison of Systems Weights for Varying ERPS Production Rates	4-45
4.8	Alternate Modes of ERPS Operation	4-48
4.9	Cost Estimates for Power Systems	4-51
4.10	Comparison of Nuclear and Solar Array/ERPS Systems for Program V	4-57
4.11	Figure of Merit Comparison for Various Solar Array Configurations	4-62
4.12	Matrix of Deployment Modes	4-79
4.13	Deployment Modes Analyzed for Time and Manual Energy Requirements	4-79
4.14	Manual Energy Expenditure for Repetitive Motions (Derived from Table 4.15 (Reference 4.10)	4-80
4.15	Manual Energy Expenditure Rates (Reference 4.10)	4-81
4.16	Sub-Array Requirements	4-83
4.17	Summary of Deployment Times	4-100
5.1	Yearly Integrated Intensities Compared for Solar Protons and Galactic Cosmic Rays	5-9
5.2	Major Solar-Proton Outburst During Years (1956-61)	5-9
5.3	Model Solar Wind	5-21
6.1	Solar Cells	6-2
6.2	Adhesives	6-4

TABLES (Continued)

6.3	Thermal Control Coatings	6-5
6.4	Protective Coatings	6-6
6.5	Wire Insulation, Interconnect and Structural Materials and Miscellaneous Items	6-7
6.6	Spectral Filter Characteristics (Reference 6.7)	6-8
6.7	Radiation Thresholds of Typical Materials	6-9
6.8	Radiation Thresholds of Typical Solar Array Materials	6-9
6.9	Temperature Thresholds of Typical Materials	6-11
7.1(a)	Comparison of Original Solar Array Configurations	7-2
7.1(b)	Various Solar Array Concepts Adapted to Flat Array Configurations	7-3
7.1(c)	Various Solar Array Concepts Adapted to Leanto Array Configuration	7-4
7.1(d)	Comparison Between Flat and Leanto Configuration	7-5
7.2(a)	Comparison of Original Solar Array Configuration	7-10
7.2(b)	Various Solar Array Concepts Adapted to the Flat Array Configuration	7-11
7.2(c)	Various Solar Array Concepts Adapted to the Leanto Array Configuration	7-12
7.2(d)	Comparison between Flat and Leanto Configuration	7-13
7.3	Comparison of Single Crystal and Thin Film Cells Between Various Parameters	7-23
7.4	Variation of Silicon Cell Parameters with Cell Efficiency	7-39
7.5	Comparison of Various Candidate Solar Array Electrical Interconnection Material Densities and Expansion Relative to Silicon	7-46
7.6	Comparison of Various Solar Array Weight-to-Area Ratio Estimates	7-50
8.1	Range of Functions for Case I (Equation 8.1)	8-11
8.3	Values of Individual Parameters used for Thermal Analysis of Solar Arrays on Lunar Surface	8-12
9.1	Reliability of Configuration P	9-34
9.2	Values for Equation (9.11)	9-36
10.1	Primary Battery Cells	10-3
10.2	Energy Density Projections for Primary Battery Cells (Reference 10.2)	10-4

TABLES (Continued)

10.3	Comparison of the State-of-the-Art of Fuel Cell Performance (References 10.3, 10.4, 10.12)	10-10
10.4	Comparison of RTG and Nuclear Reactor Thermoelectric Static Systems	10-16
10.5	Comparison of Nuclear Reactor - Dynamic Systems (Reference 10.5)	10-19
10.6	Load Electrical Power Requirements (Reference 4.2)	10-20
10.7	Lunar Environment	10-23
10.8	Estimated Total Connector Weights for Various Power Levels	10-39
10.9	Typical Specific Weights for Power System Elements	10-55
10.10	Instrumentation for Electric Power System	10-62
10.11	Weight and Efficiency Vs. Nominal Input Bus Voltage for PWM Series Regulator at 25 kw Output Power	10-71
10.12	Weight and Efficiency Vs. Nominal Input Bus Voltage for Regulator-Inverter at 12.2 kw Output	10-72
10.13	Power Loss and Line Weight for Main Cable L_B	10-72
10.14	Array Cable L_A Weight vs. Unregulated Bus Nominal Voltage	10-73
10.15	Required Array Power and System Efficiency vs. Unregulated Bus Nominal Voltage	10-73
12.1	Major Milestones for Lunar Surface Power System Development	12-12
A.1	Lunar Surface Vehicle Performance Characteristics	A-2
B.1	Load Power Requirements	B-6
B.2	Monitoring of Power System	B-11

1. INTRODUCTION

1.1 GENERAL

This technical report encompasses the work that was performed under Contract NAS8-21189, and entitled "Study to Establish Criteria for a Solar Cell Array for Use as a Primary Power Source for a Lunar-Based Water Electrolysis System". The work was essentially carried out in accordance with the approved Technical Plan (Reference 1) and the revisions outlined in Reference 2. This report fulfills the contractual requirement for preparation of a Phase I Final Technical Report and covers the period from 1 July 1967 to 30 June 1968.

1.2 STUDY OBJECTIVES

The purpose of this study was to establish the feasibility of using large solar arrays on the lunar surface. Emphasis was placed on developing parametric data, assessing the compatibility of the solar array with the lunar environment, determining its performance, and establishing the design and implementation requirements for a candidate conceptual design configuration. A summary of these objectives is given in Table 1.1. Several baseline configurations were considered. They were required to provide conditioned electrical power for a lunar-based electrolytic reactants production system (ERPS) and a manned Shelter Module. The mission requirements and overall lunar energy depot power profiles for the solar array were defined in a parallel study conducted by the Chrysler Space Division which was entitled "Study and Design Optimization of a Water Electrolysis System" (Reference 3). These are discussed in Section 4 of this report. The candidate solar array conceptual designs were based upon the analyses and parametric data generated during this study. The study was also to include the preparation of a Design Requirements Document which would establish the preliminary specifications for the overall candidate solar array system and a Preliminary Development Plan for implementation of this system.

1.3 STUDY APPROACH

The approach taken during this study was to place primary emphasis on the development of solar array system parametric performance

Table 1.1

STUDY OBJECTIVES

- TO PROVIDE PARAMETRIC MISSION, PERFORMANCE, AND DESIGN DATA FOR LARGE SOLAR ARRAYS DEPLOYED ON THE LUNAR SURFACE.
- TO PROVIDE PARAMETRIC DATA FOR POWER CONDITIONING EQUIPMENT TO BE USED IN CONJUNCTION WITH THESE SOLAR ARRAYS.
- TO PROVIDE PARAMETRIC DATA FOR THE STOWAGE, LOGISTICS, DEPLOYMENT AND ASSEMBLY OF VARIOUS CANDIDATE SOLAR ARRAY POWER SYSTEMS.
- TO PREPARE CONCEPTUAL DESIGNS OF CANDIDATE SOLAR ARRAY POWER SYSTEMS TO BE USED ON THE LUNAR SURFACE IN SUPPORT OF A LUNAR-BASED ELECTROLYTIC REACTANTS PRODUCTION SYSTEM (ERPS).
- TO PREPARE A "DESIGN REQUIREMENTS DOCUMENT" FOR THE SELECTED CANDIDATE LUNAR SURFACE POWER SYSTEM.
- TO PREPARE A "PRELIMINARY PROGRAM DEVELOPMENT PLAN" FOR THE IMPLEMENTATION OF THE SELECTED LUNAR SURFACE POWER SYSTEM.

and design data. This was essential due to the unique characteristics of the lunar surface environment and its impact on solar array system design. It also provided a broad base for future solar array system selection, transcending the constraints of program and mission requirements as defined for this study. Furthermore, it permitted the mission planner a wide spectrum for discretionary program and mission selection, while still adhering to the cardinal cost effective principles of commonality and standardization.

Concurrent with the aforementioned task, supplementary activities were undertaken to establish the various program and mission requirements as they related to the selection of the solar array configuration. In addition, data concerning the lunar environment, solar array materials, power conditioning equipment, and competitive power systems was compiled to aid in the evaluation and design of the candidate solar array systems. In addition, techniques for the utilization and conservation of energy for the lunar surface operations involved were analyzed. Finally, a series of conceptual design layouts were prepared. These layouts, together with block diagrams for various candidate electric power systems, formed the basis for the preparation of a "Design Requirements Document" and a "Preliminary Program Development Plan".

2. SUMMARY

2.1 PERFORMANCE CONSIDERATIONS

In keeping with the main objectives of this study (Table 1.1), parametric data has been generated to define the performance characteristics of solar arrays when operating on the lunar surface. It was found that array configuration, i.e.; flat, leanto, and oriented-skirted, and array equilibrium temperature were the two most important factors in establishing these characteristics. The array configuration effected the output power profile in two ways. The orientation and geometry of the array determined the magnitude of the effective intensity of the solar insolance as a function of lunar phase. In addition, the variations in view factor (both to outer space and the lunar surface) obtained from the different array configurations, directly contributed to the resulting array equilibrium temperatures.

Except in the area of the thermal effects of the shaded and unshaded lunar surface temperatures, the impact of the lunar environment on solar array performance did not differ appreciably from that experienced in Earth orbit. The magnitude of the degradation caused by particulate radiation, micrometeorites and ultra-violet radiation was found to be very nearly equivalent.

During this study consideration was given to the following array design parameters:

- oriented versus non-oriented
- insulated versus non-insulated
- skirted (shaded lunar surface) versus non-skirted (non-shaded lunar surface)

It was found, that for all three candidate array configurations, the major performance improvement was achieved by shading the lunar surface beneath and directly adjacent to the array. This was accomplished by the use of "skirting". Some increase in performance could be achieved by insulating the back of the array, so the thermal impact

of the hot lunar surface could be minimized. However, the performance gains achieved by this design technique were not nearly as great as that resulting from skirting. Array orientation results in decreased performance unless combined with skirting or insulation.

The array geometry had a pronounced effect on the array output power profile. The flat array gave rise to a sinusoidal output power profile with zero power available at lunar sunrise and sunset. The oriented-skirted array resulted in a square-wave, constant output power profile. The leanto array output power profile was continuously varying from some nominal value at lunar sunrise to a maximum value at lunar noon. By the use of misorientation or varying the array geometry (i.e. changing the leanto angle or using a "hybrid", combined leanto and flat array) various array output power profiles can be achieved.

The rapidly changing lunar surface temperatures during sunrise and sunset could result in short term perturbations to the array power output profiles arrived at in this study. These are discussed in detail in Section 8. A detailed analysis of these transients was not considered during this study phase. However, a conservative approach with respect to this phenomenon was taken in arriving at the candidate solar array configurations.

During this study, design and performance data were developed for both single crystal silicon cells and cadmium sulfide thin films. However, only silicon cell solar arrays were considered for the candidate configurations. This was based upon limiting their selection to current state-of-the-art materials. Solar cell conversion efficiencies were based upon the latest obtainable vendor data. In addition, solar array substrate structural configurations and specific weights were arrived at only after a careful review of all concepts currently under consideration by industry. In general, the substrate specific weight (lb/ft^2) selected for the candidate configurations were somewhat heavier than in Earth orbit and planetary spacecraft designs. This resulted from the necessity to make these arrays more rigid due to the one sixth "g" lunar gravity and the utilization of manual deployment and assembly techniques.

The candidate solar array configurations selected during this study were

- o flat-skirted
- o leanto-skirted
- o oriented-skirted

The unique performance characteristics of each configuration and the reasons for their selection are discussed in detail in Sections 8 and 9. The leanto and oriented-skirted output power profiles were found to most closely match the load profiles for the baseline mission (Program V of Section 4) used during this study. The determination of an optimum solar array configuration was beyond the scope of this study. A more detailed analysis of the mission requirements including the specific operating procedures to be employed during the lunar base start-up and shut-down periods is necessary. In addition, trade-off studies between the Lunar Exploration Primary Electric Power System (LEPEPS) and the Electrolytic Reactants Production System (ERPS) must also be conducted to arrive at the most cost effective approach. These factors are discussed in greater depth in Section 4.6, Study Alternatives , of this report.

2.2 MISSION CONSIDERATIONS

The baseline mission for this study was Program V of Table 4.3 (Section 4). Briefly, this was a mission involving the setting up of a lunar base for the support of lunar surface exploration activities. The mission requirements were:

Duration	- one year (3 months manned; 6 months unmanned; 3 months manned)
Crew Size	- 3 men
Total Mission Energy	- 33,000 kw-hrs (approximately)

The major lunar base equipment was:

- o Three-man Shelter Module (MIMOSA 2322-01; uprated)
- o Lunar Roving Vehicle-MOLAB (MIMOSA 2423-01)
- o Lunar Construction Trailer (MIMOSA 2432-02)
- o Portable Tools (Reference 4.2)
- o Electrolytic Reactants Production System - ERPS (References 4.2 and 4.3)

- Lunar Equipment Prime Electrical Power System - LEPEPS (Reference 4.1)
- Secondary Electrical Power System - SEPS (Reference 4.1)
- Telemetry Station System - TELSTATS (Reference 4.1)

The main emphasis in this study was to identify one or more candidate primary electric power systems (LEPEPS) to meet the required load profile for the lunar base equipment. Various load profiles (Figure 4.11 of Section 4) were possible for meeting the mission objectives. During this study, the output power profiles of several solar array configurations were determined and these were matched to the mission load profiles. Using this approach, the candidate solar array lunar surface power systems (LSPS) were selected.

The major elements of the LEPEPS as defined by references 1.1 and 4.1 for this study were:

- Solar Array - to provide raw power to the Shelter Module and ERPS during daytime operations
- Power Conditioning - to regulate the solar array power to meet the various load requirements
- Power Distribution - bus bars and cabling to distribute the power to the various loads
- Controls - to provide for load matching, peak power, and excess power dissipation

Additional equipments comprising the LEPEPS but not included during this study phase are:

- Alkaline fuel cells - to furnish power during night operations
- Secondary (rechargeable) batteries - for emergency power and some regulation requirements

A detailed analysis of these components and integration of these elements into the LEPEPS was beyond the scope of this study. However, a discussion of this equipment and its interrelationship with the lunar base requirements is provided in Reference 4.2.

An additional electric power system required for this mission was the SEPS. The major elements of this system as defined by Reference 1.1 and 4.1 were:

- Primary batteries - for launch through deployment operations
- Primary reserve batteries - for energy depot start-up and /or reactivation after dormant or standby periods.
- Radioisotope thermal generators (RTG) - two to four units for sustained power during dormant and standby periods, communications power, and initiation energy for depot activation upon remote command.

A state-of-the-art survey for the SEPS equipment was conducted and this was included in Section 10.1 of this report. An in depth analysis, of the SEPS requirements was beyond the scope of this study and has been deferred until a future study phase.

During the inception of this study several lunar mission programs were specified (reference 4.1). These programs were designated numbers I, II, III, IV, and V. These programs, together with their total mission energy requirements are summarized in Table 2.1.

Table 2.1 Total Mission Energy Requirements

Program No.	Mission Duration	Crew Size	No. of LSV's	Total Mission Energy (kw-hrs)
I II	One-14 day visit	4	1	3,960
IIIa	One-28 day visit	6	1	10,800
IIIc	Three-28 day visit over 6 month period	12	3	67,000
IV	Four-56 day visits over 12 month period	12-24	6	295,000
V	Two-90 day visits over 12 month period	3	2	32,800

Using, nominal, state-of-the-art values, four basic power systems were compared for each of these programs. They were as shown in Table 2.2.

Table 2.2 Candidate Lunar Surface Power Systems

No.	System Description
1	Solar Array and Secondary Batteries
2	Solar Array, Fuel Cells, ERPS, and Transported Initial Reactant
3	Fuel Cells and Transported Reactants
4	Solar Array, Fuel Cells, and Transported Reactant

The results of these analyses are shown in Figures 4.8 and 4.9 of Section 4. It was found that when total mission energy requirements exceed approximately 25,000 kw-hrs, that system (2) had the lowest weight. A summary of these weights for the Program V mission only is shown on Figure 2.1. Also included was a nuclear thermoelectric system (Table 4.10 of Section 4). It can be seen that as total mission energy increases, System (2) is superior, from a weight standpoint, to all the other candidate power systems considered.

During this study, several investigations were conducted to assess the use of solar arrays (with and without secondary batteries) for various lunar surface activities. These included:

- o surface mining operations
- o water extraction power requirements
- o conservation of LSV reactants

The results of these studies are described in Section 4.5 and Appendix A. The cross-over points where it becomes system effective to use solar array power systems are depicted.

The requirements for the stowage of the candidate LEPEPS in the Saturn V launch vehicle shroud are outlined in Section 4.7. The data is presented in parametric form so that it may be applied to various array configurations. Detailed operations analyses were also conducted to arrive at the deployment and assembly time required for the various candidate solar array systems. This data was used in establishing stowage volume requirements and total power systems costs

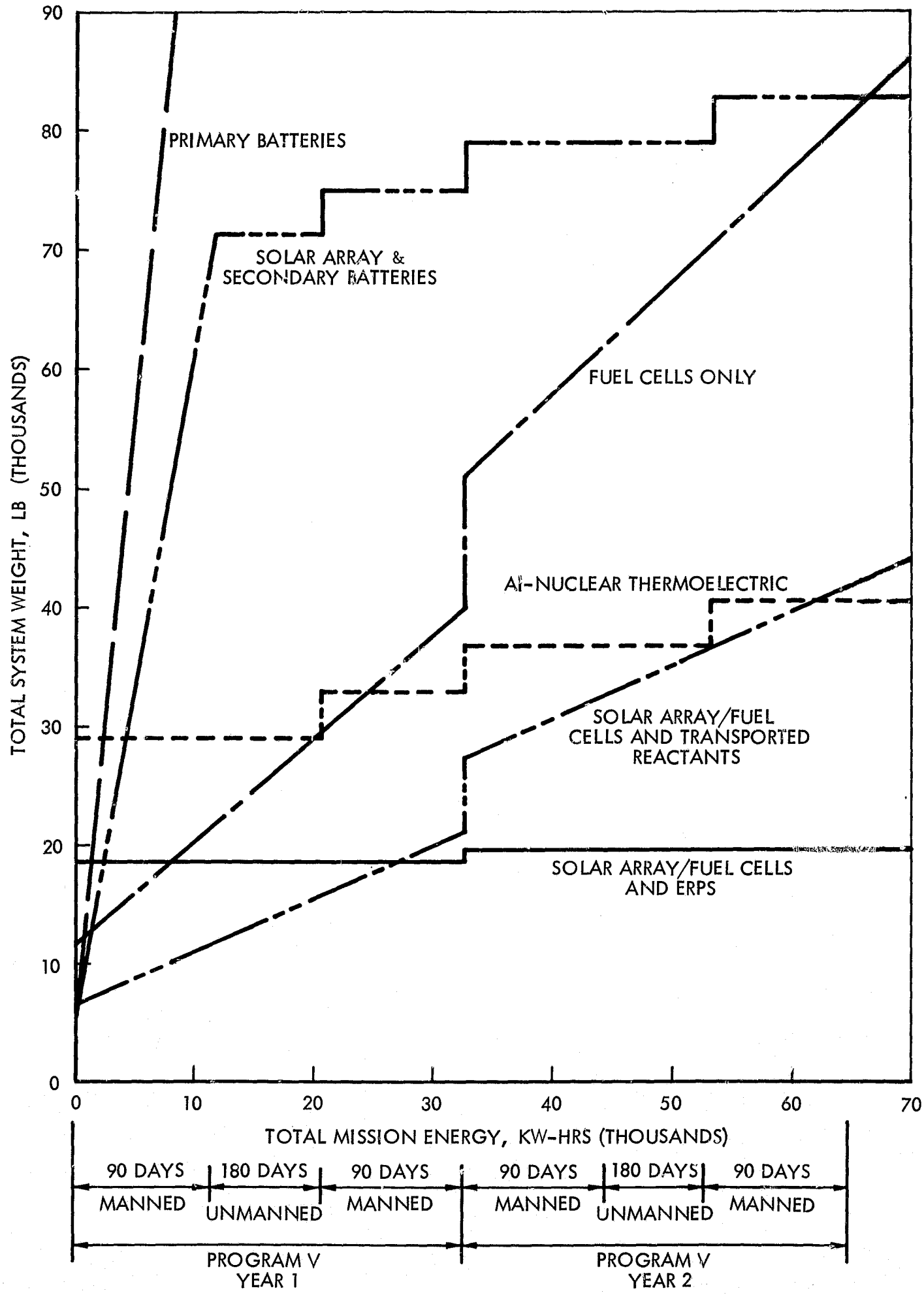

Figure 2.1 Comparison of Lunar Surface Power Systems

(Table 4.9 of Section 4). Both total power system weight and cost are depicted in Table 4.9. From this table it can be seen that the lightest candidate power system does not necessarily result in the lowest cost system for the Program V mission.

In order to analyze the other elements of the LEPEPS (power conditioning, power distribution, controls) it was necessary to synthesize an overall lunar base arrangement. A schematic of this lunar base is shown in Figure 10.28 of Section 10. The leanto solar array was depicted, but the arrangement, with slight modifications, would be equally applicable to the flat and oriented-skirted array configurations. Using Figure 10.28 as a baseline arrangement, parametric data was generated to arrive at the best solar array unregulated bus voltage level to operate at. A value of 300 vdc was selected as providing the highest power conditioning system efficiency and resulted in minimum total power system weight. This value is unique for the power levels and load characteristics for the Program V mission. Further analysis would be required to determine the preferred magnitude of this voltage for other mission requirements and load characteristics. A comparison of total LEPEPS weights as a function of array bus voltage for the various candidate array configurations is given in Figure 10.42 of Section 10. Due to the many factors discussed in Sections 4, 8, 9, and 10 of this report, these do not necessarily represent optimized systems. However, they do indicate a realistic range of achievable system weights and confirm the feasibility of the solar array power system as a candidate for the Program V mission. A pictorial representation of the Figure 10.28 lunar base arrangement is shown in Figure 2.2. This is typical of one of the many possible arrangements that might be employed in setting up the lunar base. However, because of the modular power system concept approach used during this study, various candidate solar arrays could be utilized for the lunar base. Typical examples of these are shown in Figures 2.3, 2.4, 2.5, and 2.6. Figure 2.3 depicts a flexible substrate leanto configuration. Figure 2.4 presents a rigid substrate leanto concept. Figures 2.5 and 2.6 show two

different concepts for the oriented-skirted configuration. Standardized 3.3 ft x 8.0 ft modules are used as the basic building block to make up any of the rigid substrate sub-arrays.

Another objective of this study was to prepare a "Design Requirements Document" of the candidate lunar surface power system for the Program V mission. This was done and incorporated in Appendix B of this report. This document represents a preliminary specification for the LEPEPS which must be supplemented with more specific details when additional mission data becomes available. However, by including all the criteria essential in preparing such a document, it does aid in high-lighting those technical areas where additional interface information is still required.

A final objective of this study was to prepare a preliminary Program Development Plan for implementation of the LEPEPS within a five year period. A detailed discussion of this plan is provided in Section 12 of this report. A tentative schedule for the candidate lunar surface power system is depicted on Figure 12.1. The resource requirements, normally identified with such a plan, have been omitted. It was deemed too premature to arrive at meaningful estimates for the research and development costs for the overall LEPEPS. However, cost estimates for the various candidate lunar surface power systems are given in Table 4.9 of Section 4. In addition, a Lunar Surface Power System Cost Nomograph (Figure 4.17 of Section 4) has also been prepared. This nomograph can be used in estimating both R & D and production costs for lunar surface power systems during the program planning phase.

FOLDOUT FRAME

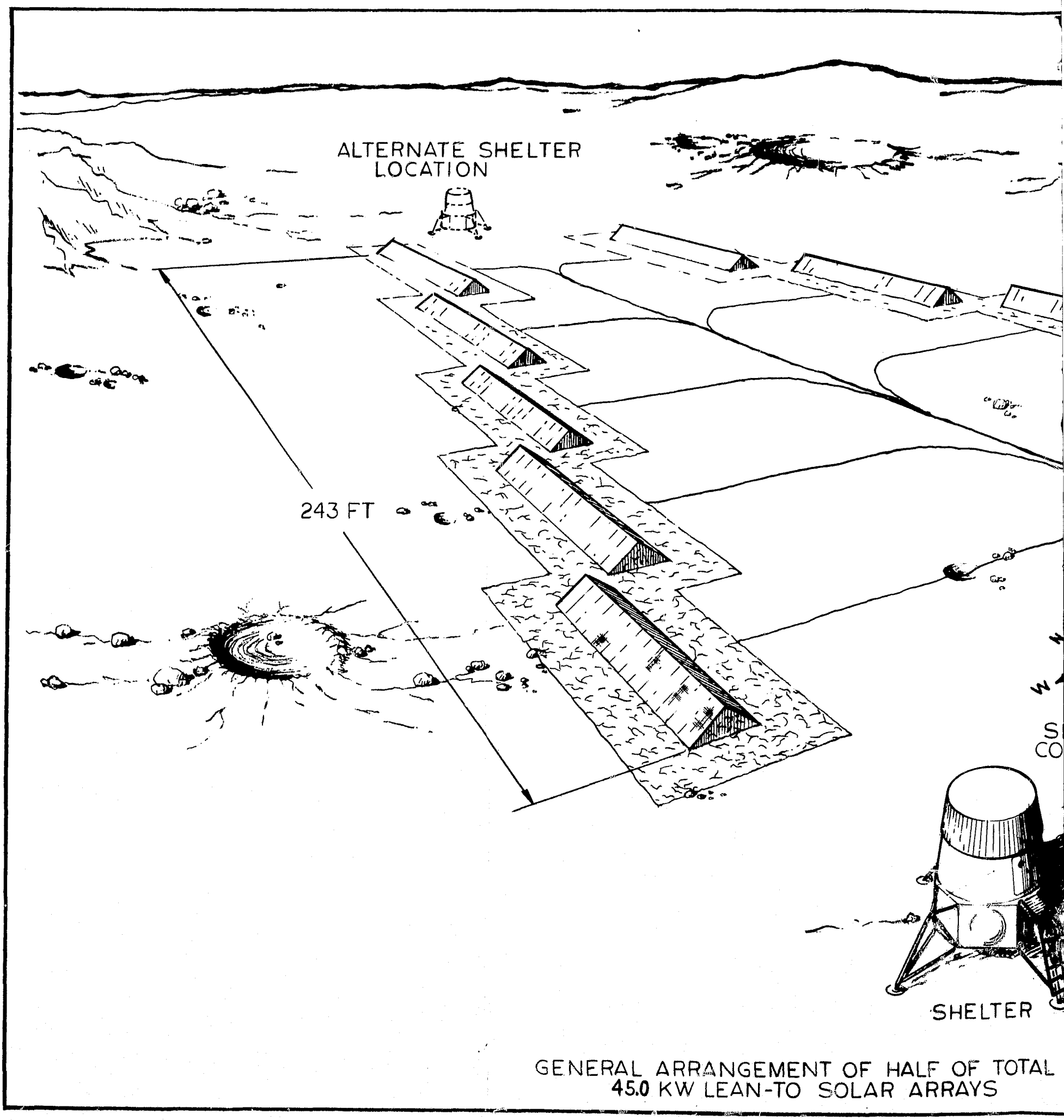

Figure 2.2 General Arrangement of Candidate Lunar Surface Power System (45 kw Leanto Solar Arrays)

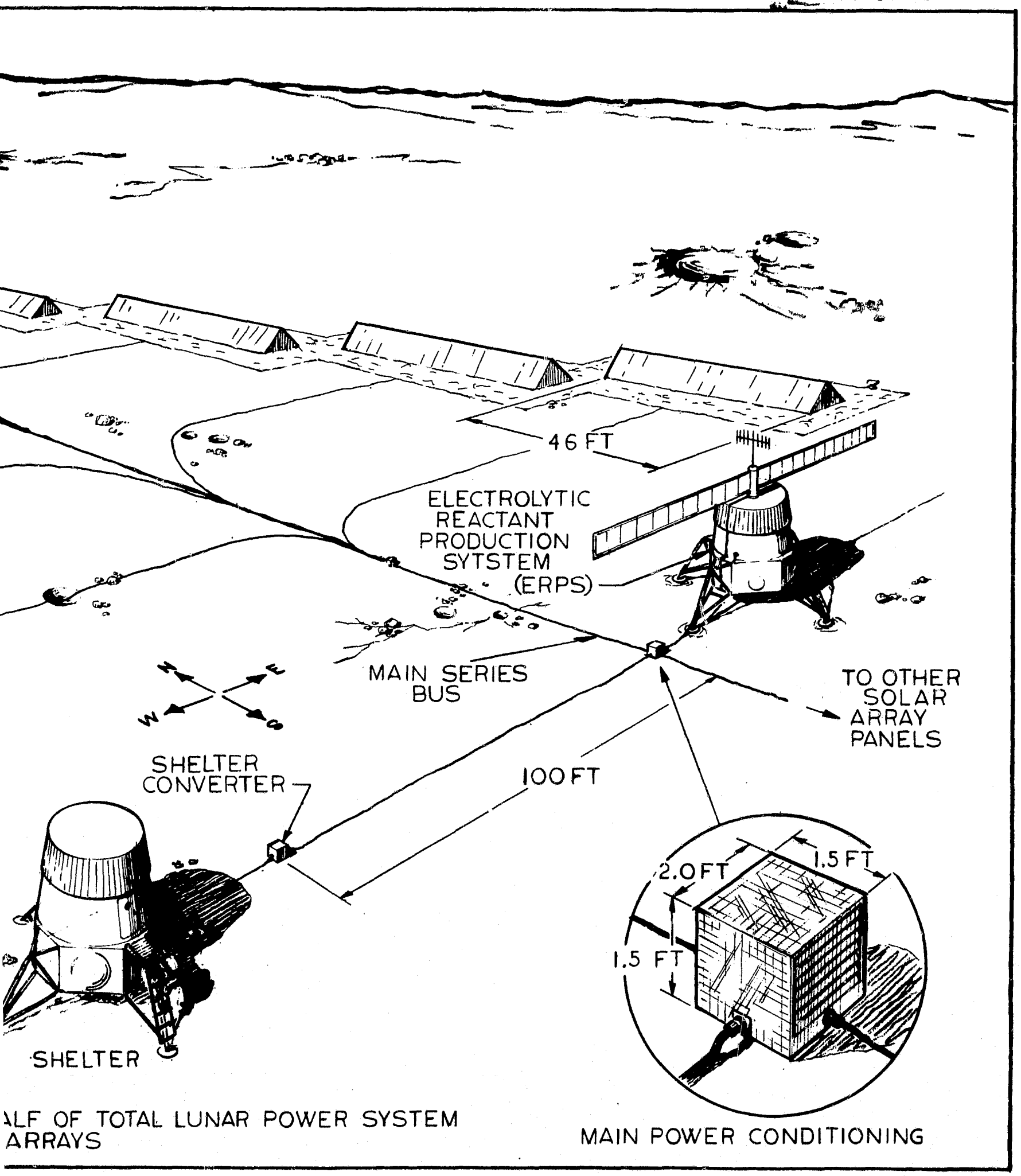
46 FT
ELECTROLYTIC
REACTANT
PRODUCTION
SYTSTEM
(ERPS)
MAIN SERIES
BUS
TO OTHER
SOLAR
ARRAY
PANELS
N
E
W
S
SHELTER
CONVERTER
100 FT
2.0 FT
1.5 FT
1.5 FT
SHELTER
ALF OF TOTAL LUNAR POWER SYSTEM
ARRAYS
MAIN POWER CONDITIONING

FOLDOUT F

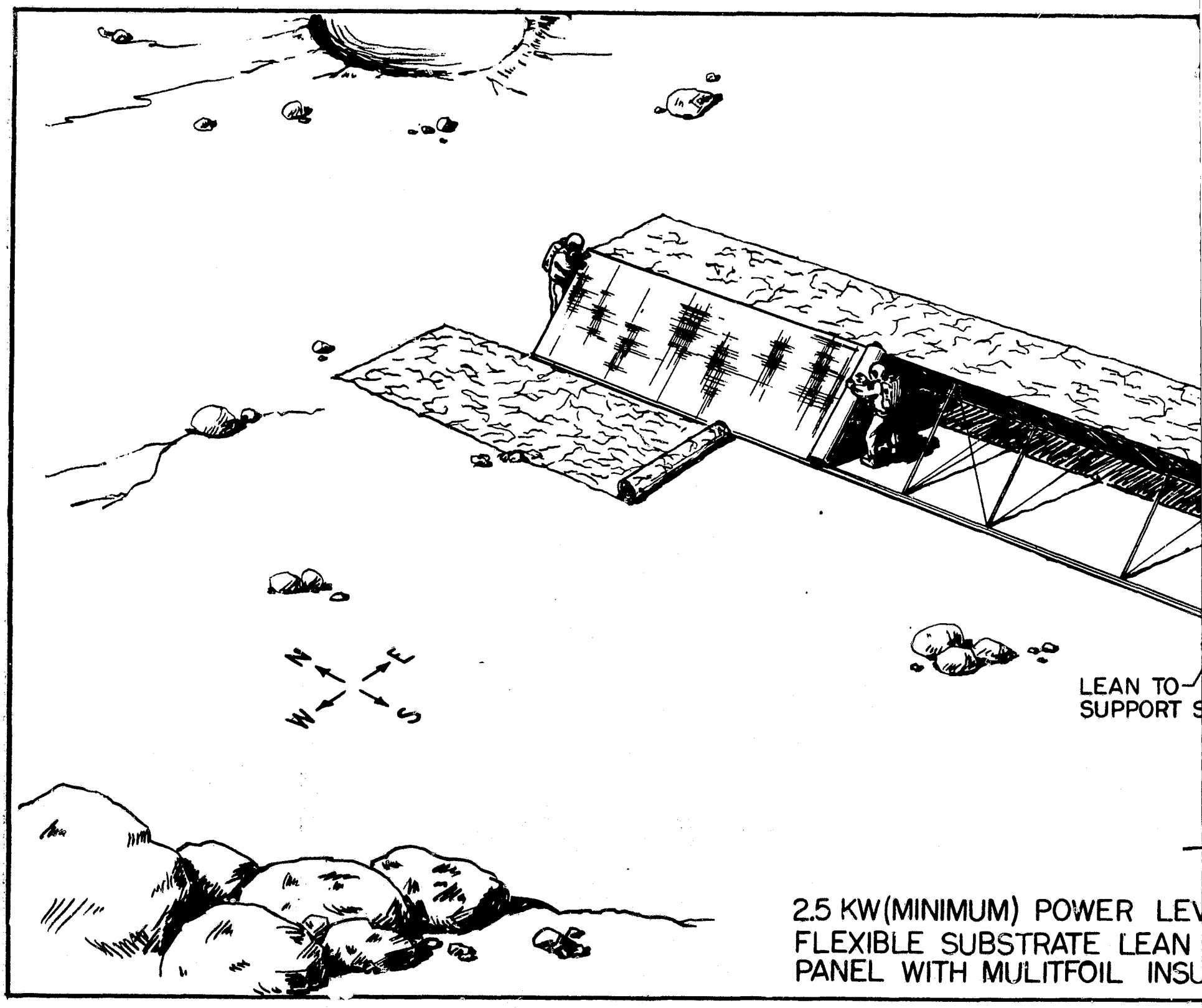

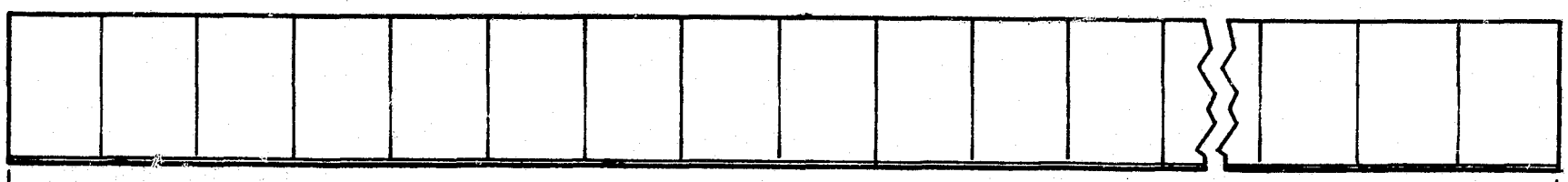

46.2 FT(14 SINGLE CRYSTAL MODULES @ 3.3 FT)
69.3 FT(21 THIN FLIM MODULES @ 3.3 FT)

DEPLOYED DIMENSIO

FOLDOUT FRAME

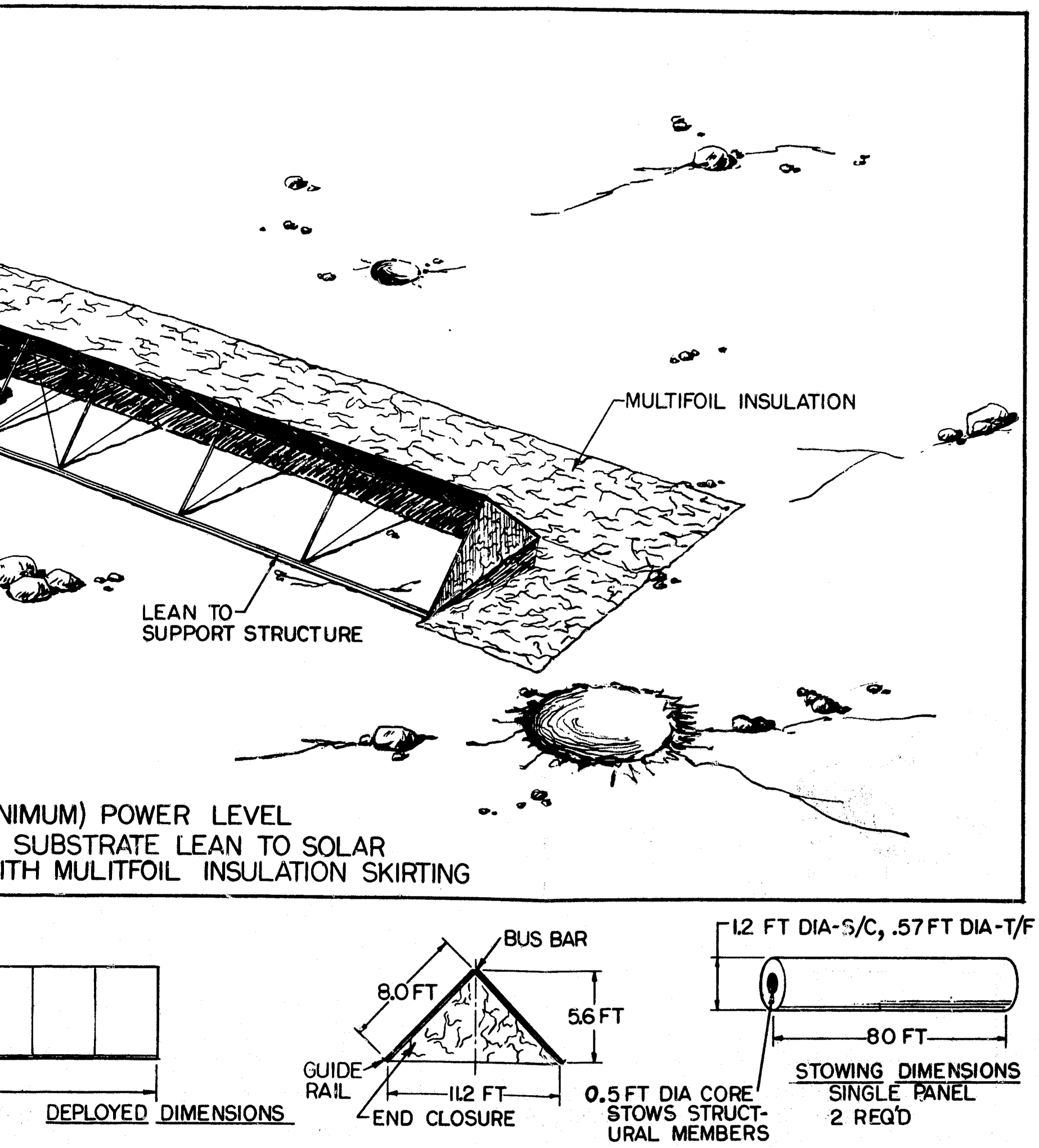

Figure 2.3 2.5 Kw Power Level Flexible Structure Leanto Solar Panel with Multifoil Insulation Skirting

FOLDOUT FRAME

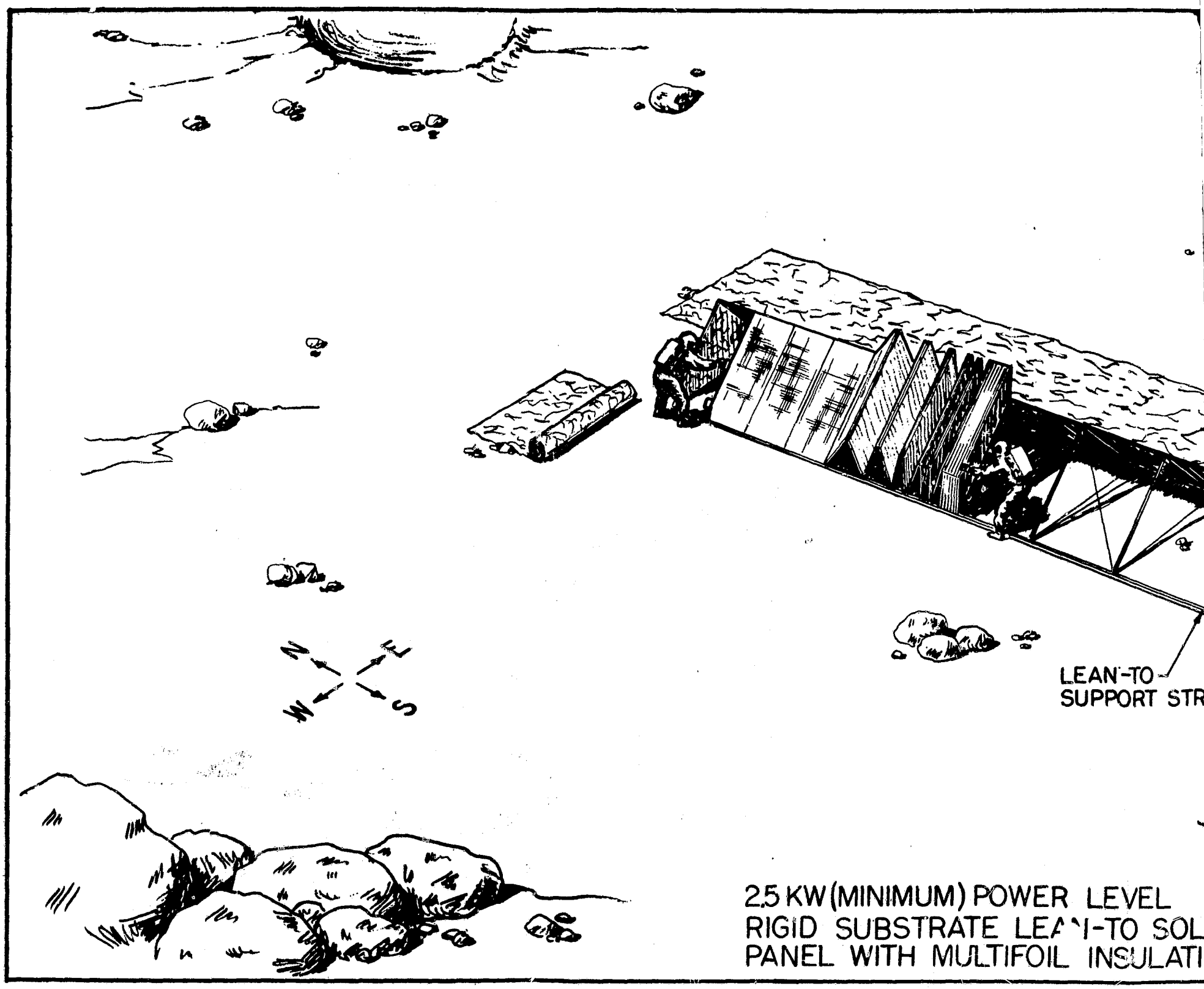

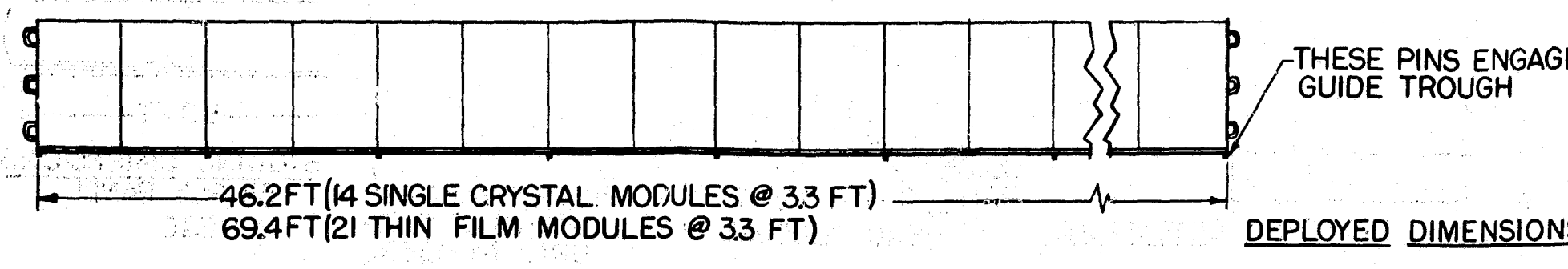

DEPLOYED DIMENSIONS

FOLDOUT FRAME

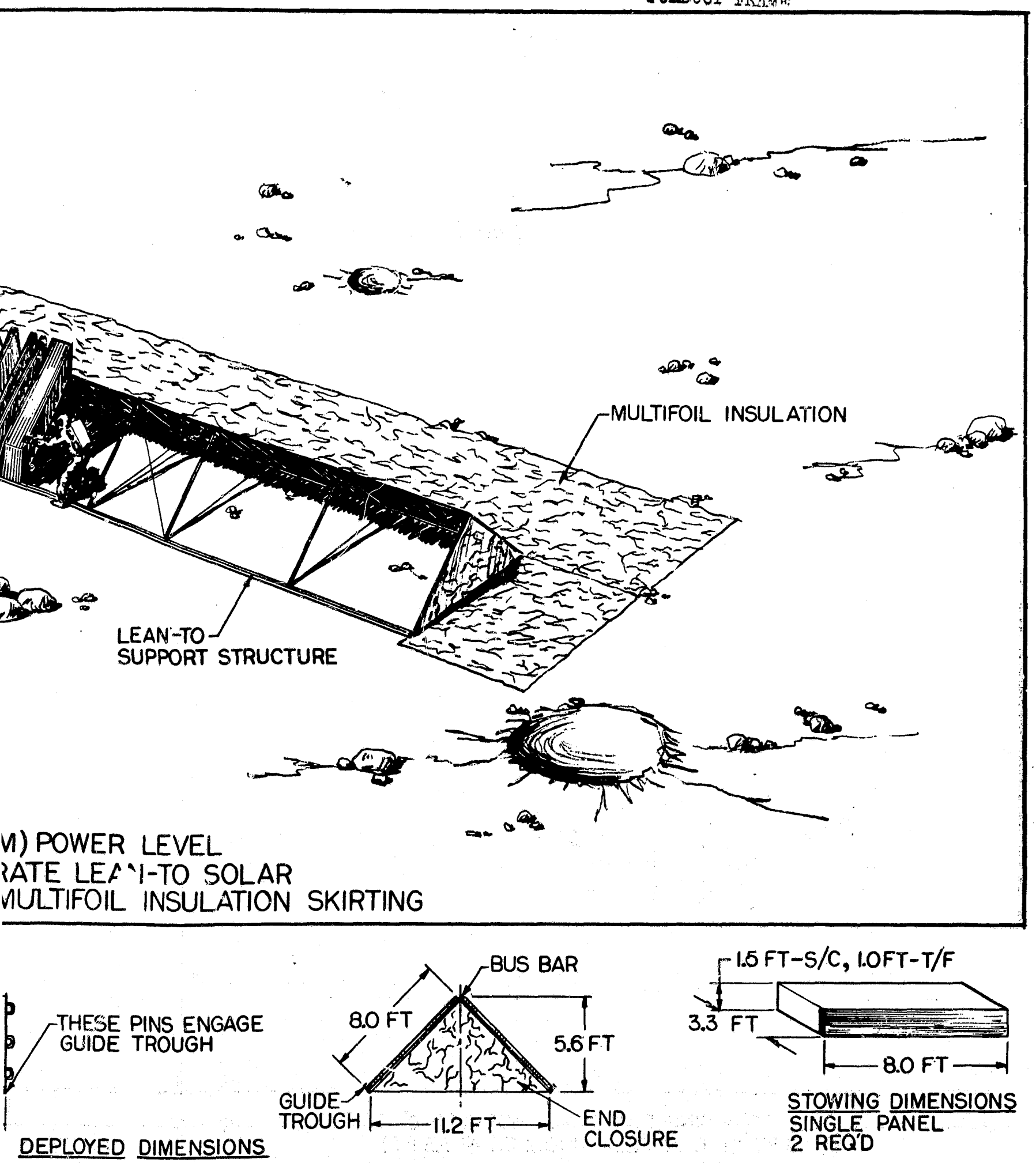

Figure 2.4 2.5 Kw Power Level Rigid Structure Leanto Solar Panel with Multifoil Insulation Skirting

FOLDOUT FRAME

POWER OUTPUT	CELL TYPE	ARRAY AREA FT^2	DUMMY PANELS	NO. OF 8' X 3.3' SUBARRAYS FOR 2.5 KW
2.5 KW	THIN FILM	668	1 AND 2	26
5 KW	SINGLE CRYSTAL	700	1	14

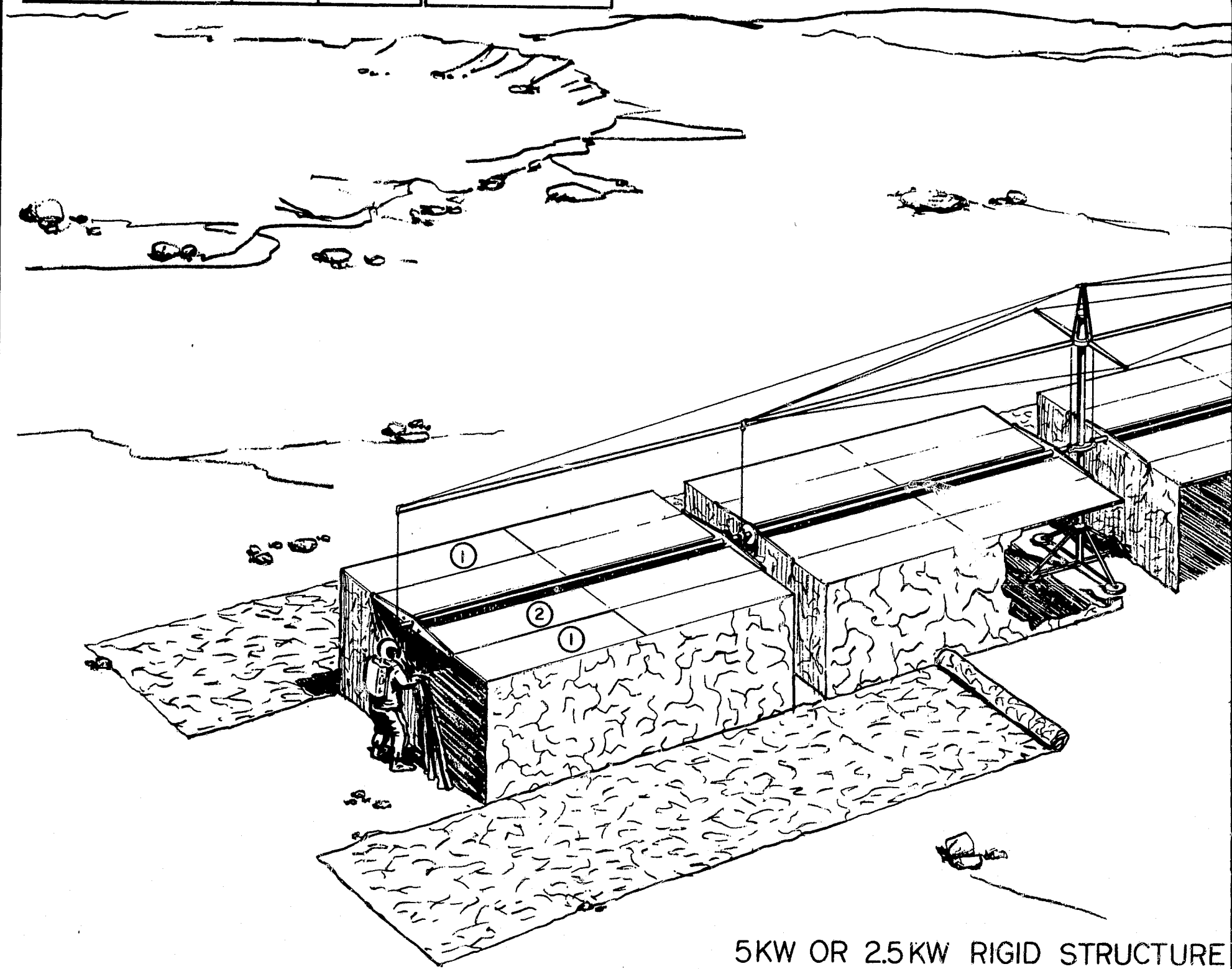

5KW OR 2.5KW RIGID STRUCTURE
ORIENTED SKIRTED SOLAR ARRAY

FOLDOUT FRAME

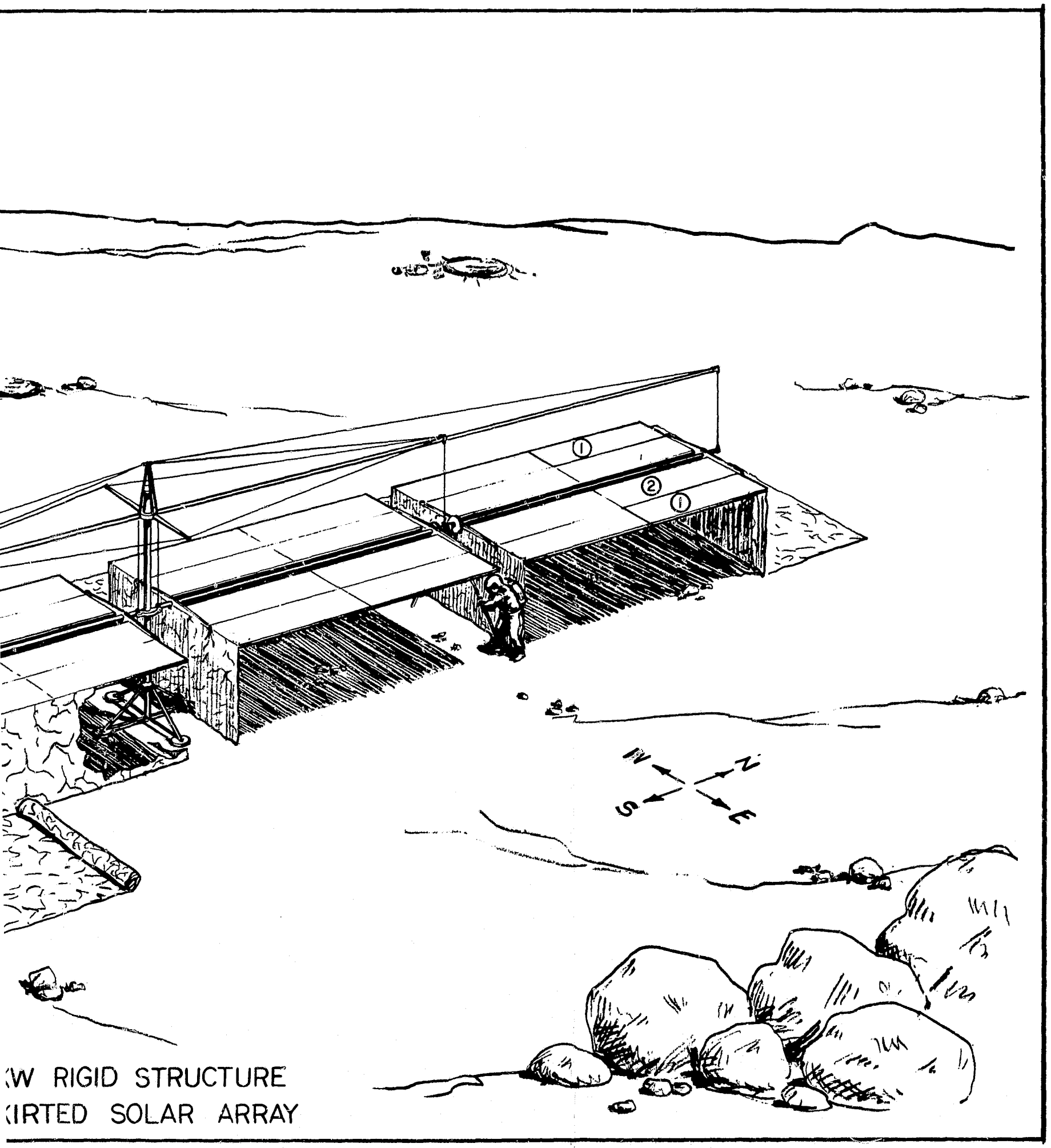

Figure 2.5 2.5 Kw or 5 Kw Power Level Rigid Structure Oriented-Skirted Solar Panel with Multifoil Insulation Skirting (Concept 1)

FOLDOUT FRAME

POWER OUTPUT	CELL TYPE	ARRAY AREA FT^2	NO. OF 8' X 3.3' SUBARRAYS	NO. OF 8' X 3.3' SUBARRAYS FOR 2.5 KW
5 KW	THIN FILM	1336	52	26
10 KW	SINGLE CRYSTAL	1400	56	14

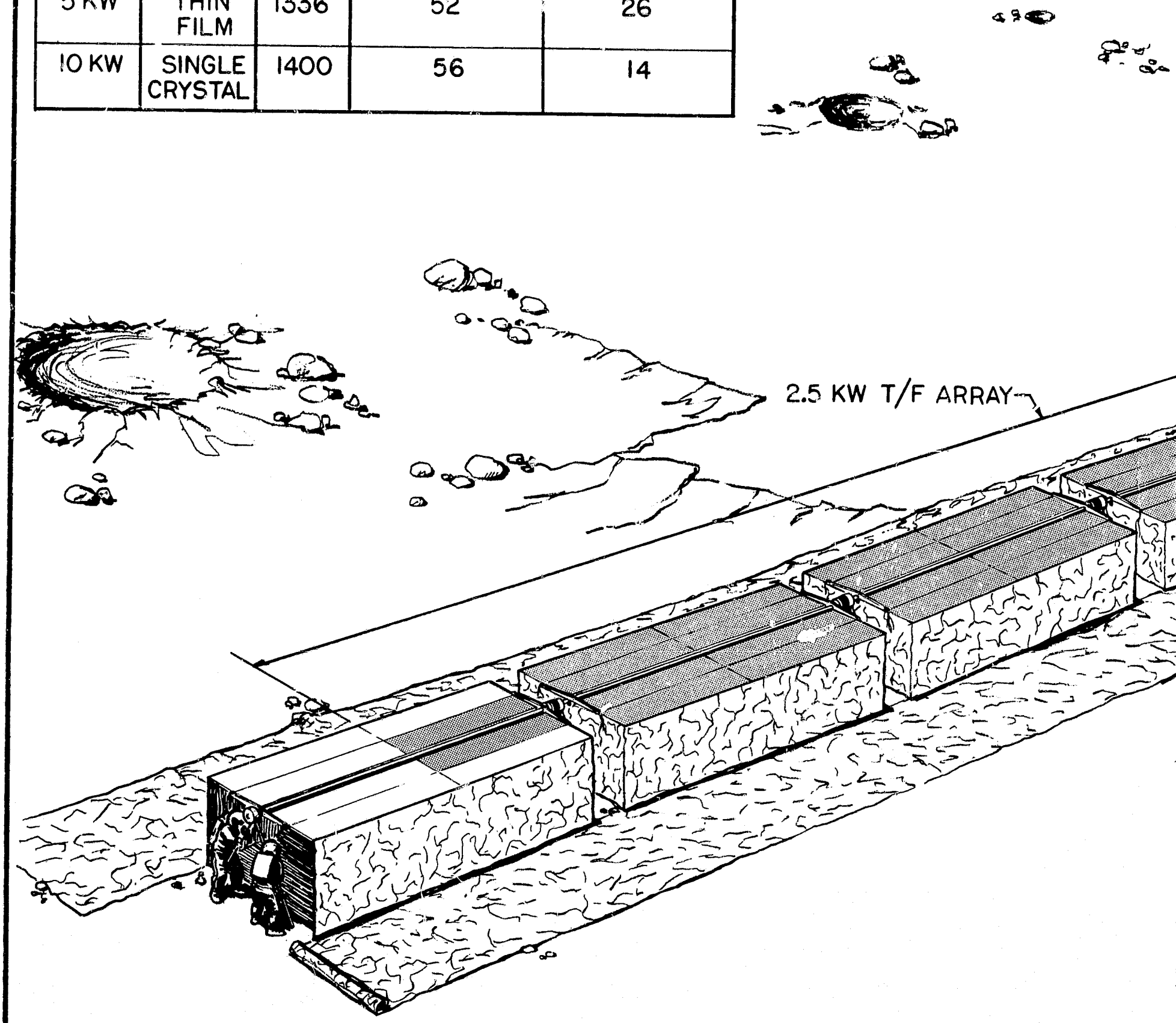

Figure 2.6 2.5 Kw or 5 Kw Power Level Rigid Structure Oriented-Skirted Solar Panel with Multi-foil Insulation Skirting (Concept 2)

10KW OR 5KW RIGID STRUCTU
ORIENTED SKIRTED SOLAR AR

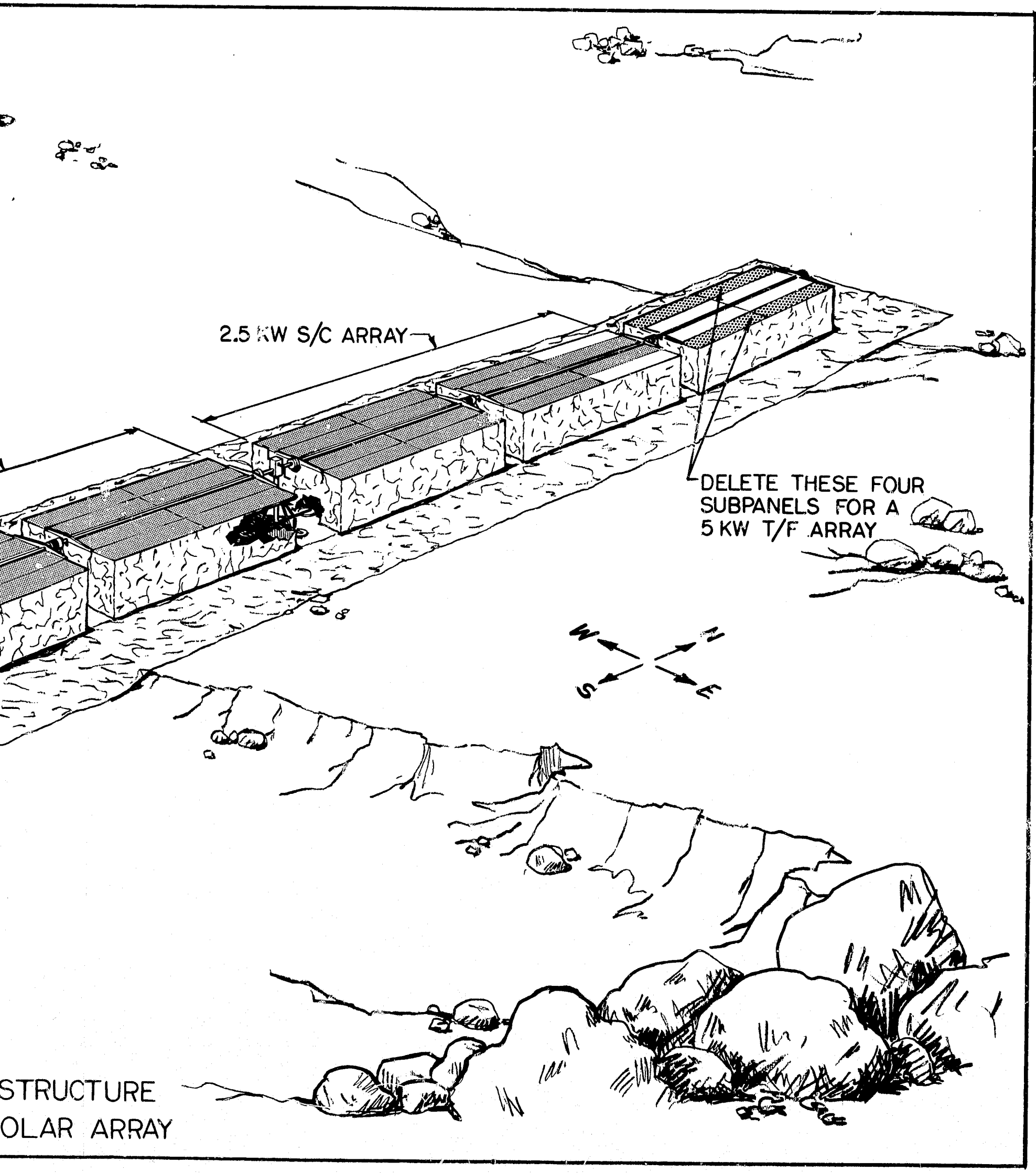

STRUCTURE
OLAR ARRAY

3. CONCLUSIONS AND RECOMMENDATIONS

3.1 CONCLUSIONS

The results of this study indicate that the use of large solar arrays on the lunar surface is feasible. Furthermore, in many instances they provide the most system effective solution for meeting the energy requirements for various lunar surface exploration missions. The following conclusions can be drawn from the work covered during this study phase.

- The use of large solar arrays on the lunar surface is feasible. They can be made compatible with the lunar environment by employing proper design techniques.
- Both single crystal silicon cells and cadmium sulfide thin films are capable of providing adequate performance.
- The solar array/fuel cell/ERPS system is an attractive concept for providing power for a lunar surface exploration base. It represents the most technologically advanced system that could be flight ready by the early 1970's. In addition, for high mission energy requirements (above 25000 kw-hrs), it represents the lightest weight system that could be employed in that time period. Based upon the results of this study, this concept is superior to other competitive systems for the Program V mission.
- The flat, leanto, and oriented-skirted solar array concepts were all capable of meeting one or more of the proposed ERPS power profiles. A more detailed system engineering study involving performance, weight, cost, and reliability tradeoffs between all elements of the lunar energy depot would be required to arrive at an optimum design configuration.

- The varying array temperature was found to be the most critical performance parameter. However, this parameter can be controlled passively by the use of various design techniques (skirting, mis-orientation, back-side insulation, etc.).

- The solar array output power profile characteristics can be modified to match the requirements of various load power profiles. This can be accomplished by the use of hybrid arrays (variable geometries), and array equilibrium temperature control (mis-orientation, skirting, insulation, active cooling). Additional flexibility in controlling array output power profiles could be achieved by the use of separate array systems. Each system would employ a different array configuration. The resulting superimposed output power profile would be designed to closely match the load power profile.

- Lunar roving vehicles will undoubtably rely on fuel cells for both motive power and environmental control and life support requirements. The use of solar arrays and secondary batteries mounted on these vehicles could reduce the propulsive power fuel cell reactant requirements by 5 to 20 percent. In addition, the need for reactant regeneration will become mandatory to minimize the overall mission payload. This will become increasingly evident when roving vehicle energy requirements begin to equal or exceed the lunar base shelter requirements.

- The use of a solar array/ERPS system for mining and water extraction becomes practical, if the water content of the lunar surface exceeds one percent.

- The solar array structural substrate can be made common to all candidate array configurations and for any lunar surface location. In addition, by use of a modular concept, lunar surface power solar arrays can be provided for a range of 2.5 to 100 kw using the same basic design elements. Finally, there does not appear to be any fundamental technology factors that would preclude achieving an operating life of at least five years. These inherent design characteristics could lead to considerable cost savings on future missions.
- The use of solar array/secondary battery systems as power oases appears attractive. They could be judiciously located along the paths to be traversed by the roving vehicles during various lunar surface exploration sorties. Utilized in this manner, they would greatly increase the reliability of the mission and considerably enhance the chances for astronaut survival in the event of failure of the lunar surface roving vehicle power system.

3.2 RECOMMENDATIONS

This study has served to confirm the feasibility of using solar arrays on the lunar surface. This conclusion is based upon the assumptions made during this study and the resulting performance characteristics, weights, and costs established for the candidate lunar surface power systems. However, there are several technology areas that should be further investigated in order to assure the adequacy of the design assumptions and to minimize development risks. The following recommendations are provided to identify these technology areas.

- Because of the criticality and sensitivity of overall solar array performance and design to the array equilibrium temperatures, additional thermal analyses should be conducted to more accurately assess this parameter.

- A detailed design and experimental test program should be conducted using an engineering test module of a typical solar array module. This development activity should be directed towards evaluating the structural dynamic characteristics of the array module and determining its ability to withstand the launch environment. In addition, the compatibility of the array materials (structural substrates, silicon cells, adhesives, cover glass, thermal coatings, etc.) with the lunar surface environment should be assessed.

- A more detailed systems engineering and tradeoff study of the various systems and subsystems comprising the overall Program V mission and lunar surface energy depot should be made to establish the most system effective approach.

- Single crystal silicon cells have been selected for the candidate solar arrays. They represent the photovoltaic material which has reached the highest state of development. They have been used extensively on both Earth orbital and planetary spacecraft. However, due to their potential for greater radiation damage resistance and reduced cost, consideration should be given to cadmium sulfide thin films. However, considerable development effort and experimental data is still required to determine their performance stability and sensitivity to temperature cycling before their use can be recommended.

- Consideration should be given to extending the stay-times of nearer-term, short duration (14 to 28 day) lunar surface exploration missions by the use of solar array/secondary battery lunar surface power systems.

4. MISSION AND SYSTEM REQUIREMENTS

4.1 MISSION OBJECTIVES

The lunar programs with which this study was concerned ranged in duration from 14 days to one year or more, involved from 3 to 24 men and one to three surface vehicles. Brief descriptions of five specific programs of progressively greater magnitude and complexity are given in Table 4.1.

The primary purpose of these missions is the exploration of the lunar surface in the vicinity of an established base, and the scientific investigation of geologic, topographic, astronomic and other phenomena within the domain of observation. While these are the principal objectives of the proposed missions, the present study is intended mainly to develop versatile, long-life, high-performance, electrical power systems that are compatible with the lunar surface environment and have the reliability and operational features needed to meet the requirements of these missions and to enhance the capabilities of lunar surface vehicles to perform extended lunar explorations. A closely related objective was the systematic study of the lunar equipment prime electrical power system (LEPEPS) which activates an electrolytic reactant production system (ERPS) for the regeneration of reactants from the water obtained from the fuel cells used at the base and on the lunar surface vehicles (Reference 4.1).

The system requirements for LEPEPS were determined for each of the programs, criteria was established for the design of solar cell array systems to provide the necessary power, and preliminary designs were prepared for the mission (Program V) and systems of greatest interest. The solar array systems were then compared with other primary power sources and modes of operation to determine which of the many candidates was most attractive from the standpoint of minimum logistic weight, stowage volume, and overall system cost. The general approach taken is outlined in Table 4.2.

The results are presented in such a form that they may be used for other missions than those specified, and for other modes of operation of

the lunar base. In general, the solar array design data are applicable to a wide variety of lunar and planetary base concepts.

4.2 STUDY GUIDELINES AND CONSTRAINTS

The primary concepts on which the solar array/electrolysis system study was based encompassed lunar base operations, surface exploration and scientific investigations. In addition to establishing the characteristics of the primary power source and adapting it to the water electrolysis system power profiles, application of solar cell arrays to the lunar mobile vehicles were also investigated to determine if mission system effectiveness would increase with the incorporation of these operations. Applications to manned space stations and long range planetary vehicles was beyond the scope of this study.

General systems analysis and tradeoff studies were used to narrow the field of candidate systems and modes of operation. Attention was focused on system interfaces, and the operational and environmental aspects which are compatible with (or independent of) the electrolysis system design. As a result of this approach, several candidate configurations were selected as preliminary baseline designs which would have a wide variety of application throughout the lunar surface exploration mission field.

Several mission concepts and modes of operation were considered at the inception of this study. The emphasis was on the selection of practical missions and systems which would be feasible for implementation during the mid-70's. Additional equipment and capabilities could be added at a later date to support more complex subsequent missions which could provide for almost continuous operation and which could take full advantage of lunar resources and future technological advancements.

The results of previous lunar surface studies (Reference 4.4) were utilized and updated in the parametric development of design procedures, environmental constraints, operational concepts and logistic interfaces, to provide a broad background of pertinent data applicable to many as yet unspecified future lunar missions. These parametric data were used to analyze in greater depth the characteristics of selected mission systems in order to illustrate the applicability of the design procedures. Finally,

Table 4.1 Specified Lunar Mission Programs

The programs for which the LEPEPS is designed are listed in Reference 4.1 (Section 2.4.7) as follows (Program V was added later in the study per References 4.2 and 4.3):

1. Program I - Establish a four-man energy depot and logistics base with the capability of supporting a one or two man mobile vehicle operation on the lunar surface for 14 days.

2. Program II - Same as Program I initially, but with provisions and additional support to sustain, subsequently, two active manned periods of 14 days. Each active period is expected to be separated by a dormant standby, unmanned period of several months.

3. Program III - Program III would establish a base for a total of 12 men for a continuous 28 day period. The base must accommodate all personnel only for short periods. During the remainder of the time, exploration parties would be deployed in vehicles. A typical operation is:

   a. Initial Period - Six men landed and one two-man vehicle available. Conduct exploration by deploying two-man crew and rotate crew as needed. Perform scientific investigations at base site. At end of 28 days, place equipment in dormant standby and return personnel to earth.

   b. Dormant Period - Unmanned base and equipment in standby for two to three months. Land two more mobile vehicles and base supplies. After deployment of equipment and checkout, proceed with additional manned activities.

   c. Active Period - Reactivate base and vehicles and provide a 12-man crew to operate base and the three mobile vehicles. Perform extensive exploration and scientific experiments for a minimum of 28 days and with the following options.

      (1) To follow up with several dormant and active periods.

      (2) To continue to operate for three to six months having the necessary logistics and crew rotation.

4. Program IV - Determine an optimum program to progressively establish a larger, more permanent energy and logistics base similar to that of Program III. This base should be sized to support between 12 to 24 persons, as determined, a larger scientific program, and either more vehicles or ones with greater capacity and range. The establishment should provide an active operational capability of at least 56 days. It should be capable of conducting a one year mission where the active periods are maximum and the intermittent dormant periods are 28 days.

5. Program V - Mission of one year duration, requiring the base to be established and used by a 3-man crew during the first 3 month period, then left unattended for 6 months with automatic operation of ERPS, followed by a final 3 month revisit by a 3-man crew.

a Design Requirements Document was prepared to describe the system believed to have the most attractive features for early development during the mid-70's. Technology requirements and near-term mission operations requirements were defined as the basis for estimating the R&D development effort needed to implement the systems by the specified flight readiness date.

The logistics and deployment aspects of the power systems were treated at some length in Section 4.7. The stowage volume constraints imposed by the Saturn V launch vehicle were examined for compatibility with the solar array areas and other subsystems constituting the LEPEPS. Labor saving methods of unloading and transporting the power system from the landing site to the selected power site were investigated. Procedures and manual energy requirements were determined for deploying the various solar array configurations in a reasonable length of time, without exceeding the work level capabilities of astronauts in space suits on the lunar surface.

4.3 ENERGY DEPOT REQUIREMENTS ANALYSIS

The power requirements of the various specified mission programs (Table 4.1) for which the energy depot will be used was determined by the analysis of the quantities of reactant consumed by the surface vehicles, plus the additional power required to service the energy depot; i.e., environmental control, lighting, communications, life support, etc. This analysis served to evaluate the total conditioned power output to be obtained from the solar array, and its distribution between the ERPS and the base facilities for day and night operations to accomplish the overall mission objectives for each of the specified programs. The power and reactant requirements for each of the programs are tabulated in Table 4.3.

A typical power profile for the energy depot during a typical 28-day lunar period is shown in Figure 4.1. Assuming a constant (or variable) output from the solar array as shown, a small percentage of the total power will be continually consumed by the base facilities; another increment will be used to charge secondary batteries, and to condition fuel cells for operation; and the remainder will be used by the ERPS to dissociate the water into H_2 and O_2 and to liquify the reactants. A portion

FOLDOUT FRAME

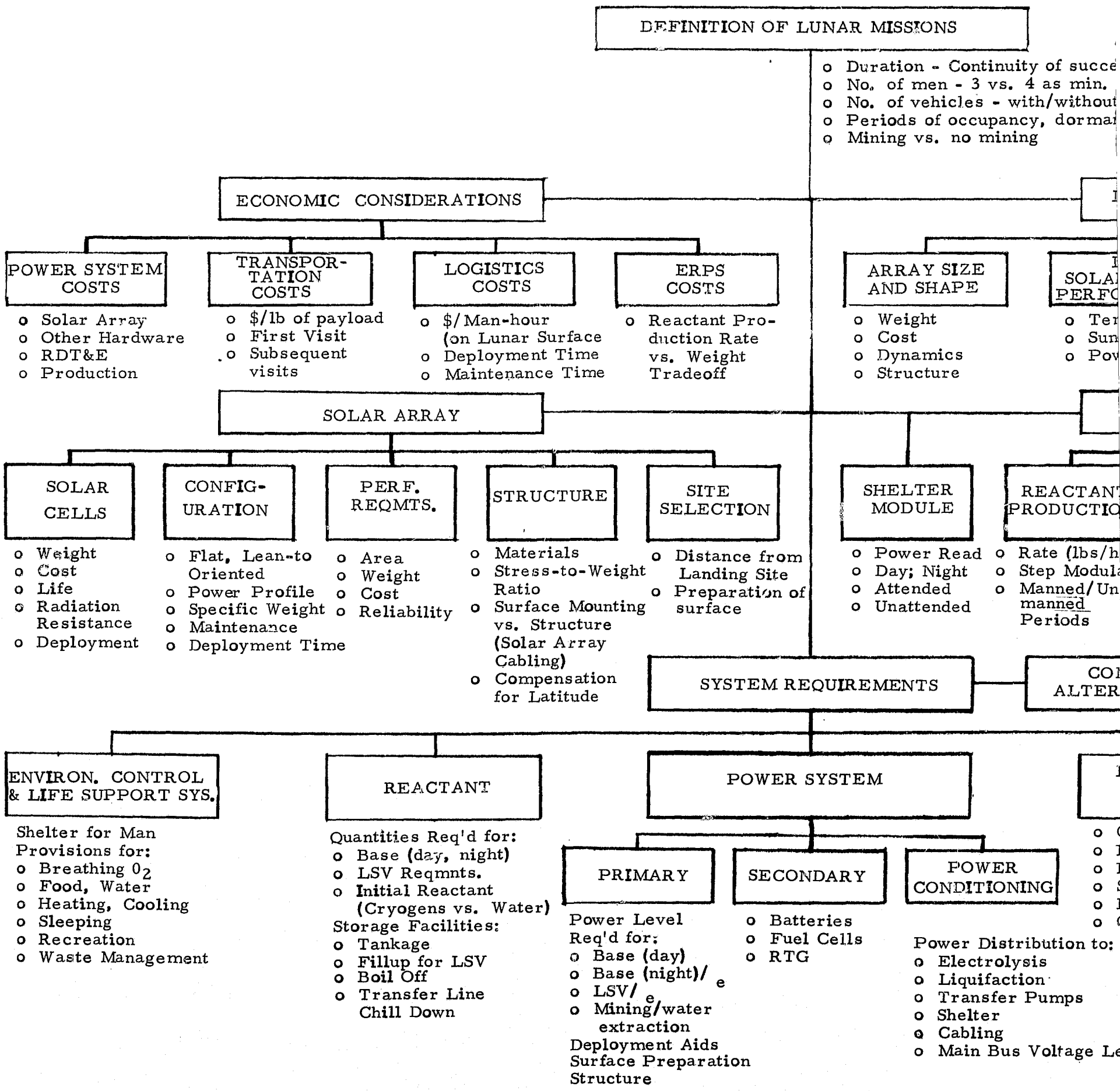

FOLDOUT FRAME

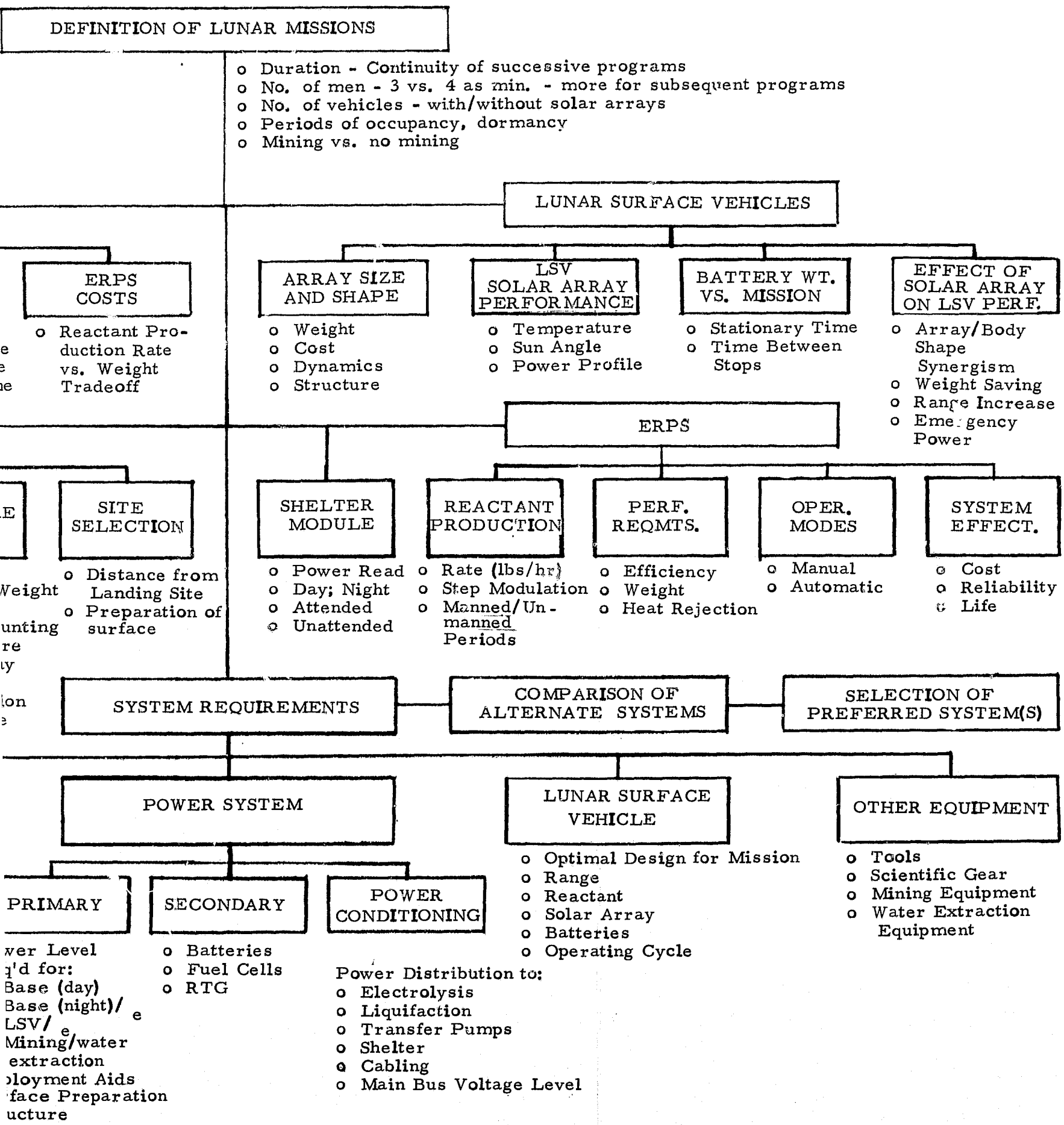

Table 4.2 Block Diagram of Lunar Mission and Systems Analysis

FOLDOUT FRAME

Table 4.3 POWER AND REACTANT REQUIREMENTS FOR SPECIFIE

PROGRAM AND DURATION	NO. OF MEN	NO. AND TYPE OF SURFACE VEHICLES	LSV FUEL (LB/HR)	CONSUMPTION TOTAL (LB)	SHELTER POWER REQUIRED (KW)	REACT	
						SHELTER	VEH
I (14 DAYS) INITIAL TRIP TO ESTABLISH ENERGY DEPOT	4	1 (ONE- OR TWO- MAN LSSM)	3	600	10	0	
II (14 DAYS) TWO RETURN TRIPS AFTER DORMANT PERIODS OF SEVERAL MONTHS*	4	1 (AS ABOVE)	3	600	10	0	
IIIA (28 DAYS) ESTABLISH BASE AND EXPLORE	6	1 (TWO- MAN LSSM)	3	1,000 (333 HOURS)	15	4,600	1,
IIIB (2-3 MOS.) DORMANT UN- MANNED*	0	LAND TWO- MAN LSSM & MOLAB	0	0	0	0	
IIIC (28 DAYS) (1) SEVERAL ACTIVE AND DORMANT PERIODS* (2) CONTINUOUS OPERATION FOR 3-6 MONTHS, WITH NECESSARY LOGISTICS AND CREW ROTATION	12	2 (TWO- MAN LSSM 1 MOLAB	2X3 1X5	1,200 1,000 2,200 TO 13,200	30 (FROM LERC STUDY, REFERR- ED TO IN ERPS RFP APPENDIX ON GUIDELINES SAMPLE)	9,200 TO 55,000	2,2 TO 13,2
IV (56 DAYS MIN) OPTIMUM PROGRAM FOR ONE YEAR MISSION. MAX. ACTIVE PERIODS WITH 28 DAY DORMANT PERIODS*	12-24	2 (TWO- MAN LSSM) 2 MOLAB 2 LONG RANGE SV	2X3 2X5 2X9	2,400 4,000 7,200 13,600 TO 60,000	50	30,600 TO 122,000	27,2 TO 120,0
V (ONE YEAR) 3 MO. ATTENDED 6 MO. UNATTENDED 3 MO. ATTENDED	3	1 MOLAB 1 CON- STRUCT'N VEHICLE	1X5	6,000	3 (DAY, ATT.) 5 (NIGHT, ATT.) 2 (DAY, UNATT.) 2 (NIGHT, UNATT.)	13,500	6,0

*DURING DORMANT PERIODS, HEATING IS ASSUMED TO BE PROVIDED BY RTG, OR PASSIVE TEMPERATURE CONTROL USED TO PROTECT CRITICAL ELEMENTS.

+THESE FUEL CONSUMPTIO DUTY CYCLE THAN OBTAIN APPENDIX A).

able 4.3 Power and Reactant Requirements for Specified Missions

ER AND REACTANT REQUIREMENTS FOR SPECIFIED MISSIONS

LSV FUEL (LB/HR)	CONSUMPTION TOTAL (LB)	SHELTER POWER REQUIRED (KW)	REACTANT (LB)			POWER REQUIRED (KW)		
			SHELTER	VEHICLES	TOTAL	SHELTER	ERPS	TOTAL
3	600	10	0	600	600	10	0	10
3	600	10	0	600	600	10	0	10
3	1,000 (333 HOURS)	15	4,600	1,000	5,600	15	73	88
0	0	0	0	0	0	0	0	0
2X3 1X5	1,200 1,000 2,200 TO 13,200	30 (FROM LERC STUDY, REFERRED TO IN ERPS RFP APPENDIX ON GUIDELINES SAMPLE)	9,200 TO 55,000	2,200 TO 13,200	11,400 TO 68,200	30	150	180
2X3 2X5 2X9	2,400 4,000 7,200 13,600 TO 60,000	50	30,600 TO 122,000	27,200 TO 120,000	57,800 TO 242,000	50	378	428
1X5	6,000	3 (DAY, ATT.) 5 (NIGHT, ATT.) 2 (DAY, UNATT.) 2 (NIGHT, UNATT.)	13,500	6,000	19,500	3	33	36

PROVIDED BY
CRITICAL ELEMENTS.

+THESE FUEL CONSUMPTIONS ASSUME A CONSIDERABLY HIGHER DUTY CYCLE THAN OBTAINED FROM LSV DATA (DISCUSSED IN APPENDIX A).

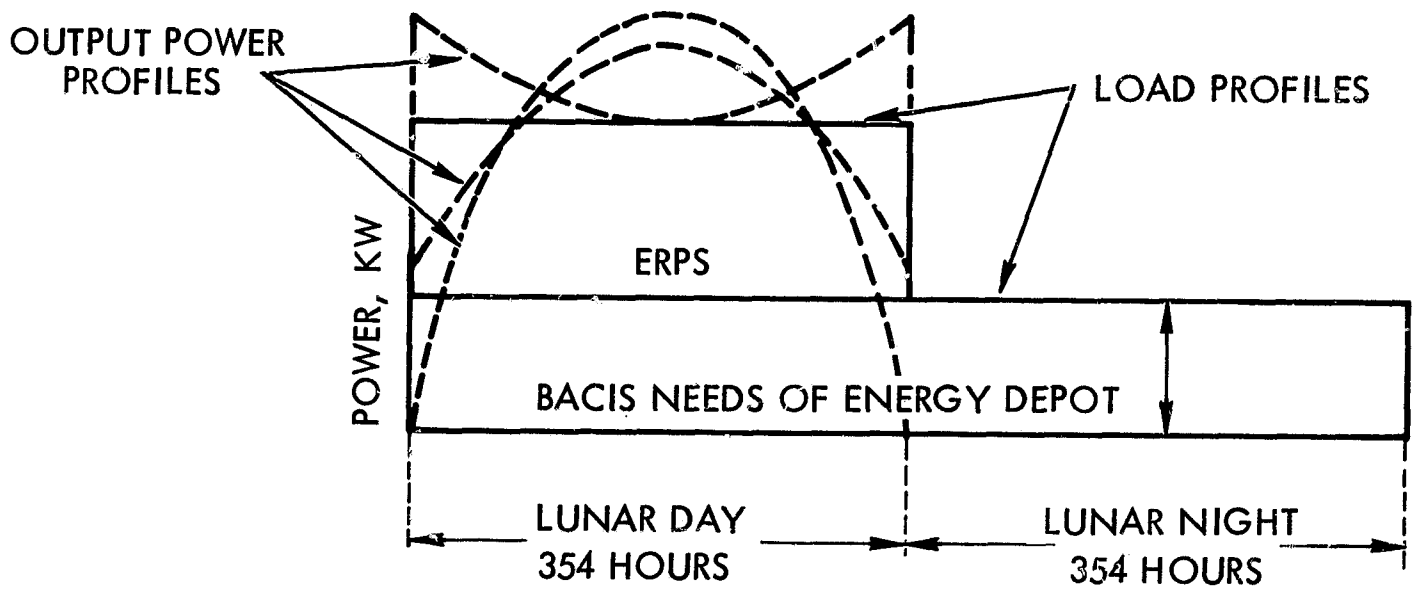

Figure 4.1 Typical Power Profile for Energy Depot

of the reactants will be reserved for use during the following night to operate the fuel cell system providing power for the base facilities. The net quantity of reactant will then be available for use by surface vehicles during the planned daytime (and possibly nighttime) operations.

4.4 ELECTRICAL POWER SYSTEM DEFINITIONS

The electrical power system for the lunar base consists of the primary electrical power system (LEPEPS), secondary electrical power systems (SEPS), lunar surface vehicle (LSV) power systems, and surface traverse emergency power. Each of these systems are now discussed to illustrate their relationship to the overall lunar mission.

4.4.1 Lunar Equipment Prime Electrical Power System (LEPEPS)

The primary electrical power system can be selected from the following power sources or combinations thereof; batteries, fuel cells, nuclear power systems and solar cell arrays. A survey of the current and projected state-of-the-art for the first three power sources is given in Section 10.1. A comparison of the relative effectiveness of each of

these systems, based on total logistic weight to accomplish the mission, is presented in Section 4.6.

Batteries capable of long duration charge/discharge cycling offer one possibility as an energy source. Several types of batteries that are commercially available were considered as follows:

- Nickel-Cadmium (Ni-Cd) batteries capable of achieving 10-15 w-hr/lb (100-67 lb/kw hr). They have a charge efficiency of about 75 percent (at the proper temperature), and can be recharged hundreds of times.

- Silver-Cadmium (Ag-Cd) batteries capable of achieving 25-30 w-hr/lb (40-33 lb/kw hr) when vented and about one-half as much when unvented. They recharge more slowly then Ni-Cd, with a charge efficiency of about 75 percent. Their non-magnetic property is favorable to many applications.

- Silver-Zinc (Ag-Zn) batteries capable of achieving 15-50 w-hr/lb (67-20 lb/kw hr) depending on cycle life. They recharge slowly with about 75 percent charge efficiency and can be discharged rapidly. While they have had little flight experience in rechargeable space applications, they offer promise of providing efficient energy storage for lunar applications.

Fuel Cells (H_2-O_2) offer another possibility as the primary energy source. Based upon inert weight only, current fuel cells generate approximately 10^3 w-hr/lb (1 lb/kw hr), but the projected energy density is expected to be 2.5×10^4 w-hr/lb (0.0 lb/kw hr). Including a reactant rate of 0.91 lb/kw hr (which allows for boil-off), an overall energy density of 0.95 lb/kw hr is projected for operation on the lunar surface. Future units with a lifetime of 2500 hours are expected to have an inert weight of 100 lb /kw or less.

Nuclear power sources are typified by the current Atomics International compact converter 23 kwe reactor-thermoelectric power system (see Reference 4.5) having a gross mission weight of approximately 25,000 pounds. Further details of the power and weight breakdown are given in Table 4.7.

Solar cell arrays for the lunar surface application offer a broad range of possible configurations, which were narrowed down to a few candidate systems in this study by the following preliminary analysis.

Various conceivable arrangements of solar arrays were compared on the basis of relative solar cell area and relative weight as shown in Figure 4.2. Both of these parameters are of equal importance. The area determines the initial cost of the solar array and the weight defines the total logistic problem and resultant overall cost of the lunar base. A brief description of each configuration follows:

- Flat Array (Type 1). The simplest configuration to deploy and activate is the rectangular array, spread out flat on the lunar surface. The relative weight and solar cell area of all other configurations are compared with this basic arrangement, which is a candidate for further detailed study.
- Tipped Flat Array (Type 2). By tipping the array normal to the sun at noon to compensate for the assumed latitude of 30°, a 14 percent reduction in solar cell area is effected at the expense of approximately 12 percent increase in total weight due to structure. This arrangement shares the disadvantage with Type 1 of providing zero power at sunrise and sunset (see diurnal power profile). For this reason, Type 2 is eliminated.
- Leanto Array (Types 3-5). By choosing the leanto configuration with a prop at the center of one side (Types 3 and 4), the power profile at dawn and dusk is improved to about 45 percent of maximum midday power and the relative weight is restored to approximate parity. Type 3 was chosen for further detailed study, and Type 4 was dropped, since a gain in performance can easily be obtained by moderate stretching. Pressurizing the leanto (Type 5) results in a considerable increase in weight, due to the addition of bottom and end closures, and gas storage weight; hence, this mode is eliminated.
- Pressurized (Hemi) Sphere (Types 6 and 7). The pressurized hemisphere and sphere will have more than twice the weight of the leanto configurations, but the power level at dawn/dusk is improved to about 50 percent maximum (for the hemisphere) and 100 percent (for the sphere). However, these modes were discarded due to their large relative weights and areas.
- Fully Oriented Array (Type 8). The fully oriented array, while requiring the least solar cell area of any of the configurations and having a more nearly constant power profile, will require considerable structural weight, more time and effort in deployment, and may have a potentially lower reliability if an automatic orientation mechanism is used. Nevertheless, it was selected for further detail study since it had the capability of requiring the smallest area for a given power profile.
- Candidate Configurations. Of the eight configurations shown in Figure 4.2, the following candidates were believed to represent the most promising systems and worthy of further study: flat array, leanto and fully oriented. These are illustrated in Figure 4.3.

FOLDOUT FRAME

TYPE	CONFIGURATION	DIURNAL POWER PROFILE (Assuming Constant Array Temp.)	
[1] FLAT ARRAY - FLAT ON LUNAR SURFACE	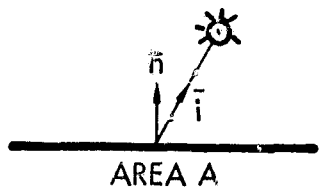	K = POWER PER UNIT AREA 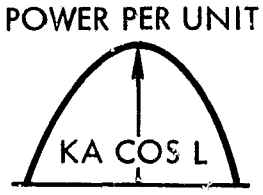	T = ∫A
2. TIPPED ARRAY- NORMAL TO SUN AT NOON	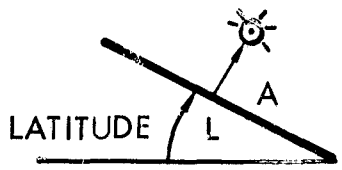	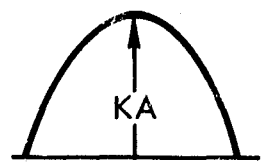	
[3] LEAN TO ARRAY - STRETCHED SINGLE PROP AT CENTER RECTANGULAR SOLAR ARRAY	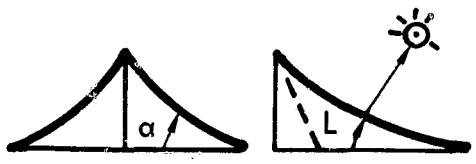	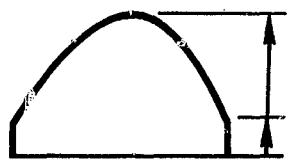	∫ = KA = 0.6
4. LEAN TO ARRAY - UNSTRETCHED SINGLE PROP AT CENTER RECTANGULAR SOLAR ARRAY	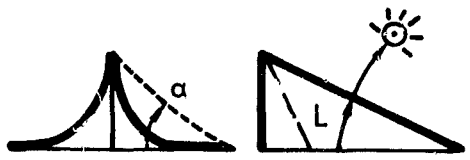	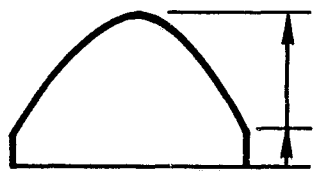	∫ = KA = 0.6
5. LEAN TO ARRAY - PRESSURIZED RECTANGULAR SOLAR ARRAY	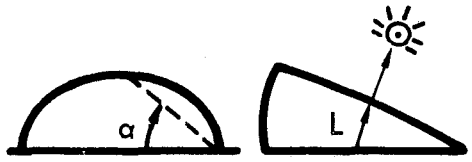	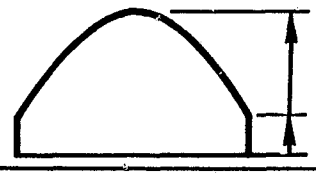	∫ = KA = 0.6
6. HEMISPHERE - PRESSURIZED	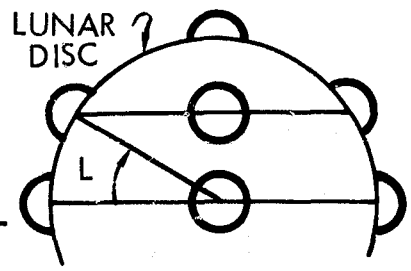	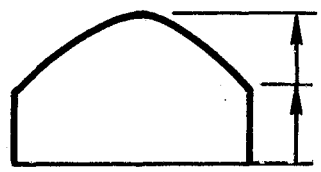	∫ = KA = 0.3
7. SPHERE - PRESSURIZED	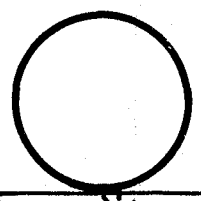	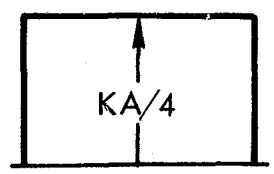	
[8] FULLY ORIENTED ARRAY	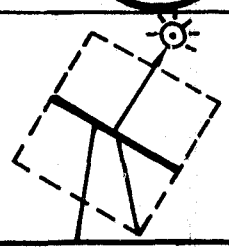	ASSUMING CONSTANT TEMPERATURE 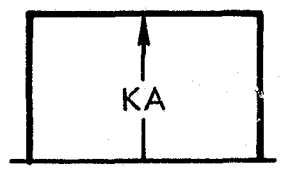	

✱ ARRAY TEMPERATURE EFFECTS NOT CONSIDERED

☐ SELECTED FOR MORE DETAILED STUDY

Figure 4.2 Relative Effectiveness of Various Configurations

DIURNAL POWER PROFILE (Assuming Constant Array Temp.)	INTEGRAL OF POWER (ONE LUNAR DAY)	REL. EFFECTIVENESS	
		REL. WEIGHT	REL. AREA
K = POWER PER UNIT AREA 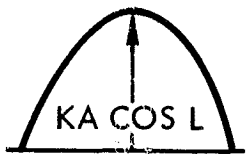	T = TIME PERIOD OF INTEGRATION $\int A\bar{n} \cdot \bar{I}\,dt = \frac{2}{\pi} KAT \cos L$ $= 0.55\ KAT;\ (L = 30°)$	1.0	1.0
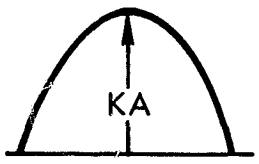	$\int = \frac{2}{\pi} KAT$ $= 0.63\ KAT;\ (L = 30°)$	1.12	0.86
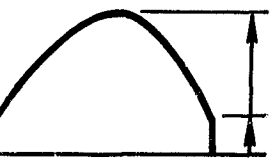	$\int = KAT\left[\frac{\sin\alpha}{4}\left(1 - \frac{2}{\pi}\right) + \frac{2}{\pi}\cos\frac{\alpha}{2}\cos\frac{L}{2}\right]$ $= 0.61\ KAT;\ (\alpha = L = 30°)$	0.97	0.90
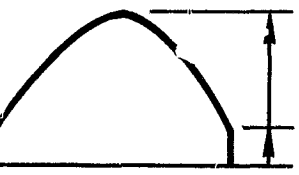	$\int = KAT\left[\frac{\sin\alpha}{4}\left(1 - \frac{2}{\pi}\right) + \frac{2}{\pi}\cos\frac{\alpha}{2}\cos\frac{L}{2}\right]$ $= 0.60\ KAT;\ (\alpha = L = 30°)$	0.96	0.92
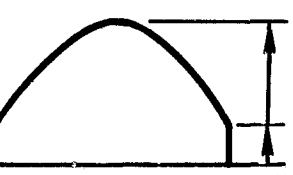	$\int = KAT\left[\frac{\sin\alpha}{4}\left(1 - \frac{2}{\pi}\right) + \frac{2}{\pi}\cos\frac{\alpha}{2}\cos\frac{L}{2}\right]$ $= 0.62\ KAT;\ (\alpha = L = 30°)$	1.72	0.89
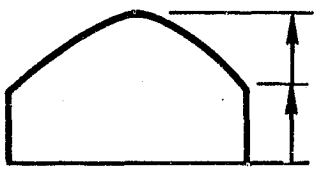	$\int = KAT\left[\frac{1}{4}\left(1 - \frac{2}{\pi}\right) + \frac{2}{\pi}(1 + \cos L)\frac{1}{4}\right]$ $= 0.39\ KAT;\ (L = 30°)$	2.13	1.43
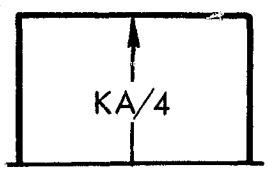	$\int = KAT/4$	2.22	2.22
ASSUMING CONSTANT TEMPERATURE 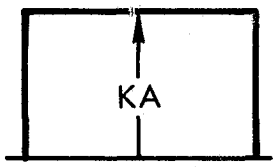	$\int = KAT$	0.71-1.38	0.55

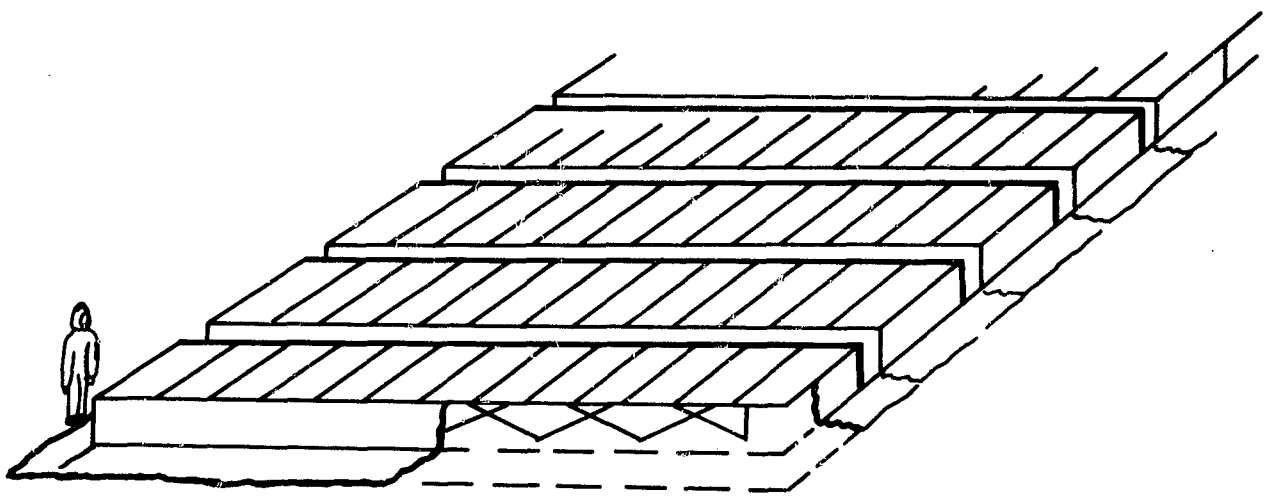

● FLAT ARRAY - PARALLEL TO LUNAR SURFACE

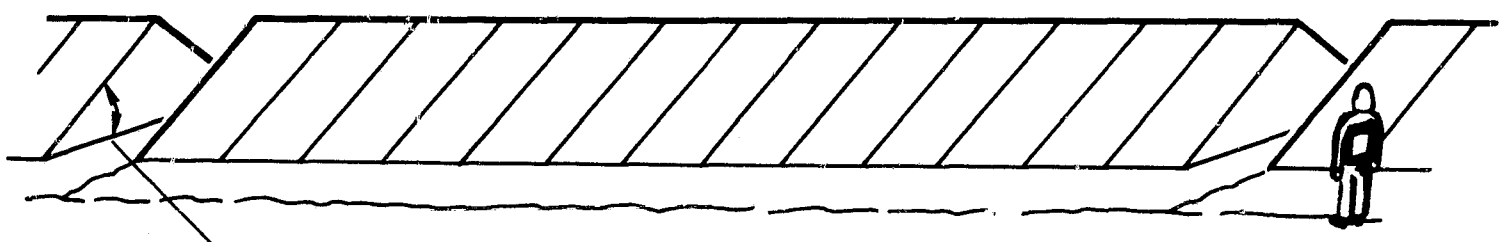

● LEAN TO ARRAY

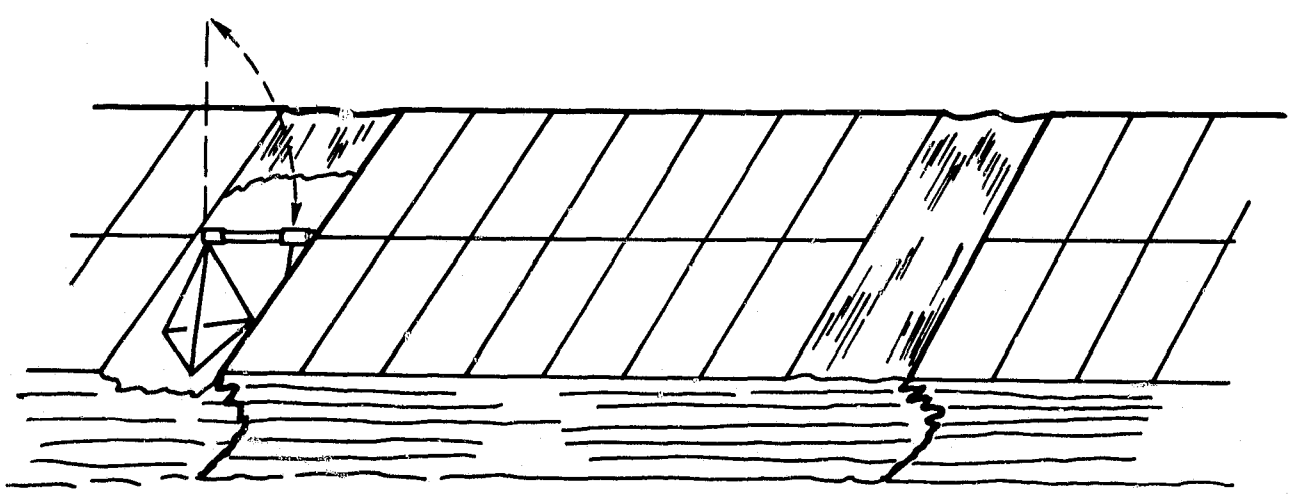

● ORIENTED ARRAY - SKIRTED

Figure 4.3 Final Solar Array Candidates
(2.5 kw Modules of Foldout Panels Shown)

4.4.2 Secondary Electric Power Systems (SEPS)

The secondary electric power system derives its energy from a primary source, distributing that energy in time to the user facilities. Examples of SEPS are as follows:

- Batteries are charged and recharged by the solar array and may be used to provide nighttime power to the base, or motive power to the roving vehicles. They may also be used to augment the primary power system for short peak-load conditions.

- Fuel Cells provide power for nighttime operation of the base and for energizing the roving vehicles. Reactants used by the fuel cells are obtained by regeneration of water through electrolysis (ERPS) or by depleting an initial reactant supply transported from Earth, as discussed in Section 4.4.3.

- Radioisotope Thermoelectric Generator (RTG) utilizes a radioactive source to provide heat and electrical energy for nighttime operation of the base, for providing motive power for the roving vehicles, and to power instruments and telemetry during dormancy periods.

- Solar Cells may be used on roving vehicles to provide additional energy, thus decreasing the quantity of reactant consumed by the fuel cells (normally used to energize such vehicles) or increasing their range (see Section 4.4.4).

Solar cells can also be used to provide emergency power for the lunar surface vehicle. In case of failure of the fuel cell system, a completely redundant source of energy is thus available to operate the environmental control and life support system, communication, and drive equipment.

4.4.2.1 Baseline System

The present concept of LEPEPS/SEPS envisions a solar array as the primary power source at the base, with fuel cells providing secondary power for nighttime operations at the base and motive power to the surface vehicles. During periods when the base in unoccupied, the ERPS system is assumed to operate automatically to regenerate reactants for nighttime use. If automatic operation of ERPS during unattended periods proves to be impractical from a reliability standpoint, additional reactants could be provided, as discussed in Section 4.6.4.2. Alternatively, an auxiliary power system such as the RTG could be provided. A detailed study of

these system tradeoffs is beyond the scope of this study but should be considered during the mission implementation study phase.

4.4.3 Alternate Modes of Reactant Supply and Power Requirements

The energy depot is initially supplied with a quantity, W_1, of cryogenic hydrogen and oxygen sufficient to satisfy the ECS, life support and initial power requirements for base operations and surface vehicle excursions. A portion of the breathing oxygen will be dissipated by air-lock cycles and other losses, but the reactant consumed by the fuel cells will result in very nearly 100 percent recovery of the water. This can then be dissociated in the ERPS to form gaseous hydrogen and oxygen, and reliquified and stored for re-use (assuming cryogenic storage is employed). The lunar base logistics problem can be minimized for the following three cases to satisfy the specified mission programs (Table 4.3):

1) No re-use of reactant (when W_1 required for the complete mission duration is less than the weight of ERPS plus liquifaction equipment)

2) Dissociation and liquifaction of recovered water (when weight of ERPS/liquifaction + W_2 is less than W_1).

3) Mining, water extraction and ERPS for large mission energy requirements justifying additional weight of equipment and complexity of operation (see Section 4.6.3).

Case 1. For daytime operation only (Programs I and II) involving relatively small amounts of reactant, W_1, for life support, surface vehicles and base power, it is evident that the minimum logistic weight is obtained by transporting the necessary reactant from Earth, without the use of ERPS.

Case 2. For day/night operation (without mining), a quantity of reactant sufficient for base power during the nighttime represents the minimum value of W_2. Surface vehicles can draw from this supply during the day, the recovered water being processed many times through ERPS/liquifaction to maintain a relatively constant value of W_2. The last excursions before sundown should conclude with sufficient time remaining to dissociate/liquify with available power; otherwise an additional increment ΔW_2 of reactant should be provided initially. The volume of reactant to be processed by ERPS the following day will be $W_2 + W_{SV}$, where W_{SV} is the reactant consumed by surface vehicles.

Case 3. With mining and water extraction from lunar surface materials, the initial quantity W_{3o} of reactant should be sufficient to satisfy the requirements until the mining/extraction/ERPS system is operative, after which the lunar generated reactant W_{3g} will build up the total supply to the amount needed for extended use ($W_{3f} = W_{3o} \times W_{3g}$). As in Case 2, the recovered water is processed through ERPS/liquifaction to maintain W_{3o} essentially constant. The volume of reactant to be handled by ERPS the following day is $W_{3f} + W_{SV} + W_{3g}$, where W_{3g} is the additional lunar generated reactant. This process continues until W_{3g} is sufficient to support the expanded exploration program.

The criterion to determine when mining and water extraction are justified is $\Sigma W_{3g} > (y + z)$, where y and z are the equipment weights required for water extraction and mining respectively, plus the added solar array and ERPS weight to support these activities (see Section 4.6.3).

4.4.3.1 Reactant Production Power Requirements

Dissociation of Water - Two Faradays of current are required to dissociate one mol of water into 2 grams of hydrogen and 16 grams of oxygen gas. 1 Faraday = 96,500 coulombs (26.8 amp-hrs). The theoretical potential required for the electrolysis of water is 1.229 v. However, because of the irreversability of the oxygen electrode, significant overpotentials are required for the liberation of oxygen from water. While these may be minimized by operation of the electrolysis apparatus at elevated temperatures and by selection of electrode materials for minimum overpotential, it seems probable that the potential required for the operation of electrolysis cells at useful rates will be not less than 2.0 v, and, depending upon the design of the cell, may be considerably higher. At the 2-v potential, 2.7 kw-hrs of electric power are required for the generation of 1 pound of hydrogen and oxygen at the correct mixture ratio (1:8) for use in fuel cells.

Liquefaction of Gases - The thermodynamic energy required for liquefaction of hydrogen and oxygen is 1.50 and 0.080 kw hr/lb, respectively, starting with gas at 25°C and 1 atmosphere pressure (see Reference 4.6). With a mixture ratio of 8:1, this amounts to 0.24 kw hr/lb of reactant. Assuming a mechanical efficiency of 14 percent, results in

a power requirement of 1.7 kw hr/lb for liquefaction. The actual efficiency of the liquefiers, and the weight of such equipment will depend on the rate of production required and the availability of equipment. The Reference 1.3 study is analyzing these requirements.

When reconverted into electrical energy via fuel cells, one pound of reactant yields 1.1 kw-hr. Hence, the overall efficiency of the ERPS/liquefaction process is $\eta_e = 1.1/(2.7 + 1.7) = 25$ percent (based upon the above assumptions).

4.4.4 Lunar Surface Vehicle Auxiliary Power

The proposal to utilize direct solar energy conversion on the LSV's (Figure 4.4) to reduce their fuel consumption can be appraised by consideration of two cases; solar cells without batteries and solar cells with battery storage.

- Solar Cells without Batteries. Typical lunar surface vehicles are described in Figure 4.4 (Reference 4.7 and 4.8). The weight and power characteristics of solar arrays were analyzed as follows:

Let, A = plan area of vehicle (ft^2)
rA = solar cell area (ft^2); i.e., r = solar cell area/plan area of vehicle
w = weight of solar array/unit area (lb/ft^2)
p = power output/unit area normal to sun-line (kw/ft^2)
θ = average angle between solar array and sun-line (rad)

Then, $prA \sin\theta$ = average power output (kw)

Let, c = average reactant consumption (without solar array) (lb/hr)
$1.1c$ = average power equivalent of reactant consumed (kw)

Then, $R = 1 - prA \sin\theta/1.1c$ = ratio of reactant consumed with/without solar array,

and, $1 - R = prA \sin\theta/1.1c$ = fraction of reactant saved by use of solar array

Thus the fraction of reactant saved is proportional to p and $\sin\theta$, both of which vary with time, as shown in Figure 4-5. The product $p \sin\theta$, integrated over the lunar day, gives an average power density of about 4.0 w/ft^2 with silicon cells; hence the integrated fraction of reactant saved in one day will be,

Data Summary		Local Surface Vehicle	Mobile Lab.	Long Range Reconn Veh
Gross Vehicle Weight (W/2-man crew)	(lb)	2200	7940	17000
Scientific Equipment	(lb)	375	750	510
Cargo (incl expendables)	(lb)	---	1990	6000
Length, Overall	(ft)	16.0	20.2	36.8
Width, Overall	(ft)	7.6	10.4	10.8
Number of Wheels		6	6	8
Wheel Diameter	(in)	48	60	80
Range	(mi)	20	250	2000
Duration	(days)	.25	14	84
Maximum Speed	(Mph)	7.5	10	10
Power System		Fuel Cells*	Fuel Cells	Fuel Cells
Max. Power Required	(kw)	3	5	9
Energy Required - Total	(kw hr)	5	525	4000
Locomotion	(kw hr)	1.5	140	2000
Navigation	(kw hr)	0.1	25	125
ECS and Life Support	(kw hr)	---	130	850
Electronics	(kw hr)	0.4	120	625
Scientific	(kw hr)	3	110	400
Cryogenics Required	(lb)	---	690	3350

*Local surface vehicle assumed to use fuel cells in this comparison

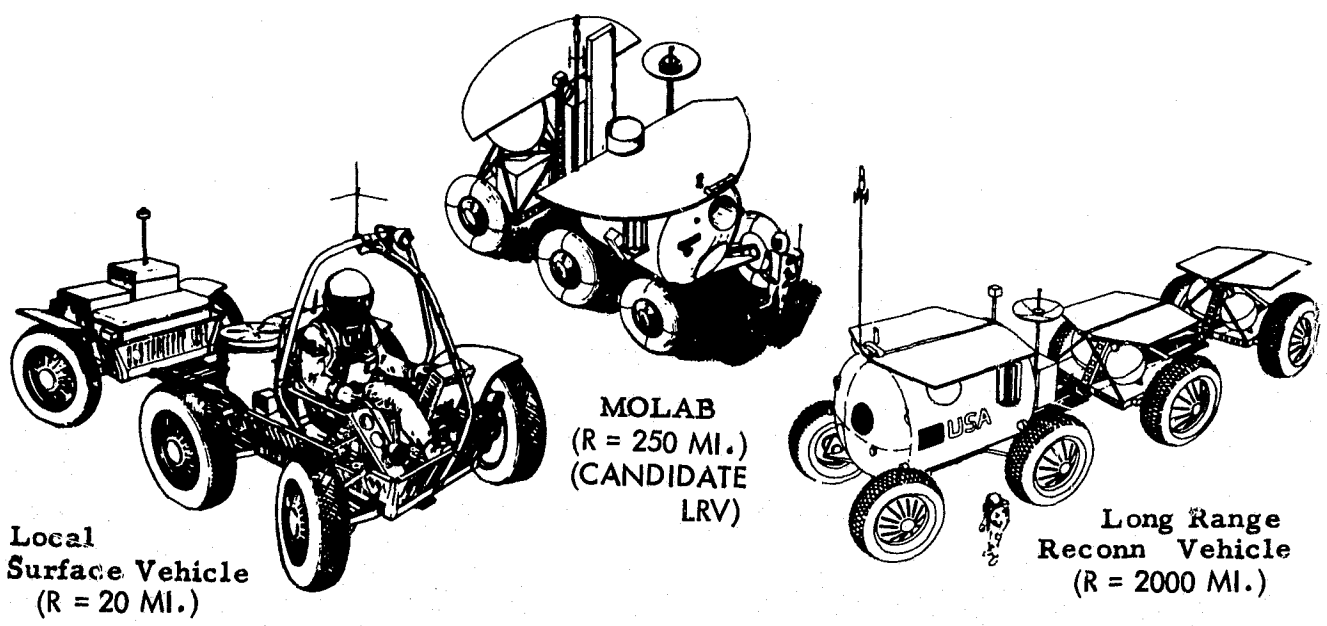

Figure 4.4 Typical Lunar Surface Vehicles for Lunar Surface Exploration

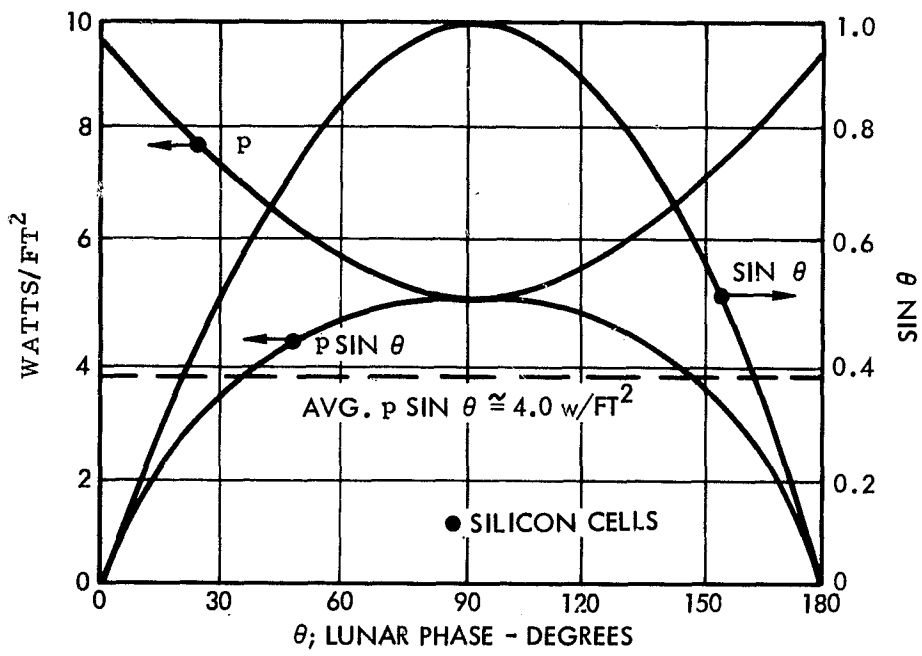

Figure 4.5 Variation of p and Sin θ During Lunar Day

$$\text{Fraction of Reactant Saved} = 1\text{-}R = .0040\ rA/1.1c \qquad (4.1)$$

$$\text{Fraction of Weight Added} = wrA/cD \qquad (4.2)$$

where D = duration of the mission, and cD = useable reactant weight. Figure 4.6 shows the variation of the above parameters, the curve labeled zero stationary time representing the case with no storage batteries.

The break even point (BEP) is defined as the total hours of vehicle operation, for equal gross weight and equal range, with or without the solar array; i.e., when the added weight of the solar array installation is equal to the reactant saved by direct conversion. The comparative weights aboard the vehicle will be:

Without solar array: $W = cBEP$ (nominal reactant weight) (4.3)

With solar array: $W = wrA + RcBEP$ (solar array plus reactant) (4.4)

Solving simultaneously gives,

$$BEP = \frac{wrA}{c(1-R)} = \frac{1.1w}{0.0040} \text{ (hours)} \qquad (4.5)$$

For example, if MOLAB is provided with a solar array weighing 0.5 lb/ft^2 (including the added weight of solar cells, power conditioning and conductors), then the break even point will be, from Equation 4.5;

$$BEP = 1.1 \times 0.5/.0040 = 138 \text{ hours}$$

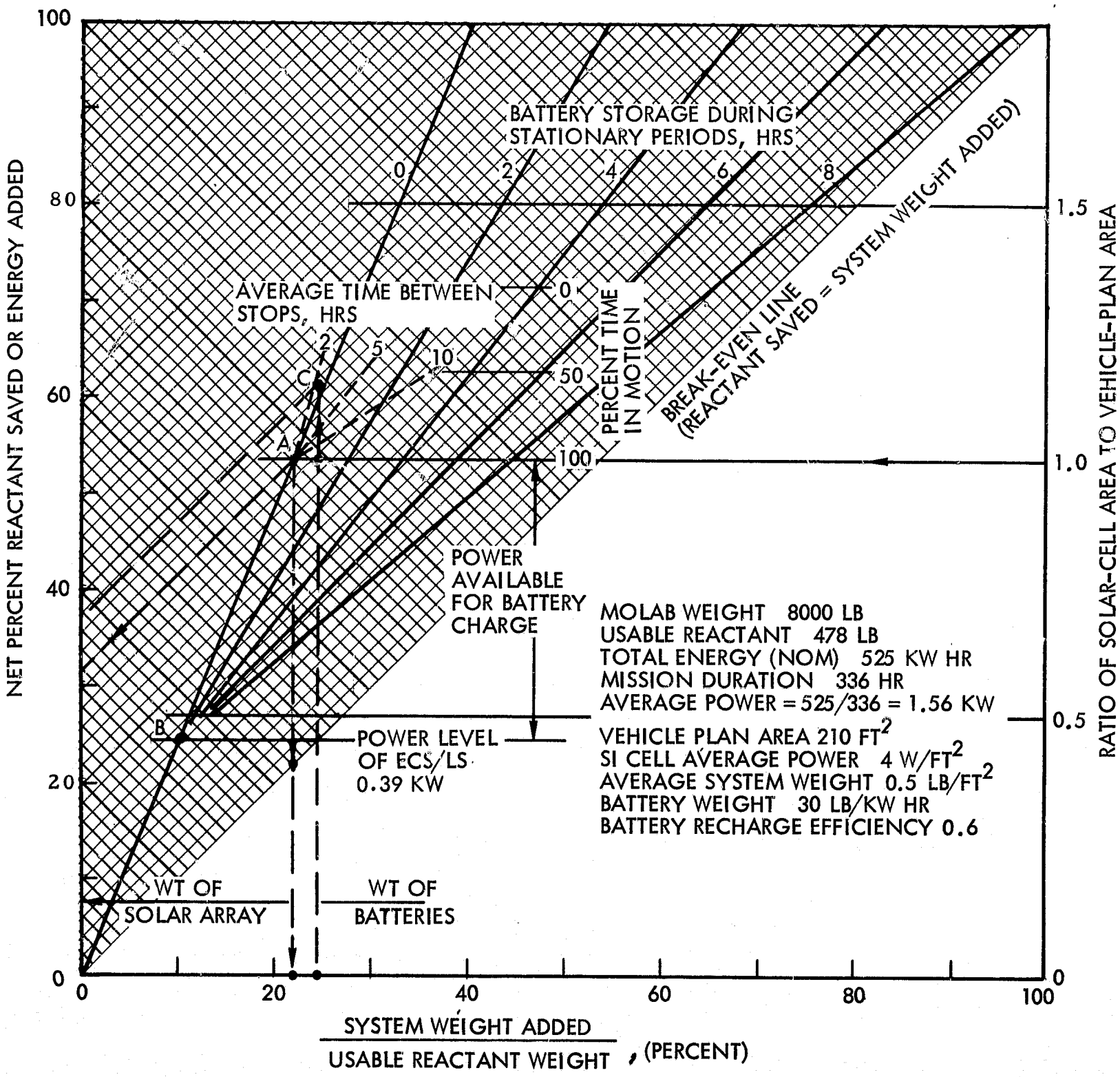

Figure 4.6 Tradeoffs with Solar Cells and Batteries on Lunar Surface Vehicles (MOLAB)

Hence, for missions of greater duration than 138 hours, the performance is increased by the addition of a solar array. Since the nominal mission duration of MOLAB is 14 days = 336 hours, the effect of the improvement will be considerable. The nominal rate of consumption, c, of reactant is obtained by dividing the useable reactant* by mission duration (Figure 4.4); i.e., 478 lb/336 hours = 1.43 lb/hr. If the solar array area is equal to the vehicle plan area, then rA = 210 ft^2. Substituting these values in Equation 4.1 gives;

Fraction of Reactant Saved = 1-R = 0.0040 x 210/1.1 x 1.43 = 0.54 or 54 percent of the useable reactant load.

The net saving after subtracting the solar array weight of 105 pounds will then be 32 percent or about 153 pounds per 14 day MOLAB mission, as shown in Figure 4.6 at point A, or 916 pounds for the 6 months operation of Program V.

When the above procedure is applied to the long range reconnaissance vehicle (Figure 4.4), the savings are considerably greater. Approximately 74 percent of the reactant load can be saved, or about 2700 pounds of reactant per 84-day mission, or 32 percent of the vehicle weight, for two missions.

- Solar Cells with Battery Storage. During stationary periods, when minimum power for ECS/LS is required, the excess power generated by the solar array could be stored in batteries, or dumped. In the MOLAB example, the minimum power is 0.39 kw or 25 percent of the average power level (Point B in Figure 4.6). The principal tradeoffs with systems using battery storage are shown in this figure. For example, the percent of reactant saved (or energy added) is plotted against system weight added by the solar array, batteries and controls. The added weight of solar cells and controls is shown along the line marked "zero stationary time" (along which the solutions to cases without battery storage will be found). Any additional weight of batteries then increases the overall system weight proportional to the length of the storage period. During the stationary periods, the solar array energy can be used to recharge the secondary batteries, the amount of energy stored depending on the number of stops and their duration as illustrated by the small triangle of dotted lines. The net savings in weight is

*Useable reactant weight = total energy required/energy per pound of reactant; i.e., 525/1.1 = 478 lb. Boiloff and other losses are not included.

measured from the break-even line (reactant saved = system weight added) to the selected value of stationary time. For example, if 210 ft^2 of solar cells are added to MOLAB, the added system weight will be about 105 pounds plus 12 pounds of batteries for a one hour storage time. The net saving in weight will be 182 pounds, or 38 percent of the useable reactant weight (Point C in Figure 4.6). If weight saving is not considered of prime importance, a corresponding increase in the nominal energy level can be attained by use of the solar array/battery system.

A more detailed analysis of the use of solar arrays on certain specified surface vehicles is contained in Appendix A. The effects of power profile are discussed, with power ranging from a minimum value (ECS/LS), through the average value for mission duration, to the maximum power available on the mobile vehicle.

4.4.4.1 Total Savings in Logistic Weight

In addition to the foregoing direct savings in reactant by the use of solar arrays on the lunar surface vehicles, an obvious indirect benefit occurs by the reduction in weight of the ERPS and the base solar array system, commensurate with the reduced reactant to be processed. Referring to the MOLAB example, the 38 percent saving in vehicle reactant represents a reduction of about 5.7 percent in total reactant. If applied to a weight of ERPS and solar array of 16,500 pounds, these systems could be made approximately 940 pounds lighter. When the above direct and indirect savings are combined, an overall reduction of more than 2000 pounds in total logistic weight can be attained for the one-year Program V mission.

It appears obvious from this analysis that a marked reduction in total system weight could be effected by the use of solar cells/batteries on surface vehicles. This could amount to a savings of approximately 11 percent in total logistic weight, or 25 percent of the LSV weight. Alternatively, for equal system weight, an improvement in LSV performance of 30 to 40 percent could be attained and converted into increased range, duration in motion, or energy available for scientific experiments.

4.4.5 Surface Traverse Emergency Power

An important feature of the use of solar arrays on lunar surface vehicles is that they represent an emergency power system, completely

redundant to the fuel cells which normally provide power for motivation, environmental control and life support (ECS/LS) and other functions on the vehicles. The secondary solar array system can thus provide the necessary power for ECS/LS in case of an emergency, and for communications with the lunar base, a lunar orbiting Command and Service Module, or Earth. Further study could result in the design of an integrated system capable of returning the vehicle to the base (at reduced power), utilizing only the solar array and battery system for motivation energy.

The availability of such an emergency power source enhances the reliability of lunar exploration missions, reducing (but not eliminating) the necessity for providing rescue capability at the lunar base for exploring parties in the field. The emergency feature of solar arrays may in itself justify the provision of such means, independent of the improved performance which they can afford, as discussed in Section 4.4.4.

4.5 MINING AND WATER EXTRACTION REQUIREMENTS

4.5.1 Water Extraction from Lunar Surface Materials

Ice or ice-soil mixtures may exist in permanently shadowed surface zones where the temperature does not rise above 120°K. In the equatorial belt, where the subsurface temperature is about 240°K, any ice near the surface will have been lost by sublimation. However, subsurface ice protected by an impermeable rock may remain from its formation to the present (Reference 4.9).

Water of hydration is considered a likely form to be expected. The moisture content may range from a few percent to as low as 0.01 percent. The energy required to heat the material to the dehydration temperature (about +800°C) is of principal concern, since this represents a major power requirement. Examples are given of cylindrical kiln and fluidized bed processing systems, for which the power required to extract water from material having one percent moisture content is 4.9 kw hr/lb and 4.1 kw hr/lb respectively (Reference 4.9). These values are about 1.7 times as great as the power required to dissociate the water into H_2 and O_2. When the moisture content is reduced to 0.1 percent, the power required for water extraction is increased by a factor of 7, whereas for 10 percent moisture content, the factor is decreased to about one third.

The above values illustrate the extreme importance of the moisture content and the water extraction process to the LEPEP system design and the effect it could have on the selection of optimal systems for accomplishing various specified missions. In the absence of data on the moisture content of the lunar surface materials, a range of values from 0.1 to 10 percent was investigated during this study to carry out the systems comparisons (Section 4.6.3).

4.5.2 Mining of Surface Material

Various mining techniques and the power required to collect a quantity of surface material are discussed in the literature. Assuming that 10^4 pounds of water are to be extracted from material having a moisture content of 1 percent, a quantity of 10^6 pounds of surface material would have to be mined by blasting or other means and made ready for pickup. If the rock weighs 120 lbs/ft^3, 8340 cubic feet of rock must be picked up and transported an assumed distance of 500 ft to the water extractor.

A reasonable estimate of the product of blade width and scraping depth might be 3 ft^2. The pickup vehicle must move through a distance of at least 8340/3 = 2780 feet under maximum power and return an equal distance at reduced power. If we let cruise power = 1.5 kw (1112 ft-lb/sec), cruise velocity = 1 mph (1.5 ft/sec), max thrust available = $\frac{\text{thrust}}{\text{wt}}$ wt = (1/2) (2200) = 1100 lbs, and maximum power available = 5 kw (2690 ft-lb/sec), then,

Energy consumed in pickup = (max power) (time) = (3960)(2780/.75)
= 14.7×10^6 ft-lb = <u>5.5 kw-hrs</u>

Energy consumed in transport and return = (power)(time) = (1112)(2780 x 1000/1.5)
2060×10^6 ft-lb = <u>776 kw-hrs</u>

Total energy to pickup and transport 10^6 rock = <u>782 kw-hrs</u>
or approximately <u>800 kw-hrs</u>

The total energy required to pickup and transport 10^6 pounds of surface material is then on the order of 800 kw hr, or 0.08 kw hr/lb of water (1 percent moisture content); i.e., about 1.8 percent of the energy (4.5 kw hr/lb) required to extract the water, and an equal percentage of the energy (4.4 kw hr/lb) required to dissociate/liquify the water. From

these preliminary calculations, it appears that unless extremely difficult mining conditions are encountered, the energy required for mining operations will be considerably less than other processes associated with water regeneration. However, the above results represent fairly optimistic values for lunar mining since no allowance has been made for the probable non-homogenity of the surface materials.

4.6 STUDY ALTERNATIVES

During the course of this study, various system analyses were performed to investigate several alternate modes of operation. The impact on the overall system weight was determined. The following studies are included:

	Section
o Weight comparison of alternate systems (no mining)	4.6.1, 4.6.2
o Added weight for mining and water extraction	4.6.3
o Analysis of Program V	4.6.4
Power profiles for 3 solar array configurations	4.6.4.1
Reducing ERPS production rate to 50 percent of baseline value	4.6.4.2
Effect of initial (transported) reactant weight	4.6.4.3
Economic comparison of various solar array/ ERPS systems	4.6.4.4
o Comparison of nuclear system with solar array/ ERPS system	4.6.5
o Figures of Merit for comparing various power systems	4.6.6

4.6.1 Comparison of System Weights to Perform Program I

Program I (Table 4.3) requires electric power to support four men and a surface vehicle for 14 days (336 hours). The power required to support the base is 10 kw. The surface vehicle draws 3 kw average. The base will be operating for 336 hours, which results in a mission energy requirement of 3360 kw-hrs. The surface vehicle will operate for 200 hours, thus requiring 600 kw-hrs. The 200 hours have been broken up into 10 trips of equal duration (20 hours).

There are various ways of supplying the required power. Compared here are systems using:

1) A solar array and secondary batteries

2) Solar array, ERPS, and initial reactant

3) Fuel cells (only) with transported reactant

4) Solar array and transported reactant.

These are evaluated in the sections that follow.

4.6.1.1 Solar Array and Secondary Batteries

4.6.1.1.1 Solar Array and One Set of Lunar Surface Vehicle Secondary Batteries

In this system, the solar array supplies a constant power of 10 kw to the base and in addition, also recharges the batteries when the LSV returns to the base. The maximum power required from the array is inversely proportional to the time allowed to recharge. Since the array must be sized to produce maximum power at all times, the allowable recharge time is critical. The following analysis was used to arrive at the variation in system weight as a function of allowable recharge time:

Total system weight is: $W_t = W_{solar\ array} + W_{batt.\ on\ vehicle}$

$W_{batt.\ on\ vehicle} = P_v H w_b = 3 \times 20 \times 25 = 1500$ lb

$W_{solar\ array} = W_s (p_b + p_v H/R\eta_c) = 120 (10 + 60/R\eta_c)$

The power (kw) needed = $10 + 60/R\eta_c$ where R = recharge time allowable, and η_c = charging efficiency (assumed to be 60 percent). Then total weight will be,

$$W_t = 1500 + 120 (10 + 60/.6R) = 2700 + 12000R$$

Typical values for Program I are as follow:

R (hrs) =	20	10	5.7	1
W_t(lbs) =	3300	3800	4800	14,700

and these results are plotted on Figure 4.7.

Obviously, the fast charge (R = 1 hr) is undesirably heavy. In addition, the total weight is lower when R < 5.7 hrs, if a second set of batteries is provided (see cross-over point on Figure 4.7).

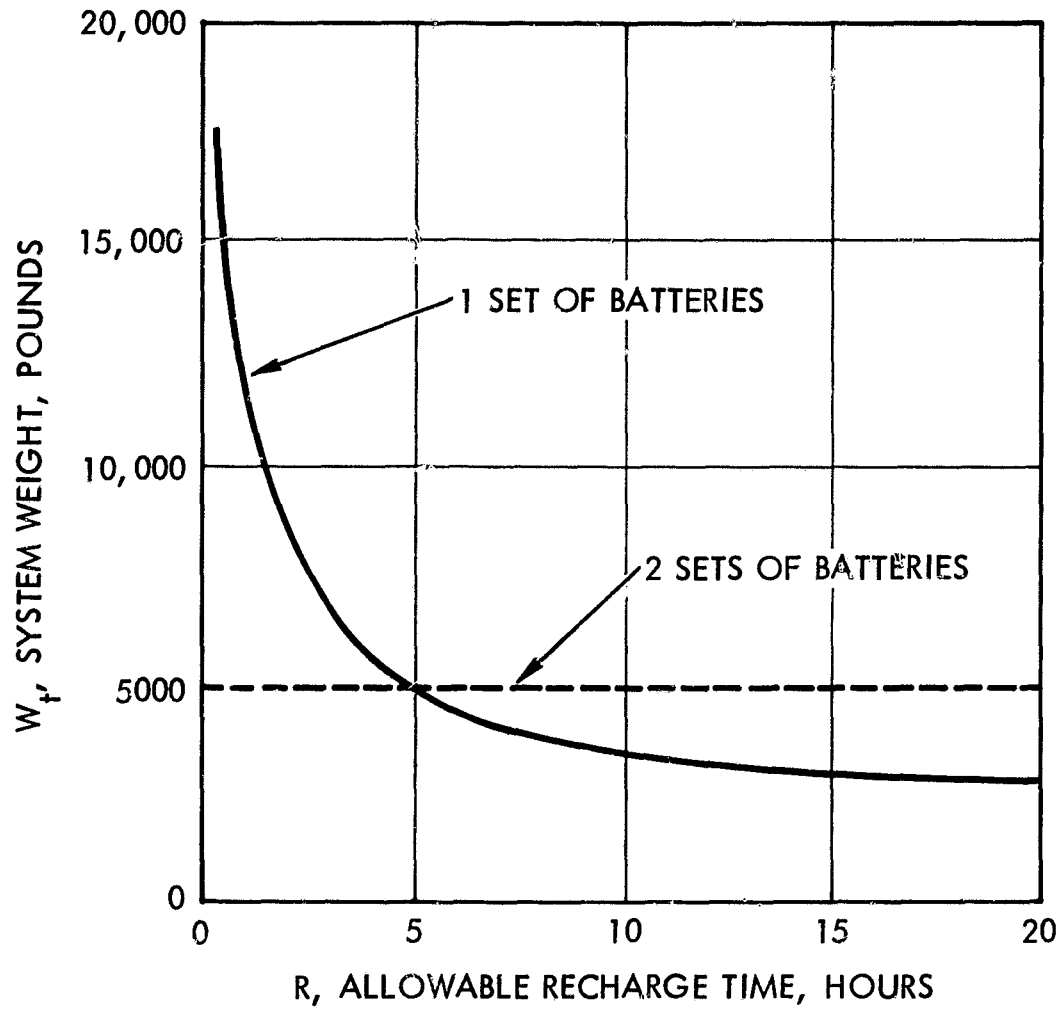

Figure 4.7 Total System Weights Vs. Time to Recharge Batteries

4.6.1.1.2 Solar Array and Two Sets of Lunar Surface Vehicle Secondary Batteries

With two sets of LSV batteries, the solar array can take the full 20 hours to supply the needed 60 kw-hrs per trip. This means the solar array must be sized to produce a total of 15 kw at all times (10 for the base, 5 for the battery charging). Therefore, this total system weight is,

$$W_t = 1500 + 1500 + 1200 + 12000/20 = 4800 \text{ lbs}$$

In this case, the vehicle stay-time at the base is only that required to exchange its batteries for recharged batteries. From the above comparison, it appears desirable to provide two sets of secondary batteries to minimize the total system weight and the stay-time of the lunar surface vehicle at the lunar base.

4.6.1.2 Solar Array, ERPS and Initial Reactant

Fuel cells need to put out 600 kw-hrs of power in 200 hours of lunar surface vehicle operation. Reconverting 1 pound of reactant gives 1.1 kw-hr, or a total propellant weight of 550 lbs. Thus in 20 hours the system must produce 60/1.1 = 55 pounds or about 2.73 lbs/hour. However, the overall regeneration cycle is only 25 percent efficient. Hence, it requires 3/0.25 = 12 kw from the solar array to process the reactant (to produce 3 kw of power) in the form of H_2 and O_2 in the same length of time (20 hours).

The power demand on the solar array is thus,

$$10 \text{ (base)} + 12 \text{ (ERPS)} = 22 \text{ kw}$$

The array weight will be,

$$22 \times 120 = 2640 \text{ lb}$$

Assuming now that the weight of the ERPS equipment depends on the pounds of propellant per hour needed to be processed, the total system weight is then,

$$W_t = W_{\text{solar array}} + W_{\text{prop}} + W_{\text{tanks}} + W_{\text{ERPS}}$$
$$= 2640 + 550 + 165 + W_{\text{ERPS}} = 3355 + W_{\text{ERPS}}$$

The value for W_{ERPS} should be obtained from the Reference 1.3 study. However, when $W_{\text{ERPS}} \leq 1445$ lb, the above system is competitive with the solar array plus battery system discussed in Section 4.6.1.1.2.

4.6.1.3 Fuel Cells and Transported Reactant

Since Program I is only a 14-day mission (daytime only) and no fuel cells or ERPS are provided in this system, the solar array supplies power for the base only (10 kw) and the array weight is 10 x 120 = 1200 lb (compared with 2640 lb when ERPS is used). Transported reactant and storage tanks weigh 550 and 165 lb respectively. Hence for this system,

$$W_t = 1200 + 550 + 165 = 1915 \text{ lb}$$

4.6.1.5 Comparison of System Weights

A summary of the above results is as follows:

1) Solar array + secondary batteries

   1 set of batteries: W_t = 4800 lb (5.7 hr turnaround)

   2 sets of batteries: W_t = 4800 lb (immediate turnaround)

2) Solar array, ERPS, fuel cells: $W_t = 3355 + W_{ERPS}$

3) Fuel Cells, transported fuel: W_t = 5680 lb

   For ERPS to be best of above modes,

   $3355 + W_{ERPS}$ must be less than 4800 lb, or

   $$W_{ERPS} < 1445 \text{ lb}$$

4) Solar array for base power (10 kw array) = 1200 lb

   Transported propellant for surface vehicle = 550

   Propellant storage (on LM taxi) = 165

   ∴ Total Weight, W_t = 1915 lb

4.6.1.6 Program I Evaluation

The total logistic weight to be transported to the lunar base is minimized when the solar array is used to provide power for the base, and the propellant for the surface vehicle operation is transported from Earth. Some reduction in the latter item can be effected by providing a solar array on the surface vehicle (see Figure 4.6).

4.6.2 Alternative Power Systems Weight Comparison (No Mining)

To evaluate the relative merits of various alternative power systems for the specified missions, it is necessary to visualize each system in sufficient detail to determine the relative transportation weights from Earth to the lunar energy depot. Specific systems to be compared are as follows, and the results are shown in Table 4.4 and Figure 4.8 for the case of no mining.

- Solar array and secondary batteries
- Solar array, ERPS and fuel cells (plus initial reactant)
- Fuel cells and transported reactant
- Solar array, fuel cells and transported reactant

Another system (primary batteries for all power needs) was eliminated as being far too heavy to be competitive. A solar dynamic system (at approximately 200 lb/kw) was somewhat heavier and more complex than the solar cell system; hence, it was not considered to be competitive.

This comparison is based upon the mission analysis as shown in Table 4.3, which lists the power and reactant requirements for each of the specified programs. In addition, the following values for weights and efficiencies are basic inputs to the analysis and derived from other sections of this report. (Note: approximate values shown should be modified to reflect results of detailed studies.)

$\eta_e = 0.25 = p_v/p_e$ = kw fuel cells/kw ERPS (for dissociation & liquifaction)

$\eta_c = 0.60 = p_v/p_s$ = kw vehicle/kw recharge = recharge efficiency

$w_s = 120$ lb/kw = weight of solar array/kw generated ($\pm$ 30%)

$w_b = 25$ lb/kw hr = weight of batteries/kw hr (recharge 20 times)

$w_f = 100$ lb/kw = weight of fuel cells/kw generated

$w_p = 0.91$ lb/kw hr* = weight of reactant/kw hr generated by fuel cells

$w_t = 0.3$ lb/lb** = weight of storage tanks/lb reactant

$x + y + z$ = weight of ERPS equipment (lb) for water dissociation/liquifaction, water extraction and mining, resp. (from Reference 1.3 and other studies)

The weight of transported reactant should be selected in accordance with the requirement for day/night operation discussed in Section 4.4.3.

In the above comparison, items such as redundant units and breathing oxygen have been omitted for simplicity, since these items are believed to be sufficiently small so as to have little effect on the results of the comparison. They should, of course, be included in the overall weight of the final system, or in the comparison of candidate systems having essentially the same total weight.

---

* The reactant consumption of fuel cells is nominally 0.8 lb/kw hr; however, the value of 0.91 is used to provide a 14% allowance for boiloff.

** Flight weight hardware, designed for <100 psi tank pressure, with superinsulation.

Table 4.4 Comparison of Alternate System Weights (No mining, no solar arrays on LSV)

Program Number		I & II	IIIa	IIIc	IV	V
First Visit (days)-Mission Duration(days)		14-14	28-28	28-180	56-365	90-365
Basic Data from Mission Analysis (from Table 4.2)		(Sect. 4.6.1)				
p_b = Base power required	(kw)	10	15	30	50	5
p_v = Vehicle power*	(kw)	3	3	11	34	3
p_e = ERPS power = $(p_b+p_v)/\eta_e$	(kw)	12**	72	164	336	32
D = Mission duration	(hrs)	336	672	672	1344	8760
NH = Vehicle trips x trip duration	(hrs)	10x20	13x20	10x20	10x20	6x200
1. Solar Array and Secondary Batteries						
W solar array (base) = $w_s p_b$	(lb)	1200	1800	3600	6,000	600
W solar array (batt) = $w_s(p_b+p_v)/\eta c$	(lb)	600	3600	8200	16,800	1600
W 2 sets batt's for LSV=$2p_v H w_b$	(lb)	3000	3000	11,000	34,000	30,000
W batt's for nighttime=$w_b p_b D_{night}$	(lb)	0	75,500	151,000	252,000	44,000
W_{total}	(lb)	4800	83,900	173,800	308,800	76,200
2. Solar Array, ERPS, Fuel Cells and Initial Reactant						
W solar array (base) = $w_s p_b$	(lb)	1200	1800	3,600	6,000	600
W solar array (ERPS) = $w_s p_e$	(lb)	1440	8,600	19,700	40,300	3840
W ERPS equipment = x + y + z	(lb)	Not defined →				6400
W reactant = $w_p p_b D_{night}$***	(lb)	550	4600	9,200	15,300	3350
W storage tanks = $w_t W_{prop.}$	(lb)	165	1400	2,800	4,600	1000
W fuel cells for nighttime = $w_f p_b$	(lb)	0	1500	3,000	5,000	500
W_{total} (less ERPS)	(lb)	3355	17,900	38,300	71,200	15,690+
3. Fuel Cells and Transported Reactant						
W fuel cells (base) = $p_b w_f$	(lb)	1000	1500	3,000	5,000	500
W reactant = $(p_b D + p_v HN) w_p$	(lb)	3600	9900	20,400	67,500	19,700
W storage tanks = $w_t W_{prop.}$	(lb)	1080	2970	6,120	20,250	5,900
W_{total} (for first visit++)	(lb)	5680	14,370	29,520	92,750	26,200
4. Solar Array, Fuel Cells and Transported Reactant						
W solar array (base) = $w_s p_b$	(lb)	1200	1800	3,600	6,000	600
W reactant = $(p_b D_{night} + p_v HN) w_p$	(lb)	550	5300	11,200	36,800	11,180
W storage tanks = $w_t W_{prop.}$	(lb)	165	1600	3,360	11,040	3,350
W fuel cells for nighttime = $w_f p_b$	(lb)	0	1500	3,[illegible]	5,000	500
W_{total}(for first visit++)	(lb)	1915	10,200	21,160	58,840	15,630

*Average power to be supplied by reactant
**$p_e = p_v/\eta_e$ in this case
***Minimum reactant for base power (nighttime)
+Weight includes ERPS
++Transport additional reactant and storage tanks for subsequent visits

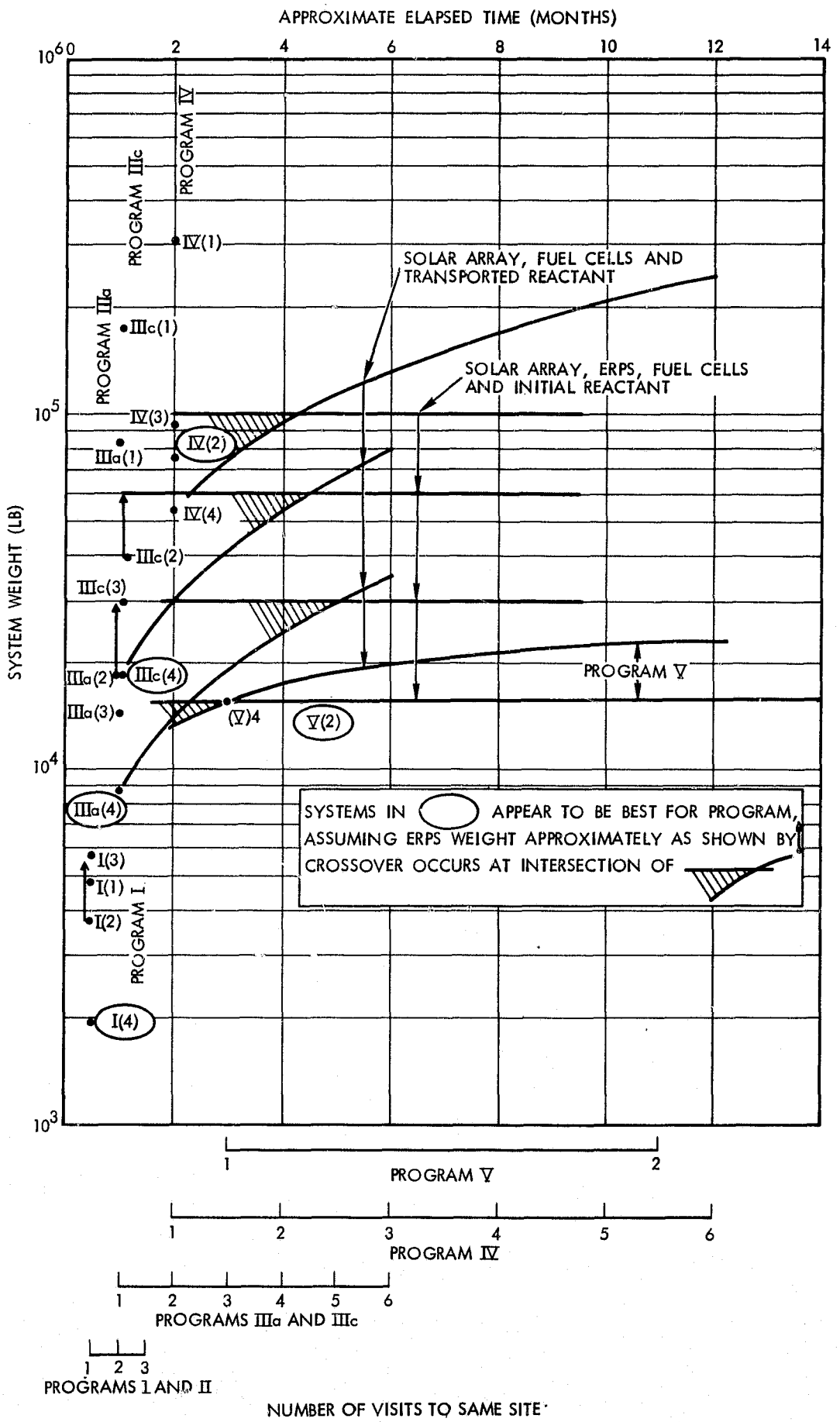

Figure 4.8 Comparison of Alternate System Weights

The results of the system comparison shown in Figure 4.8 are replotted in bar chart form in Figure 4.9, for four different operational systems and five programs. For Programs I and II, the solar array with transported reactant (system 4) is far lighter than any of the other alternates, even for several revisits to the same site. For Programs IIIa and IIIc, the ERPS/solar array/fuel cell (system 2) becomes competitive in weight with systems 3 and 4 only after several revisits are considered. For Program IV, transportation of fuel for fuel cells is no longer competitive with the solar array/ERPS combination beyond two visits. For this program, the combination of solar array/ERPS/fuel cells and initial reactant (System 2) is superior to all other systems. For Program V, the solar array/ERPS/fuel cell system is superior for missions longer than 90 days, with a weight saving of 14,470 lbs for the 1-year program.

The quantities of reactant required for LSV operation are shown for each program at the top of bars for system 4 in Figure 4.9. It should be noted that these propellant weights are relatively small compared with the total system weight in all cases.

4.6.3 Total System Weights (Including Mining and Water Extraction)

Considering the possibility of extracting water from the lunar surface materials, the system weights should include the additional equipment for mining and water extraction, as well as the added power system and ERPS weights to support these operations.

The buildup of weights to satisfy Program IV with solar array, ERPS, fuel cells and initial reactant (System 2) are given in Table 4.4 for no mining. An additional quantity of reactant (10,000 lbs in the following example), will be produced by mining and processing the lunar surface materials over a period of time (two lunar days in the example). Hence, the same weight of propellant is added to the total system weight, W_{tsw}, for the case of no mining, as follows:

$$W_{\text{solar array (base)}} = 6,000 \text{ lbs}$$

$$W_{\text{solar array (ERPS}} = 40,300$$

$$W_{\text{initial reactant}} = 15,300$$

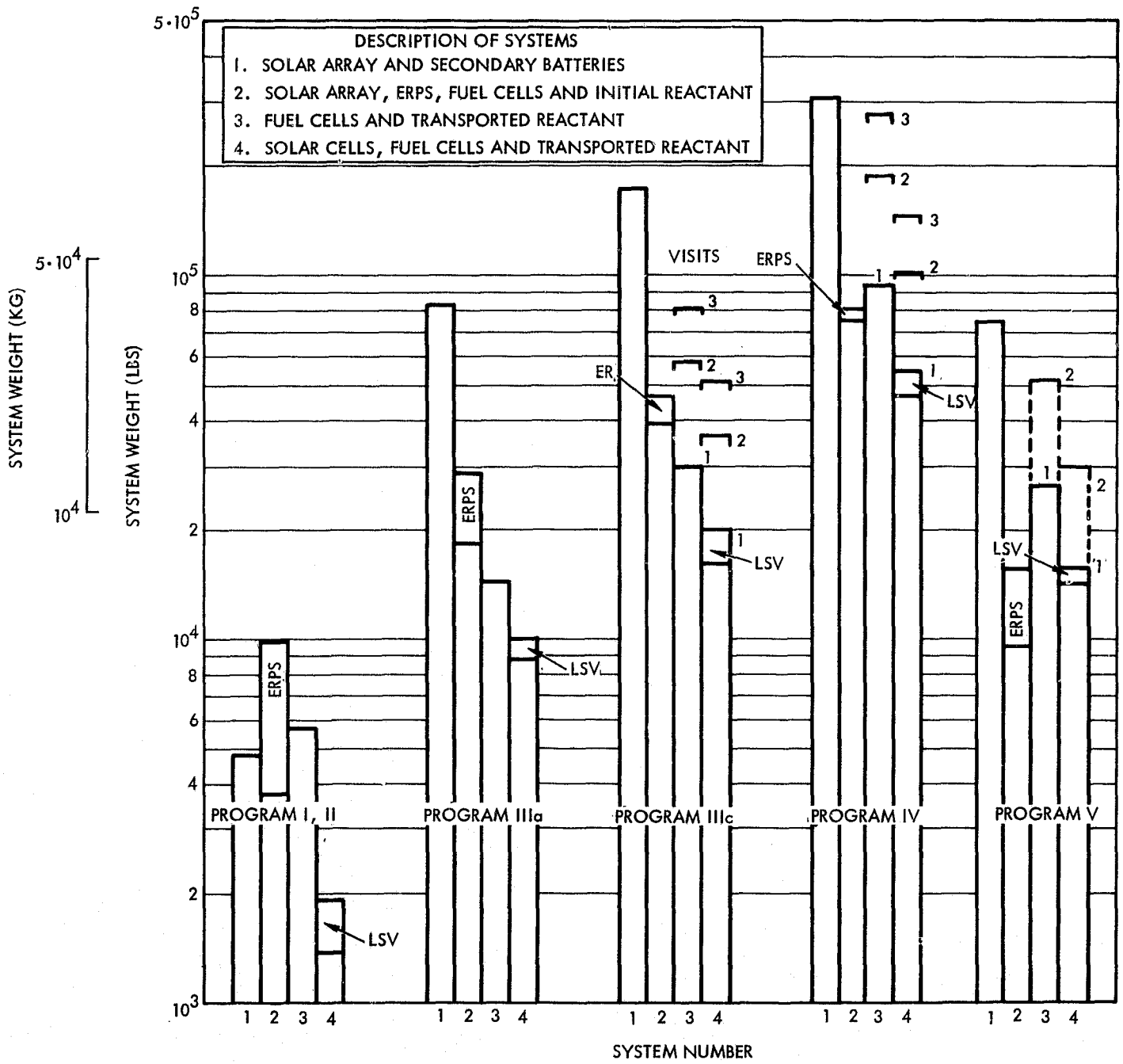

Figure 4.9 Comparison of Alternate Power System Weights

$W_{storage\ tanks}$	= 4,600
$W_{fuel\ cells}$	= 5,000
$W_{tsw\ (no\ mining)}$	71,200
W extra reactant	10,000
W total (no mining)	81,200 lbs

For the case of mining and water extraction, the above system weights will be supplemented by the weight of special equipment plus the added weight of the solar array and ERPS to support these operations. It should be noted that the above table of weights applies to Program IV, whereas the following discussion is general, applying to any program.

Solar array size and weight are dependent on the power demand. The portion of solar array power allocated for the surface vehicles and night-time base operation will be obtained through use of the ERPS system, subject to a efficiency factor, η_e. Daytime base power, mining and water extraction power are assumed to be supplied directly by the solar array. The total power, P_t, required from the solar array will then be,

$$P_{t(mining)} = \left\{ \left[(P_{b(night)} + P_v)/\eta_e \right] + P_{b(day)} \right\} + P_m + P_{ex}$$

$$P_t(mining) = P_t\ (no\ mining) + P_m + P_{ex}$$

where P_t (no mining) = terms in brackets above, P_m = mining power and P_{ex} = water extraction power. It is noted that the last two terms represent the additional power required for the mining and water extraction operations.

The solar array weight, W_{sa}, is proportional to power required; hence,

$$W_{sa\ (with\ mining)} = W_{sa\ (no\ mining)} + 120\ (p_m + p_{ex})$$

The power required for mining and water extraction depends on the weight of water, W_w, to be generated, the energy per pound (e_m or e_{ex}) required for mining and water extraction and the duration, D, of the mining and water extraction operating period. For example, for two lunar days

(daytime only), D = 672 hours. Using data developed in Section 4.5 for e_m and e_{ex}, and assuming lunar rocks having 1 percent moisture by weight, p_m and p_{ex} are then,

$$p_m = W_w(\text{lb})\ e_m\ (\text{kw hr/lb})\ /\ D(\text{hrs}) = (10^4)(0.08)\ /\ 672 = 120\ \text{kw}$$

$$p_{ex} = W_w(\text{lbs})\ e_{ex}(\text{kw-hrs/lb})\ /\ D\ (\text{hrs}) = 10^4\ (4.5)\ /\ 672 = 67\ \text{kw}$$

Thus, $W_{sa\ (\text{with mining})} = W_{sa\ (\text{no mining})} + 120\ (1.2 + 67) = W_{sa\ (\text{no mining})} + 8180$ lb.

The total system weight, W_{tsw}, will then be,

$$W_{tsw(\text{with mining})} = W_{tsw(\text{no mining})} + 120\ (p_m + p_{ex}) + W_m + W_{ex} + \Delta W_{ERPS}$$

The above equation for total system weight distinguishes between items common to both systems (no mining and mining) and those required only in the latter case. For equal logistic weight, the latter items can be compared with W_w to determine the relative effectiveness.

System weight is plotted in Figure 4.10 with respect to the no mining case, for various lunar soil moisture contents of from 0.1 to 10 percent. The weight tradeoffs between transported propellant and mining/water extraction/ΔW_{ERPS} equipment are illustrated by the shaded areas. The lower horizontal line (X-axis) represents the total system weight with no mining. Additional reactant can be transported from Earth (designated by the parallel horizontal lines), or it can be produced by mining and water extraction (designated by the various curves). The difference between the horizontal lines and the curves represents the maximum permissible weight of mining/water extraction/ΔW_{ERPS} equipment to break even with the weight of transported reactant. As can be noted, for a given amount of water produced, the time available to produce the water and the moisture content of the lunar soil markedly effect the maximum additional system weight allowable.

4.6.4 Analysis of Program V

Program V was defined as a mission of one year duration scheduled for the 1975 time period (references 4.2 and 4.3 in which the lunar base, ERPS and solar array system will be established and used by a 3-man

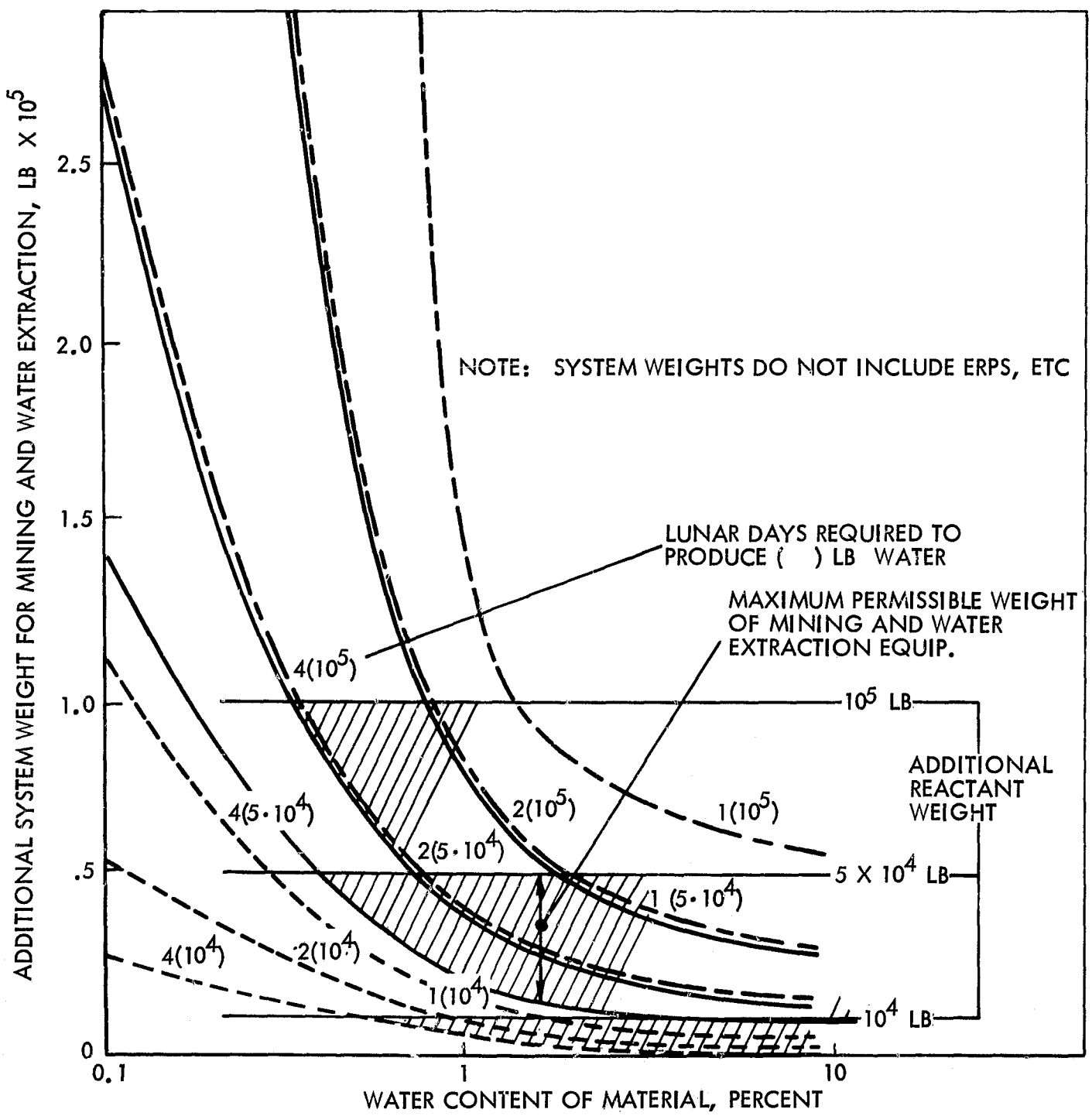

Figure 4.10 Power System Weights with Mining and Water Extraction

crew during the first 3-month period. It will then be left unattended for 6 months with automatic operation of the ERPS system. Finally, it will be followed by a final 3-month revisit by a 3-man crew. During the two periods of manned operation, the base power consumption was assumed to be 3 kw (daytime) and 5 kw (nighttime), plus an amount of energy equivalent to the surface vehicles consuming 1000 lbs of reactant per month. During the 6-months of unattended operation, the base power consumption was assumed to be 2 kw (day and night).

The reference 1.3 study estimated the power required for the above operation to be approximately 36.1 kw as the constant solar array output during periods of daylight. This power level permits the ERPS system to electrolyze and liquify 3.43 kg/hr (7.55 lb/hr) of reactant, in addition to supplying the daytime power needs of the base. The solar array design to satisfy these conditions, to conserve and reprocess the initial quantity of reactant consumed by fuel cells (all in a near-optimal manner for minimum total logistic weight) can now be considered for the suggested new program.

4.6.4.1 Solar Arrays for Program V

Program V power load profiles are shown in Figure 4.11 and were based upon the data in Reference 4.2. Power output profiles for various candidate solar array configurations are shown in Figures 4.12 to 4.14, using silicon cells and with proper allowance made for the effect of array temperature variations during the lunar day and for radiation/micrometeoroid degradation after one year (See Section 8.3).

- Flat Array. Power profiles for arrays deployed flat on the lunar surface are shown in Figure 4.12. The envelope power output curve would require 86 kw to match power profile No. 3 of Figure 4.11, with no secondary batteries required. A 78 kw peak power array would be 227 kg (600 lb) lighter, but would require 273 kg (600 lb) of rechargeable batteries to fill out the triangular shaded areas of the power profile. A total weight equaling the 86 kw array results. A reduction of 290 kg (640 lb) could be made by using the modified multi-step) power profile, shown by the dotted lines on Figure 4.12, rather than the original two-step power profile No. 3 proposed in Reference 4.2. Power profile No. 2, with a 10 day working period, requires a 94 kw array, with 273 kg (600 lb) of batteries, to produce the specified quantity of reactant. The flat array is not compatible with power profile No. 1 and no consideration was given to its use in this case.

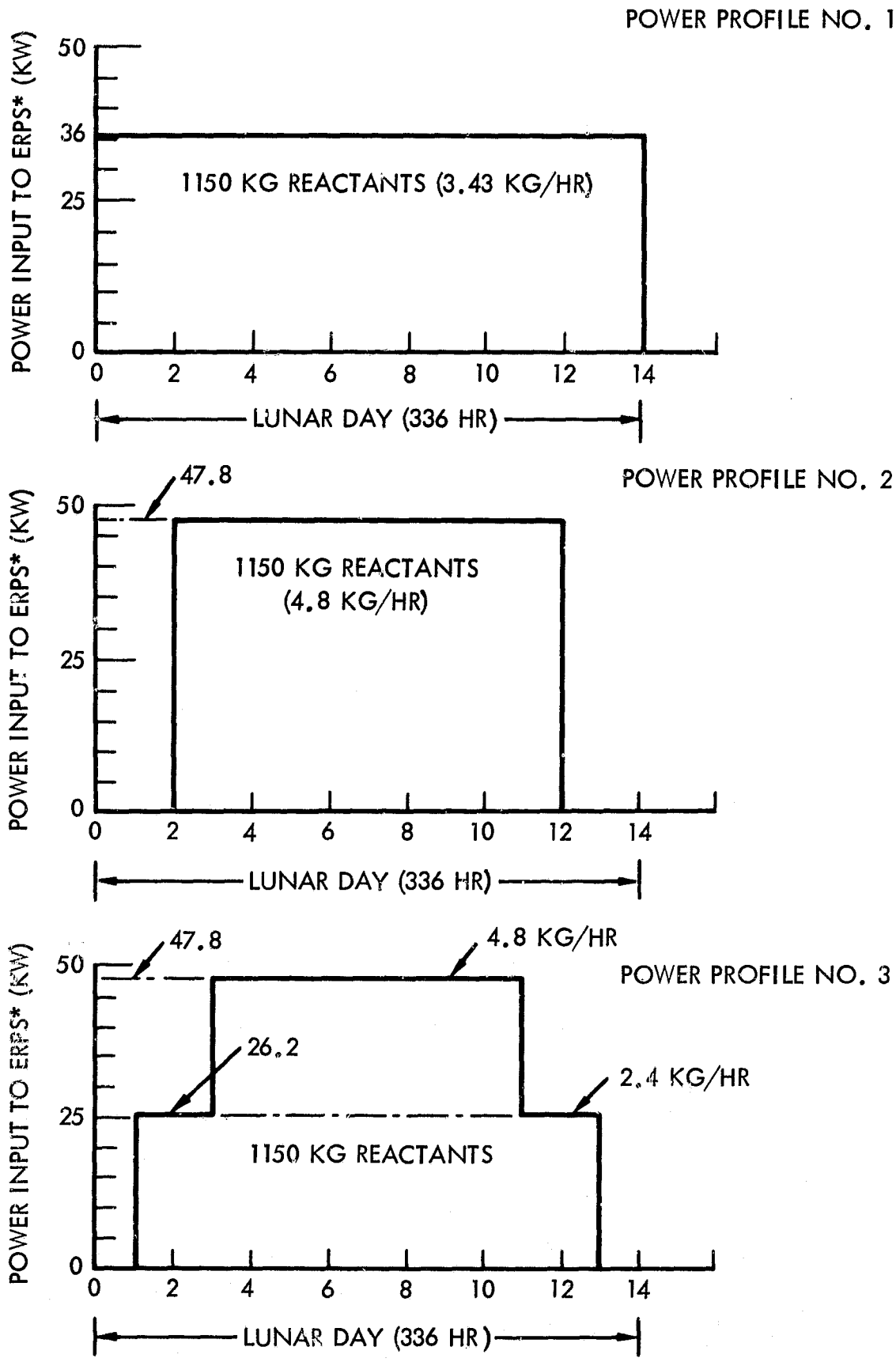

* INCLUDES APPROXIMATELY 3 KW AVERAGE FOR SHELTER POWER

Figure 4.11 Typical Program V Power Load Profiles

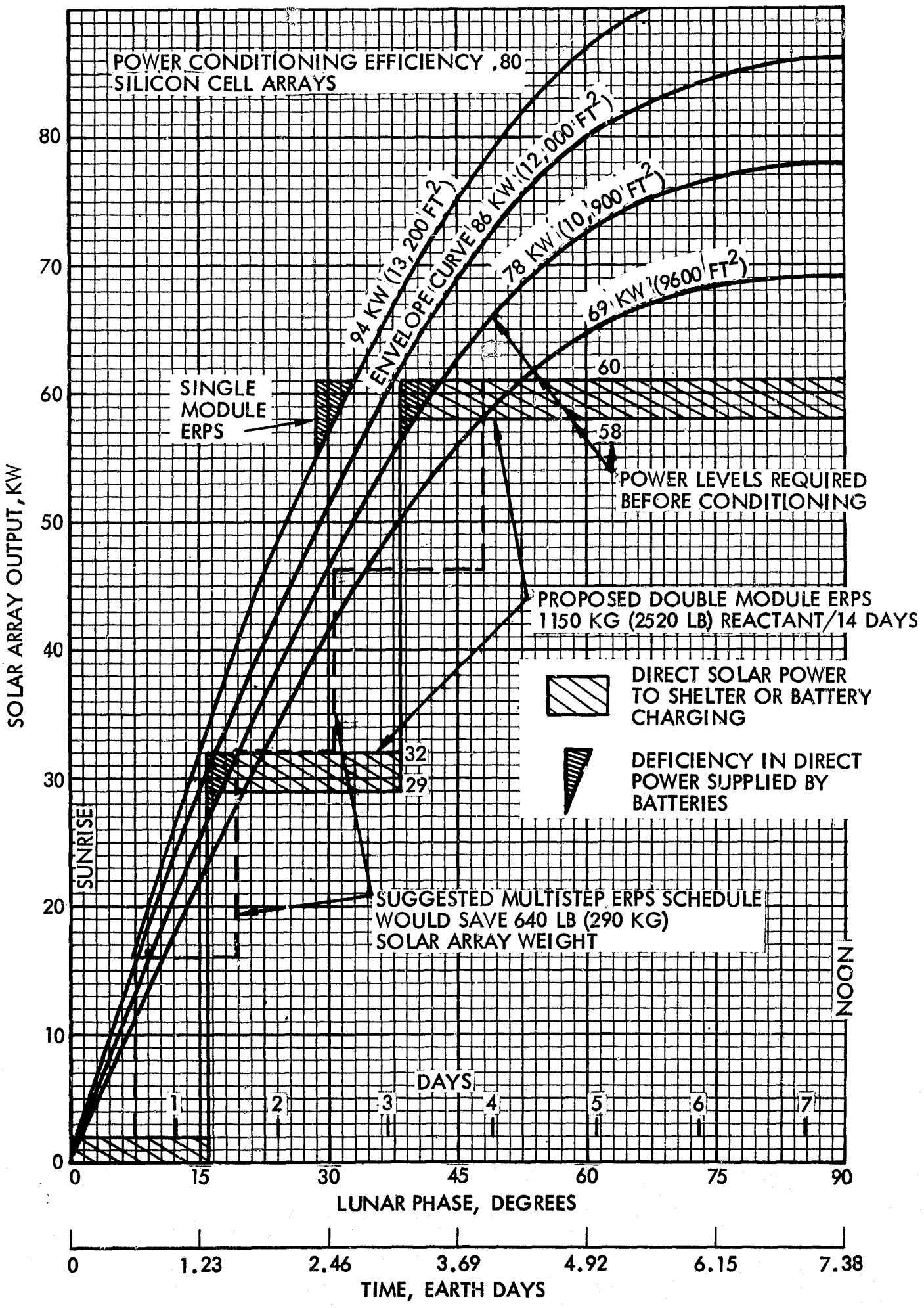

Figure 4.12 Power Profile for Flat Solar Array

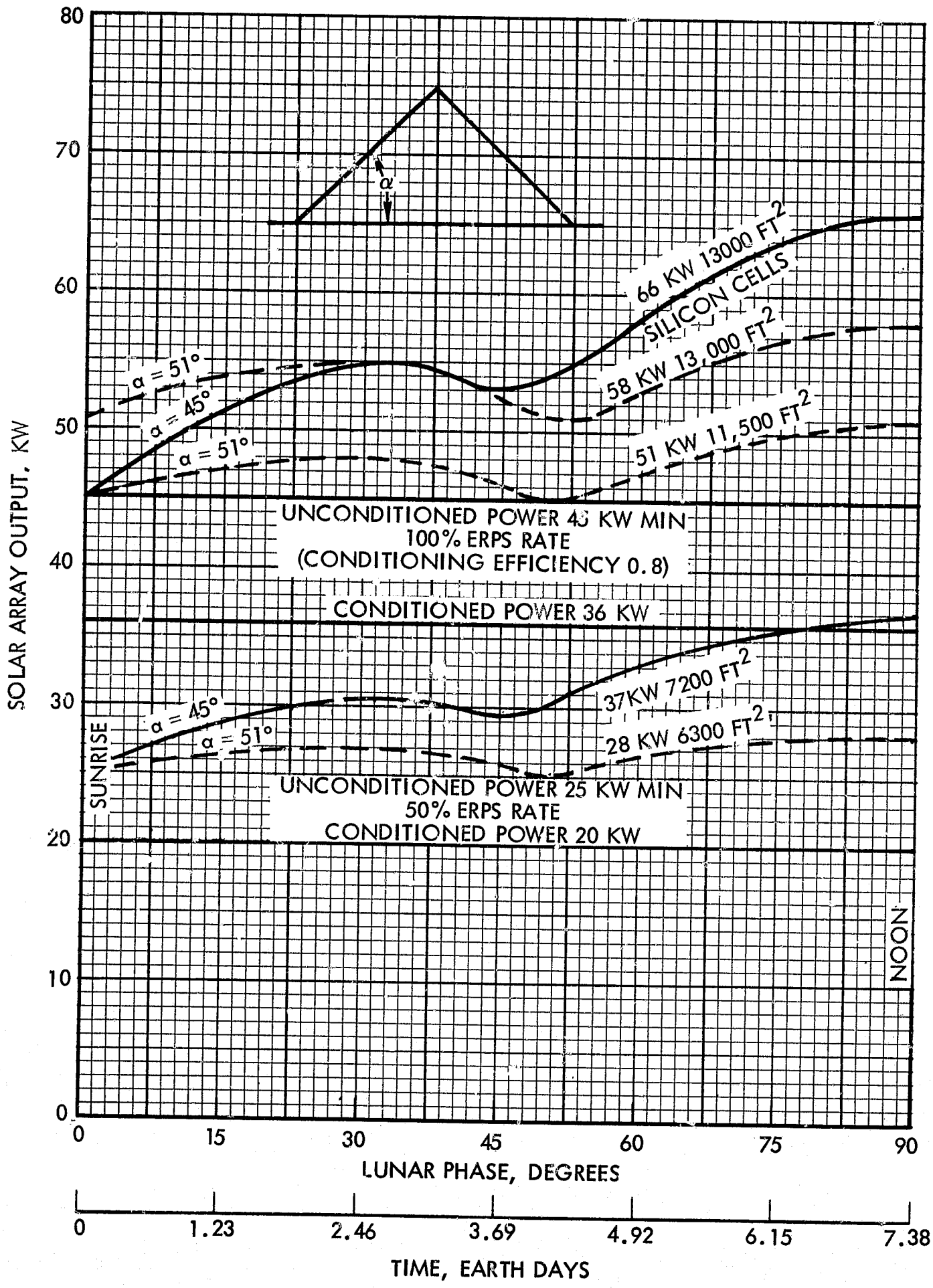

Figure 4.13 Power Profile for Leanto Array

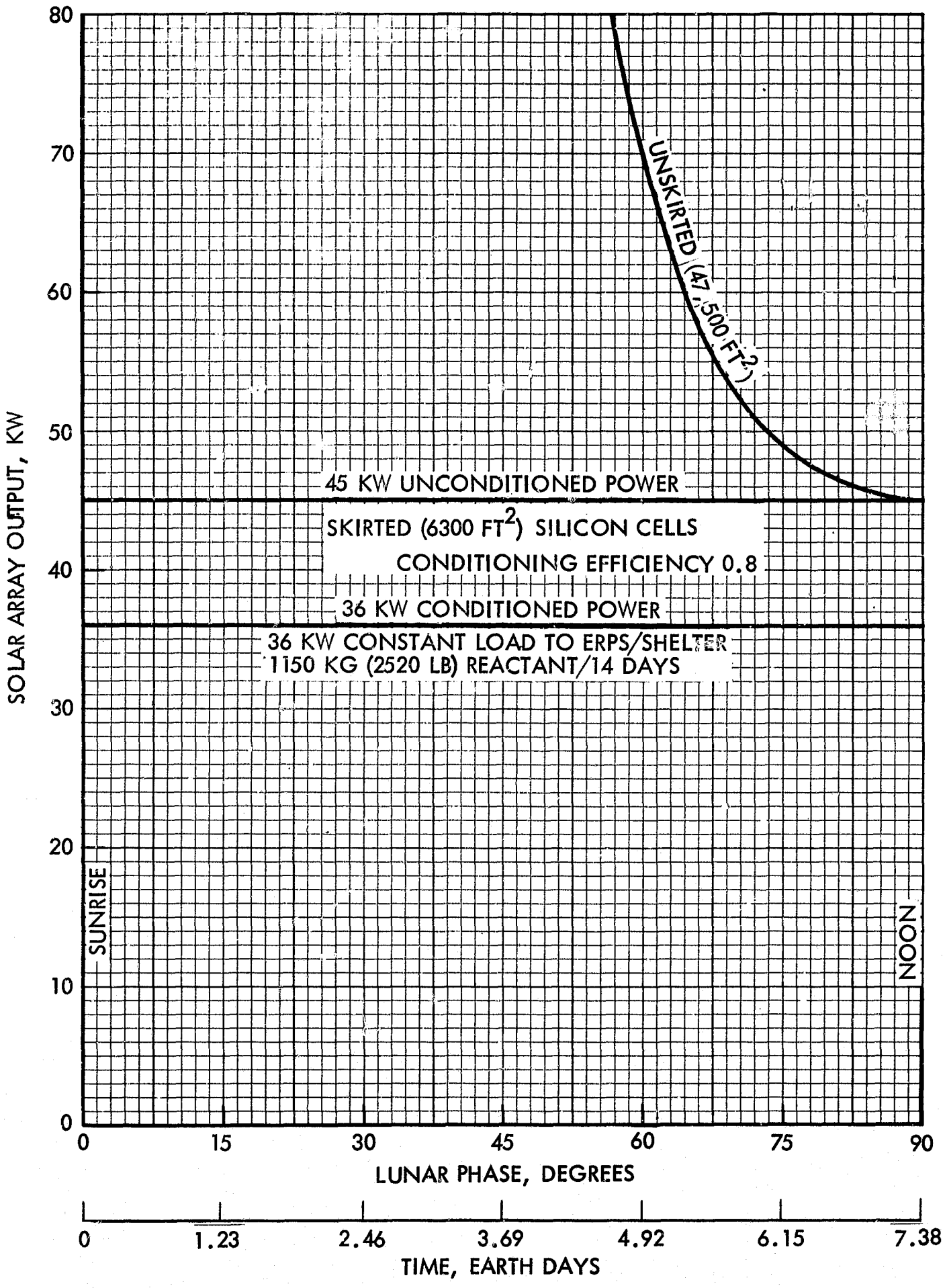

Figure 4.14 Power Profiles for Oriented Arrays

- Leanto Array. By elevating the center of the array (leanto configuration), its power profile is considerably improved at lunar dawn and dusk, when compared to the flat array. Figure 4.13 shows the power output profile of a 66 kw leanto (45°) array superimposed on power load profile No. 1. The 66 kw array is capable of supplying a minimum of 45 kw throughout the lunar day, thus permitting the ERPS system to operate at constant output and still provide 3 kw of power to the base. The varying output from this array is converted to 36 kw constant output by the power conditioning system (see Section 10.2), which has an efficiency of approximately 0.80.

It was noted during this study that an ascending power profile is obtained with the candidate leanto (Figure 4.13) having panels placed at an angle of α = 45 deg to the lunar surface. A flatter power profile would result if the panel angle was made slightly steeper. For example, if α = 51 deg, the dawn/dusk power will be increased to 51 kw, while at noon the power will be decreased to 58 kw. Since the minimum power required is only 45 kw, the area of this array could be decreased to approximately 45/51 = 0.88 of the original size; i.e., from 13,000 ft^2 to 11,500 ft^2 with a weight saving of about 324 kg (710 lbs). This important design consideration, together with further detailed thermal modeling could lead to further weight reductions for the leanto configuration.

It was also determined during this study that 28 to 37 kw leanto arrays shown by the lower set of curves in Figure 4.13 are adequate to operate the ERPS system at a constant processing rate of 50 percent of the original rate. This mode of operation is discussed in Section 4.6.4.2. The corresponding array weight could be reduced to 55 percent of the original value, thereby saving approximately 1270 kg (2800 lb) by using the lower processing rate.

- Oriented Array. Figure 4.14 shows power profiles for the fully oriented array. The unskirted oriented array, due to its high average temperature and resulting large area, is excessively heavy. The skirted oriented array, with a skirt to block out the adverse effects of the hot lunar surface, and a structural factor of 0.3 times solar cell weight, has a total weight of 1870 kg (4100 lb). This is the lightest array capable of meeting the Program V requirements. However, when viewed with respect to the overall mission economic considerations (see Section 4.6.4.4), this array configuration may not be the most cost effective.

The weights of the above solar array systems are summarized in Table 4.5 below. These values are based on single crystal silicon cells (8 mil thick), with one-year degradation due to radiation/micrometeoroids taken into account and for various assumed temperatures of the lunar surface.

Table 4.5 Solar Array Weights for Program V

Array Config.	P_{max} kw	Min P/A w/ft^2	T Array ^oC	T Surf ^oC	Area ft^2	Array wt-lb	Batt. wt-lb	Total wt-lb
Flat (One Step)	94	7.15	35	-6 Avg.	13,200	6,010	600	6,610
Flat (Two Step)	78	7.15	35	-6 Avg.	10,900	5,580	600	5,580
45° Leanto	66	5.05	35	-6 Avg.	13,000	6,160	-	6,160
51° Leanto	51	4.44	35	-6 Avg.	11,500	5,450	-	5,450
Oriented (unskrtd)	240	.8	160	-173 to + 122	47,500	30,800	-	30,800
Oriented (skirted)	45	7.15	57	-6 Avg.	6,300	4,100	-	4,100

The above estimates for solar array systems to satisfy the specified ERPS processing rate of 3.43 kg/hr (7.55 lb/hr) give a weight range from 1860 to 14,000 kg (4100 to 30,800 lbs). However, if an ERPS rate of 50 percent lower is assumed, the corresponding 45° leanto solar array will weigh approximately 1560 kg (3420 lb).

Of the three candidate solar array configurations shown in Figure 4.3, the oriented skirted array was found to have the lowest logistic weight. However, a consideration of total cost as given in Section 4.6.4.4, leads to different conclusions regarding the preferred choice of the various candidate configurations.

4.6.4.2 Schedule for Reactant Production and Consumption

In reviewing the power requirements for Program V, it became necessary to consider the time variation of reactant utilization and production during the one year mission (Figure 4.15). Each of the duty cycles specified in the program requirements represents a net depletion or accumulation of reactant. For example, during the first 3-month period, the cumulative effect on the initial reactant weight, W_o, is to deplete it to a value of approximately 0.15 W_o (i.e., 15 percent margin). The reactant supply is then restored during the 6-month unattended period to approximately, W_o, (boil-off losses not being considered) in readiness for

the second 3-month visit. The same schedule is then repeated for the next 3-month manned period.

The above process of analysis serves two purposes. It can aid in selecting a minimum weight solar array and also provides to insure that sufficient initial reactant and storage tank volume have been provided for the program. These two design factors are interrelated and should be optimized to result in a minimum total logistic weight. This optimization analysis was beyond the scope of this study, but the impact of a 50 percent ERPS production rate on the mission is described below.

The various power requirements associated with various phases of the Program V mission operations can be converted to reactant rates as shown in Table 4.6, with the negative values representing consumption.

Table 4.6 Reactant Production/Consumption Rates for Program V

Power Requirements Phase	kg/hr	lb/hr	kg/14 days	lb/14 days
ERPS rate (attended)	3.43	(7.55)	1150	(2530)
6 kw daytime (attended)	included in 36 kw to produce ERPS rate above			
5 kw nighttime (attended)	-2.07	(-4.55)	-695	(-1530)
2 kw daytime (unattended)	included in 36 kw to produce ERPS rate below			
ERPS rate (unattended)	3.67	(8.05)	1230	(2710)
2 kw nighttime (unattended)	-.83	(-1.82)	-278	(-610)
MOLAB avg. rate (daytime)	-1.35	(-2.98)	-453	(-1000)

These values are shown plotted versus time in Figure 4.15 for two values of the ERPS processing rate; 3.43 kg/hr and 50 percent of this rate. In the former case, the initial reactant is completely replenished about 10 days after the beginning of the dormant (unattended) period, after which a reduced duty cycle serves to maintain this condition. With the 50 percent ERPS rate, the reactant is restored gradually during the dormant period by the same processing rate but with the ERPS operating continuously during each lunar day. This results in full replenishment of reactants at the end of the 6-month period. Additional weight of initial reactant (plus tankage) required in the latter case is more than offset by savings due to a reduction in solar cell area requirements and ERPS system weight. An additional weight saving results from the elimination

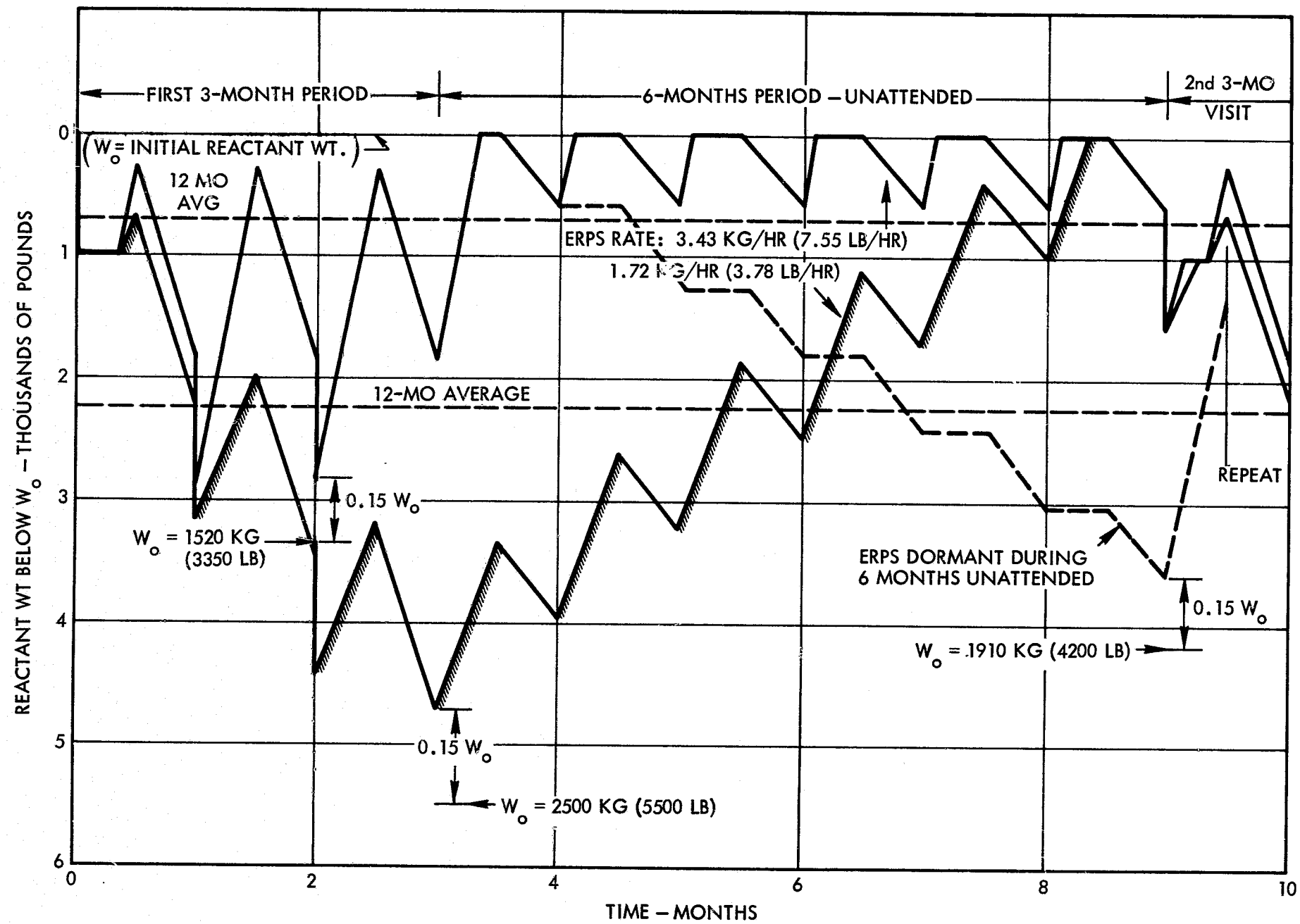

Figure 4.15 Reactant Schedule for Program V - Comparison of Alternate Modes

of a parasitic load bank. In the latter case, the ERPS system operates at its full capacity at all times and hence, excess power generated by the solar array is reduced to a minimum. The relative weights of the two systems assuming the 45° leanto array, are shown in Table 4.7.

Table 4.7 Comparison of Systems Weights for Varying ERPS Production Rates

System Components	Weight at Full ERPS Rate kg (lbs)	Weight at 50% ERPS Rate kg (lbs)
Solar Array	2800 (6160)	1560 (3420)
Initial Reactant	1520 (3350)	2500 (5500)
Tankage	455 (1000)	750 (1650)
ERPS System	2910 (6400)	1820 (4000)
Total Weight	7680 (16,910)	6600 (14,570)

Weight Savings Due to ERPS Rate. The above comparison of alternate modes of operating the ERPS system for Program V shows that approximately 1063 kg (2340 lb) less logistic weight would be required for the lower ERPS rate. When using the high ERPS rate, the quantity of reactant is maintained at a high level during the 6-months unattended period and hence, the base is in a state of readiness at all times. However, during the unattended period, the high ERPS rate system is inoperative for long periods during each lunar day, thus posing considerable thermal control problems with a potential lowering of overall system reliability. On the other hand, when using the reduced ERPS rate system, reactant is processed continuously during each lunar day (after the first one) throughout the first 3-month period and the 6-month unattended period. This is indicated by the shaded black lines in Figure 4.15. While the advantage of this steady-state operation must be determined by a detailed analysis of the ERPS/power system when using this mode, it is inherently felt that it would result in a higher level of reliability.

Cryogenic Boiloff Loss. The average weight of cryogenics stored at the base during the one-year mission amounts to 2650 lb for the high ERPS rate, and 3250 lb for the low ERPS rate (see dashed horizontal lines on Figure 4.15). This represents a difference of 600 lb between the

two systems. If the cryogenic boiloff is assumed to be 10 percent for the 12-month period, the low rate ERPS system will then lose 60 lb more reactant than the high rate ERPS system. However, this boiloff loss is small compared to the 2340 lb weight saving to be derived by use of the low ERPS rate as shown on Table 4.7.

Automatic ERPS Operation. The above discussion assumed that the solar array/ERPS system would operate automatically during the 6-month period when the base was unoccupied. If this proves to be impractical from a reliability standpoint, the following alternate procedure could be followed. The solar array would operate automatically to supply daytime needs of the shelter and dormant ERPS, while nighttime needs would be supplied by reactant through fuel cells. The dotted lines in the lower right hand section of Figure 4.15 show the change in reactant consumption. Initial reactant, W_o, would be 1910 kg (4200 lb), compared with 1520 kg (3350 lb) for the automatic ERPS mode. While this represents an increase of 386 kg (850 lb) in logistic weight for the one-year Program V mission, the elimination of the necessity to operate the ERPS during the unmanned period might considerably increase overall mission reliability.

4.6.4.3 Operation of ERPS on the First Lunar Day

The ERPS production rate is based on 336 hours of operation during each lunar day (14.75 x 24 = 354 hrs). Hence, an allowance of 18 hours elapsed time is available for deployment of the power system and ERPS, to accomplish full production for the first lunar day. In subsequent days, this 18 hour margin could be used for maintenance, adjustment of equipment and unexpected shutdown periods.

During the first lunar day, reactant consumption is at a minimum, since only the LSV's are generating water (approximately 1000 lb) to be reprocessed when the vehicles return to base near the close of the day. After the first lunar night, an additional 1530 lb of water is awaiting processing by the ERPS system. Hence, at the beginning of the second lunar day, the system has a full charge of 2530 pounds of water for processing.

To permit ERPS to operate at full capacity during the first lunar day, an initial weight of 2530 pounds of water should be transported. This would permit the initial reactant weight to be reduced by an equal amount.

The total volume of tankage would remain the same, since a water tank of 2530 pound capacity is needed to operate ERPS, and the reactant tanks should be capable of storing the full amount of initial reactant plus reprocessed water.

It should be noted that mission requirements can be accomplished without the necessity for ERPS to attain full production during the first lunar day. For example, with no water available initially, the ERPS system can stand by until the LSV's have operated for a period of time and returned water for reprocessing. Depending on the percentage of LSV water which is returned to ERPS in time for processing during the first lunar day, a number of conceivable cases are analyzed in Table 4.8 (the start up time for ERPS depending on the availability of water). A comparison of several modes of operation, involving different choices in weight of initial reactant (plus water), result in weight differences affecting the optimization of overall logistic weight. Table 4.8 shows four cases for the full ERPS production rate, and two cases for the one-half ERPS rate previously discussed.

4.6.4.4 Economic Considerations for Program V

A comparison of the relative costs of various power systems for Program V includes the procurement cost of the hardware, transportation cost from Earth to moon, cost of deploying and activating the system at the lunar base and cost of maintaining the system. The following basic cost numbers were used for the economic evaluations:

- Cost of RDT&D (to build and qualify first 2.5 kw array) — $10M
- Silicon cell array production cost — $1,500/ft^2
- Other hardware costs, in general — $300/lb
- Transportation cost to lunar site $230M cost per launching/23,000 lb lunar payload — $10,000/lb
- Value of astronaut time, assuming; — $300,000/man-hr

  a) $1B total mission cost for Program V/3333 man hrs of productive astronaut time and,

Production Mode	Initial Conditions		Production	Consumption	Final Conditions		Total Initial Weight,
	Water (lb)	Reactant (lb)	Reactant (lb)	Reactant (lb)	Water (lb)	Reactant (lb)	W_o (lb)
100% ERPS Rate							
Case I	2530	1150	2530(1)	2530	2530	1150	3680
Case II-1st Mo.	0	2910	1000(2)	2530	1530	1380	2910
-2nd Mo.	1530	1380	2530	2530	1530	1380	
*Case III-1st Mo.	0	3350	700(3)	2530	1830	1520	3350
-2nd Mo.	1830	1520	2530	2530	1830	1520	
Case IV-1st Mo.	0	4060	0(1)	2530	2530	1530	4060
-2nd Mo.	2530	1530	2530	2530	2530	1530	
50% ERPS Rate							
Case I-1st Mo.	1265	4370	1265(1)	2530	2530	3105	5635
-2nd Mo.	2530	3105	1265	2530	3795	1840	
-3rd Mo.	3795	1840	1265	2530	5060	575	
-4th-9th	5060	575	6x1265	6x610	1130	4505	
* Case II-1st Mo.	0	5500	350(4)	2530	2180	3320	5500
-2nd Mo.	2180	3320	1265	2530	3445	1955	
-3rd Mo.	3445	2055	1265	2530	4710	790	
-4th-9th	4710	690	6x1355	6x610	240	5160	

(1) This production does not require delivery of water generated by LSV until end of lunar day.

(2) This production requires that all water generated by LSV be delivered to ERPS in time for processing.

(3) This production requires that 70 percent of the water generated by LSV be delivered to ERPS in time for processing.

(4) This production requires that 35 percent of the water generated by LSV be delivered to ERPS in time for processing.

* These two cases are shown plotted in Figure 4.15

Table 4.8 Alternate Modes of ERPS Operation

b) Three astronauts x 14.75 x 24 x 0.525 x 6 = 3333 man hrs (assuming 52 percent of the daylight hours are spent in productive activity and the balance are spent in sleeping, eating and recreation).

The RDT&E cost of $10M is an initial estimate for the development and qualification of a 2.5 kw array (plus foldable structure and packaging/deployment details). This minimum size array can be used in a building block manner, to satisfy lesser power requirements for lunar missions. Such a unit can be built, development tested and qualified for operational use. This universal size array would then be applicable to missions requiring larger amounts of power, with only minor changes in packaging and deployment techniques required to meet the requirements of much larger systems (i.e., up to 100 kw).

The production cost of multiple quantities of this 2.5 kw array (20 or so per mission) will decrease with an increasing number of arrays, according to an exponential learning curve as shown in Figure 4.16. It should be noted that each 2.5 kw array consists of 10-20 foldout modules, produced separately and then hinged together to form the array. Hence, there would be 200-400 modules produced to make up a 50 kw solar array.

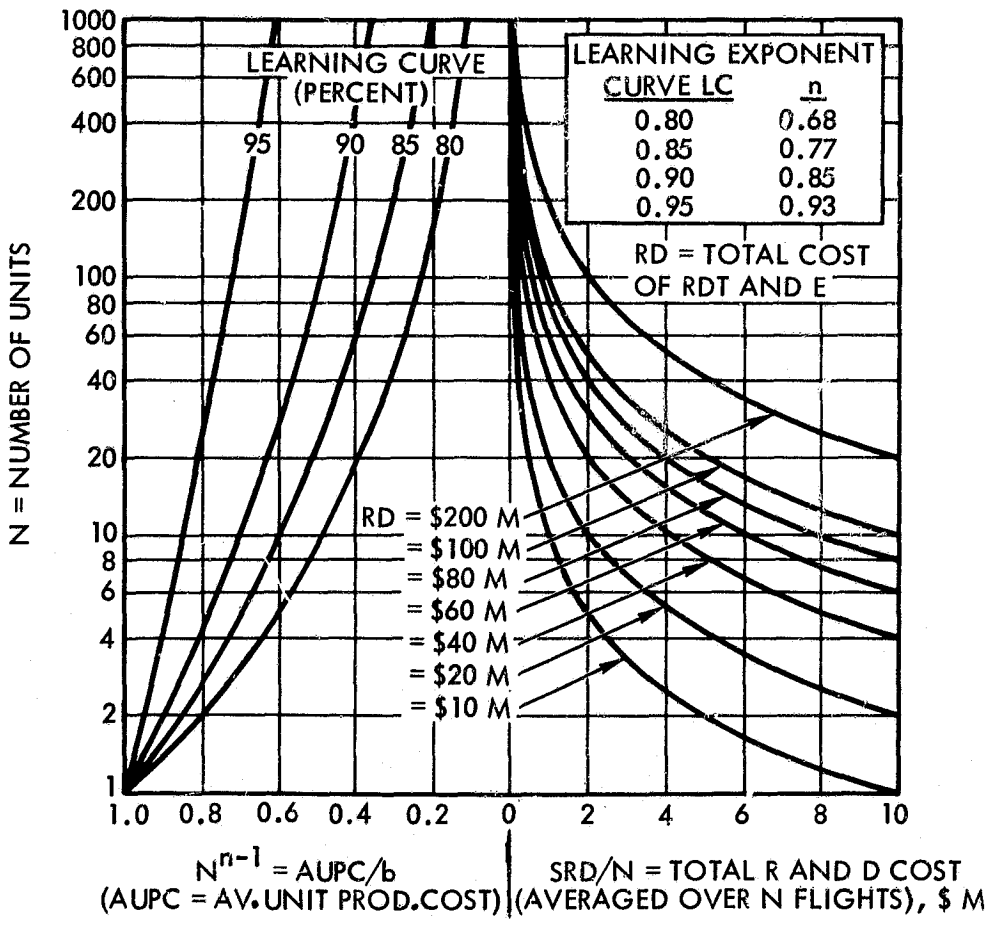

Figure 4.16 Average Cost of Solar Arrays

The average 2.5 kw array cost, AUC, when produced in quantities of N, is then AUC = bN^{n-1} + RD/N, where b = first unit production cost, n = exponent of learning curve = 1 + log LC/log 2, and RD = total cost for RDT&E averaged to RD/N by use of the right side of Figure 4.16. The learning curve LC for production costs is by definition the ratio (average cost of 2N units)/average cost of N units. Then the average unit production cost AUPC = bN^{n-1} can be determined from the left side of the figure. On a 90 percent learning curve, the average array cost will then be 40-45 percent of the first unit production cost. Current state-of-the-art first unit production costs (OGO and others) give rise to a value of b = \$2500/ft^2. Hence, the average array production cost would be expected to drop to \$1000 to \$1200/ft^2 for large quantities. To be conservative, a solar array production cost of \$1500/ft^2 was assumed in this study.

Using the above basic values, the cost of solar arrays were computed on the basis of the total (unconditioned) power required to satisfy the mission requirements. Additional hardware costs included the structure to support the solar array, power conditioning equipment, cabling, batteries, etc. The transportation cost was based on the total logistics weight to be transported from Earth to the lunar base site. The cost of astronaut time was based on the total elapsed time in man-hours after landing to deploy, activate and maintain the power system (during which period the astronauts are precluded from the accomplishment of scientific and exploratory objectives for which the mission is primarily intended).

Cost calculations for various power systems are shown in Table 4.9. It should be noted that transportation and deployment costs constitute a major portion of the total power system costs. The maintenance costs for the oriented-skirted array also contributed greatly to the overall cost of this system. Furthermore, while minimum total power system costs usually coincided with minimum total power system weight, this was not the case for the oriented-skirted configuration. The calculation procedure is illustrated in nomographic form in Figure 4.17. Starting with the total unconditioned power, one must follow the dashed lines downward to the w/ft^2 at lunar noon, then horizontally across to the array area and continue on to the solar array unit production cost, \$/ft^2. The initial array

DOUBLE FRAME

Category \ Array Configuration	Flat (2 step ERPS)		Flat
Panel type	Flexible	Rigid	Flex
Mounting	Surface	Structure	Surf
Power (unconditioned) - kw	78	78	94
watts/ft^2 at lunar noon	7.15	7.15	7.15
Array Area - ft^2	10,900	10,900	13,2
Array weight - lb(3)	880	880	1,07
Other hardware wt - lb	4,670	5,300	5,40
Structure(3)	(3,470	(4,100)	(4,20
Batteries	(600)	(600)	(6
Power Conditioning and Cabling	(600)	(600)	(60
Total Power System Weight - lb	5,550	6,180	6,47
Time to Deploy - man hours	18(1)	15	18(1)
Time to Maintain - man hours	--	--	--
Cost of Solar Array(4) - $M	26.4	26.4	29.8
Cost of other Hardware - $M	1.5	1.6	1.6
Cost of transportation - $M	55.5	61.8	64.7
Cost of Deployment - $M	5.4	4.5	5.4
Cost of Maintenance - $M	--	--	--
Total Power System Cost - $M	88.8	94.3	101.5

(1) The longer deployment time in this case is due to preparation of lunar surface
(2) Assuming manual actuation. Total cost reduced by automatic motor controls
(3) The unit weights of the silicon cell modules were taken as follows (see Section 8)

Configuration	Array Weight lb/ft^2	Struc lb/
Flat (flexible) on surface	.081	.3
Flat (rigid) on structure	.081	.3
Leanto (rigid) on surface	.081	.3
Leanto (rigid) on structure	.081	.4
Oriented (rigid) skirted	.081	.5

(4) Includes $10M for RDT&E

Flat (2 step ERPS)		Flat (1 step ERPS)		45° Leanto		51° Leanto	Oriented (skirted)
Flexible Surface	Rigid Structure	Flexible Surface	Rigid Structure	Rigid Surface	Rigid Structure	Rigid Surface	Rigid Structure
78	78	94	94	66	66	51	45
7.15	7.15	7.15	7.15	5.1	5.1	4.4	7.15
10,900	10,900	13,200	13,200	13,000	13,000	11,500	6,300
880	880	1,070	1,070	1,060	1,060	930	510
4,670	5,300	5,400	6,140	5,550	6,450	4,970	4,000
3,470	(4,100)	(4,200)	(4,940)	(5,100)	(6,000)	(4,520)	(3,600)
(600)	(600)	(600)	(600)	--	--	--	--
(600)	(600)	(600)	(600)	(450)	(450)	(450)	(400)
5,550	6,180	6,470	7,210	6,610	7,510	5,900	4,510
18(1)	15	18(1)	15	20	45	20	120
--	--	--	--	---	---	--	177(2)
26.4	26.4	29.8	29.8	29.5	29.5	27.3	19.4
1.5	1.6	1.6	1.8	1.7	1.0	1.5	1.2
55.5	61.8	64.7	72.1	66.1	75.1	59.0	45.1
5.4	4.5	5.4	4.5	6.0	13.5	6.0	36.0
--	--	--	--	--	--	--	53.0
88.8	94.3	101.5	108.2	103.3	120.0	93.8	154.7

of lunar surface
motor controls
ws (see Section 8)

Array Weight lb/ft^2	Structure lb/ft^2	Total lb/ft^2
.081	.319	.400
.081	.375	.456
.081	.394	.475
.081	.458	.539
.081	.569	.650

Table 4.9 Cost Estimates for Power Systems

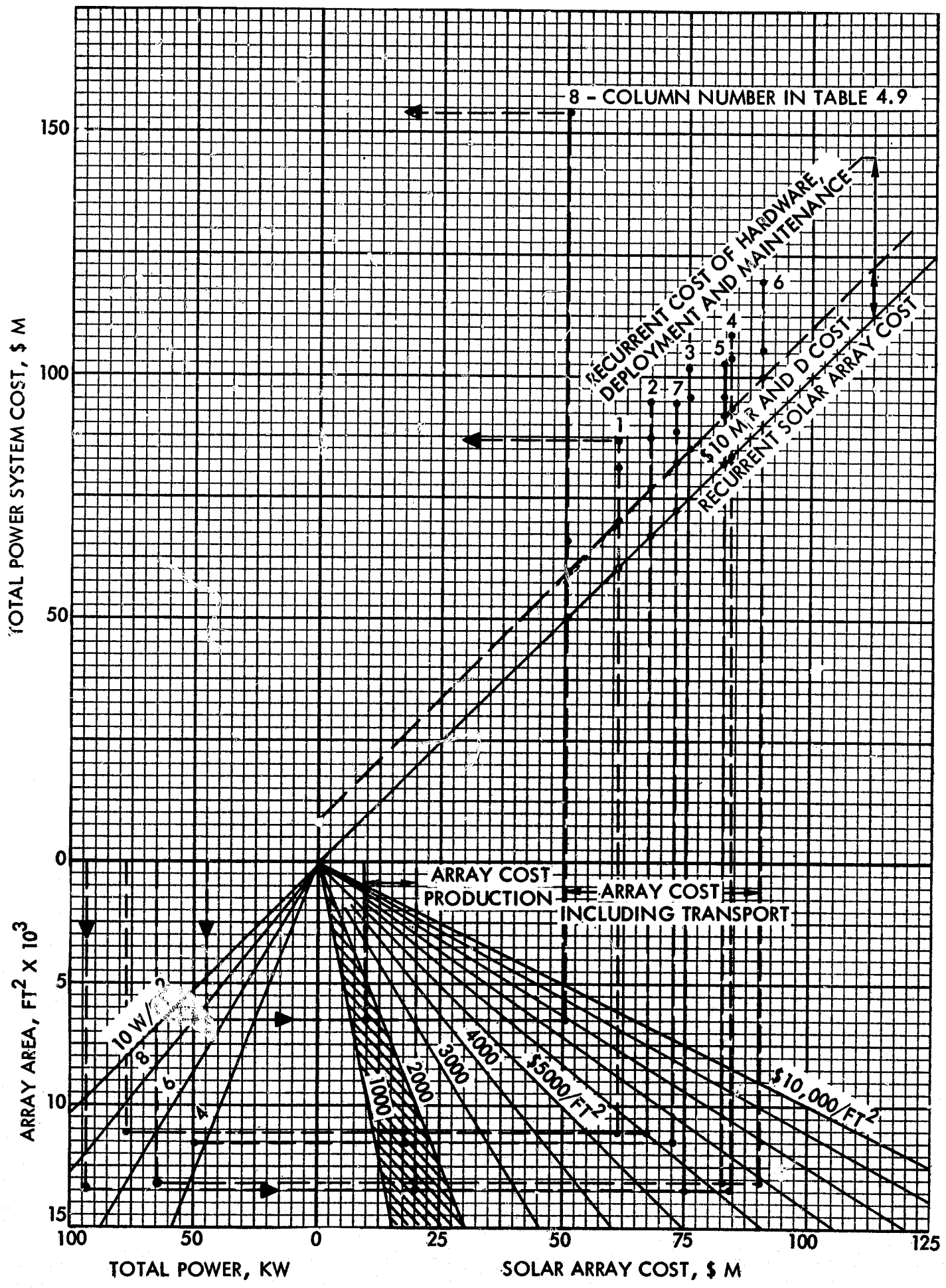

Figure 4.17 Power System Cost Nomograph

production cost can then be read from the horizontal scale. Continuing horizontally across to include the cost of transporting the array to the lunar surface gives the total recurrent cost attributable to the solar array alone. Now, following the dashed lines upward to the 45° line, these solar array costs can now be read from the vertical cost scale. Additional costs shown above the 45° line include the initial $10M R&D cost (which could be amortized over a number of missions), recurrent hardware cost including their transportation cost, and total system deployment/maintenance cost. The uppermost point for each case equals the total power system cost as shown on Table 4.9.

The solar array production cost was assumed to be $1500/ft^2 in the above example. This is believed to be a conservative value, and may be expected to ultimately decrease to about $1000/ft^2, depending upon how much is invested in manufacturing development. If the production cost of $1000/ft^2 proves to be attainable, the resulting savings in total power system costs could amount to $3M to $7M, after amortization of the additional R&D costs over a number of missions. These considerations illustrate the potential cost savings to be derived when the use of large quantities of the standard size 2.5 kw array is required and emphasizes the need for a more comprehensive study to evaluate R&D and production costs, to confirm the validity of the above conservative estimates.

Cost Sensitivity. The sensitivity of total power system cost to variations in the cost inputs is shown in Figure 4.18, based on the data shown for the 51° leanto configuration of Table 4.9. It can be seen that for this case, the transportation cost is the most significant parameter affecting total power system cost. Since this value is related directly to the cost of the launch vehicle and launch operations, any reductions in this area could materially lower the total power system cost. A reduction in array production costs also could contribute greatly to reducing the cost of the solar array and hence, the overall total power system costs.

A discussion of the reasons for the specific difference in total power systems costs as shown in Table 4.9 and Figure 4.17 are outlined below.

One-Step ERPS vs. Two-Step. The total power system cost for the flat array with the two-step ERPS mode is approximately $20M lower than when utilizing the one-step ERPS mode (not including the cost of the ERPS

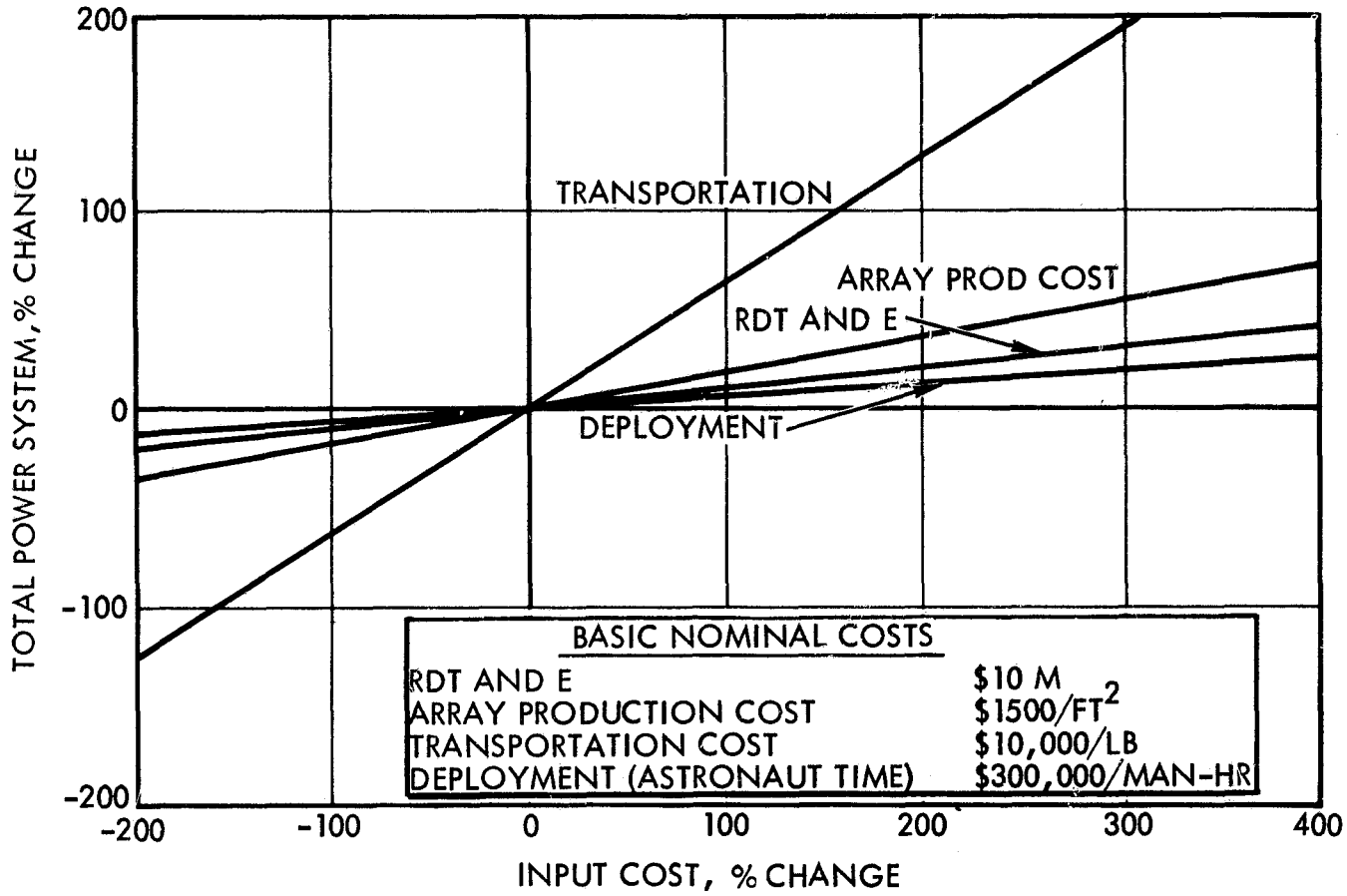

Figure 4.18 Cost Sensitivity to Input Values

itself, which is not a part of the power system). The one-step ERPS, designed for continuous operation at 33 kw for 14 days, weighs 6400 lb (References 4.2 and 4.3). The two-step ERPS, designed for operation at both a 23 kw and 46 kw level, would be expected to be somewhat heavier due to the requirement for two modules or staging. A weight increase of 2000 pounds would correspond to a $20M increase in transportation cost (at $\$10^4$/lb). Hence, the two-step ERPS could be as much as 2000 lb heavier, and still be competitive with the one-step ERPS as far as total cost is concerned. A more detailed analysis of the ERPS weights would be required to determine whether one-step or two-step operation is preferable.

Flat Array vs. 45° Leanto. When both arrays are mounted on structure, the total power system cost is $10M lower for the flat array due to its lighter, simpler structure. However, the weight of ERPS should again be considered. A weight increase up to 1000 lbs would be permissible for the 46 kw ERPS to be used with the flat array, to break even in

total system cost with the 33 kw ERPS used with the leanto. Scaling up the 6400 lb ERPS weight by the ratio of 46/33 gives 8900 lb, or a 2500 lb increase. Therefore, the leanto is evidently to be preferred. The 51° leanto provides further proof of this conclusion since a further reduction in the leanto system cost is potentially possible with this configuration.

Leanto - Surface vs. Structure Mounting. The leanto using rigid panels can be made a self supporting structure, as described in Section 7.5.2.4. Its total power system cost is $16.7M lower than the leanto mounted on structure, due to a saving in weight and deployment time. This potential cost saving justifies a considerable amount of design effort to develop a self-supporting, surface-mounted leanto array.

Improved Leanto with Steeper Slope. It was noted in Section 4.6.4.1 that an increase in the slope of the leanto panels from 45° to 51° could result in reduced array area and weight. This change (which must be confirmed during the next study phase) could reduce the solar array cost about $2M, and the transportation cost by about $7M. The total power system cost of the 45° leanto array shown in Table 4.9 can therefore be reduced by about $9M, thus making them comparable to the low cost flat arrays. If the increased weight and resulting transportation costs of the two-step ERPS are taken into account, then the leanto system is definitely to be preferred.

Oriented Skirted Array. The oriented-skirted array has a total power system cost $25M to $66M higher than the other systems, due primarily to the higher deployment and maintenance costs. The oriented array requires about 2 man-hours every 24 hours to re-orient the array with respect to the sun. The total cost of this maintenance activity amounts to $53M over a one-year period. The cost of actuation could be reduced somewhat by providing automatic motor controls, but the resulting total system cost would still only be comparable with that of the other fixed arrays, which are still to be preferred for reliability reasons.

Solar Array/ERPS vs. Transported Reactant. When the above overall economic criteria are applied to the various systems compared in Table 4.4, the relative merit of the alternative systems are viewed more realistically than when compared on the basis of logistic weight alone.

For example, with Program V, the solar array/ERPS/fuel cells with initial reactant (System 2) was found to have 14,470 lb lower logistic weight than the solar array/fuel cell with transported reactant (System 4) for the one-year mission. This means that System 2 would cost $145M less than System 4, if transportation cost were the only criterion. However, even when the costs of the larger solar array and the ERPS are considered, there is still a net saving of $95M by the use of the solar array/ERPS/fuel cells with initial reactant system for the one-year Program V mission. The economic analysis thus confirms the superiority of the solar array/ERPS/fuel cells with initial reactant system.

4.6.4.5 Cost and Weight Considerations

The solar array/ERPS system provides not only the lowest logistic weight, but also the lowest cost approach of accomplishing Program V. The leanto array configuration mounted on the lunar surface shows promise of resulting in the lowest cost system for use with the minimum weight 33 kw, one-step ERPS mode. However, additional thermal analyses are required to confirm the selection of an optimum leanto angle. The oriented-skirted array is more costly than other fixed arrays when manual control is used for orientation. With automatic motor control, the costs would be essentially equal. However, the oriented array is potentially less reliable than the fixed array and hence, the latter configuration is to be preferred. The flat array configuration with the two-step ERPS mode offers promise of providing a low cost system for Program V. However, the potential increased weight and cost of the two-step ERPS more than offsets any cost advantages to be derived from this system. In addition, a widely varying power output profile results in a large voltage excursion, thus imposing performance penalties on the related power conditioning equipment.

4.6.5 Nuclear Power vs. Solar Array/ERPS for Program V

During the course of this study, the use of a 20 kwe nuclear-thermoelectric power plant (Reference 4.5) for Program V was proposed. This system requires the logistic transport of 79 percent more equipment to the moon than the solar array/ERPS system, as shown in Table 4.10. For the initial landing, the relative weights are 13,200 kg (29,010 lb) for

Table 4.10 Comparison of Nuclear and Solar Array/ERPS Systems for Program V

	REACTOR-THERMOELECTRIC POWER PLANT (Reference 4.5)		NEAR TERM SOLAR ARRAY/ERPS	
Electric Power				
Gross, initial (kwe)	24.3		51 kw leanto	
Gross, final (kwe)	23.3			
Net, final (kwe)	20.0		36 kw	
Reactor Power (kwt)	900			
System Efficiency (%)	2.2			
Temperature (^{o}F)	Inlet	Outlet		
Reactor	1100	1300		
Converter	1272	1078		
Radiator	766	574		
Design Life				
Reactor (yr)	1.7			
Power conversion system (hr)	20,000		10,000	
Radiator Area (sq. ft.)				
Converter	1360			
Pumps and shield cooling	167			
TOTAL	1527			
Weights (lb)				
Reactor	1,100		Power system	5900
Radiation Shield	13,900		Prop & tanks	4350
Power conversion system	6,870		Array trailer	400
			ERPS system	6400
Structure	1,915		Extra fuel cell	500
Miscellaneous	1,325		Misc. (5%)	800
Reactant for LSV (incl. storage tanks)	3,900(1)			
TOTAL	29,010(1)			18,350
Available payload to lunar surface	23,300			23,300
Design margin	-5,710			4,950

(1) LSV reactant supply for 3 month staytime. Second landing after 9 months must include similar amount of reactant plus tankage.

nuclear system (including shielding), and 8330 kg (18,350 lb) for the solar array/ERPS system. For the second landing (9 months later) the nuclear system will require 1770 kg (3900 lb) more payload (LSV reactant plus storage tanks). Hence, the ratio of the weight of total equipment transported for the one-year mission is 32910/18,350 = 1.79.

The principal reason for the nuclear system being so much heavier is that its net power output is far greater than needed to meet the base power requirements of Program V; i.e., 20 kwe available where only 5 or 6 kw are required. The quantity of reactant consumed by the LSV in one year is 2730 kg (6000 lb), hardly sufficient to justify the use of an ERPS system for this function only. Hence, the only remaining requirement for this nuclear power plant is to satisfy the 5-6 kw power needs of the shelter, communications, experiment, etc.

Therefore, this nuclear system would be a poor choice for Program V for the following reasons:

- It requires the transport of 79 percent more logistic weight
- Its weight exceeds the 10,600 kg (23,300 lb) specified as the maximum payload weight for a soft lunar landing. The negative margin is 2950 kg (5710 lb) or -24 percent.
- It provides no redundancy for the reactor component.
- It introduces the problem of nuclear hazards jeopardizing mission safety and increasing the complexity of system maintenance.

By contrast, the solar array/ERPS system is lighter than the specified maximum payload by 2250 kg (4950 lb), giving a margin of 21 percent. Multiple redundancy is obtained by using many independent 2.5 kw modules, the loss of any one imposing only a minor decrease in the total power output. Redundancy of the fuel cells is provided by replacement units having a lifetime of 2500 hours. A weight allowance of approximately 227 kg (500 lb) was included in the weight statement of Table 4.10 for fuel cell replacement.

A comparison between these two systems and other systems considered during this study for the Program V mission is shown on Figure 4.19. The superiority of the solar array/fuel cell/ERPS is evident.

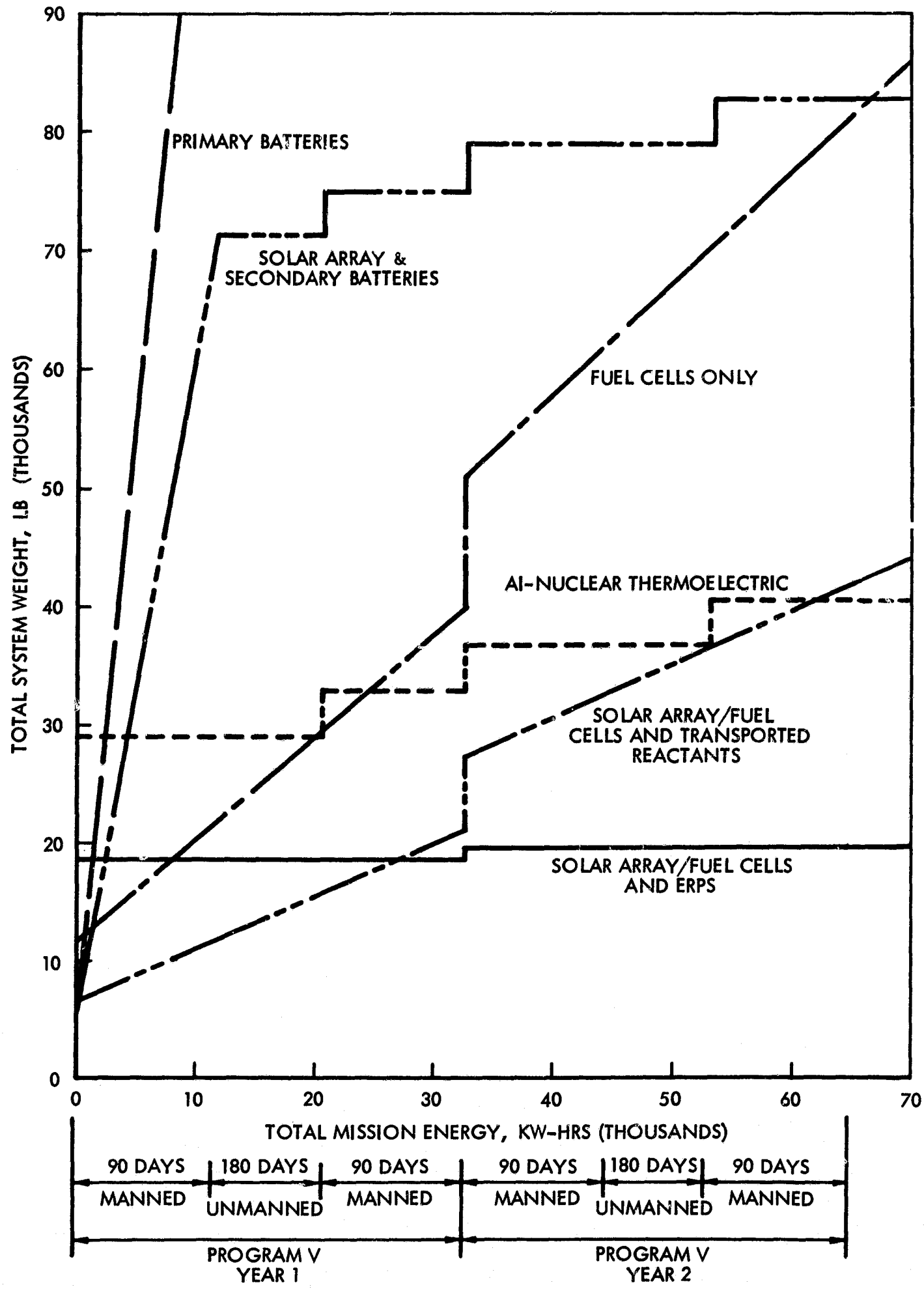

Figure 4.19 Comparison of Lunar Surface Power Systems

Only if lunar base nighttime power requirements increased sharply, thus requiring the processing of additional quantities of reactant for fuel cell operation, would the solar array/fuel cell/ERPS system begin to approach the weight of the nuclear system. However, since current mission planning envisions most surface exploration and experimentation activities taking place during the lunar day, a large increase in nighttime power requirements would not be contemplated.

4.6.6 Figures of Merit

The vast power available from solar radiation at 1 AU is equivalent to 444 Btu/hr/ft^2 or 0.13 kw/ft^2. This energy, when converted by silicon solar cells, generates electrical power which represents only 10 to 14 percent (η_c) of the solar constant. In addition, the power profile efficiency η_{pp}, of the solar array can be envisioned as the ratio of power utilized/power generated and in a sense represents a measure of the efficiency of the solar array to match the power demand (excess power being dissipated into resistance elements as unusable). The flow of high voltage output direct current must be converted to lower voltage dc and to ac power to meet the load characteristics by a power conditioning subsystem having an overall efficiency of η_{pcs}. The above factors result in a total useful power $P = 0.13\, A\, \eta_c\, \eta_{pp}\, \eta_{pcs}$ (kw), where A is the area of the solar array.

When this power is utilized over a period of time, H (hrs), the total useful energy is $E = P \cdot H$ (kw-hr). The relative merit of the electrical power system can then be measured in terms of the useful energy per unit of logistic weight. The total logistic weight W of the power system includes the weight of the solar array plus structure, cabling and power conditioning subsystem. The relative merit, m, then becomes,

$$m = \frac{P \cdot H}{W} = \frac{0.13\, A\, \eta_c\, \eta_{pp}\, \eta_{pcs} \cdot H}{W} \quad \left(\frac{\text{kw-hr}}{\text{lb}}\right)$$

The above value of merit can be compared with that of a corresponding ideal system of the same type but without power profile and power conditioning losses or structure.

$$m' = \frac{0.13\, A\, \eta_c \cdot H}{k\, W}$$

where k is the ratio of $(W_{\text{less structure}})/W)$.

An overall Figure of Merit, M, can then be postulated by the ratio of m/m'. This ratio denotes the relative merit of the actual system to that of the ideal system and is represented by the following relationship,

$$M = \frac{m}{m'} = \eta_{pp}\eta_{pcs} K \text{ (non-dimensional)}$$

Now, if for example we let $\eta_{pp} = 0.82$, $\eta_{pcs} = 0.85$, and $k = 0.30$, then $M = 0.209$. Hence, the actual system develops 21 percent of the energy/unit weight of the ideal system. This form of the Figure of Merit provides a convenient means to compare similar electrical power systems, with proper allowance for power profile efficiency, power conditioning efficiency and structural efficiency.

For comparing dissimilar power systems, the Figure of Merit is simply the ratio of energy/unit weight of the two systems, i.e.,

$$M' = \frac{m_1}{m_2} M_2 = \frac{(P \cdot H/W_1)}{(P \cdot H/W_2)} M_2 = \frac{W_2}{W_1} M_2$$

since the useful power P and duration H are essentially equal for two systems designed to accomplish the same mission.

The relative cost can be introduced into the Figure of Merit by computing the relative merit as a function of the useful energy per unit cost, where the cost is taken as the sum of transportation cost and solar array cost (R&D and production). Therefore,

$$m_c = \frac{0.13A\ \eta_c \eta_{pp} \eta_{pcs}}{\frac{\$}{lb} + \frac{\$}{lb}\ \frac{A}{W}\ W}$$

and,

$$m'_c = \frac{0.13A\ \eta_c\ (1.0)(1.0)}{\frac{\$}{lb} + \frac{\$}{A}\ \frac{A}{kW}\ kW}$$

where,

$$\frac{\$}{lb} = \$10^{4}/lb \text{ (transportation cost)}$$

and,

$$\frac{\$}{A} = \text{solar array cost in } \$/ft^2 \text{ from Table 4.9.}$$

Then the Figure of Merit M_c based on cost is

$$M_c = \frac{m_c}{m'_c} = (\lambda_{pp}\ \lambda_{pcs}\ k)\ \frac{1 + \frac{\$}{A} / \frac{kW}{A}}{1 + \frac{\$}{A} / \frac{W}{A}}$$

Figures of Merit for the various arrays considered for Program V are compared in Table 4.11.

Table 4.11 Figure of Merit Comparison for Various Solar Array Configurations

Array Type	η_{pp}	η_{pcs}	k (1)	M	M_c	Total Cost ($\$ \times 10^6$)
Flat (1 step ERPS)	.62	.80	.87	.44(4)	.46(4)	108(3)
45° Leanto	.81	.80	.84	.55(2)	.59(2)	103(2)
51° Leanto	.93	.80	.84	.62(1)	.66(1)	94(1)
Oriented(skirted)	1.0	.80	.62	.49(3)	.58(3)	155(4)

(1) In this comparison, the weight less structure $kW/A = 0.40\ lb/ft^2$ in all cases, while the total weight W/A is as shown in Table 4.9.

It should be noted that the leanto arrays rate first and second (1 and 2) of the four candidates, whether compared on the basis of M, M_c, or total cost in millions of dollars (from Table 4.9).

The Figure of Merit for the nuclear thermoelectric system (Table 4.10) when compared to the best solar array/ERPS system is,

$$M = \frac{18350}{32910}(0.62) = 0.35$$

thus providing further evidence that the solar array/ERPS system is superior for Program V.

4.7 OPERATIONS ANALYSIS

This section describes the operations relating to the logistics, stowage, transport and deployment of solar array power systems. The parametric data developed was used in assessing the total power system costs in Section 4.6.4.4 of this report.

4.7.1 Logistics and Stowage of Solar Array Power Systems

Several steps must be considered in appraising the logistics operations for the solar array power system. These are as follows:

- Procurement of vendor-supplied components, assembly, development and qualification testing.
- Transport of factory inspected and acceptance tested components to the launch site.
- Receiving inspection, preflight testing and checkout, and storage at launch site.
- Preparation and packaging of various components for loading on launch vehicle.
- Loading of lunar base components aboard LM taxi or truck.
- Countdown, launch and lunar trajectory insertion, including continuous monitoring of the payload compartment.
- Lunar landing at selected site.
- Unloading of components from landed vehicle.
- Site selection and layout of energy depot.
- Transport of components to site with surface vehicle(s).

Since the solar array itself represents the major portion of the power system (other items such as the support structure (if used), controls, power conditioners, cabling, etc., being of lower weight, bulk and cost), the principal technical problems related to logistics are believed to be the packaging of the solar array, its loading and unloading from the lunar logistics vehicle, and its transport from the landing site to the lunar base. Such characteristics are closely interrelated with deployment operations at the lunar base, which are discussed in Section 4.7.2.

Packaging designs are planned to accomodate the following deployment schemes; (1) hand-carried spools or foldout arrays, (2) vehicle-deployed foldout arrays, (3) strips unrolled from the back of surface vehicles, and (4) large integrated arrays, pre-assembled on Earth. These were analyzed from the standpoint of packaging volumes and sizes, to fit in the space available in the logistics vehicle, with provisions for unloading to the lunar surface and transporting to the selection lunar base site.

4.7.1.1 Packaging the Foldout Array

Foldout panels of silicon cells were sized to provide multiples of 500w modules for a nominal 10 w/ft^2 power density (NLW = 50 ft^2). These could be constructed as single modules or subdivided into N = 2, 3 or 4 modules to provide 500w. The length L of the modules parallel to the folds would be in the range from 4 to 10 ft, with the optimum length to be selected for convenience in handling. Figure 4.20 illustrates the module dimensions for the 500w level. Larger power output can be obtained by connecting N number of selected modules in parallel.

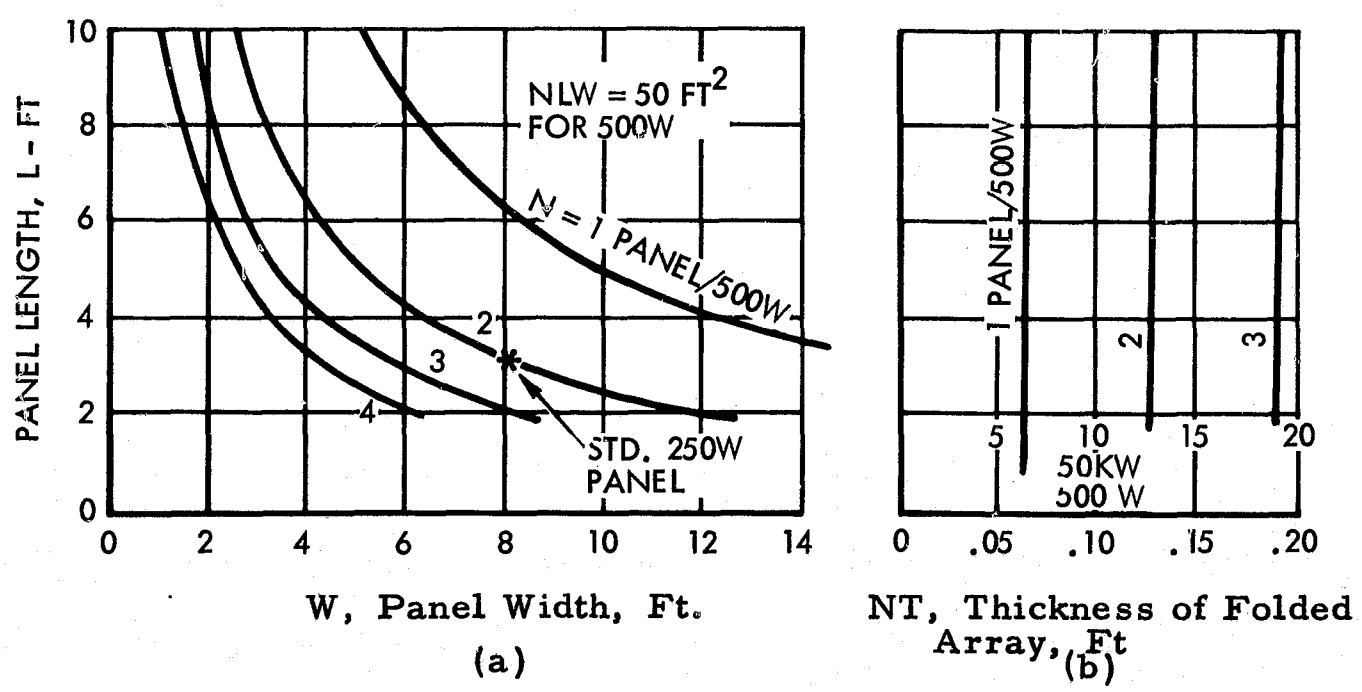

Figure 4.20 Dimensions of Foldout Panels

The module length was selected with consideration for packing efficiency in the logistic vehicle, unloading and transportation to the power site, and deployment of the foldout array in readiness for operation. Since the transportation distance from landing site to lunar base site was estimated to be 600 meters or more, and since a nominal 50 kw array would weigh

at least 5000 Earth pounds, the construction trailer or LSV would be used to tow the folded array to the base and to aid in its deployment. For convenience in unloading and transport, the use of a wheeled dolly is recommended having a tread equal to that of the surface vehicle to be used; i.e., 7.6 ft for the LSSM and 10.4 ft for the MOLAB. This would suggest a module length of about 6 ft for the smaller vehicle and about 8.0 ft for the MOLAB.

Using the latter value, a 500w module would then be 6.5 x 8 ft (see Figure 4.20(a)), which is considered too large for convenient handling by two space-suited astronauts. A 250w module would be half as large and more convenient to handle. Therefore, a 3.3 x 8 ft (1 x 2.4M) module was selected as the standard foldout element from which all the larger arrays would be assembled.

The 3.3 x 8 ft standard modules of 250w nominal power output would be assembled to form a 2.5 kw array, which is the key building block unit for making up larger power arrays. A 10 kw array could be obtained by deploying 4 identical 2.5 kw arrays. Similarly, a nominal 50 kw array would require 20 such arrays. The versatility and development savings of such a concept are obvious.

By selection of a standard 2.5 kw size array (which could also satisfy missions with smaller power requirements than Program V), it would only be necessary to build, development test, and qualify one unit for operational use. This standard size qualification unit could then be applied to missions requiring larger amounts of power, with only minor changes in packaging and deployment techniques required.

The thickness, NT, of the folded array is shown in Figure 4.20(b) for an assumed module thickness, T, of 3/4 in (0.0625 ft) for a 500w and 50 kw array size. The total array volume is then the product of length, width and thickness, LWNT (3.3 ft^3 for 500w; 333 ft^3 for 50 kw). With a panel length of 8 ft, the corresponding width of the 500 kw array is 6.5 ft and the thickness is 6.4 ft, assuming 1 module/500w. For the standard 250 w module, the dimensions are 8 ft x 3.3 ft x 12.5 ft respectively. From these dimensions, the size of the transport dolly can be readily determined.

The foregoing sizes and volumes were based on a nominal power density of $10 w/ft^2$ for a 28^oC average array temperature. At higher temperatures, the power density will be reduced and the corresponding number of modules, N_t, can be determined by reference to Figure 4.21.

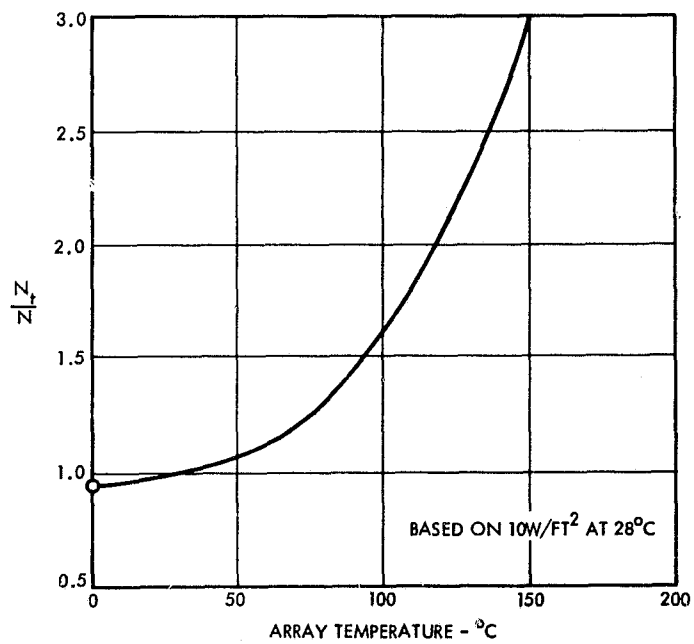

Figure 4.21 Temperature Correction for Number of Panels

For convenience in loading, unloading and transporting of the 50 kw foldout solar array, typical trailers are illustrated in Figure 4.22(a) and (b). These would be towed by the LSV or construction trailer to the site of the lunar base. Figure 7.5-3(c) shows a trailer for a flexible strip-roll array which is described in Section 4.7.1.2.

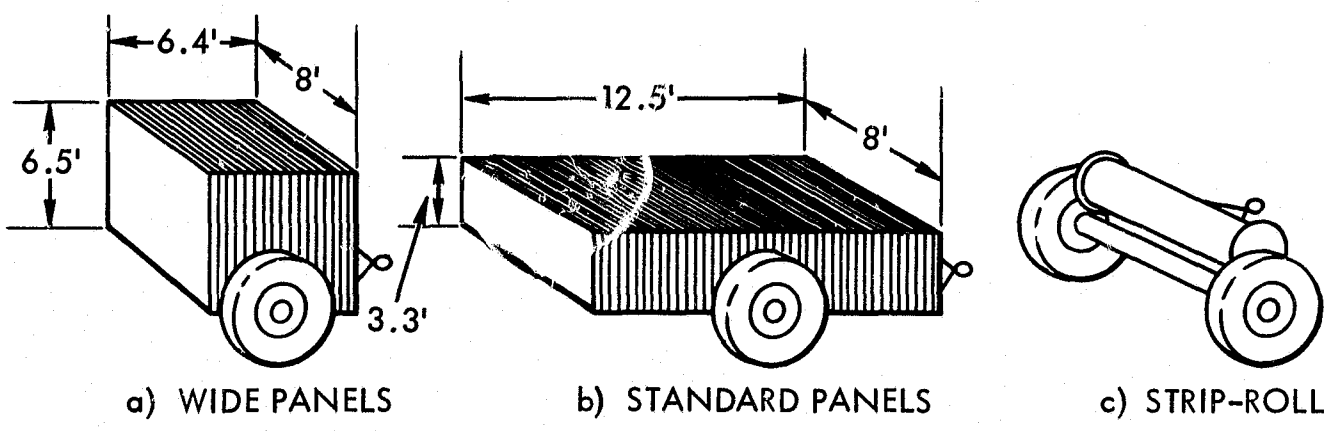

Figure 4.22 Typical Transport Trailers for 50 kw Arrays

4.7.1.2 Packaging the Strip-Roll Solar Array

Single arrays or multiple arrays using CdS thin film solar cells and of area, A, can be stored compactly by winding around a mandrel of

diameter, D, and length, L, (the latter term representing the width of the strip array). The outside diameter, D_o, of the roll thus formed will then be,

$$D_o = \sqrt{D^2 + 4At/\pi L} = D + 2Nt; \; N = (D_o - D)/2t$$

where t is the thickness occupied by each layer on the roll, and N, the number of layers required to contain the area A. Values of D_o and N are plotted in Figure 4.23 as a function of mandrel diameter D, for the case where L = 8 ft, t = 0.012 in. and a nominal array power density of 5 watts/ft^2.

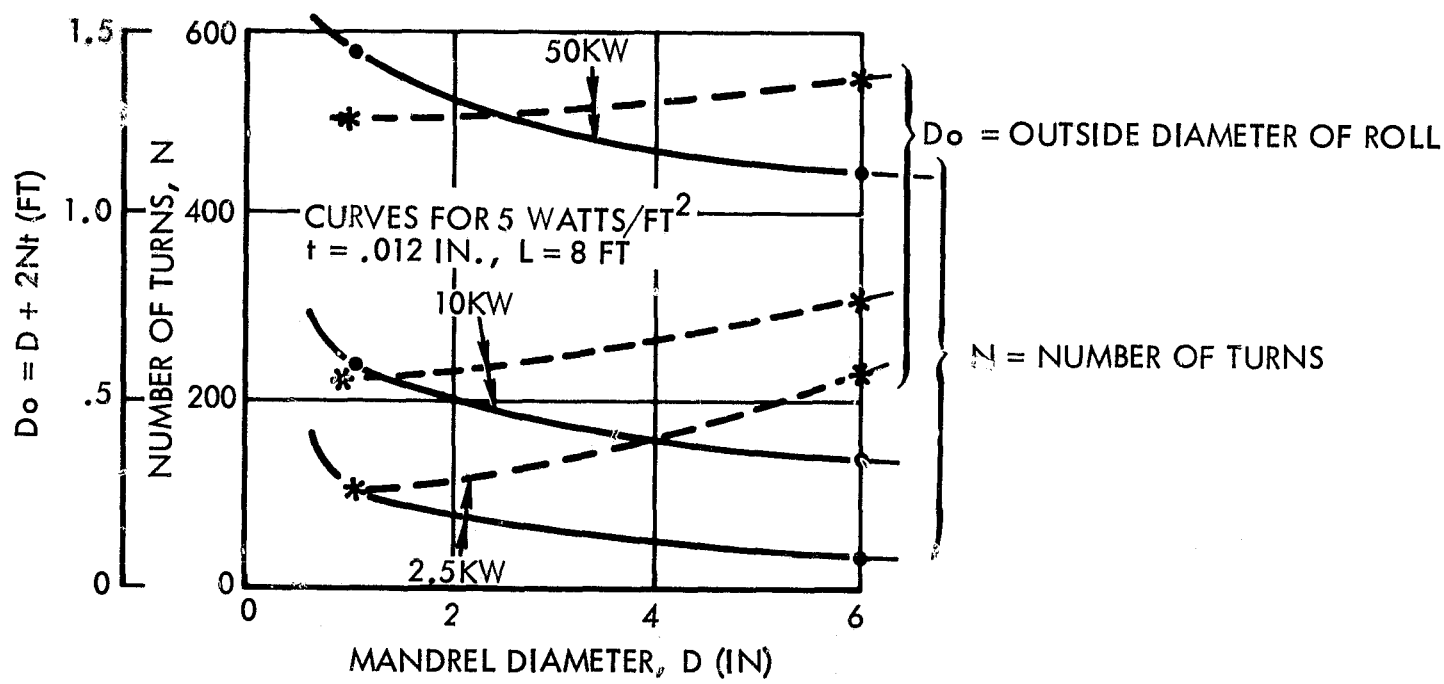

Figure 4.23 Roll Diameter and Number of Turns

It should be noted that a 2.5 kw array strip (area = 8 ft x 63 ft) can be stored on a 1 inch diameter mandrel. This results in a cylinder with an outside diameter of 3.54 inches (N = 106 turns) and a stowed volume of about 1 cu ft. A 50 kw array (area 8 x 63 ft x 20) stored on a 1 inch mandrel will be approximately 15 inches in diameter (N = 585 turns) and occupy a stowed volume of about 18 cu ft.

The selection of mandrel diameter is largely a matter of bending strength to support the array weight during Earth handling and launch operations. For example, the 2.5 kw array weighing about 125 lbs, can easily be handled on a light weight metal tube of 1 inch diameter. However, a 50 kw array, weighing about 2500 lb would require a somewhat heavier tube of larger diameter to meet the bending strength requirements.

The number of modules to be wound on a single mandrel would depend upon the handling facilities for unloading and deployment. For manual handling by two men on the lunar surface (Figure 4.32), the Earth weight of the roller should not exceed about 500 lbs. However, if the roller can be wheel-mounted for unloading and deployment, a weight of 2500 lb or more is permissible (Figure 4.22c).

The strip-rolls can be stored in the launch vehicle with their axes either parallel or normal to the vehicle centerline. Lightweight rolls are probably most conveniently stored fore-and-aft, while the heavy, wheel-mounted rolls should be stored laterally for ease of unloading.

The foregoing sizes and volumes were based on a nominal power density of 5 w/ft^2 at 0°C. At other array temperatures the power density will vary and the corresponding number of turns, N_t, and outside diameter, D_{ot}, may be determined by reference to Figure 4.24.

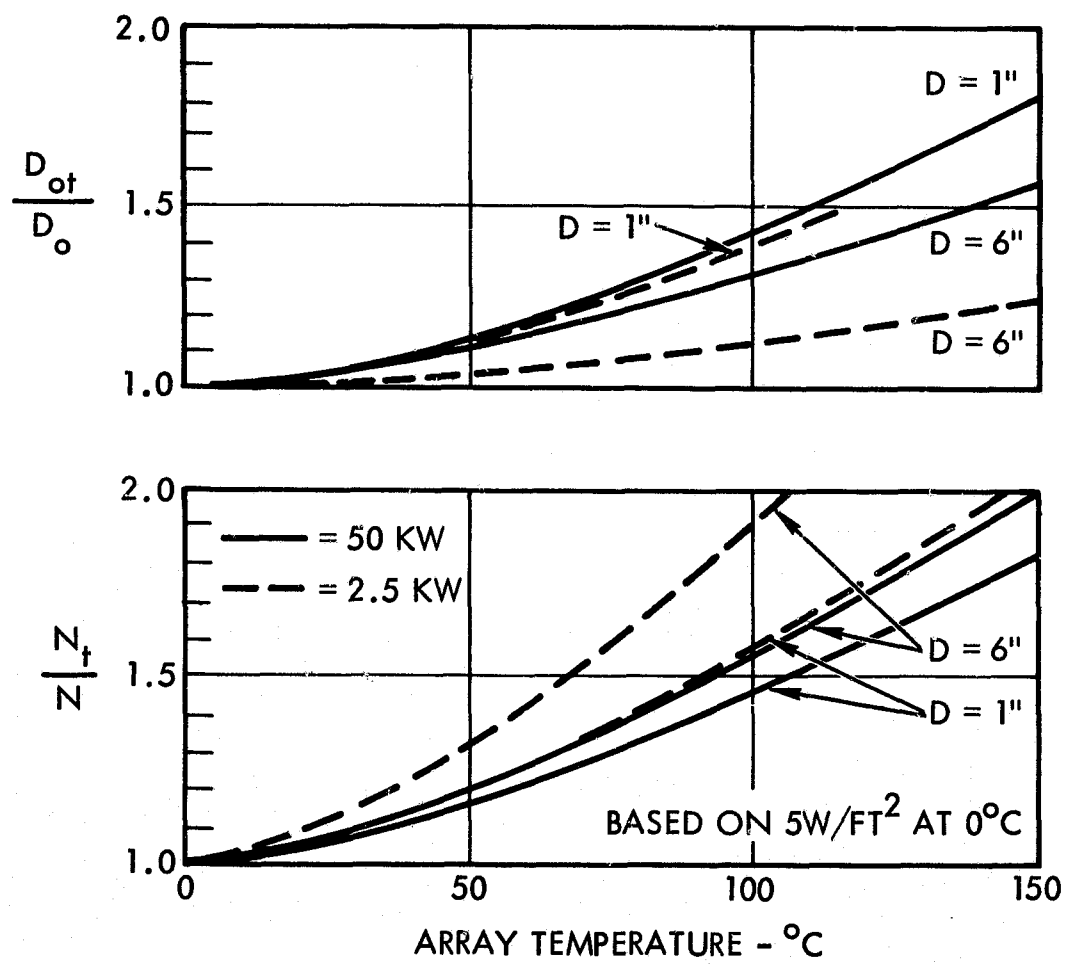

Figure 4.24 Temperature Correction for Number of Turns and Diameter

4.7.1.3 Stowage of Foldout Solar Array in Launch Vehicle

The space allocated to the solar power system in the forward end of the Saturn V adaptor cone is shown in Figure 4.25. The aft end of the cone is occupied by the construction trailer. This combined cargo is mounted on the LM descent vehicle, which lands on the lunar surface near the site selected for the ERPS/Electric Power System installation.

One mode of stowage of the power system is indicated in Figure 4.25. The solar array foldout modules are mounted on a trailer, ready for unloading and transport to the lunar base site. Adequate clearances are provided for the corners of the rectangular solar array packages from the skin line of the adaptor cone, as illustrated in the upper plan view of Figure 4.25.

Silicon Cell Volumes and Areas. The volume and solar panel area which can be stowed above Station A are indicated in Figure 4.26 for a cone-cylinder or a straight-cylinder adaptor section. It should be noted that 9500 ft^2 of 3/4 in thick solar array modules can be stowed within the conical section (7 ft above Station A), thus providing for a 95 kw array at a nominal power density of 10 w/ft^2. By adding a 3 ft cylindrical section to the top of the cone, the stowable solar array area can be increased to 13,000 ft^2. This provides ample stowage volume for all the candidate solar array configurations discussed for Program V in Section 4.6.4.1.

If a straight cylindrical shroud of 6.6m diameter is used instead of the conical section, the above stowage volumes are more than doubled. Thus it would be possible to stow a 300 kw solar array in a 9 ft high cylinder (above Station A) at a nominal power density 10 w/ft^2.

Cadmium Sulfide Thin Film Stowage Volumes. The space required to stow the Cadmium Sulfide thin film array is markedly less than for the silicon cell array. As determined in Section 4.7.1.2, a 50 kw thin film array could be wound around a mandrel to give a total volume of less than 20 ft^3, compared to 500-600 ft^3 for the foldout type array. The trailer for the thin film array could be stowed in the upper end of the adaptor cone, or it could be stowed directly above the LM descent vehicle (figure 4.27). This would permit the upper cone to be used for less dense cargo and keep the center of gravity of the total cargo as low as possible.

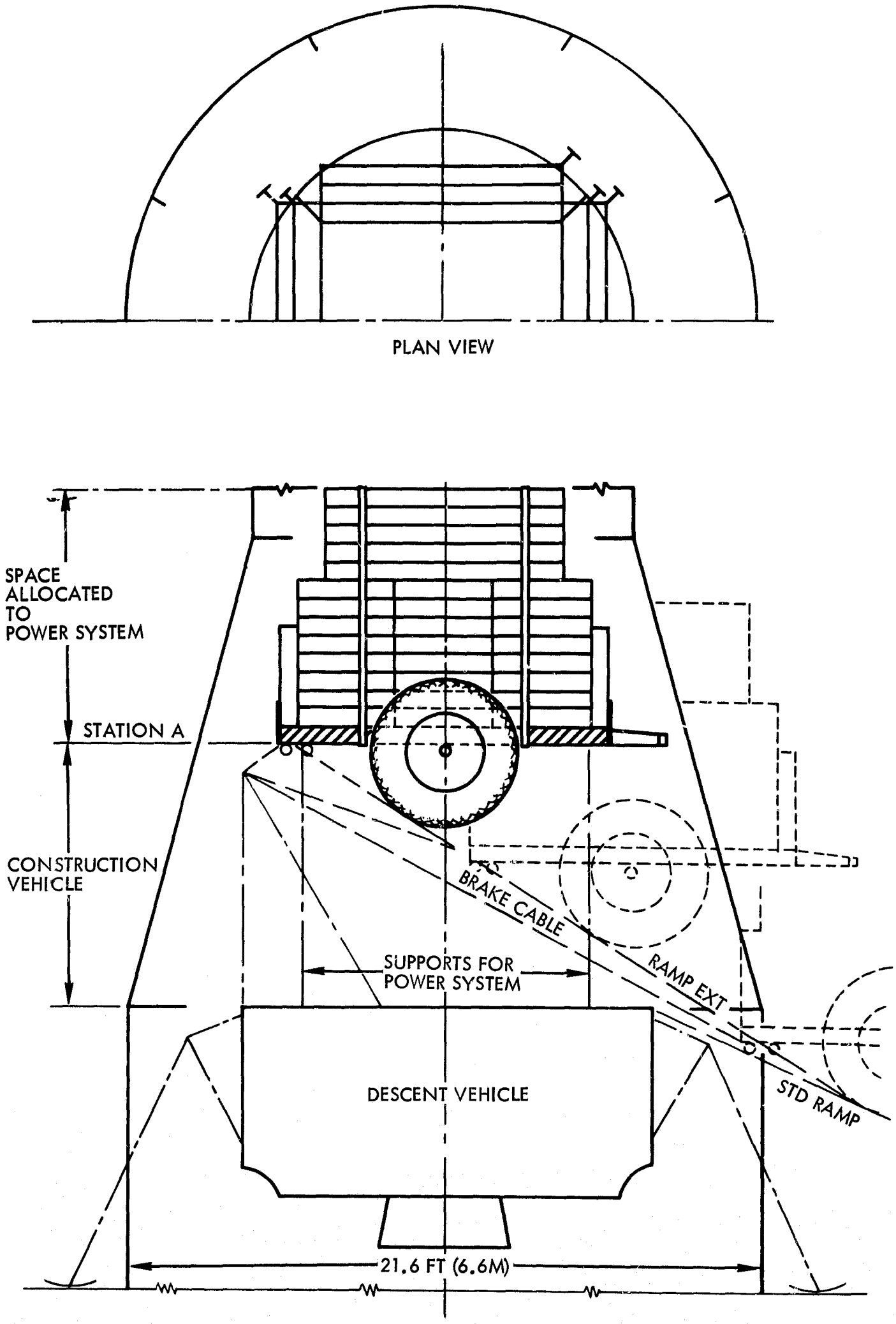

Figure 4.25 Stowage and Unloading of Foldout Solar Array

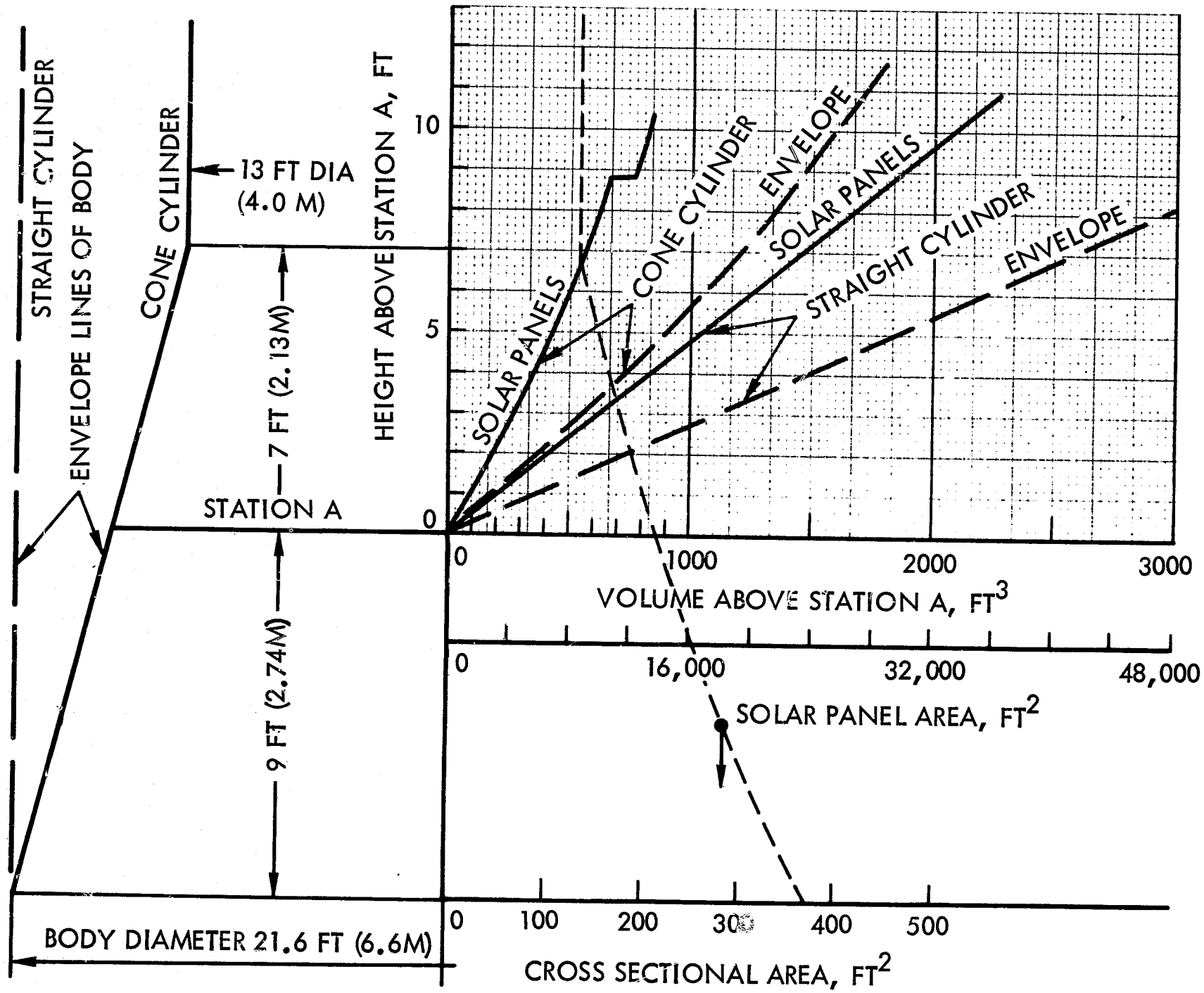

Figure 4.26 Stowage Volume Available

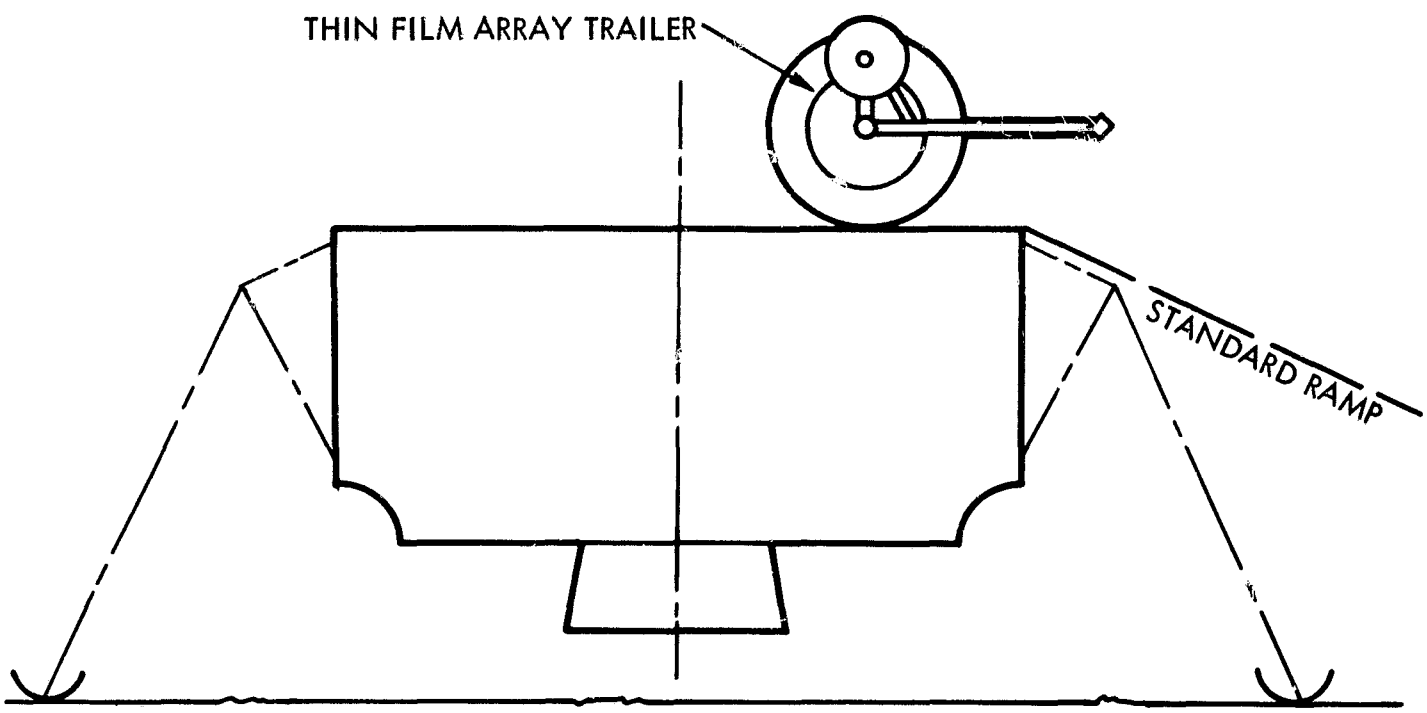

Figure 4.27 Stowage and Unloading of Flexible Solar Array

Stowage of Other Equipment. The foldable structure for supporting the solar array was estimated to have a volume of less than 20 percent of the solar array modules. Power conditioning equipment and cabling would have a volume of less than 5 percent of the solar array. The total volume of such equipment in the stowed condition was estimated to be less than 35 percent of the solar array volume. Since the solar array occupies only about 50 percent of the space available within the envelope (see Figure 4.26), there is ample room for stowing other equipment in the peripheral regions.

4.7.1.4 Unloading the Solar Array Trailer

Foldout Module Trailer. It was assumed that the payload (construction trailer, etc.) stowed directly above the LM descent vehicle (Figure 4.25) would be unloaded first after the lunar landing, thus permitting the solar array trailer to utilize the ramp normally employed for unloading other portions of the payload. The ramp extension would have been installed and the braking cable activated. The support members for the power system could then be removed, leaving the trailer free to roll down the ramp to the lunar surface but under constraint of the braking cable.

Guide rollers would be installed on the aft end of the trailer bed to prevent tipping of the trailer as it moved down the ramp.

Flexible Array Trailer. Due to the small size and high density of the trailer for the flexible array (Figure 4.27), it may be desirable to place it directly above the LM descent vehicle, with other less dense cargo placed in the upper compartment of the adaptor cone. In this case, the standard ramp could be used for unloading, without the need for a ramp extension (as described above for the foldout array). This plan has the threefold advantage of simplicity of the unloading operations, low c.g. of the total payload, and minimum weight.

4.7.1.5 Selection and Layout of the Lunar Base Site

The lunar base site would be selected for reasonable flatness and smoothness from surface irregularities, and within a few hundred meters from the landing site. It would be deployed near the selected ERPS location. The lunar surface area required for flat arrays of various power levels is shown in Figure 4.28. These configurations could be readily adapted to the surface characteristics, to minimize the effort required to attain the smoothness/area requirements.

Leanto assemblies made up of 2.5 kw arrays must be oriented in a north and south direction to attain the desired power profile, and the individual arrays must be spaced sufficiently far apart to avoid excessive shadowing of each other at lunar sunrise and sunset. The ridgepole of these unit would be approximately 6 ft from the lunar surface. Hence, an adjacent unit 100 ft away will not be completely free of shadow until approximately 6.7 hours after sunrise. Allowing for both sunrise and sunset conditions, the total loss in hours of full radiation will then be 3.8 percent of the lunar day. This condition poses a tradeoff in the layout of such arrays; i.e., additional array area to make up for the loss in hours vs. spacing of the arrays to give a compact layout with moderate length of transmission lines, as shown in Figure 4.29. At the distance of 220 ft, no appreciable shadowing will occur.

4.7.1.6 Packaging the Large Integrated Arrays

The foregoing discussions have been concerned primarily with small arrays (2.5 kw) which are to be deployed separately on the lunar

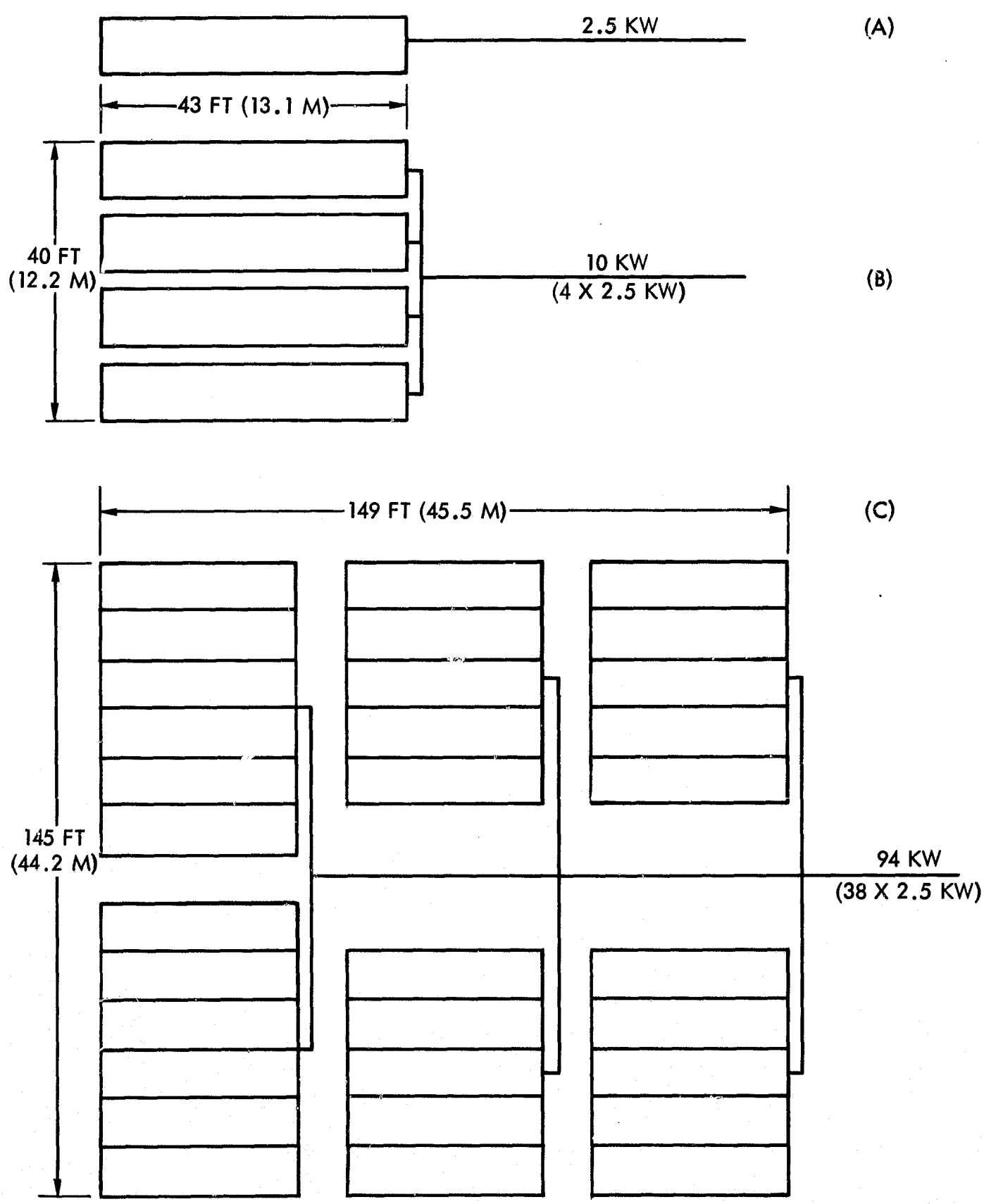

Figure 4.28 Typical Assemblies of 2.5 kw Flexible Silicon Cell Flat Arrays to Provide Various Power Levels

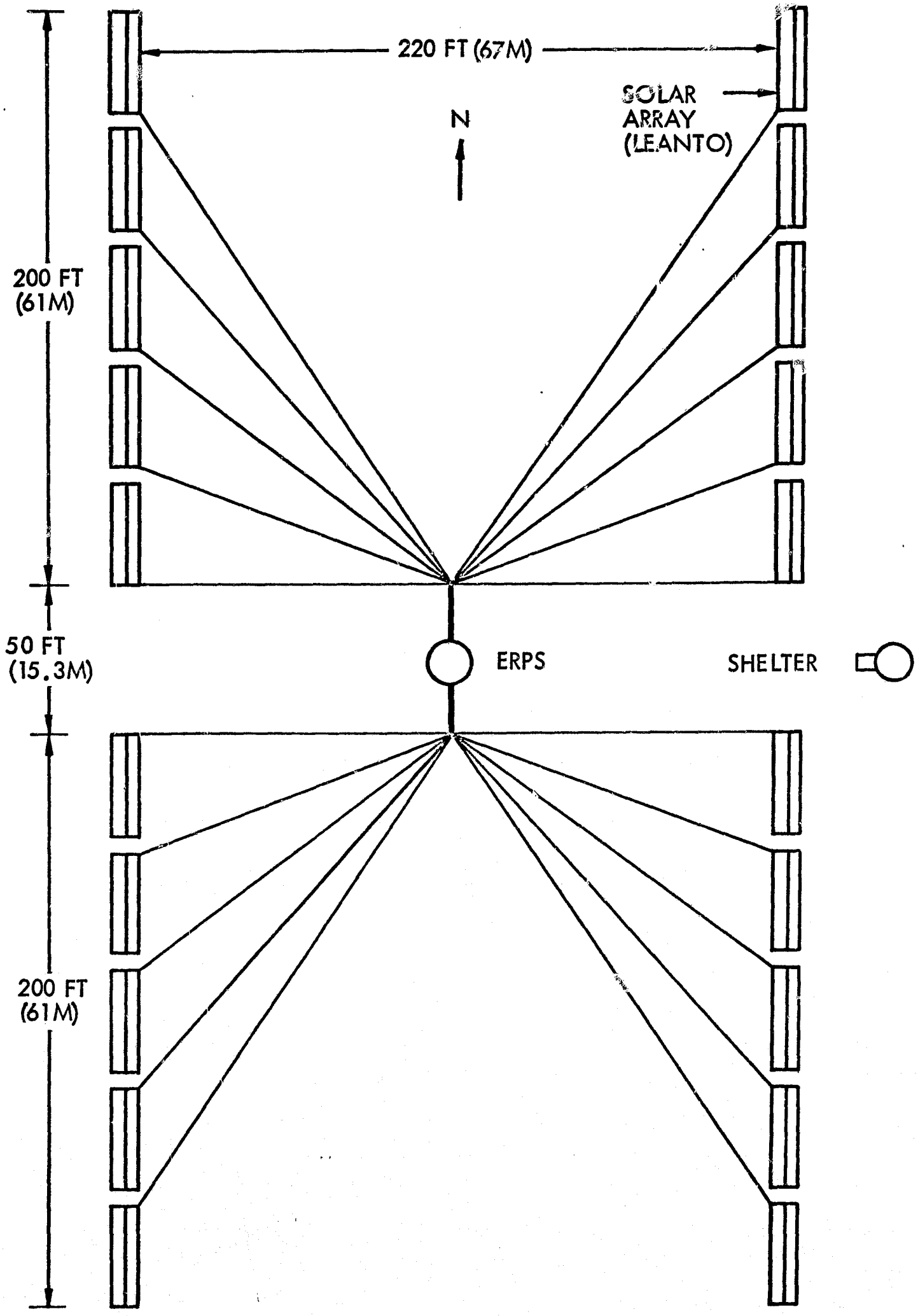

Figure 4.29 Typical Layout of Lunar Base with Leanto Solar Array

surface and then interconnected to provide larger power systems of the order of 50 kw. This concept is compatible with the use of rigid panels of silicon cells, and offers the most convenient method of packaging, handling and deployment of such units.

The thin film solar array lends itself to being completely assembled on Earth, and folded into a compact package which could then be deployed as a complete system upon arrival at the lunar base site. This mode of packaging has the advantage of eliminating a large number of detail assembly operations on the lunar surface which reduces the manual effort and deployment time required, and potentially improves mission reliability.

Configurations which can be assembled on Earth include the large rectangular array, to be deployed either flat on the lunar surface or as a leanto, and the hemispherical inflatable array. Upon completion of the Earth assembly and checkout of such arrays, they would be multifolded into a long narrow strip about 8 ft wide and a few inches thick. This strip would then be folded into a package having a length 10 ft or 12 ft and would be suitable for mounting on a wheeled trailer which would be used for unloading from the logistic vehicle, and for transport to the lunar base site.

Figure 4.30 illustrates the typical steps required in packaging these large integrated arrays. Further details of the folding procedure are given in Figure 4.34, in which the deployment steps, taken in reverse order, illustrate the packaging plan for the rectangular array.

Packaging Volume for a 94 kw Thin Film Array. The area of a thin film flat array capable of providing 94 kw at lunar noon is approximately 19000 ft^2, giving an array about 115 ft square. The first fold as described in Figure 4.30 results in a strip 3 in thick x 8 ft wide x 138 ft long. The second fold gives a spiral roll of diameter $D_o = \sqrt{D^2 + 4tL/\pi} = 7.3$ ft, where D_o = outside diameter of roll, D = inside diamter = 3 ft, t = thickness of strip = 0.25 ft, and L = length of strip = 138 ft. This alternate mode, laid flat on a 10 ft long trailer would build up to a height of about 7.6 ft above the trailer bed. Therefore, the compartment shown in Figure 4.25 provides ample space to stow the folded array when using either the spiral roll or the flat folded mode.

a) FIRST FOLD

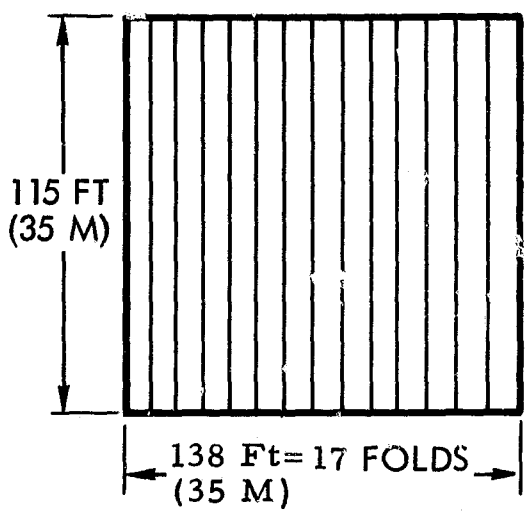

PACKAGE 3 IN. X 8 FT WIDE X 138 FT LONG

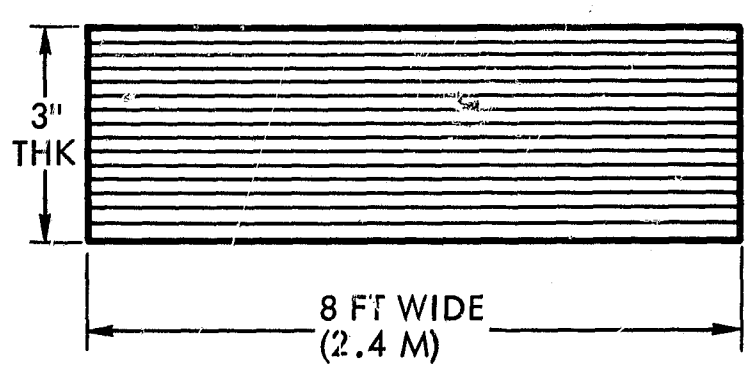

b) SECOND FOLD

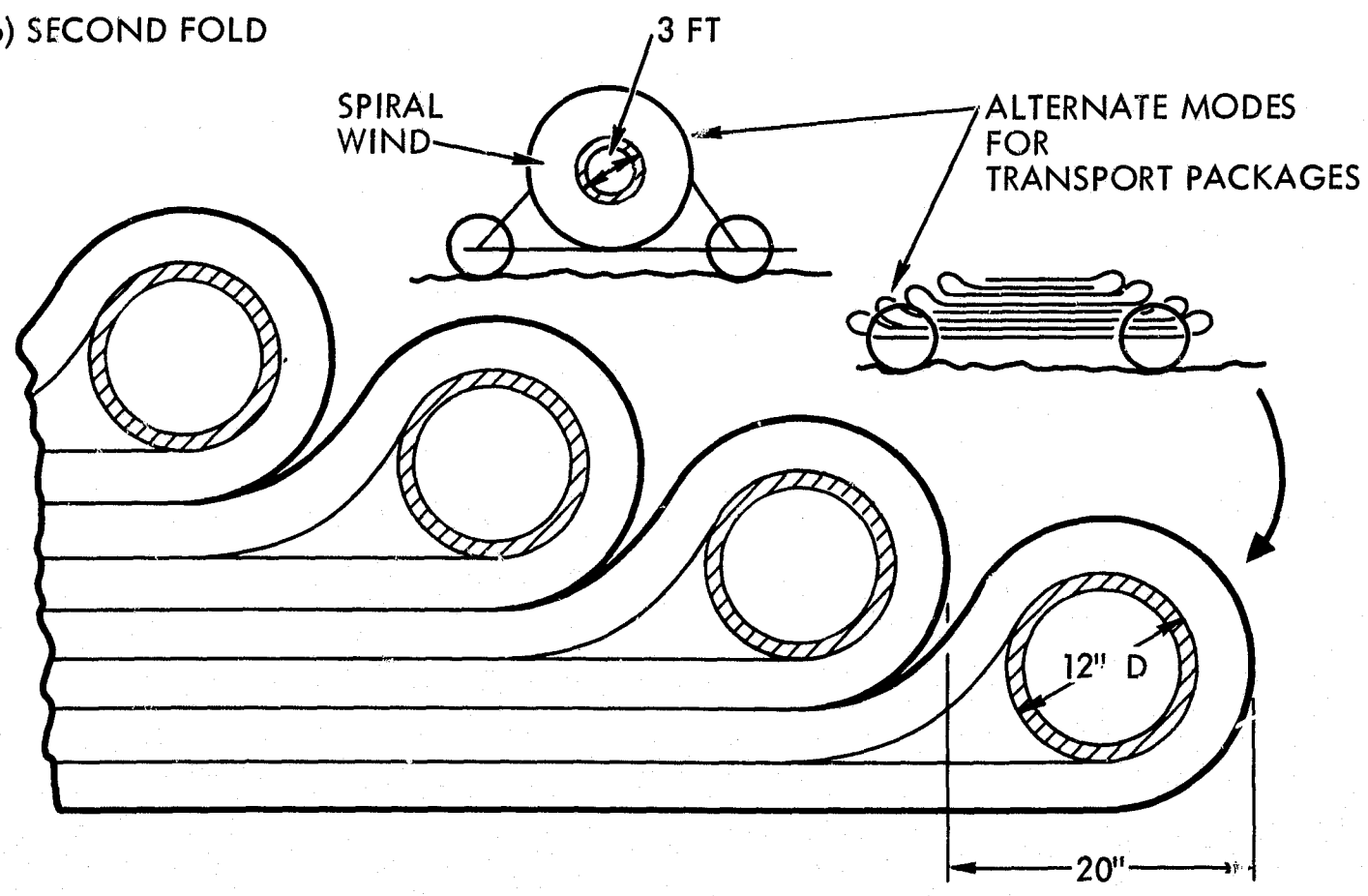

Figure 4.30 Roll-up Solar Array Packaging Detail

4.7.2 Deployment of Solar Array Power Systems

After delivery of the solar array to the selected lunar site, the following operations would be implemented for its deployment and integration with the user equipment.

(1) Preparation (smoothing) of the lunar surface for solar array, if necessary

(2) Deployment of packaged solar array to lunar surface

(3) Erection of solar array to operative configuration

(4) Installation of other components, equipment and controls

(5) Connection of power leads to ERPS and LM Shelter control center

(6) Activation of controls, sensors, auxiliaries, etc.

(7) Functional check and adjustment of entire system

(8) Preliminary shakedown operation of entire system

(9) Final adjustments and modifications, if necessary

(10) Initiate regular operation of overall power system.

The time and energy required for deployment of the flat, leanto and oriented arrays can be determined by an analysis of the routine steps required to transport and assemble the packaged array (as received at the landing site) into an operational power system at the selected lunar site. The above three configurations can be implemented with solar arrays consisting of flexible panels, rigid panels, or integrated (i.e., arrays completely assembled on Earth). The array can be placed directly on the lunar surface or mounted on a separate built-up structure which would be assembled on arrival at the site. Combinations of the above variables are summarized in a matrix of deployment modes shown in Table 4.12. Twelve of these modes are considered worthy of further analysis to determine their deployment procedures and times, and to identify any special equipment required in the process (see Table 4.13).

The flexible roll-strip or "wax paper" scheme is the simplest mode of deployment with the least manual effort, since it only requires the fastening of an end of the solar array to the ground and then driving

Table 4.12 Matrix of Deployment Modes

Solar Array	Flat		Leanto		Oriented
	On Surface	On Structure	On Surface	On Structure	On Structure
Flexible	√	√	x	√	√
Rigid Panel	√	√	√	√	√
Integrated	√	x	x	√	√

Table 4.13 Deployment Modes Analyzed for Time and Manual Energy Requirements

1 - Flat/Flexible/Surface	7 - Leanto/Flexible/Structure
2 - Flat/Rigid/Surface	8 - Leanto/Rigid/Structure
3 - Flat/Integrated/Surface	9 - Leanto/Integrated/Structure
4 - Leanto/Rigid/Surface	10 - Oriented/Flexible/Structure
5 - Flat/Flexible/Structure	11 - Oriented/Rigid/Structure
6 - Flat/Rigid/Structure	12 - Oriented/Integrated/Structure
NOTE: Modes 1, 2, 3, 4 and 9 require preparation of the lunar surface, while the others do not.	

forward, unrolling the array from the back of a surface vehicle. The fully oriented array is the most difficult and time consuming to deploy, because of the extra structure required and to checkout the orientation mechanisms to achieve the specified reliability. Other intermediate modes, such as the rigid module and the integrated array, are attractive for various reasons, and the relative effort required for their deployment was also determined.

As indicated in Section 4.7.1, the method of deployment is closely related to the logistic plan for packaging, unloading and transport of the solar array to the lunar base site. The transport trailer, towed by a surface vehicle, is considered a necessity, to relieve the astronauts of having to hand-carry the arrays any great distance. By using the trailer to deliver elements of the array as near as possible to their deployment location, the manual effort to be exerted by the astronauts would be minimized, as well as the transit time in hand-carrying the modules to their final location.

Upon arrival at the lunar base, the first step would be to prepare the lunar surface (for those modes requiring a relatively smooth surface). Next, the trailer would be maneuvered to the desired location and precede the men in their deployment operations. This could include spreading out the array, which would be the case for the flat array mounted on the lunar surface. For other configurations, such as the leanto and the fully oriented array, additional assembly and erection procedures are involved, and the sequence of operations would be different.

Manual Energy Expended in Various Routine Motions. The manual energy expended by a group of astronauts in deploying the solar array was estimated by reference to the energy required for repetitive motions, as listed in Table 4.14, which was derived from Table 4.15 (Reference 4.10).

Table 4.14 Manual Energy Expenditure for Repetitive Motions (Derived from Table 4.15 (Reference 4.10)

Walking slowly (on Earth, in shirt sleeves)	= 600 Btu/hr
o Walking 1 mph at 2 ft/step	= 2640 steps/hr at 1.47 ft/sec
o Energy per step = 600/2640	= 0.228 Btu/step
o Energy spent on gravity = $W\Delta h$	= 0.054 Btu/step
o Remainder spent on inertia & muscles	= 0.174 Btu/step
o Plus lunar gravity energy	= 0.009 Btu/step
o In shirt sleeves on moon	= 0.183 Btu/step
o In space suit on moon (x 4)	= 0.73 Btu/step (1 step = 2 ft)
Walking slowly (on moon, in space suit	= 1.0 Btu/step
Carrying object (W/W_{man} = 1/3) = walking x 2.5	= 2.5 Btu/step
Pulling on line (F/W_{man} = 1/3) = walking x 2.5	= 2.5 Btu/step
Pulling on line (Distance = 20 steps)	= 50 Btu/pull
Waist bend (assume equivalent to 10 steps)	= 10 Btu/stoop

Preparation of Lunar Surface. A location for the solar array will have been selected having a reasonably level surface area of (typically) 15,000 ft^2, to provide the space for assembly of the array configuration as shown in Figures 4.28(c) or 4.29. It was assumed that the area will

FOLDOUT FRAME

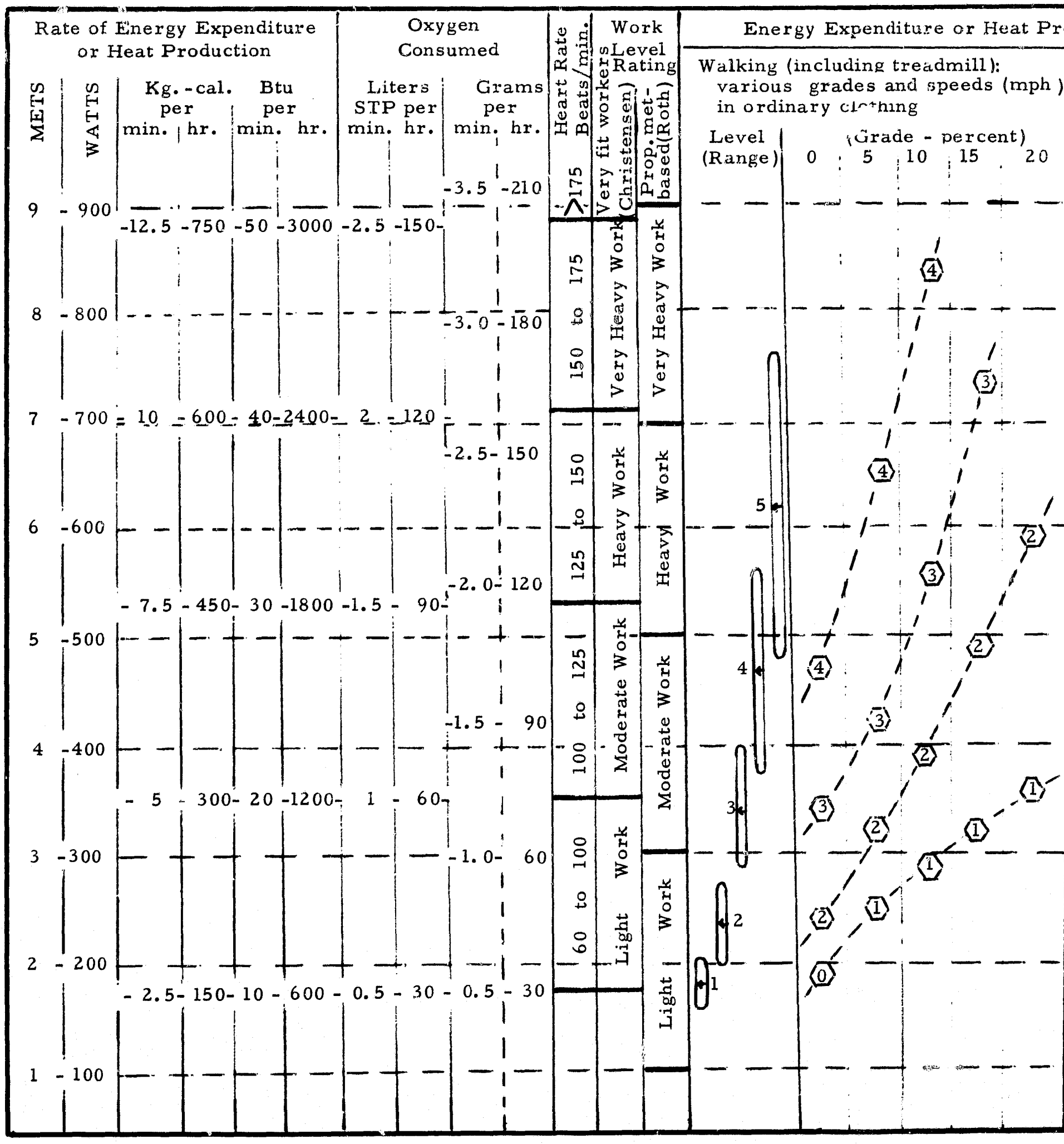

FOLDOUT FRAME

Expenditure or Heat Production for Various Working, Recreational, or Other Physical Activities

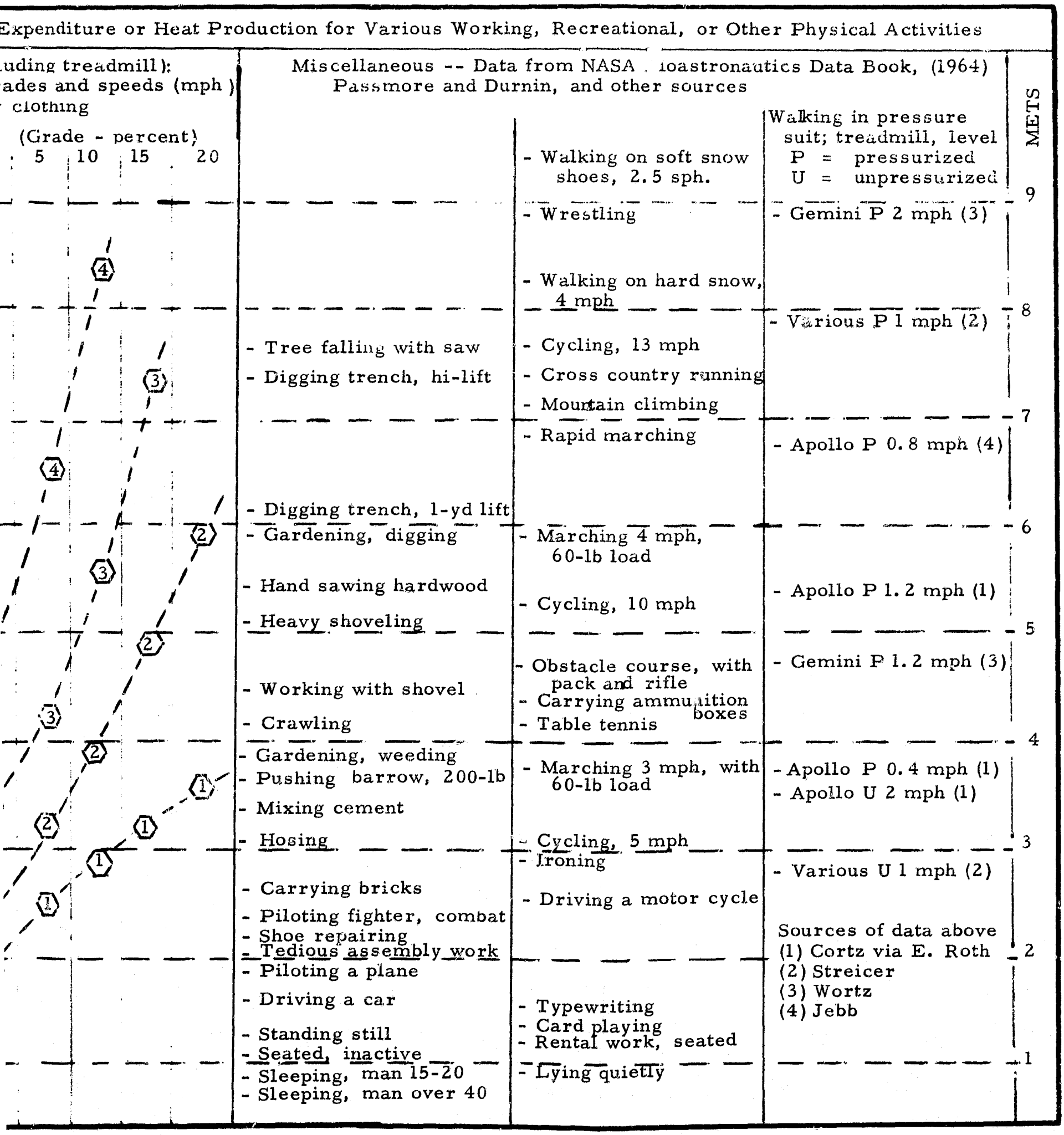

Table 4.15 Manual Energy Expenditure Rates (Reference 4.10)

be strewn with rubble (distributed randomly with a 1 ft average spacing) ranging in size from 1 inch to 20 inches, as shown in Figure 4.31a. The volume to be moved is plotted in Figure 4.31b as a function of size, and this curve was summed up for each one inch increment of rubble size to give a total volume of about 700 ft^3. This material would be removed from the surface and deposited in craters and holes as necessary (for modes requiring a smooth surface).

The lunar surface vehicle with a 10 ft wide rubble collector would make approximately 15 passes over the site, picking up pieces smaller than 10 in. enroute. At 1 mph average, this would take about 30 minutes (including turns at the ends) and also result in 1200 Btu expended by the surface vehicle operator. Two astronauts would assist him by riding on the collector and loading pieces larger than 10 in., of which there is estimated to be about 250 pieces according to Figure 4.31a. It is assumed that each of these will consume 0.3 minutes on the average, or a total time of 75 minutes with a total of 3500 Btu expended by the astronauts. Rubble can be deposited in craters and holes that require filling, and the time to do this is estimated as 60 minutes, assuming 60 stops at 1 minute each (for a hole spacing of approximately 20 ft). The energy to unload the rubble would be about 3000 Btu. The total time to accomplish the above operations would then be 165 minutes or about 2.75 hours. The total energy expended by three astronauts would be about 8000 Btu, or 1000 Btu/hr/man. The above procedure should be adequate to level the surface to a degree of smoothness sufficient for the deployment of the flat solar arrays mounted directly on the surface. It should be noted that the other modes of deployment would not require as complete a smoothing operation (see Table 4.13).

Number of Small Arrays to be Deployed. The total power to be provided by the solar array was determined in Section 4.6.4. Rigid modules of 3.3 ft x 8 ft can be assembled into foldout panels (and flexible modules into rollout strips) with each subassembly providing a few kilowatts to form a small array. Table 4.16 shows the panel area in each small array for easy handling, and the number of these subarrays needed to meet the total power requirements for Program V.

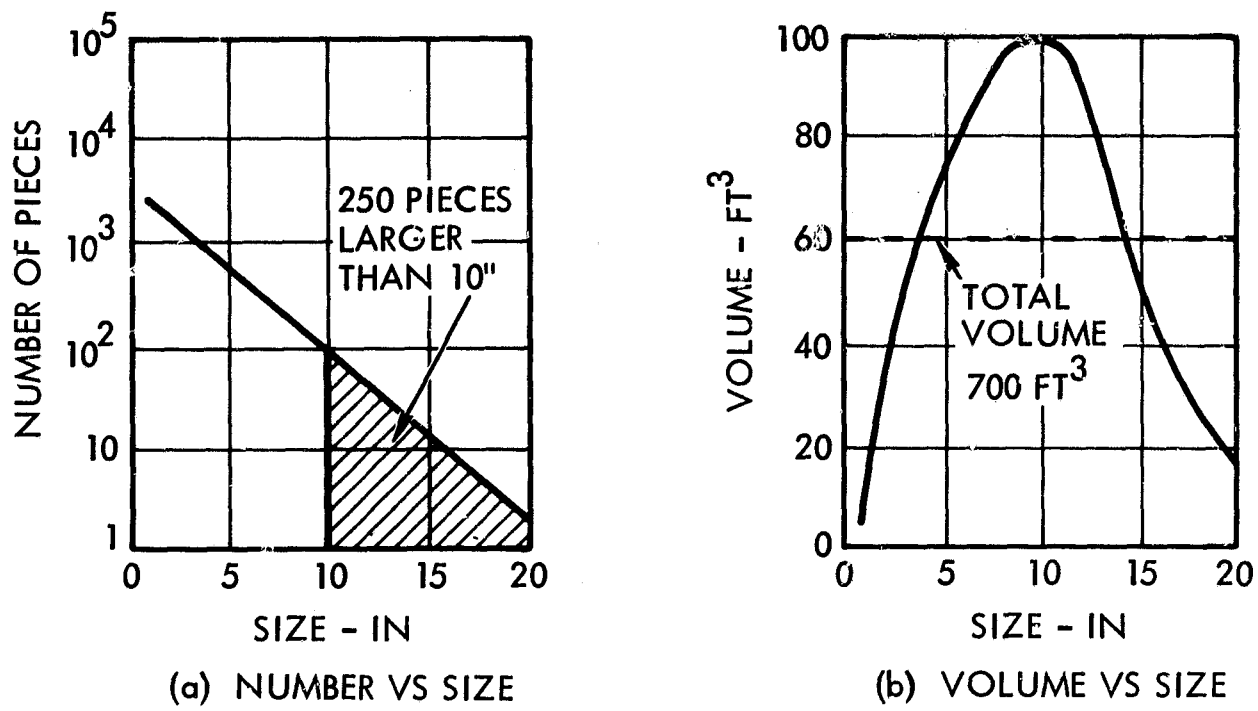

(a) NUMBER VS SIZE (b) VOLUME VS SIZE

Figure 4.31 Surface Rubble to be Removed

Table 4.16 Sub-Array Requirements

Configuration	Power (kw)		No. of Sub-Arrays	Panel Size No. (ftxft)	Panel Weight (lb)	Total Array Area(ft^2)
	Total	Panel				
Flat	94	2.5	38	1 (8x43)	140-160	13200
51° Leanto	51	2.55	20	2 (8x36)	240-274	11500
Oriented-Skirted)	45	2.65	17	2 (8x23)	240	6300

4.7.2.1 Flat Array of Flexible Panels Deployed on Lunar Surface

A 2.5 kw array of flexible solar cells would be approximately 8 ft x 43 ft in size (at a power density of 7.15 w/ft^2) and would weigh approximately 140 Earth pounds. By fastening one end of the array to the lunar surface and moving forward (on foot or in a trailer), the array could be quickly unrolled from its spirally wound spool (Figure 4.32).

The "wax paper" deployment scheme promises advantages in deployment ease and packaging weight which would compensate to a degree for the lower power/weight ratio of the thin film cells. The strips would be unrolled from a mandrel mounted on a moving vehicle or (for small arrays) carried by two men. The free end of the strip would be fastened to the

ground. This would be done in order to pull the strips from the roll or to aid in pulling the strips loose when used in conjunction with a powered roller as shown in Figure 4.32.

It would be desirable to prevent the array from scraping on the ground during deployment, to avoid possible tearing on surface irregularities. The roller feed should therefore be designed to lower the strip gently to the lunar surface, and the equipment should be guided along a straight path until the strip is fully deployed.

After laying down the required number of strips, their ends would then be inter-connected in a manner appropriate to the efficient transmission of power to the user equipment.

A typical deployment procedure would be:

(1) Two men attach trailer to rear of surface vehicle

(2) Surface vehicle is driven to power site

(3) End of first strip staked to surface

(4) Vehicle is driven forward to end of strip

(5) Vehicle stops, astronauts fasten end of strip to surface

(6) Next strip is deployed in similar manner

(7) Repeat above operations until all strips are laid out

(8) Interconnect ends of strips to main bus cable

(9) Surface vehicle returns to base, laying main bus cable enroute

The time and energy requirements to deploy the 43 ft strips are as follows (Note: rollout time will be reduced if longer strips, >2.5 kw, are used):

(1) Surface vehicle and 3 astronauts clear the surface of rubble, as previously described. This will require approximately 3 hours with a work rate of 1000 Btu/hr/man.

(2) Two astronauts ride on trailer during periods when the solar array is being unrolled from spool. For each 2.5 kw array, they will stake down the front and back end of each strip. Each man will walk a distance of 10 feet twice (20 sec; 20 Btu) and stoop twice (20 sec; 20 Btu). This would be repeated 38 times to lay down a 94 kw array. Total surface vehicle driving time would be 30 minutes.

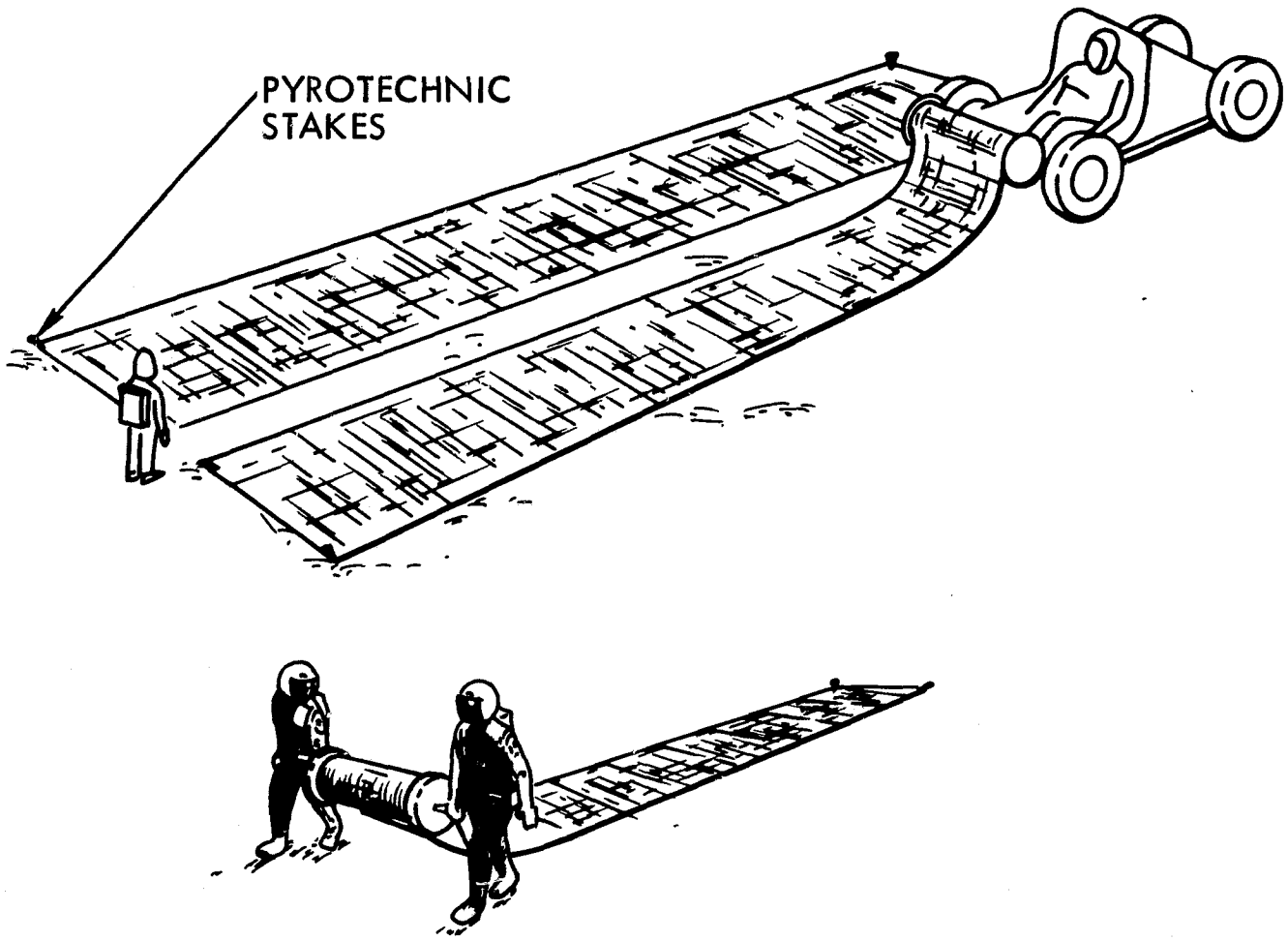

Figure 4.32 Deployment of Flexible Solar Arrays

Total time and energy for operations (1) and (2) =

	4 hr	4500 Btu/man

(3) Connect transmission line to ends of strips =

	1.3 hr	760 Btu/man
Total for 94 kw array =	5.3 hr	5260 Btu/man

Therefore, the rate of energy expended for these operations = 1000 Btu/hr/man

4.7.2.2 Flat Array of Rigid Panels Deployed on Lunar Surface

Deployment of a large solar array utilizing 2.5 kw foldout arrays is illustrated in Figure 4.33. The panels would be preconnected to form integral units of approximately 2.5 kw, and would be deployed separately on the lunar surface from a transport trailer as shown. The panels are progressively moved to the rear of the transport trailer, where their deployment is monitored and manually assisted by two astronauts as the surface vehicle moves forward. The astronauts can hand-carry the 27 moon-pound, 2.5 kw array, deploying the panels as they walk along, while the trailer moves on to the next station. After the individual arrays are deployed and assembled in the operative configuration, they are interconnected by suitable transmission lines to the power system.

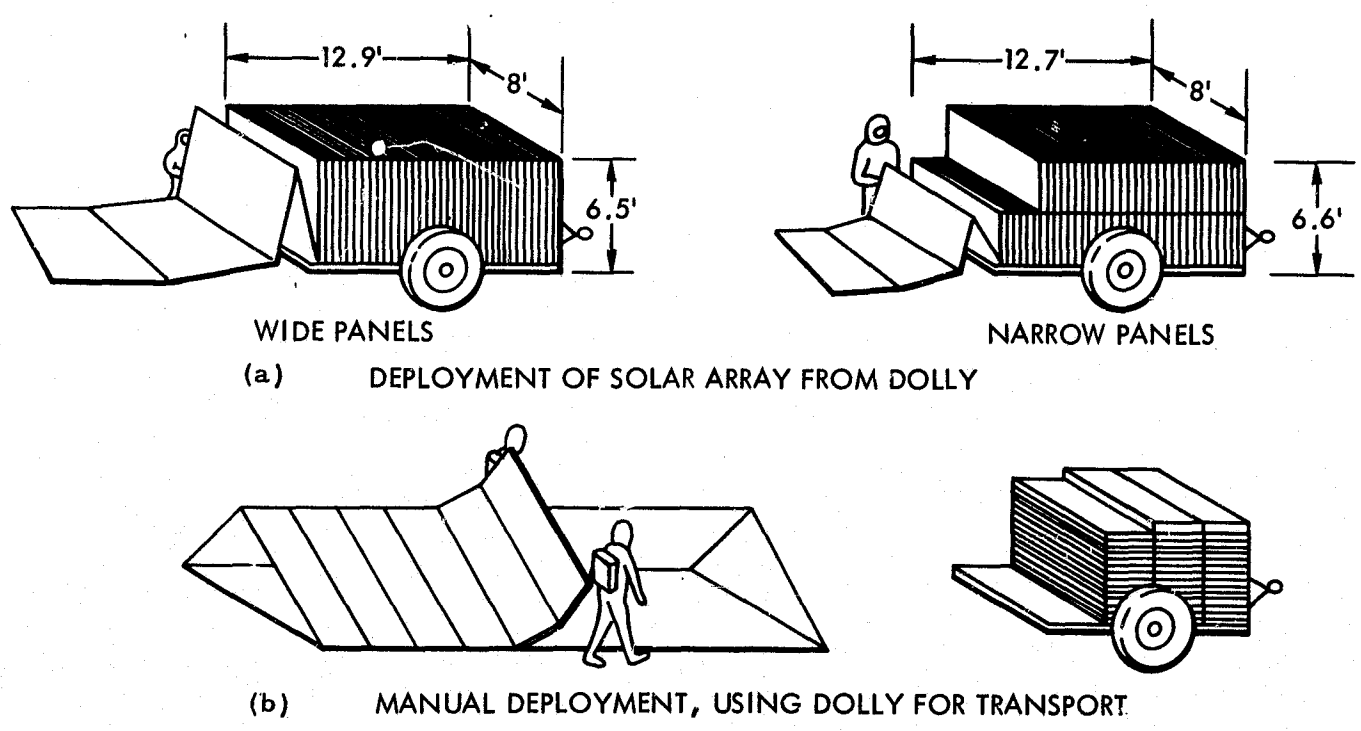

Figure 4.33 Deployment of Rigid Panel Arrays

If the 2.5 kw arrays are hand-carried, the deployment times and energies will be as follows:

(1) Surface vehicle and 3 astronauts clear the site of rubble. This will require	3.0 hrs	1000 Btu/hr/man
(2) For each 2.5 kw array, 2 men carry 14 lb each 25 steps (25 sec, 30 Btu) then walk back 25 steps to surface vehicle (25 sec, 25 Btu). Driving time 1 min. Total time & energy for each 2.5 kw array	1.8 min	55 Btu/man
(3) Connect transmission line to end of array	2 min	20 Btu/man
Total for each 2.5 kw array	3.8 min	75 Btu/man
Totals deployment of 94 kw array	5.4 hrs	1080 Btu/hr/man

4.7.2.3 Deployment of Integrated Flat Array (On Lunar Surface)

When the 94 kw array is completely assembled on Earth, and packaged as described in Figure 4.30, it constitutes a rectangular array approximately 145 x 149 ft (at 7.15 w/ft^2) weighing about 5300 lb. Proceeding according to the deployment sequence shown in Figure 4.34,

1) Surface vehicle and 3 astronauts will clear site of rubble, requiring	3 hrs	3000 Btu/man
2) Two astronauts unfold substrate. Walk 600 ft (300 Btu), stoop 4 times (40 Btu)	10 min	340 Btu/man
3) Two astronauts unfold solar array, assisted by surface vehicle. Vehicle operator expends 600 Btu. Astronauts walk and pull 600 ft (800 Btu), stoop 12 times (120 Btu)	1 hr	920 Btu/man
4) Connect transmission line to edge of array	5 min	100 Btu/man
Totals for 3-man crew	= 4.3 hrs	4360 Btu/man

Therefore, the rate of energy expended for these operations = 1010 Btu/hr/man

a) UNROLL THE PACKAGED ARRAY FROM TRAILER TO THE LUNAR SURFACE, GIVING THE FOLLOWING FOLDED STRIP CONFIGURATION.

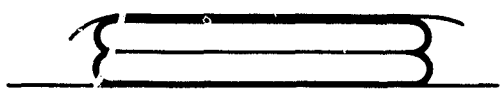

b) UNFOLD A SUBSTRATE (TO PROTECT THE ARRAY FROM INJURY DURING DEPLOYMENT.

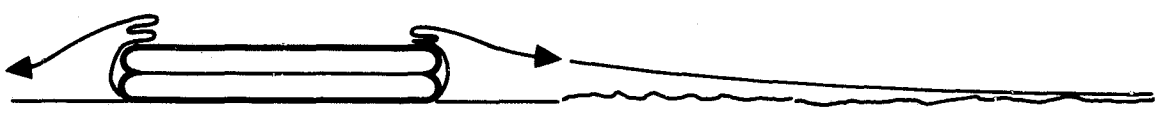

c) UNFOLD ARRAY (ONE-HALF AT A TIME)

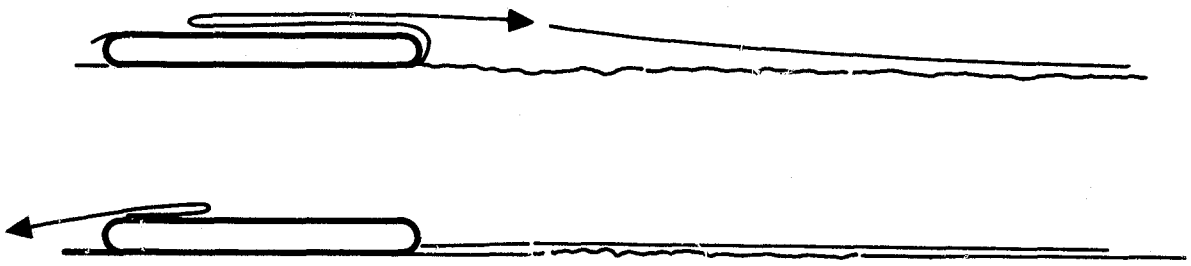

d) ERECT ARRAY (FOR LEANTO, SEE SECTION 4.7.2.8)

e) SECURE ARRAY IN FINAL POSITION BY RIGGING.

Figure 4.34 Details of Deployment of Flexible Integrated Arrays

4.7.2.4 Leanto Arrays of Rigid Panels Mounted on Surface

The 2.55 kw array of rigid panels will have an area of 575 ft^2 (at 4.44 w/ft^2), and will weigh about 274 earth pounds. The size of the array will be about(2)(8 x 36 ft) when unfolded on the ground as shown in Figure 4.35a.

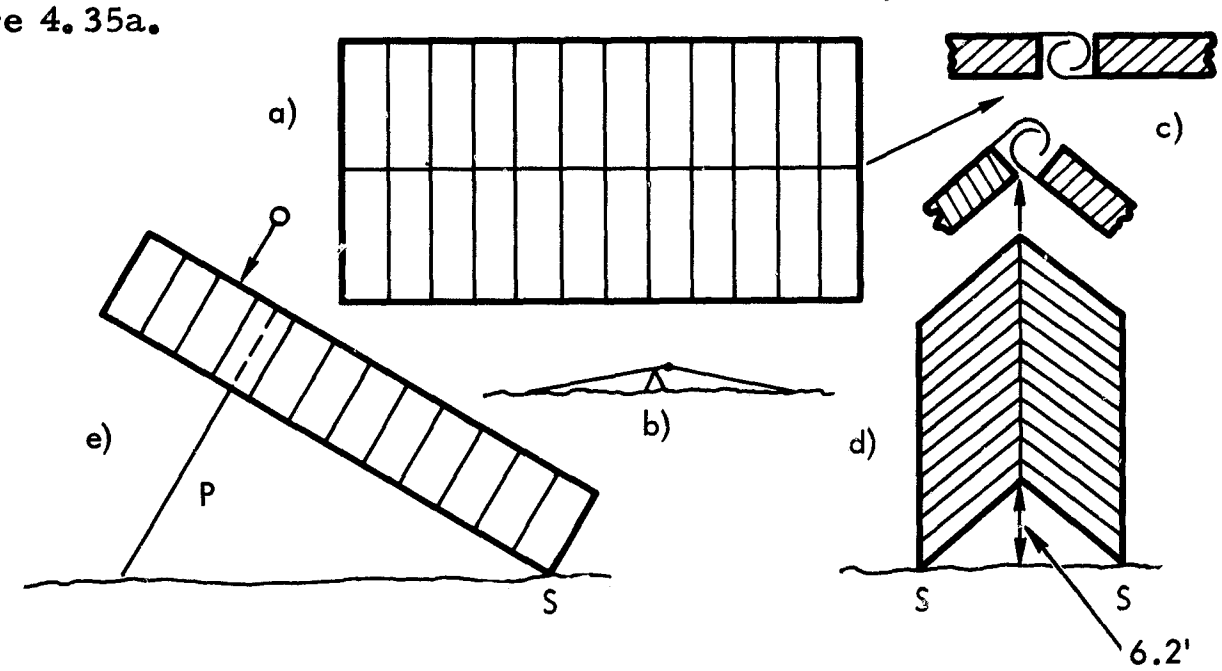

Figure 4.35 Deployment of 2.55 kw Foldout Leanto

The deployment and assembly are facilitated by the use of a light-weight triangular-shaped (Δ) beam which is placed on the lunar surface near the centerline of the array as shown in Figure 4.35b. The first set of modules are rested on this beam, which affords a means for aligning the edges of the modules. The second set of modules permits arrangement of the mating hooks on the edges of both sets of modules as shown in Figure 4.35c. The ridge is then lifted to its proper elevation of 6.2 ft by means of the Δ-beam which holds the hinge line straight during the lifting operation (Figure 4.35d). The total lifting force to be exerted by each of the astronauts is approximately 32 pounds, including the 18 pound Δ-beam and the 45 pound solar array. In the inverter-V shape, the leanto then becomes a stable structure, and the Δ-beam can be removed for use at the next assembly station. If the lunar base is located at a latitude, L, with respect to the lunar equator, the assembly can be elevated further, hinging about S-S, to provide the maximum projected area at lunar noon. Finally, it can be secured in that position with a pole P under the ridge (Figure 4.35e).

The deployment times and energies for each 2.55 kw leanto array are as follows:

(1) Surface vehicle and 3 astronauts will clear site of rubble, requiring 3 hours and 1000 Btu/hr/man.		
(2) First lay. 2 men carry 12 lb each 50 ft (1 min, 50 Btu) then walk back 50 ft (.5 min, 20 Btu)	1.5 min	70 Btu/man
(3) Second lay. 2 men carry 12 lb each 50 ft (3 min, 50 Btu) one man walks back 50 ft (.5 min, 20 Btu)	3.5 min	70 BTU/man
(4) Lift Array. 2 men lift 32 lb each 6 ft (3 min, 20 Btu), release end skirts, one man walks back 50 ft (.5 min, 20 Btu)	3.5 min	40 BTU/man
(5) Connect transmission line to end of array	2 min	20 BTU/man
(6) Attach Δ-beam to rear of vehicle and proceed to next station	.5 min	20 BTU/man
Totals for each 2.55 kw array =	11 min	220 Btu/man
Totals for 51 kw array =	6.7 hrs	1100 Btu/hr/man

4.7.2.5 Flat Array of Flexible Panels Mounted on Structure

The problem with this combination is to build up a structure of closely spaced members to properly support the flexible array. Due to the larger number of longitudinal and lateral members to be assembled, the deployment time for this configuration will be greater than the 15 hrs required for the leanto described in Section 4.7.2.8. An estimate of 20 hrs is made, based on the comparison of the two cases.

4.7.2.6 Flat Array of Rigid Panels Mounted on Structure

The structure for a 2.5 kw array of rigid foldout panels will consist of a pair of pantographic linkages (Figure 4.36) unfolded from their compact, stowed condition, and joined together with a few crosswise diagonals to hold the linkages in the vertical position after deployment.

The 2.5 kw array of foldout panels will have an area of 350 ft^2 (at 7.15 w/ft^2) and will measure 8 x 43 ft when extended. Its weight will be about 160 Earth pounds. The high points of the linkages will rest under

the foldout joints which tend to sag, the alternate joints having sufficient bending stiffness to support themselves.

Deployment times and energies will be as follows:

1) Remove pantograph linkage from trailer, walk 50 ft while unfolding (1 min, 25 Btu), lock ends and fold out crosswise diagonals to hold linkage upright (1.4 min, 10 Btu), walk back 50 ft (5 min, 25 Btu)		2.9 min	60 Btu/man
2) Two astronauts carry 13 lb each 50 ft (2.0 min, 75 Btu) unfolding the array panels on the structure, walk back (1 min, 25 Btu) releasing skirt enroute		3.0 min	100 Btu/man
3) Connect transmission line		2.0 min	20 Btu/man
Totals for each 2.5 kw array	=	7.9 min	180 Btu/man
Totals for 94 kw array	=	5.0 hrs	1360 Btu/hr/man

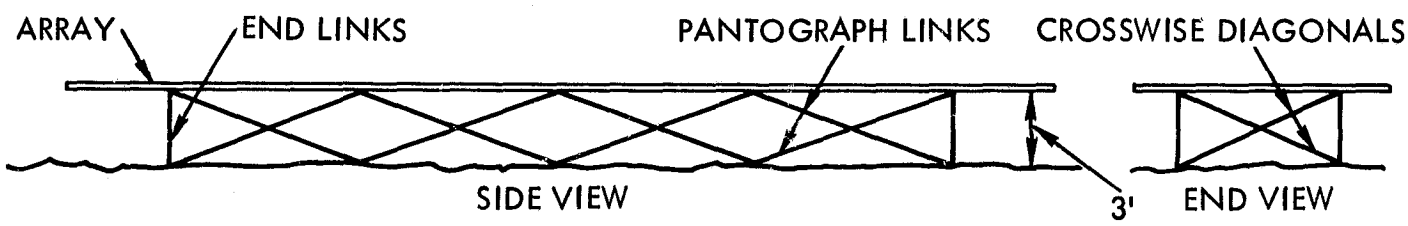

Figure 4.36 Structure for Flat Arrays of Rigid Panels

4.7.2.7 Leanto of Flexible Panels Mounted on Structure

This case is similar to Section 4.7.2.5 and an estimate of 20 hrs deployment time is made.

4.7.2.8 Leanto of Rigid Panels Mounted on Structure

A-Frame Structure. When a structure is assembled on which to mount the solar array panels, it is unnecessary to clear the site of rubble, since the structure will ride over such protuberances. One concept for the structural design envisions a system of A-frames, unfolded from their packaged condition and set up vertically on the lunar surface. To these are attached longitudinal rails which are unfolded from their stowed condition and attached to the A-frames to support the foldout panels (Figure 4.37a).

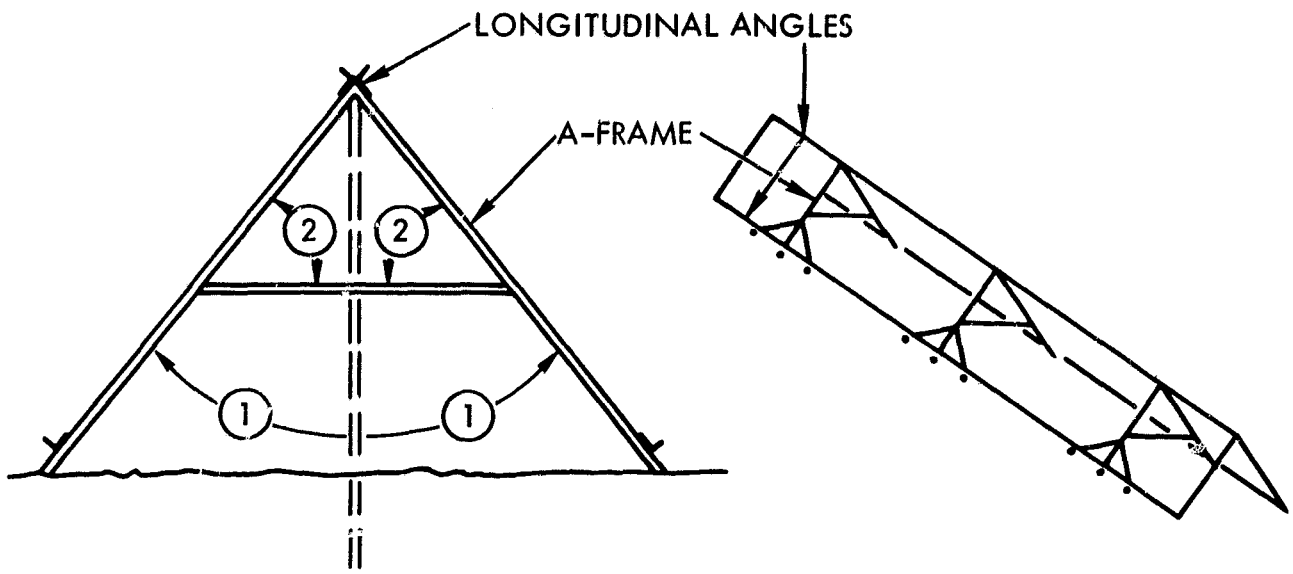

a) FOLDOUT A-FRAMES AND LONGITUDINAL ANGLES

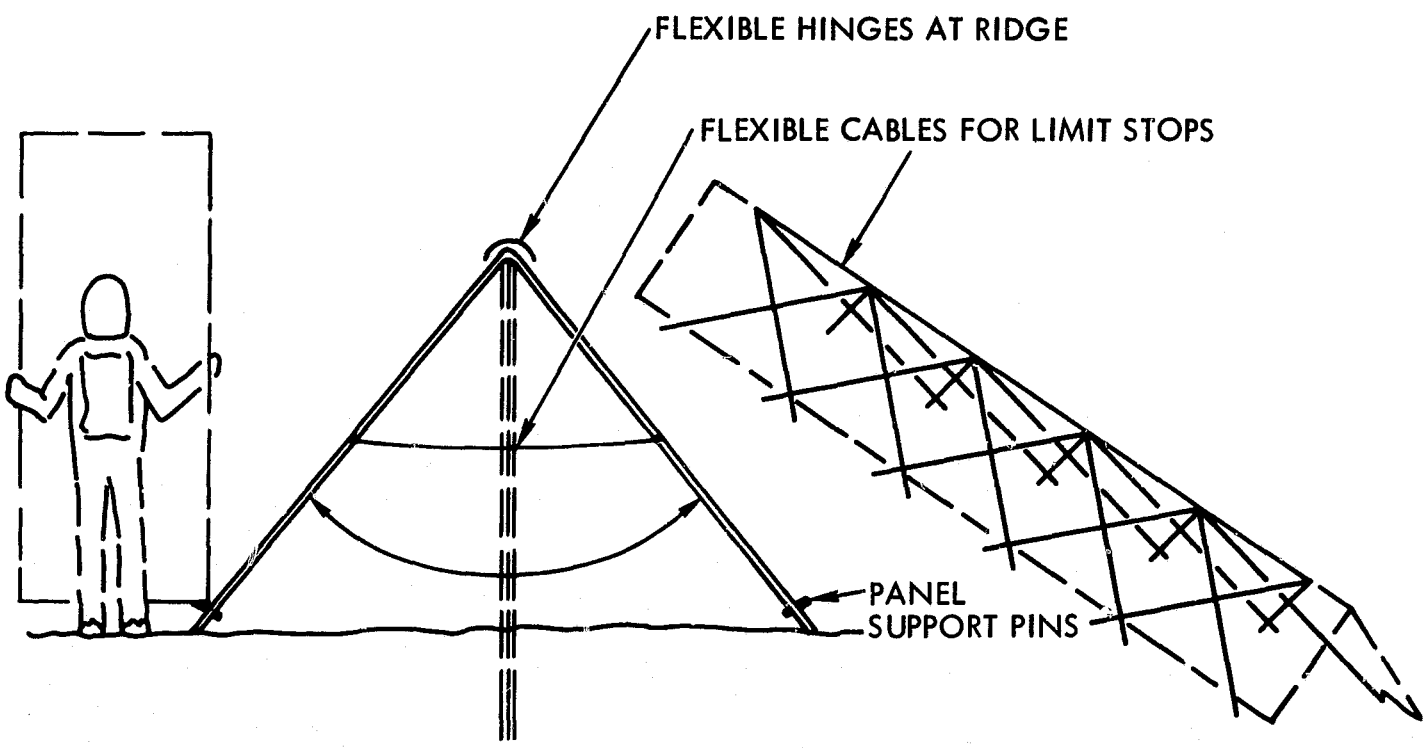

b) DOUBLE PANTOGRAPH STRUCTURE

Figure 4.37 Typical Leanto Structures

The time and energy requirements for deploying leanto arrays in this manner are as follows:

A. A-Frames

1. Remove A-frame from trailer and walk 15 steps	15 sec	15 Btu
2. Open A-frame and attach cross-bar	30	5
3. Open feet and set A-frame in position	60	10
4. Walk back 15 steps	15	15
Total per A-frame	120 sec	45 Btu
Total for 3 A-frames/ 2.55 kw array =	6 min; =	1350 Btu/hr/man

B. Longitudinal Beams

1. Remove spacer bar from trailer, attach to A-frames	90 sec	25 Btu/man
2. Remove beam from trailer and walk 25 steps	25	25
3. Unfold beam	60	10
4. Attach beam to A-frames	200	20
5. Walk back 25 steps	25	25
Total per beam	400 sec	105 Btu
Total for 4 beams/ 2.5 kw array =	27 min; =	930 Btu/hr/man

C. Solar Cell Panels

1. 2 men carry 10 lb each, unfold panels on structure	240 sec	50 Btu/man
2. Walk back 25 steps after releasing end skirts	85	25
3. Repeat 1 and 2 for other side	265	75
4. Connect transmission line	120	20
Total for solar panels/ 2.55 kw array	710 sec	170 Btu/man
	12 min	170 Btu/hr/man
Total of A, B, C for each 2.55 kw array =	45 min; =	725 Btu/man
Overall total for 51 kw array (20 x 2.55) =	15 hrs; =	970 Btu/hr/man

Double-Pantograph Structure. The preceding section shows that considerable time is required to perform the many assembly operations for A-frame structures with longitudinal angles. By using the double-pantograph illustrated in Figure 4.37b, the structure is completely assembled on Earth, thus requiring only an unfolding operation upon arrival at the lunar base. Using this concept, the time and energy required for deployment would be as follows:

(1) Remove folded structure from trailer, walk 40 ft while unfolding until flexible cables at ridge are taut (2 min, 40 Btu), spread sides apart to form inverted V as determined by cross-wise flexible cables (2 min, 10 Btu) then set structure down and walk back, making final adjustments enroute (1 min, 30 Btu)	5 min	80 Btu/man
(2) Two astronauts carry 12 lb each 40 ft (1 min, 60 Btu), unfolding the panels on support pins near the surface (2.7 min, 70 Btu) walk back 1 min, 40 Btu, releasing end skirts enroute. Repeat for other side of leanto. Move on to next station (30 sec)	10 min	170 Btu/man
(3) Connect transmission line	2 min	20 Btu/man
Totals for each 2.55 kw array =	17 min;	270 Btu/man
Totals for 51 kw array =	5.7 hrs;	950 Btu/hr/man

4.7.2.9 Leanto Array Using Integrated Assembly (Leanto/Integrated/Structure)

A 51 kw leanto array (51° leanto) will require approximately 11,500 ft^2 of solar cell area, with proper allowance for temperature effects and radiation/micrometeorite damage for one year. If this is erected to form an inverted V whose height at the ridge is 0.61 times the width of the base, the desired power profile would be obtained (i.e., nearly constant throughout the lunar day). For various ridge heights, the corresponding length of the array will be as follows:

o	Ridge height (ft)	20	30	40	50
o	Array length (ft)	225	149	112	89

Using 30 ft poles to elevate the ridge, the assembly would appear as in Figure 4.38. The erection procedure would be accomplished in the following steps, which are identified by number in Figure 4.38:

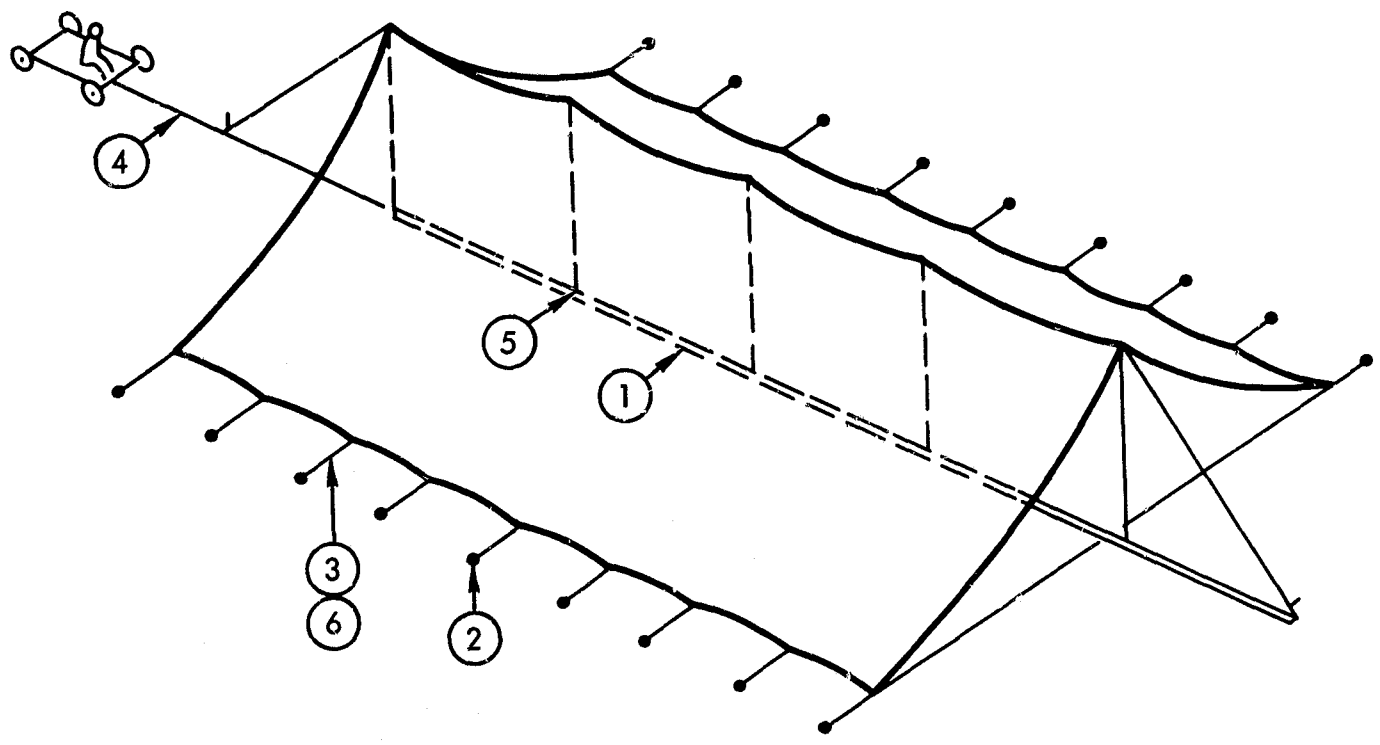

Figure 4.38 Leanto Array Using Flexible Integrated Assembly

1 After preparation of the site to avoid excessive roughness, lay out pole guide, poles and ridge cable, stake down guide, then unfold the rectangular array on the surface, as described in Figure 4.34.

2 Drive stakes into lunar surface adjacent to two sides of the array.

3 Attach trim lines at two sides of the array to the stakes. Allow sufficient trim to stabilize the poles during erection, but avoid excessive tautness which could impede erection.

4 Hoist poles to erect position with the line pulled by surface vehicle.

5 Secure lower ends of poles after stressing ridge cable.

6 After poles are secured, tighten trim lines at sides to remove excessive sag from array.

Deployment times and energies to perform sequence of steps in Figure 4.39 are as follows:

(1) Vehicle operator and two astronauts will clear site of rubble requiring	3 hrs	3000 Btu/man
(2) Tow poles and pole guide into position, and unfold solar array. Astronauts will expend approximately 3710 Btu (pole guide 950 Btu, poles 650 Btu, cable 300 Btu, solar array 1760 Btu)	4 hrs	3710 Btu/man
(3) Man walks around site (250 steps) carrying 50 lb stake driver (400 Btu), stoops 20 times (20 Btu)	20 min	600 Btu/man
(4) Man walks around site (250 Btu), stoops 20 times (200 Btu), pulls on trim lines 18 x 50 Btu/pull = (900 Btu)	40 min	1350 Btu/man
(5) Two men control tension on ends of longitudinal cable (100 Btu). VO hoists prop to erect position (5 min, 200 Btu)	30 min	200 Btu/man
(6) Man walks 100 steps (50 Btu), stoops 5 times (50 Btu) and secures poles to pole guide	15 min	100 Btu/man
(7) Man walks around site (250 Btu), stoops 20 times (200 Btu) and pulls trim lines (900 Btu) including end skirts	40 min	1350 Btu/man
(8) Connect transmission line to edge of array	5 min	100 Btu/man
(9) Two men standing still when not working	--	1200 Btu/man
Totals for 3-man crew =	10 hrs;	=11600 Btu/man
Therefore, the rate of energy expended for these operations =		1160 Btu/hr/man

4.7.2.10 Oriented Flexible Array Mounted on Structure

The structure in this case will be similar to that described in Section 4.7.2.11, except that more longitudinal and lateral members would be required to properly support the flexible array. The deployment time is estimated to be 45 hours.

4.7.2.11 Oriented Rigid Array Mounted on Structure

Each 2.65 kw array would be supported by a rectangular frame. The ends would have trunnions on the longitudinal centerline to permit orientation. Several of these arrays (weighing about 240 lb each) would be joined together by universal couplings, thus permitting several arrays to be controlled from the end unit, as illustrated in Figures 7.24 and 7.25.

Due to the requirement for rotation about the longitudinal trunnions, the frame structure and trunnion supports must be sufficiently stiff to avoid binding as the frame rotates back and forth.

The operations required for assembly of the structure are similar to those described under Section 4.7.2.5, with the exception that considerably greater care must be exercised in the design of this array to attain reliable, low friction operation. Because alignment of the structure is more critical, it is estimated that three or four times as much deployment time would be required for the oriented array as for the fixed array. Each of the 2.65 kw modules is estimated to require about 2.4 hours to assemble, align, and integrate, or 40 hours for the 45 kw candidate array using a 3-man crew.

4.7.2.12 Oriented-Integrated Array

The feasibility of this mode of deployment is considered satisfactory for solar arrays of a few kw, but additional design effort would be required to confirm that a 45 kw array could be packaged into the limited space available when using this technique. If this proved to be feasible, a considerable reduction in deployment time would be possible. A 2.65 kw array, weighing about 240 lbs could probably be deployed and integrated in 15 minutes, or 45 kw in less than 5 hours. However, at this time, this mode is not considered a likely candidate for large kw arrays, due to its poor packaging efficiency.

4.7.2.13 Summation of Time and Manual Energy Expended in Deploying Solar Arrays

Twelve alternate combinations of deployment modes were selected for solar arrays having the flat, leanto or oriented configurations; using either flexible or rigid panels; and mounted either directly on the lunar surface or mounted on a foldout structure above the surface. Time and motion studies were conducted for these 12 modes, to determine the time required for three astronauts, assisted by a construction vehicle, to accomplish the deployment operations.

The rates of energy expenditure for various repetitive motions (walking, carrying, stooping, driving, etc.) by an astronaut in a space suit were derived from Reference 4.10. The nominal work level in all cases was maintained at 1000 Btu/hr, to stay within the category classified as "light work" by Reference 4.10.

Five of the 12 deployment modes required that surface rubble be cleared away to provide a relatively smooth surface for those cases where the array was deployed directly on the lunar surface. The time to accomplish this task was determined by a detailed study involving lifting, loading and unloading, transit time, etc.

The time to deploy the foldout structures and solar arrays was estimated with the aid of conceptual drawings of the structural configurations. The time and energy to accomplish the various mechanical operations were analyzed individually and these were integrated to provide an estimate of total deployment time. The total number of standard 2.5 kw arrays to be deployed to attain the total power required for the Program V mission was taken into account during this analysis.

The results of these time and motion studies are summarized in Figure 4.39 and Table 4.17 showing that the flat arrays could be deployed in the least time (about 5 hours), the leantos were next (6 to 20 hours due to added structure) and the oriented arrays required the most time (about 40 hours, due to the added orientation mechanism, large skirt and the extreme care required to assure reliability).

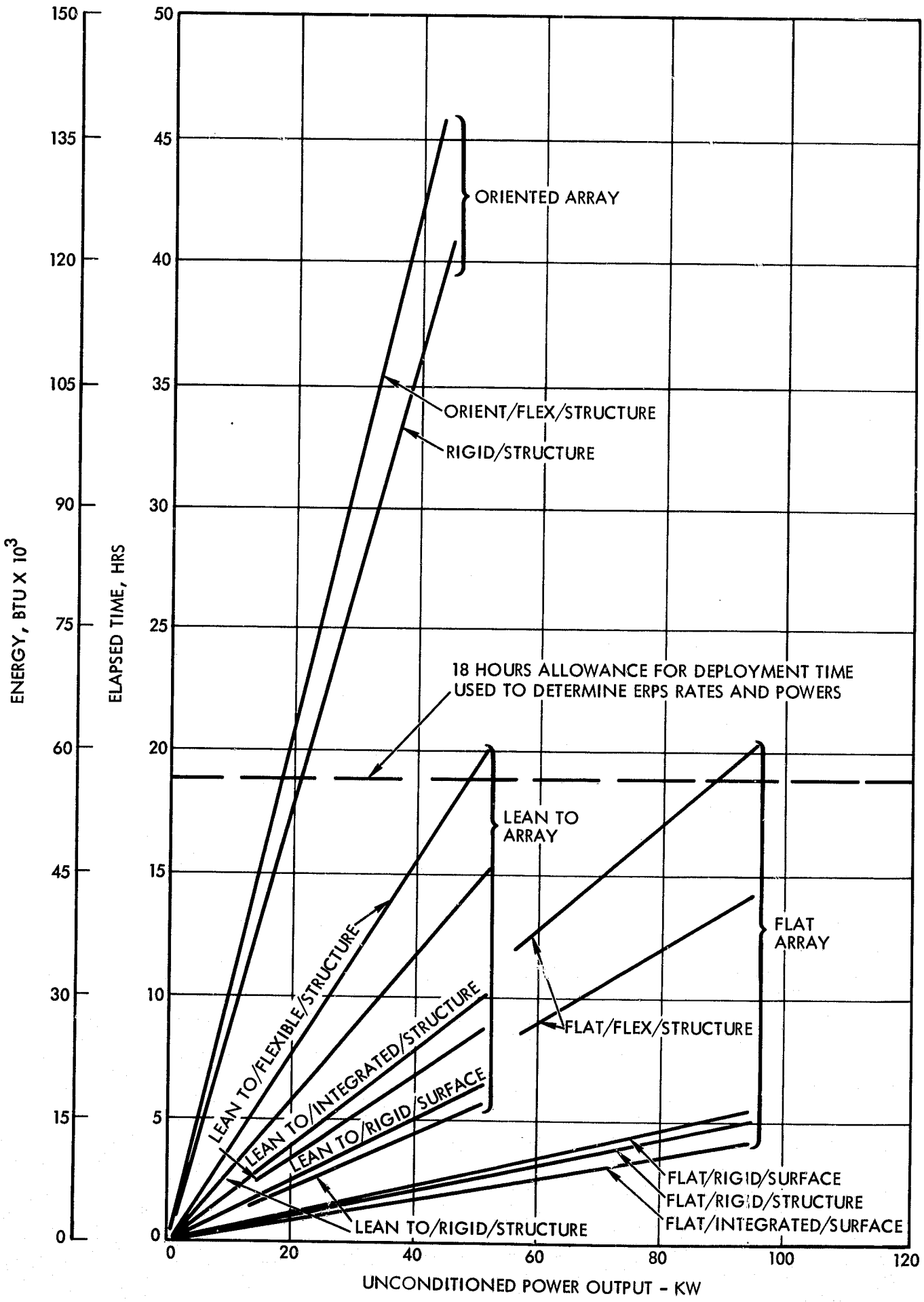

Figure 4.39 Deployment Time and Energy Required for Solar Arrays

FOLDOUT FRAME

Configuration[a] No.	Type	Surface Preparation (hours)	Structure Assembly (min)	Solar Array (min)	Skirt Deployment (min)	T
1.	FFsu	3	--	1.6	-- (See Figure 4.32)	
2.	FRSu	3	--	1.8	-- (See Figure 4.33)	
3.	FLSu	3	--	70	-- (See Figure 4.34, b and	
4.	LRSu	3	.5 (Δ-beam)	7.5	1.0 (See Figure 4.35)	
5.	FFSt	--	26.7	2.5	.5	
		(a) (Pantograph base with bed of foldout longitudinals and laterals)				
			17.9	2.5	.5	
		(b) (Pantograph on pantograph plus longitudinals)				
6.	FRSt	--	2.9	2.5	.5	
		Pantograph structure supporting rigid panels as in Figure 4.36)				
7.	LFSt	--	40	17	1.0	
		(a) Structure like Configuration 8(a) with more members to support f				
			6	17	1.0	
		(b) (Double pantograph with cables at ridge and base)				
8.	LRSt	--	33	9	1.0	
		(a) (A-frames and longitudinals like Figure 4.37a)				
			5	9	1.0	
		(b) (Double Pantograph like Figure 4.37b)				
9.	LISt	3	145	260	10	
		(Circus tent configuration like Figure 4.38)				
10.	OFSt	--	117	10.3	30	
		(Rigid, bolted structure with orientation mechanism and large skirt)				
11.	ORSt	--	100	9.7	30	
		(Less structure than required for Configuration 10)				
12.	OISt	--	This configuration is not feasible for large kw arrays			

(a) Configuration Code (See Table 4.13)

(b) Add 5 hours for ERPS deployment and cable connections to PCS and ERPS

1. Flat/Flexible/Surface
2. Flat/Rigid/Surface
3. Flat/Integr/Surface
4. Leanto/Rigid/Surface
5. Flat/Flexible/Structure
6. Flat/Rigid/Structure
7. Leanto/Flex/Structure
8. Leanto/Rigid/Structure

Table 4.17 Summary of Deployment Times

FOLDOUT FRAME

Skirt Deployment (min)	Connect Tr. Line (min)	Number of Units	Total Less Surface Prep. (hours)	Total[b] Deployment Time (hours)
-- (See Figure 4.32)	2	38	2.3	5.3
-- (See Figure 4.33)	2	38	2.4	5.4
-- (See Figure 4.34, b and c)	5	1	1.25	4.3
1.0 (See Figure 4.35)	2	20	3.70	6.7
.5 udinals and laterals)	2	38	20	20
.5 als)	2	38	14	14
.5 as in Figure 4.36)	2	38	5.0	5.0
1.0 re members to support flexible array)	2	20	20	20
1.0 nd base)	2	20	8.7	8.7
1.0 .37a)	2	20	15.0	15.0
1.0	2	20	5.7	5.7
10	5	1	7.0	10.0
30 anism and large skirt)	2	17	45	45
30 on 10)	2	17	40	40

ible for large kw arrays, due to its poor packaging efficiency

S

Flexible/Structure	9. Leanto/Integr/Structure
Rigid/Structure	10. Oriented/Flex/Structure
to/Flex/Structure	11. Oriented/Rigid/Structure
to/Rigid/Structure	12. Oriented/Integr/Structure

The deployment time for the assembly of structure is generally greater than that required for the solar array, skirt and connection to the transmission line. Pantograph structures are easier and faster to deploy than other structures, due to the lesser number of mechanical operations involved. The flexible arrays require more structural members and more connections to the structure to prevent excessive sagging; hence, the deployment time for flexible arrays tends to be greater than for rigid panels. The oriented arrays require considerably more time to deploy than the flat and leanto arrays, due to the need for structural rigidity and the installation/checkout of the orientation mechanism. In addition, the large flexible skirts require more time to install and stake down to the lunar surface. The need to achieve high reliability for the more complex oriented arrays also accounts for additional deployment time, when compared with the passive arrays.

The analysis of deployment times is seen to be closely related to the detail design of the structures, the various connects and mechanical operations required, and the transit times for men and vehicles to traverse the lunar surface. Normalization of the results is difficult because of the many configurations and parameters involved. The foregoing results are believed to be reasonably accurate and comparable, but further refinement will depend upon the accomplishment of more detailed design studies and the corresponding detailed scheduling of operations.

4.7.2.14 Final Deployment Operations

After deploying the solar array as described above, the final operations include the laying of cable from each array module to the ERPS unit, mounting the power conditioning equipment, and connecting off all cables. These operations were estimated to require approximately 2 hrs. The ERPS unit requires about 3 hours to deploy and the sequence of operations between ERPS and LEPEPS can be scheduled in any convenient manner.

It should be noted that a 336 hour working period was used in computing the nominal ERPS production rates. Since the lunar day is actually 354 hours, an allowance of 18 hours is available for deployment time or for other purposes. In the case of the leanto configuration (see Section

4.7.1.5), approximately 7 hours are required to unshadow the array; hence, a 9 hour period at dawn and dusk is appropriate.

Systems which require more than 18 hours for deployment will have a disadvantage, in that their power levels must be set higher, with an attendant increase in weight of solar array, power conditioning equipment, etc. Table 4.17 shows the total deployment time in hours. In those cases where the time exceeds 18 hours, an increase in array power level would be required to meet the Program V reactant production rates.

5. LUNAR SURFACE ENVIRONMENTAL MODEL

5.1 GENERAL CONSIDERATIONS

Ideally, an environmental model should be based upon established data. The model should consist of tables, graphs, and charts from which can be abstracted all the physical parameters necessary for the design of a specific system. At present, when lunar surface exploration models are being considered, the design engineer has learned not to expect this ideal. Although recent Surveyor, Ranger, and Lunar Orbiter missions have made valuable data available, their limited number and their degree of sophistication have not, as yet, resulted in a complete and infallible set of data. However, despite the few data points which have been measured and with extrapolation and interpolation of these data, systems can be designed to be reliable enough to result in successful missions as long as conservative estimates are utilized.

The data in this report is based on the most recently measured data (as of July 1967) and on past experiences as outlined in references 5.1 to 5.6. The data presented should be considered merely as a guide to the solar array designer to acquaint him with the range and probable magnitude of the environmental parameters. This information will make him aware of when the design limits of materials, performance, and mission life are being reached.

As lunar surface exploration (manned and unmanned) increases in complexity and duration, periodic updating of this data will become necessary. Eventually, as the quantity of high quality measured data received from future lunar surface missions is increased, a more precise and exact lunar model will evolve.

Materials selected for evaluation in this study were based upon the successful performance of those materials during Surveyor, Ranger, and Lunar Orbiter missions as well as on Earth orbiters and deep-space probes. To date, no lunar surface mission has survived more than three lunar days (three Earth months). However, degradation has not, to our knowledge, been reported for solar array performance or materials. Degradation has occurred, however, to other power subsystem

components such as the electrochemical energy storage batteries. They seem to degrade because of the temperature extremes experienced during the cycle from lunar night to lunar daytime. The fact that no degradation of the Surveyor solar array has been observed during the three lunar days of electric power system operation does not preclude the possibility of the occurrence of such degradation at longer exposure times to the lunar environment.

The assumption made in this study was that the recommended materials themselves do not degrade noticably in the lunar environment for a time period of up to 5 years. However, improper selection of material combinations from the recommended materials could result in adverse effects on performance and an acceleration of various degradation phenomenon.

The most important consideration, then, for any solar array design, is to accurately define the environment in which it will be required to operate and to insure that despite the uncertainties involved, that its end of mission (EOM) performance will still meet mission requirements. With this concept in mind, the most recent NASA/MSFC, JPL, and other documents were used to establish a lunar environmental model and to define those conditions which would be expected to adversely affect the operation of a lunar-based solar array. The resultant lunar surface environmental model definition was the criterion upon which the proper selection of materials to be used for solar array construction was based. Several alternate materials for each solar array element were identified and conservative estimates of combined environment and time effects on mechanical and/or electrical functioning of the array were made. This lunar environmental model includes the environment from the surface of the moon to a height where the atmospheric density is that of interplanetary space, i.e., 10^{-23} gm/cm^3.

5.2 LUNAR THERMAL MODEL

The lunar surface environment is the dominant factor in effecting the material selection, performance, and operation of lunar-based solar arrays. The various environmental parameters affecting solar array system operation are:

- temperature
- radiation levels
- micrometeoroid bombardment
- dust
- vacuum level
- g-level.

By far the most critical of these, from the standpoint of affecting solar array performance, is the thermal environment and the resultant effect on array temperature. This has been amply demonstrated by the parametric analysis of Section 7 and 8 of this report, data obtained in laboratory tests, and operation data obtained from Earth orbital and interplanetary spacecraft.

The average day/night variation in lunar surface temperature due to the presence or absence of the solar constant (I_{sol}) of approximately 140 mw/cm^2 is shown in Figure 5.1. Subsurface temperatures are considerably more moderate due to the insulating effect of the surface materials. Theoretical lunar surface temperature variation parametric curves are shown in Figure 5.2 for a point at the lunar equator where the lunar material thermal inertia (γ) varies from 20 to 1000°C-cm^2-sec$^{1/2}$/cal. Figure 5.3 depicts the lunar surface temperature variation with latitude.

The equation $T = T_{\text{subsolar point}} \cos \psi / 4$ (Reference 5.1) was used to establish these curves (ψ is the latitude angle) and since radiation is the principal heat transfer mechanism, variation in surface material properties can cause hot spots of re-reflected solar energy. The light scattering properties of the moon are such that there is no limb darkening regardless of latitude or longitude during a full moon, at which time each part attains maximum brightness.

Figure 5.4 is considered a best estimate of a lunar thermal model due to the fact that it is based on experimental means rather than actual measurement. The range of thermal parameters of surface materials (Reference 5.1) are:

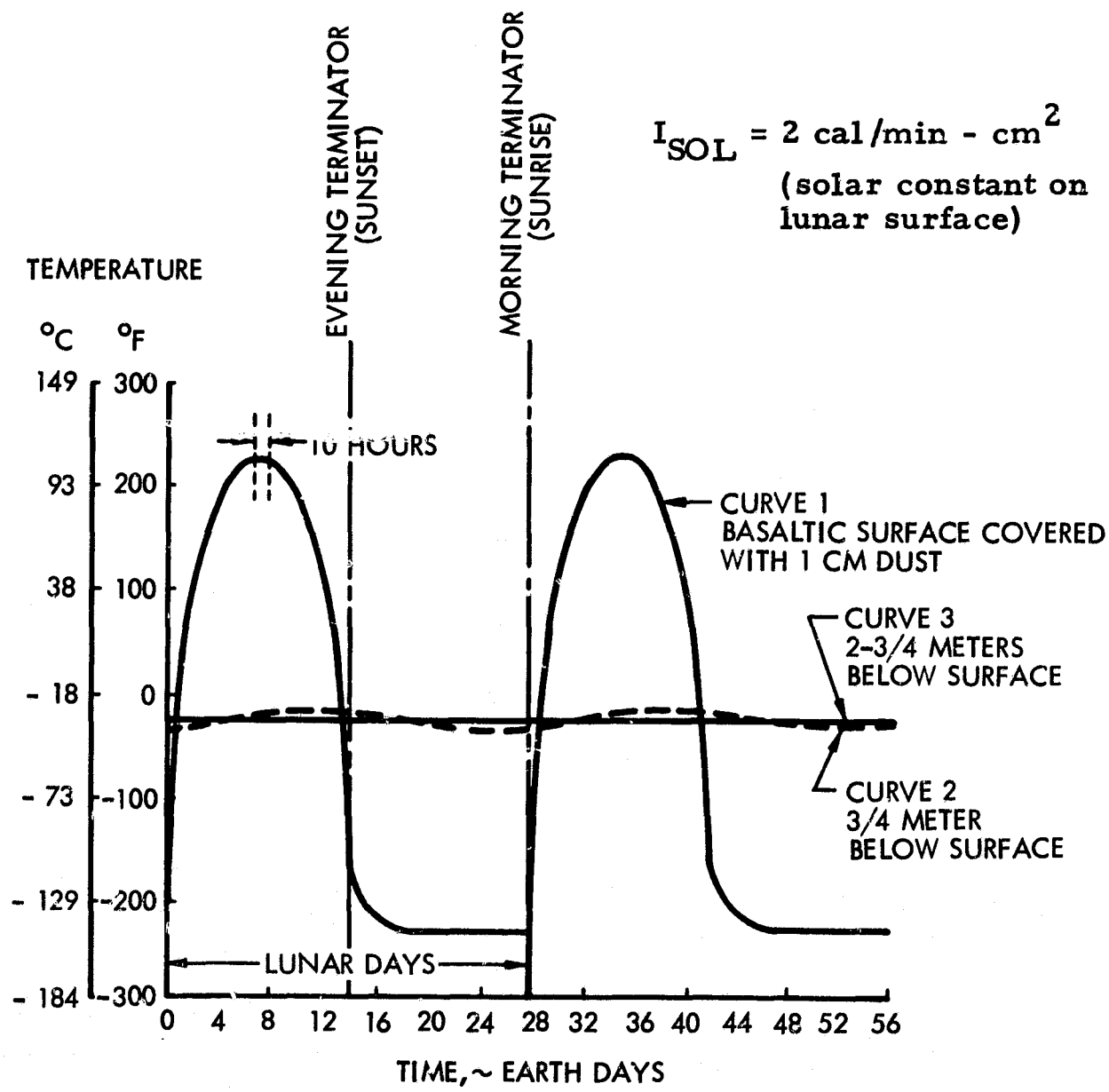

Figure 5.1 Typical Temperature Variation of the Lunar Surface (Reference 5.4)

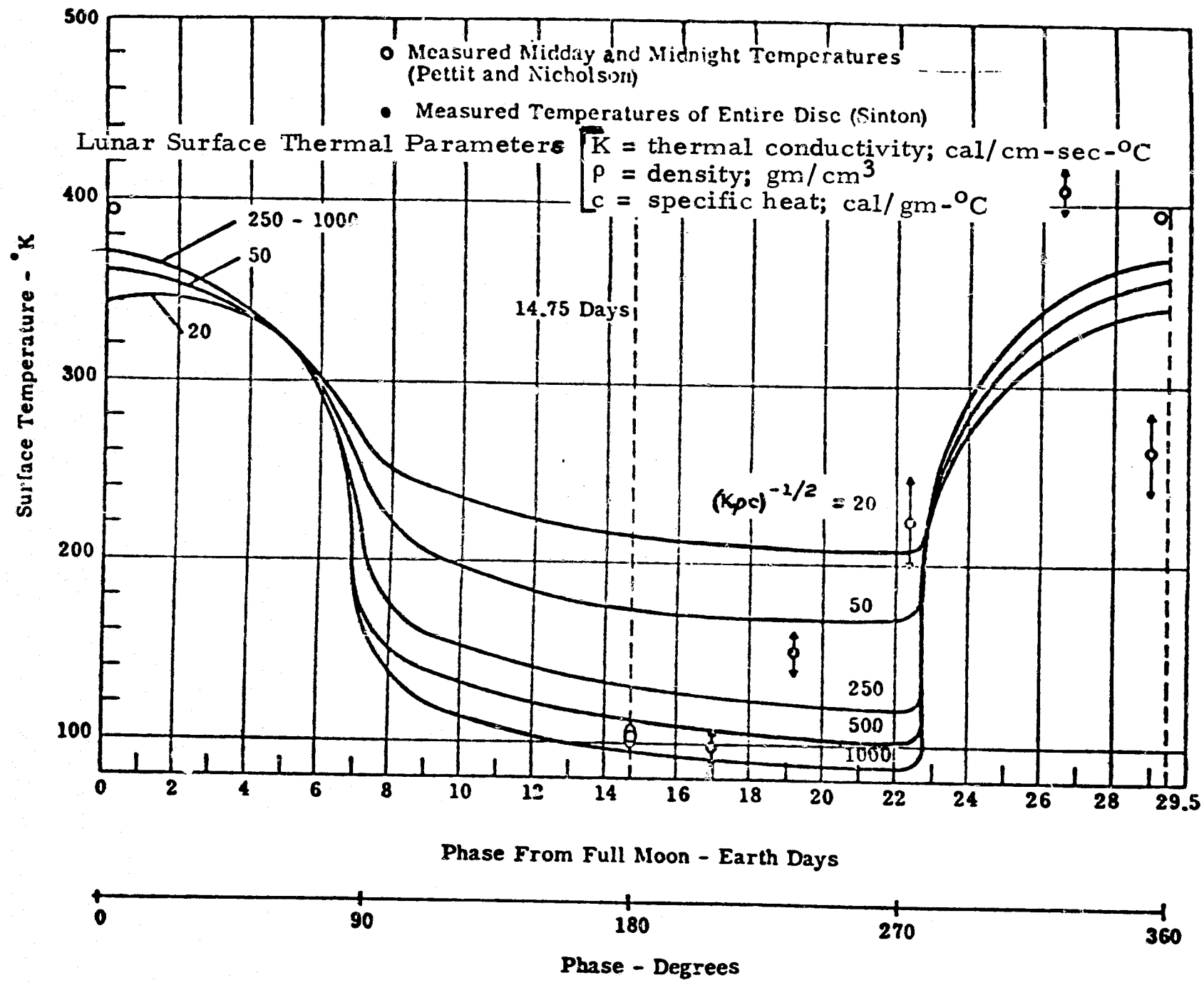

Figure 5.2 Theoretical Lunar Surface Temperature Variation for a Complete Lunation (Reference 5.1) at the Lunar Equator (where the lunar thermal inertia, $\gamma = (K\rho c)^{-1/2}$)

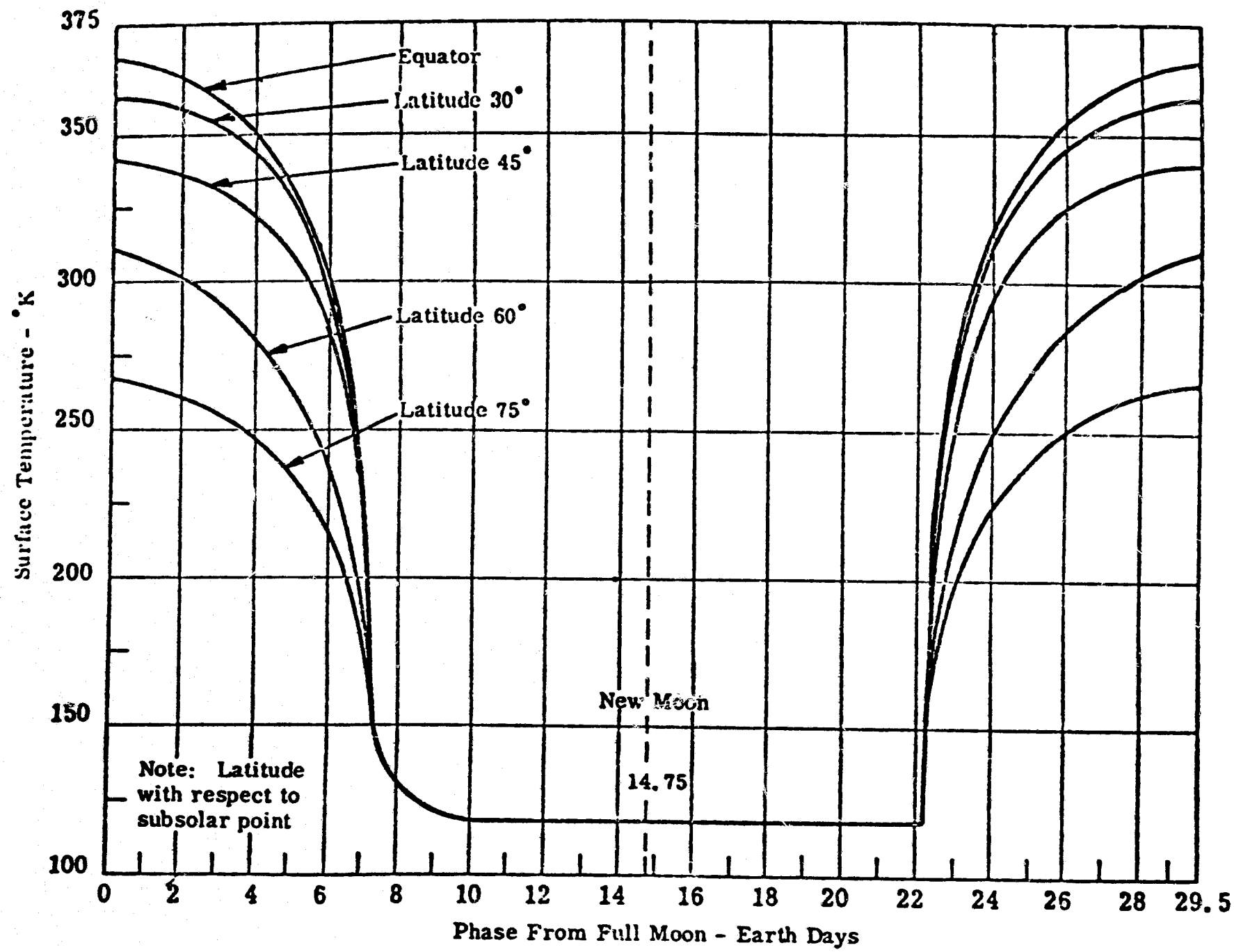

Figure 5.3 Theoretical Lunar Surface Temperature Variation for a Complete Lunation on Lunar Central Meridian (Reference 5.1)

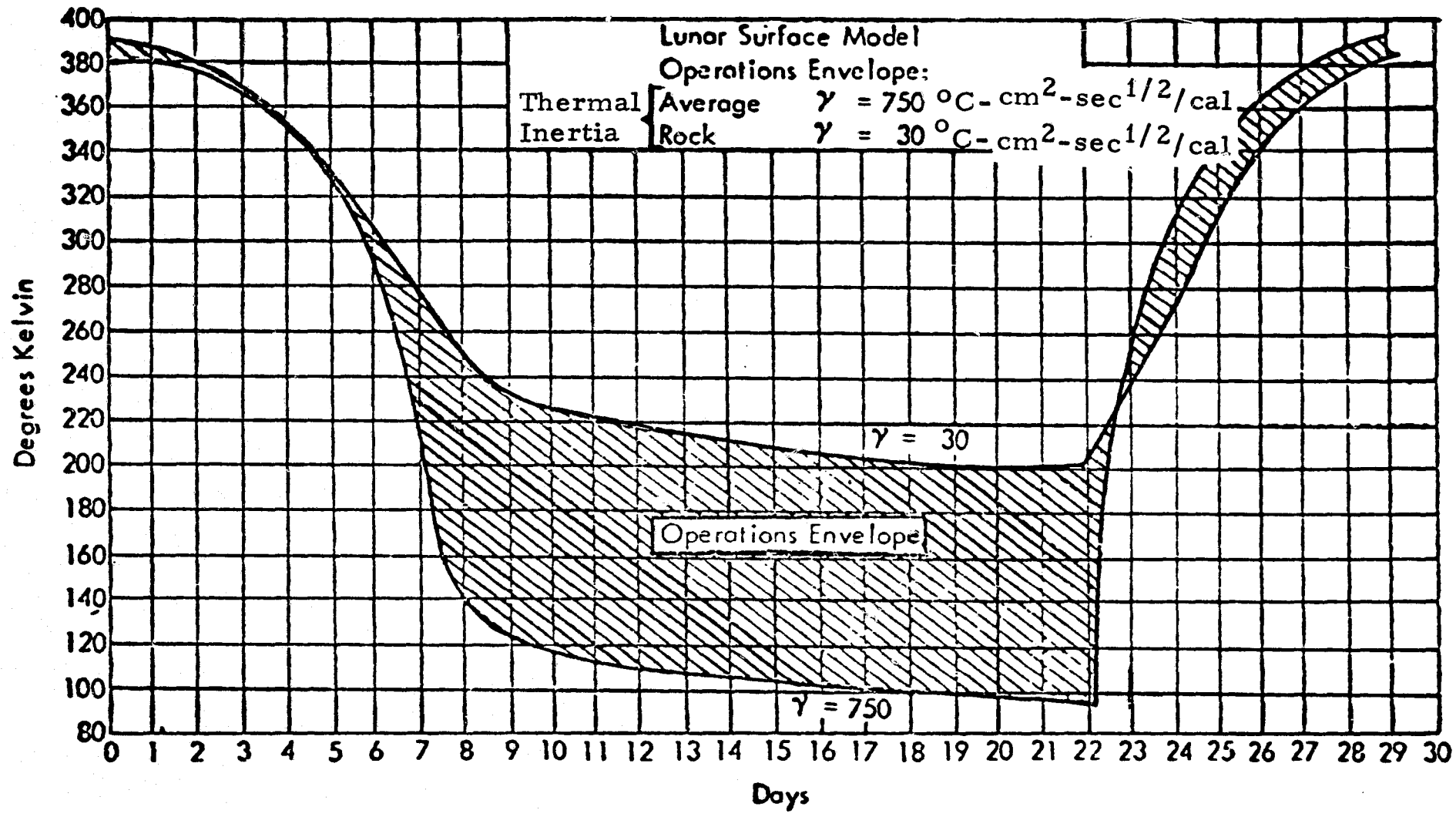

Figure 5.4 Variation of Lunar Surface Temperature During a Complete Lunation (Reference 5.1)

K (thermal conductivity) = 1.676 to 2.514 w/^{o}C-m

ρ (density) = 350 to 2500 kg/m^3

c (specific heat) = 838 w-sec/^{o}C-kg

γ (thermal inertia) = 1.43×10^{-2} to 4.3×10^{-2} ^{o}C-m^2/w-sec$^{1/2}$

It should be noted that the lunar surface material density range is similar to that of cometary meteoroid and secondary ejecta particles.

5.3 RADIATION ENVIRONMENT

The radiation environment to be encountered on the lunar surface consists of particulate radiation and the solar illumination intensity. The particulate radiation is composed of galactic cosmic rays, solar-protons, and electrons. While the galactic radiation maintains a relatively constant level with time, the solar particulate radiation rises occasionally by several orders of magnitude during solar flare disturbances, as shown in Tables 5.1 and 5.2. For exposed equipment, such as the solar array, the integrated flux can be determined by statistical data of this type, with due regard to the phasing of the operational period with respect to the 11-year solar cycle. The effect of the integrated flux on components and materials can then be determined by reference to threshold data presented in Section 6.

The solar high energy particle radiation on the lunar surface consists predominantly of protons (H^+) and alpha (He^{++}) particles. The maximum and minimum curves for these particles are shown in Figure 5.5.

The probability that solar flare (proton) events will occur near equinox rather than solstice (Reference 5.1) is high. Figure 5.6 shows the probability (p) of experiencing solar flares having integrated flux levels with energies greater than 30 MEV in any one day (n_f is the number of flares, n_t the time over which the flare is recorded).

The solar illumination intensity on the lunar surface is assumed to be equal to the value of the solar constant at 1.0 AU. This value is 1396 w/m^2 (2.0 cal/cm^2/min). The solar spectrum is considered to follow that of Johnson for AMO and 1 AU (Reference 5.1). During periods of solar activity, the x-ray flux may increase by 1 to 2 orders of magnitude. Generally, it is in the 10^{-8} to 10^{-11} w/cm^2 range in the region

Table 5.1 Yearly Integrated Intensities Compared for Solar Protons and Galactic Cosmic Rays

Year	No. of Events	Solar-Proton Integrated Intensity (10^7 particles/cm^2) >30 Mev	>100 Mev	Galactic Cosmic-Ray Integrated Intensity (10^7 particles/cm^2)
1956	2	70	32	10
1957	4 or 5	40	1	7
1958	6	70	1	6
1959	4	360	34	6
1960	8	200	50	8
1961	5	32	6	10
Total	30	772	124	47

Table 5.2 Major Solar-Proton Outburst During Years 1956-61

Date	Time of Optical maximum	Time of RF maximum	Max RF Signal 3-10kMc (10^{-19}w/m^2/cps)	Onset + Rise Time (hr) >30 Mev	>100 Mev	Decay Time (hr) >30 Mev	>100 Mev	Peak Intensity (10^3 protons/cm^2/sec) >30 Mev	>100 Mev
2/23/56	0340	0341	20	6-8	3-4	30	16	6.2	5
1/20/57	1120							2-3	0.15
7/7/58	0115	0112	2			32	16-20	1.5-2	0.08
7/14/59	0349	0352	6.3	16-20	12-18	18	9-12	10-12	1.2
11/12/60	1329	1329	10	12-16	8-10	18-24	14-18	12	2.5
7/18/61	1010		5	6-10	2-3	24	12	2.5	0.6

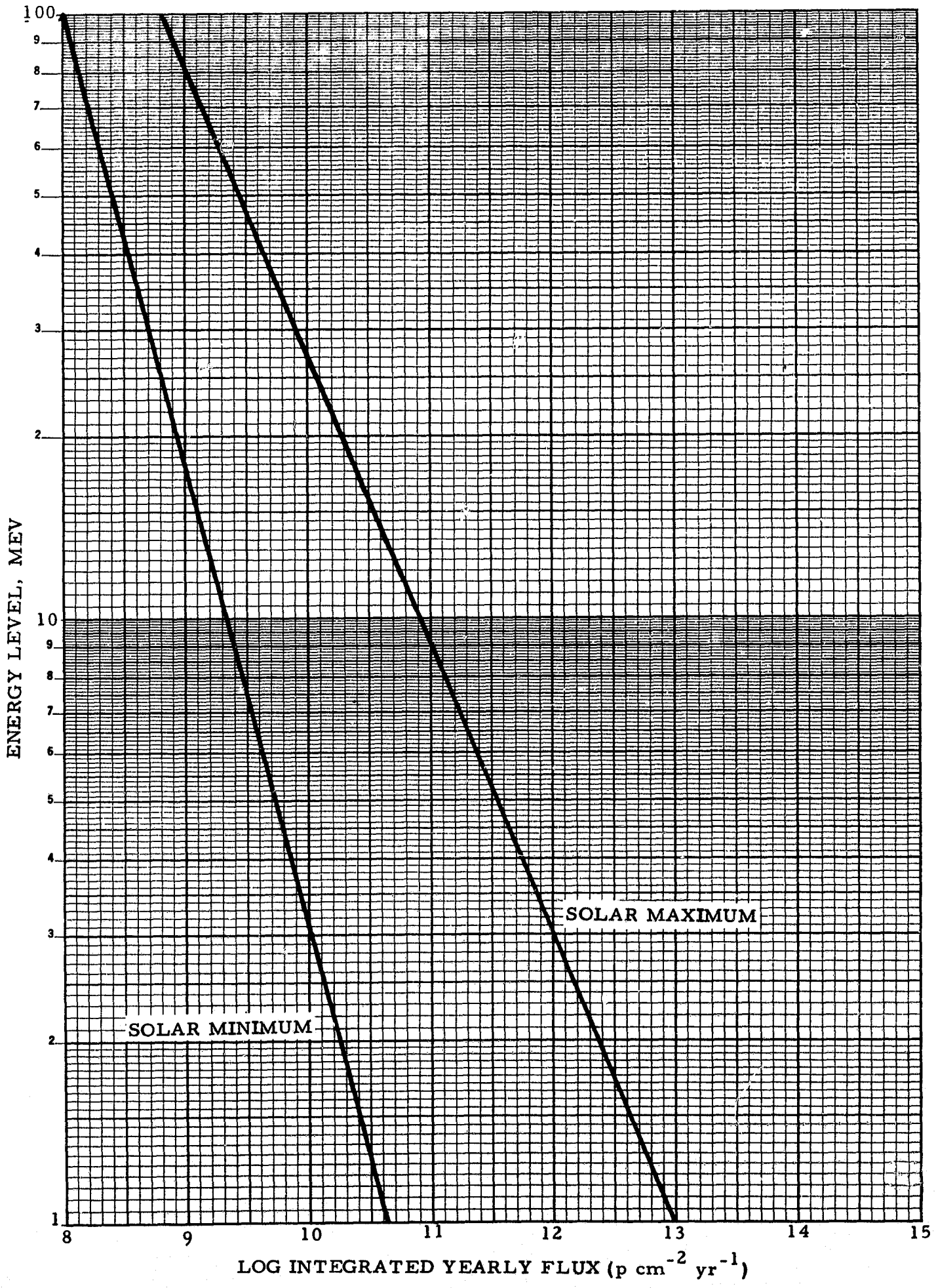

Figure 5.5 Solar High Energy Particle Radiation Energy Level Versus Yearly Integrated Flux for 1 AU (Estimate Based on Reference 5.1)

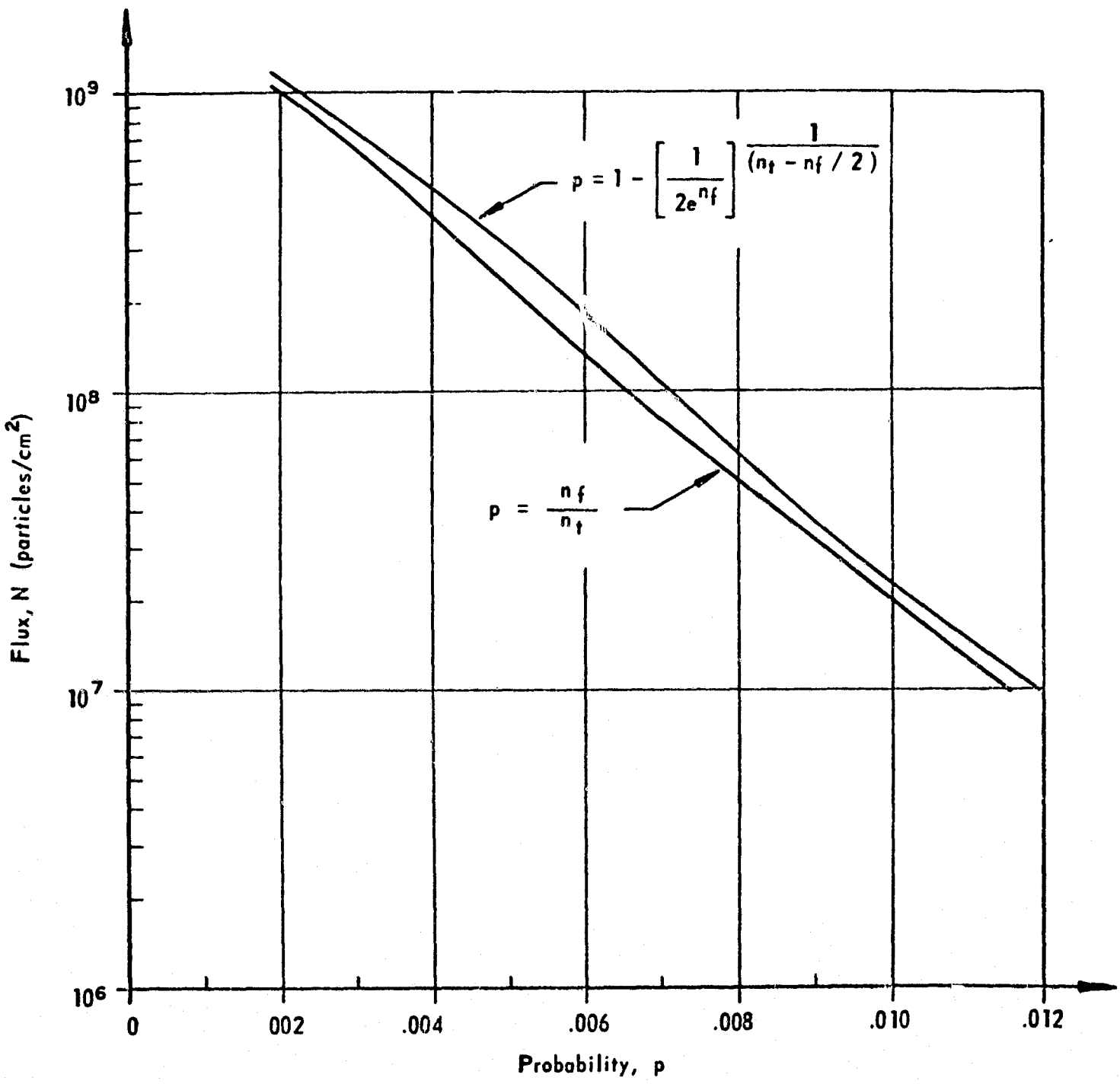

Figure 5.6 The Probability, p, of the Occurrence of a Flare Whose Flux is Equal to or Greater Than N, and Whose Individual Particle Energies are Equal to or Greater than 30 MEV (Reference 5.1)

from 100 Å to 2 Å, respectively. The solar radiation pressure, Figure 5.7 is shown to vary from 4.5×10^{-5} to 9×10^{-5} dyne/cm^2 for reflecting bodies whose reflectivity varies from 0 to 100 percent (7×10^4 dynes/cm^2 = 1 lb/in^2). Solar wind pressure is 10 orders of magnitude less than that value and thus its effect on large area solar arrays is considered negligible.

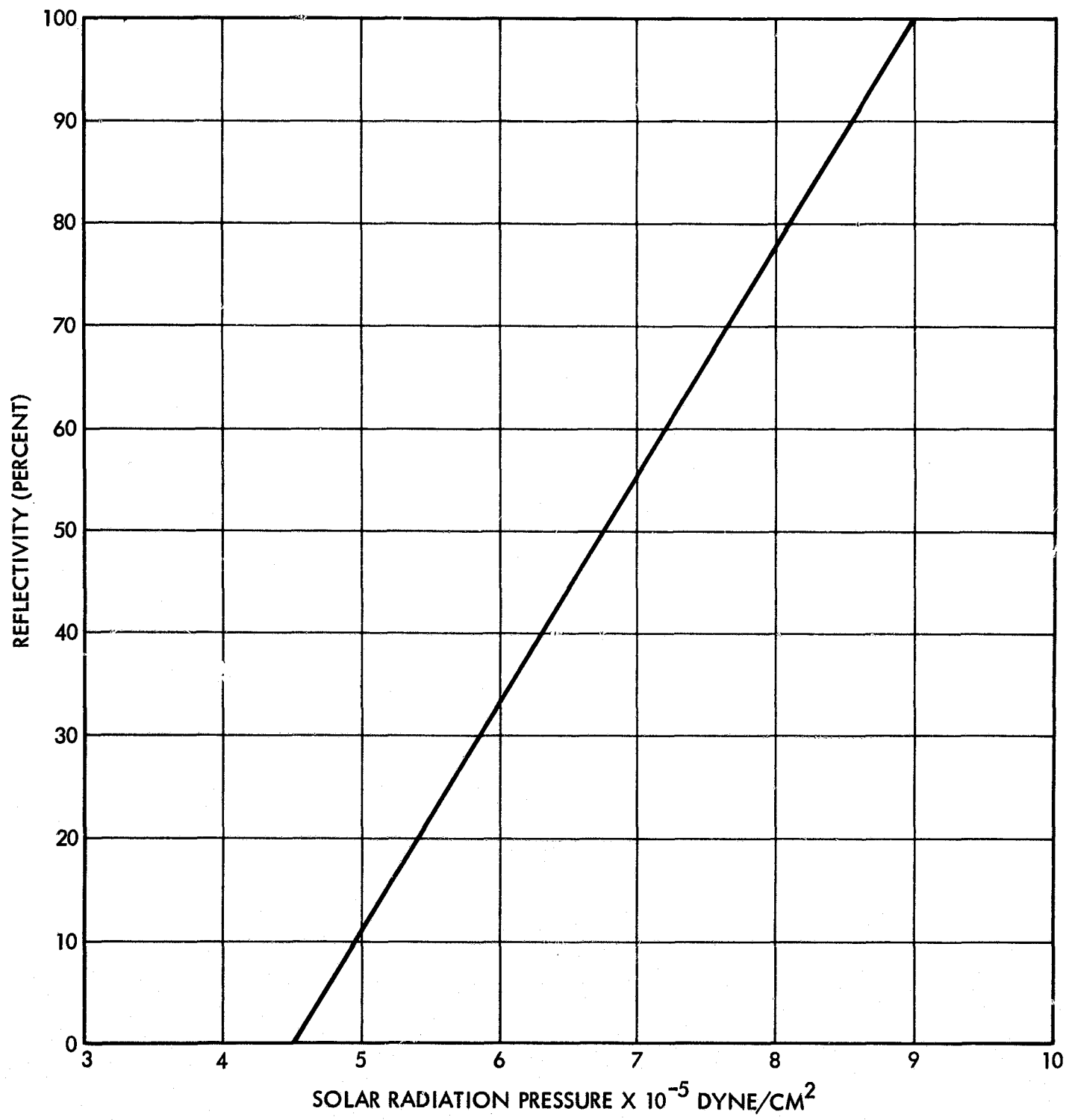

Figure 5.7 Solar Radiation Pressure at 1 AU Versus Reflectivity

5.4 METEOROID ENVIRONMENT

The cumulative meteoroid flux per unshielded m^2sec of cometary materials at the lunar surface with a mass greater than m grams, is shown in Figure 5.8 and is based on data presented in Reference 5.1. Cislunar flight data is included for comparison purposes. The cometary micrometeroid flux (F) shown in Figure 5.8 is calculated per Reference 5.1 from:

$$\text{Log } F = -14.20 - 1.386 (\text{Log } m) - 0.0331 (\text{Log } m)^2 + 0.00051 (\text{Log } m)^3$$

The secondary ejecta (F') is determined from:

$$F' = 10^{3.75} F$$

Typical variations in meteoroid flux over a 1-year period are shown in Figure 5.10. The average photographic meteoroid density is taken as 0.34 gm/cm^3 with a mean velocity of 22 km/sec. Secondary ejecta from meteoroid impacts is shown in Figure 5.8 with densities of 2.5 gm/cm^3 and average velocities of 0.2 km/sec. Figure 5.9 shows particle diameter and weight for these densities.

The depth of penetration D for meteoroids is given by the following equation:

$$D/d = 2.78 (\rho_m/\rho_t)^{2/3}(V_m/V_t)^{2/3} \qquad \text{(Reference 5.2)}$$

where d = diameter of particle, ρ_m = density of meteoroid (mean value of 0.44 gm/cm^3), ρ_t = density of target material, V_m = velocity of meteoroid (mean value of 22 km/sec), and V_t = speed of sound in target material. To apply the above formula to thin sheets, a factor of 1.5 is used to convert from a semi-infinite target to a thin sheet of a thickness which will not be punctured; i.e., t = 1.5D. The above equation may be rewritten:

$$t = 4.25(\rho_m/\rho_t)^{1/3}(M/\rho_t)^{1/3}(V_m/V_t)^{2/3}$$

where M = micrometeoroid mass (grams).

The above equation provides the basis for the design of a lunar surface solar array to a desired level of reliability from the standpoint of micrometeoroid effects.

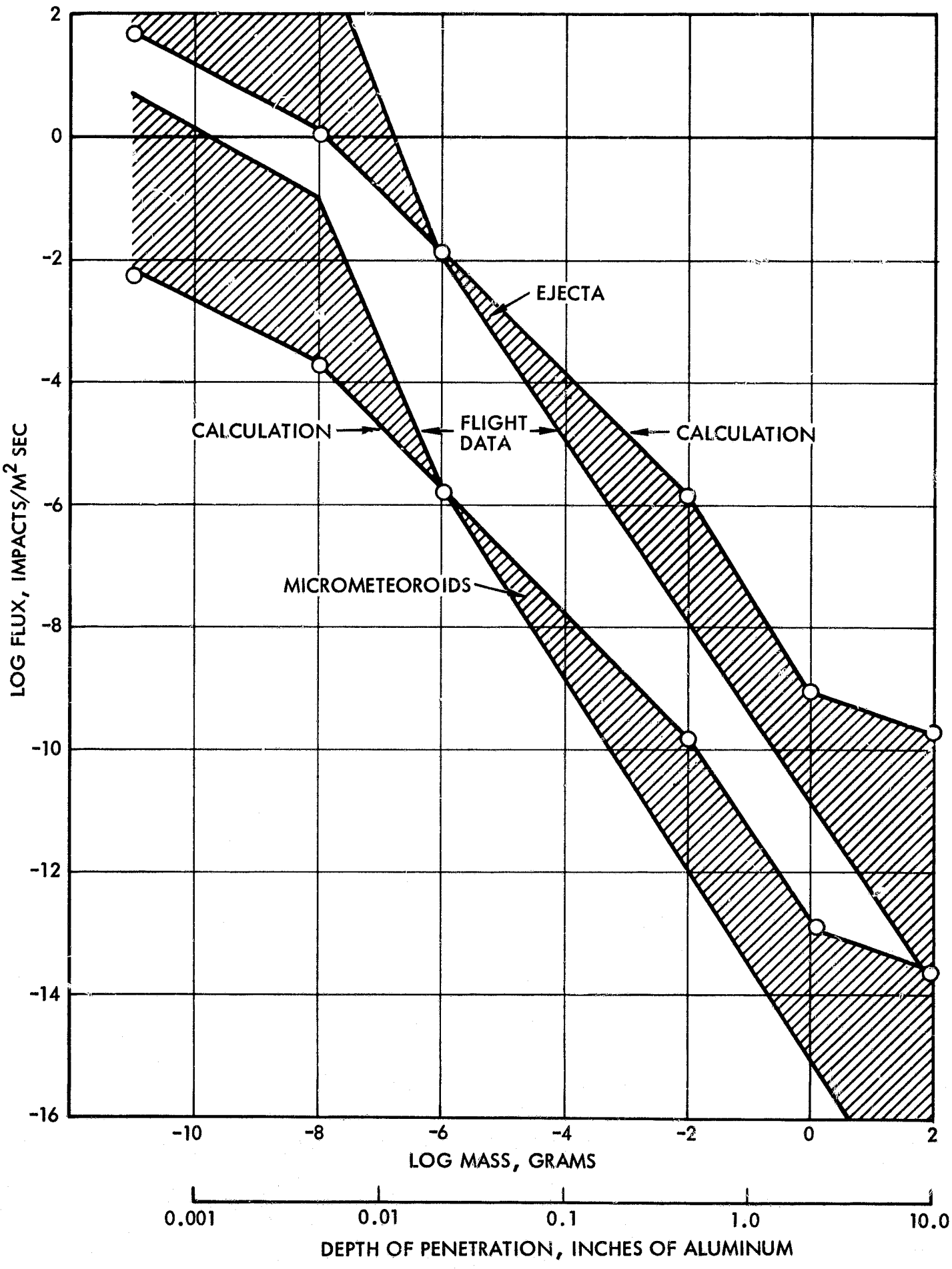

Figure 5.8 Cometary Micrometeoroid Flux and Secondary Ejecta Flux Vs. Particle Mass and Depth of Penetration into Aluminum

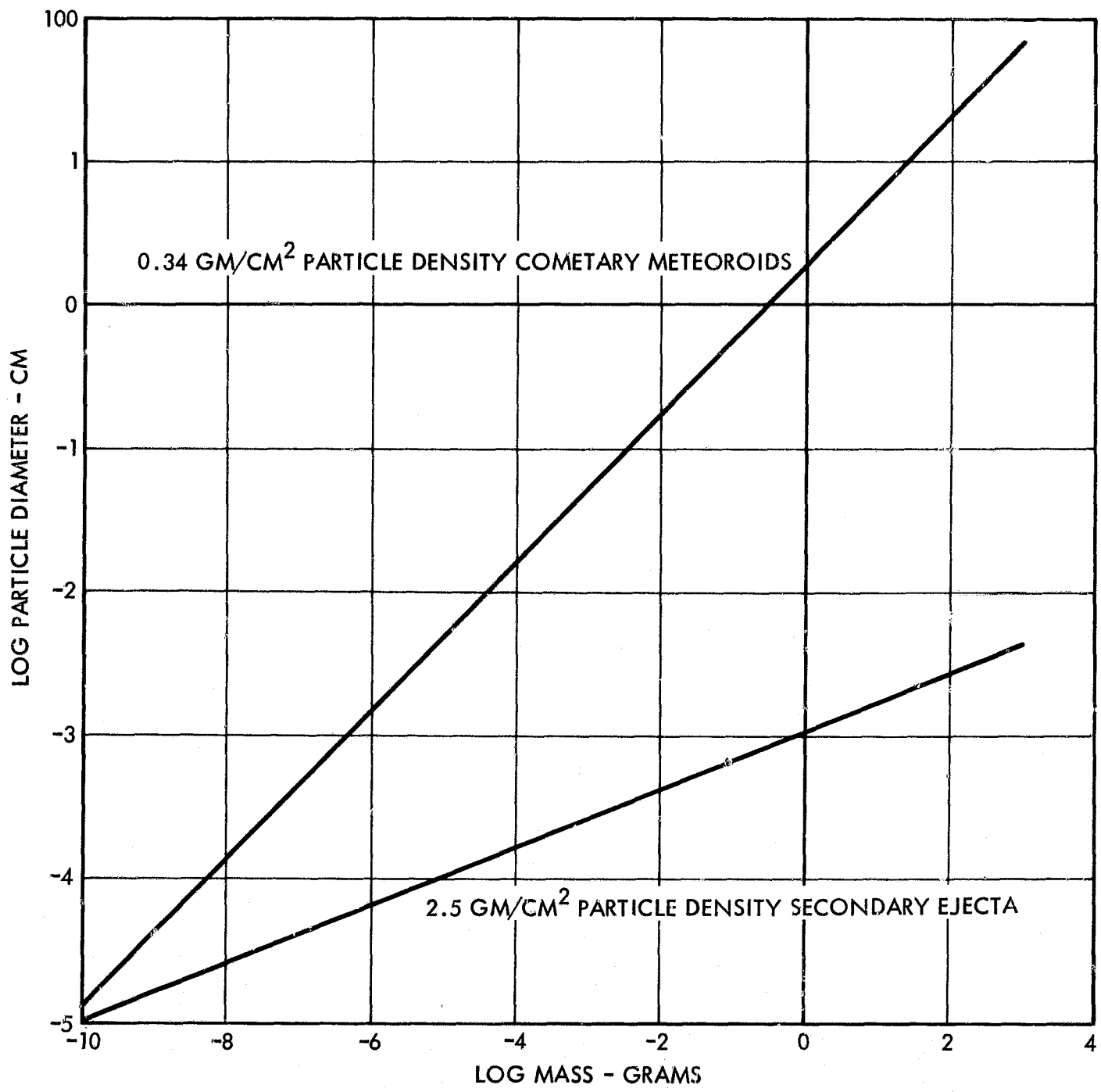

Figure 5.9 Particle Diameter Versus Mass for Typical Micrometeorite and Secondary Ejecta Particle Densities

For thin materials, where

$\rho_m = 0.34\ gm/cm^3$

$\rho_t = 1.40\ gm/cm^3$

$V_m = 22\ km/sec$

$V_t = 1.5\ km/sec$

d = particle diameter, cm

D = depth of penetration, cm

The depth of penetration becomes:

$D = d(6.474)$ for micrometeoroids

and

$D = d(1.059)$ for secondary ejecta

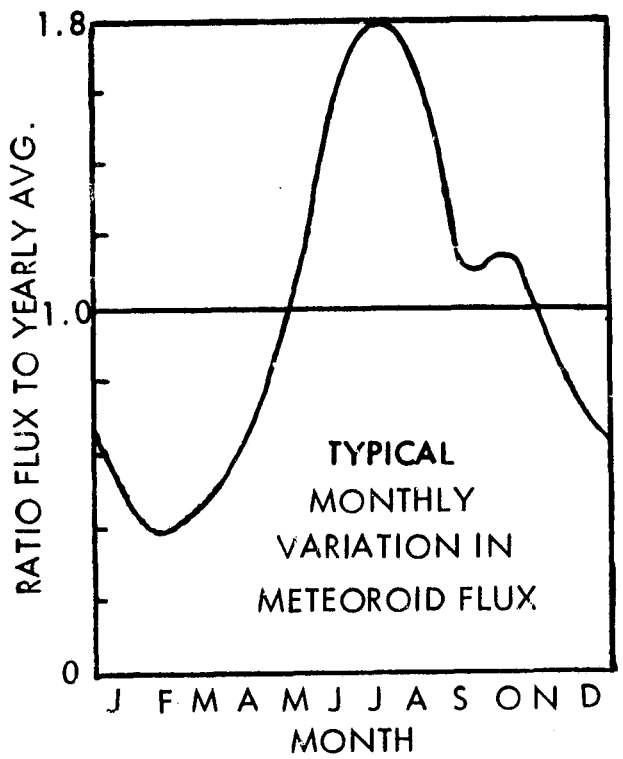

Figure 5.10 Micrometeoroid Frequencies

this data is presented in Figure 5.11.

The mean number of punctures (puncture flux) per unshielded m^2 sec for cometary meteoroids is given by the equation (reference 5.1)

$$\text{Log}\ \phi = -13.03 - 3.81(K_t + \log p) - 0.384\ (K_t + \log p)^2 - 0.017(K_t + \log p)^3$$

where the target material parameter K_t is:

$$K_t = -1.36 + \log\left(\epsilon_t^{1/18} \rho_t^{5/6} C_t^{2/3}\right)$$

With the known values for thin-film solar cells of

1. p (thickness) = 0.005 in. = 0.0127 cm
2. ϵ_t(elongation) = 0.70
3. ρ_t(density) = 1.42 gm/cm^3 Kapton
   1.39 gm/cm^3 Mylar
4. C_t (sonic velocity) = 1.500 km/cm^3 (assumed)

$$\text{Log}\ \phi = -5.14656$$

Calculation shows, $\phi = 1.4 \times 10^{-6}$ punctures/m^2 sec through 0.005-in.-thick material. K_t approaches -1.36 for plastic materials.

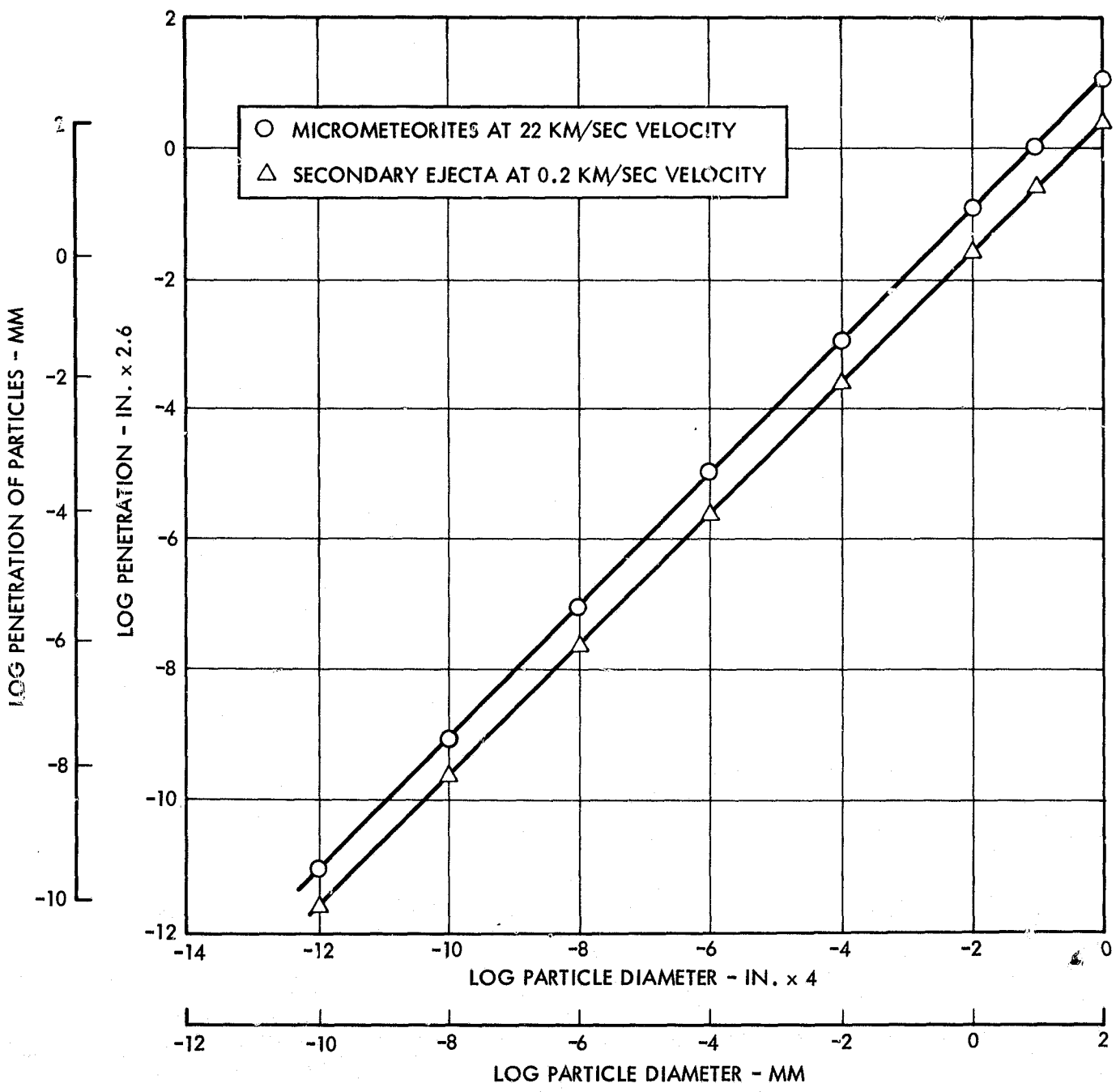

Figure 5.11 Micrometeoroid and Secondary Ejecta Particle Penetration Depth for Thin Materials

Secondary ejecta puncture flux is considered negligible, compared to the primaries, at this time. However, when ejecta particle velocities become low (m/sec), some considerations should be given to structures of bumper or multiwall design so as not to absorb debris.

Figure 5.12 is data from Reference 5.5 which, when used in conjunction with data in Figures 5.8, 5.9, and 5.11 permits an indication of the level of debris and/or dust which may be experienced by a lunar-based solar array. As an example, Figure 5.8 shows the maximum cometary meteoroid flux (impact/m^2 sec) to correspond to particle weights of 10^{-10} to 10^{-10} grams. Figure 5.9 tells us that the diameter of a particle having this weight is 1.94×10^{-5} cm (1.94×10^{-7}m). Figure 5.11 then tells us that particles traveling at 22 km/sec velocity and having 2×10^{-7} m diameter will not penetrate to any appreciable depth into array material (10^{-7} to 10^{-6} mm or 10^{-8} to 10^{-7} inches) thus indicating the possibility of a dust condition. However, 1 impact/m^2 sec indicates that at this flux level for 1 year (31,526,000 sec) a total of 3.1526×10^7 impacts/m^2 will have occurred. This number of impacts of particles having 1.94×10^{-7} m diameter indicates than ($\pi d^2/4$) $9.114 \times 10^{-7} m^2$ of area will be covered by debris over that 1 year period or some 10^6 years to completely cover a 1-m^2 area with microscopic particles. At the other extreme, particles whose mass is 1 gram (dia = 3 cm) have a flux level of 10^{-16} impacts/m^2 sec and will penetrate up to 10^{-1} mm (0.001 inch). Over a 1 year period 3.1×10^{-9} impacts/m^2 will occur or $9.114 \times 10^{-10} m^2$ of area covered or degraded by abrasions over the 1-year period.

Figure 5.12 shows that from 100 to 1000 particles of (1 gram) 3-cm diameter impact per 100 m^2 area of lunar undisturbed surface over a given period of time. This data is a plot of the equation $N = 3 \times 10^{-5} y^{-1.77}$ where N = cumulative number of particles, y = particle diameter in millimeters. Also shown by Figure 5.12 is the probability that for every 100 m^2 a boulder of 1 meter diameter (3400 gm, 7.4 lb) could exist which would require removal.

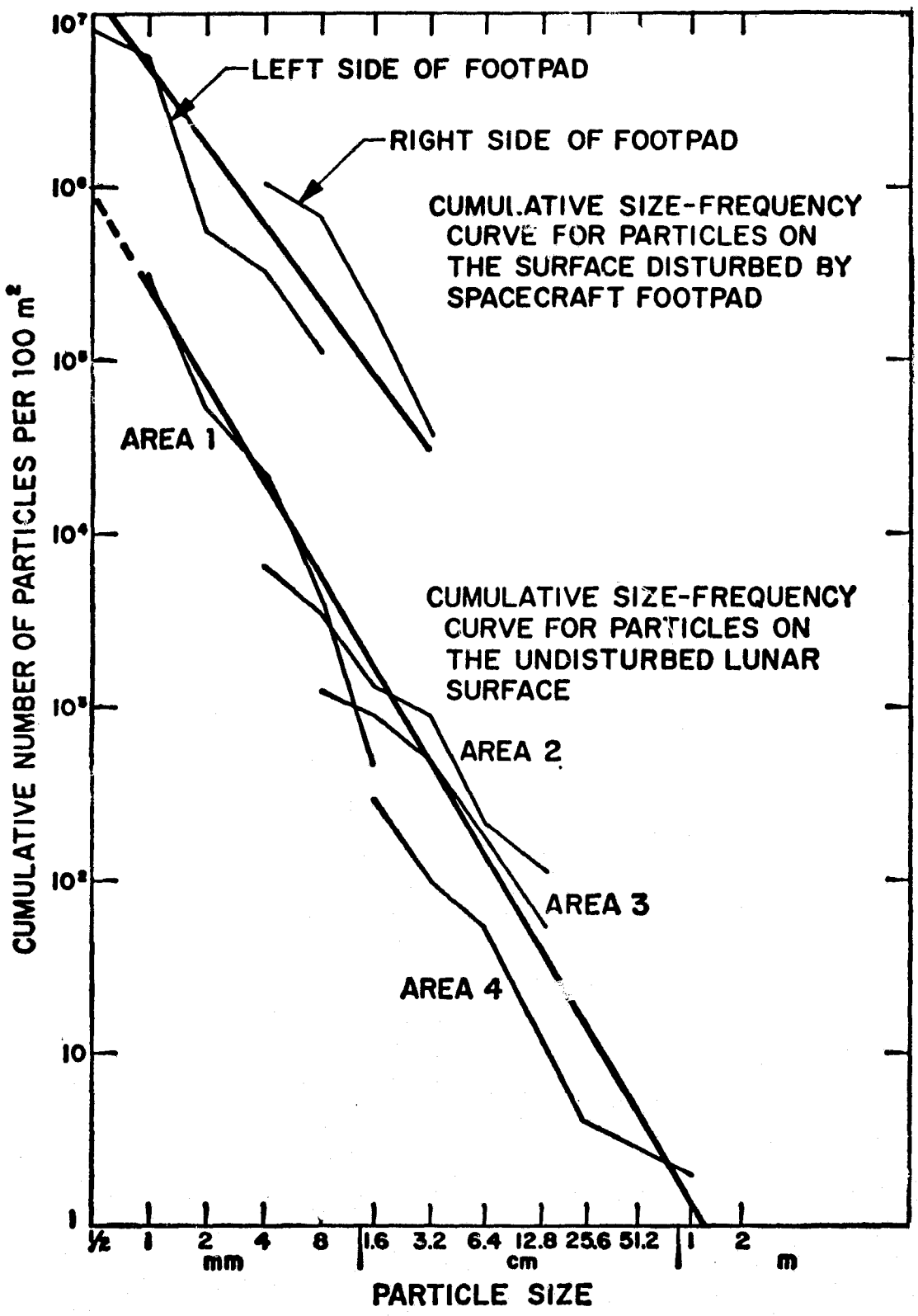

Figure 5.12 Cumulative Frequency Distribution of Particles on the Lunar Surface Determined from Surveyor I Observation Photographs (Reference 5.5)

5.5 ATMOSPHERIC PROPERTIES

Based on data in Reference 5.1, the atmospheric pressure and density are estimated to be 10^{-13} times that of earth at sea level. Based on these estimates, the depth rate of meteoric erosion for aluminum and magnesium is on the order of 1.5×10^{-13} cm/sec (at this rate approximately 10,000 years is required to erode 1.5 cm of material) ith similar times required for significant corpuscular spattering at a rate of 2×10^{-13} gm/cm^2-sec and sublimation at a rate of 10^{-13} gm/cm^2-sec. Assuming each effect was occurring at the maximum rate simultaneously, it will take approximately 3,000 years for a 1.5-cm depth of material erosion to occur. Thus it is reasonable to assume negligible effects from pressure, atmosphere, and erosion for solar arrays located on the lunar surface.

The range of lunar albedo values is from 0.065 to 0.105 for an average of 0.073 and this value was used during this study to determine albedo effects on the temperatures of surface structures such as the solar arrays.

Table 5.3 is the minimal model for solar wind (Reference 5.1) while Figure 5.13 is a plot of mean values of solar wind data for various AU distances from the sun. For 1 AU, there seems to be no unusual effects resulting from solar wind. Both particle (H^+) flux and density are relatively low and should not cause problems, especially at the velocity at which they are traveling.

The earth radiation decreases as the square of the distance from earth and varies with position angle. The average albedo has been established as 0.39. Based on this fact and the following equations, the effect of earth shine on the lunar surface is considered to be negligible.

Thermal Radiation, $Q = FAI$

Albedo Radiation, $Q = FASa$

where:

Table 5.3 Model Solar Wind

Quantity	Unit	Electrons e^-	Protons H^+	Helium Ions He^{++}
Solar wind flux	$\frac{\text{Particle}}{\text{cm}^2\ \text{sec}}$	10^9	0.93×10^9	7×10^7
Average Velocity	$\frac{\text{km}}{\text{sec}}$	500	500	500
Kinetic energy per particle	Joule	1.1×10^{-19}	2.1×10^{-16}	8.3×10^{-16}
Particle density	$\frac{\text{Particle}}{\text{cm}^3}$	20	18.6	1.4
Number density times kinetic energy per particle	$\frac{\text{Joule}}{\text{cm}^3}$	2.16×10^{-18}	3.87×10^{-15}	1.6×10^{-15}
Temperature,	^{o}K	10^5	10^5	10^5
3kT/2	Joule	24×10^{-19}	24×10^{-19}	24×10^{-19}

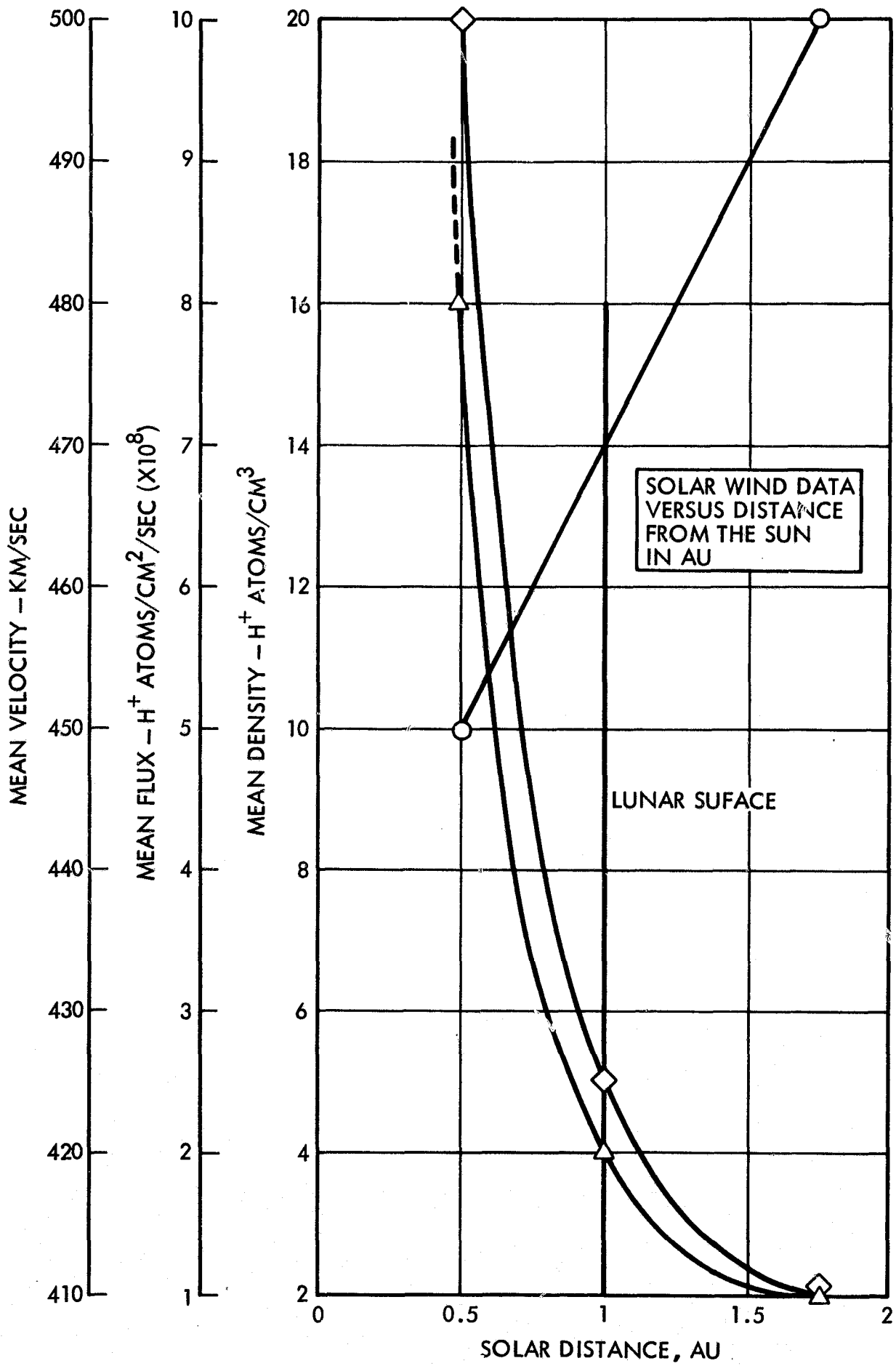

Figure 5.13 Solar Wind Data Vs. Distance from the Sun in AU

Q = radiation flux(w/ m^2)

F = view factor

A = cross section (m^2)
area of spherical
surface

I = earth radiant flux (w/ m^2)

S = solar constant (w/ m^2)
(1 AU)

a = albedo

5.6 LUNAR SURFACE PROPERTIES

The load-bearing strength of the lunar surface high porosity material is such that a static load of 7×10^4 dynes/cm^2 (1 lb/in^2) (Reference 5.1) will penetrate to a maximum depth of 10 cm (3.9 in). Figure 5.14 permits estimate of the depth of penetration for various degrees of static load. A dynamic load of 8.3×10^5 dynes/cm^2 (12 lb/in^2) will penetrate to a maximum of 60 cm (24 inches) into the surface material. No loads of this magnitude are expected to be imposed by the solar array at any time. Recent Surveyor data indicates that even these numbers may be made more negligible as at the landing site a bearing strength of 5 lb/in^2 3.5 cyne/cm^2) was realized. Also soil composition was found to be similar in consistency as wet beach sand.

Based on data in Figures 5.15 and 5.16 (Reference 5.1) as well as data from the Ranger and Survey programs, various lunar crater diameters and heights have been determined. Using these data as a base, Figure 5.17 was developed to indicate the percentage of sunlight time available when obstacles (craters, etc.) of various heights are in the sunline between sunrise and sunset and when these obstacles are at various distances from the viewer (solar array). These values can be reduced to as low as 0.5 if the obstacle is not symetrical and/or the viewer is not centered between obstacles of equal height. For these cases, various combinations of the family of curves shown would be used to establish total sunlight time available. This consideration (location of array) could significantly affect array sizing and power output as a function of lunar phse.

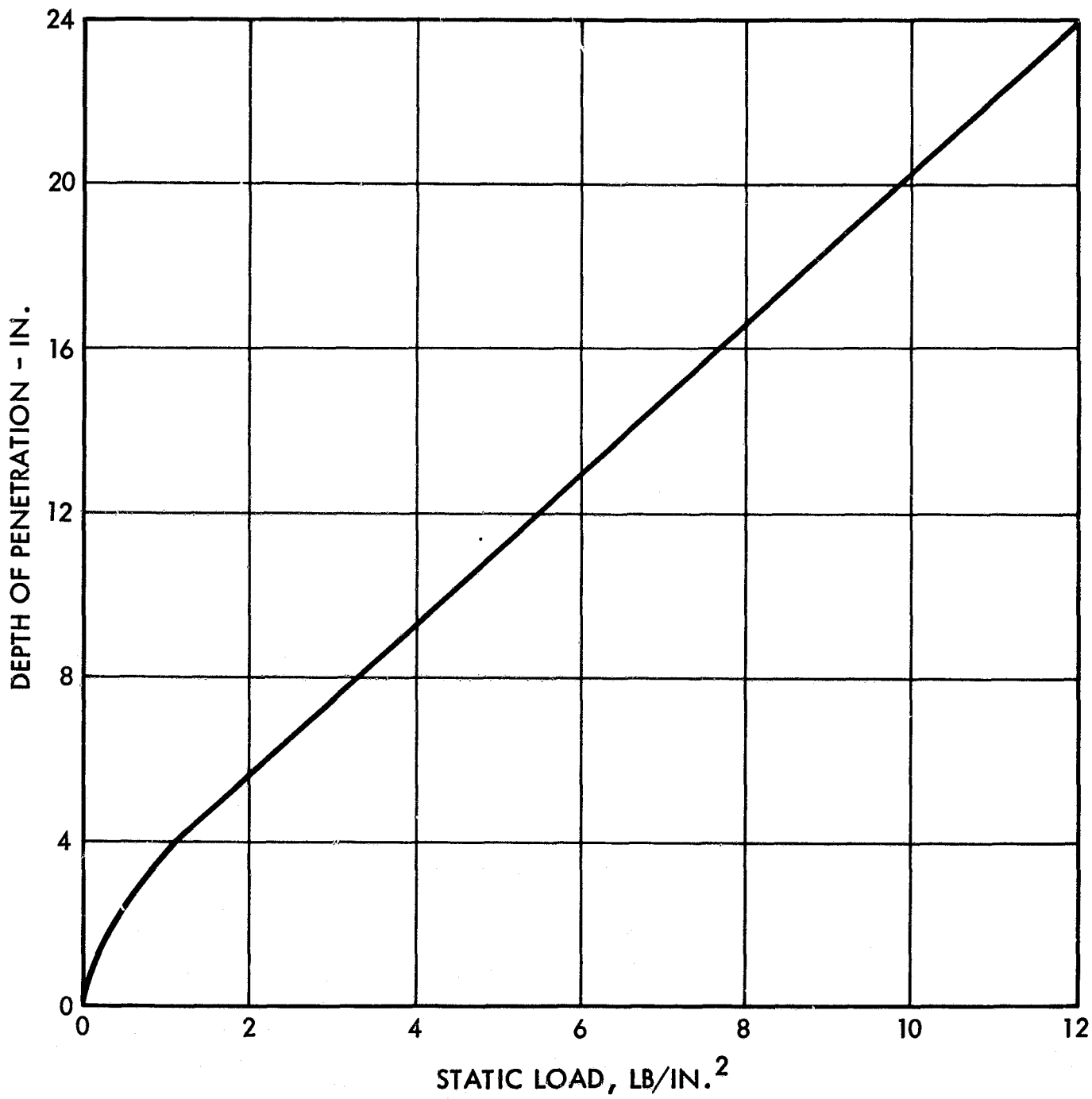

Figure 5.14 Estimated Depth of Penetration of Lunar Surface Versus Static Load Based on Minimum Bearing Strength of the High Porosity Lunar Material

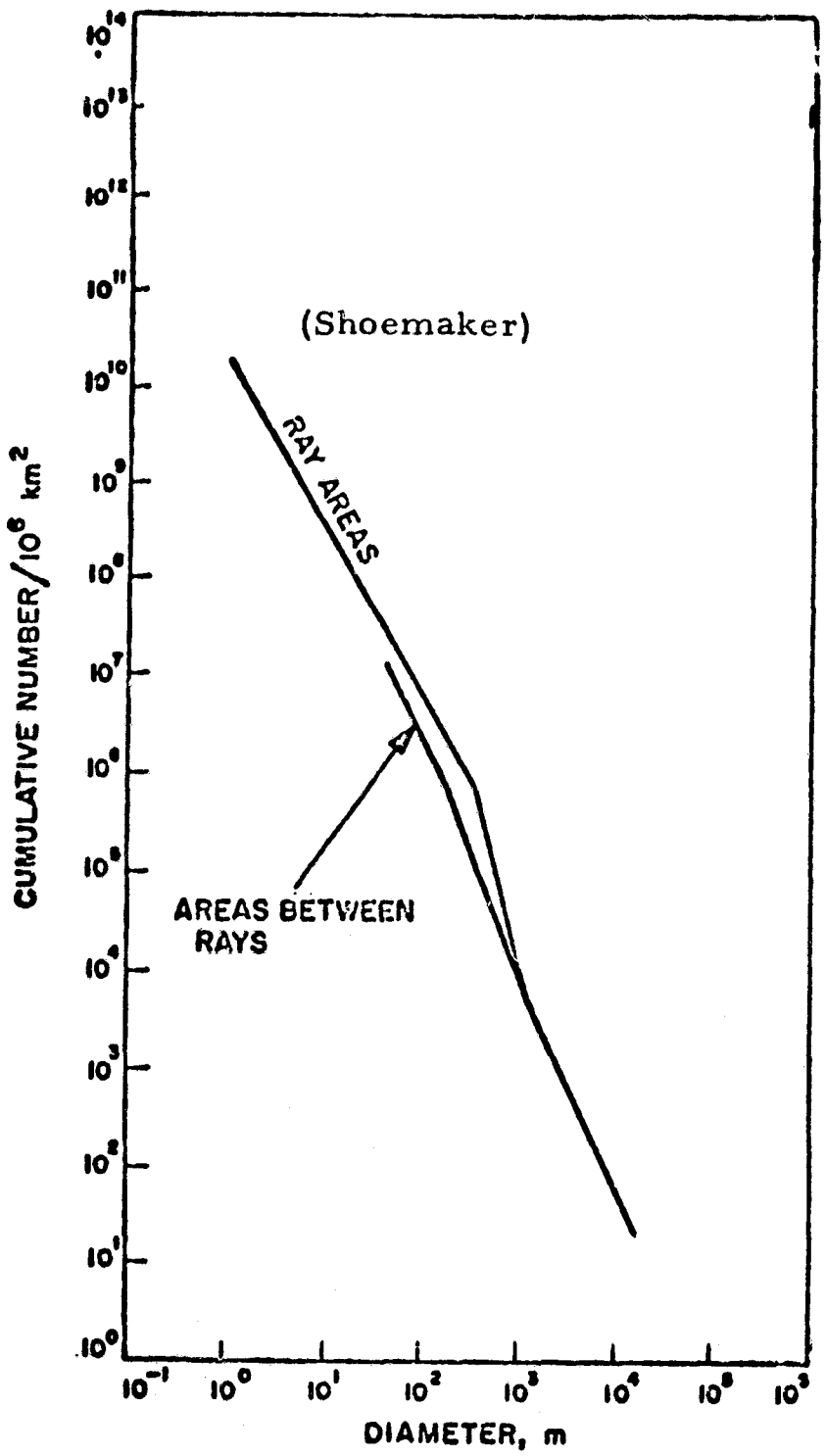

Figure 5.15 Cumulative Size-Frequency Distribution of Craters in Mare Cognitum (Based on Distribution of Craters Observed in Ranger VII Photographs) (Reference 5.1)

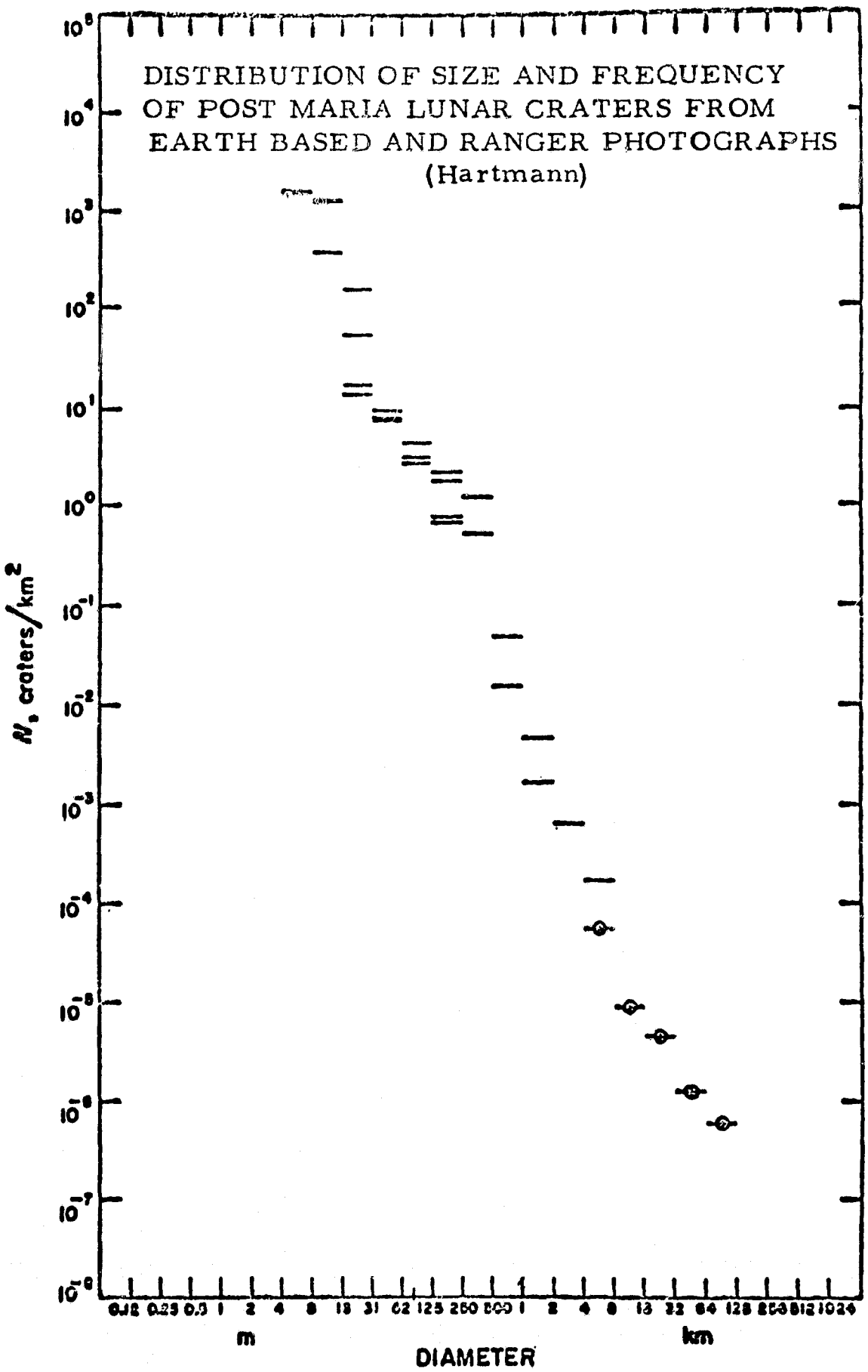

Figure 5.16 Distribution of Size and Frequency of Post Maria Lunar Craters From Earth-Based and Ranger Photographs (Reference 5.1)

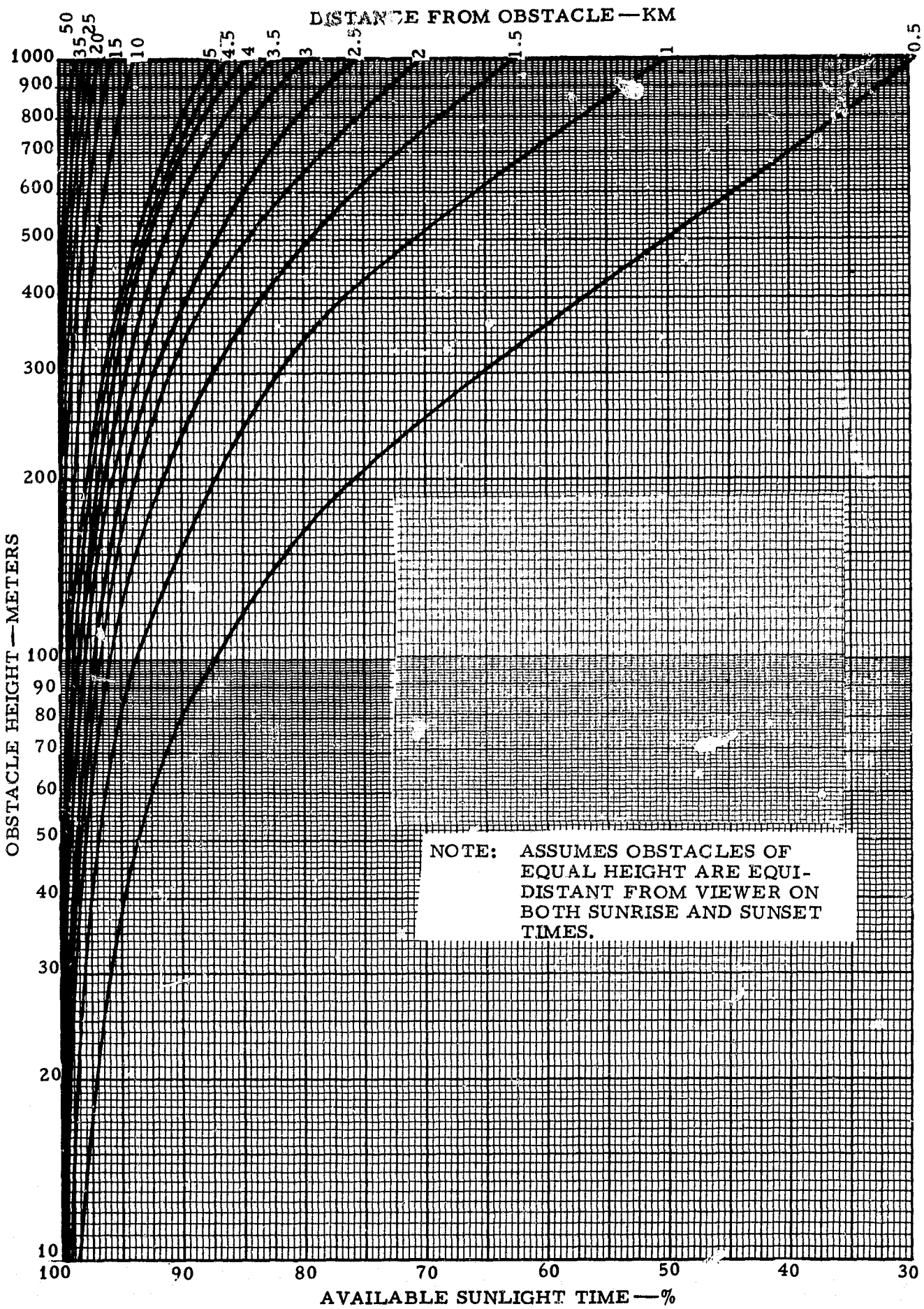

Figure 5.17 Percentage of Sunlight Portion (14.75 Days) of Lunar Day Available Due to Obstacles of Various Heights for Various Distances from the Obstacle

5.7 IMPACT ON SOLAR ARRAY

The moon has a tenuous atmosphere and the principal environmental conditions which could affect the operation of a lunar based solar array were found to be:

- Temperature
- Radiation Levels
- Micrometeoroid bombardment and dust

The most significant environmental parameter effecting solar array operation on the lunar surface is temperature. Solar array equilibrium or average temperatures are a function of lunar surface temperatures, lunar surface properties, lunar phase angle, lattitude and albedo radiation. All these parameters must be evaluated in depth to accurately determine the resulting equilibrium temperatures of the solar array panels. Both radiation and conduction interactions with the lunar surface surroundings must be considered. The thermal modeling utilized must be sufficiently flexible so that a wide range of specific designs and lunar surface environmental conditions can be evaluated. During this study, realistic estimates of array thermal properties (solar absorption, emittance, efficiency, conduction paths, insulation, thermal mass, packing density, etc.), lunar surface properties (absorptance, emittance, conductivity, etc.), and the lunar terrain were made to arrive at a determination of solar array performance (see Section 8.2).

The effects due to radiation levels, micrometeorites and vacuum level on solar arrays when located on the lunar surface do not appear likely to differ very much from those experienced in Earth orbit. Hence, these effects on solar array performance and life were readily extrapolated from data obtained from these type missions. During this study program, these effects were evaluated using previous experimental and operational data and the results of Reference 5.1. By superimposing these environmental effects on the data obtained from the thermal environmental analyses, a more precise assessment of these combined effects on solar array performance and life was obtained.

The major impact of lunar surface g-level (1/6 g) is the influence it has on the selection of the solar array panel size and the techniques and energy requirements associated with array deployment and assembly. The study results (see Section 7.5) indicated it would be desirable not to exceed the physical capabilities of two space-suited astronauts. In addition, manual deployment and assembly were found to be the simplest and most reliable approach to solar array logistic operations.

6. SOLAR ARRAY MATERIALS

6.1 MATERIAL SURVEY

From the lunar environment model presented in Section 5, there are four criteria which must be employed in lunar based solar array materials and processes selection. These are:

- Pressure - The materials discussed have vacuum outgassing characteristics compatible with the environment
- Meteoroids - Erosion rates for the materials discussed are considered to be minimal and it is assumed that detailed design of a solar array will reflect a conservative approach in the form of joint redundancy, etc.
- Radiation - Particulate radiation is considered less severe, except as a result of solar flares, than for earth orbiting or solar probe missions and degradation due to this parameter is expected to be minimal.
- Temperature - The materials discussed were selected for a three-year operation while thermal cycling between minimum - 175°C and +120°C, accumulating approximately 40 thermal cycles during this period.

It was beyond the scope of this study to present a complete listing of materials information in this report. However, Tables 6.1 through 6.9 represent a limited abstract of detailed data presented in Reference 6.1 through 6.7. Though these referenced sources are far from complete, they were sufficiently adequate to permit selection of the various materials making up the solar array and to determine array weights. In the case of the solar arrays, this included not only the cells themselves, but also the cover slide or encapsulant.

The addition of a cover slide to the solar cell has these functions:

a) to protect against micrometeorite errosion;

b) to protect against particulate radiation;

c) to provide the cell with a high thermal emission surface allowing the cell to operate at more moderate temperatures and thus higher performance.

Table 6.6 shows the effects of spectral filter characteristics on the cell performance.

Table 6.1 Solar Cells

TRW Specifications	Material	Application	Single-Crystal or Thin Film	Remarks
None	Silicon $\alpha = 0.70$ $\epsilon = 0.83$	Solar energy Conversion to Electric Power	Single-Crystal	Thickness from 0.004 in. to 0.014 in. and 2 to 10 Ω cm
None	Cadmium Sulfide $\alpha = 0.84$ $\epsilon = 0.87$	Same as Above	Thin-Film	0.001 in. Kapton or Mylar Encapsulated Plastic Substrate
None	Cadmium Telluride $\alpha = 0.85$ $\epsilon = 0.86$	Same as Above	Both	Requires Development Not Now Available

As shown in Figure 6.1, integral covers may not be usable for long lifetime missions due to the effect of micrometeoroids on performance. Covers of at least 0.006 inch thickness will be required. The α and ϵ values of Table 6.1 for silicon cells has already included the use of a red and antireflecting cover slide for its characteristics.

As with all space missions, materials that are selected, even flight proven materials, must undergo qualification in an environment similar to that which it will experience, either individually or as part of the composite system. There are also some materials which must be subjected to special testing programs before they can be considered for use. This situation holds true for the lunar-based solar array except that the quantity of materials requiring special tests is less than for most space applications. In general, materials presently used on Earth orbiting, space probes and for Surveyor type arrays are directly applicable to lunar surface use.

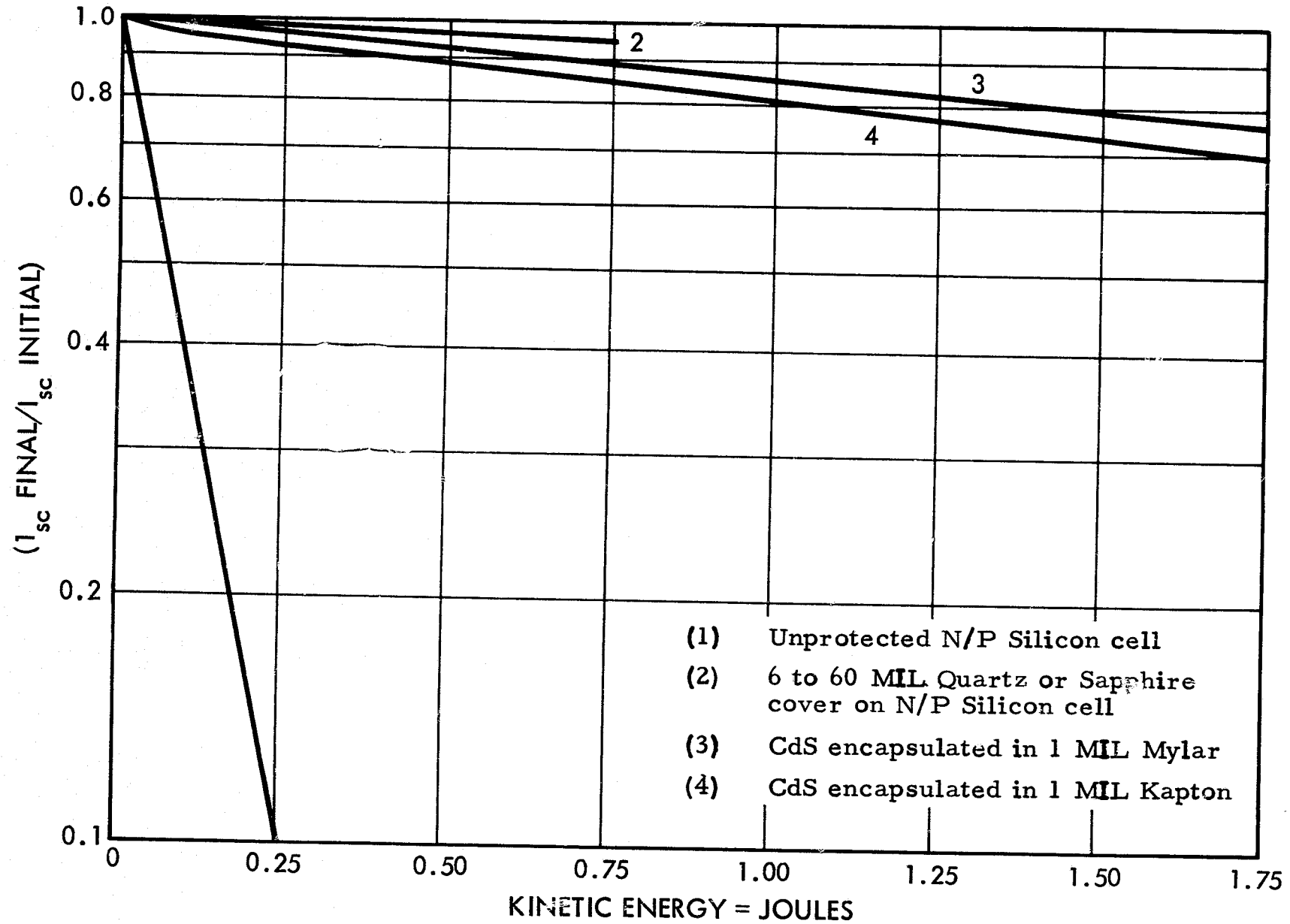

Figure 6.1 Estimate, Based on Laboratory Data, of the Ratio of Initial I_{sc} to Final I_{sc} for Silicon and CdS Solar Cells Versus Kinetic Energy of Cloud of Impinging Micrometeoroid Particles Weighing 10^{-8} to 10^{-12} grams Whose Average Velocity is 2.65 km/sec (Reference 6.6)

Table 6.2 Adhesives

TRW Systems Specification	Material	Application	Single Crystal or Thin Film	Remarks
PR4-1, Type V	General Electric RTV 511, SS4004 Primer	Solar cell to substrate, component wire spot bonds	Mainly single crystal, some thin film applications	Material has demonstrated acceptable low temperature flexibility in rapid cycling. Long term effects of low temperature require evaluation.
None	Urethane	Same as above	Same as above	Certain urethane polymers have known good low temperature properties. Long cure cycles, etc., would make these a candidate only if RTV is unacceptable.
PR4-15, Type I	Dow Corning XR6-3489 XR6-3466 Primer	Cover Glass Adhesive	Single Crystal	Primer use is predicated on design, solar cell parameters.
PR4-28	Narmco 7343 Urethane Adhesive	Semistructural Adhesive Bonds	Both	Each structural bond will require review, however there should be little difficulty in bonding similar materials.
PR10-7, Type I MMM-A-132, Type I	American Cyanamid FM-1000 Epoxy-Polyamide	Structural Substrates, etc.	Both	Mismatched expansion characteristics may fail bonds over this temperature range.
MMM-A-132, Type III	American Cyanamid HT 424, Epoxy	Structural	Both	
MT3-35	Schjeldahl GT 421, 321 Kapton-Polyester Adhesive	Mechanical Interconnect of Solar Cells	Thin Film	High temperature bond strength requires evaluation. May require substitute adhesive.

Table 6.3 Thermal Control Coatings

TRW Systems Specification	Material	Application	Single Crystal or Thin Film	Remarks
MT6-7	Dow Corning 92-007 (Silicone based)	White Thermal Control $\alpha = 0.14 - 0.20$ $\epsilon = 0.84 - 0.9$	Both	Good general properties. Low temperature adhesion requires evaluation.
--	IIT S-13G (Silicone based)	White Thermal Control $\alpha = 0.18 - 0.25$	Both	Same as above
Dwg. C243235	Minnesota Mining Y-9184S Pressure Sensitive Tape	High Reflective Gold Tape $\epsilon = 0.03$	Both	Silicone adhesive version of tape (Y-9184S) is appropriate for low temperature use.
Dwg. C243236	Mystic 7462 Pressure Sensitive Tape	High Reflective $\alpha = 0.11$ $\epsilon = 0.03$ (Aluminum)	Both	Low temperature performance of tape requires evaluation.
MT6-2	Silicate Based Inorganic Paint	White, $\alpha = 0.13$ $\epsilon = 0.85$	Single Crystal	Paint requires high temperature cure cycle complicating assembly.
PR5-13	Minnesota Mining Velvet Black	Black $\alpha = 0.98$ $\epsilon = 0.98$	Both	Probably best UV resistant black. Low temperature adhesion on some substrates requires evaluation.
--	CAT-A-LAC 463-3-8	Black $\alpha = 0.98 \epsilon = 0.98$	Both	
--	Laminar X500	Black $\alpha = 0.98 \epsilon = 0.98$	Both	

Table 6.4 Protective Coatings

TRW Systems Specification	Material	Application	Single Crystal of Thin Film	Remarks
MT3-21, Type I Class 2	Dow Corning Sylgard 182	Conformal Coating of Circuit Board, Components, etc.	Both	Minimum use recommended. Low temperature brittleness of all coatings is known to stress (and fail) diodes, etc.
MIL-A-8625, Type II	Sulfuric Anodize	Aluminum Protection	Both (Supporting Structure)	Preferred over chromic anodize (Type I). Required for dyed coatings.
PR6-6, Type I	Hard Anodize	Aluminum Protection Dielectric Coating	Both (Supporting Structure)	Specify for best abrasion resistance and as dielectric where required.
MIL-C-5541, Class 3	Iridite, Alodine, etc.	General Corrosion Protection of Aluminum	Both (Supporting Structure)	Recommended for general corosion protection and some organic finish pretreatment. Coating is electrically conductive.
MIL-M-45202 Type I, Class C, Type II, Class D	Dow 17	Magnesium	Both (Supporting Structure)	Magnesium corrosion protection.
PR6-5	Solder Plating	Bus Bars	Thin Film	Copper bus bars require plating to insure solderability.
MIL-T-10727, Type I, Fused	Tin Plating	Kovar Interconnect Plating	Single Crystal	Kovar interconnects require plating to insure solderability.

Table 6.5 Wire Insulation, Interconnect and Structural Materials and Miscellaneous Items

TRW Systems Specification	Material	Application	Single Crystal or Thin Film	Remarks
WIRE				
PT3-38	Polyolefin with PVF jacket	Hookup Wire	Both	Wire will not survive flexing at low temperature.
MIL-W-81381/1 or /2	Polyimide Jacketed FEP Tape Wrapped Wire	Hookup Wire	Both	Most radiation resistant wire.
MIL-W-22759 MS 21985	Teflon Insulation	Hookup Wire	Both	Radiation resistance may be marginal in unprotected applications.
INTERCONNECT AND STRUCTURAL MATERIALS				
QQ-C-576	OFHC Copper Foil	Bus Bars	Thin Film	Solder plated for thin film bus bars.
--	Molybdenum	Interconnects	Single Crystal	Best match of expansion characteristics but difficult to solder.
MIL-I-23011, Class 1	Kovar	Interconnects	Single Crystal	Preferred material for this use (small number of temperature cycles).
QQ-S-571, SN63	Solder	Hookup and Electronic Soldering	Thin Film	Solder for gold plated cell contacts.
QQ-S-571, SN62	Solder	Interconnect	Single Crystal	Solder for silver plated cell contacts.
MIL-F-14256, Type A	Flux	Solder Flux	Both	
Various	Aluminum Alloys, 1100, 3003, 2024, 4043, 5052, 5086, 6061, 6062, 6063, 7075, 7158, 356	Support Structure Frames, etc.	Both	All alloys listed are suitable.
Various	Magnesium Alloys, AZ31B, ZK60A, AZ80A, AZ91C	Support Structure, Fames, etc.	Both	All alloys listed are suitable. Special corrosion protection may be applicable.
AMS 7901, 7902	Beryllium	Support Structure, Fames, Substrates, etc.	Both	High fabrication cost makes use practical only for extreme design and weight problems.
MISCELLANEOUS				
MIL-P-13949	Epoxy Laminate Copper Clad	Etched Circuit Boards	Both	Fabricate etched circuits per PR7-5.
MIL-P-18177	Epoxy Laminate	Terminal Boards	Both	Type GEE (general purpose).
MT13-4, Type I and Type II	Sleeving, Heat Shrinkable	Electrical Insulation	Both	Type I is irradiated polyolefin. Type II is polyvinylidene fluoride.
PR4-7, Type IV	Urethane Potting Material	Connector Potting	Both	
PR12-1, Type II, Class 1A	Epoxy Ink	Marking, Identification	Both	
AM 3136	Dry Film	Lubricant	Both	Use for articulation and deployment mechanisms

Table 6.6 Spectral Filter Characteristics (Reference 6.7)

Cell/Filter Combinations	α	ϵ	α/ϵ	T° C	% Po at 28° C	% Power Gain from Bare Cell
Ideal cell	0.700	1.00	0.700	28° C	100	—
Typical bare cell	0.935	0.368	2.54	85° C	77	—
Cell with 0.001 inch SiO coating	0.874	0.642	1.36	63° C	86	4.3
Cell with glass and anti-reflecting coating	0.813	0.835	0.974	46° C	92	15.8
Cell with glass, 1.15 micron red and anti-reflecting coating	0.700	0.835	0.84	35° C	96	11.2

As a guide in material selection, Surveyor solar array data is very useful. From this data it is known that silicon adhesives such as RTV-40, RTV-60, RTV-602 can survive the 260°C (455°F) maximum temperature excursion experienced between lunar noon and lunar midnight. RTV-511 and 577, however, are more desirable (increased reliability) due to their excellent low-temperature characteristics. Silicon solar cells faced with 0.006-in-thick coverglass and thin film cells with plastic encapsulant can withstand (Survey Ground Test and Telemetry Data) the temperature extremes (-240°F to +215°F)(-150°C to +110°C) without significant degradation, and a 0.006-in thick coverglass or 0.001-in thick plastic (Mylar or Kapton) is adequate to survive lunar micrometeoroid showers (Reference 6.6 and Figure 6.1) as well as electron and proton radiation bombardment with no more than the normal percentage degradation as experienced during any space mission (and considerably less than that experienced within the Van Allen Belt).

The radiation thresholds at which various plastic materials and some electronic components can continuously operate and not degrade are shown in Tables 6.7 and 6.8. This data is useful in designing solar arrays and

Table 6.7 Radiation Thresholds of Typical Materials

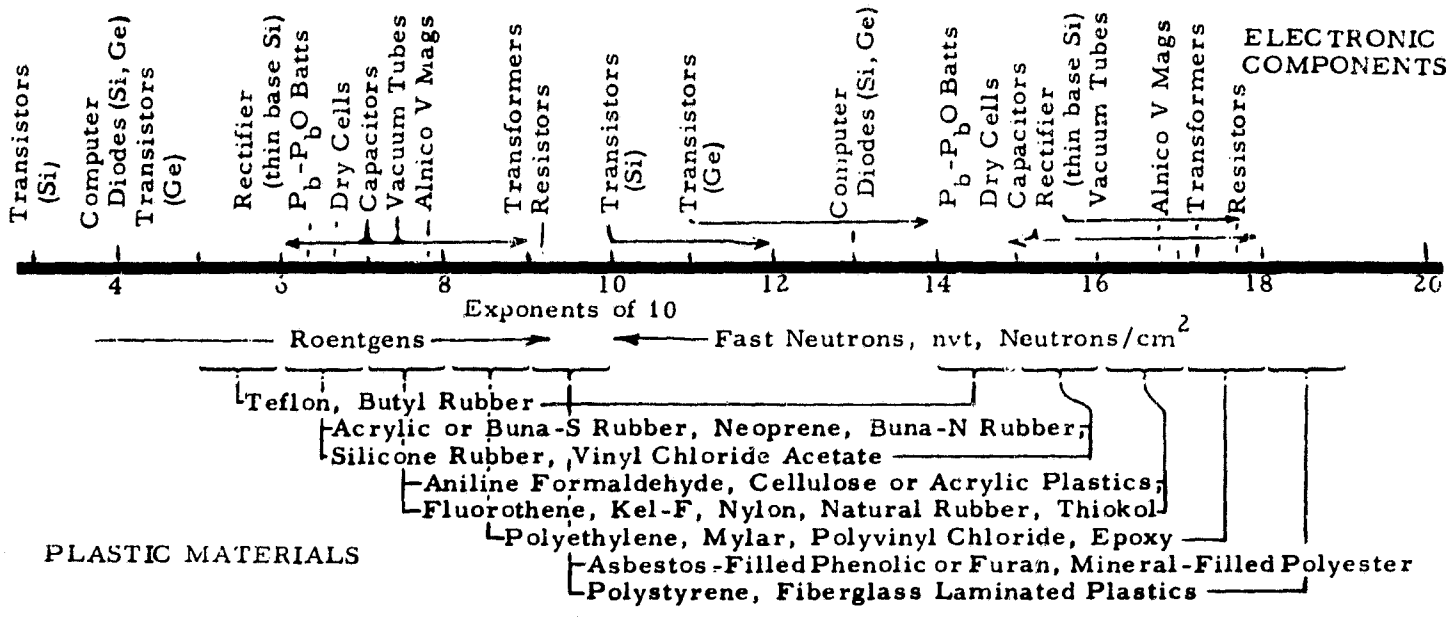

Table 6.8 Radiation Thresholds of Typical Solar Array Materials

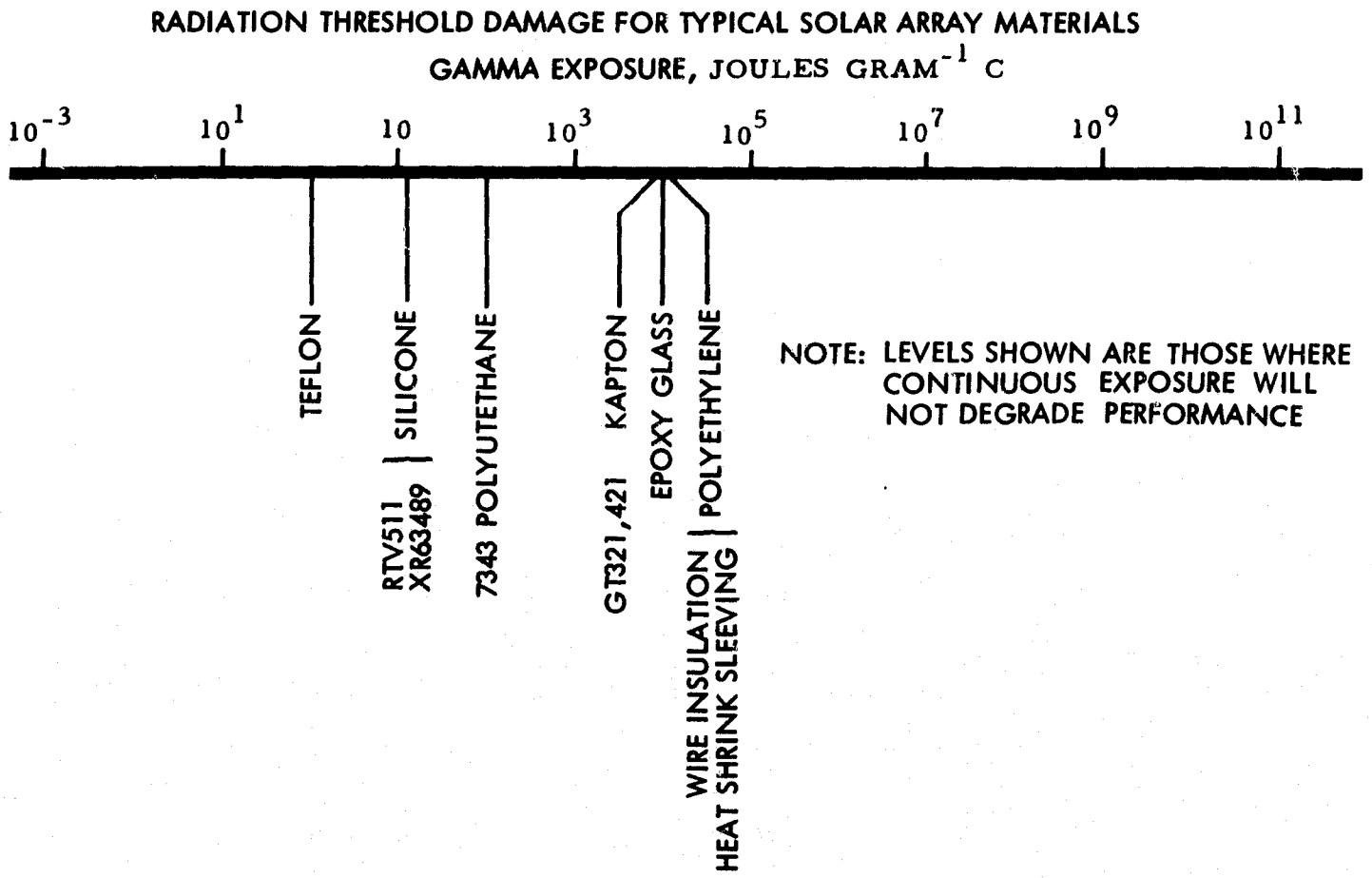

in selecting components which are resistant to the lunar radiation environment.

Both dielectric insulation, when required, and thermal control coating of the array have been satisfied on Surveyor with the use of PT-401, white pigmented, epoxy, paint. Structural materials such as titanium, magnesium, and aluminum have also been used satisfactorily for the Surveyor missions.

Analysis performed for Surveyor, which considered lunar temperature excursions and rapid shock rates (50 to 100°F/min), have demonstrated that although material degradation is not necessarily a problem, components such as copper for cell interconnects are not usable on silicon arrays. Because of the mismatch in differential thermal expansion coefficients between silicon and copper, the electrical contact is severely degraded during deep thermal cycles. Molybdenum, the most acceptable alternative to Kovar A for interconnects, requires investigation (soldering to molybdenum is difficult) before it can be specified for use on arrays which require the maximum use of nonmagnetic materials. Table 6.9 shows the threshold temperatures of typical solar array materials.

TRW Systems has investigated on several in-house programs the possibility of using nonmetallic substrates for single crystal arrays to eliminate separate dielectric insulation requirements. This investigation has been successful and nonmetal structures are being currently used on some recent TRW solar array programs. This technology was considered for use on lunar-based arrays during this study.

The substrate requirement can possibly be eliminated entirely by the use of thin-film cell arrays where the substrate is integral with the cell and is usually made of Kapton, a high-temperature, radiation and ultraviolet resistant, polyamide or similar high temperature space-proven film.

Power transmission cabling deployment and orientation mechanisms (fused) will require engineering optimization during actual design. However, there does not appear to be any basic material problems that would adversely limit the solar array design.

Table 6.9 Temperature Thresholds of Typical Materials

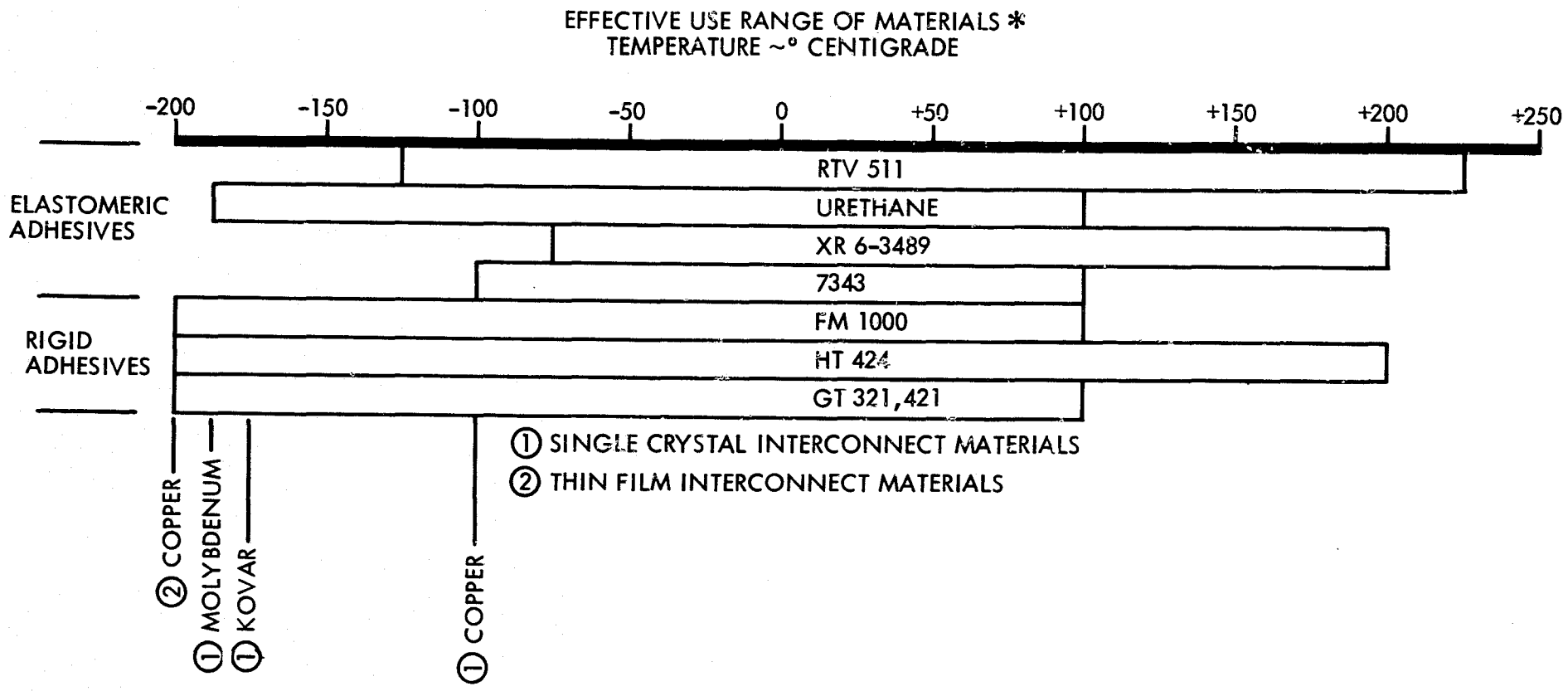

NOTE: TEMPERATURES SHOWN ARE THOSE WHERE CONTINUOUS OPERATION DOES NOT DEGRADE PROPERTIES.

* ELASTOMERIC ADHESIVES, EFFECTIVE USE RANGE FOR BONDING DISSIMILAR MATERIALS. LOW TEMPERATURE REPRESENTS LOSS OF ESSENTIALLY ALL ELASTOMERIC PROPERTIES. HIGH TEMPERATURE LIMIT REPRESENTS LOSS OF ADHESIVE PROPERTIES.

RIGID ADHESIVES, EFFECTIVE USE RANGE FOR BONDING SIMILAR MATERIALS (MATCHED COEFFICIENTS OF THERMAL EXPANSION. LOW AND HIGH TEMPERATURE LIMITS REPRESENT LOSS OF ADHESIVE PROPERTIES.

INTERCONNECT MATERIALS, EFFECTIVE LOW TEMPERATURE USE RANGE FOR INTERCONNECTION OF SINGLE CRYSTAL CELLS. HIGH TEMPERATURE LIMIT IMPOSED BY USE OF SOLDER AND CELL EFFICIENCY LOSS.

7. SOLAR ARRAY DESIGN CONSIDERATIONS

In order to arrive at realistic concepts for the candidate solar arrays, it was essential that available data from industry be evaluated. This included an assessment of the structural, mechanical, and electrical components that are utilized to design a solar array. This section of the report addresses itself to these considerations and establishes the criteria upon which the solar array design concepts were based. In addition, in keeping with the objectives of this study, parametric design data was developed for future lunar surface power system applications.

7.1 STRUCTURAL CONCEPTS

The various structural concepts from industry, as described in References 7.1 to 7.24, cannot be directly compared on a mass-to-area ratio basis, since each configuration has been designed to satisfy various specific spacecraft system requirements. Array size, load power profile, vibration and shock environment, and stowage and deployment techniques all differ for each case. Therefore, in order to arrive at a meaningful comparison, each of the array concepts has been resized to place them on a common basis.

7.1.1 Comparison of Candidate Concepts

There are several companies who are currently actively engaged in solar array development. These include Hughes, Ryan, Fairchild-Hiller, General Electric, Boeing, Electro-Optical Systems, and TRW Systems. During the course of this study, the work being conducted by these companies was evaluated. The results are summarized in Tables 7.1 and 7.2. The following assumptions formed the basis under which these concepts were compared:

Rigid Panels

1) Individual panel size: 39.00 x 96.00 inches

2) Weight of cells, wires, etc., to be uniform distributed load of 0.24 lb/ft^2 (6.25 lb/panel)

3) Maximum allowable stress to be 75 percent of structure yield stress when subjected to 1 Earth "g" with panel horizontal and supported at each of 4 corners (2 man-hand carry)

FOLDOUT FRAME

Table 7.1(a) Comparison of Original Solar Array Configurations

Structure Array Type	Concept Contractor	Descriptive Sketch	Construction Description	Ce Ty
F L E X I B L E	Hughes	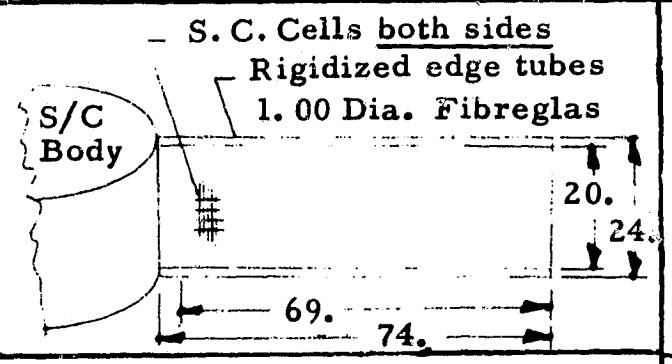	Substrate: 0.0012 Teflon impreg. fiberglass Edge tubes stiffened chemically after inflation Stowed by wrapping on S/C body with 0.150 thick cushion Stowed Volume 0.16 ft^3	Sing Cry
	Ryan	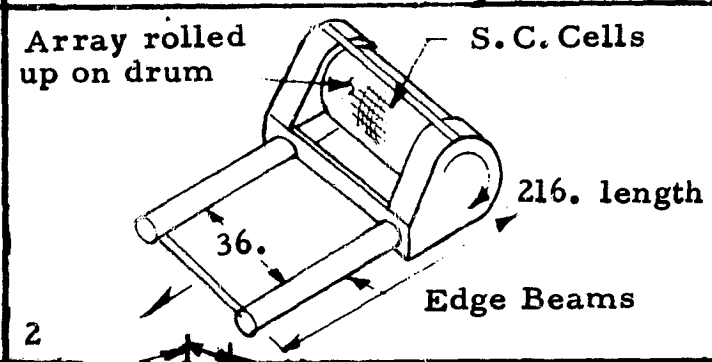	Substrate: 0.003 epoxy fiberglass drum: 1 ft. dia. x 43 long x 0.025 mag. sht. Mech. const.: Alum, Mag, Plastic Deployment: Electric motor drive Beams: Titanium - Flattened for roll up Stowed Volume 10 ft^3	Sing Crys
	Fairchild Hiller	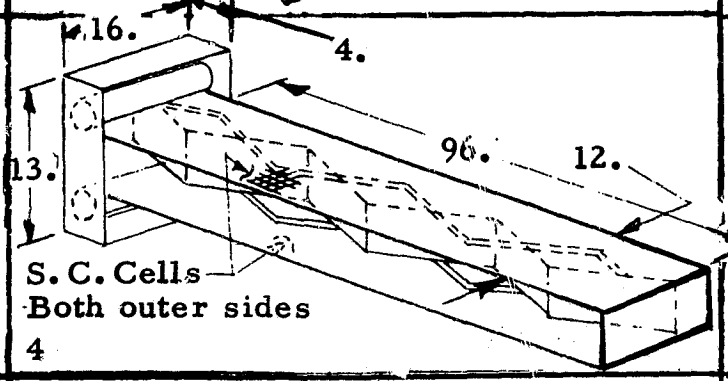	Substrate: Mylar film/with lateral stiffener strips of fiberglass Mech. Const.: Alum, Mag, Plastic Deployment: Electric motor driven scissors Stowed Volume 0.48 ft^3	Sing Crys
	General Electric	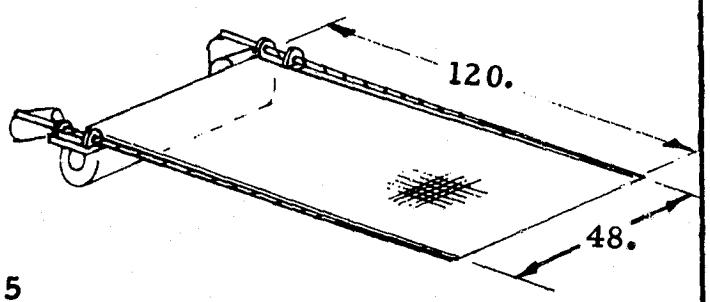	Substrate: Kapton film Drum: 4 ft. long Deployment: 2 Hunter-Stacer spiral tubes with synchronized electric motor drive Stowed Volume 6ft^3 (est)	Cadm Telu Thin Film (7.15 ft^2 on G repo
	TRW Systems	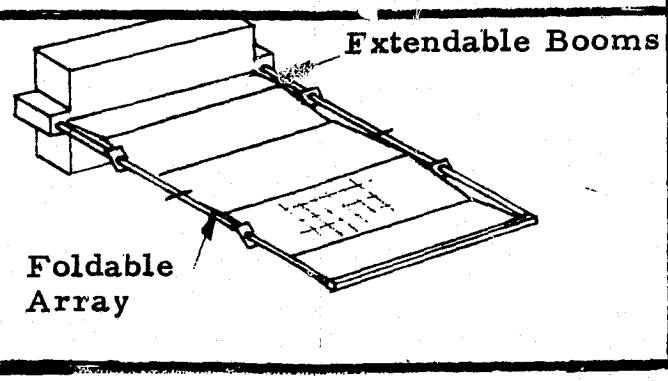	Substrate: Kapton film-stiffened by metal strips bonded at fold lines and by maintaining corrugated pattern Deployment by DeHaviland Booms Stowed Volume 2 ft^3	Cadm Sulfi Thin Film

FOLDOUT FRAME

tions

scription	Cell Type	Design Power Level Watts	Array Total Weight Lbs	Total Array Area Ft^2	Power to Weight Goal W/Lb ; W/Kg	Total Array Density Lb/ft^2 Kg/M^2	Approx Dens. Less Deployment System Lb/ft^2 Kg/M^2	Stowage Effic. Ft^2/Ft^3
on impreg. fiber- emically after S/C body with	Single Crystal	29	6.6	19.2	9.2 / 4.16	2.9 / 1.42	2.9 / 1.42	120
y fiberglass drum: 025 mag. sht. Mag, Plastic motor drive attened for roll up	Single Crystal	500	34.6	50	14.5 / 6.58	0.69 / 3.38	0.30 / 1.47	5.0
/with lateral rglass Mag, Plastic motor driven 3	Single Crystal	80 (est)	12.86	16 (8 ft^2 per side)	6.24 / 2.83	0.80 / 3.92	0.43 / 2.11	33.0
n -Stacer spiral d electric t)	Cadmium Teluride Thin Film (7.15 W/ ft^2 based on GE report)	135 (est)	35.45	40	3.8 / 1.72	0.89 / 4.36	0.18 / 0.88	8.0 (est)
n-stiffened by fold lines and ated pattern iland Booms	Cadmium Sulfide Thin Film	2	92.5	491	27 / 12.2	0.19 / 0.93	0.09 / 0.43	246

Table 7.1 (b) Various Solar Array Concepts Adapted to Flat Array Configuration

Structure Array Type	Concept Contractor	General Adaptability	Array Power to Area Ratio at Lunar Noon W/ft^2; W/M^2	Density $\frac{Lb}{Ft^2}$; $\frac{Kg}{M^2}$	Additional Mounting Structure Lb/ft^2	For 2.5 KW Array Total Area Ft^2; (M^2)	For 2.5 KW Tot. Array Weight Lb;Kg	Stowage Efficiency Ft^2/Ft^3	Total Array Specific Weight W/Lb; W/Kg
FLEXIBLE	HUGHES	Inflatable-Chemical rigid Tubes not considered as suitable for Astronaut actuation	7.15 / 79.4	0.29 / 1.42	0.01	350 / 31.5	101 / 223	33	24.8 / 11.2
	RYAN	Automatic stiffening Beams are suitable Drive motor not required Stow in 8 ft. x 3 ft. dia. rolls	7.15 / 79.4	0.30 / 1.47	0.01	350 / 31.5	105 / 231	33	23.8 / 10.8
	FAIRCHILD HILLER	Highly mechanized Deployment not required Substrate concept alone suitable for Astronaut rollout	7.15 / 79.4	0.43 / 2.11	0.01	350 / 31.5	150 / 330	33	16.6 / 7.5
	GENERAL ELECTRIC	Highly mechanized deployment not required Substrate not stiff	- / -	0.18 / 0.88	0.01	- / -	- / -	3.2	- / -
	TRW SYSTEMS	Highly mechanized deployment not required Substrate suitable for Astronaut deployment	3.75 / 41.6	0.09 / 0.43	0.01	668 / 60.2	60 / 132	206	41.7 / 18.9

Table 7.1 (c) Various Solar Array Concepts Adapted to Leanto Array Configuration

Structure Array Type	Concept Contractor	General Adaptability	Array Power to Area Ratio at Lunar Sunrise W/ft^2 W/M^2	Density Lb/ft^2 ; Kg/M^2	Additional Mounting Structure Lb/ft^2	Array Total Area Ft^2;M^2	Total Array Weight Lb ; Kg	Stowage Efficiency Ft^2/Ft^3	Total Array Spec. Wt. W/lb;W/Kg
FLEXIBLE	HUGHES	Inflatable-Chemical rigid Tubes not considered as suitable for astronaut actuation	6.94 / 77	0.29 / 1.42	0.03	360 / 32.4	104 / 228	33	23.9 / 10.8
	RYAN	Automatic stiffening Beams are suitable Drive motor not required Stow in 8 ft. x 3 ft. dia. rolls	6.94 / 77	0.30 / 1.47	0.03	360 / 32.4	108 / 237	33	23.1 / 10.5
	FAIRCHILD HILLER	Highly mechanized Deployment not required Substrate concept alone suitable for astronaut rollout	6.94 / 77	0.43 / 2.11	0.04	360 / 32.4	155 / 341	33	16.2 / 7.35
	GENERAL ELECTRIC	Highly mechanized Deployment not required Substrate not stiff	- / -	0.18 / .88	0.03	- / -	- / -	3.2	- / -
	TRW SYSTEMS	Highly mechanized Deployment not required Substrate suitable for Astronaut deployment	4.56 / 50.7	0.09 / 0.43	0.03	545 / 49	49 / 108	206	50.7 / 23

Table 7.1(d) Comparison Between Flat and Leanto Configurations

Structure Array Type	Concept Contractor	Total Array Area (ft^2)	Stowage Efficiency (ft^2/ft^3)	Stowed Total Array Volume (ft^3)	Deployed Power/ Stow. Vol. (kw/ft^3)	Total Weight of Array lbs.; Kg
FLEXIBLE	Hughes	355	33	10.7	233	102.5 / 47.7
	Ryan	355	33	10.7	233	106.5 / 48.3
	Fairchild Hiller	355	33	10.7	233	152.5 / 69.3
	General Electric	--	3.2	--		--
	TRW Systems	606 1/2	206	2.68	930	226 / 102.8
	Average	416	76 1/4	8.7	407 1/4	146 1/2 / 66.5

Rollup Arrays (Single Crystal and Thin Film Solar Cells)

1) Rollup on 8 ft long, 6 in diameter cores

2) Maximum rollup diameter 3 ft

3) Silicon cell rollups to include foam cushion of 0.25 in thickness per rolled up layer

4) Thin film cell rollups are sufficiently durable to rollup and stow without interlayer cushions

A sketch of each concept is shown on Tables 7.1(a) and 7.2(a) and a brief description of each design concept is outlined below:

(a) Hughes (Flexible)

This panel concept consists of a single crystal silicon cells on a 0.0012 in thick Teflon impregnated Fiberglas substrate. The substrates are rolled up on the body of a cylindrical spacecraft. No mechanization is required other than holding straps, as deployment is accomplished by centrifugal force from the spacecraft rotation. Panel rigidization is achieved by inflation and chemical rigidization of lengthwise Fiberglas tubes. This method of rigidization is not considered a suitable or desirable method of manual deployment on the lunar surface.

(b) Ryan (Flexible)

The substrate for this concept consists of an 0.003 in thick epoxy Fiberglas sheet on which single crystal silicon cells are mounted. The substrate is stowed on a cylindrical drum 12 inches in diameter by 43 inches long. Deployment is implemented by motor/geartrain actuation. The deployed substrate is rigidized by extendible edge beams similar to the TRW Systems' closed-section boom. This type of boom, because it rigidizes automatically when unrolled, is considered suitable for astronaut deployment.

(c) Fairchild-Hiller (Flexible)

The substrate for this concept consists of a Mylar film with lateral rigidizing strips of Fiberglass (longitudinal in the rolled-up mode) on which single crystal silicon cells are mounted. The substrate is stowed on a cylindrical drum. Deployment is accomplished by a multi-element pantograph mechanism. The Fiberglass strip method of stiffening one direction of the rollup is considered suitable for astronaut deployment and is considered applicable to the leanto support structure as shown in Figure 7.22.

(d) General Electric (Flexible)

The substrate for this concept consists of a Kapton film on which thin film solar cells are mounted. The substrate is stowed on a cylindrical drum 12 inches in diameter by 48 inches long. Extendible boom deployment is utilized. The substrate, without the booms, is flexible in all directions and is considered to be difficult for astronaut deployment without the addition of stiffeners in one direction.

(e) TRW Systems (Flexible Foldup)

The substrate for this concept consists of rectangular Kapton film panels, 31 inches by 88 inches, accordian hinged to stow in a flat stack. The substrate has thin film solar cells mounted on it, but the concept is equally capable of mounting single crystal silicon cells as well, providing a necessary protective cushion between cell layers is incorporated. Deployment is accomplished by a pair of synchronized extendible booms, one located on each edge of the stowed array. Each of the rectangular panels is connected to the booms with sliding loops or "oarlocks". The booms and loops provide edge stiffening for the extended array. The accordion folded panels, with added stiffening at the panel hinges, is considered suitable for astronaut deployment.

(f) Electro-Optical Systems (Rigid Panel with Electroformed Core)

This substrate concept consists of a pair of facesheets separated by tubular non-tangent separators, with the facesheets within the diameter of the tubes removed. The substrate is formed as segments of a sphere (biconvex) by electroplating over a mandrel which is subsequently etched away. The substrate is supported by a beamed frame made up of 57 inch square modules. A demonstration model, fabricated on a nickel substrate with aluminum frame is planned, with the final units fabricated of an aluminum substrate with a beryllium frame.

It should be noted that the high stiffness-to-weight ratio of this structure depends on the biconvex configuration. EOS reports (Reference 7.14) show that the weight becomes excessive at slope angles of less than 5°, indicating that this structural concept is efficient only in spherical curved panels.

The stress analyses related to this type of structure are sufficiently complex as to require computer solutions. Therefore, the resizing of this type of thin shell to the lunar base requirements was considered beyond the scope of this study. Hence, Table 7.2 reflects values in the "adapted" columns that are identical with the "original configuration" parameters.

(g) Boeing (Rigid Panel with Beryllium Box Beam)

The panels for this concept consist of a main edge frame formed of double box beams with secondary beams dividing the panel into smaller, square, open sections. The open sections are cross-laced with Fiberglass tapes, 0.2 in wide by 0.003 inch thick, on a 0.8 inch grid. The gridwork of tapes forms the substrate on which are mounted single crystal silicon cells.

In the original configuration, multiples of the panels are stowed in a stack on the spacecraft, and are hinged to deploy into "wings" 65 feet long. The panel structures are designed to accommodate attitude control maneuver loads, which results in a weight increase on the inboard panels.

(h) TRW Systems (Rigid Panel with Beryllium Cap Aluminum Honeycomb Core Beam)

The substrate for this concept is similar to the Boeing-type and consists of Fiberglass tapes cross-laced to form a supporting web for the single crystal silicon cells. The arrangement of the frame beams would also be the same. The main difference between TRW Systems' concept and the Boeing configuration is the construction of the beams. The TRW Systems beams are formed of flat beryllium cap strips (to take the bending loads) separated by an aluminum honeycomb core. The advantage of this design over the Boeing beryllium box beam is the elimination of a complicated hot-creep forming operation for the channels and a weight reduction due to the honeycomb core being more structurally efficient in shear than the shear webs of the box beams. This concept is considered to be very suitable for astronaut deployment.

(i) TRW Systems (Rigid Panel with Boron Cap Aluminum Honeycomb Core Beam)

This concept is similar to the TRW Systems Beryllium Cap rigid panel except that the caps consist of boron filaments in an epoxy Fiberglass laminate with the cross-laced tape substrate consisting of boron filaments with an epoxy binder. Preliminary weight versus area calculations indicate an efficiency for this construction equal to the TRW Systems Beryllium Cap beam but with an estimated much lower cost for future fabrication. Detail stress analyses have resulted in an extremely low weight design. The much higher value of Young's modulus of elasticity (E) for boron permits an increase in the allowable tensile stress for the substrate lattice, thus effecting a significant weight reduction in the beam design along the axis designed to support the tape pretension loads. This structural concept is also considered to be highly suitable for astronaut deployment.

(j) TRW Systems (Rigid Panel for SIVB Orbital Workshop (AAP)

The substrate for this concept consists of panels formed of aluminum honeycomb core and epoxy Fiberglass factsheets. The panels are then supported within a larger structure by aluminum channels and "T" sections. This configuration was designed to more demanding criteria than the other rigid panels. Therefore, the weight-to-area ratio is somewhat higher. The basic honeycomb panels are considered to be slightly less efficient on a weight per unit area basis than the cross-laced substrate panels. The concept is considered suitable for astronaut deployment.

(k) TRW Systems (Rigid Panel with Boron Tube)

The basic structural concept of the TRW Systems Boron Tube array is similar to the previous listed frame and cross-laced substrate concepts in that the basic structural support is provided by a system of square tubular members supporting a network of cross-laced substrate ribbons with support of the single crystal silicon cells. The basic difference between this concept and the other cross-laced panels is in the construction of the beams. In this concept, a beam construction has been implemented that consists of square tubes formed of lengthwise boron filaments in a laminate of epoxy resin and Fiberglass cloth arranged at $\pm 45^{\circ}$ angle to the boron filaments. Preliminary stress calculations indicate a structural efficiency equal to the other cross-laced substrate concepts. Similarly, this concept is also considered to be a suitable candidate for astronaut deployment.

(l) Boeing - V-Ridge Concentrator

The V-Ridge concentrator concept studied by Boeing for NASA is not considered applicable to this mission for several reasons. The most important of these are discussed briefly.

Although solar energy concentration can achieve an increase in array performance, it can also result in an increased array temperature. In an environment such as on the lunar surface where high daytime temperatures are a major design consideration, the overall effect would be a decrease in performance. This concept is primarily applicable for missions to Mars and beyond, where concentration of solar energy is required to maintain array performance despite a decreasing solar radiation intensity and to provide for thermal control.

FOLDOUT FRAME

Table 7.2(a) Comparison of Original Solar Array Configurations

Structure Array Type	Concept Contractor	Descriptive Sketch	Construction Description		Cell Type
R I G I D	E.O.S.	R = 163.25 Spherical Radius 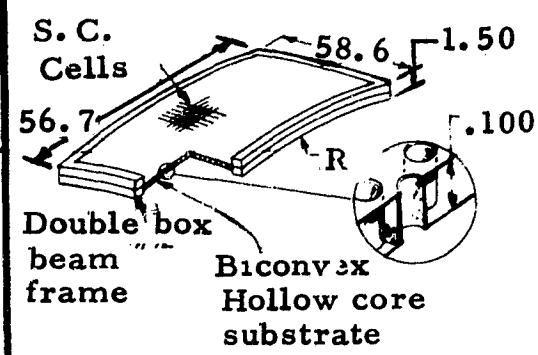 6	Box beam frame: Sheet metal fab hollow core substrate: Electro deposited on a mandrel which is subsequently removed by etching	Demo. module: .010 alum. beams .002 nickel Hollow core S towed vol. 2.9 ft^3	Demo. Model
	E.O.S.		Box beam frame: Sheet metal fab hollow core substrate: Electro deposited on a mandrel which is subsequently removed by etching	10 Kw jupiter flyby: 0.010 beryllium beams 0.002 alum. hollow core	Single Crystal
	Boeing	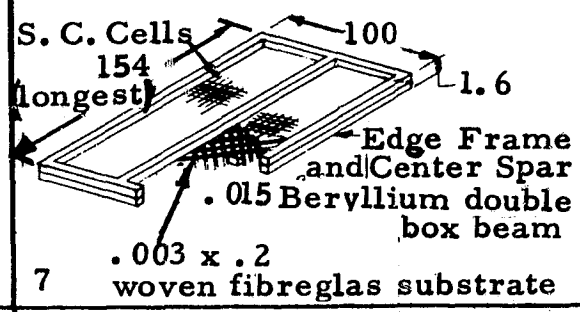 7	Substrate: .003 x .2 woven fiberglass tapes on .8 pitch. mech. const.: .015 hot creep formed beryllium box beams-epoxy bonded edge frame and center spar; double box intercostals; single box deployment; 13 panels, hinged, and winch and cable deployed to form wing 777" long x 300" wide Stowed Volume: 575 ft^3		Single Crystal
	TRW Systems Beryllium Honeycomb Beam	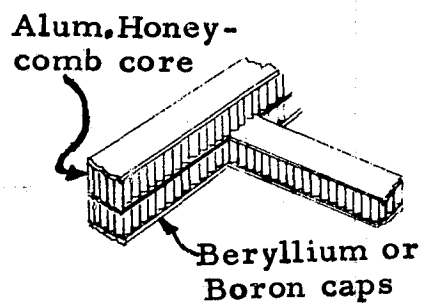 8	Substrate: Same as Boeing Beams: Alum. Honeycomb Core Beryllium Caps. Stowed Volume: 575 ft^3		Single Crystal
	TRW Systems Boron Honeycomb Beam		Substrate: Same as above except tapes are boron filaments Beams: Alum. honeycomb core boron filament caps Stowed volume: 575 ft^3		Single Crystal
	TRW Systems S 14 B Panel	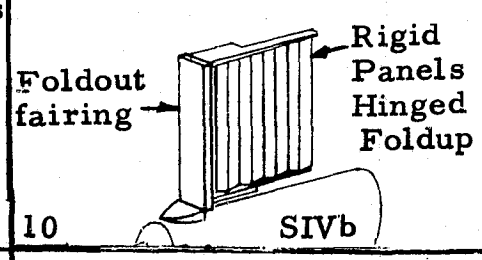 10	Substrate: Subpanels approx. 6.3 ft^2 consisting of .375 honeycomb 3.1 lb/ft^3 core; .016 alum. face sheets. 14 subpanels formed into each rigid panel by alum. alloy channel and "T" beams. Stowed volume: 575 ft^3		Single Crystal
	TRW Systems Boron Tube	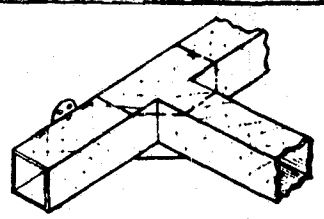	Substrate: Same as TRW Systems Boron Honeycomb beams: Square tubes formed of boron filaments lengthwise; with 2 wraps at + 45° of fiberglass Gussets: Beryllium sheet Stowed volume: 575 ft^3		Single Crystal

	Cell Type	Design Power Level Watts	Array Total Wt. Lbs	Total Array Area Ft^2	Power to Weight Goal W/lb; W/Kg	Total Array Density Lb/ft^2 Kg/M^2	Approx Dens. less Deployment System Lb/ft^2 Kg/M^2	Stowage Efficiency Ft^2/Ft^3
le: beams 2.9 ft^3	Demo. Model	--	9.0	23	-- / --	0.39 / 1.52	-- / --	7.9
r m beams ollow	Single Crystal	10 kw	285	1239	36.6 / 16.6	0.23 / .90	0.26 / 1.27	7.9
rglass : .015 beams- nter ngle ed, and n wing	Single Crystal	45.9 kw	2101	4590	21.8 / 9.9	0.46 / 1.79	0.16 / .78	8.0
ms: um	Single Crystal	--	1858	4590	24 (est.) / 10.9	0.40 / 1.56	0.14 / .69	8.0
t	Single Crystal	--	1858	4590	24 (est) / 10.9	0.40 / 1.56	0.14 / .69	8.0
.3 ft^2 1 lb/ . 14 l panel beams.	Single Crystal	10 kw	1266	1214	8.24 / 3.74	1.04 / 5.10	0.17 / .83	15.8
ns e tubes wise; ss	Single Crystal	--	1858	4590	24 (est) / 10.9	.40 / 1.56	0.14 / .69	8.0

Table 7.2 (b) Various Solar Array Concepts Adapted to the Flat Array Configuration

Structure Array Type	Concept Contractor	General Adaptability	Array Pwr to Area Ratio at Lunar Noon W/ft² / W/M²	Density Lb/ft² / Kg/M²	Add. Mounting Structure Lb/ft²	Array Total Area Ft² / M²	Total Array Wt. Lb / Kg	Stowage Efficiency Ft²/Ft³	Total Array Spec. Wt. W/Lb / W/Kg
RIGID	E.O.S.	Generally suitable subject to denting Biconvex bulge (req. for stability) could cause handling and stowage difficulties	7.15 / 79.4	0.39 / 1.52	0.02	350 / 31.5	136 / 300	16	19.6 / 8.9
	E.O.S.		7.15 / 79.4	0.23 / .90	0.02	350 / 31.5	80 / 176	16	33.4 / 15.1
	Boeing	Highly suitable for deployment-stowage efficiency is poor	7.15 / 79.4	0.50 / 2.45	0.02	350 / 31.5	175 / 385	16	15.3 / 6.9
	TRW Systems Beryllium Honeycomb Beam	Highly suitable for deployment-stowage efficiency is poor	7.15 / 79.4	0.40 / 1.56	0.02	350 / 31.5	140 / 308	16	19.1 / 8.7
	TRW Systems Boron Honeycomb Beam	Highly suitable for deployment-stowage efficiency is poor	7.15 / 79.4	0.40 / 1.56	0.02	350 / 31.5	140 / 308	16	19.1 / 8.7
	TRW Systems S IV B Panel	Highly mechanized deployment not req'd Sub panel concept suitable with possible addition of edge	7.15 / 79.4	1.04 / 5.10	0.02	350 / 31.5	364 / 802	16	7.35 / 3.33
	TRW Systems Boron Tube	Highly suitable for deployment-stowage Efficiency is poor Structural weight is lower than other rigid panels	7.15 / 79.4	0.40 / 1.56	0.02	350 / 31.5	140 / 308	16	19.1 / 8.7

Table 7.2(c) Various Solar Array Concepts Adapted to the Leanto Array Configuration

Structure Array Type	Concept Contractor	General Adaptability	Array Power to Area Ratio at Lunar Sun-Rise W/ft² / W/M²	Density Lb/ft² / Kg/M²	Add. Mounting Structure Lb/Ft²	Array Total Area Ft² ; M²	Total Array Wt Lb ; Kg	Stowage Efficiency Ft²/Ft³	Total Array Spec. Wt W/Lb / W/Kg
RIGID	E.O.S.	Generally suitable subject to denting Biconvex bulge (req. for stability) could cause handling and stowage difficulties	6.94 / 77	0.39 / 1.52	0.04	360 / 32.4	140 / 310	16	17.8 / 8.10
	E.O.S.		6.94 / 77	0.23 / .90	0.04	360 / 32.4	83 / 183	16	30.0 / 13.6
	Boeing	Highly suitable for deployment-stowage efficiency is poor	6.94 / 77	0.50 / 2.45	0.05	360 / 32.4	180 / 397	16	13.8 / 6.27
	TRW Systems Beryllium Honeycomb Beam	Highly suitable for deployment-stowage efficiency is poor	6.94 / 77	0.40 / 1.56	0.05	360 / 32.4	144 / 317	16	17.3 / 7.85
	TRW Systems Boron Honeycomb Beam	Highly suitable for deployment-stowage efficiency is poor	6.94 / 77	0.40 / 1.56	0.05	360 / 32.4	144 / 317	16	17.3 / 7.85
	TRW Systems S IV B Panel	Highly mechanized deployment not req'd. Sub panel concept suitable with possible addition of edge	6.94 / 77	1.04 / 5.10	0.06	360 / 32.4	375 / 825	16	6.68 / 3.03
	TRW Systems Boron Tube	Highly suitable for deployment-stowage efficiency is poor Structural weight is lower than other rigid panels	6.94 / 77	0.40 / 1.56	0.05	360 / 32.4	144 / 317	16	17.3 / 7.85

Table 7.2(d) Comparison Between Flat and Leanto Configurations

Structure Array Type	Concept Contractor	Total Array Area (ft^2)	Stowage Efficiency (ft^2/ft^3)	Total Array Volume (ft^2)	Deployed Power/ Stow. Vol. (Kw/ft^3)	Total Array Wt. (lbs)
RIGID	E.O.S.	355	16	22.2	113	138
	E.O.S.	355	16	22.2	113	81.5
	Boeing	355	16	22.2	113	177.5
	TRW Systems Beryllium Honeycomb Beam	355	16	22.2	113	142
	TRW Systems Boron Honeycomb Beam	355	16	22.2	113	142
	TRW Systems S IV 8 Panel	355	16	22.2	113	369
	TRW Systems Boron Tube	355	16	22.2	113	142
	Average	355	16	22.2	113	170

7.1.2 Concept Considerations

Both flexible and rigid panel solar arrays can be considered for the lunar surface application. The advantages and disadvantages of each type is discussed below:

(a) Flexible Arrays

Mechanized deployment as shown in the original configurations of Table 7.1(a) is not considered suitable for the lunar surface array for the following reasons:

(1) The large areas involved would require providing numerous and/or large mechanisms for one-time use.

(2) Most mechanisms do not lend themselves to efficient stowage in boost vehicle.

(3) Mechanism reliability would tend to lower overall mission reliability.

(4) With astronaut manual deployment capability available, mechanisms are redundant and impose an unnecessary weight penalty.

If the deployment mechanisms are deleted, leaving only the flexible substrates, these concepts are nearly identical with respect to area ratio and other design parameters. The only major distinction would be whether single crystal silicon or thin film solar cells were used, since the single crystal silicon cells would require foam cushion protection during stowage.

Flexible arrays can be manually deployed by the astronauts following the procedures outlined in Section 4.7 and usually require less time than for rigid panel arrays. However, flexible arrays which are not placed directly on the lunar surface will require added structure. This additional support structure, however, can be easily stowed within the 6-inch diameter core tubes, which provides a very high stowage efficiency.

(b) Rigid Panel Arrays

For reasons similar to those outlined for the flexible arrays above, mechanized deployment is not considered desirable for rigid panel array configurations. However, they lend themselves readily to the use of manual fold-out techniques described in Section 4.7. The EOS biconvex provides the lightest structure. The cross-laced substrates are somewhat heavier and very nearly equal on a specific density basis. It is estimated that by judicious design, the cross-

laced substrate panel could all be resized to give virtually the same panel weights. However, due to the required thickness of the rigid panels, the stowage volume requirements for these configurations are much larger than for the flexible arrays.

7.1.3 Candidate Structural Configurations

The flexible array structures provide the most efficient stowage, on the basis of the total area (ft^2) to total stowed volume (ft^3) ratio. Of these types, the TRW Systems thin film foldup array exhibits the highest stowage efficiency. It should be noted, however, that this stowage efficiency is contingent upon the use of thin film solar cells. If this array were adapted to the use of single crystal silicon cells, the stowage efficiency would be lower and approach that of rollup type arrays.

The rigid panel configurations, although exhibiting a lower stowage efficiency when compared to the flexible panels, are competitive, on a power-to-weight ratio basis, with the flexible arrays. If stowage efficiency is a critical mission requirement, flexible concepts seem to have a significant advantage over rigid panels. If power density (watts/lb) is found to be the critical mission parameter, the flexible concepts indicate a slight advantage over rigid panels only if thin film solar cell performance can be maintained in the 5 percent conversion efficiency range. With respect to ease of deployment, flexible panels are only advantageous if located on the lunar surface. However, time to prepare the lunar surface eliminates this advantage and makes rigid panels more attractive (see Section 4.7). For the various flexible array concepts, the TRW Systems foldup array exhibits a deployed stiffness most nearly equal to that of rigid panels, by virtue of the hingeline design. However, the Fairchild-Hiller rollup array with lateral stiffener strips also exhibits, to some extent, the desirable stiffness characteristics of the rigid panels.

With respect to the rigid panel concepts, the Boeing design appears quite attractive on the basis of near future developments in materials and design. Refinement of this design to include the TRW Systems Boron and Honeycomb Beam or the Boron Tube would result in a reasonable stowage efficiency, high power-to-weight ratio, and relatively low fabrication costs when compared to the other rigid concepts considered. Figure 7.1 compares each industry concept on a density basis.

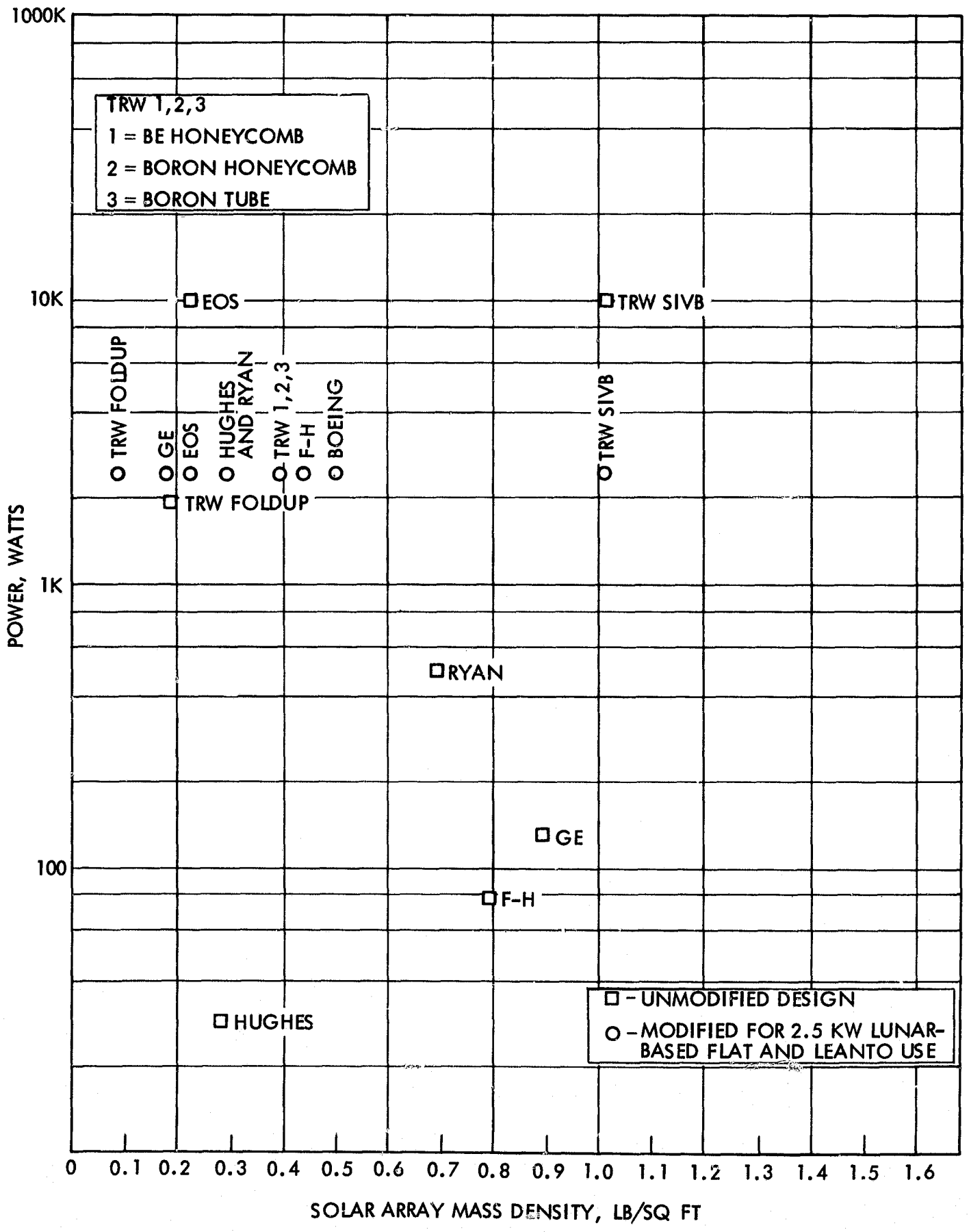

Figure 7.1 Comparison of Industry Large Area Solar Array Concepts (Mass Density of Original Design and as Modified for Lunar Surface Application)

From the foregoing, it is obvious that both flexible and rigid structure concepts have unique advantages depending upon the critical mission tradeoff parameter selected. The rollup configurations for the flexible concepts provide highly efficient stowage capabilities when considering the ancilliary structure that may be required. The rigid structure concepts seem equally acceptable. However, at this time the Boeing concept is by far the most developed of both approaches. If development cost and early availability become important mission planning criteria, this design approach would be the one that is recommended.

Appendix C of this report discusses the detailed criteria for redesigning a rigid panel of the Boeing type to be compatible with the lunar surface power system requirements and constraints. Appendices D and E provide the analyses for incorporating the TRW Systems Boron-Honeycomb and Boron Tube refinements into the Boeing structural concept.

7.1.4 Lunar Surface Handling and Assembly

Astronaut human factors are an important consideration in the design of any large, deployable space structure. This factor is especially significant for the large solar arrays envisioned for Program V of this study. The astronaut would be expected to manually transport the solar array panels over short distances while encumbered by his space suit, which would include a back pack, hand protection (gloves), and limited vision through his face visor. These factors, when coupled with the array size, coordinated team assembly and handling, surface obstacles, and lunar gravity formed the basis for the evaluation of the design concepts which are discussed in this report.

The array size should be such that in the stowed condition, the width (or diameter) does not exceed single astronaut handling capabilities (arm spread, cantilever length, weight and ability to overcome inertia effects). A module area 8 ft long by 3.3 ft wide was established as the limit compatible with these criteria.

Each 2.5 kw array is formed from several modules which can be readily removed and replaced for array maintenance. Stowage debris has been minimized and maximum use of all structural elements has been considered. This included such features as using the core of the flexible array stowage drums for superstructure stowage.

A detailed analysis associated with the logistics problems associated with stowage and deployment of the candidate solar arrays is provided in Section 4.7 of this report.

7.2 MECHANICAL

There are various mechanical features associated with the design of the array mounting structure. Their unique characteristics could affect array weight, stowage volume, deployment time, and maintenance. Several attractive design concepts are discussed.

7.2.1 Candidate Concepts

7.2.1.1 Mounting Structure - Non-Oriented Arrays

This category encompasses the leanto and flat arrays and includes both rigid panel and flexible design approaches.

With respect to the leanto array configuration (see Figures 7.22 & 7.23) the members forming the structure that support either the rigid panels or the rolled-out flexible structure may consist of one of several concepts. These are as follows:

(1) 90° Angle Members. This type of construction would consist of angle members of manufactured lengths and would be equipped with easily assembled snap-in end fittings. The end fittings may be bending moment resistant, or simple pin-ends. If pin-ended, the trusses must be provided with diagonal tension ties in at least one bay of each 2.5 kw array. This type of member would provide good stowage efficiency as the members can be nested within each other to achieve low stowage volume.

(2) Round or Square Rigid Tubes. This type of construction would consist of thin-walled tubes manufactured to specific lengths, and would be equipped with easily assembled snap-in fittings. This type of tube would be more amenable than the 90° open angle members described above, to the use of end fittings that have both bending and torsional resistance. Therefore, diagonal tension ties would not be required. The round or square tubes, however, would occupy more stowage volume than the 90° angle members, since they cannot be stowed within each other.

(3) Roll-Stowed Tubular Members. This configuration consists of tubular members such as the de Havilland (now SPAR) "Stem" or "Bistem" booms, or the TRW System closed-section boom.

These sections are designed to form straight tubular members when in the released or free state. By collapsing or flattening them laterally, they may then be rolled up lengthwise on to a cylindrical stowage drum.

These types of members are fabricated from thin, spring-quality sheet metal which has been formed and heat treated to produce the shape of the extended members in their free or unstrained state. Strain energy can be introduced to provide the deformation forces necessary to flatten and roll up the tubes for stowage.

One method of utilizing this type of tube consists of stowing a long continuous length on a drum that is contained in a framework or housing and that also contains a hand crank or other motive power to extend the boom from the drum.

In use, the housing would be carried by the astronaut or placed adjacent to the construction site. As construction proceeds, lengths of the tube as required are unrolled from the dispenser. Lengths are measured by footage or guide marks printed on the boom, and these lengths are cut off by a shear cutter attached to the dispenser.

Joints for this type of tube are made by prefabricated fittings carried separately. The fittings have stub posts to plug into the tubing ends and/or means to friction grip the outside of the tube.

Another technique for utilizing this type of tube with flexible arrays consists of attaching the tubes, in a lengthwise and and transverse grid, to the backside of the flexible substrate. Thus, when the array is rolled up for stowage, the tubes are simultaneously flattened and rolled up with the array. During deployment, as the flexible array is unrolled, the tubes automatically and simultaneously spring from the flattened condition to the stiff tubular form.

7.2.1.2 Mounting Structure - Materials

Referring to the materials described below for the rigid panels, it was determined that some of these would be suitable for the mounting structure where the 90° angle members and round or square tubes are used. However, the mounting structure material would not necessarily be limited to those listed for rigid panel construction.

The candidate materials selected during this study for rigid panel construction are as follows:

(1) Beryllium Tube (Boeing)

The square tubes utilized for this concept are formed of "hot-creep-formed" U-shaped beryllium sheet channels bonded together in pairs to form a closed section tube. The basic material, beryllium is considered highly desirable as it exhibits the highest modulus of elasticity to density ratio of any of the metals.

The "hot-creep-forming" technique is fairly well developed, but at this time is still very costly. The metal cannot be cold-formed, so this cost must be anticipated if this material is selected. For the various mounting structure types, the hot-creep-formed beryllium is adaptable to the 90° angle members, and the square or round tubes. This metal is not suitable for use with the roll-stowed tubular members as it cannot be heat treated to provide spring type material.

(2) Beryllium Cap-Aluminum Honeycomb Core Beam (TRW Systems)

The beams for this concept are formed from flat beryllium cap strips provided to take bending loads and spaced by an aluminum honeycomb core with its cells perpendicular to the cap strips. This core provides resistance to shear loads.

This type of construction takes advantage of the stiffness of beryllium for the bending loads and eliminates the need for the costly hot-creep forming required for the beryllium box beams. However, this type of beam has its major bending stiffness only in one direction or axis, since it is not considered feasible to bond flat strips to the sides of the honeycomb core cells to provide bending stiffness in the 90° direction or other axis. This type of construction could be considered as a candidate for the mounting structure if the characteristic of single-axis bending stiffness could be accommodated in the handling and deployed loads envelope.

(3) Boron Filament Cap-Aluminum Honeycomb Core Beam (TRW Systems)

The structural factors regarding the beryllium cap-aluminum honeycomb core beam are also applicable to the TRW Systems boron filament cap-aluminum honeycomb core beam with the additional feature that the boron filament cap could result in a slightly lighter weight structure than the beryllium cap beam. However, the technique for fabricating the boron filament cap beam is not as well developed as the beryllium cap beam.

(4) Boron Tube Beam (TRW Systems)

This concept consists of hollow tubes (round or square) fabricated of boron filaments in the lengthwise direction to provide bending stiffness and with Fiberglass filaments or cloth, wrapped in both 40° directions, for shear and torsional stiffness.

The boron tube beam is functionally equivalent to the beryllium tube in that it has equal stiffness in either axis of bending, and the construction principle is adaptable to a 90° angle member. The fabrication techniques for this concept have not been developed as yet. However, the use of boron filaments to fabricate tube type beams is considered to be fairly straightforward. The main area of concern currently is the development of long, slender mandrels on which to form the tubes.

Preliminary calculations indicate that the TRW Systems boron filament tube would yield a weight-to-area ratio as good as the best of the beryllium structures, and indications are that future material cost reductions, plus reduced tooling and fabrication costs could result in the boron filament construction becoming the best candidate concept, not only for rigid panel construction, but also for the mounting structure construction.

(5) Miscellaneous Materials

Of the various materials not previously mentioned, several others are worthy of comment. Aluminum alloy is in wide use and tube and structural elements, of the type required for the lunar based solar arrays, are in a highly developed state. Use of aluminum would result in the lowest fabrication costs but only at the expense of an increased weight penalty.

Fiberglass, like aluminum, is also in widespread use and has well-developed fabrication techniques. The use of this material would be more economical than beryllium or boron filaments, but also at a considerable weight penalty.

7.2.2 Concept Selection

Of the various candidate materials discussed above, the boron filament construction offers the lightest weight structure. In addition, there are strong indications of future reductions in material costs and fabrication costs, once the techniques are developed.

Beryllium results in an excellent lightweight structure, but indications are that the material and fabrication costs will continue to remain

high. Aluminum and fiberglass offer the lowest material and fabrication costs, but at the expense of increased weight. Finally, if rollup stowed tubular members are used, stainless steel appears to be the most attractive material selection for the earlier time periods.

7.3 ELECTRICAL

7.3.1 Solar Cells

There are several types of photovoltaic energy conversion devices available or under development at this time. Table 7.3 lists several single crystal and thin film types and compares them for both physical and environmental parameters. Based on the data presented in this table, as well as other factors such as availability, state of development, etc., single crystal silicon solar cells of 3.9 cm^2 active area are considered to be the cell type best suited for the Program V mission. Cadmium sulfide (CdS) thin film solar cell data is included in this report for comparison purposes only and for possible future consideration.

Figure 7.2 compares the AMO, 28°C current-voltage characteristics of both 2 ohm-cm and 10 ohm-cm silicon solar cells of various thicknesses. From this data, as well as cell handling durability, availability, cost, etc., a cell thickness of 0.008 inch was selected for use in performance analysis. In addition, the 10 ohm-cm base resistivity cell was selected to be conservative. An increase of approximately 5 percent in solar cell conversion efficiency could be realized if an 0.008 inch thick, 2 ohm-cm solar cell was used for this mission and should be considered in future studies.

Figure 7.3 indicates the variation in current-voltage characteristic with temperature. The temperature range shown includes the expected solar array temperature envelope between the terminator (-30°C) and lunar noon (60°C), assuming a shaded lunar surface temperature of -6°C. Figures 7.4 to 7.6 are the current/voltage envelope curves for terminator to noon conditions for the insulated and non-insulated array conditions of either the oriented or non-oriented silicon solar cell arrays. Figures 7.7 to 7.9 are similar envelope curves for typical CdS thin film solar celled arrays.

	Single Crystal (Silicon)			
	Unit	Present	Dendritic	Future
Maximum Efficiency Claimed (AM0/28°C)	%	12	8-11	9
Maximum Efficiency Measured by TRW (AM0, 28°C)	%	11	8.65	-
Maximum Area	cm^2	9	30	2
Thickness	inch	0.012	0.015	0.004
Type	-	N/P	N/P	N/P
Contact Material	-	TiAg	TiAg	TiAg
Effects on output of:				
Humidity	-	None	None	None
Temperature Cycling	-	None	None	-
1 Mev 10^{13} partials/cm^2 (e/cm^2)	%	None	None	None
1 Mev 10^{16} partials/cm^2 (e/cm^2)	%	50 loss	50 loss	50 loss
1.8 Mev 10^{11} partials/cm^2 (e/cm^2)	%	35 loss	35 loss	35 loss
1.8 Mev $3x10^{12}$ partials/cm^2 (P/cm^2)	%	> 60 loss	> 60 loss	> 60 loss
Simulated 0.5 - joule micrometeoroids (10^{-8} to 10^{-12} gm particles)	%	w/6 mil glass 3 loss	w/6 mil glass 3 loss	w/6 mil glass 3 loss
	%	< 6 mil glass 100 loss	< 6 mil glass 100 loss	< 6 mil glass 100 loss

FOLDOUT FRAME

	Single Crystal (Silicon)				Thin Film		
Unit	Present	Dendritic	Future	Wrap Around	CdS	CdTe	GaAs
%	12	8-11	9	11.7	3-6	4-5	3-5
%	11	8.65	-	10.5	3.97	2.46	-
cm^2	9	30	2	4	55	56	4
inch	0.012	0.015	0.004	0.008	0.005	0.002	0.004-0.009
-	N/P	N/P	N/P	N/P	P/N	P/N	P/N
-	TiAg	TiAg	TiAg	TiAg	CuAu	Au	Au
-	None	None	None	None	Degrade	Degrade	Degrade
-	None	None	-	None	Degrade	-	-
%	None	None	None	None	Degrade	-	-
%	50 loss	50 loss	50 loss	50 loss	10 loss	-	-
%	35 loss	35 loss	35 loss	35 loss	1 loss	-	10 loss
%	> 60 loss	> 60 loss	> 60 loss	> 60 loss	3 loss	-	> 60 loss
%	w/6 mil glass 3 loss	w/6 mil glass 3 loss	w/6 mil glass 3 loss	w/6 mil glass 3 loss	w/1 mil Mylar 4 loss	-	-
%	< 6 mil glass 100 loss	< 6 mil glass 100 loss	< 6 mil glass 100 loss	< 6 mil glass 100 loss	w/1 mil Kapton 10 loss	-	-

Table 7.3 Comparison of Single Crystal and Thin Film Cells Between Various Parameters

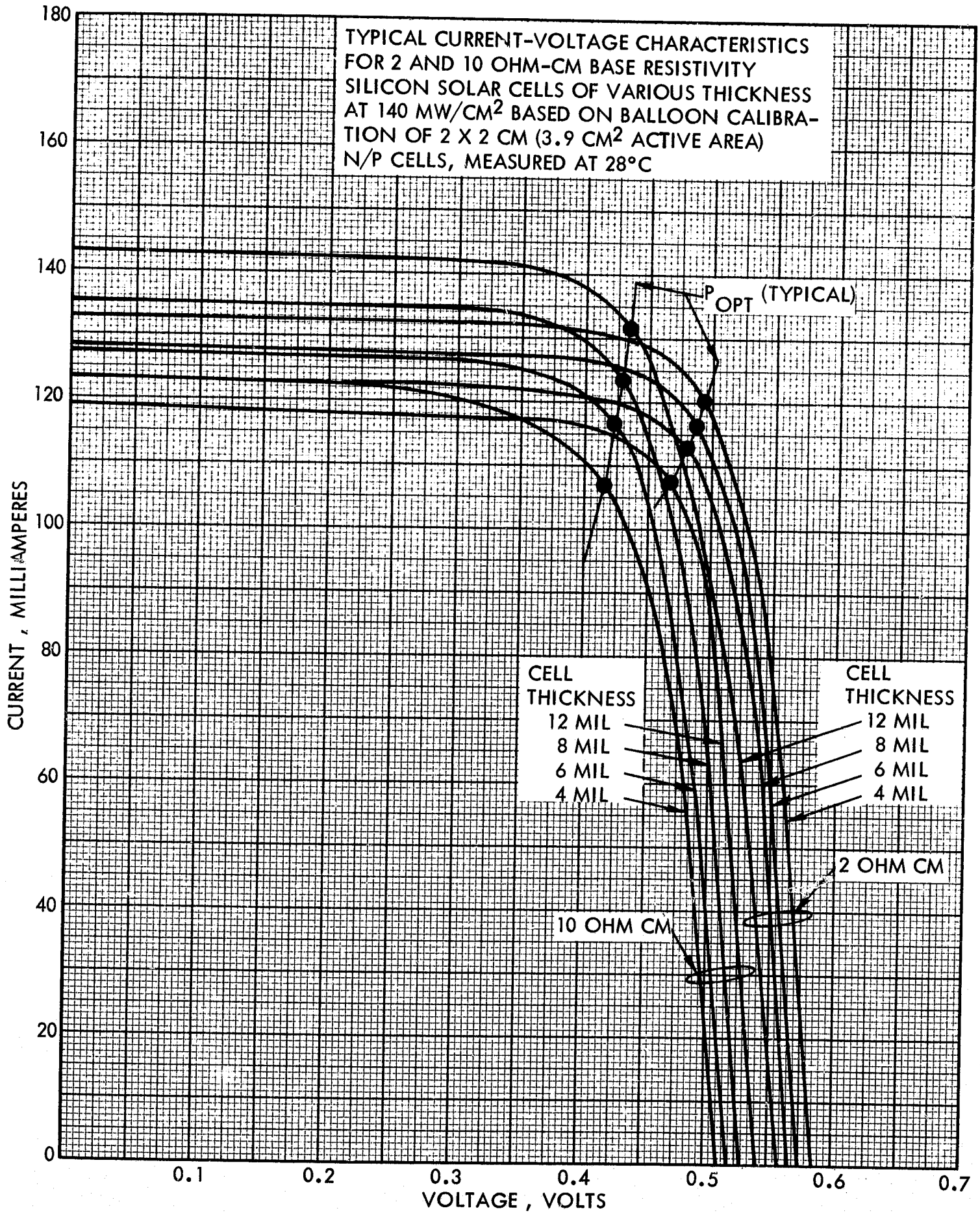

Figure 7.2 Typical Current-Voltage Characteristics for 2 and 10 ohm-cm Base Resistivity Silicon Solar Cells of Various Thicknesses

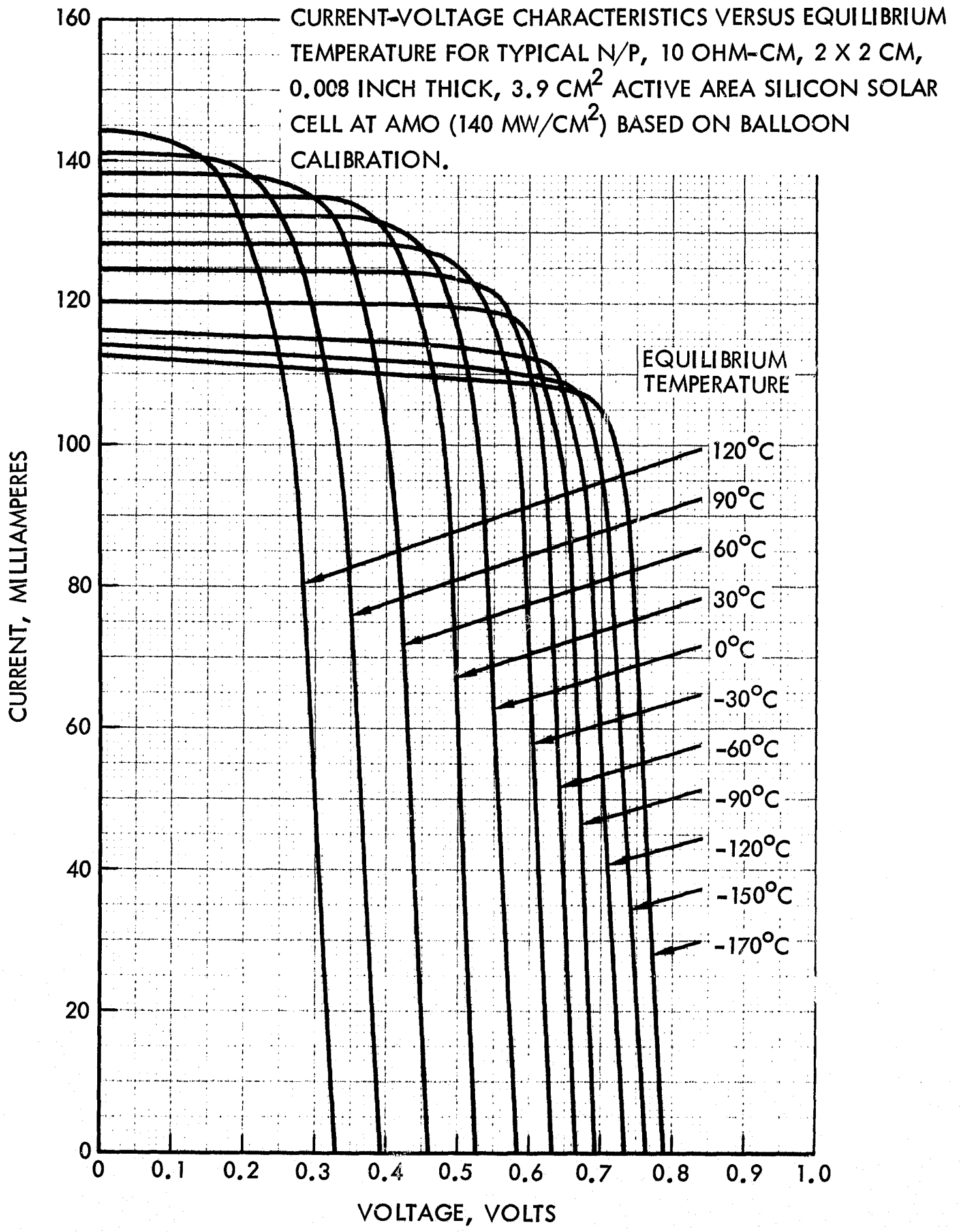

Figure 7.3 Current-Voltage Characteristics for Silicon Solar Cells Versus Equilibrium Temperature

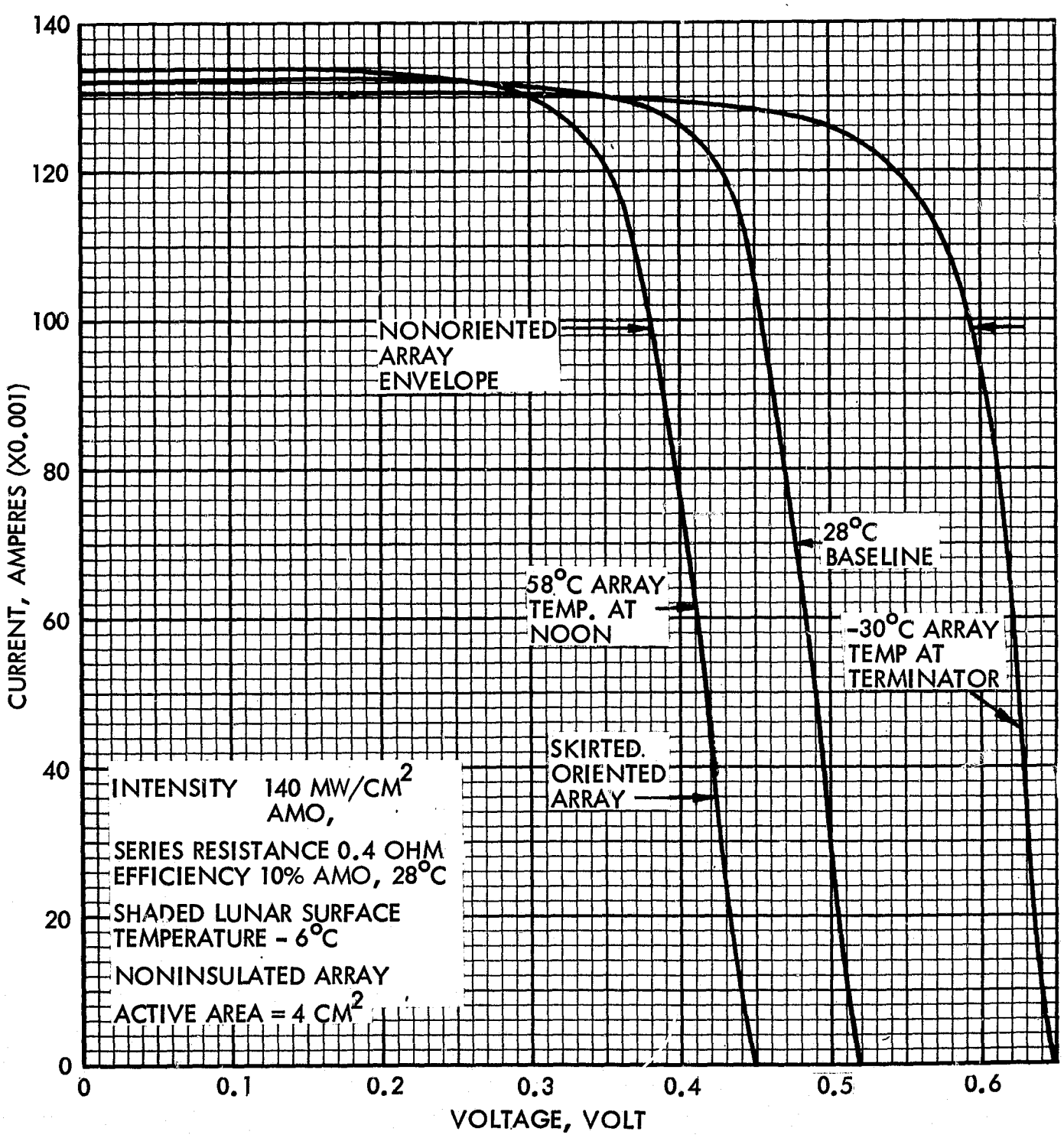

Figure 7.4 Typical 10 Ohm-CM Single Crystal Silicon Solar Cell Current-Voltage Characteristic Curves for Lunar Noon and Terminator Conditions

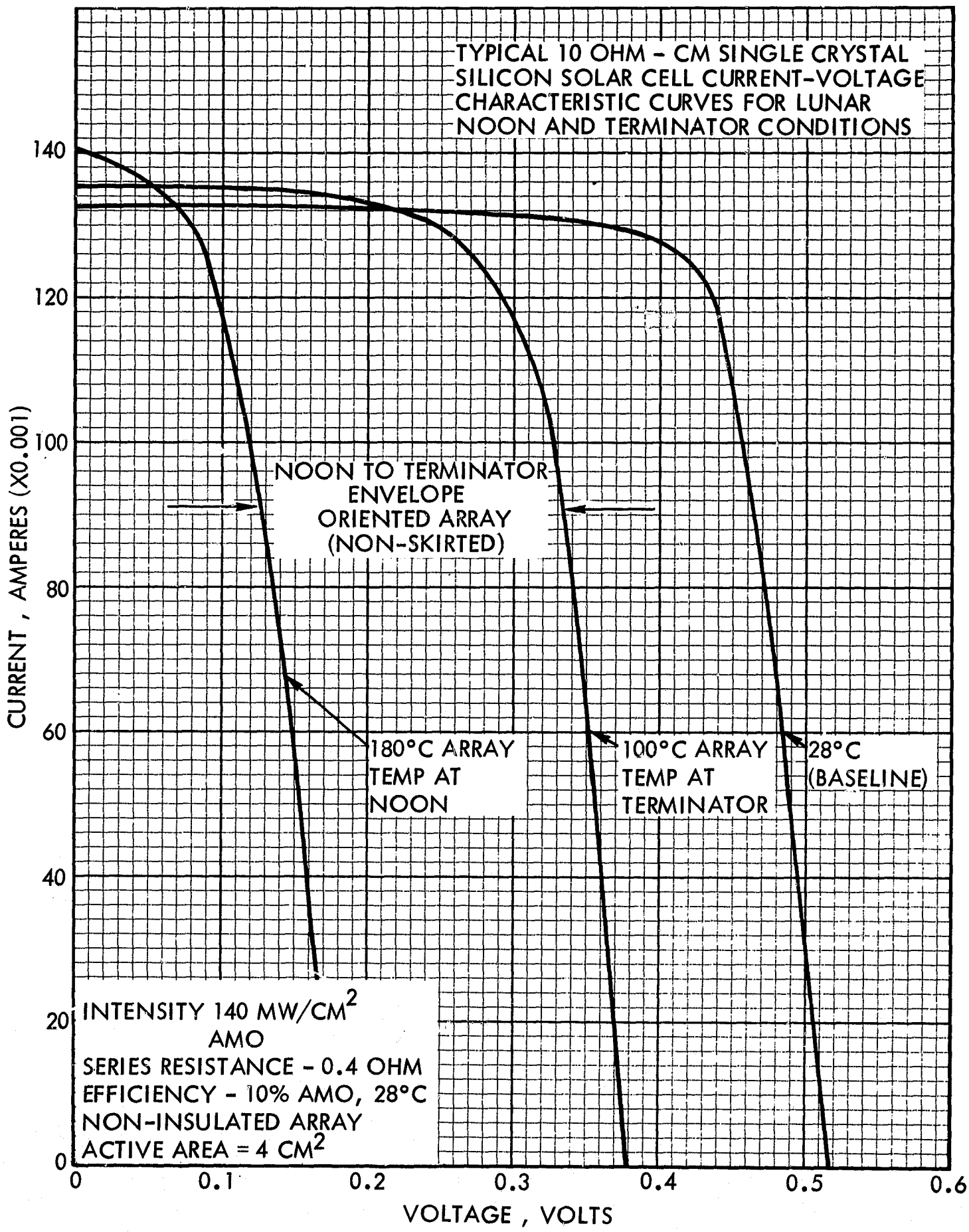

Figure 7.5 Typical 10 ohm-cm Single Crystal Silicon Solar Cell Current-Voltage Curves

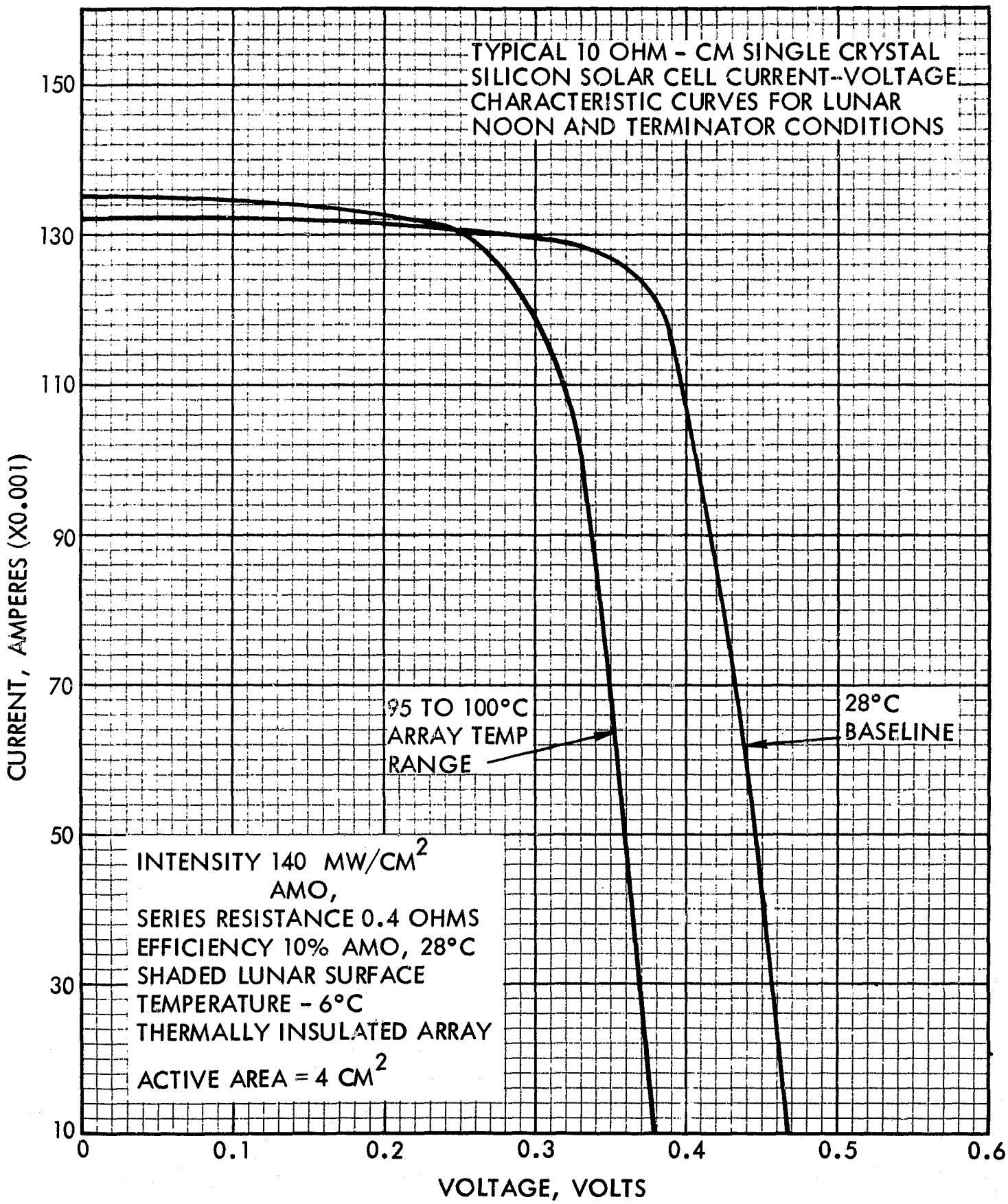

Figure 7.6 Typical 10 ohm-cm Single Crystal Silicon Solar Cell Current-Voltage Curves

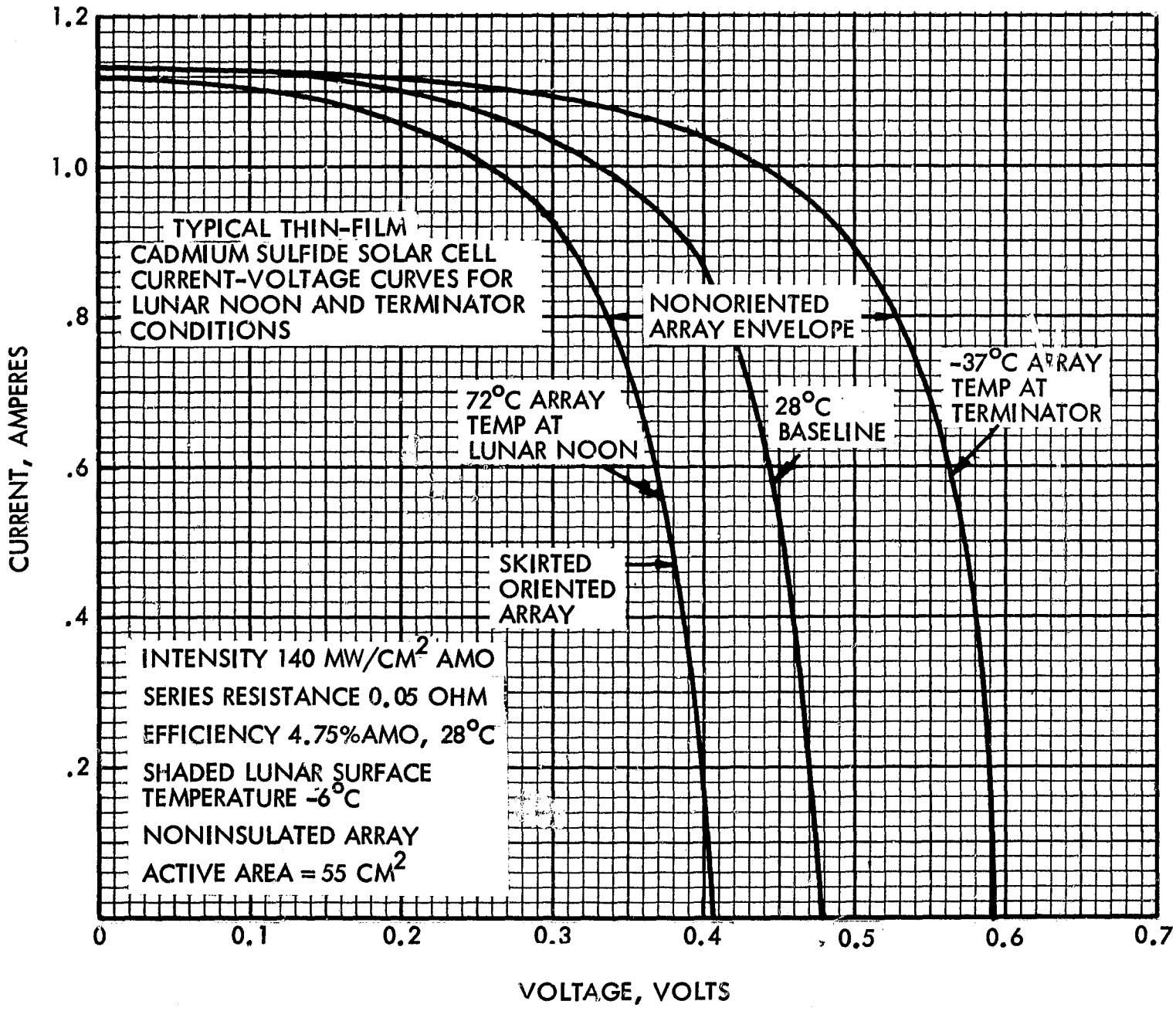

Figure 7.7 Current-Voltage Characteristics for Thin Film Cadmium Sulfide Solar Cells for Array Temperature Operating Range

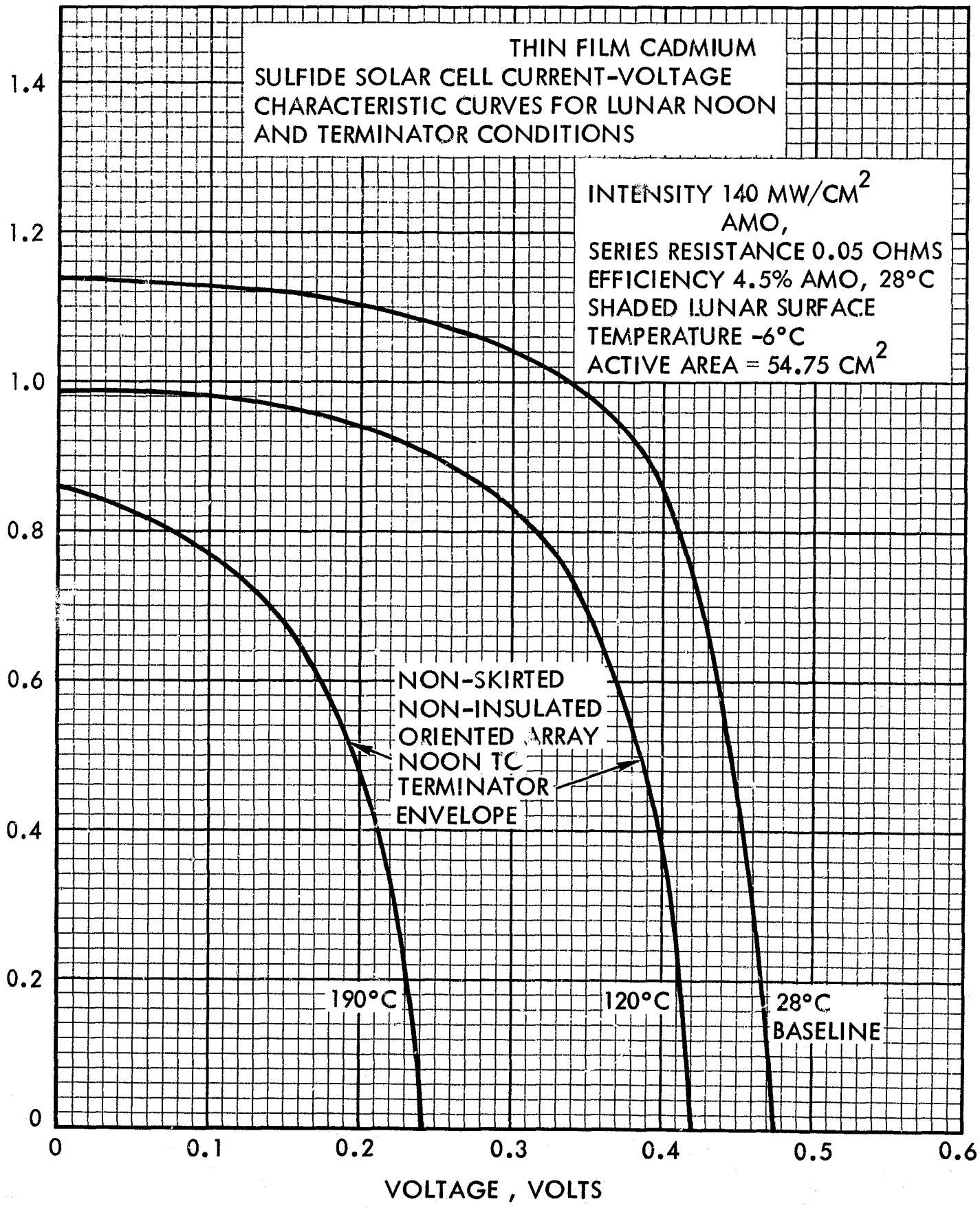

Figure 7.8 Typical Cadmium Sulfide Thin Film Current-Voltage Curves

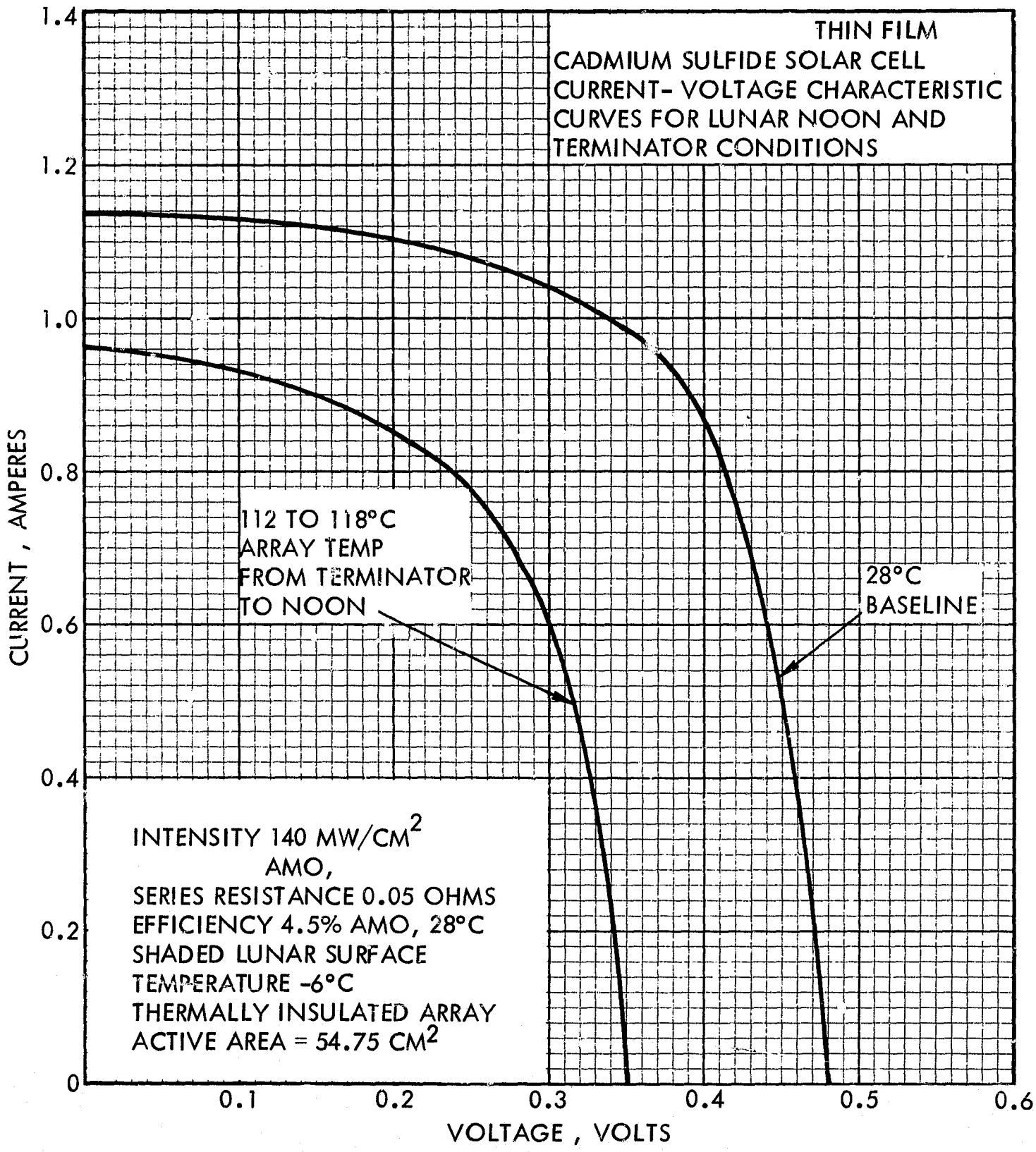

Figure 7.9 Typical Cadmium Sulfide Thin Film Current Voltage Curves

The single crystal and thin film open-circuit voltage variation with temperature is plotted for comparison in Figure 7.10. It can be seen that the voltage variation of a thin film solar cell is less than that for a single crystal cell, which indicates that for large temperature variations, such as would be experienced on the lunar surface, thin film cell arrays may require less power conditioning than would single crystal cell arrays.

The selection of a 10 ohm-cm solar cell, as seen in Figure 7.11, allows the array designer two latitudes of flexibility, should he ultimately decide on the use of a 2 ohm-cm solar cell for his array. As stated earlier, a cell thickness of 0.008 inch was selected for this study. Should the 2 ohm-cm solar cell be utilized, the overall cell thickness could be reduced (assuming handling would not become a problem) to between 5 and 6 mils, thus resulting in a lighter array. The second design alternative would be to maintain the cell thickness at 0.008 inch for handling ease but to increase array performance, and hence reduce array area and weight, by taking advantage of the increased efficiency gained by the use of the lower base resistivity cell. The relative gains in power-to-weight ratio are also given in Figure 7.11 for both the single crystal silicon and thin film CdS solar cells. It should be noted that the CdS thin film cell of 4 percent efficiency (presently available) compares (on a cell basis) with the 0.008 inch thick (with 0.006 inch cover glass) single crystal silicon solar cell. Figure 7.12 is a plot of the inverse of Figure 7.11.

The change in solar cell efficiency as a function of temperature is shown in Figure 7.13 for both single crystal silicon and CdS thin film cells.

Figure 7.14 compares the single crystal silicon and CdS thin film solar cells on a cost basis and depicts the predicted cost variation over the next few years. It should be noted that based on 4 percent CdS thin film cell efficiencies, a cost savings of over 50 percent on the cells (protected) alone could be realized when compared to 10.25 percent efficient silicon cells. This savings may be even greater when structural costs are considered. It is estimated that by 1969, assuming available cell efficiencies have not materially increased, that the saving in solar cell costs could approach nearly 70 percent of silicon cells.

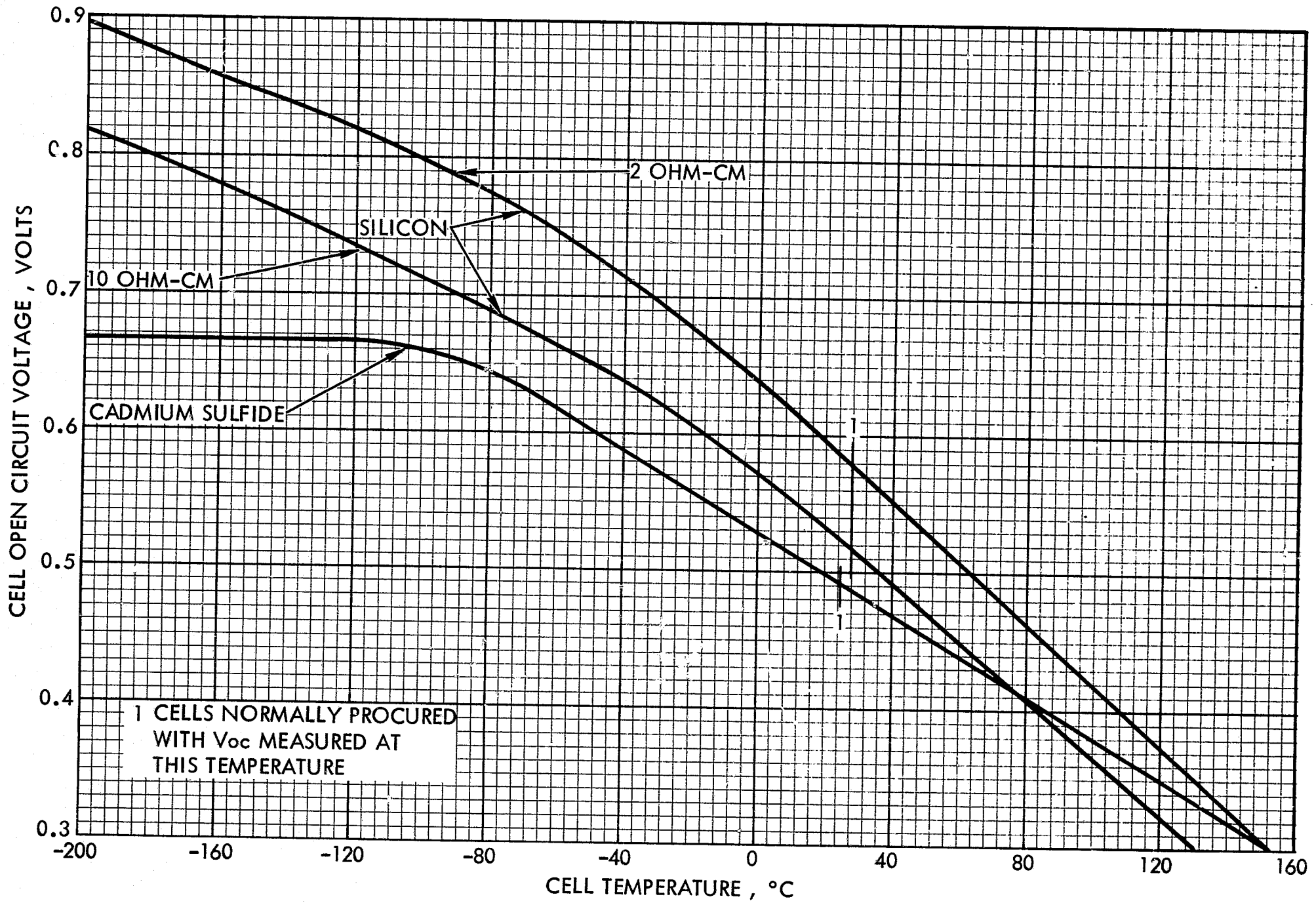

Figure 7.10 Cell Open Circuit Voltage Versus Temperature for Silicon and CdS Thin Film Solar Cells

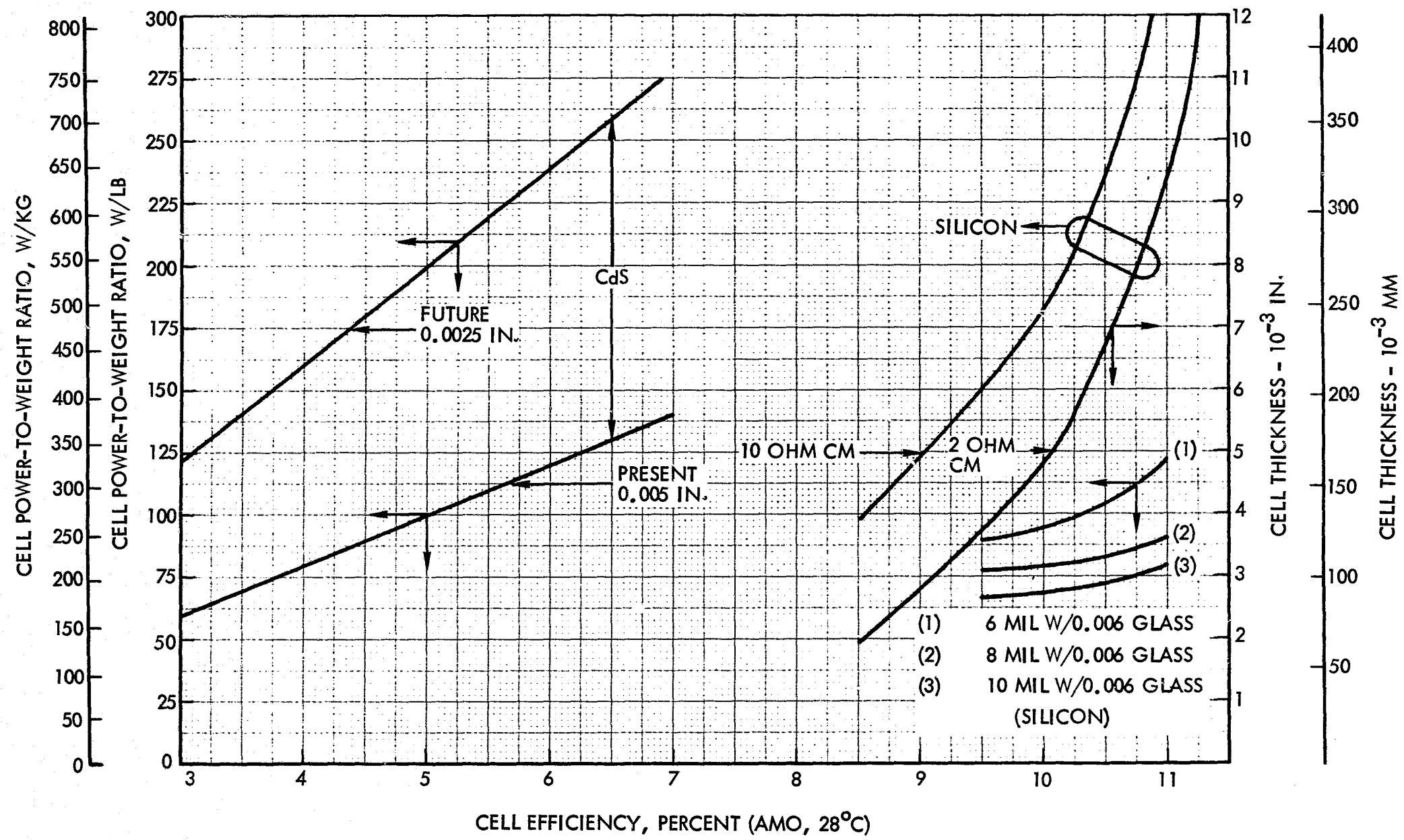

Figure 7.11 Power-to-Weight Ratio Versus Efficiency for Silicon and Thin Film Solar Cells

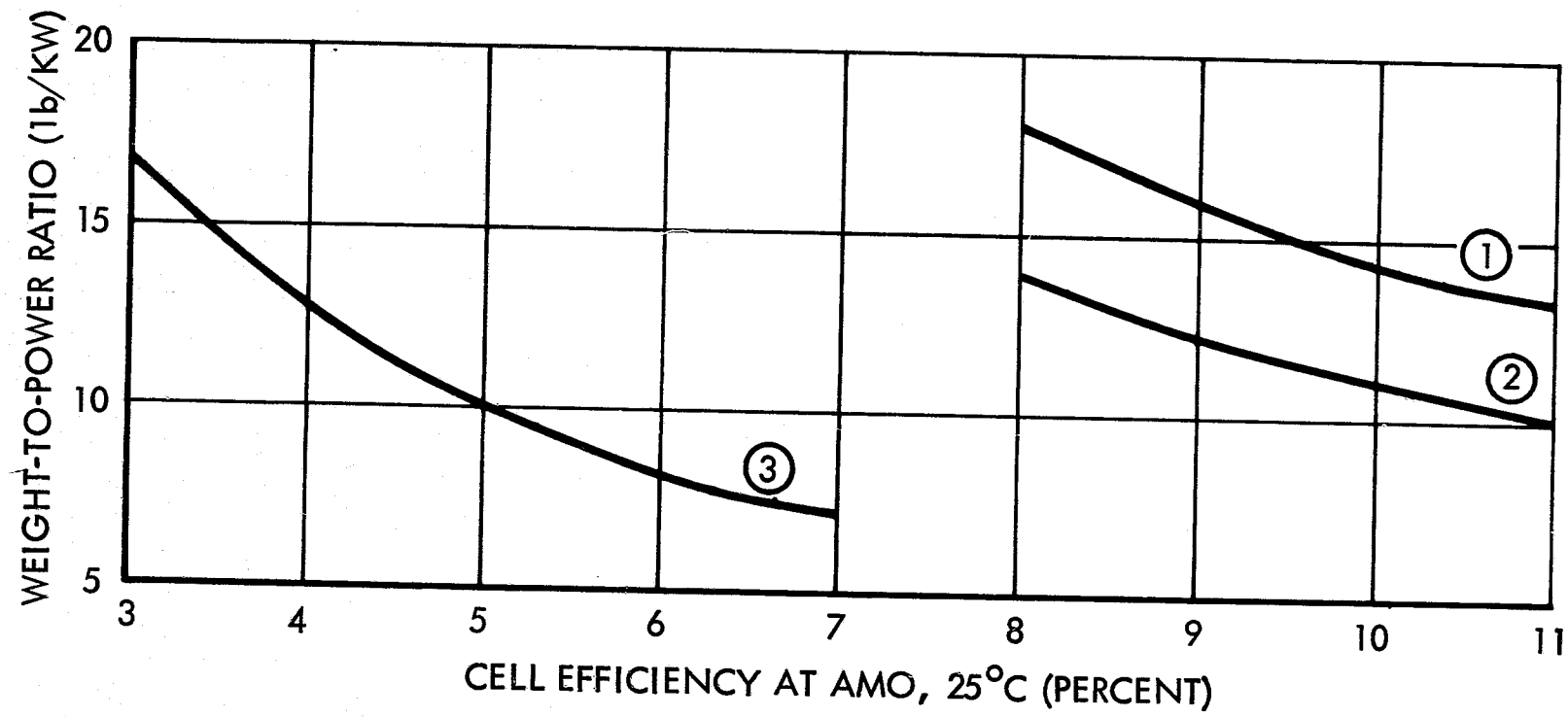

1. 0.010-INCH-THICK Si WITH 0.003-INCH-THICK GLASS
2. 0.008-INCH-THICK Si WITH 0.003-INCH-THICK GLASS
3. 0.004-INCH-THICK KAPTON ENCAPSULATED CdS

Figure 7.12 Cell Efficiency versus Weight-Power Ratio

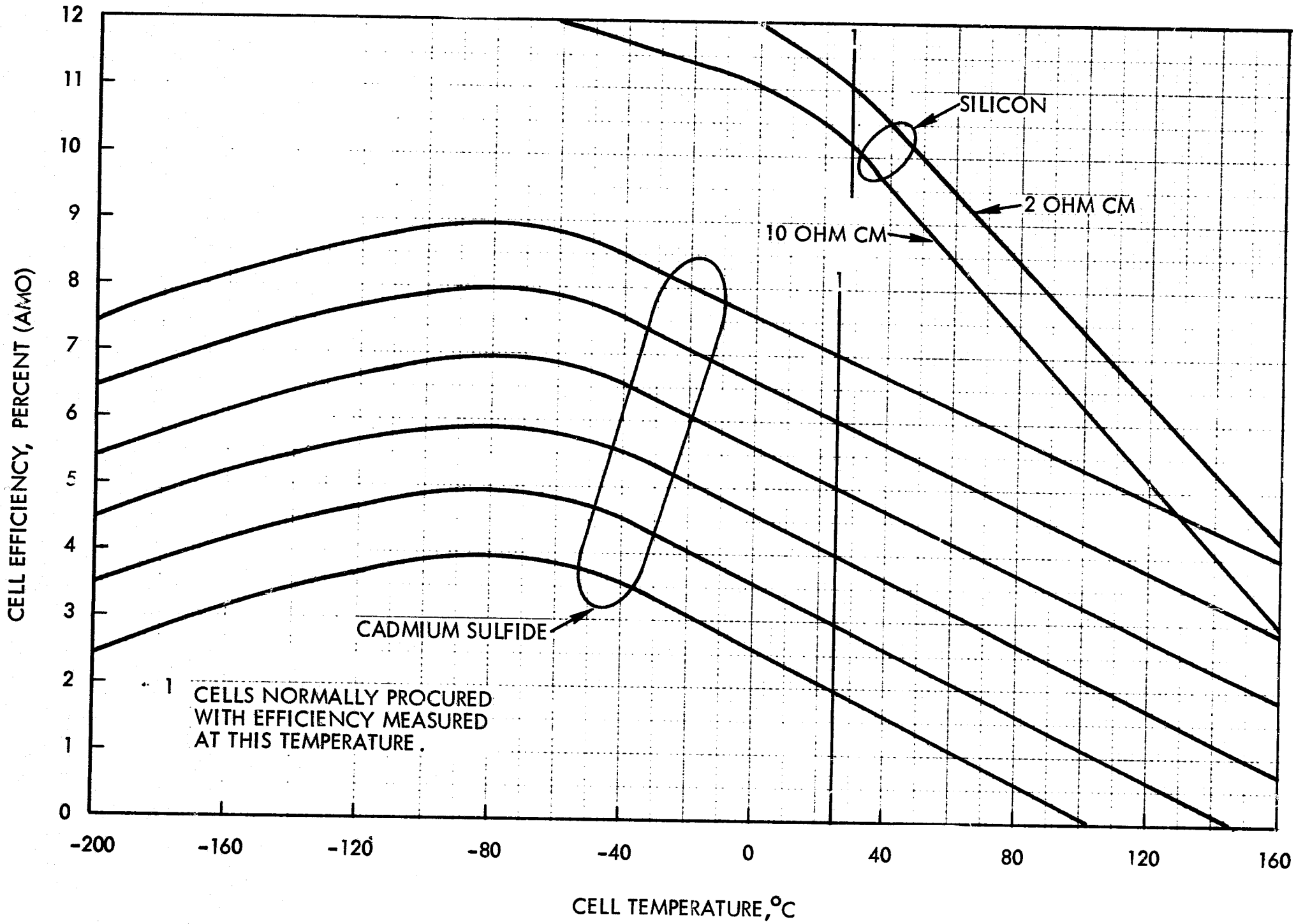

Figure 7.13 Cell Efficiency Versus Temperature Comparison for Silicon and Thin-Film Solar Cells

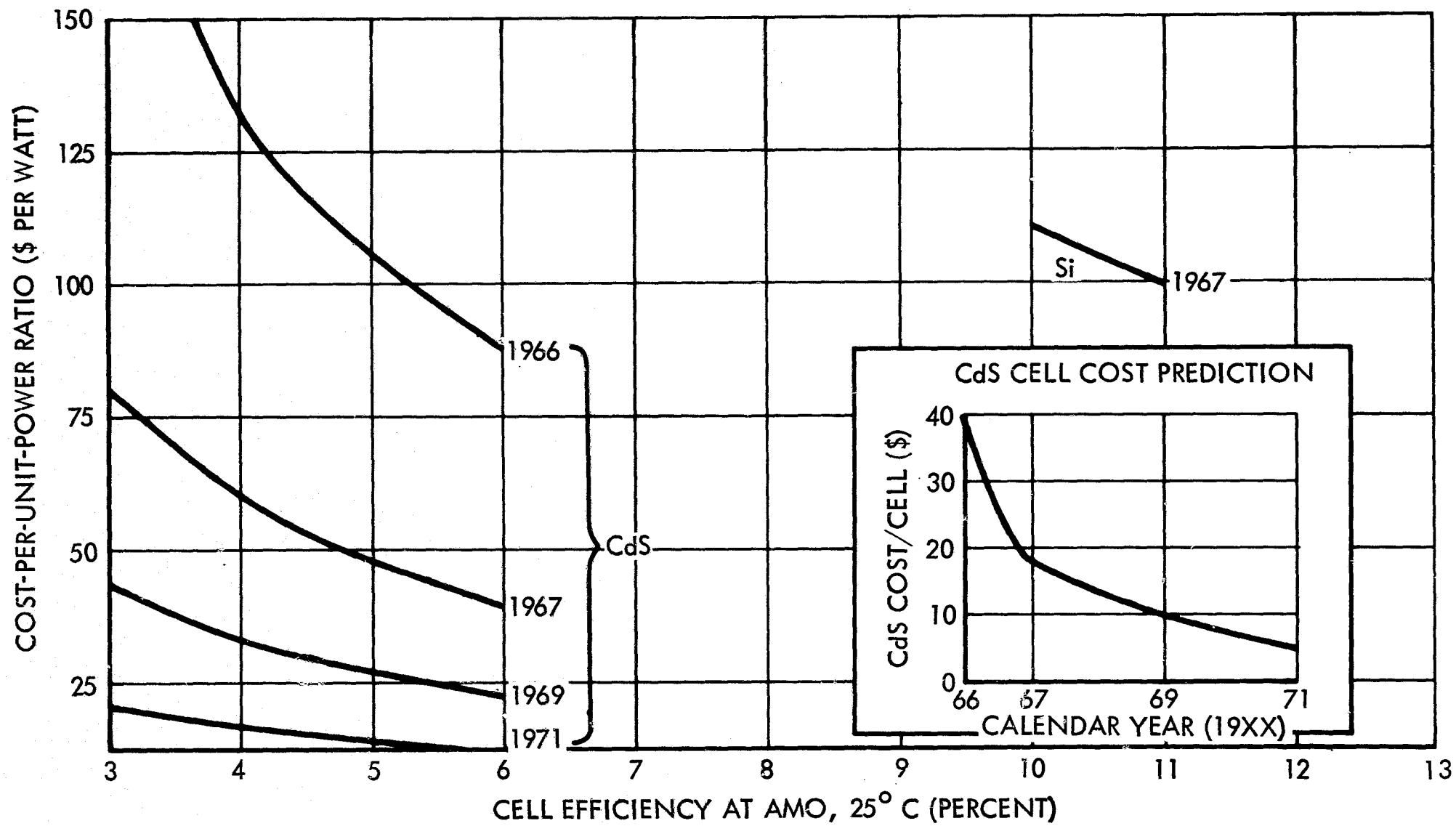

Figure 7.14 Silicon Cell and CdS Thin Film Cost Projections

Table 7.4 is a comparison of silicon and CdS thin film cells of various efficiencies for several design parameters.

7.3.2 Cover Slides

Reference 7.1 (Table VIII) shows the effect of various spectral filter characteristics on cell absorptivity and emissivity as well as output power. In this study, combination 5 (α/Σ = 0.84) was selected for thermal analysis as this is the type commonly used today and offers the best temperature/power tradeoff of those shown.

The relative radiation degradation effect on cell power-to-area ratio for various cell cover thicknesses is shown in Figure 7.15, showing that for a 0.006 inch cover, less than a 10 percent performance loss per year would be expected in a radiation environment comparable to that of Earth space. The lunar surface radiation environment is expected to be less than that of Earth space (Reference 7.1) and hence, 0.006 inch covers are considered adequate for radiation protection on the lunar surface. Due to the low radiation levels, cells with values lower than 10 ohm-cm base resistivity are considered usable on the lunar surface. Figure 7.16 (Reference 7.1) shows that a significant decrease in solar cell performance may be experienced in a micrometeorite environment similar to that anticipated on the lunar surface, if covers of less than 0.006 inch were used. However, unlike radiation protection, which increases with increased cover thickness (Figure 7.15), no significant increase in array micrometeorite protection is realized by the use of thicker covers. Based upon this data, the 0.006 inch thick silicon solar cell cover was considered to provide the required micrometeorite protection to achieve the Program V mission requirements while still permitting the use of lightweight solar arrays.

7.3.3 Circuit Interconnections

The cell interconnects and the main power bus are array components which must be designed for a specific requirement (i.e., power level, array geometry, circuit loss, etc.). Figure 7.17 shows the many possible voltage and current combinations for several array power levels. Based upon power conditioning limitations, user requirements, circuit weight, array percent power loss, and other important system design

FOLDOUT FRAME

Parameter	Cell Type*	Cell Effic			
		3	4	5	6
w/cell	SC	-	-	-	-
	TF	0.231	0.308	0.385	0.462
cells/kw	SC	-	-	-	-
	TF	4330	3250	2600	2170
Cells/ft^2	SC	-	-	-	-
	TF	15	15	15	15
lb/ft^2	SC	0.195	-	-	-
	TF	0.059	0.059	0.059	0.059
lb/kw	SC	-	-	-	-
	TF	15.21	11.42	9.14	7.63
w/lb	SC	-	-	-	-
	TF	65.7	82.5	109.5	131.2
ft^2/kw	SC	-	-	-	-
	TF	289	217	173	145
w/ft^2	SC	-	-	-	-
	TF	3.46	4.62	5.79	6.90
$/cell with cover	SC	-	-	-	-
	TF	15.00	15.00	15.00	18.00
$/w	SC	-	-	-	-
	TF	65.00	48.75	39.00	39.00
$/ft^2	SC	-	-	-	-
	TF	225	225.00	225.00	270.00
K$/lb	SC	-	-	-	-
	TF	3.82	3.82	3.82	4.58

Cell Efficiency at AMO, 28°C in Percent							
4	5	6	7	8	9	10	11
-	-	-	-	-	0.050	0.056	0.062
0.308	0.385	0.462	0.539	-	-	-	-
-	-	-	-	-	19850	17900	16250
3250	2600	2170	1860	-	-	-	-
-	-	-	-	-	221.1	221.1	221.1
15	15	15	15	-	-	-	-
-	-	-	-	-	0.195	0.195	0.195
0.059	0.059	0.059	0.059	-	-	-	-
-	-	-	-	-	17.50	15.80	14.34
11.42	9.14	7.63	6.54	-	-	-	-
-	-	-	-	-	57.8	63.3	69.8
82.5	109.5	131.2	153.0	-	-	-	-
-	-	-	-	-	100.0	89.4	81.3
217	173	145	124	-	-	-	-
-	-	-	-	-	10.0	11.2	12.3
4.62	5.79	6.90	8.07	-	-	-	-
-	-	-	-	-	4.00	5.00	6.00
15.00	15.00	18.00	18.00	-	-	-	-
-	-	-	-	-	125.00	112.00	97.50
48.75	39.00	39.00	33.50	-	-	-	-
-	-	-	-	-	885	1105	1825
225.00	225.00	270.00	170.00	-	-	-	-
-	-	-	-	-	4.53	5.68	6.80
3.82	3.82	4.58	4.58	-	-	-	-

Table 7.4 Variation of Silicon Cell Parameters with Cell Efficiency

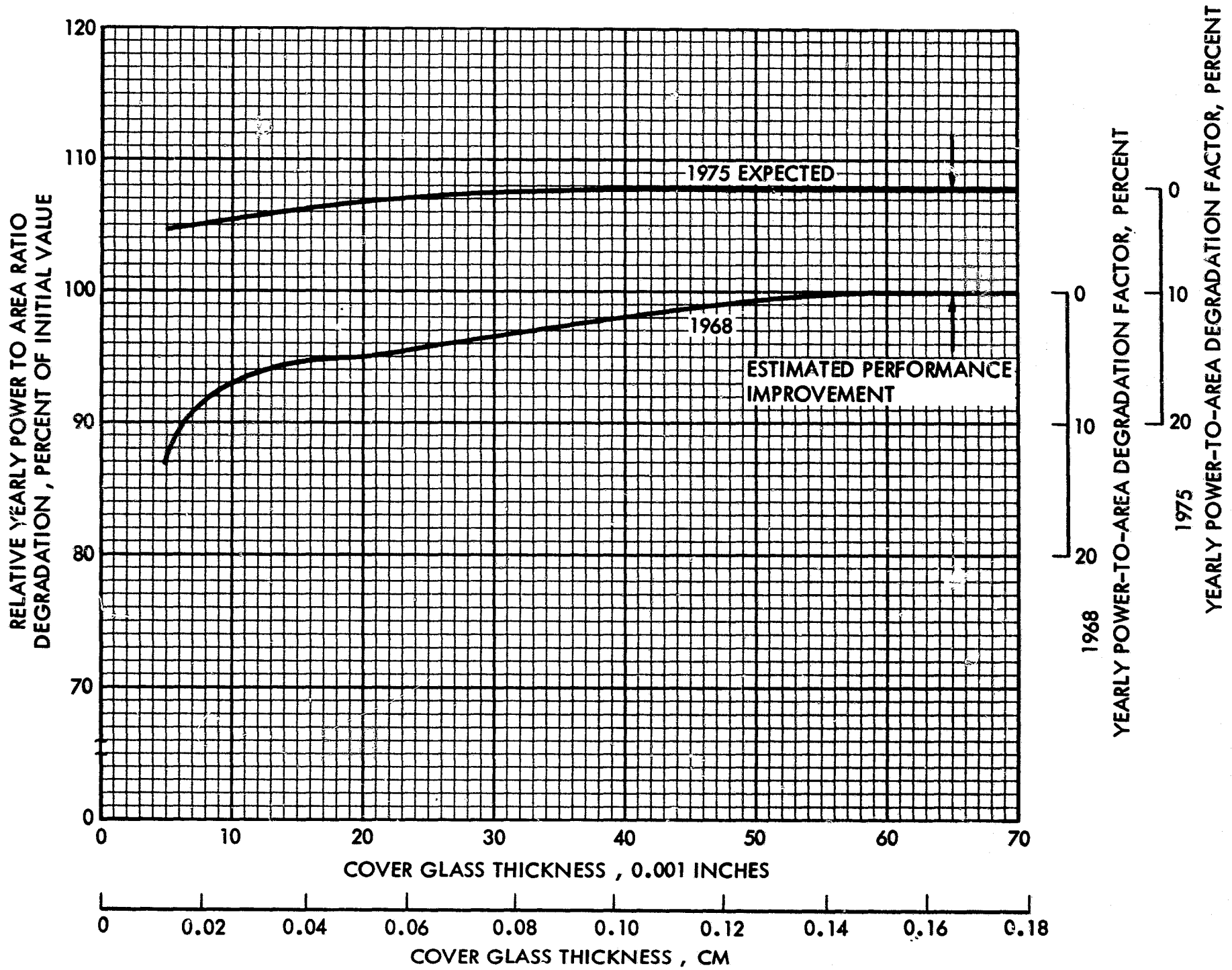

Figure 7.15 Percent Power to Area Ratio Remaining After Ratiation Bombardment (Yearly) Versus Cover Thickness

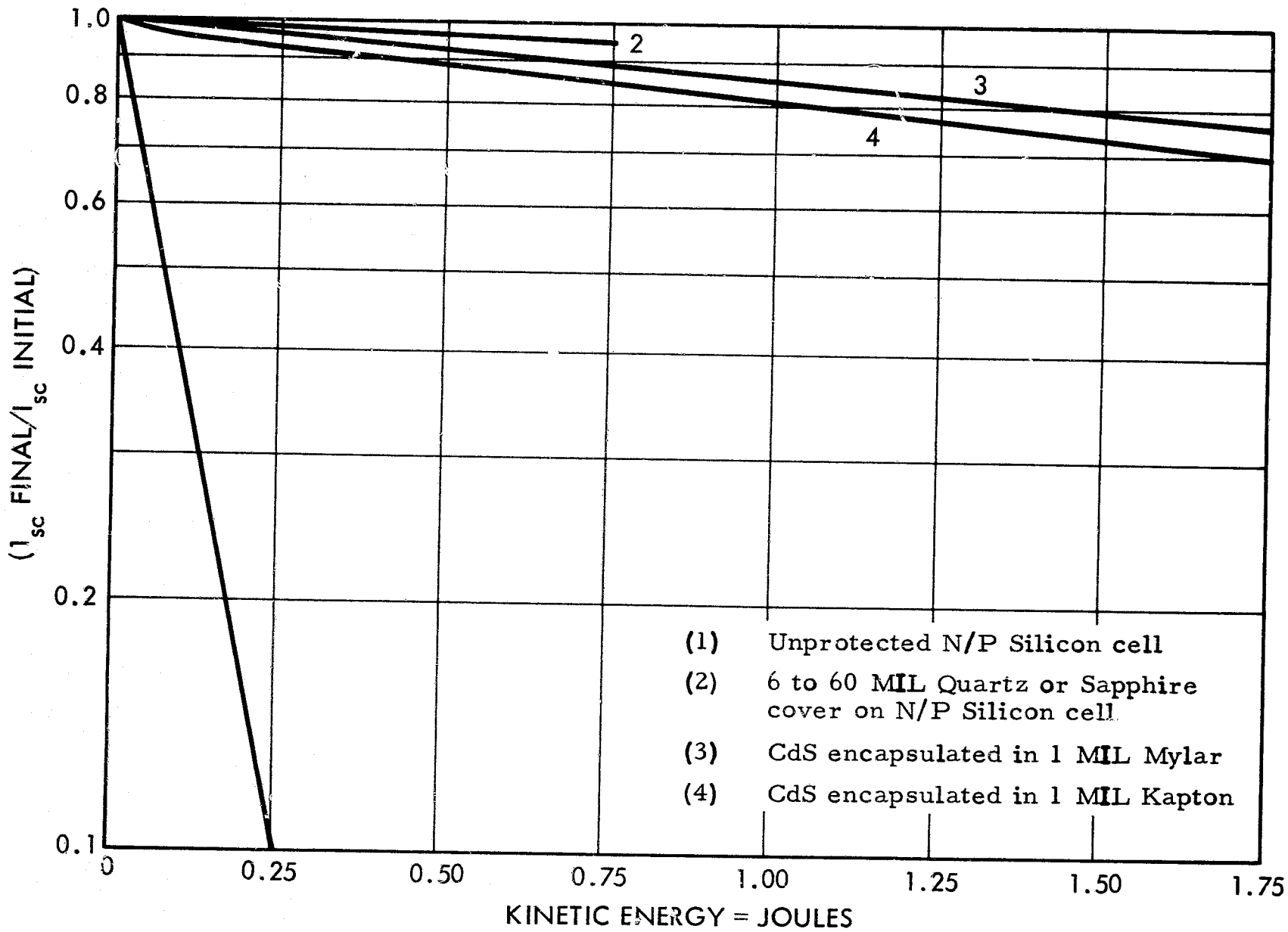

Figure 7.16 Estimate, Based on Laboratory Data, of the Ratio of Initial I_{sc} to Final I_{sc} for Silicon and CdS Solar Cells Versus Kinetic Energy of Cloud of Impinging Micrometeoroid Particles Weighing 10^{-8} to 10^{-12} grams Whose Average Velocity is 2.65 km/sec (Reference 6.6)

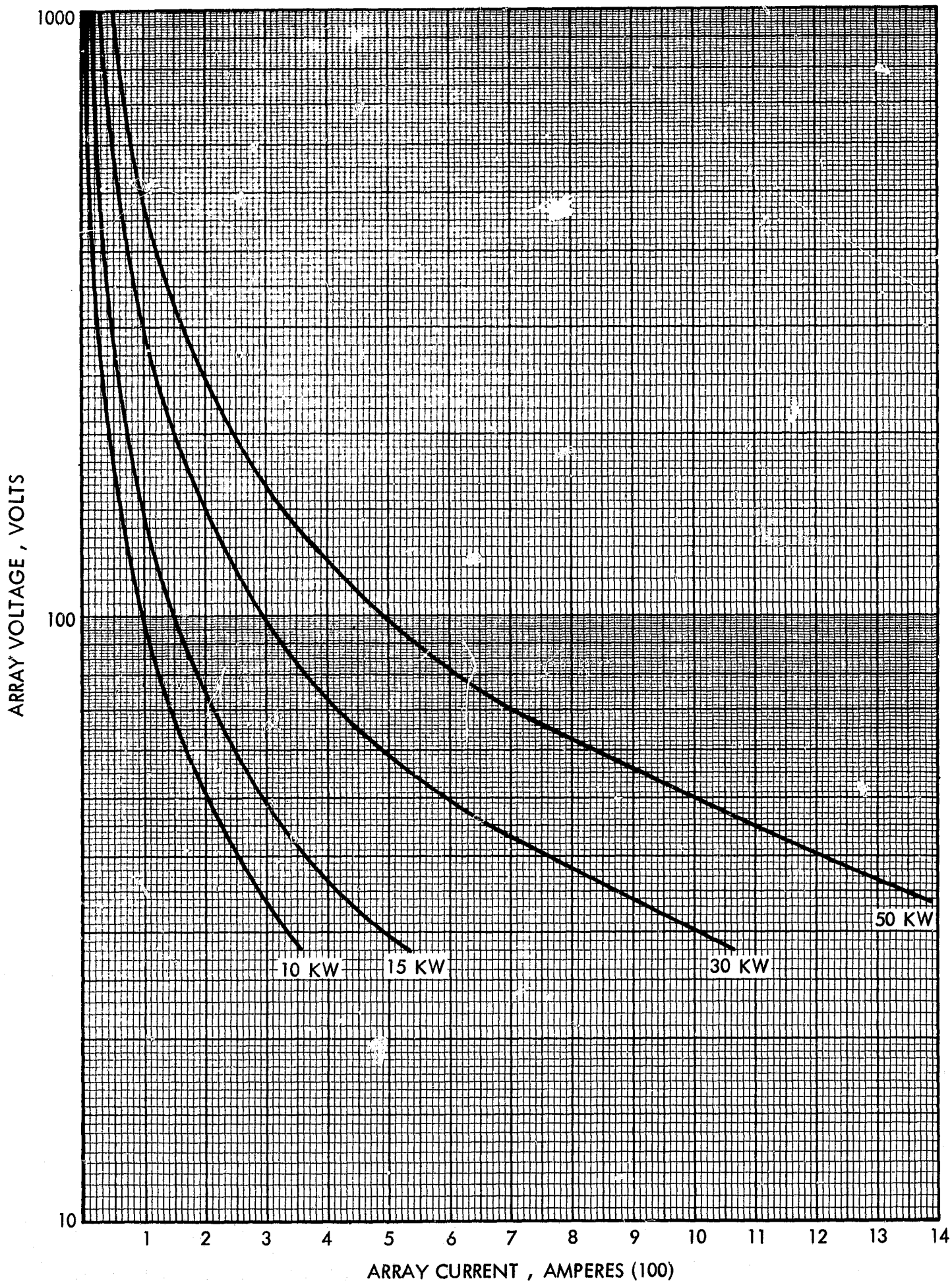

Figure 7.17 Solar Array Voltage Versus Current for Various Power Output Levels at Normal Solar Insolance and Constant Temperature

considerations, a main bus voltage of 300 volts was selected for this study (see Section 10). Figures 7.18 and 7.19 show the effect of array voltage on circuit power loss and circuit weight (assuming copper as the conductor in all cases) for various array power levels for both single crystal silicon and CdS thin film arrays.

In the case of CdS thin film solar cell arrays, copper can be used throughout for the circuit interconnection as there is no material compatibility problem of differential thermal expansion between components (thin film cells use copper contacts). There is a requirement, however, as a result of the wide thermal excursions and rapid thermal shock rates to be expected, to use a material other than copper for the direct interconnections of silicon cells on the arrays. There are two alternative materials available today in this area. These are goldplated Kovar and molybdenum. Kovar is the most commonly used material, because of the relative ease with which it can be applied to array fabrication. At present, molybdenum cannot be attached to the silicon cell contacts by conventional means. However, Kovar, being an iron-nickel alloy, could create electromagnetic interference problems. Hence, this characteristic should be investigated prior to its use to insure compatibility with the overall mission requirements. This restriction could dictate the use of molybdenum and thus, necessitate the requirement to develop cell interconnect attachment techniques.

The main bus, on the other hand, should be made of copper to minimize power losses between the solar array, the power conditioning equipment, and the load. Table 7.5 indicates that a significant weight savings could be realized if aluminum were used, even with the additional material gauge required to maintain low power losses. Hence, consideration should be given to use of this material also. Figure 7.18 has only considered copper as the circuit material. Thus, for aluminum, the weight and/or percent power loss values would change, depending on the particular design.

All weights for silicon cell arrays discussed throughout this study were based upon the use of Kovar interconnects and a copper main bus. CdS thin film arrays considered the use of copper throughout.

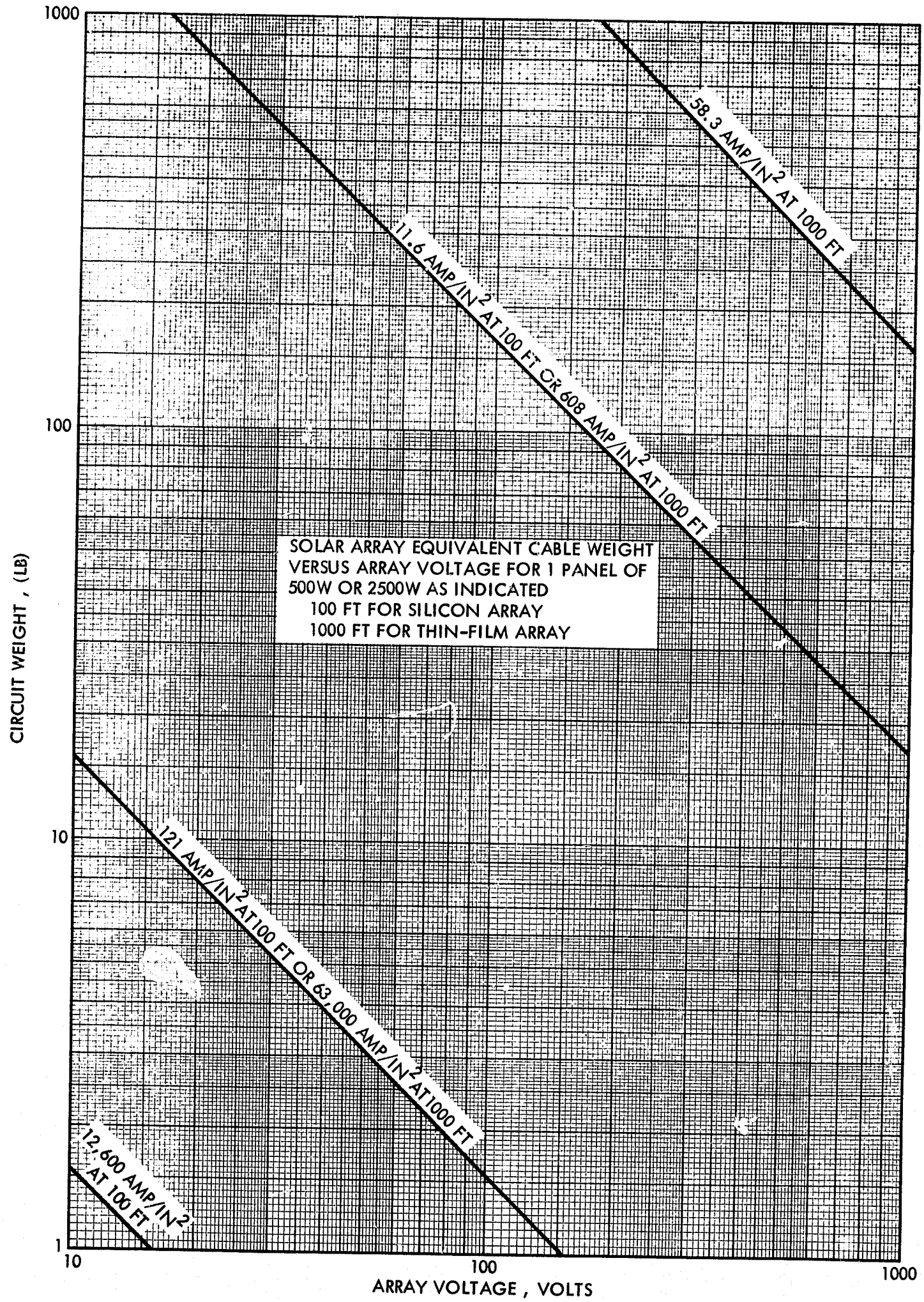

Figure 7.18 Solar Array Equivalent Cable Weight Versus Array Voltage

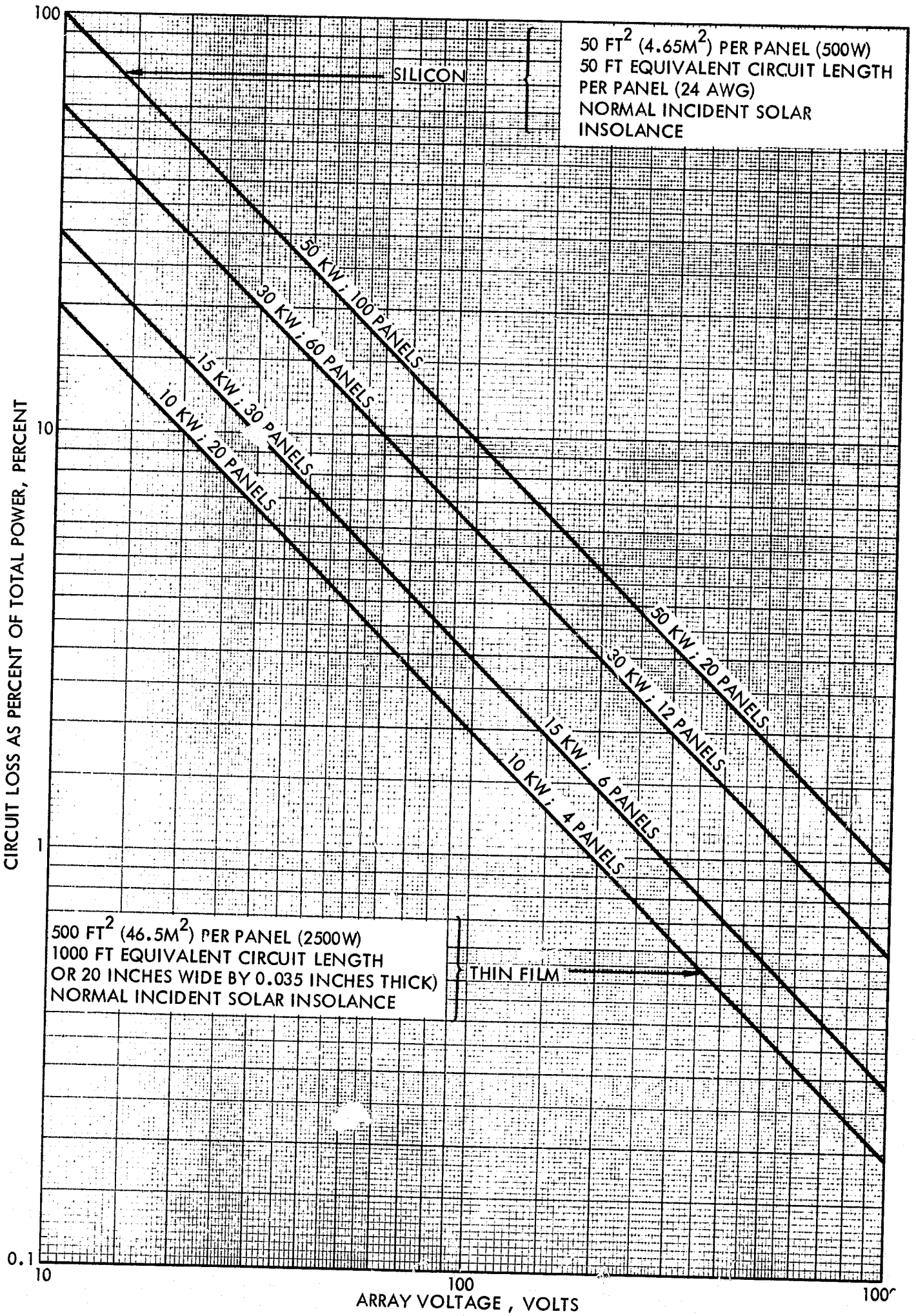

Figure 7.19 Solar Array Power Losses Versus Array Voltage

Table 7.5 Comparison of Various Candidate Solar Array Electrical Interconnection Material Densities and Expansion Relative to Silicon

	Relative Thermal Expansion	Density	
		lb/ft^3	m/cc
Silicon	1	151	2.33
Copper	4.1	555	8.89
Kovar	1.18	521	8.35
Molybdenum	1.20	562.5	10.20
Iridium	1.4	1400	22.42
Platinum-Iridium	1.87	1335	21.4
Tantalum	1.62	1036	16.6
Aluminum	4.6	168	2.7
Brass	4.9	527	8.44
Beryllium	3.5	113.5	1.82

Figure 7.20 compares the thermal expansions coefficients of several candidate silicon cell interconnect materials (0.003 inch thick) to that of the cell itself. It should be noted that at low temperatures (i.e., below $0^{\circ}C$) molybdenum more closely matches the expansion coefficient of silicon, while at high temperatures (i.e., $0^{\circ}C$ to $400^{\circ}C$) Kovar is more closely matched. The coefficients of each of these materials (i.e., Kovar and molybdenum) are much better than all others considered. However, until satisfactory production assembly techniques are developed for using molybdenum, Kovar is currently recommended for use.

7.4 WEIGHT

7.4.1 Structural

The weight of a 2.5 kw array, including the substrate and mechanical support frames and mechanisms for each candidate configuration were based on estimates of various industry designs (see Section 7.1) and use materials and components which would be available in the 1968-1970 time period.

The substrate was assumed to have a specific weight of 0.15 lb/ft^2 (based on the Boeing concept) and the frame, mechanical assembly, and support structures were varied depending on configurations as follows:

- o flat 0.120 lb/ft^2
- o leanto 0.203 lb/ft^2
- o oriented 0.314 lb/ft^2

All arrays were also assumed to include multifoil insulated skirting for lunar surface thermal control.

The total array densities, including 0.169 lb/ft^2 for electrical components, then become:

- o flat 0.438 lb/ft^2
- o leanto 0.522 lb/ft^2
- o oriented 0.633 lb/ft^2

The flat array is lightest, as it has the least support structure. The leanto has an increased density due to the fact that it requires a two-sided support structure. The oriented array requires a more

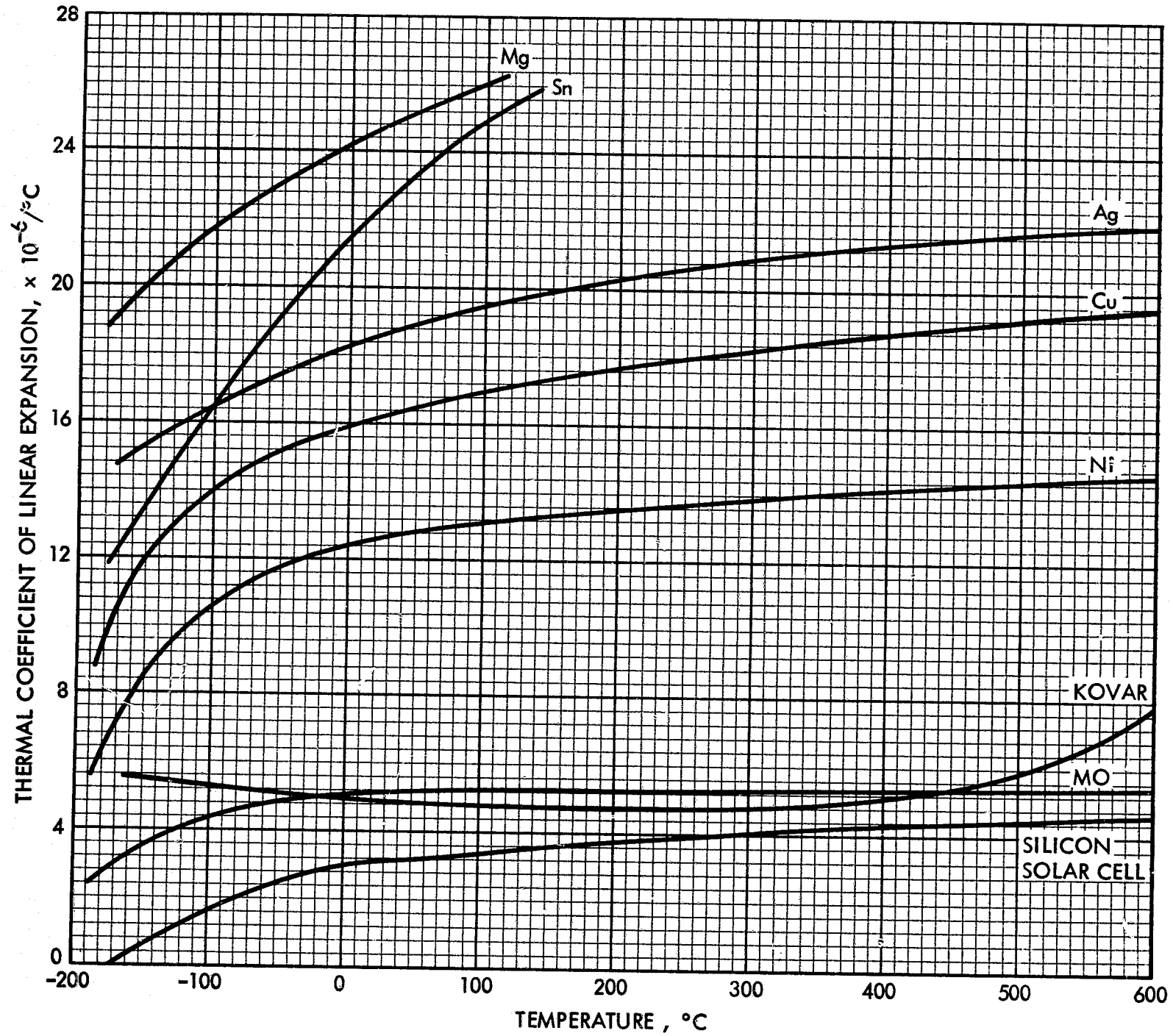

Figure 7.20 Comparison of Candidate Silicon Solar Cell Interconnect Material Thermal Expansion Coefficients with Single Crystal Silicon Cells

sophisticated structure to minimize bending due to both static and dynamic loading in the 1/6 gravity environment. Also, this array requires automatic or manual actuators to provide the required oriented capability.

Weight-to-power ratios for each configuration including electrical components are:

- o flat 63.5 lb/kw
- o leanto 94.5 lb/kw
- o oriented 91.0 lb/kw

These values are based on the noon power-to-area ratios of each configuration, discussed in Section 8 of this report.

7.4.2 Electrical

The photovoltaic assembly is considered to consist of the following:

- o cell to structure adhesive (0.004 inch thick)
- o cabling (0.03 lb/ft^2)
- o interconnects (0.003 lb/ft^2)
- o solar cells (silicon 0.008 inch thick)
- o cover slide adhesive
- o cover slides (0.006 inch thick)

The adhesives considered for a lunar environment application are:

- o RTV-511 or 577 (cell-to-substrate bonding)
- o RTV 602 or equivalent (cover slide-to-cell bonding)

Power cabling weights are assumed to be included as part of the power conditioning systems and are taken into consideration in Section 10 of this report.

Table 7.6 was included to permit a comparison of the estimates made in this study (Tables 7.1 and 7.2) for lunar surface arrays, with those for contemporary deep space application arrays. Since the Lunar Environment Model (reference 7.1) upon which this study was based, does not suggest the need for any new or exotic materials for solar array electrical and mechanical assemblies, the "common" materials and techniques

FOLDOUT FRAME

Array Type	Single Crystal Silicon Cell (lb/ft^2)					
Supplier	Boeing	Hughes	EOS	Ryan	General Electric	
Data Base	50 kw	20 kw	10 kw	2 kw	2.5 kw	1
Cell Thickness	8 mil	8 mil	4 mil	8 mil	8 mil	1
Cell Stack	0.1699	0.1560	0.0968	0.1560	0.1560	0.
cover adhesive cell interconnect adhesive dielectric						
Structure	0.1500	0.0120	0.1111	0.1689	0.1500	0.
substitute frame						
Deployment	0.0407	0.2075	0.0376	0.3224	0.0500	0.
structure mechanisms						
Main Electrical Cabling and Miscellaneous Hardware	0.0353	0.0065	0.0050	0.0073	0.0350	0.
TOTAL	0.3959	0.3820	0.2505	0.6546	0.3910	0.

*TRW Cell Stack and Cabling Weights with Hughes-Ryan Structure Respectively

Table 7.6 Comparison of Various Solar Array Weight-to Area Ratio Estimates

FOLDOUT FRAME

on Cell (lb/ft^2)			CdS Thin Film (lb/ft^2)				
Ryan	General Electric	TRW	Boeing	General Electric	TRW	*TRW/ Ryan	*TRW/ Hughes
2 kw	2.5 kw	1 kw	50 kw	2.5 kw	2.5 kw	2.5 kw	20 kw
8 mil	8 mil	10 mil	5 mil	5 mil	5 mil	5 mil	5 mil
0.1560	0.1560	0.2120	0.0665	0.1500	0.0665	0.0665	0.0665
0.1689	0.1500	0.1680	0.1240	0.0220	0.0134	0.1689	0.0120
0.3224	0.0500	0.1130	0.0420	0.0500	0.1206	0.3224	0.2075
0.0073	0.0350	0.005	0.0305	0.0350	0.0040	0.0040	0.0065
0.6546	0.3910	0.4980	0.2630	0.2570	0.2045	0.5618	0.2925

spectively

normally used for spacecraft arrays have been assumed to arrive at the above array densities.

7.4.3 Ancillary Components

Several structural and support elements will be required for lunar based solar arrays that are not required for space applications. These would include handles, attached to the array structure. This would permit astronaut handling without damage to the structure and/or solar cells and also provide insulation to protect the astronaut from the potential danger of handling a high voltage, high power array.

Another ancillary component would be the interface pad between the array support structure and the lunar surface. Figure 7.21 shows that the depth of array penetration into the lunar soil as a function of bearing surface area. Thus, a low surface bearing pressure must be included in this interface structure design.

Of considerable importance in lunar surface solar arrays is the requirement to insure astronaut safety. Thus, some method of insuring against electrical injury must be considered involving a structural barrier, such as a fence around the array, or by establishing detail operating and maintenance procedures to be followed when working near illuminated arrays.

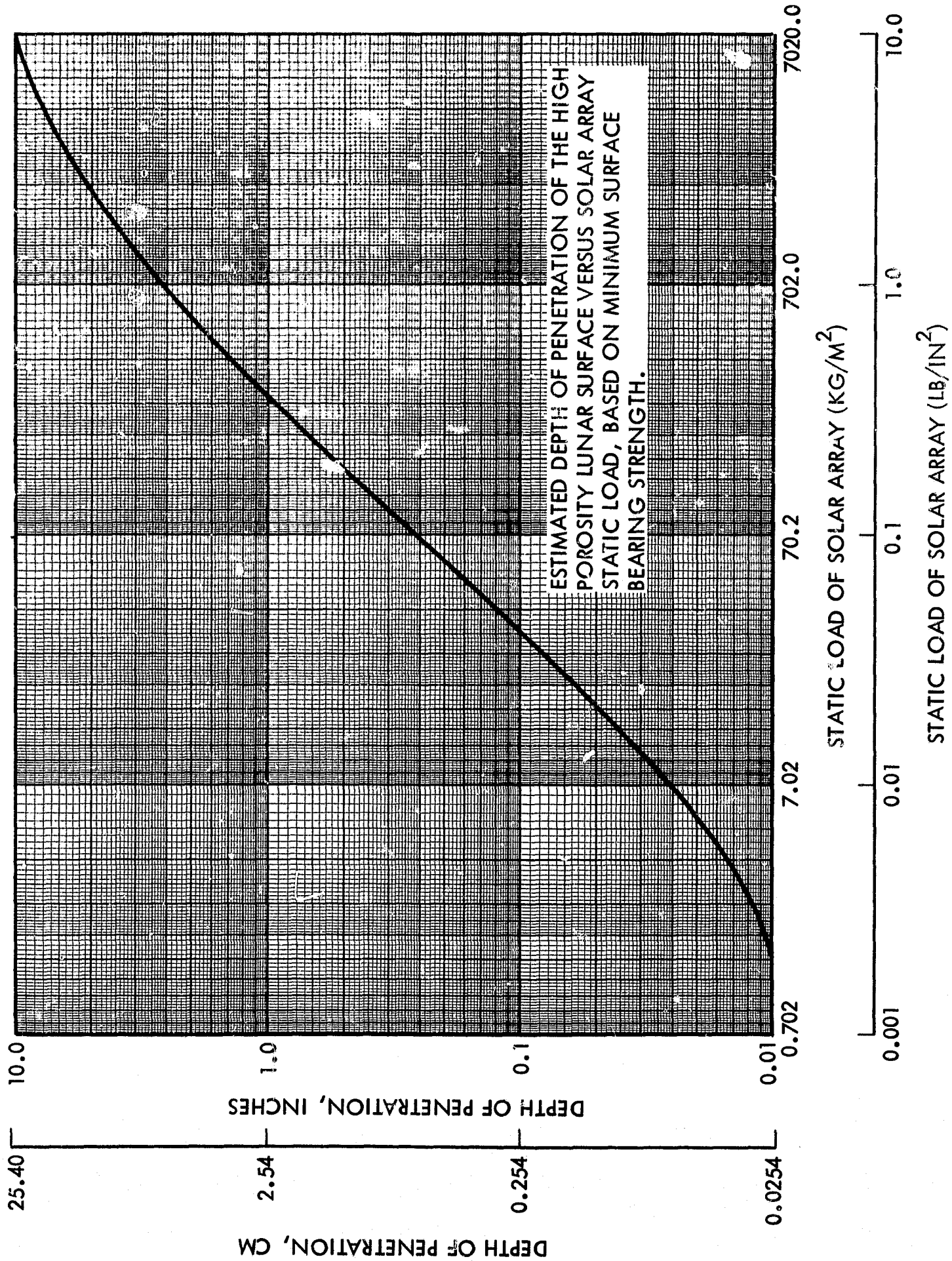

Figure 7.21 Estimated Depth of Penetration of the High Porosity Lunar Surface Versus Solar Array Static Load

8. SOLAR ARRAY PERFORMANCE CONSIDERATIONS

8.1 INTRODUCTION

There were three categories of solar arrays considered during this study. These categories were non-oriented, semi-oriented (non-articulated), and fully oriented. The various configurations that were of interest during this study are shown in Figure 8.1, and the reasons for their selection are discussed in Section 4.6. The thermal analyses and parametric data used in estimating the performance of the baseline solar array concepts is discussed in this section.

8.1.1 Baseline Configurations

8.1.1.1 Non-oriented Array

This concept applied to a flat configuration (Type 1 of Figure 8.1) which was normal to the Sun at lunar noon (at the lunar equator) and thus, produced maximum power only at that time. For other latitudes, it would be necessary to adjust the array to achieve the equivalent performance. It represents the simplest of all the configurations to put into operation. However, the power output profile is a function of the cosine of the solar incidence angle and hence produces no power at the terminator (sunrise and sunset) conditions. Thus, it is not always possible to match the load profile for various applications without the supplementary use of electrochemical power (batteries, fuel cells).

8.1.1.2 Semi-oriented (non-articulated) array

This array concept is depicted by Types 2 through 7 of Figure 8.1 and permits non-articulated shaping of the output power profile by the use of various fixed-array geometries.

- Tipped flat array

  This concept (Type 2 of Figure 8.1) is identical with the non-oriented flat array except that it can be adjusted during lunar assembly to compensate for latitude angle. This permits the array to be normal to the Sun at lunar noon at any latitude on the lunar surface. This attitude adjustment can result in as much as a 10 to 15 percent increase in power at lunar noon. However, this performance improvement is offset by a 10 to 15 percent increase in array weight due to the additional supporting

Type	Configuration	Diurnal Power Profile (Including Temperature effects)	Relative Effectiveness at 30° Latitude	
			Relative Weight	Relative Solar Cell Area
* 1. Fixed Array— Flat on Lunar Surface	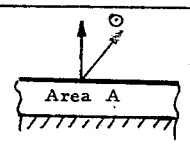	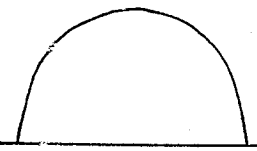	1.0	1.0
2. Fixed Array—Normal to Sun at Noon	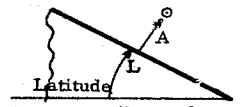 L = array tilt equal to latitude angle	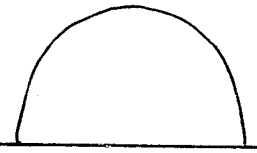	1.12 (Weight of structure = 0.3 x weight Solar Cells)	0.863
3. Fixed Lean-to -Stretched Single Prop at Center Rectangular Solar Array	α = slope of lean-to-sides		0.97 (Weight of structure = 0.07 weight Solar Cells)	0.90
* 4. Fixed Lean-to-Unstretched Single Prop at Center Rectangular Solar Array	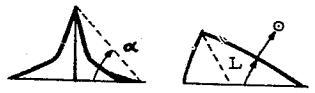	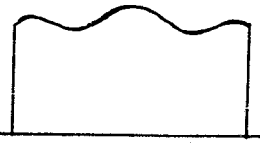	0.96 (Weight of structure = 0.05 weight Solar Cells)	0.92
5. Fixed Lean-to-Pressurized Rectangular Solar Array	α = slope angle	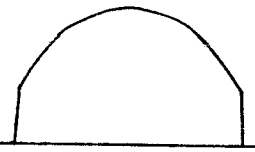	1.72	0.89
6. Hemisphere-Pressurized	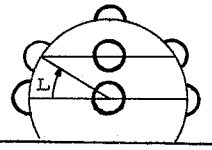	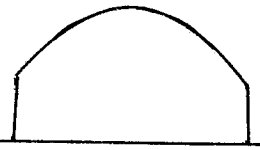	2.13	1.43
7. Sphere-Pressurized	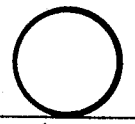		2.22	2.22
8. Fully Oriented Array (nonskirted)	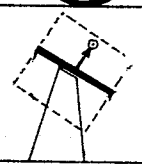	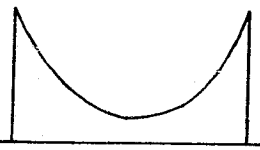	0.71 to 1.38 (Weight of structure = 0.3 to 1.5 x weight Solar Cells)	0.55
* 9. Fully Oriented Array (skirted)		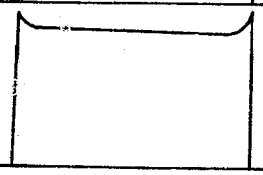	0.71 to 1.38 (Weight of structure = 0.3 to 1.5 x weight Solar Cells)	0.55

*Array configurations being evaluated in detail.

Figure 8.1 Baseline Solar Array Configurations

structure required. The net result is that on an overall weight basis the Type 2 concept is equivalent to Type 1.

- Leanto array

  These concepts (Types 3, 4, and 5 of Figure 8.1) have all the advantages of the tipped flat concept (Type 2). However, they can be made more effective in increasing the power output of the terminators by orienting the tilt angle in both the north-south and east-west directions and by incorporating a second array as a mirror image. This concept results in a much improved output power profile compared to the flat array, in that there is a significant increase in the power produced at the terminators. In addition, approximately 40 to 50 percent more power is available at lunar noon. The leanto concept can easily be made operational by either one or two astronauts. In addition, no adjustments are required during manned or unmanned periods of operation for power optimization.

- Hemisphere array

  This concept (Type 6 of Figure 8.1) is similar to the leanto configuration, except that it would utilize inflation or geodesic dome construction for erection. The area required for this configuration is approximately two times that of the leanto array and results in only a slightly improved lunar noon power output profile. The inflatable design requires a hermetically sealed base and gas storage, as well as, pressurization controls to compensate for the gas volume change during the extreme temperature excursions between lunar noon and midnight. All inflatable concepts by virtue of being gas filled are heavy, difficult to repair, and extremely vulnerable to micrometeroid damage. Geodesic type structures are very inefficient solar array configurations unless they are used for multi-purpose requirements, such as to house personnel and for equipment storage. Array weight, cost and area requirements can then be pro-rated with other sub-systems, in which case, they become extremely attractive. However, the time required for erection can become prohibitive if the cost factor of $300, 000/astronaut hour (see Section 4) is applied.

8.1.1.3 Fully Oriented Arrays

This category includes the sphere (Type 7 of Figure 8.1) and the articulated flat array configurations (Type 8 and 9 of Figure 8.1).

- Spherical array

  This concept is similar to the hemisphere (Type 6) and would also utilize either gas pressurization or geodesic type construction for erection. The comments made for the hemisphere concept also apply to the spherical array. In addition, for both cases the array circuitry would become extremely complex due to the continuously changing sun angle. Array weight and cost would also be probhibitive due to the large total area involved.

- Articulated flat array

  This concept, was found to be very attractive due to its power output profile (significant power at terminators). However, there were several shortcomings associated with this configuration. These included increased structural weight, longer deployment time, redundant automatic drive mechanisms required to achieve necessary reliability or the use of several hundreds of astronaut hours per mission for manual orientation or maintenance.

The lunar phase changes at a rate of 0.51 degrees per hour (12.2 deg/Earth day). Therefore, to maintain a pointing accuracy of $\pm$ 10 degrees ($\pm$ 4% power variation), which is considered a minimum to maintain solar array performance, orientation at 40 hour intervals would be required. Each array produces 2.5 kw (20 arrays required for 50 kw) and assuming 0.5 hours per array for orientation, a total of 10 hours out of every 40 hours would be required for orientation of the solar array. This was felt to be prohibitive. If synchronized automatic orientation was employed, this time period could be reduced. However, this would increase the complexity of the array design since additional consideration for the use of special lubricants, seals, thermal control techniques and cabling designs would also have to be included. These latter requirements could also adversely effect overall system weight and reliability. Nevertheless, the articulated flat configuration does result in the smallest array active

area of all candidate concepts considered, and its power profile can be made very nearly constant throughout the lunar day by the use of passive thermal control techniques (i.e., skirting).

8.1.2 Concept Selection

Based upon the qualitative assessments for the above candidate configurations, Types 1, 3 and 9 of Figure 8.1 were selected for further analysis. These concepts appeared to represent the most attractive configuration from each category investigated.

The flat array (Type 1) was selected because of its relatively simple construction. The leanto array (Type 3) was chosen for its improved, passively controlled power profile. Finally, the articulated flat array (oriented, Type 9) was included, due to smaller area requirements and its correspondingly attractive power output profile.

Inflated concepts (Types 5, 6, and 7) were discarded for the reasons discussed in Paragraph 8.1 above, as well as the fact that this concept was potentially costly, and also incompatible with the use of single crystal silicon solar cells. The Type 4 (Figure 8.1) leanto configuration was dropped since the Type 3 concept was more compatible with single crystal silicon cell array designs. In addition, with moderate stretching or as a rigid configuration, it offered gains in performance not possible with Type 4, which had been considered primarily for use with CdS thin solar cells.

These candidate solar array configurations are depicted schematically in Figure 8.2. The concept of skirting to passively control the lunar surface temperature was included for each configuration. Its function is discussed in detail in Thermal Analysis, Section 8.2 which follows.

8.2 THERMAL ANALYSIS

Having selected the three candidate array concepts on a rather qualitative basis, it now became necessary to investigate the solar array thermal characteristics. This was essential since the performance of solar arrays is highly dependent upon the resultant solar cell equilibrium temperature as discussed in Section 7.3. A generalized, albiet fairly simplified, thermal model was devised to aid in this analysis and is discussed below.

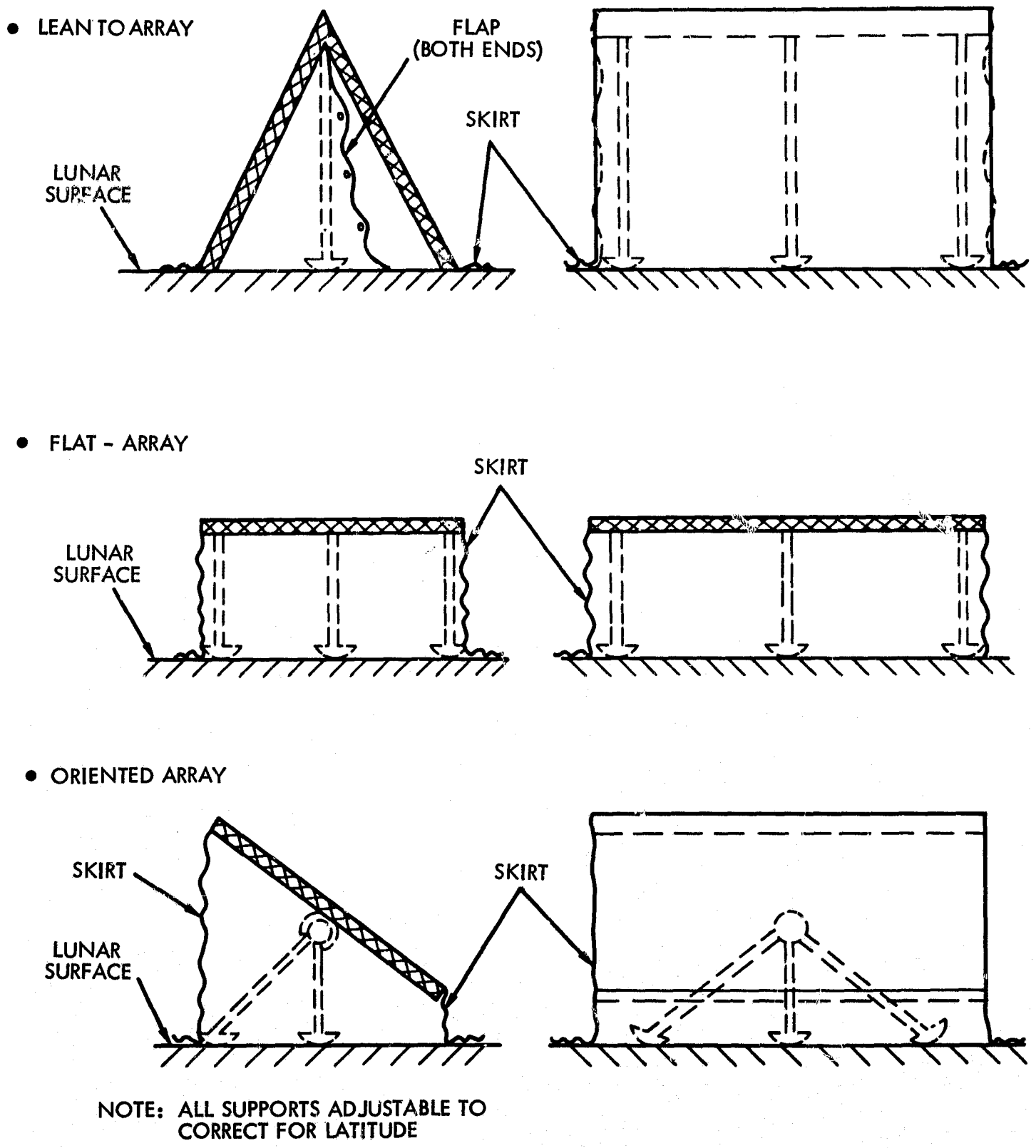

Figure 8.2 Candidate Solar Array Configurations

8.2.1 Thermal Model

Accurate calculation of solar array temperatures during the lunar day involves equations and parameters which are a function of many variables. Due to the large number of variables involved, a comprehensive computer program was required to arrive at reasonably accurate solutions. To keep the effort associated with the thermal analysis within the scope of this study, it was necessary to make several simplifying assumptions, but which would still result in a reasonably accurate, first order approximation solution for solar array equilibrium temperatures. The approach taken and the conditions assumed are shown in Figures 8.3 and 8.4. These equations and values were used for calculation of array equilibrium temperatures. Three separate conditions were considered. Case I was for a non-insulated condition in which the thermal resistance between the front and the back surfaces of the array was assumed negligible (such as when light gauge materials are used for cell mounting). Case II was for insulated arrays where the rear surface of the array consisted of multi-foil insulation which permitted neither cooling nor heating by the lunar surface. A third case which was a special condition of Case I, incorporated array skirts, which limit the view factor of the back surface of the array to the shaded lunar surface directly under the array. With this portion of the lunar surface completely shaded from direct and/or reflected solar input, the only thermal input to the shaded lunar surface would be that which radiates from the rear of the solar array during operation. The skirting would be made from multi-foil aluminized Mylar insulation.

Typical values of conductance and specific weight for ten layers of 0.00025 in. aluminized Mylar are 0.01 BTU/hr-ft^2-$^\circ$F and 0.045 lb/ft^2 respectively. The view factors given in Figure 8.4 are for flat plate elements and are given as a function of the angle between the lunar surface and the solar array rear surface. The values in this figure may also be used for curved surfaces by considering the surface to be made up of a series of flat plate chords. The temperature can then be computed as a function of position on the curved surface.

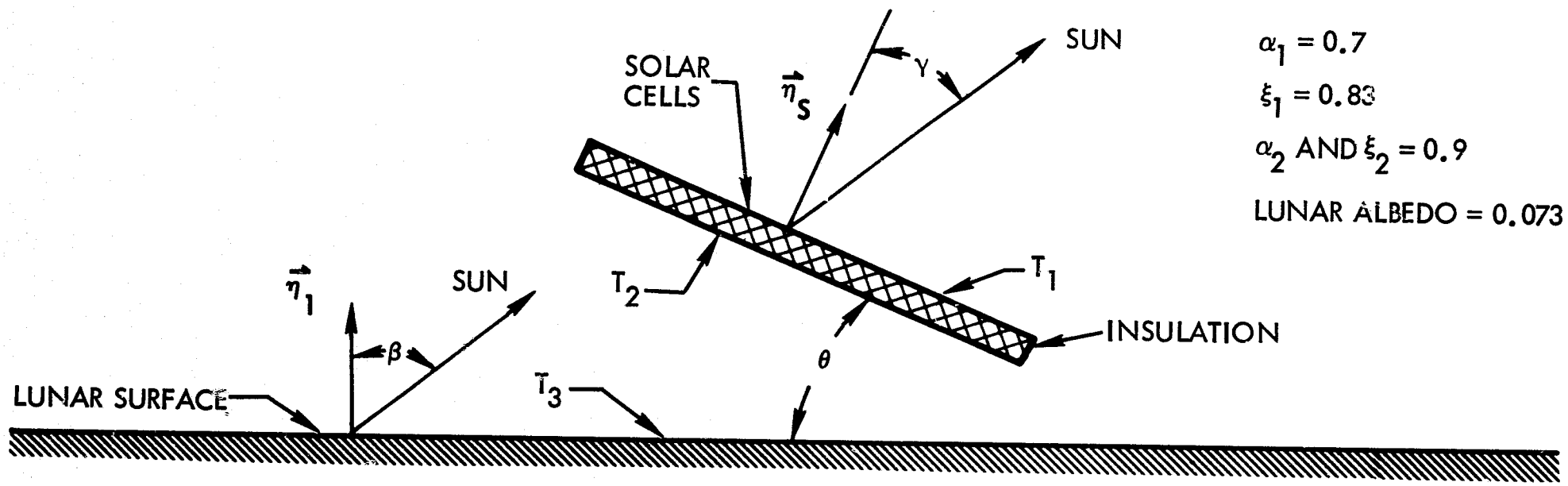

CASE I: NEGLIGIBLE THERMAL RESISTANCE BETWEEN FRONT AND BACK SURFACES (NONINSULATED)

$$T_1 = \left\{ \frac{B + C \cdot T_3^{\,4} + D}{(G + C)} \right\}^{1/4}$$

CASE II: PERFECT INSULATION BETWEEN FRONT AND BACK SURFACES (INSULATED)

$$T_1' = \left\{ \frac{B + C_1 \cdot T_3'^{\,4} + D_1}{(G_1 + C_1)} \right\}^{1/4}$$

Figure 8.3 Thermal Model for Temperature of Lunar Surface Solar Arrays

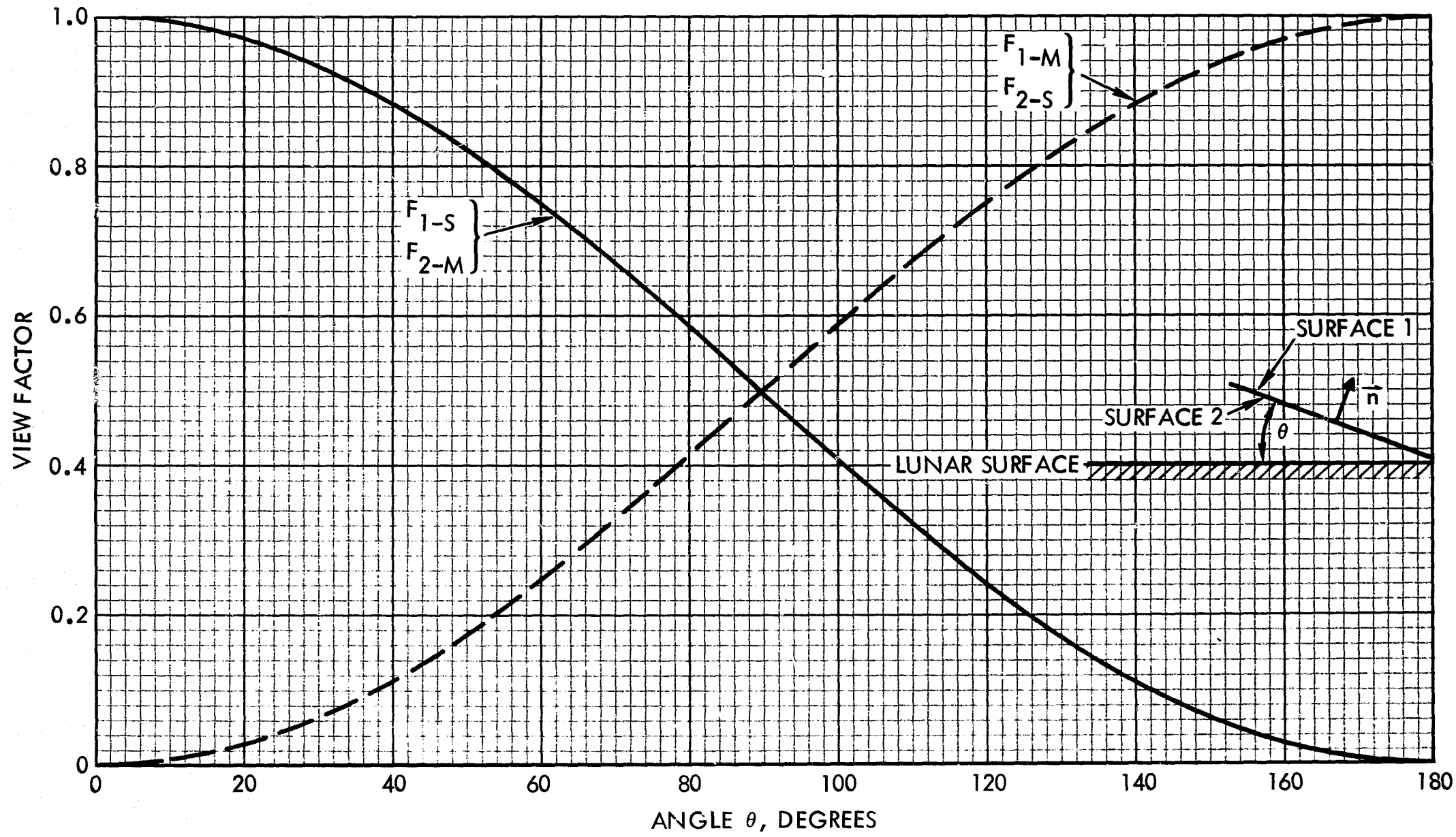

Figure 8.4 Flat Plat View Factors

The array equilibrium temperature temperature for Case I, where negligible thermal resistance exists between array front and rear surfaces ($T_1 = T_2$), is given by the equation,

$$\alpha_1 \cdot S \cdot (1-\eta) \cdot \cos\gamma \times A + A\,[\epsilon_1 F_{1-m} + \epsilon_2 F_{2-m}] \cdot [T_3^4 - T_1^4] + A \cdot [\alpha_1 F_{1-m}(1-\eta) + \alpha_2 F_{2-m}] \cdot S \cdot \cos\beta \cdot E = A\,\sigma\, T_1^4\,[\epsilon_1 F_{1-S} + \epsilon_2 F_{2-S}] \qquad (8.1)$$

The variables in equation 8.1 can be grouped into functions. These have been designated by symbols B, C, D, and G and together with a range of values for silicon cells and CdS thin films are listed in Table 8.1.

Hence, when solving for T_1, Equation (8.1) can be rewritten as;

$$T_1 = T_2 = \left[\frac{B + C \cdot T_3^4 + D}{(G + C)}\right]^{1/4} \qquad (8.2)$$

For the case of perfect insulation between front and rear surfaces (Case II) of the solar array, Equation 8.1 becomes;

$$\epsilon_1 \cdot F_{1-S} \cdot \sigma \cdot T_1^4 A = \alpha_1 \cdot S \cdot (1-\eta) \cdot \cos\gamma \cdot A + \sigma \cdot \epsilon_1 \cdot F_{1-m} \cdot \left[T_3^4 - T_1^4\right] \cdot A + \alpha_1 \cdot F_{1-m}(1-\eta) \cdot S \cdot E \cdot \cos\beta \cdot A \qquad (8.3)$$

and the equivalent range of values for grouped functions is given in Table 8.2. Equation (8.3) rewritten to solve for T_1 becomes:

$$T_1 = \left[\frac{B_1 + C_1 \cdot T_3^4 + D_1}{(G_1 + C_1)}\right]^{1/4} \qquad (8.4)$$

where $T_1 \neq T_2$ and $K/X \rightarrow 0$

Table 8.2 gives the data used to obtain values of B_1, C_1, D_1 and G_1 in the above equations.

Table 8.3 lists values used for array temperature calculation by euqations (8.2) and (8.4).

Table 8.1 Range of Functions for Case I (Equation 8.1)

Thermal Component	Symbol	Range of Values	
		Silicon Cells	CdS Thin Films
$\alpha_1 \cdot S \cdot (1-\eta) \cdot \cos\gamma$	B	0 to 378	0 to 356
$\sigma \cdot \left[1 F_{1-m} + \epsilon_2 F_{2-m}\right]$	C	0.143×10^{-8} to 0.154×10^{-8}	0.149×10^{-8} to 0.154×10^{-8}
$S \cdot E \cdot \cos\beta \cdot \left[\alpha_1 F_{1-m} (1-\eta) + \alpha_2 F_{2-m}\right]$	D	0 to 22.7	0 to 26
$\sigma \cdot \left[\epsilon_1 F_{1-S} + \epsilon_2 F_{2-S}\right]$	G	0.142×10^{-8} to 0.149×10^{-8}	0.149×10^{-8} to 0.152×10^{-8}

Table 8.2 Range of Functions for Case II (Equation 8.3)

Thermal Component	Symbol	Range of Values	
		Silicon Cells	CdS Thin Films
$\alpha_1 \cdot S \cdot (1-\eta) \cdot \cos\gamma$	B_1	0 to 278	0 to 356
$\sigma \cdot \epsilon_1 \cdot F_{1-m}$	C_1	0 to 1.43×10^{-9}	0 to 1.49×10^{-9}
$\alpha_1 \cdot F_{1-m} \cdot (1-\eta) \cdot S \cdot E \cdot \cos\beta$	D_1	0 to 22.7	0 to 26
$\sigma \cdot \epsilon_1 \cdot F_{1-S}$	G_1	0 to 1.43×10^{-9}	0 to 1.49×10^{-9}

TABLE 8.3

VALUES OF INDIVIDUAL PARAMETERS USED FOR THERMAL ANALYSIS OF SOLAR ARRAYS ON LUNAR SURFACE

Parameter	Units	Values	
		Silicon Cell	CdS Thin Film
E	Non-dimensional	0.073	0.073
S	BTU/hr-ft^2	444	444
T_3	^oR	180 to 780	180 to 780
α_1	Non-dimensional	0.70	0.84
α_2	"	0.90	0.90
ϵ_1	"	0.83	0.87
ϵ_2	"	0.90	0.90
η	%	10.5	4.5
σ	BTU/hr-ft^2 - ^oR	0.1714×10^{-8}	0.1714×10^{-8}
F_{1-m}	Non-dimensional	Dependent on configuration - obtain from Figure 8.4	
F_{1-S}	"	"	
F_{2-m}	"	"	
F_{2-S}	"	"	

The values of E, S, α_1 and ϵ_1 were taken from Reference 7.8 and represent the latest data available for the lunar surface. The cell efficiencies were selected from Figure 7.13 and are considered to be 1968 state-of-the-art values. The values of α_2 and ϵ_2 are considered achievable values for state-of-the-art thermal control coatings. The lunar surface temperature, T_3, was obtained from the profile shown in Figure 8.5(a), curve No. 1 and 8.5(b).

By utilizing equations 8.2 and 8.4, and substituting the proper values of the individual parameters from Table 8.3 it was possible to determine the variation in the solar array equilibrium temperature as a function of the lunar surface temperature. The corresponding lunar phase in degrees, or time in Earth days, was also depicted upon the resulting curves.

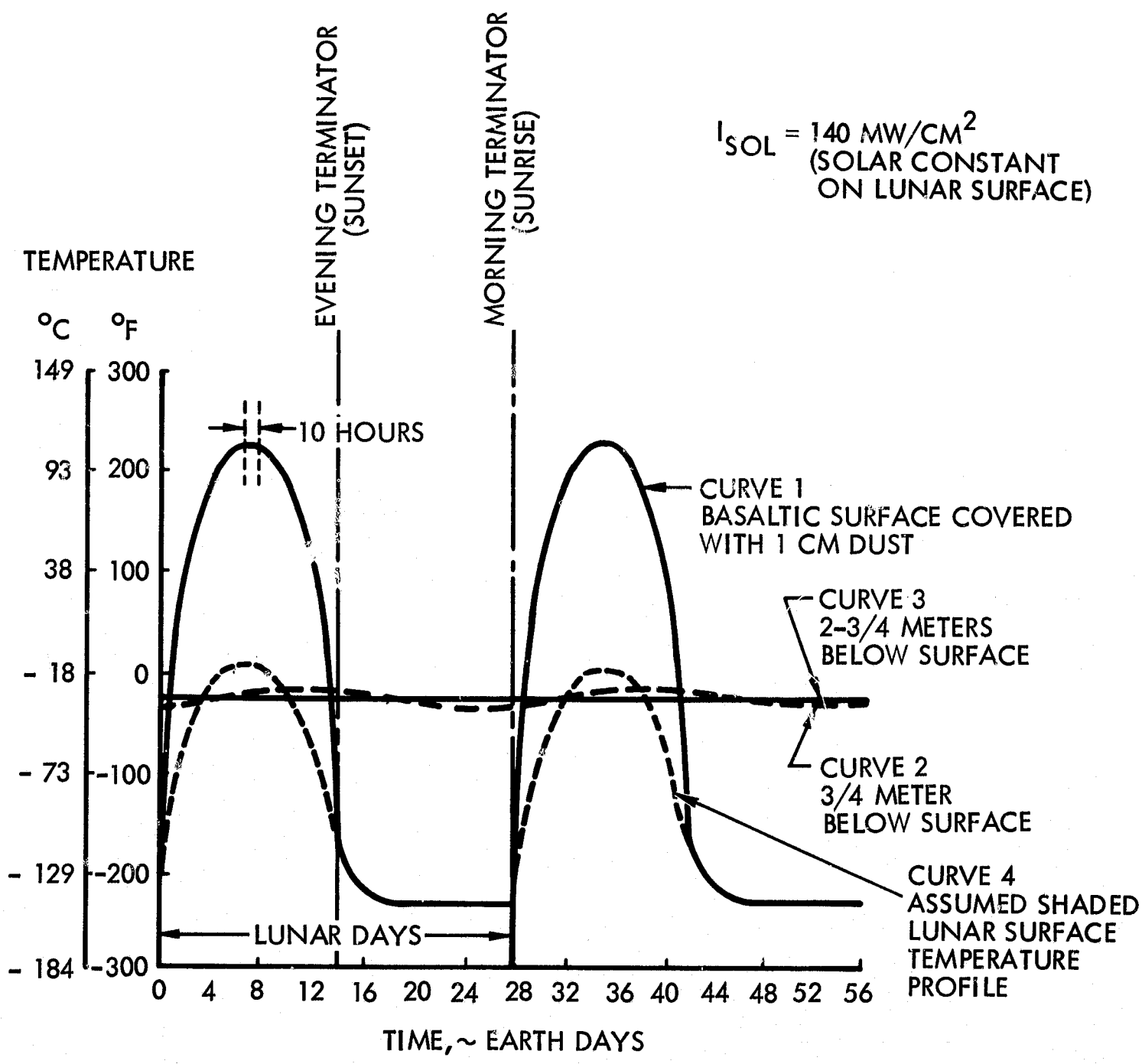

Figure 8.5(a) Typical Temperature Variation of the Lunar Surface

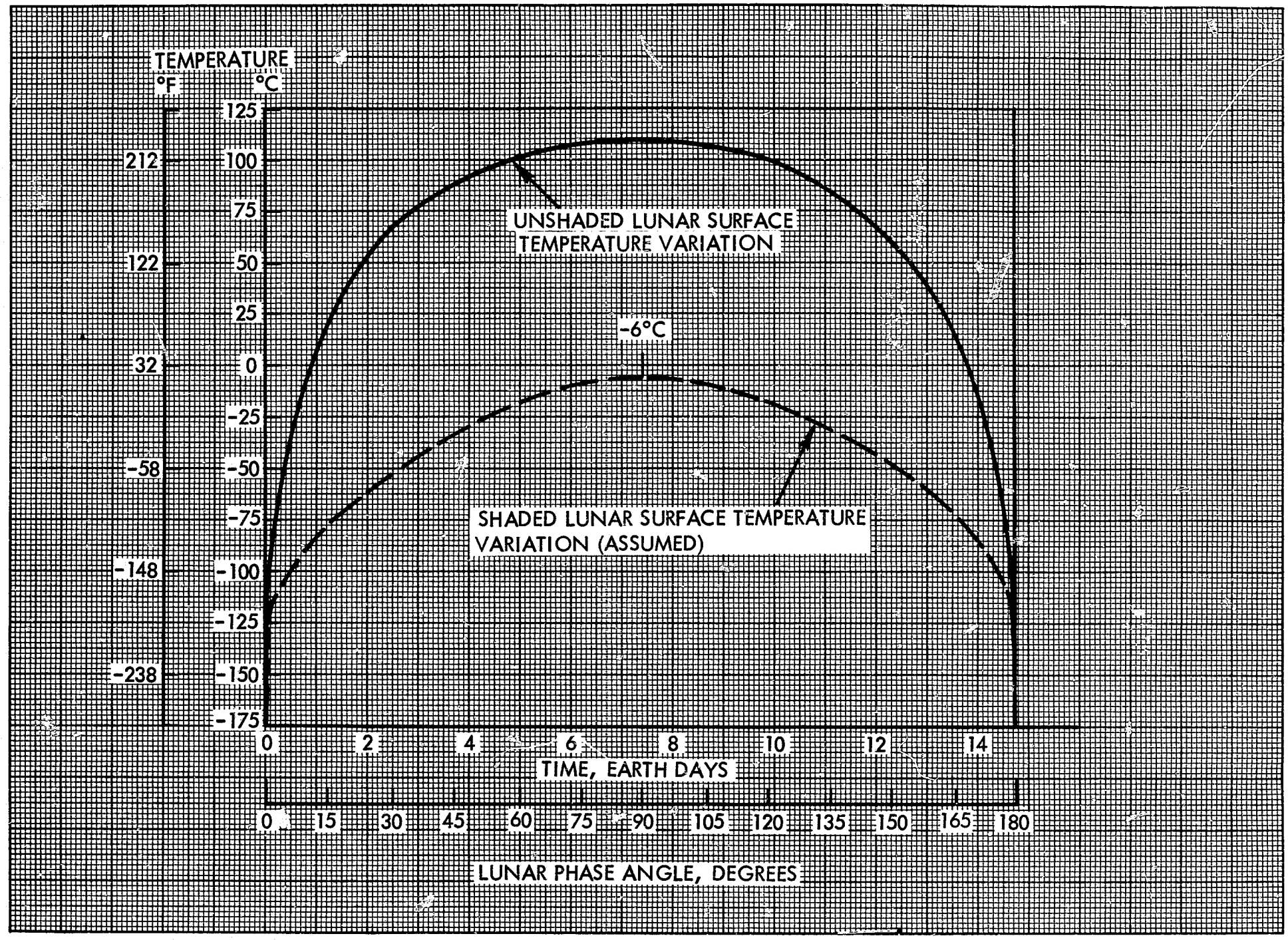

Figure 8.5(b) Comparison of Shaded and Unshaded Lunar Surface Temperature (Lunar Equator)

8.2.2 Oriented Arrays

As previously discussed, there were three thermal models considered in this study, namely:

- Case I - non-insulated
- Case II - insulated
- Case III - non-insulated (skirted)

The results obtained for the oriented array and the difference in array equilibrium temperature between cases I and II, are shown in Figures 8.6 and 8.7 respectively. The high array equilibrium temperatures obtained for Case II result from the inability of the solar array to reject heat from its rear surface due to the use of multi-foil insulation. In Case I (negligible insulation) the rear surface of the oriented array has a poor view factor with respect to outer space and lacks any other heat sink to which it may reject heat. In addition, despite its relatively high temperature, it is a cool surface when compared to the lunar surface temperature. Also, having a good view factor with respect to the lunar surface, results in the array being heated by both the solar energy on the front surface and by the reradiated energy from the hot lunar soil on the back surface.

There are, several design options which could be exercised that would result in a reduction in the oriented array equilibrium temperatures. One solution would be to maintain an orientation lead or lag of approximately 45° with respect to the solar insolance angle. The decreased energy input on the front surface due to the cosine effect, would lower the array temperature. This apparent advantage, however, may be offset by the increased area required to satisfy a given minimum power level. Hence, although a more satisfactory array temperature would be realized, a considerable increase in array area, weight, and cost would still occur. Another design option would be to shade the rear surface of the solar array and the lunar surface, directly beneath and adjacent to the array. Figure 8.8 schematically depicts the energy input for Cases I and II and indicates the effect of "skirting" on the thermal energy input.

It was seen in Case I (Figure 8.6) that the average array equilibrium temperature profile for oriented arrays using single crystal silicon cells varied between $100^{\circ}C$ and $190^{\circ}C$. For CdS thin film arrays, the corresponding temperature variation was from $125^{\circ}C$ to $195^{\circ}C$. For Case II the

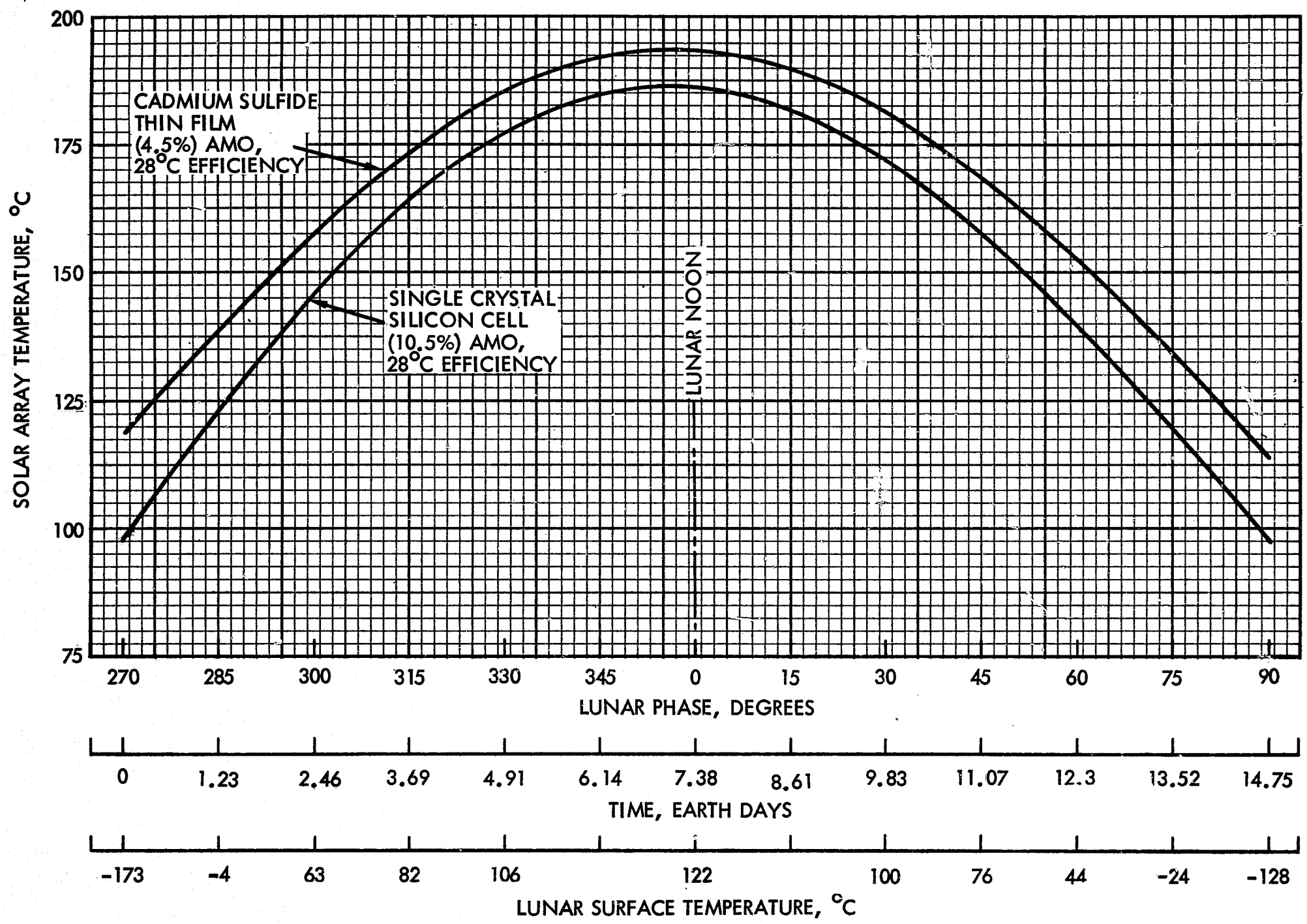

Figure 8.6 Average Solar Array Temperature Variation with Lunar Phase for Oriented Arrays (Non-insulated and Non-skirted)

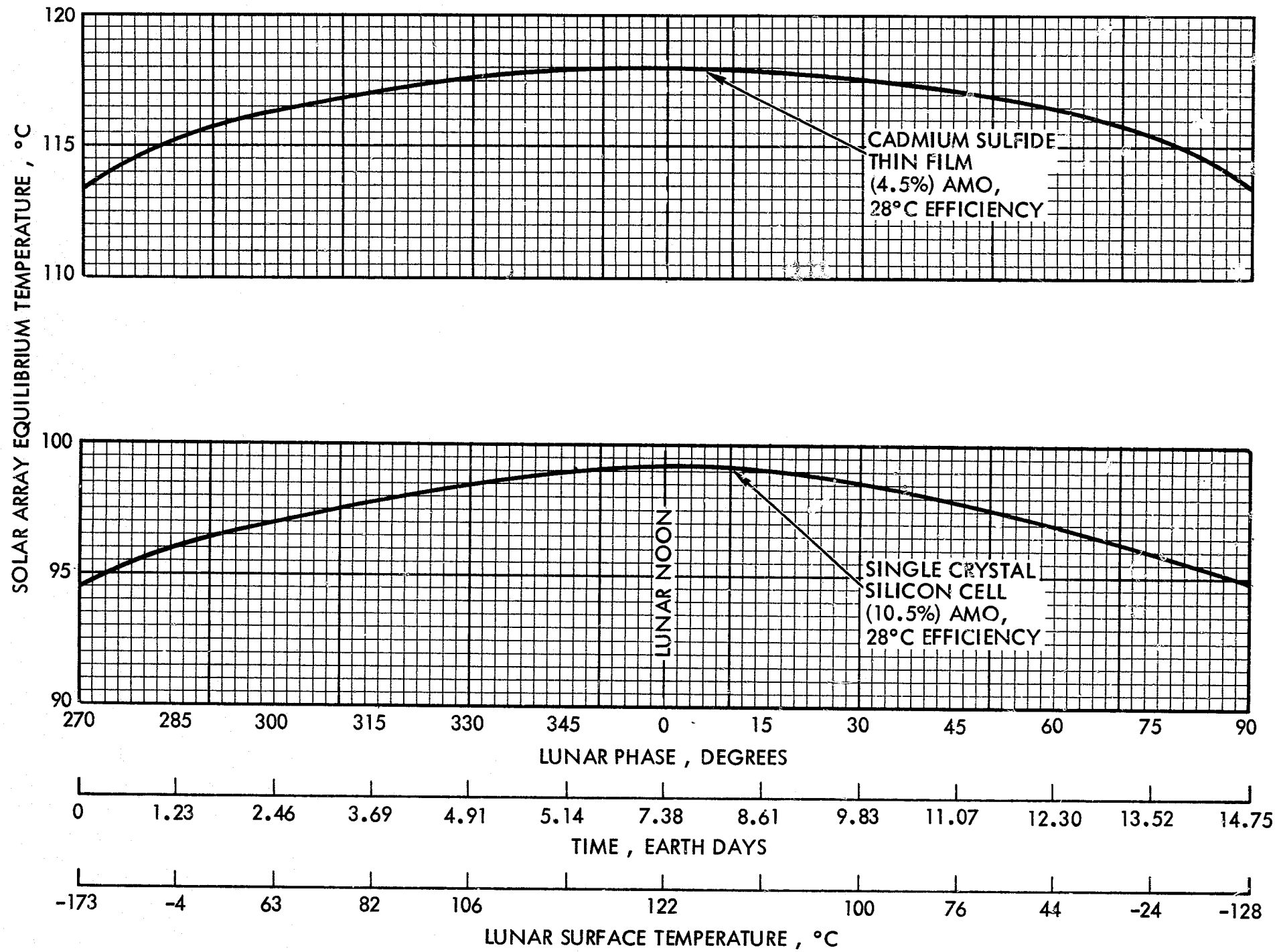

Figure 8.7 Average Solar Array Temperature Variation with Lunar Phase for Oriented Arrays (Insulated and Non-Skirted)

peak values were 99°C and 118°C, for single crystal silicon cells and CdS thin films respectively. Thus, insulating the back of the array considerably reduced these peak temperatures but they still remained relatively high. The effect of adding "skirting" (case III) to the oriented array is shown in Figure 8.9, where the shaded lunar surface was assumed to reach the peak temperature indicated at lunar noon. Array equilibrium temperature is shown for several values of shaded lunar surface temperature and cell efficiency. It should be noted, that a considerably lower average array temperature can be achieved if the peak shaded lunar surface temperature can be maintained at a corresponding low temperature.

In order to use Equation 8.2 for Case III, without greatly increasing the complexity of the analysis, it was necessary to assume that the shaded lunar surface temperature remained constant at the various peak temperatures shown in Figure 8.9. This approach, though not necessarily depicting the actual condition on the lunar surface, can be made quite conservative by a judicious selection of the peak shaded lunar surface temperature. It also permits one to make the assumption that the equilibrium temperature for the oriented-skirted array is equivalent to the non-oriented, skirted, flat array at lunar noon. The rationale behind these assumptions was as follows.

Figure 8.10 represents a simplified approximation of the thermal energy balance for a oriented-skirted or non-oriented, skirted flat array at lunar noon. For the array properties indicated, 30% of the incident solar energy is initially reflected to outer space. From the remaining 70%, approximately 10% is converted to electric power. This leaves 60% of the solar energy available for heating up the array and the shaded lunar surface. It was estimated that 30% of this remaining energy would be radiated to space by the front surface of the array. This leaves only 30% of the initial incident solar array energy available for heating up the shaded lunar surface temperature. In addition, the lunar surface has a thermal conductivity similar to that of Earth soil (1.676 to 2.514 W/°C-m per reference 7.8), which is significantly better than the perfect insulation assumed for Case III. Hence, a portion of the solar energy reaching the shaded lunar surface below the array can be conducted to the adjacent

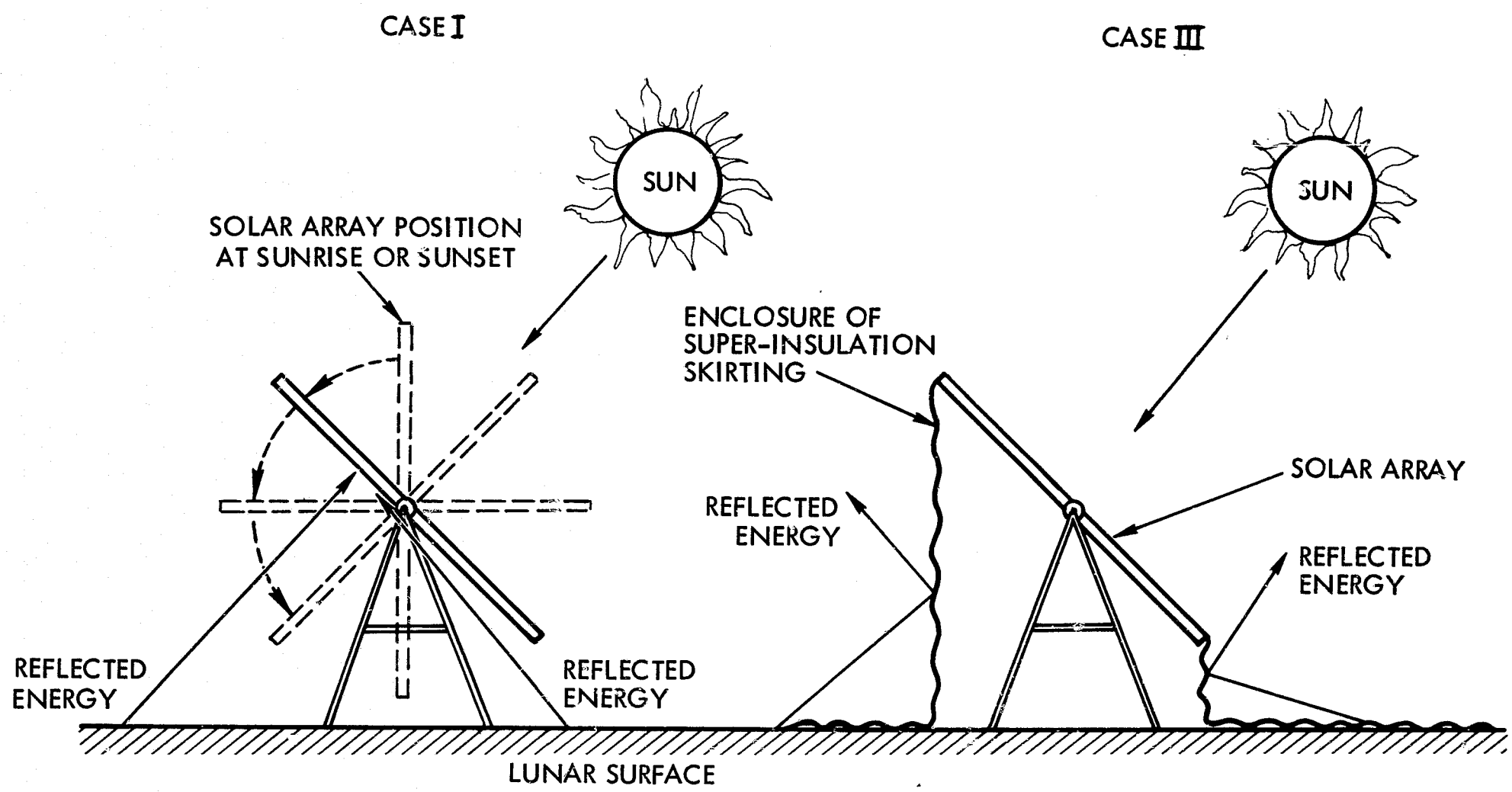

Figure 8.8 Oriented Solar Array Thermal Energy Inputs for Two Design Concepts

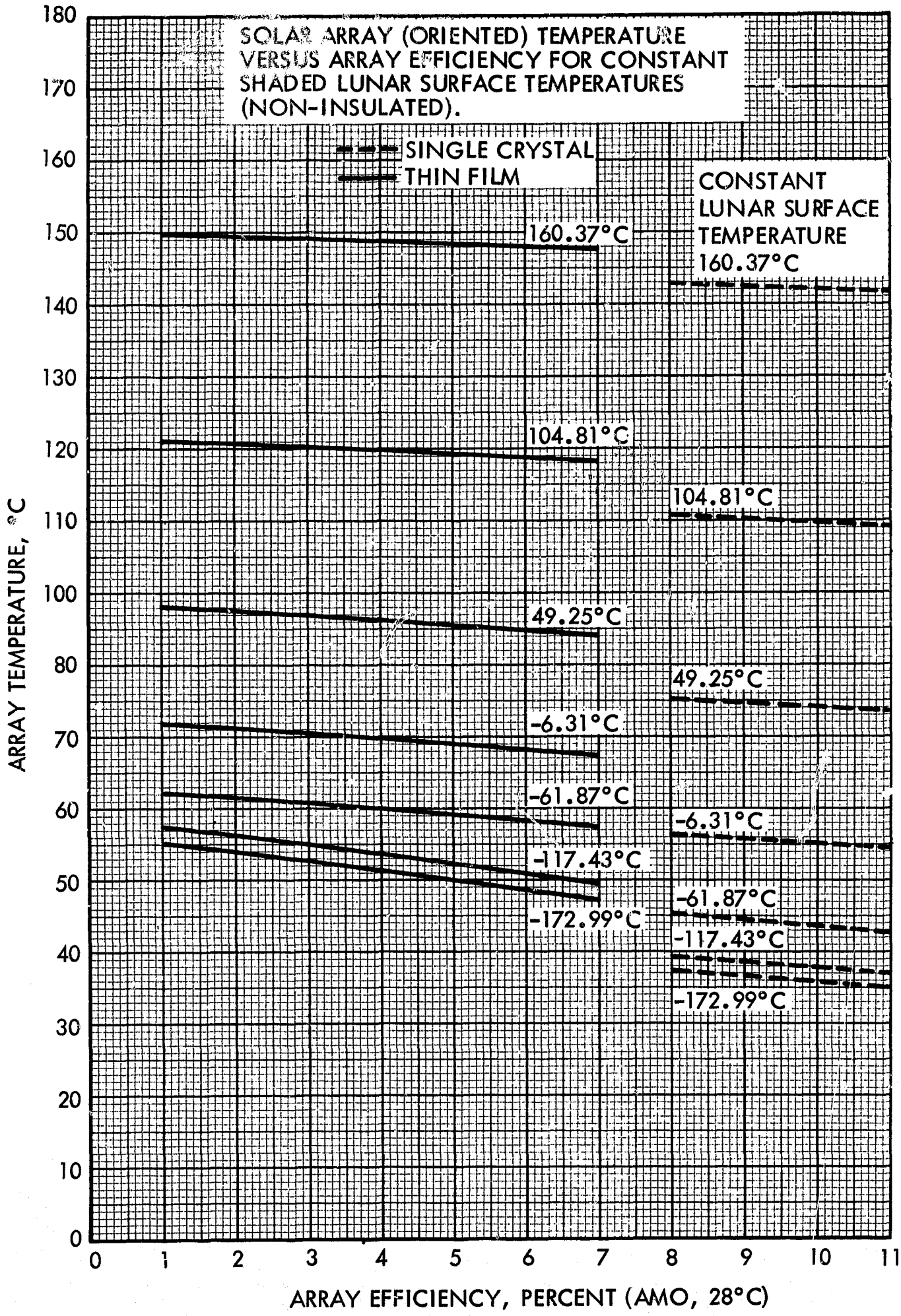

Figure 8.9 Oriented-Skirted (Non-insulated) Solar Array Temperature vs. Array Efficiency for Various Shaded Lunar Surface Temperatures at Lunar Noon

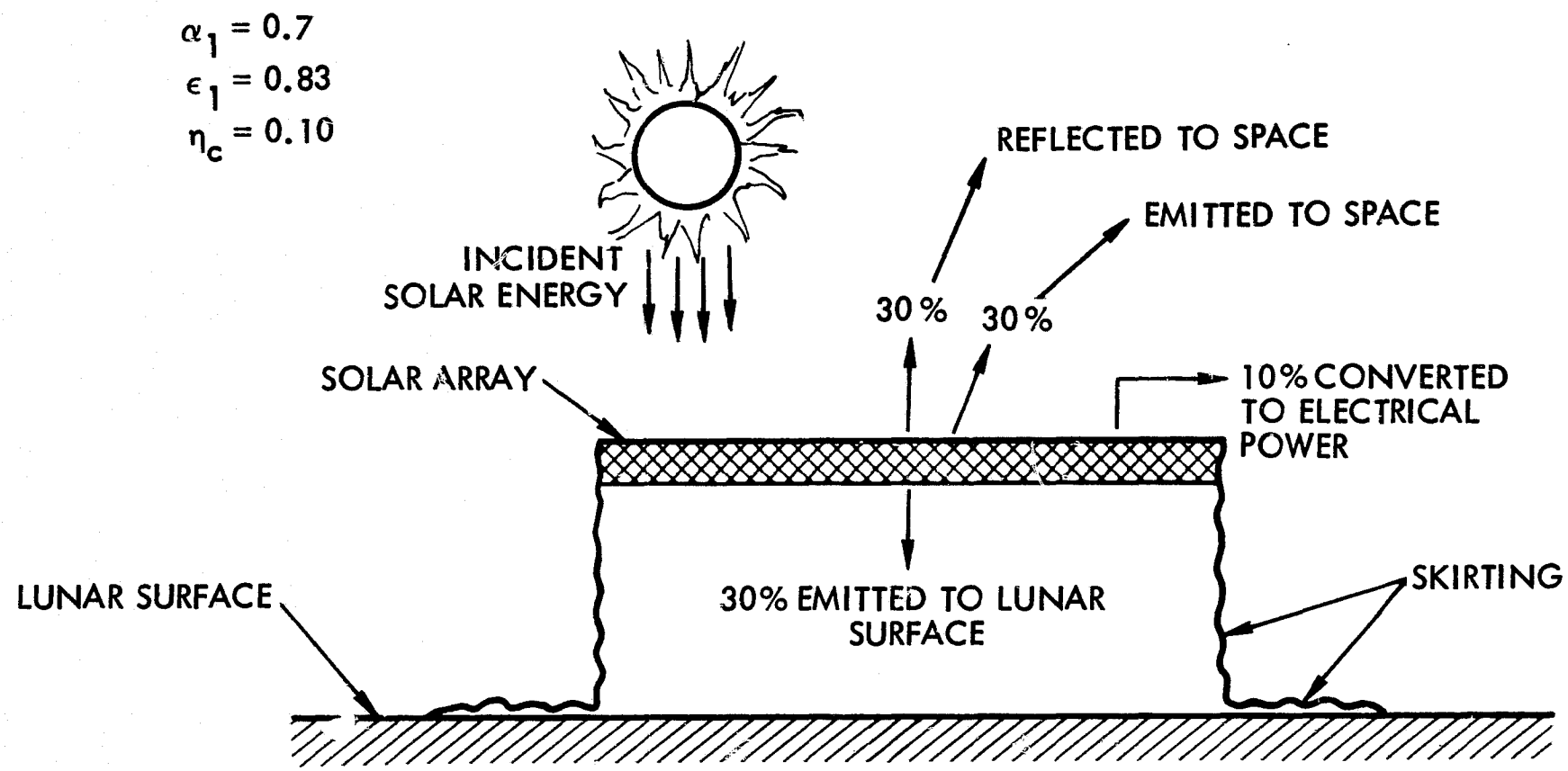

Figure 8.10 Schematic of Solar Thermal Energy Dissipation for a Silicon Cell Solar Array on the Lunar Surface

lunar surface which is also being shaded by an appropriate width of skirting. Finally, the unshaded lunar surface temperature varies from -173°C at sunrise and sunset, to 122°C at lunar noon (at the lunar equator). Hence, it is reasonable to assume that the shaded lunar surface would vary in a similar manner, but due to the reduced thermal energy input would reach a lower peak temperature at lunar noon. The assumed shaded lunar surface temperature variation used in this study is shown on Figure 8.11. A peak shaded lunar surface temperature of -6°C is indicated. This corresponds to an oriented-skirted solar array temperature of 55°C as shown in Figure 8.9 and (as will be discussed later in Section 8.2.3) to the non-insulated, non-oriented, skirted flat array temperature at lunar noon.

It is recognized that a more detailed thermal analysis is required to more accurately establish the shaded lunar surface temperature variation. If it is found to be greater than -6°C at lunar noon, the array temperature profile would also change. However, the upper temperature limit for a oriented skirted array would not exceed the temperatures shown for the non-skirted, insulated array (Figure 8.7), since the latter case is equivalent to negligible thermal energy being rejected to the lunar surface. Hence, for a silicon cell array the peak temperature at lunar noon might be as high as 95°C (versus 55°C).

The sensitivity of array operating temperature to changes in lunar surface temperature and other array performance parameters is shown in Figures 8.12 and 8.13 for silicon cells and CdS thin films. It should be noted that the array operating temperature is affected most by changes in the value of, T_S, the shaded lunar surface temperature. For example, an increase of 55°C in T_S would result in an increase in the silicon cell array equilibrium temperature of 19°C or an increase from the nominal 55°C temperature (for T_S = -6°C) to 74°C. However, this temperature is still 25°C less than the peak temperature experienced by the insulated array (Case II: Figure 8.7) and 116°C less than the non-insulated array (Case I: Figure 8.6). Hence, there appears to be little doubt about the benefits to be derived by skirting both oriented and non-oriented arrays for use on the lunar surface. The impact of array equilibrium temperature on electrical performance is discussed in Section 8.4.2 of this report.

8.2.3 Non-oriented Arrays

The non-oriented array concepts selected for this analysis (see Section 8.1) were the flat and leanto configurations. The rationale and assumptions used to determine oriented array equilibrium temperatures were also applied to the non-oriented configurations. Thus, the three cases, namely: non-insulated, insulated, and non-insulated (skirted) were investigated. The results of these analyses are shown in Figures 8.14, 8.15, and 8.16. Figure 8.14 depicts the resultant array temperatures for the non-insulated case for both single crystal silicon cells and CdS thin films. In addition, it shows the lunar noon array temperatures for the insulated case. Since there was no significant reduction in the peak lunar noon temperatures between the non-insulated and insulated cases, no analytical effort was expended to obtain a curve of array temperature versus lunar phase for the insulated case. Figures 8.15 and 8.16 depict the array equilibrium temperatures for the non-insulated, skirted case for single crystal silicon cells and CdS thin films respectively. The temperature profiles are shown between lunar noon and the evening terminator. During this study, array performance analyses were based upon assuming these profiles are symmetrical about the lunar noon period. The short duration transients at lunar sunrise and sunset are not depicted. These are expected to be of short duration (< 1 hour or approximately 0.25 degrees of lunar phase) and would usually coincide with lunar base ERPS start-up and shut down periods. The effect would be to lower the array temperatures during these periods which would result in increasing the power output. Hence, the results shown on Figures 8.15 and 8.16 are conservative for the sunrise and sunset terminator conditions. Thermal heating rates of the arrays at sunrise are estimated to be in the range from $10^{\circ}C$ to $20^{\circ}C$ per minute and this rate is not expected to degrade array structural integrity or electrical performance.

The concept of skirting discussed earlier in this report would not only attenuate the rate of increase in the lunar surface temperature (Figure 8.11) but with proper design could reduce the peak lunar noon magnitude of this temperature. To achieve this, the skirting would be designed not only to shade the lunar surface below the array but also the surrounding adjacent surface areas. For example, the skirting could

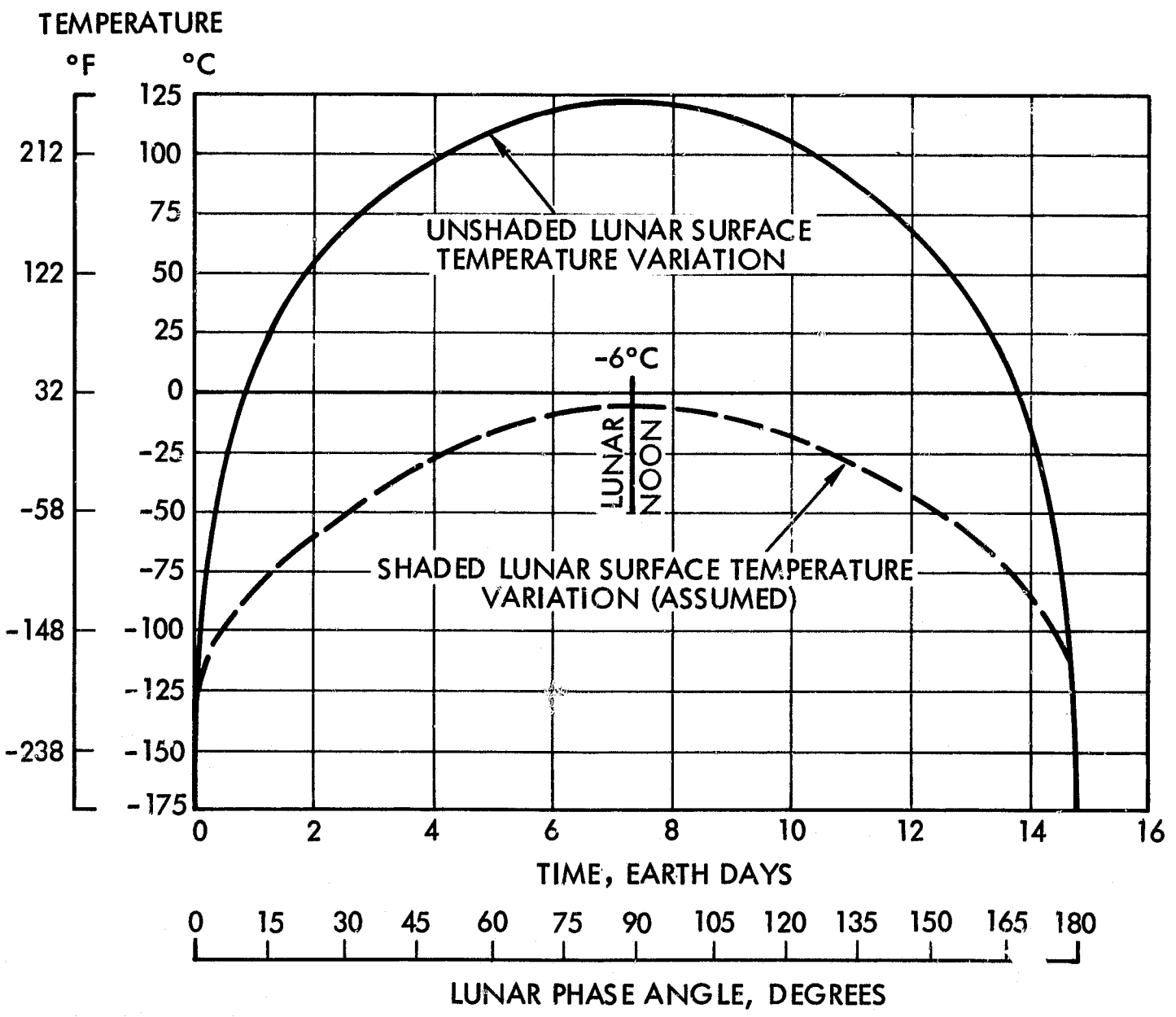

Figure 8.11 Assumed Lunar Surface Temperature Variation (Lunar Equator)

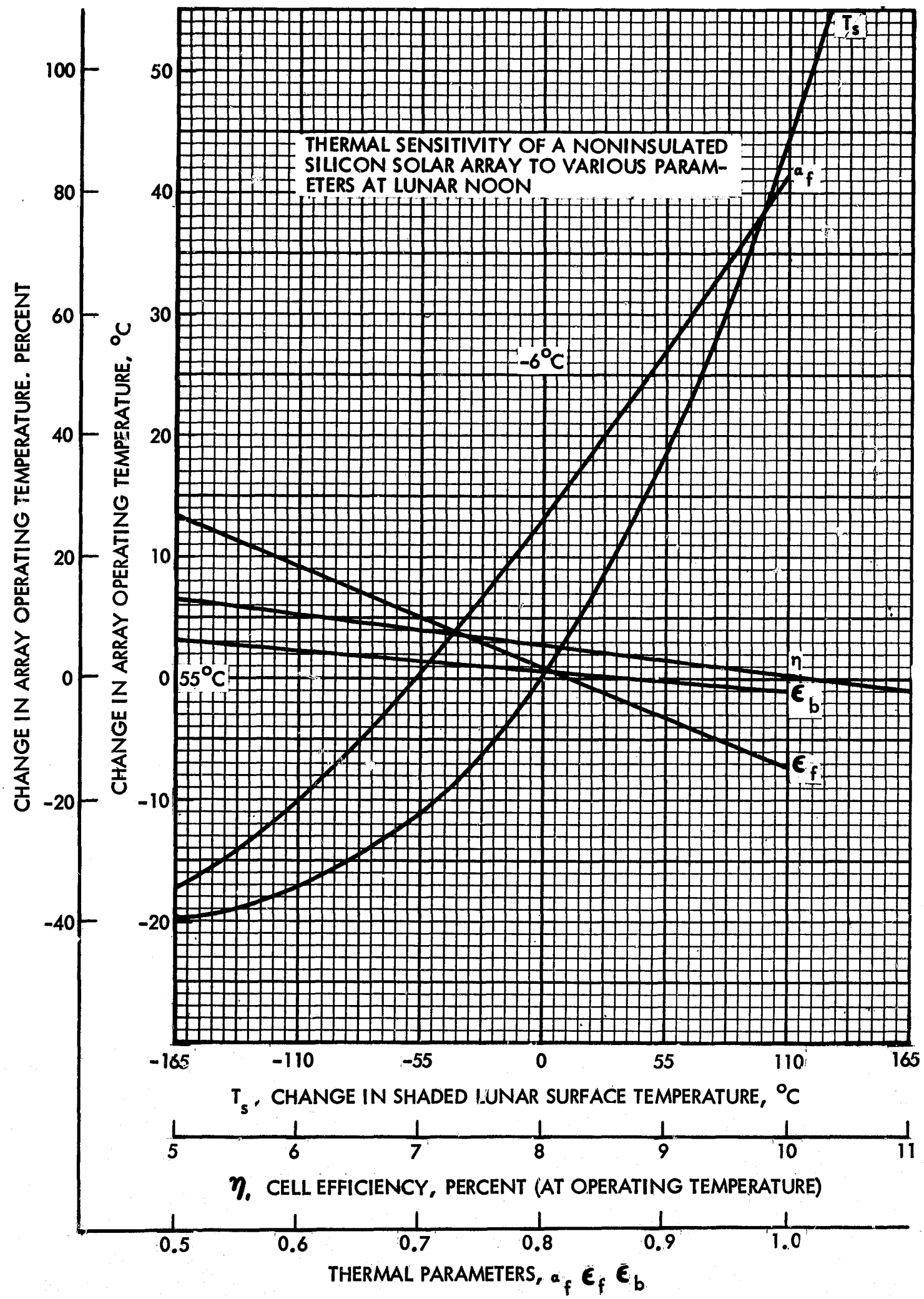

Figure 8.12 Thermal Sensitivity of a Non-insulated Silicon Cell Solar Array to Various Parameters at Lunar Noon

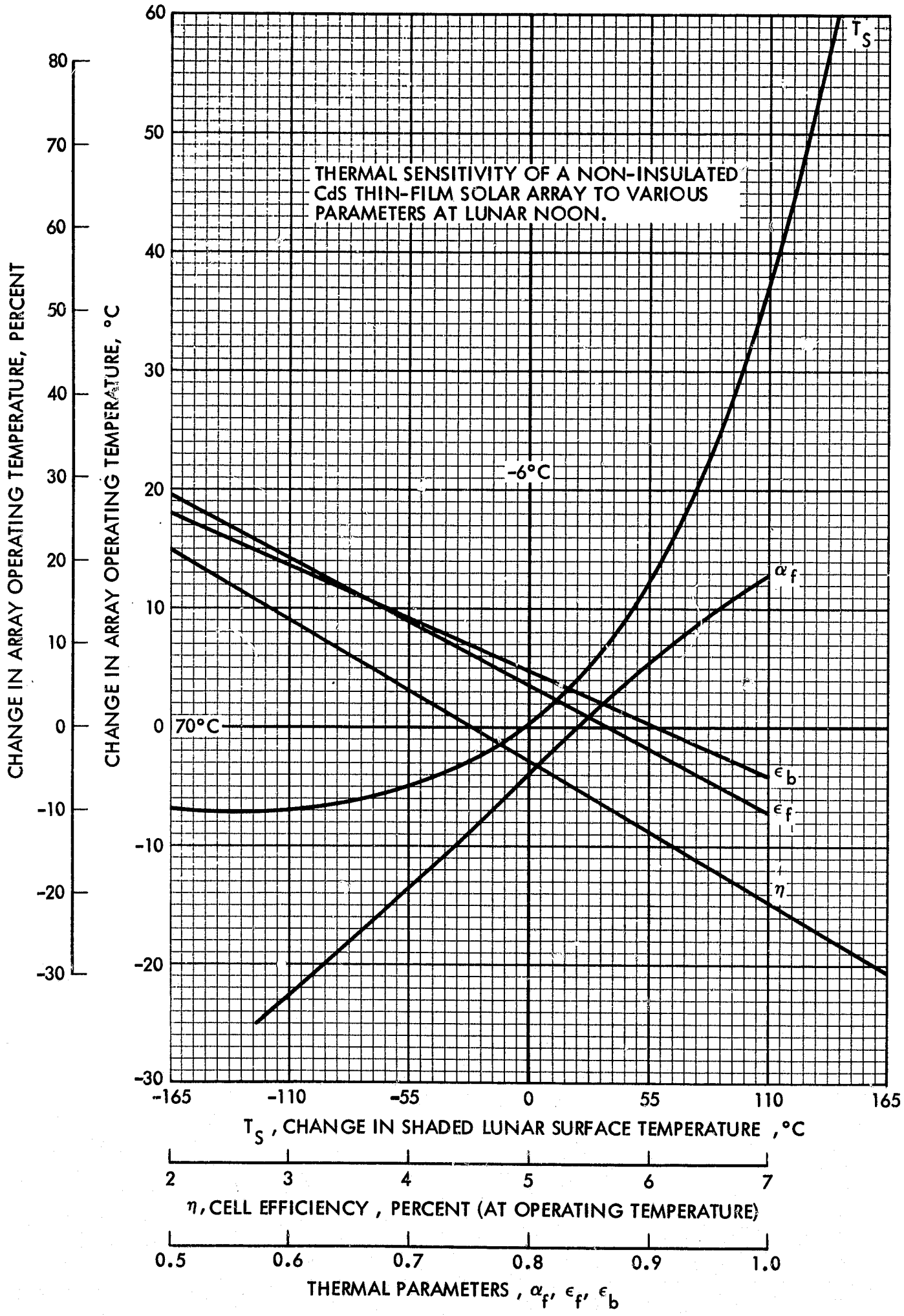

Figure 8.13 Thermal Sensitivity of a Non-insulated CdS Thin Film Solar Array to Various Parameters at Lunar Noon

extend 5 to 10 feet from the base of the array. This would increase the thermal gradient region between the shaded surface under the array and the unshaded lunar surface. This skirt would also be constructed so as to have a poor view factor with respect to the array. This would be accomplished by using a highly diffused (irregular or crinkled) reflective surface or by inclining the skirt. This would greatly reduce lunar albedo effects and prevent the creation of hot spots on the active array surface.

8.3 PERFORMANCE ANALYSIS

The determination of solar array performance on the lunar surface is a function of many factors. The data required and the sequence of its utilization during this study are shown in Figure 8.12. As can be noted, a combination of experimental vendor data and a detailed thermal analysis are required to establish actual solar cell conversion efficiencies. These efficiencies vary with array equilibrium temperatures and for lunar surface applications are a function of lunar phase or time. The additional factors required to determine the power to area ratio for solar arrays from which overall array area requirements are determined are shown in Figure 8.18. These factors are placed in two groups. The first group, which are independent of mission duration, are primarily a function of array design parameters. The second group are intimately related to the lunar environment and are also affected by elapsed mission time. The relationship used to determine the power-to-area ratio from these factors are:

$$\frac{P_o}{A} = \left[\eta_p \times \eta_c \times \eta_o \times \eta_{reg} \times \eta_{conv}\right] \times \left[I_{sol} \times \eta_{rad} \times \eta_{uv} \times \eta_{nm}\right] \qquad (8.5)$$

Because of the temperature dependency of the solar cell conversion efficiency and the variation of the solar insolance intensity due to the cosine effect, the power-to-area ratio will vary with respect to array configuration and lunar phase.

8.3.1 Efficiency and Voltage Variations with Lunar Phase

Solar array cell conversion efficiency is an important factor in power subsystem design and greatly affects total area requirements. Cell conversion efficiency, in turn, is dependent upon the array equilibrium temperature as shown in Figure 7.13. In addition, Figure 7.10 shows the effect of temperature on open circuit voltage which is another parameter which influences array design. Sections 8.2.2 and 8.2.3 presented

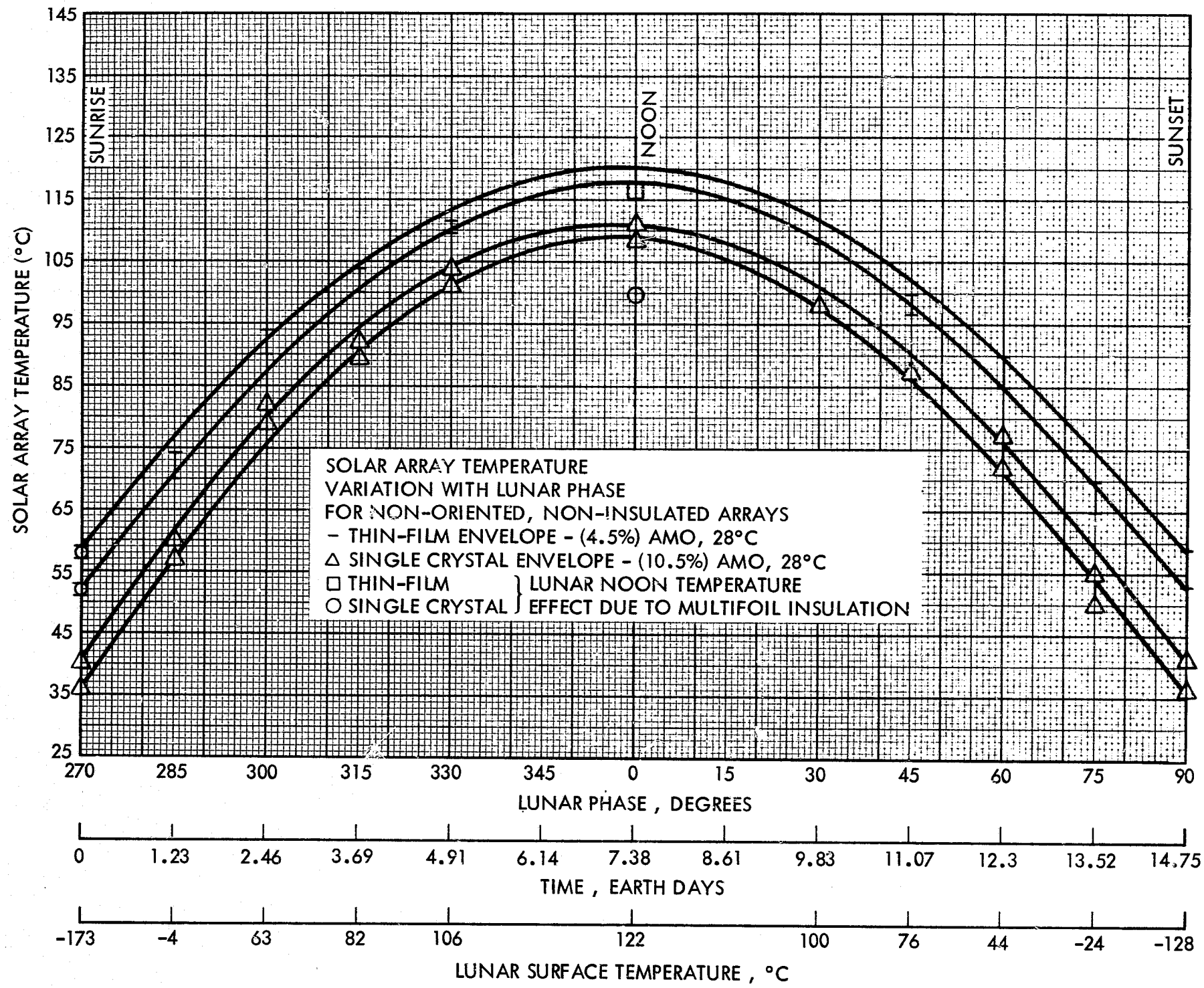

Figure 8.14 Solar Array Temperature Variation with Lunar Phase for Non-oriented, Non-insulated Arrays

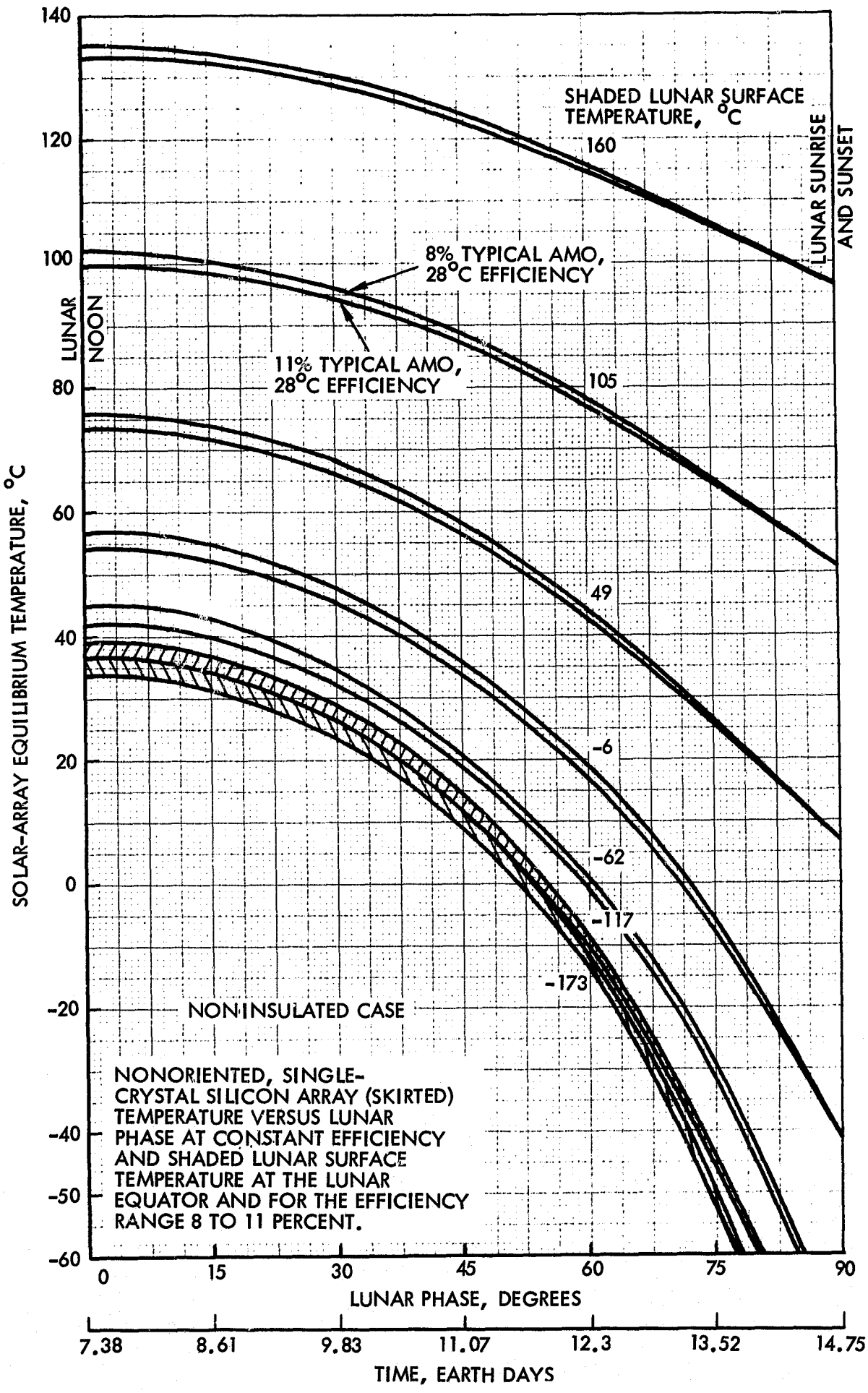

Figure 8.15 Silicon Cell Solar Array Equilibrium Temperature Versus Lunar Phase

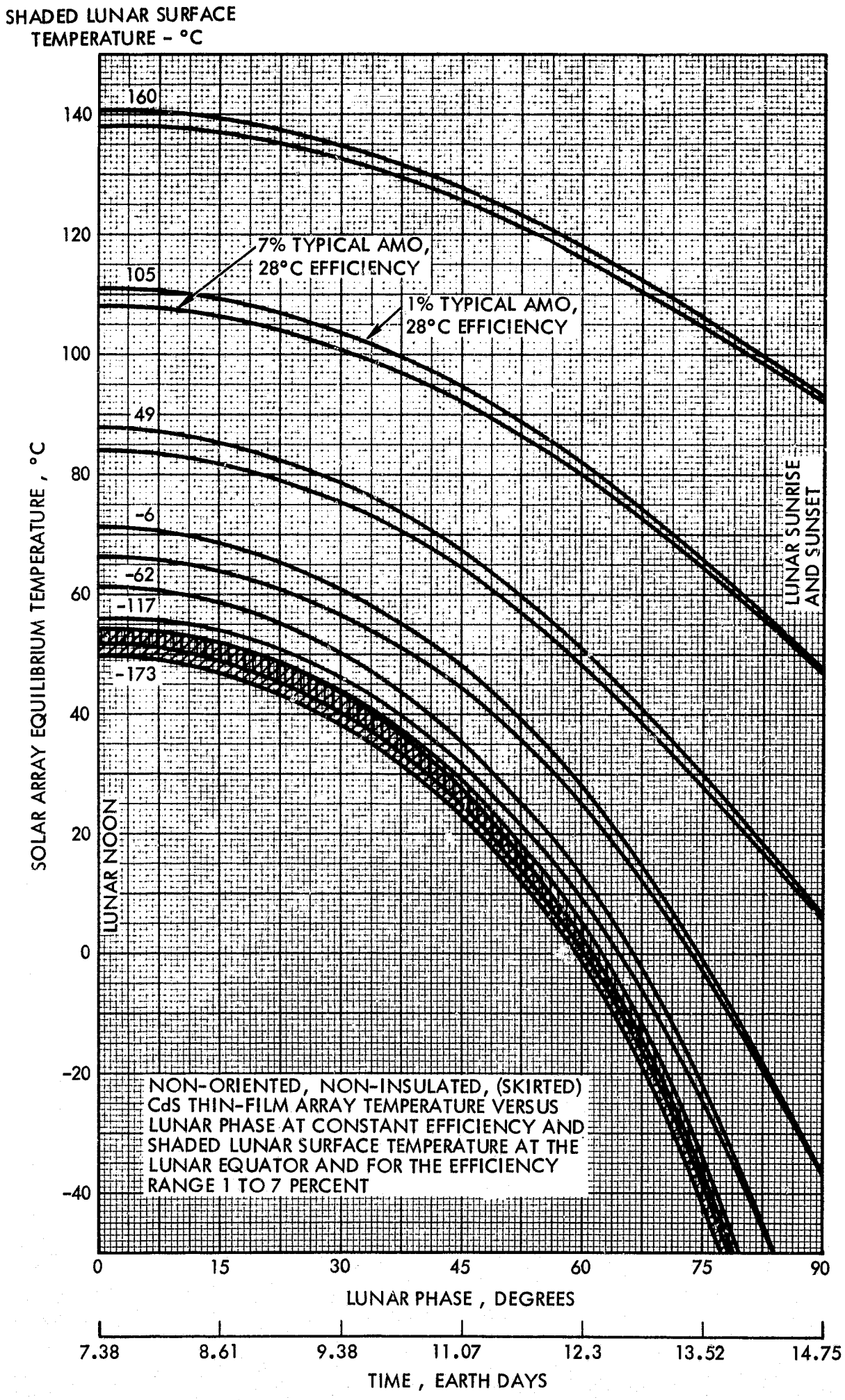

Figure 8.16 CdS Thin Film Solar Array Equilibrium Temperature Versus Lunar Phase

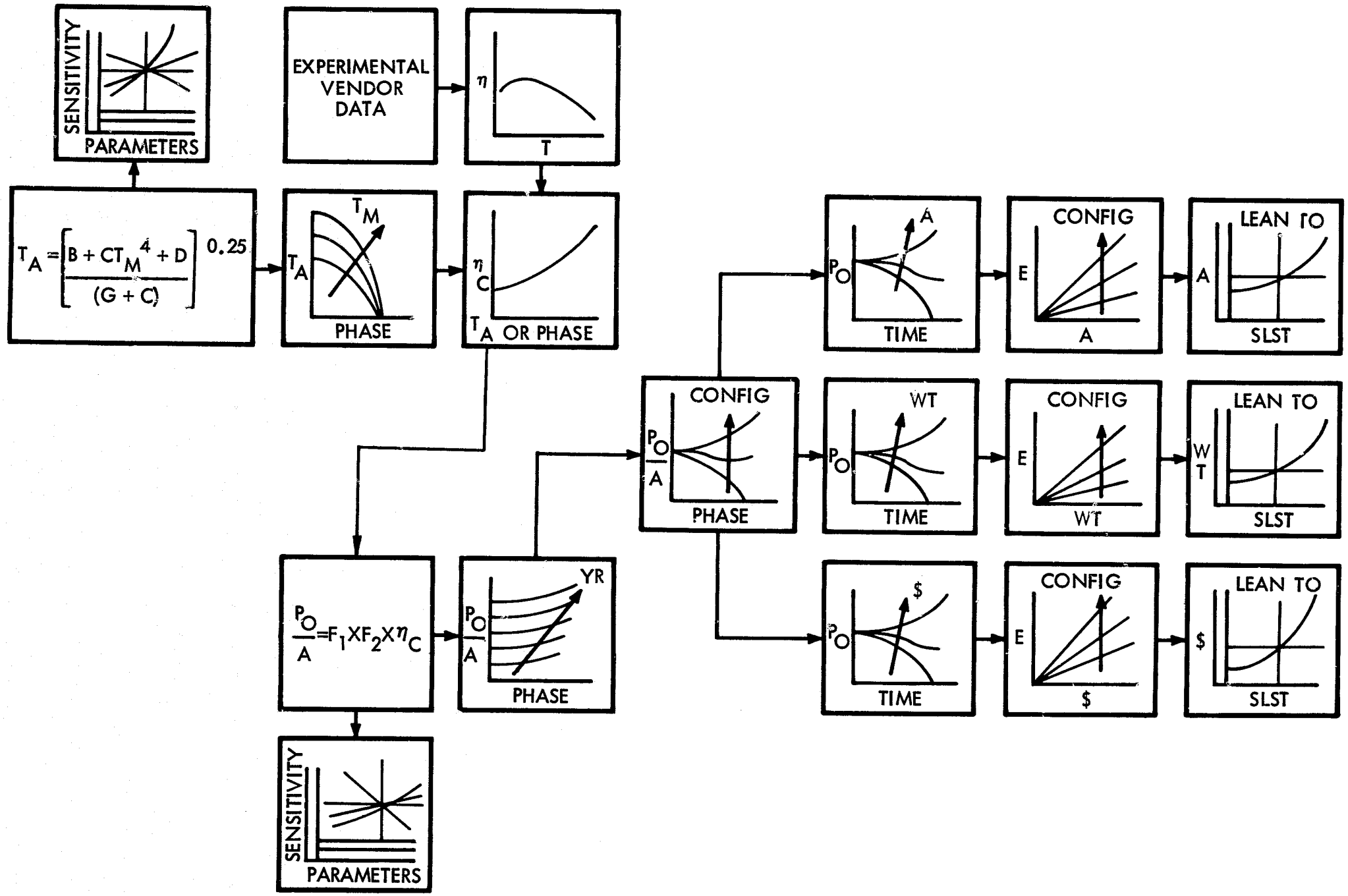

Figure 8.17 Flow Diagram Showing Sequence of Data Derivation for Lunar Array Performance Analysis

$$P_O/A = \left[\eta_P \times \eta_C \times \eta_M \times \eta_O \times \eta_{REG} \times \eta_{CONV}\right] \times \left[I_{SOL} \times \eta_{RAD} \times \eta_{UV} \times \eta_{MM}\right]$$

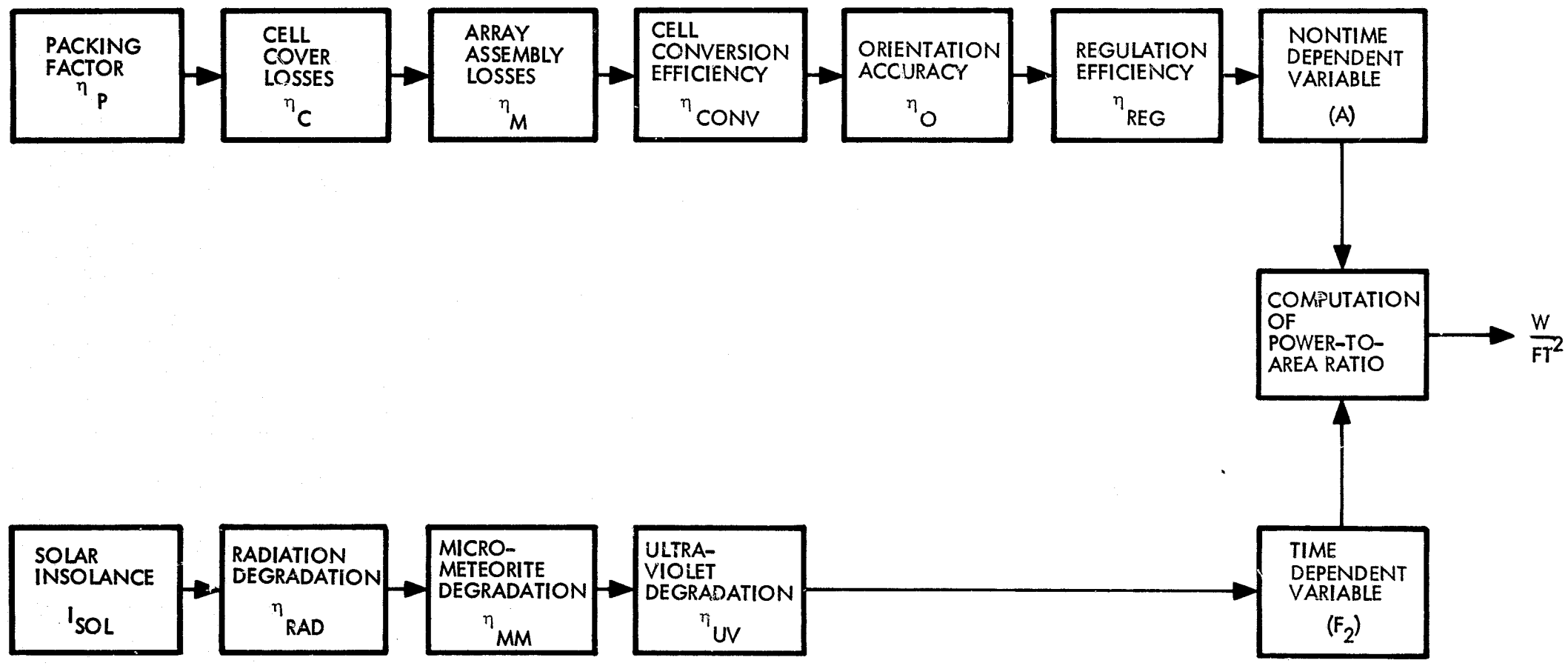

Figure 8.18 Factors Considered in Power-To-Area Ratio Computation for Lunar-Based Solar Arrays

the expected array temperatures for three candidate array concepts. Using this data together with the experimental vendor data presented in Section 7.3.1, it was now possible to plot array efficiency and open circuit voltage as a function of lunar phase. These results are shown in Figures 8.19 to 8.27.

Figures 8.19 and 8.20 show large excursions of cell efficiency and open circuit voltage for the oriented, non-insulated, non-skirted case. Due to the high array temperatures experienced in this case, the nominal array cell efficiency is so much lower at lunar noon that extremely large area arrays would be required to produce several kilowatts of power during the entire lunar day. Hence, this concept was not considered competitive as a candidate array. The cell efficiency at lunar noon was considerably improved by adding a super insulating layer between the hot lunar surface and the back face of solar array, as shown in Figures 8.22 and 8.23. In addition, this concept offers possible power conditioning weight savings due to the smaller voltage excursion experienced. Therefore, this concept was retained for further consideration as a candidate array.

The oriented, non-insulated, skirted array concept performance at lunar noon is similar to the non-oriented, non-insulated, skirted flat array at lunar noon. The array geometry, solar incidence angle, (γ), and shaded lunar surface temperature are identical. Hence, for this case, the non-oriented, non-insulated, skirted performance at lunar noon (see Figures 8.26 and 8.27) was utilized. In addition, since for the oriented concept the solar incidence angle remains constant and since the shaded lunar surface temperature was assumed to remain constant (a conservative assumption as previously discussed), the cell efficiency and open circuit voltage were also assumed to remain constant at the lunar noon values over the entire lunar day.

An important factor regarding oriented solar array performance, which must be taken into consideration, is that of orientation accuracy. The cell efficiency and open circuit voltage profiles previously discussed, are only valid if the orientation accuracy can be maintained at $\pm$ 10% of the required normal solar incidence angle. This implies the need for complex tracking equipment which must be redundant to achieve the required reliability, as well as introducing potential sealing, bearing, and

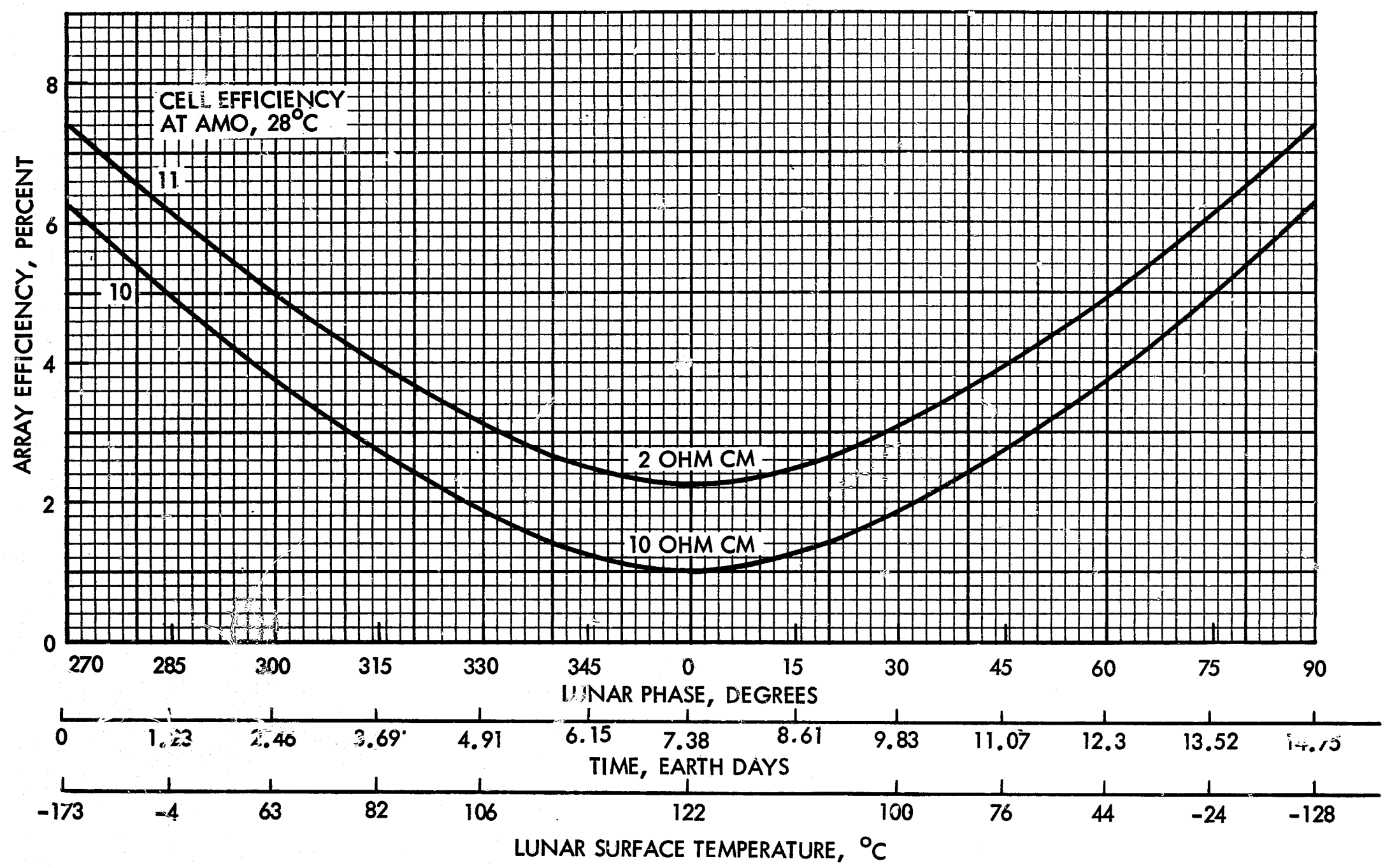

Figure 8.19 Oriented Array (Non-Skirted and Non-Insulated) Efficiency Variation with Lunar Phase for Average Array Temperature (Using Single Crystal Silicon Cells)

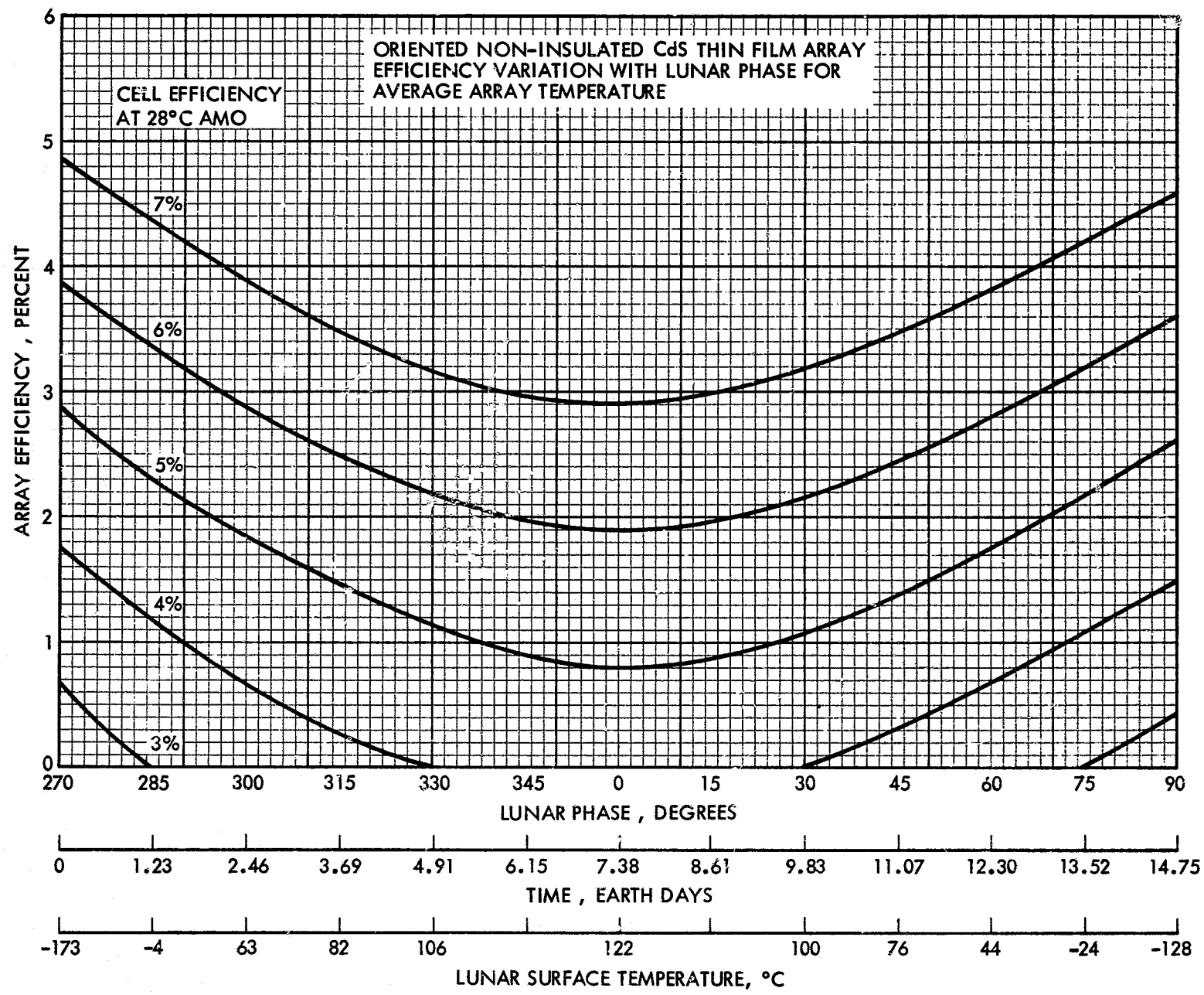

Figure 8.20 Oriented (Non-Skirted, Non-Insulated) CdS Thin Film Array Efficiency Variation with Lunar Phase for Average Array Temperature

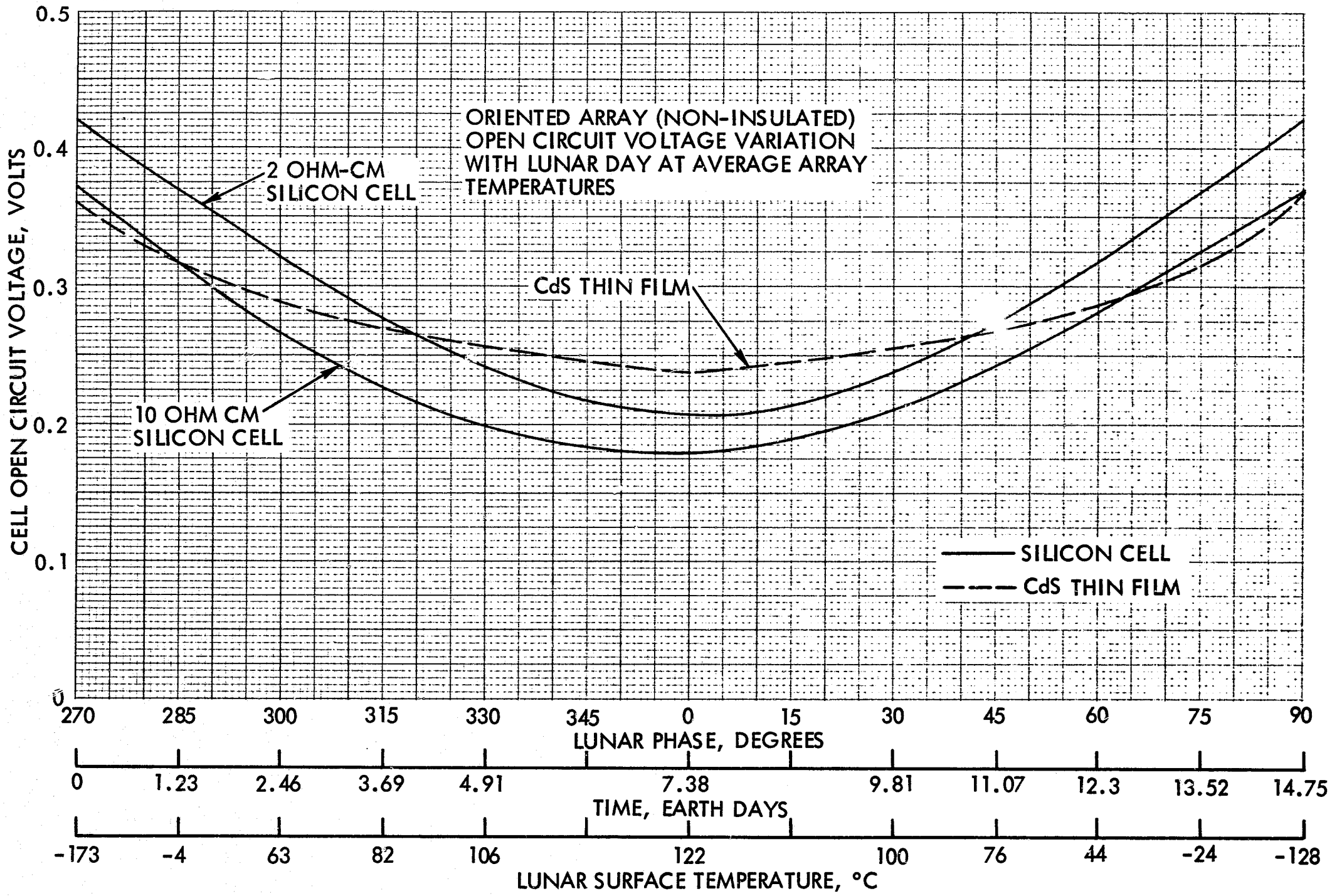

Figure 8.21 Oriented Arrays (Non-insulated) Open Circuit Voltage Variation With Lunar Day at Average Array Temperature

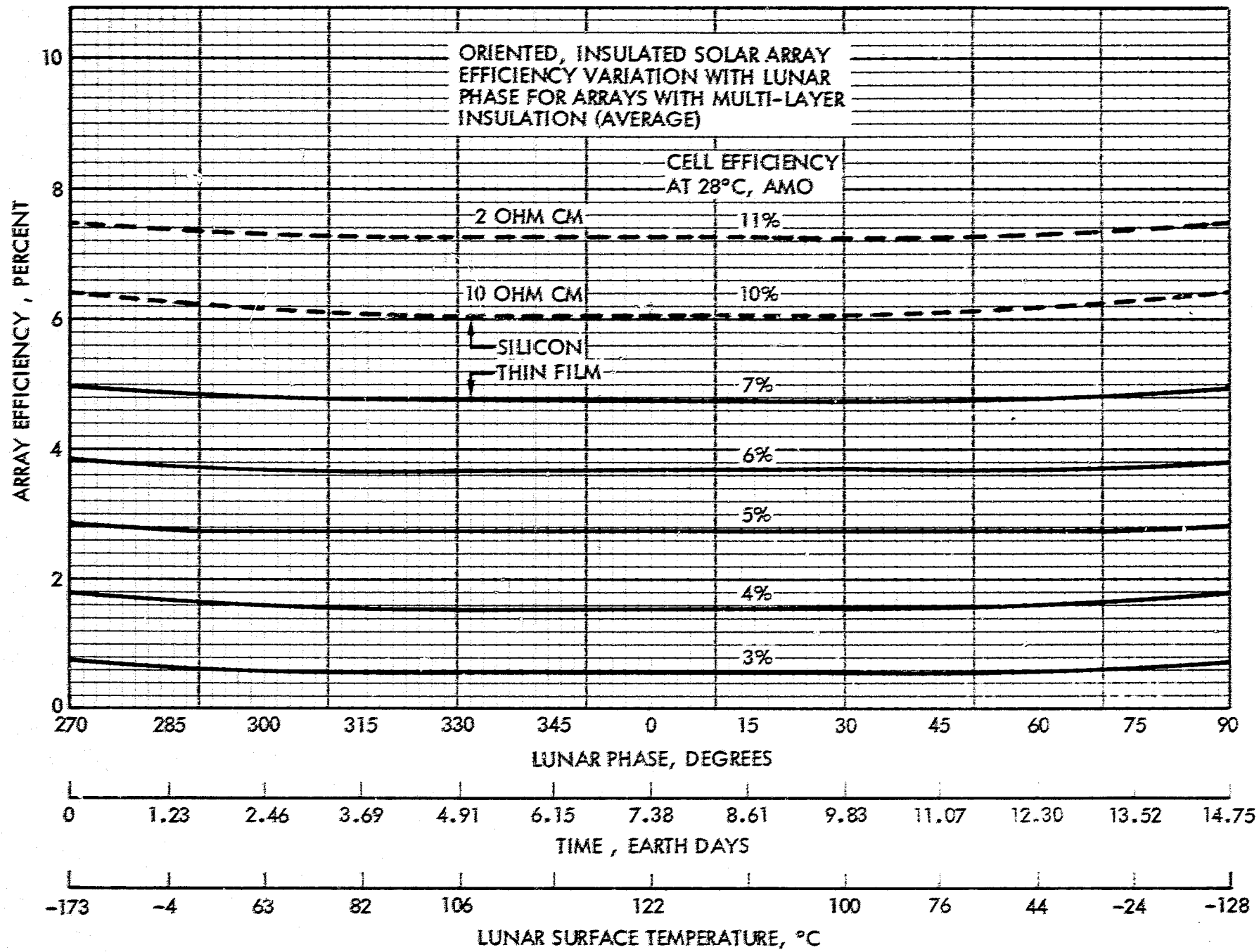

Figure 8.22 Oriented, Insulated Solar Array Efficiency Variation with Lunar Phase for Arrays with Multi-layer Insulation (Average)

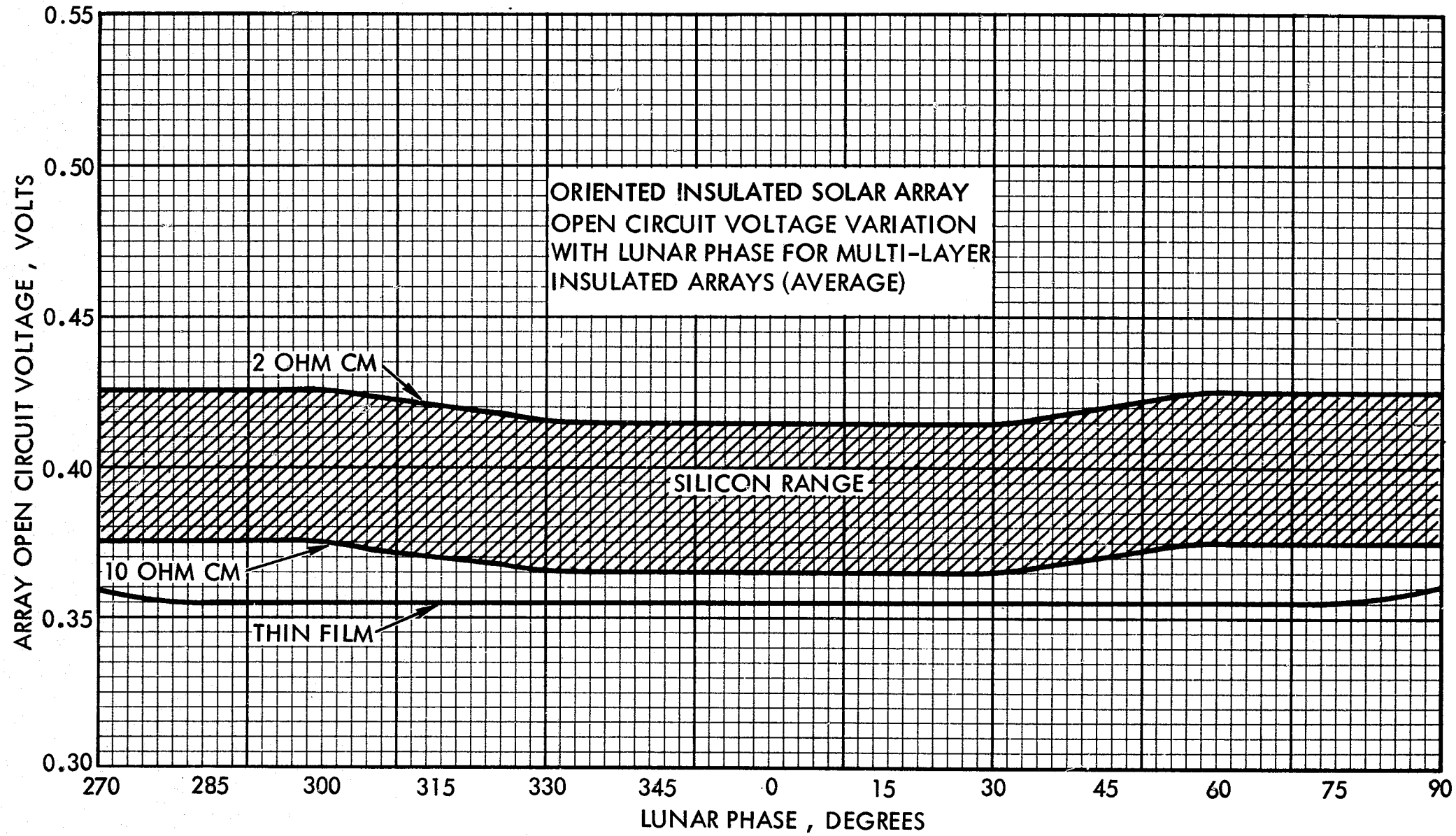

Figure 8.23 Oriented, Insulated Solar Array Open Circuit Voltage Variation with Lunar Phase for Multi-insulated Arrays (Average)

lubricating problems associated with rotating large structures in the lunar surface environment. In addition, periodic preventative maintainance would be necessary to meet the 1 to 5 year system life requirements. The possibility of mechanism failure during the unmanned portion of the mission would also exist. Manual orientation might be utilized but would be required at intervals of no less than every 10 hours. For a multi-panel 50 kw array, this could consume up to 25% of an astronaut's time and greatly reduce the system effectiveness of the mission. Despite these potential disadvantages, the oriented array concept was retained in this study because of the apparent advantages of its constant output power profile and the resultant reduced total array area and power conditioning requirements. However, the static (non-oriented) array concepts do not have the operational shortcomings of the oriented arrays and still retain many attractive overall mission characteristics. A discussion of the performance of non-oriented arrays follows.

Figures 8.24 and 8.25 show that for the non-insulated, non-skirted, flat and leanto arrays the lunar noon cell efficiency and open circuit voltage are equivalent to those predicted for insulated, oriented arrays (Figures 8.22 and 8.23). The cell efficiency at the terminators (sunrise and sunset), however, are higher than for the oriented array, resulting in a higher average array performance. Non-oriented, insulated array concepts were not considered since it was obvious from their geometries and the data for oriented arrays that they would result in much lower cell conversion efficiencies. Finally, Figures 8.26 and 8.27 show the achievable cell efficiency to be highest for non-oriented, non-insulated, skirted arrays. These results are contingent upon the assumption that the shaded lunar surface temperature does not exceed -6°C as shown in Figure 8.11. However, Figures 8.12 and 8.13 show the sensitivity of the array performance parameters, and as previously discussed, a 55°C error in this assumption would result in only a 19°C change in array equilibrium temperature. This could lower the cell conversion efficiency from 8.6% to 7.5% which could be compensated for in the initial array design.

On the basis of the foregoing study results the non-oriented, skirted arrays are competitive from a performance standpoint with the oriented concepts (insulated and non-insulated, skirted), and possess the additional advantages of a static system.

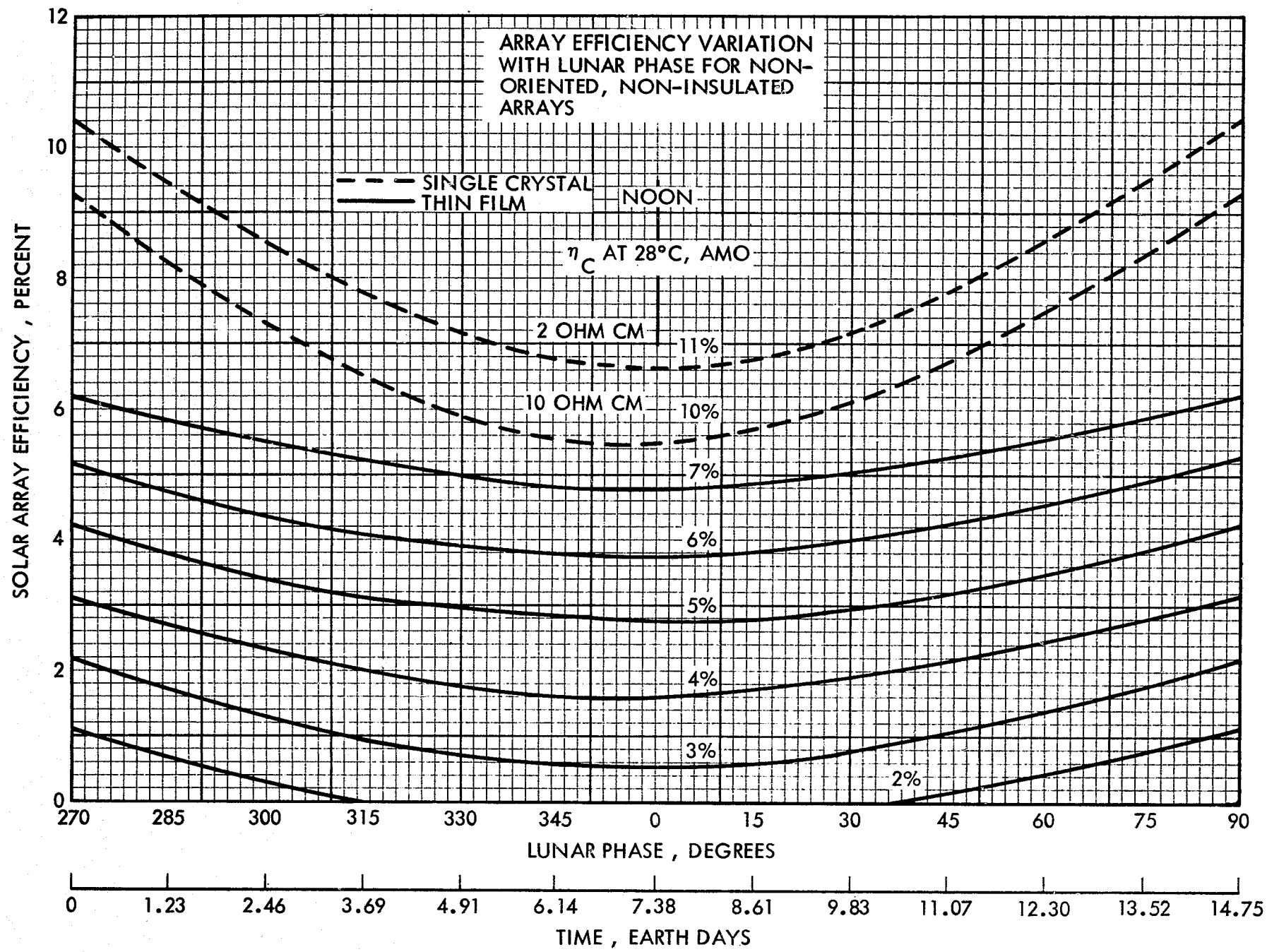

Figure 8.24 Array Efficiency Variation with Lunar Phase for Non-oriented, Non-insulated arrays

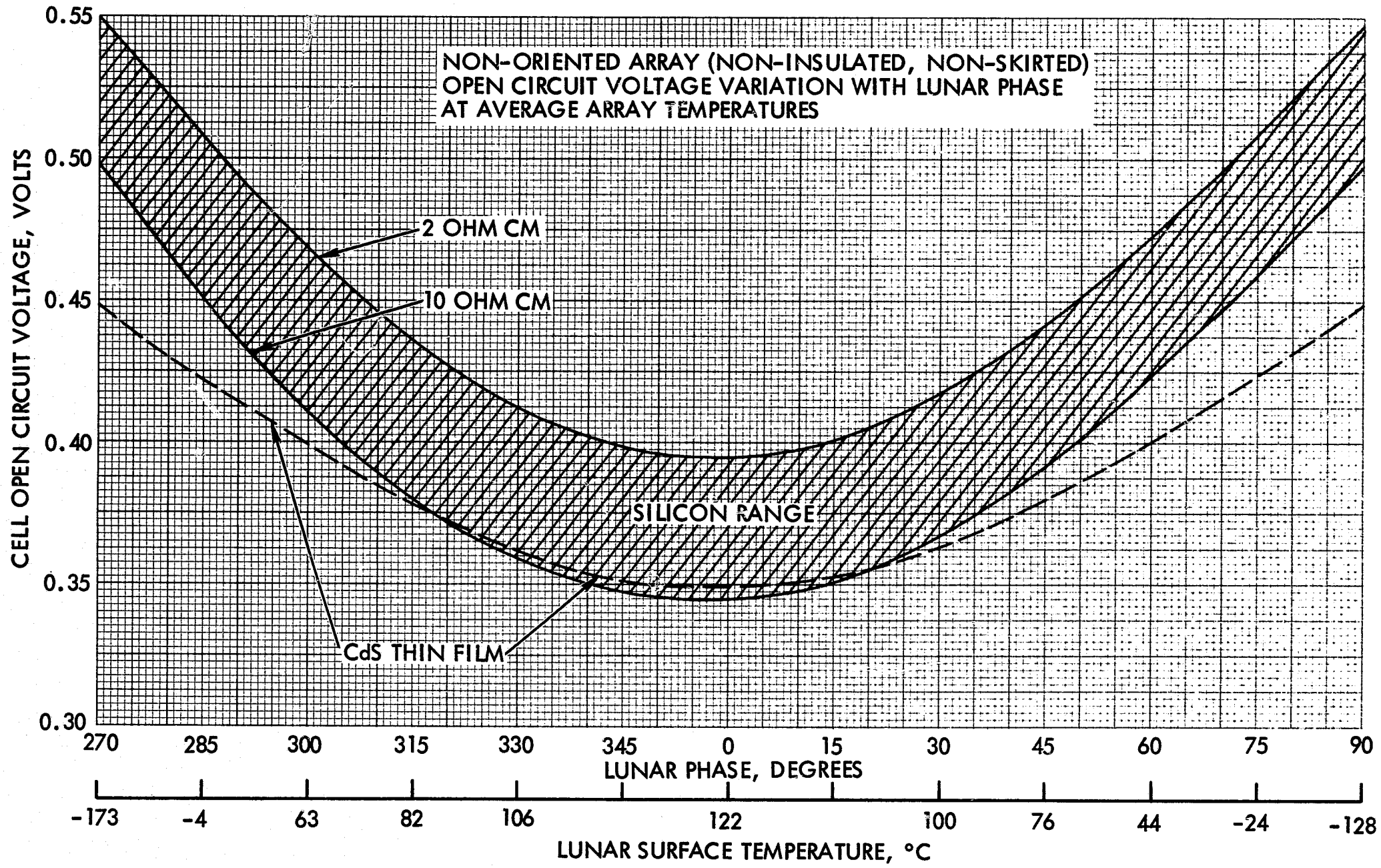

Figure 8.25 Non-oriented Array (Non-insulated, Non-skirted) Open Circuit Voltage Variation with Lunar Phase at Average Array Temperatures

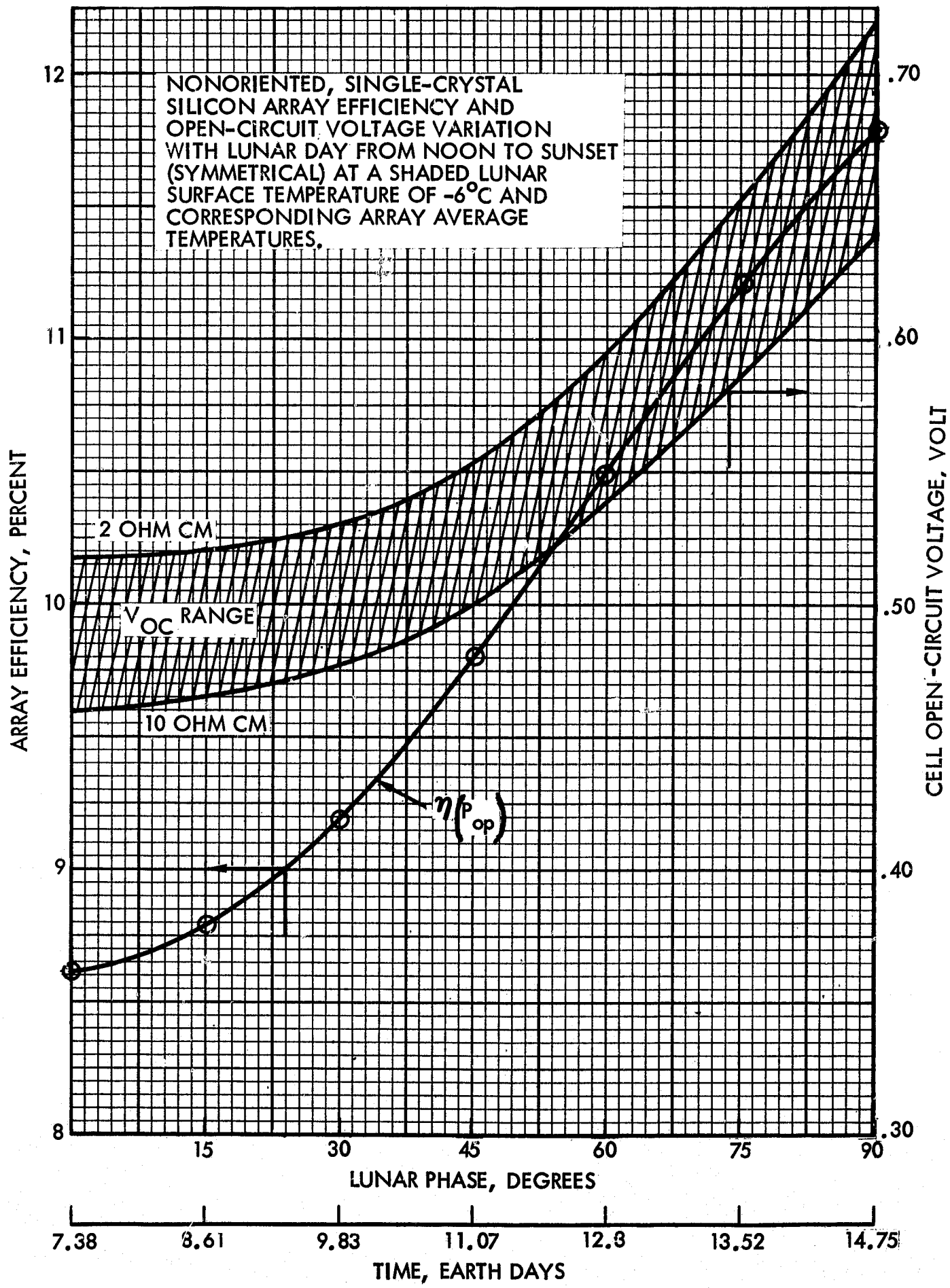

Figure 8.26 Silicon Cell Array (Non-Oriented) Efficiency and Open-Circuit Voltage Versus Lunar Phase

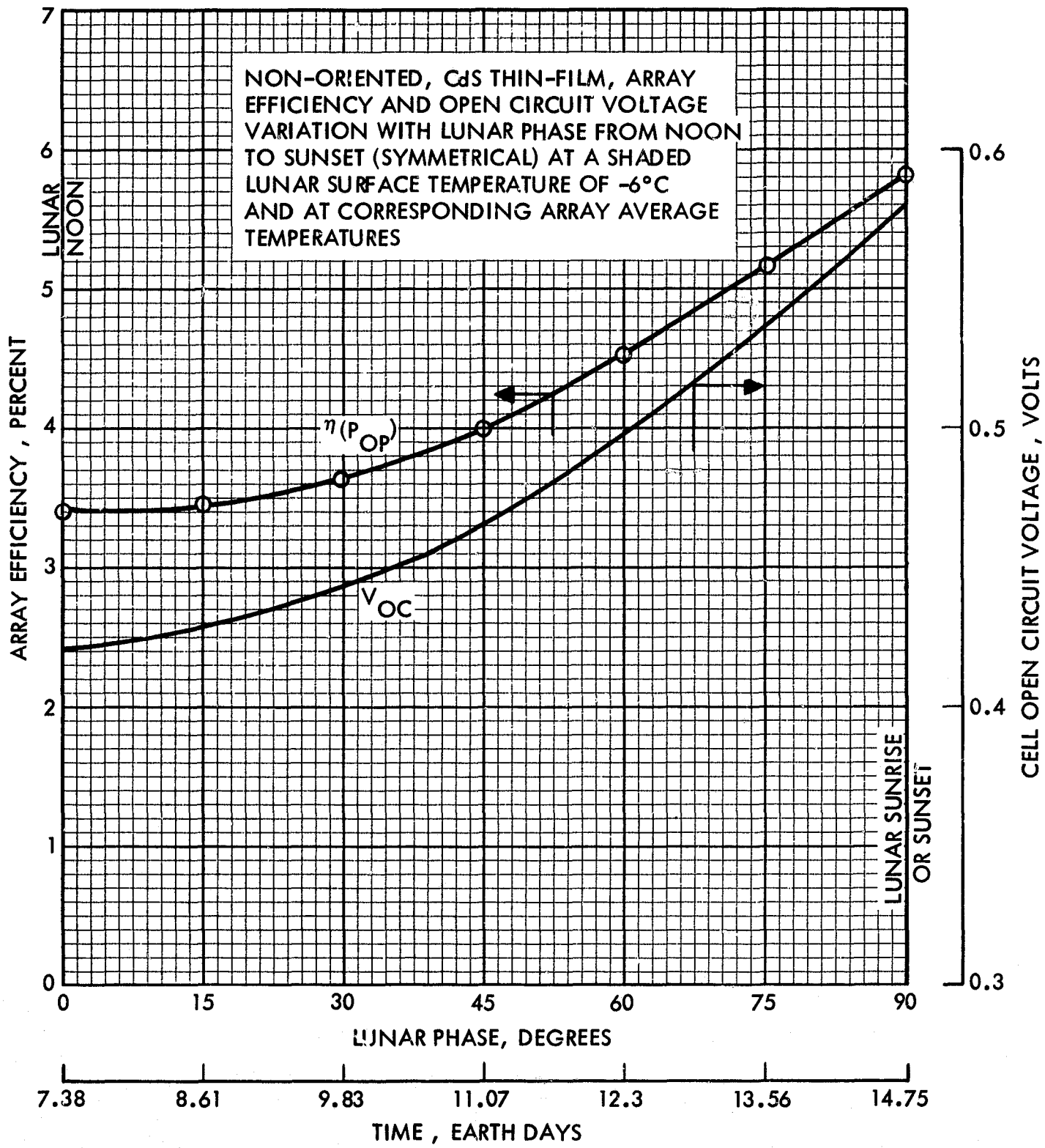

Figure 8.27 Non-Oriented, CdS Thin Film Array Efficiency and Open Circuit Voltage Variation with Lunar Phase

8.3.2 Power-to-Area Ratio for Various Mission Durations

The assessment of the overall solar array design characteristics is contingent upon the determination of the power-to-area ratio. This parameter, in turn, is a function of the various time dependent and non-time dependent variables of equation (8.5), and is usually expressed in watts/sq. ft. or watts/sq. meter depending upon which system of units are being used. From this parameter, the solar array raw power output profile can be generated. By matching the output power profile to the load profile, the total array area, weight, and cost can be established. Hence, this parameter becomes very important in solar array design. The equation expressed in Figure 8.18 was used in this analysis to compute the array power-to-area ratio and includes all the degradation factors known to effect array performance. The effect of temperature was considered from the results of Section 8.31 in determining the cell conversion efficiencies (η_{conv}). Table 8.4 lists the values for the other factors used in Equation 8.5 for various intervals of time during a 5 year mission. The adjusted solar insolance is also included and represents the effective solar energy available for conversion to electric power after all degradation factors have been considered. Using these values equation 8.5 can be simplified to:

$$\frac{P_o}{A} = I'_{sol} \times \left| \eta_{conv} \right|_{f(T_A)} \qquad (8.6)$$

where I'_{sol} = adjusted solar insolance

$\left| \eta_{conv} \right|_{f(T_A)}$ = actual cell conversion efficiency (as function) of array equilibrium temperature)

The non-time dependent variables were based upon nominal values utilized in industry and data presented in Reference 7.3. The time dependent variables were based on extrapolation of data presented in Figures 8.28 and 8.29, as well as values presented in Reference 7.3. All performance degradation factors were selected to result in reasonable but conservative values for the adjusted solar insolance. The resulting values for the adjusted solar insolance were based on the assumption that all degradation factors were at their maximum level

TABLE 8.4

LIST OF VALUES USED TO DETERMINE ARRAY POWER-TO-AREA RATIO FOR VARIOUS MISSION DURATIONS (Up to 5 Years)

Parameter	Symb.	Units	Silicon Cells				CdS Thin Film			
			Mission Duration - Years							
			0	1	3	5	0	1	3	5
Max. Solar Insol.	I_{sol}	W/FT^2	140	(Constant)			140	(Constant)		
Packing efficiency	η_p	1-loss factor	0.9				0.95			
Cover losses	η_c		0.92				1.00			
Mfg. losses	η_m		0.96				0.96			
Orientation losses	η_o		0.98				0.98			
Diode losses	η_{reg}		0.95				0.95			
Radiation losses	η_{rad}		1.00	0.84	0.76	0.71	1.00	0.98	0.92	0.88
Ultra-violet losses	η_{uv}		1.00	0.98	0.95	0.93	1.00	0.95	0.90	0.85
Micro-meteorite losses	η_{mm}		1.00	0.98	0.95	0.93	1.00	0.95	0.90	0.85
Adjusted Solar Insol.	I'_{sol}	W/ft^2	104	83.8	71.2	63.7	119	111	98.4	84
		W/M^2	1119	900	765	685	1280	1195	1059	903

during the entire mission. This approach is consistent with meeting the end-of-mission (EOM) power requirements. However, since there is approximately a 25% reduction in the adjusted solar insolance, between a one year and five year mission, this becomes an important consideration for the mission planner.

Figures 8.30 and 8.31 show the sensitivity of the array power-to-area ratio to the values assumed for each of the variables involved. All non-time dependent variable values used were state-of-the-art and consistent with current industry practice. The time dependent variables may vary to some degree depending upon the individual designers basic assumptions and the amount of conservatism included in his analysis. The results of the analyses for both the oriented and non-oriented arrays are shown in Figures 8.32 through 8.39. These figures are plotted as a function of lunar phase only and must be further adjusted to include the variation of the solar insolance angle, (γ), for each array configuration. The resultant power-to-area ratio profiles are shown in Figures 8.40 through 8.47. The oriented array data remains unchanged since the solar incidence angle remains constant for this configuration.

The power density profile for the 45° leanto configuration is shown to be ascending in two phases from sunrise to lunar noon (Figure 8.42 is typical). This profile results from the leanto geometry and reflects ideal temperature and matched load conditions. However, in actuality, the profile slopes becomes shallower due to several second-order temperature effects not considered in the analyses. As stated in Section 8.2.1, a simplifying assumption of the analysis was that the -6°C shaded lunar surface temperature was constant throughout the lunar day. It is known, however, that at the terminators (sunrise and sunset) the lunar surface is much colder (see Figure 8.11). Hence, the array electrical performance predicted will be higher than that shown. The lunar noon performance is also expected to be lower than predicted due to load matching and radiation interaction between the back sides of the array. These factors will cause the array equilibrium temperatures to be higher than predicted at lunar noon, thus reducing the power output. The general trend of this revised power profile is shown on Figure 8.48. The net effect of this change would be to reduce the leanto area requirements for the Program V load profile.

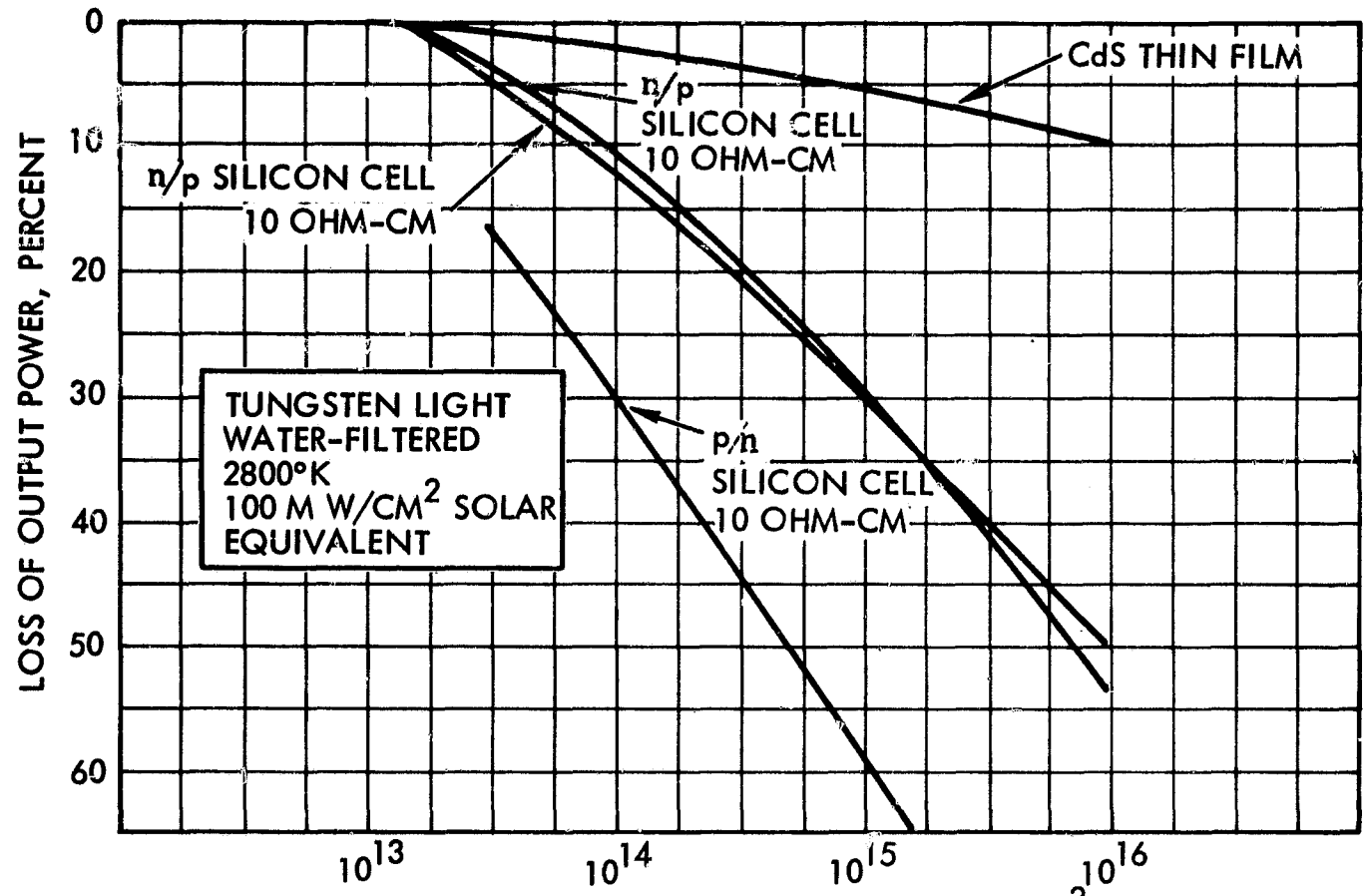

PERCENTAGE CHANGE IN OUTPUT POWER FOR ELECTRON-BOMBARDED SOLAR CELLS FROM AN INTEGRATED FLUX OF 10^{13} (e/CM^2)

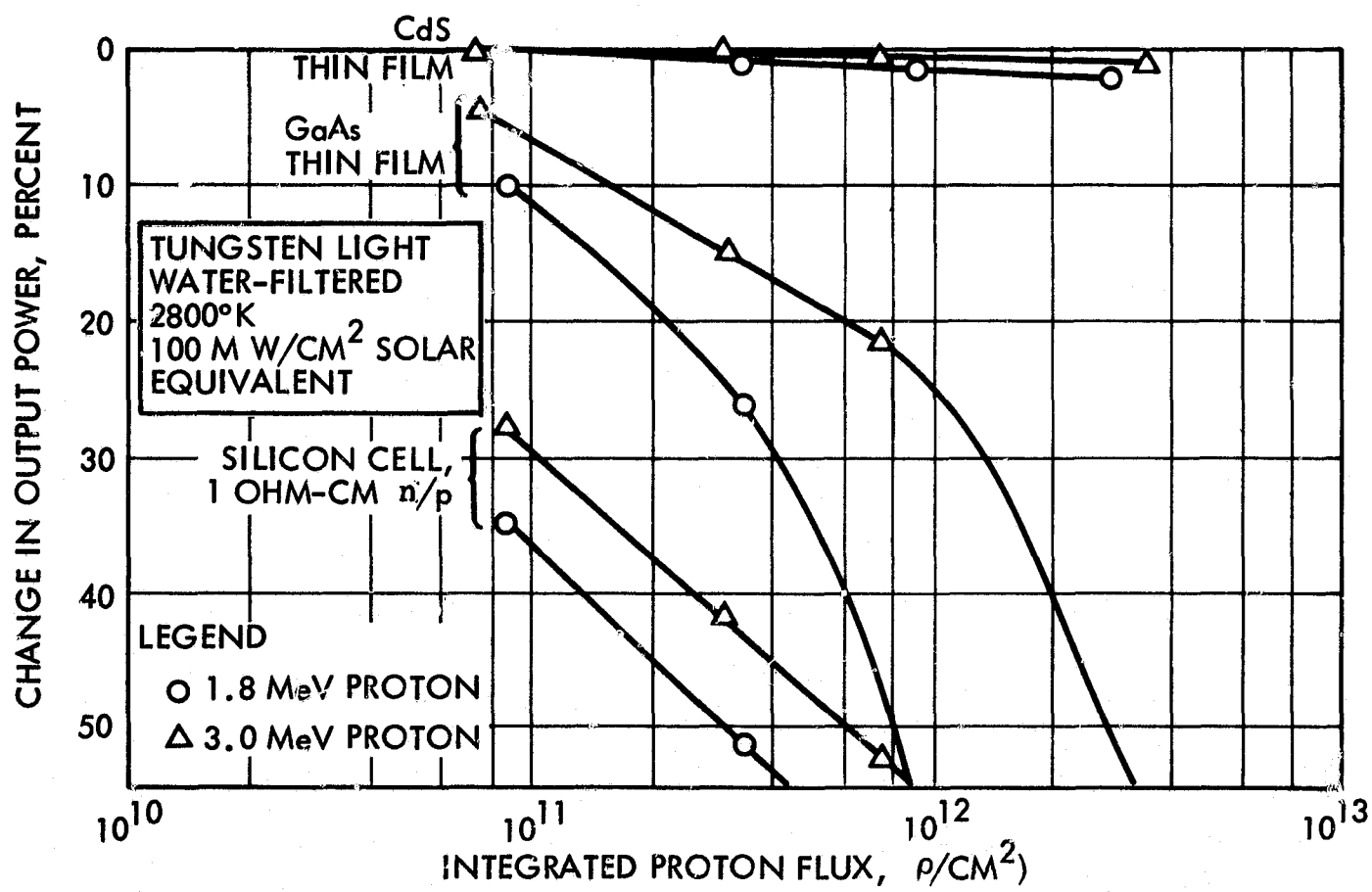

PERCENTAGE CHANGE IN OUTPUT POWER FOR PROTON-BOMBARDED SOLAR CELLS

Figure 8.28 Percent Change in Output Power for Electron-Bombarded and Proton-Bombarded Solar Cells

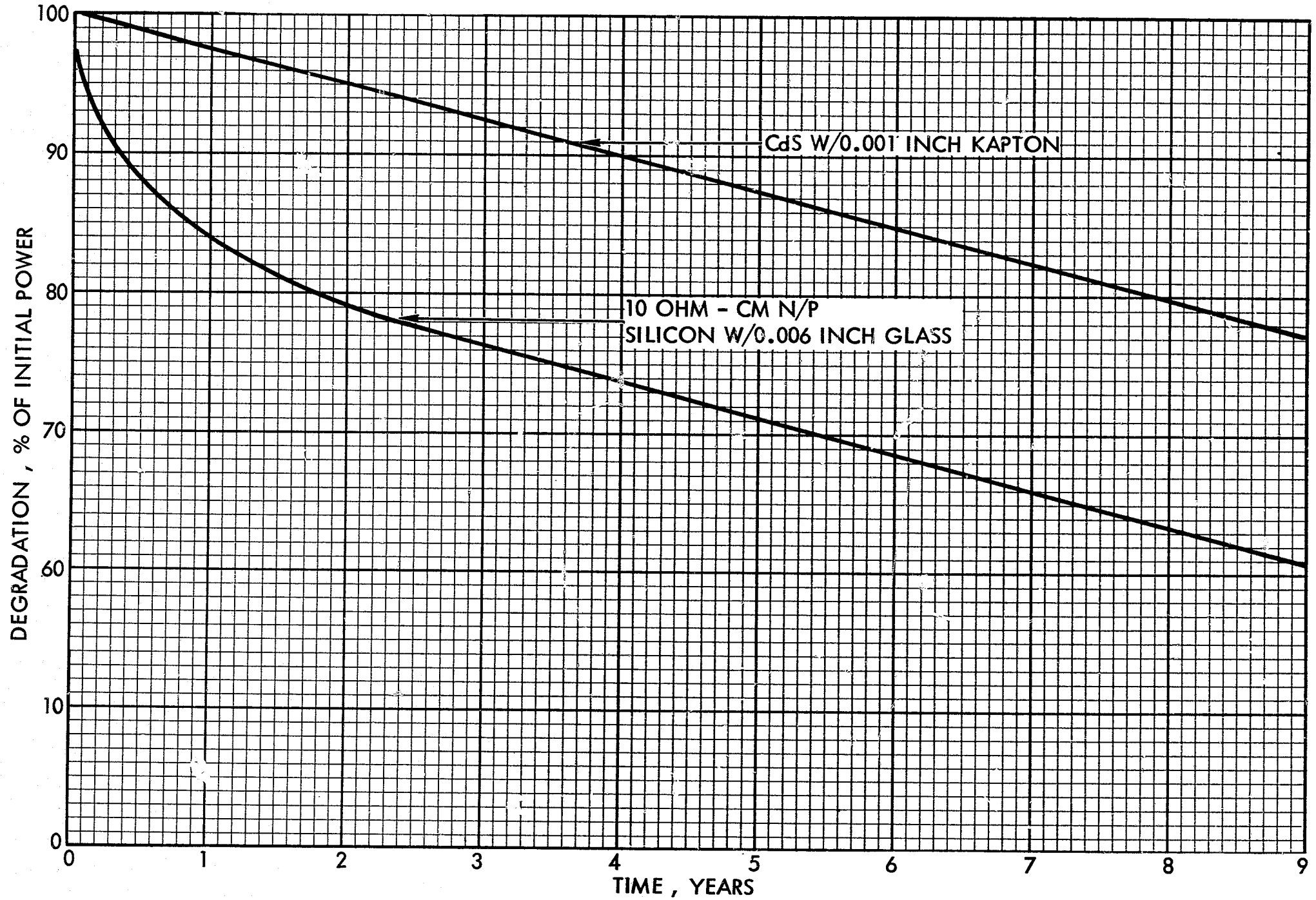

Figure 8.29 Silicon and CdS Thin Film Solar Cell Degradation Due to the Space Environment

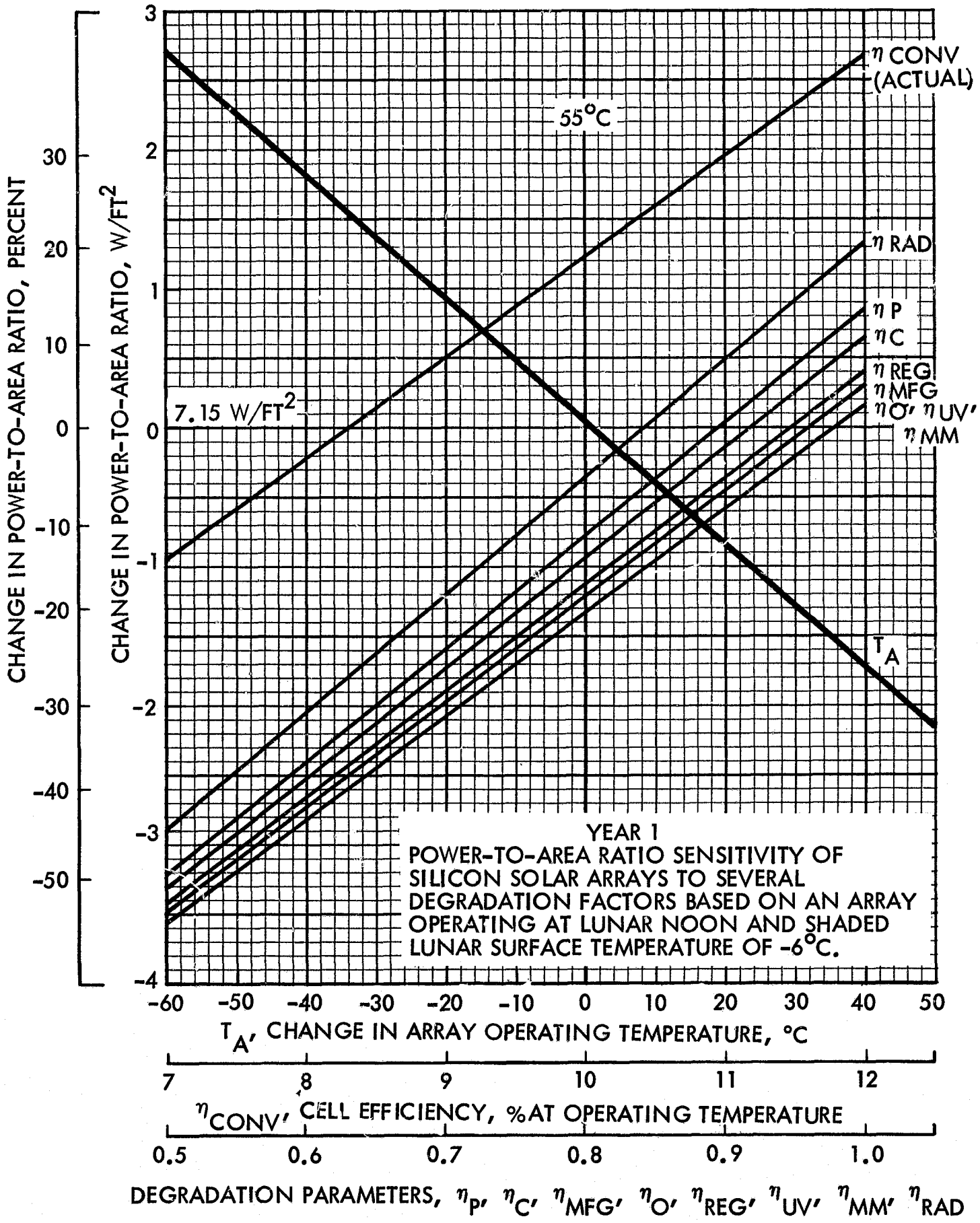

Figure 8.30 Power-To-Area Ratio Sensitivity Curves (Silicon Cell Solar Arrays)

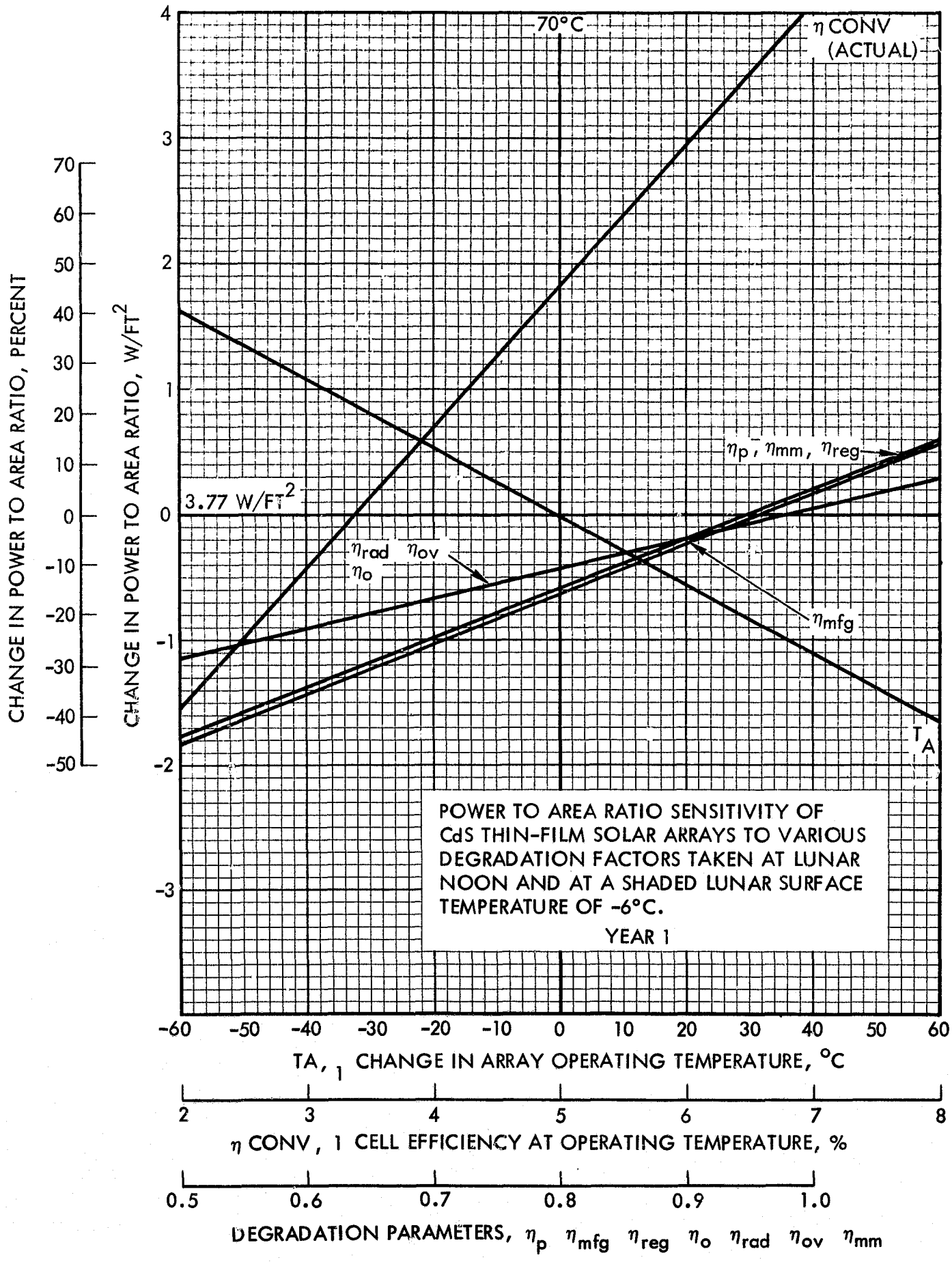

Figure 8.31 Power-To-Area Ratio Sensitivity Curves (CdS Thin Film Arrays)

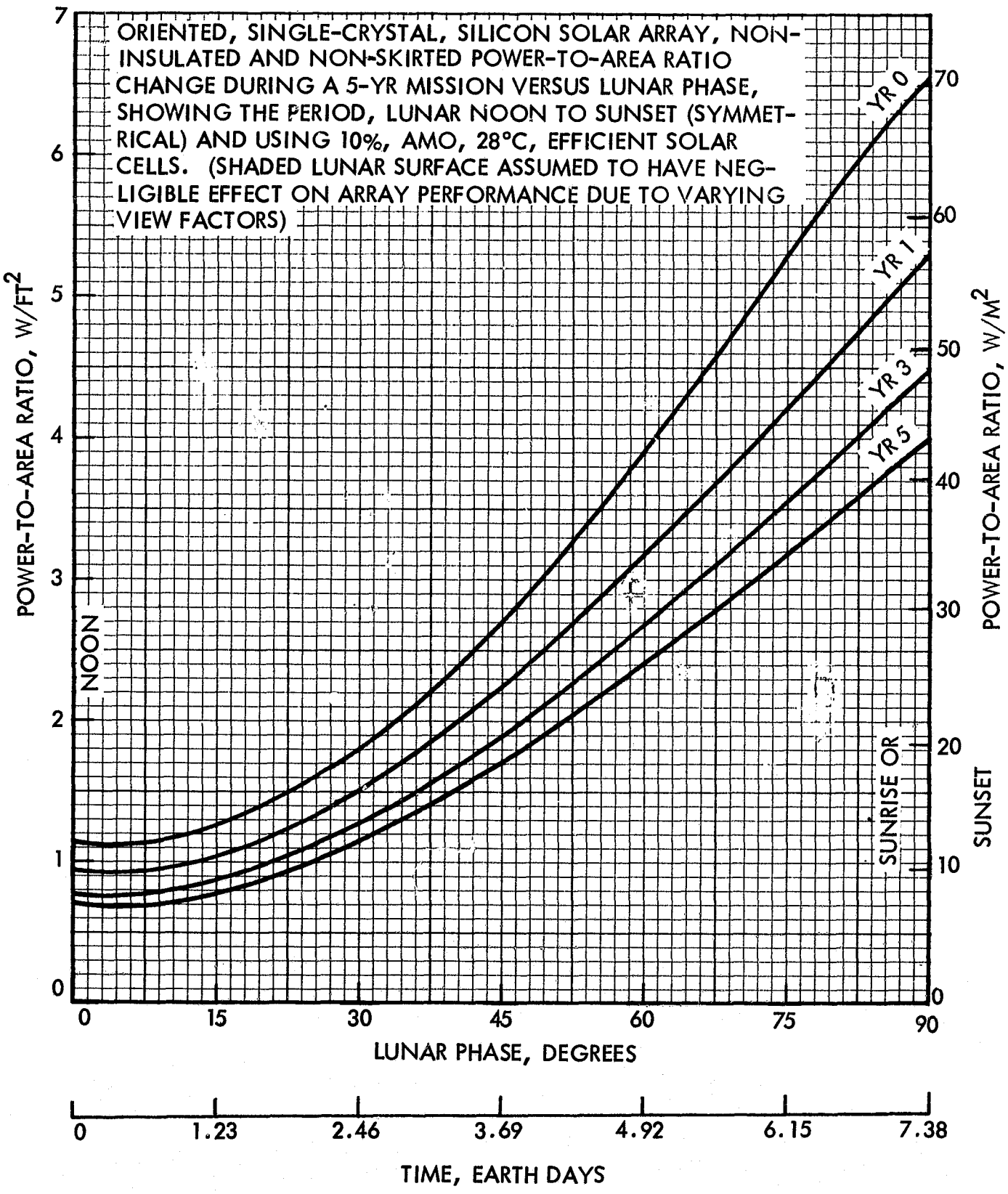

Figure 8.32 Power-To-Area Ratio Versus Lunar Phase for Silicon Cell Solar Arrays (Oriented, Non-Insulated and Non-Skirted)

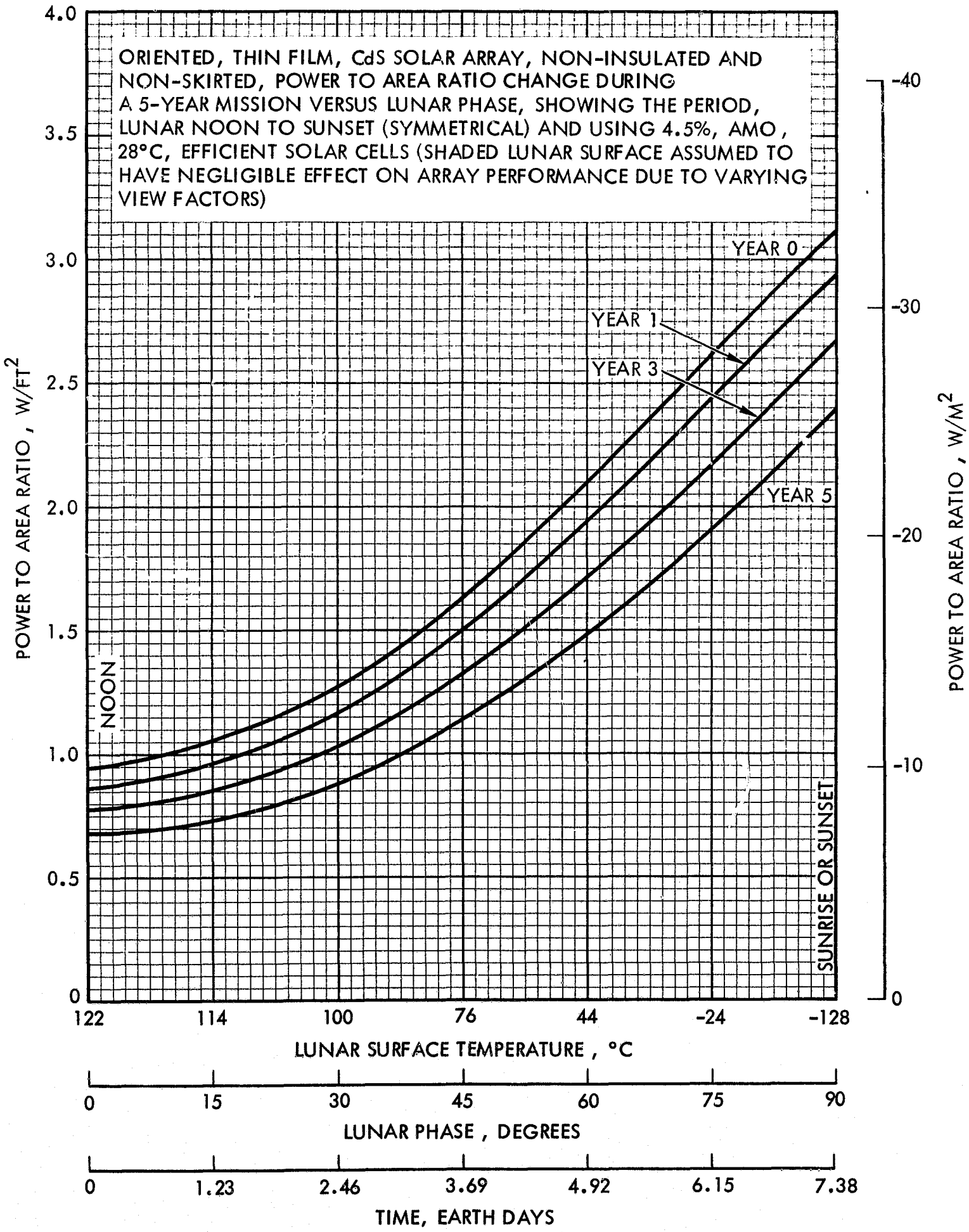

Figure 8.33 Power-To-Area Ratio Versus Lunar Phase for CdS Thin Film Solar Arrays (Oriented, Non-Insulated, Non-Skirted)

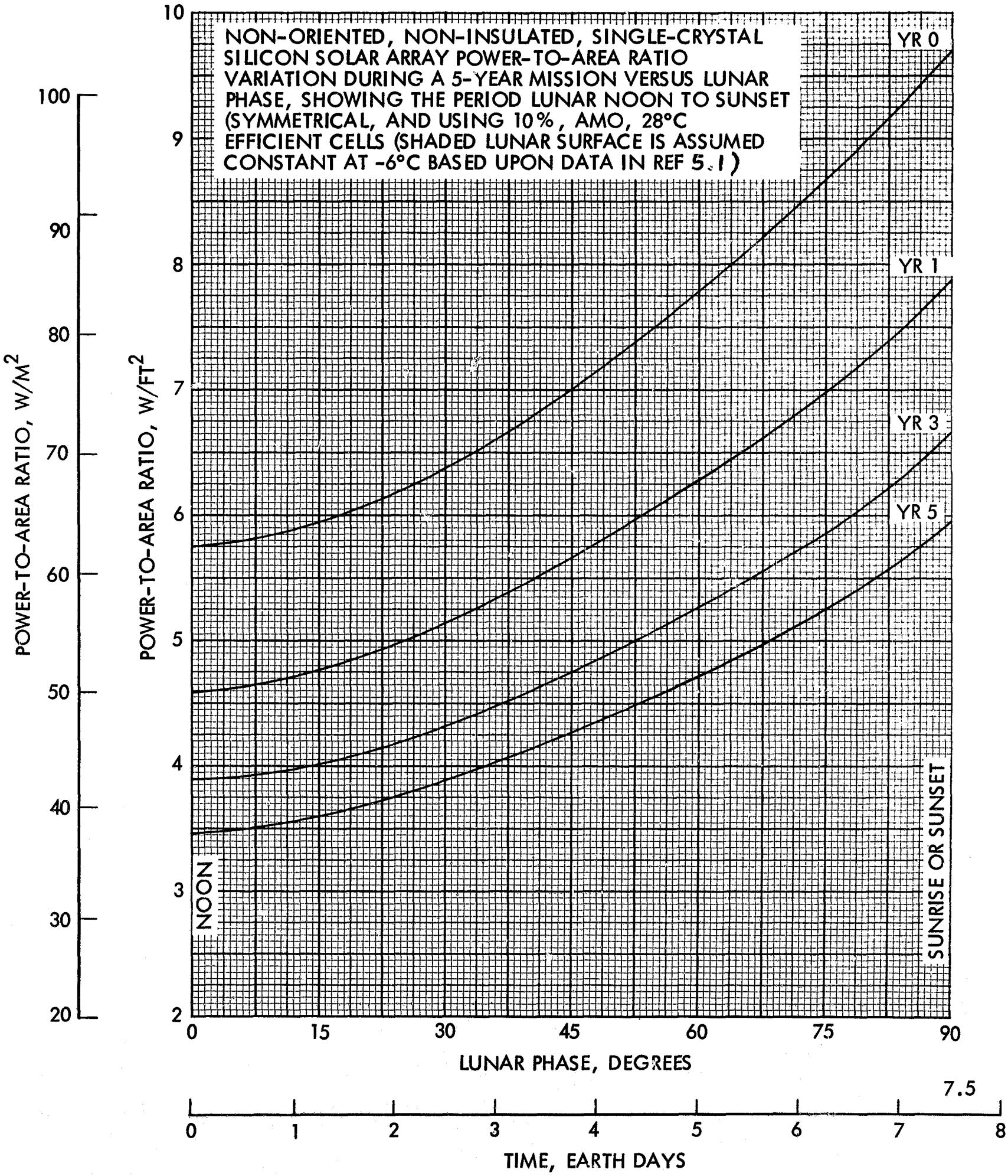

Figure 8.34 Power-To-Area Ratio Versus Lunar Phase for Silicon Cell Solar Arrays (Non-Oriented, Non-Insulated, Non-Skirted)

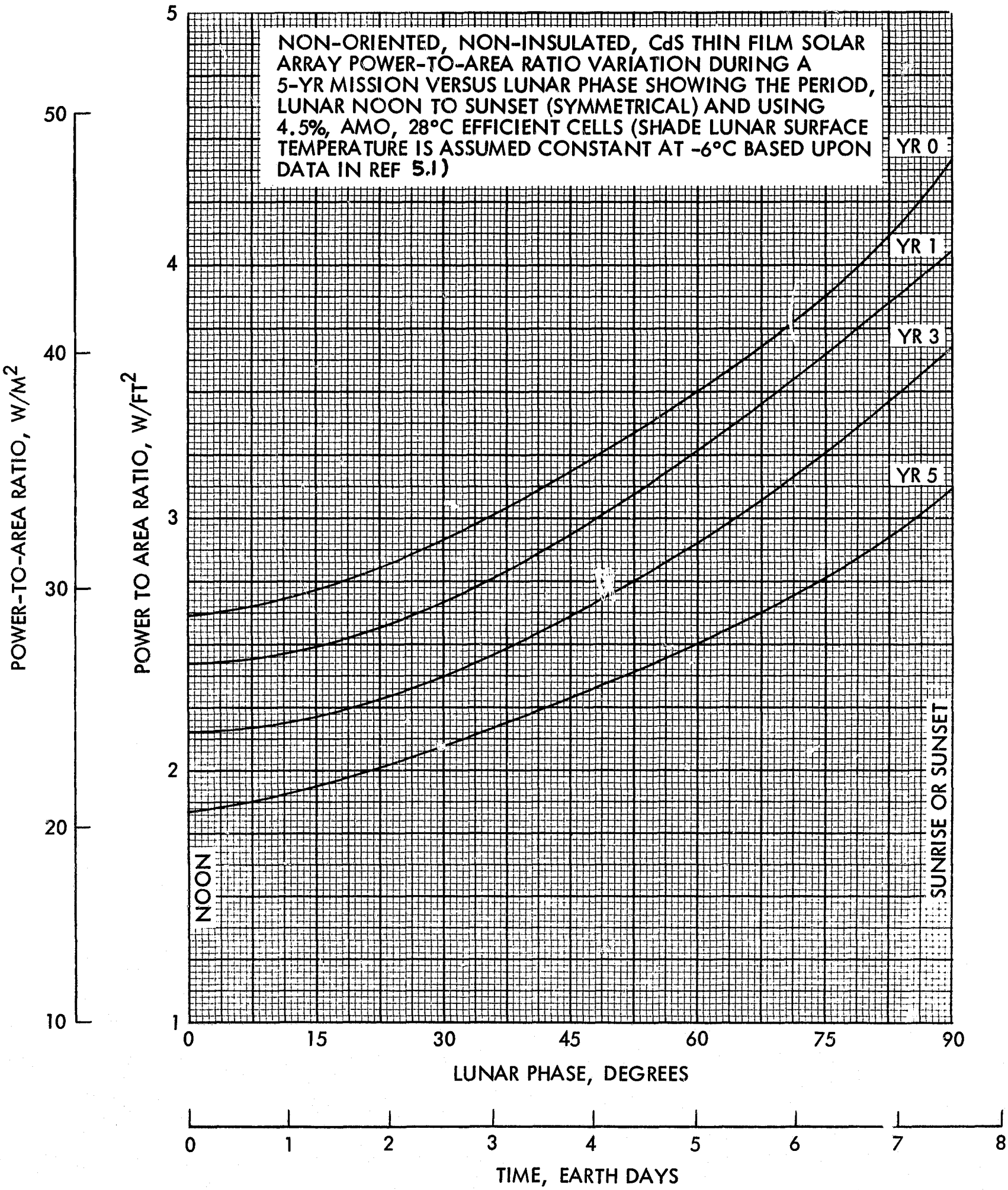

Figure 8.35 Power-To-Area Ratio Versus Lunar Phase for CdS Solar Arrays (Non-oriented, Non-insulated Non-skirted)

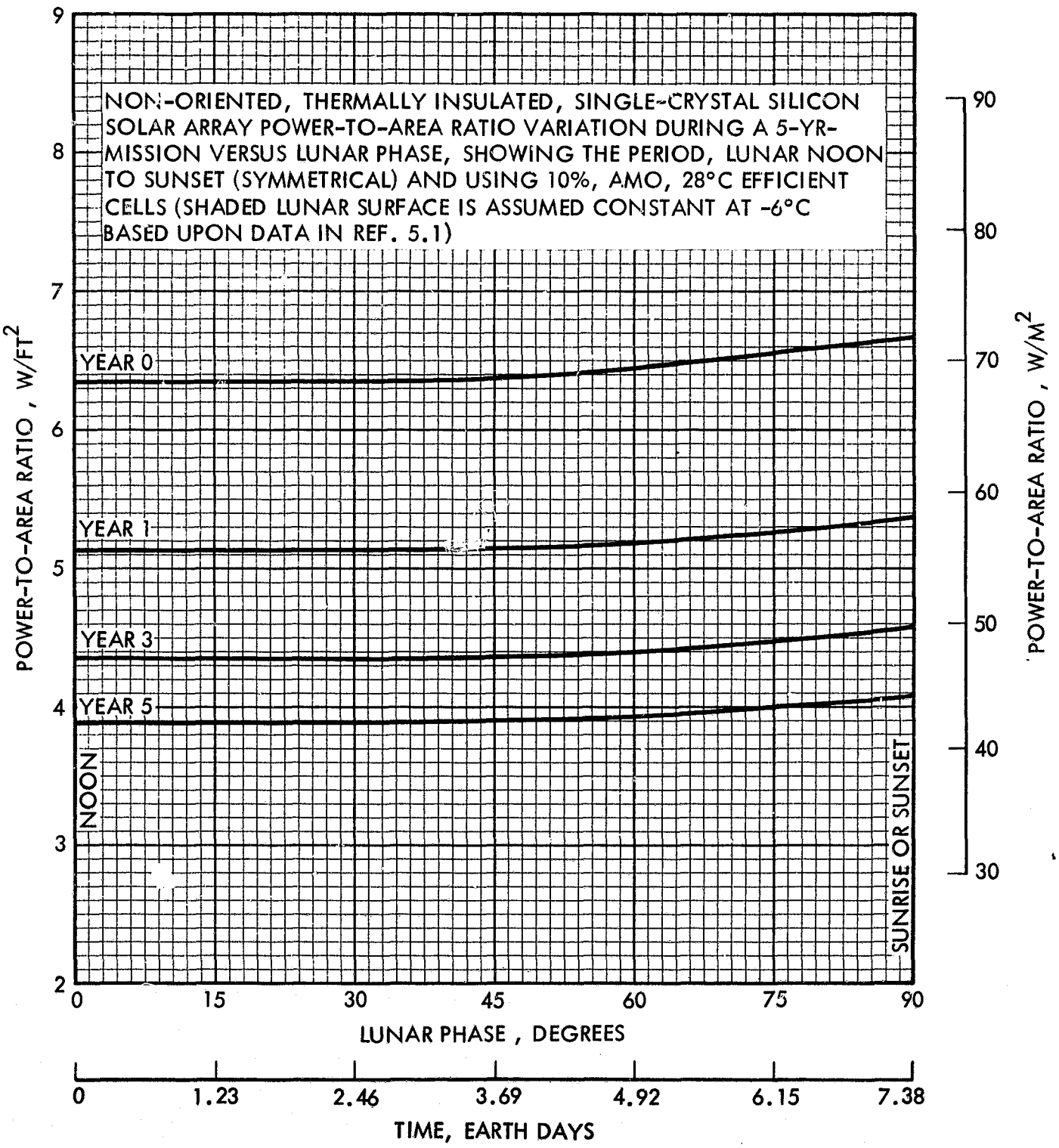

Figure 8.36 Power-To-Area Ratio Versus Lunar Phase for Silicon Cell Solar Arrays (Non-oriented, Thermally Insulated)

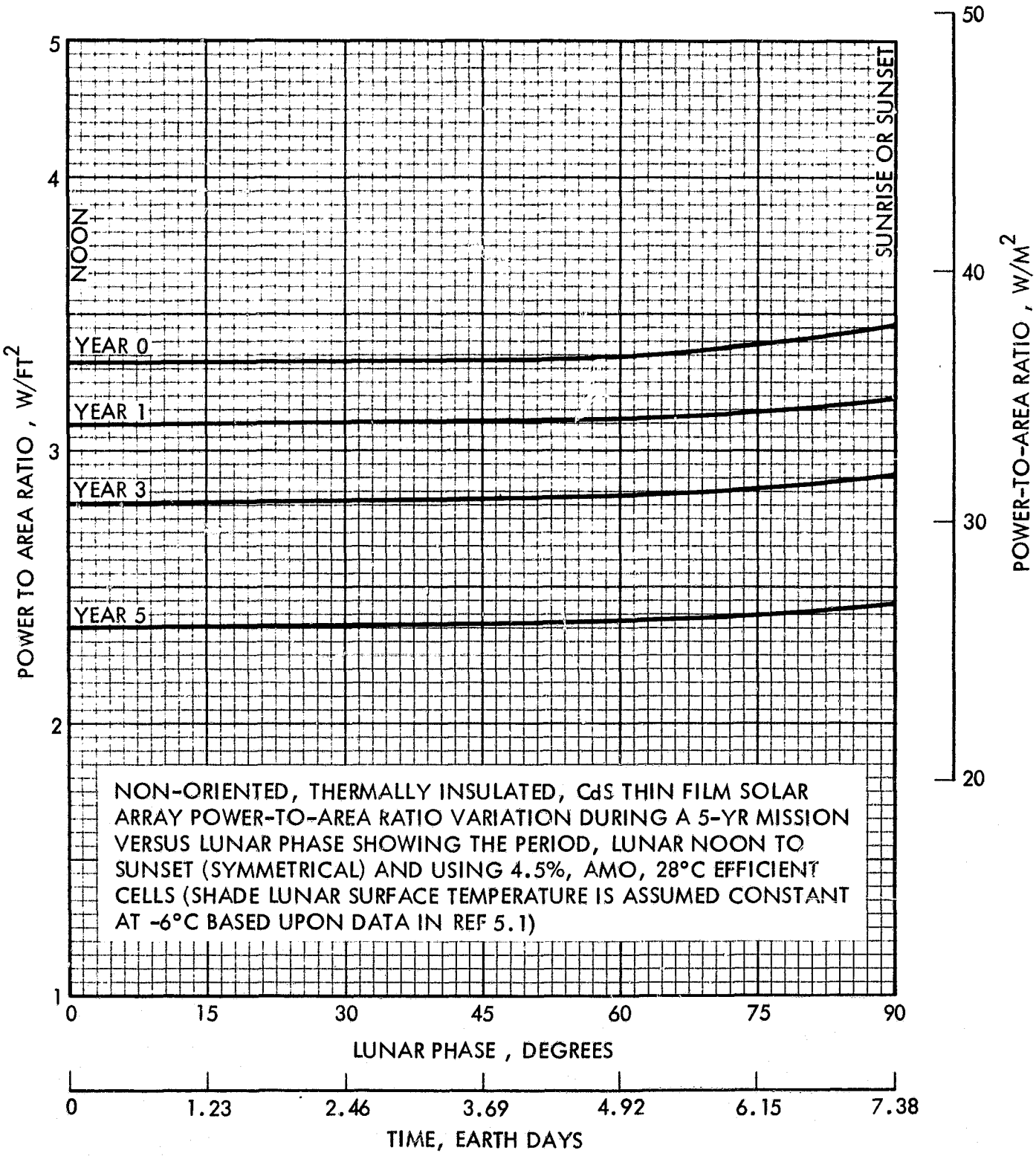

Figure 8.37 Power-To-Area Ratio Versus Lunar Phase for CdS Thin Film Solar Arrays (Non-oriented, Thermally Insulated)

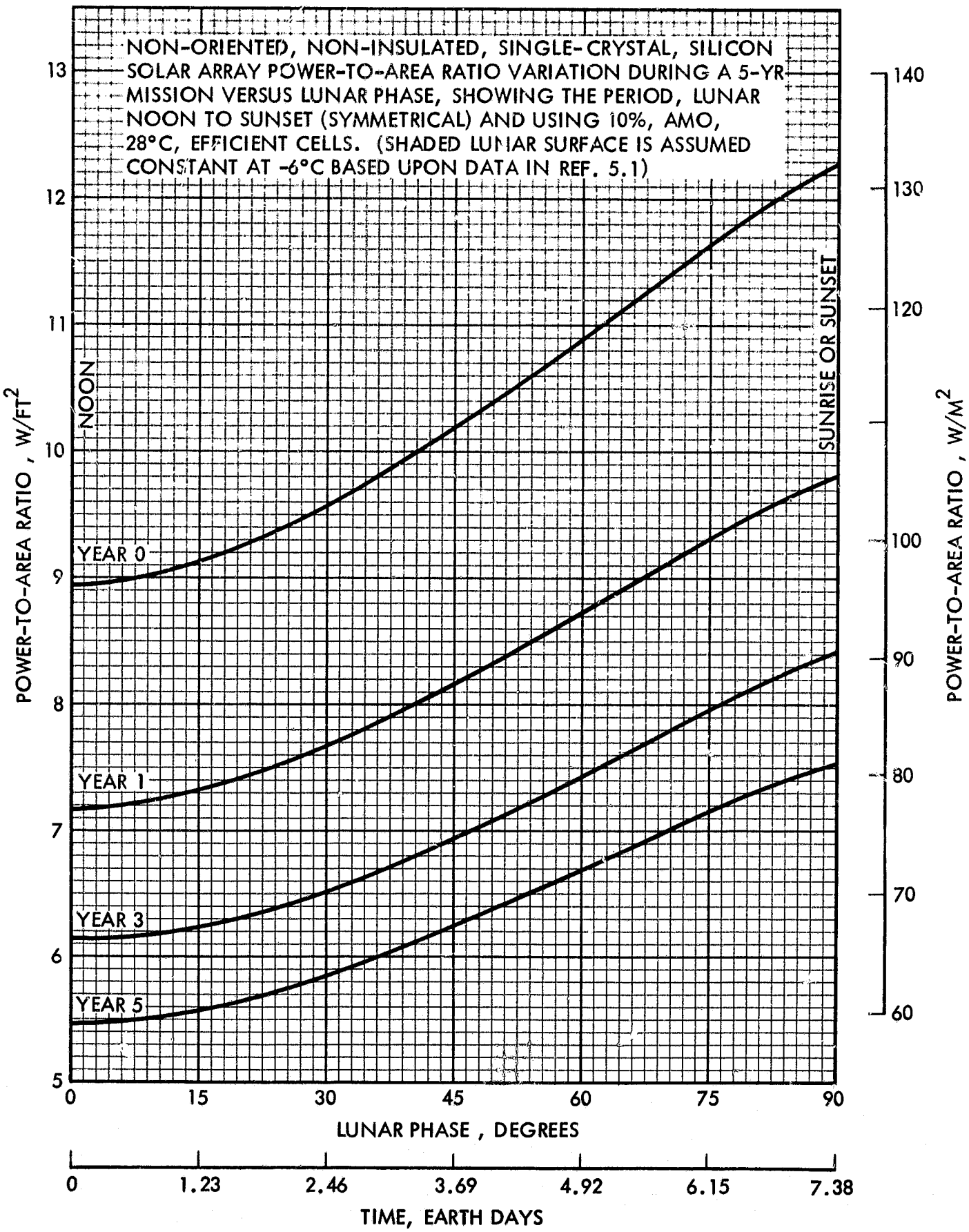

Figure 8.38 Power-To-Area Ratio Versus Lunar Phase for Silicon Cell Solar Arrays (Non-oriented, Non-insulated, skirted)

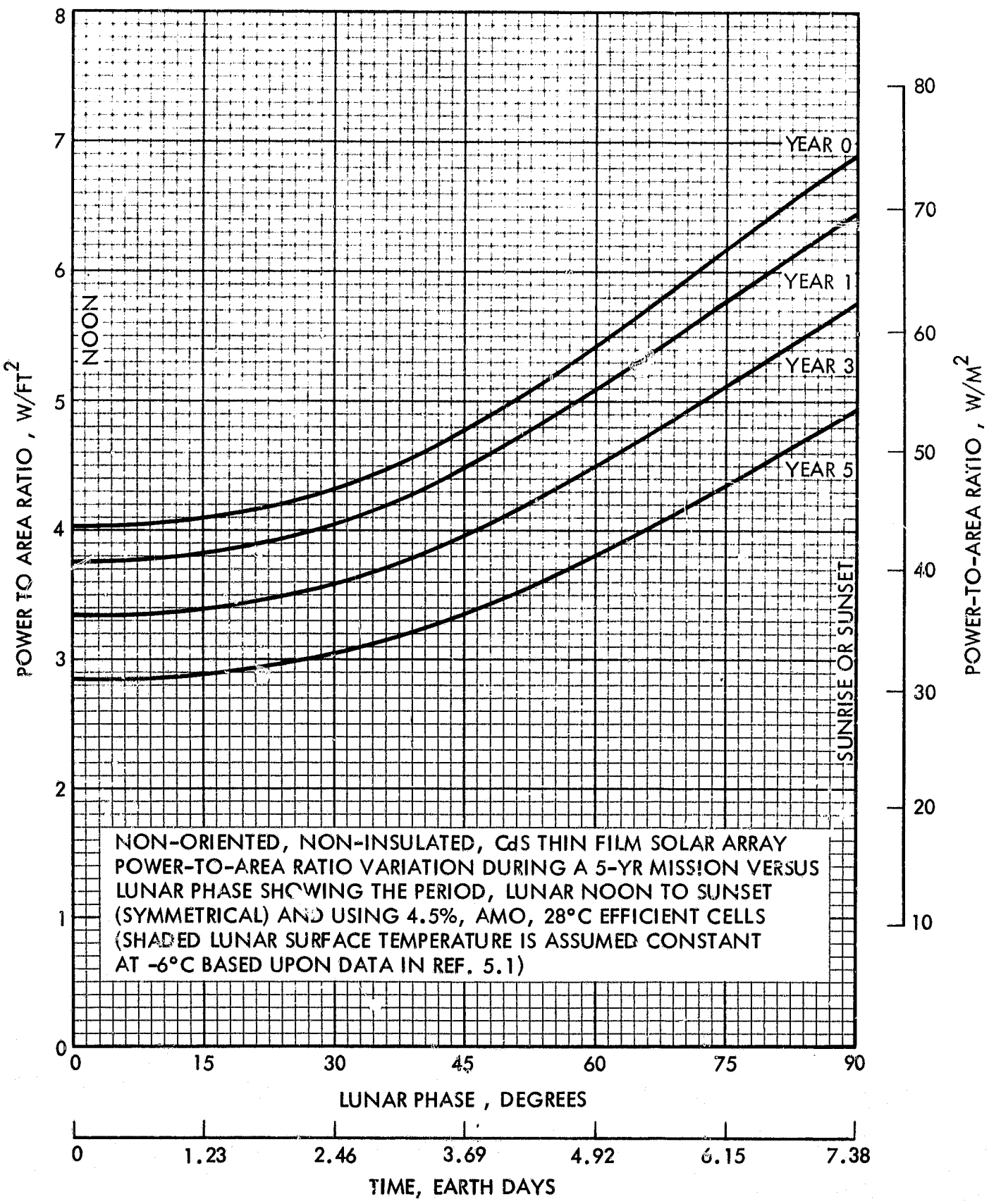

Figure 8.39 Power-To-Area Ratio Versus Lunar Phase for CdS Thin Film Solar Arrays (Non-oriented, Non-insulated, Skirted)

Another way to modify the output power profile of the leanto array would be to change the angle. Increasing the angle also tends to flatten the array output power profile as shown on Figure 8.49. This figure indicates that the leanto configuration can be tailored to provide any desired power profile by compensating for temperature and load effects through variations of the array tilt angle. Leanto angle optimization would vary from mission to mission, and would be influenced by the results of the detailed design requirements. This would include load profile matching and a comprehensive thermal analysis supplemented by extensive heat transfer testing. Transients as well as non-steady state operating conditions would have to be considered in detail. The leanto configuration can be tailored to a wide variety of output power profiles. This is also true, to some extent, for the flat and oriented-skirted arrays. For example, by leading or lagging the solar insolence angle, i.e., mis-orienting, the equilibrium temperatures of the oriented array could be reduced. Hence, despite a decrease in solar radiation intensity the net result could be to increase the output power. Another technique that could be applied to power profile shaping would be to use a "hybrid" array. Included in this category would be a combination of the flat and leanto array (Figure 8.50a), a semi-cylindrical array (Figure 8.50b), or a non-symmetrical leanto array (Figure 8.50c). By a judicious selection of array geometry coupled with a detailed analysis of array equilibrium temperatures, it would be possible to closely match a wide variety of base load profiles. The overall result could lead to a reduction in total array area, weight and cost for a specific mission requirement by use of several, standardized hybrid array configurations.

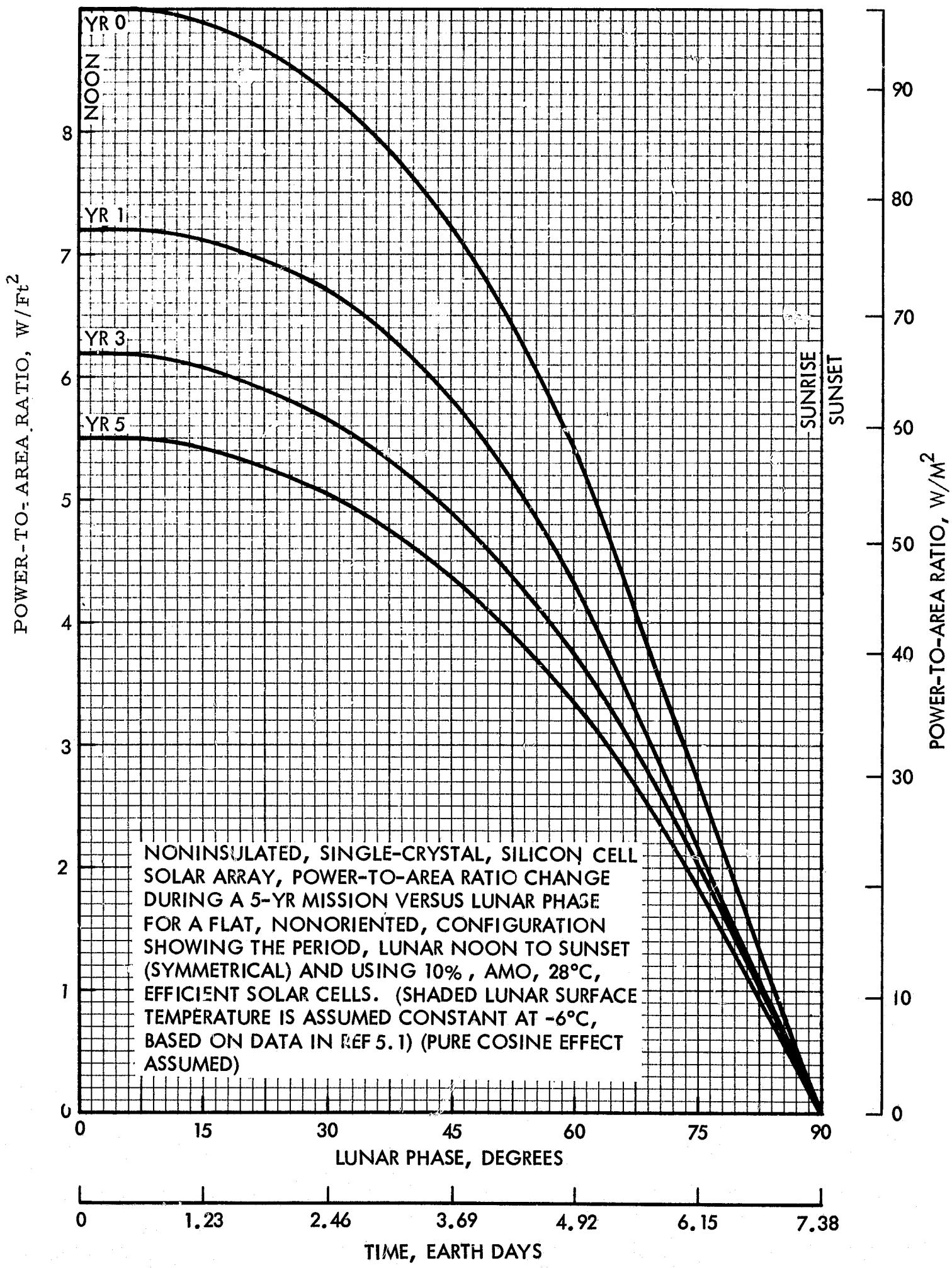

Figure 8.40 Power-To-Area Ratio for a Flat Silicon Cell Solar Array Configuration (Non-insulated, Non-oriented, Skirted)

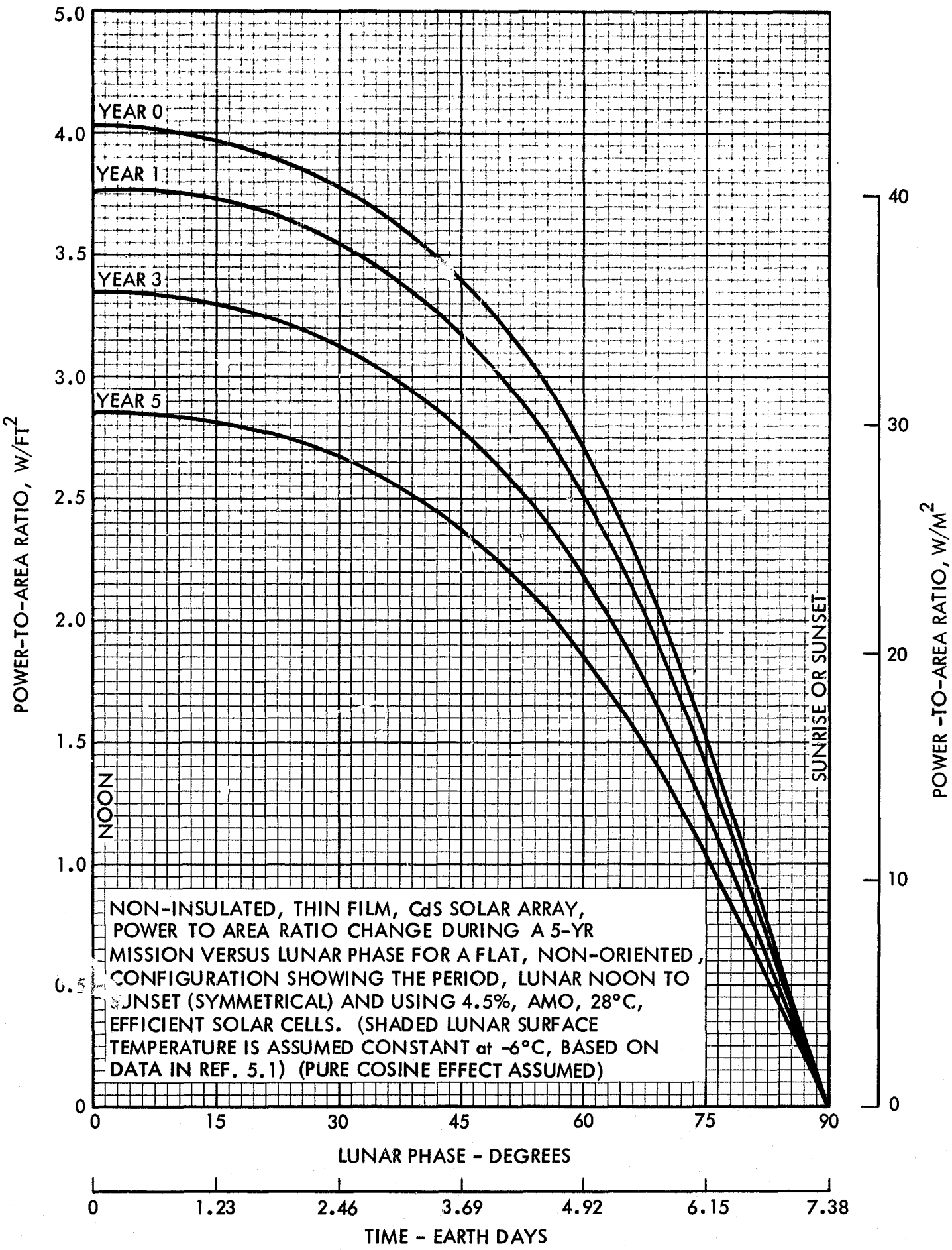

Figure 8.41 Power-To-Area Ratio for a Flat CdS Thin Film Solar Array Configuration (Non-insulated, Non-oriented, Skirted)

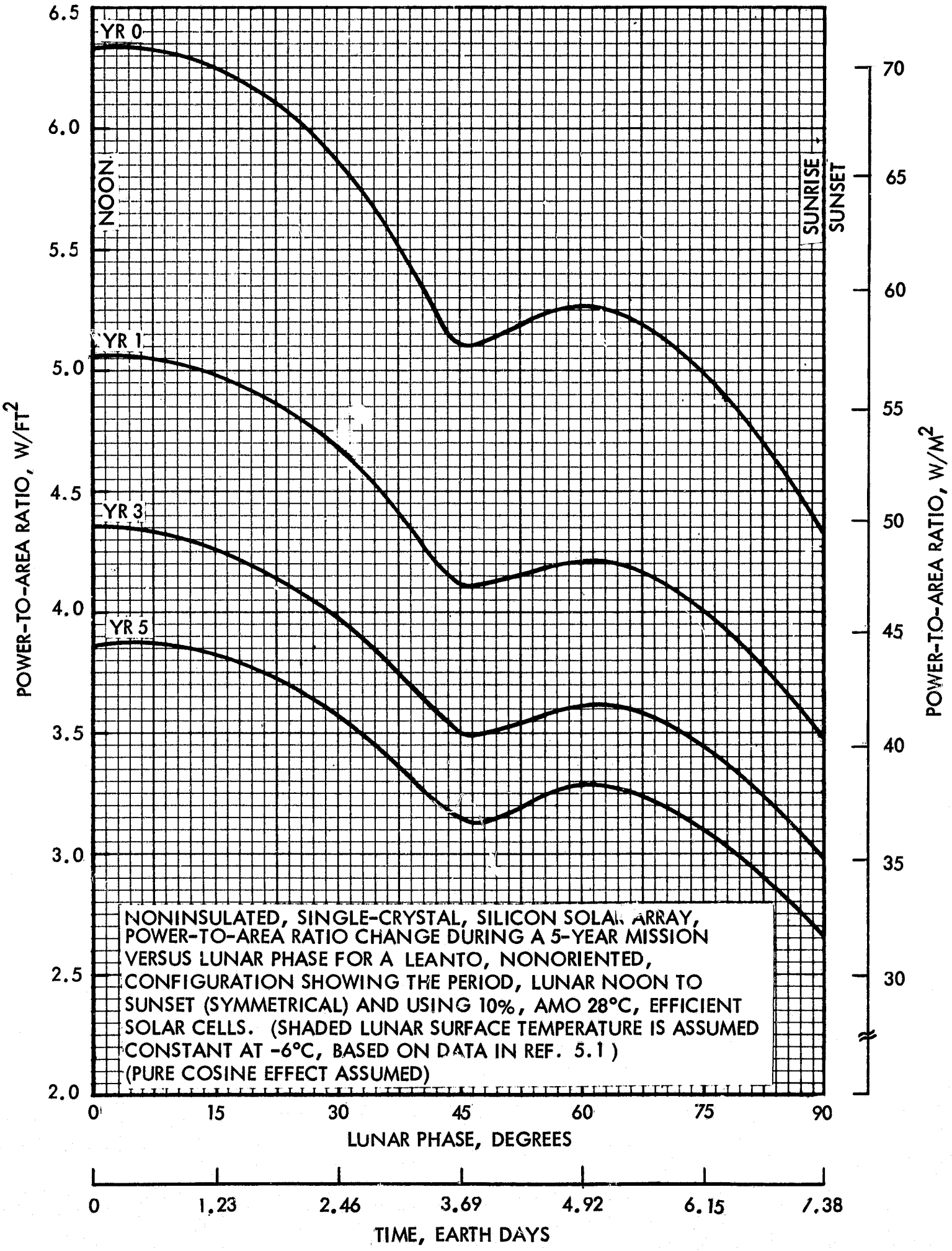

Figure 8.42 Power-To-Area Ratio for a Leanto Silicon Cell Solar Array Configuration (Non-Insulated, Skirted)

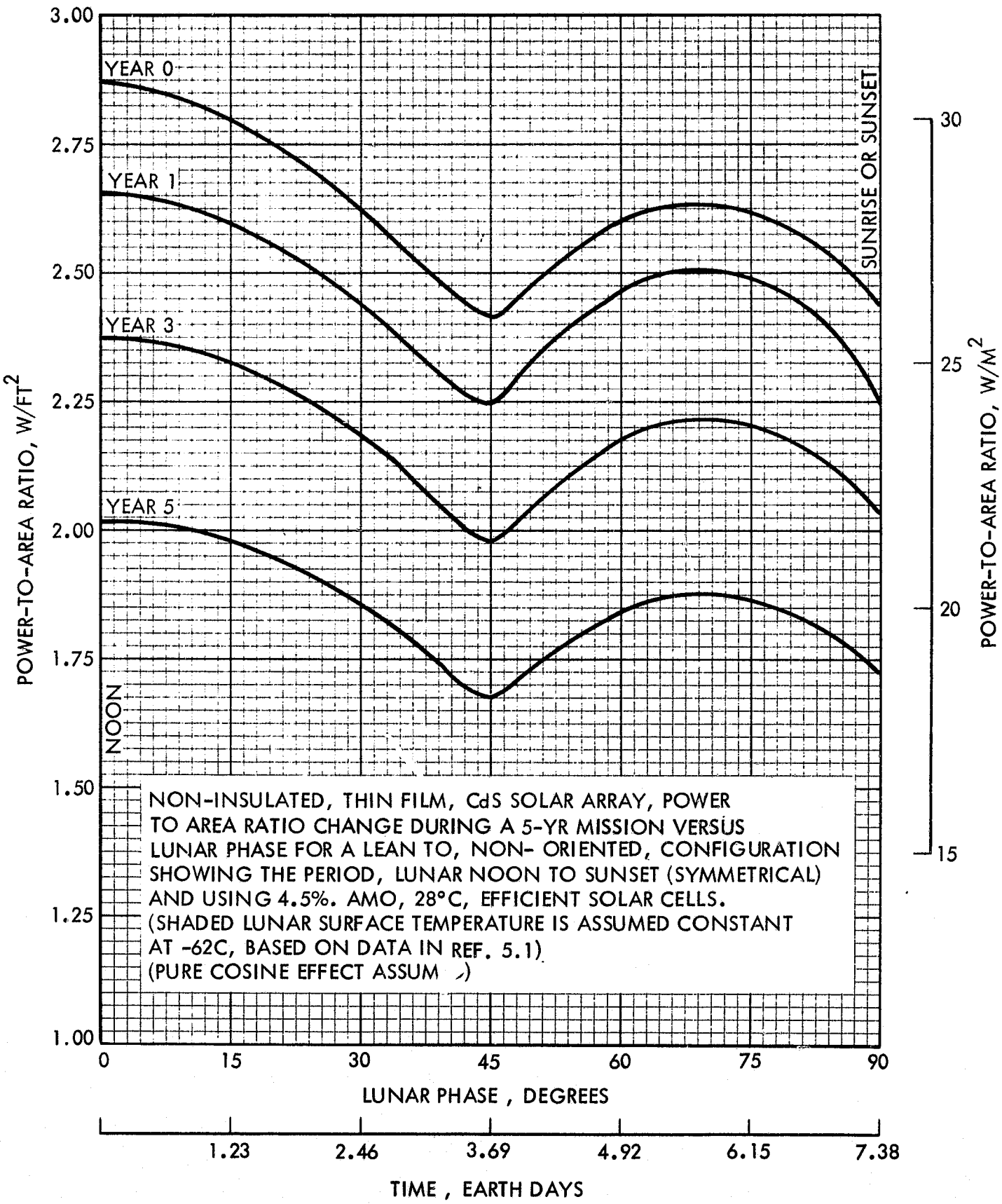

Figure 8.43 Power-To-Area Ratio for a Leanto CdS Thin Film Solar Array Configuration (Non-Insulated, Skirted)

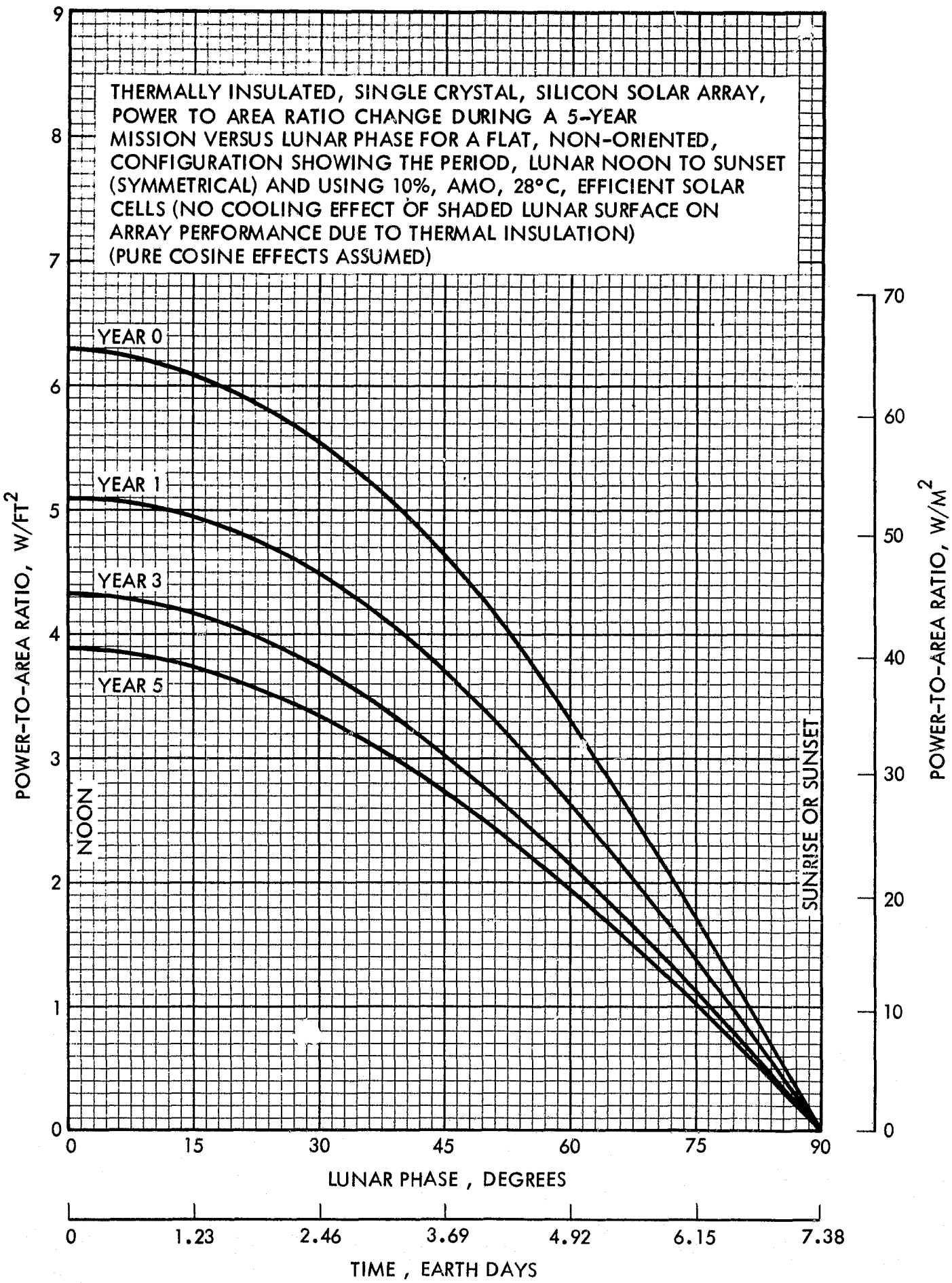

Figure 8.44 Power-To-Area Ratio for a Flat Silicon Cell Solar Array Configuration (Thermally Insulated, Non-Oriented)

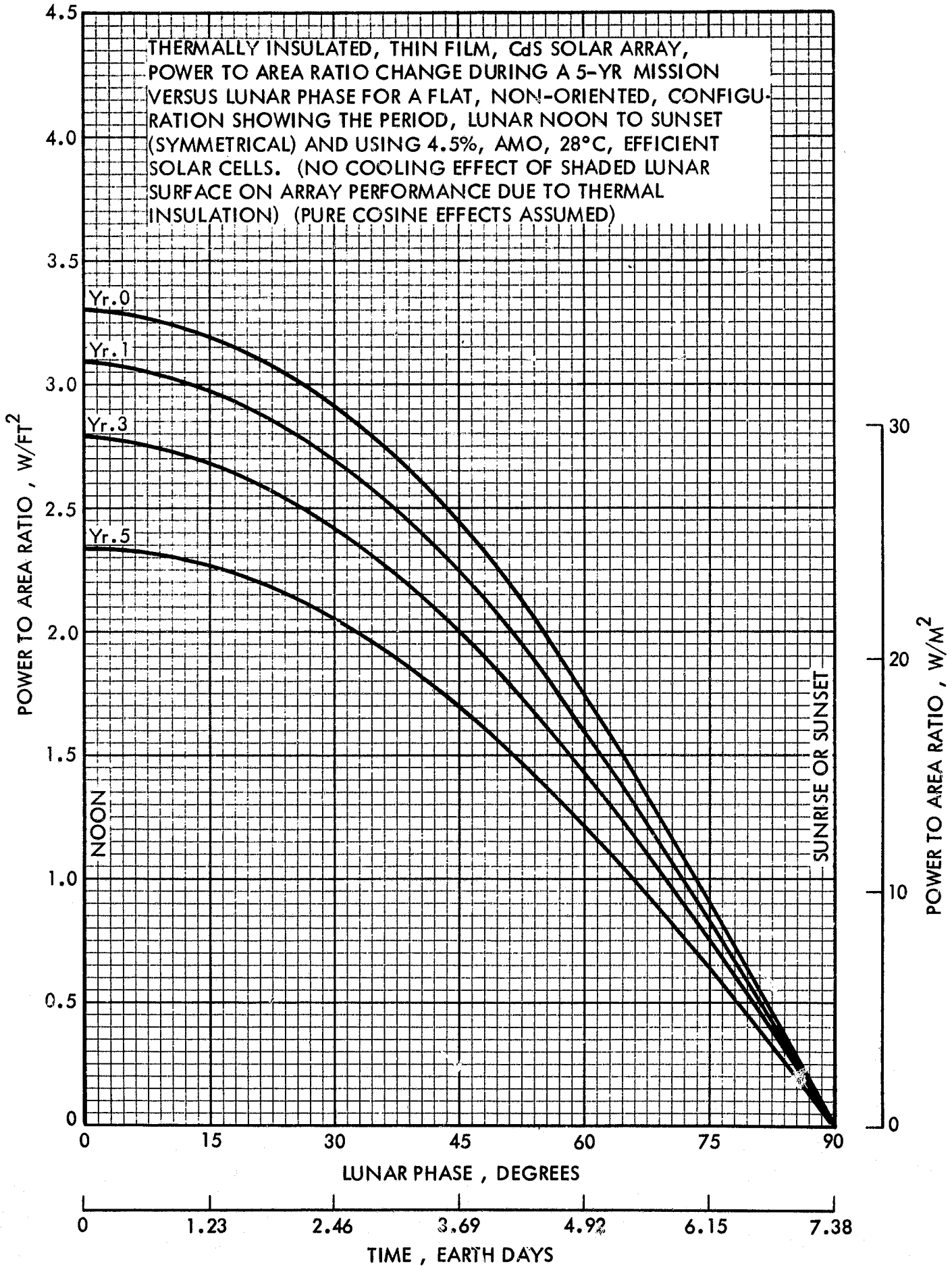

Figure 8.45 Power-To-Area Ratio for a Flat CdS Thin Film Solar Array Configuration (Thermally Insulated, Non-Oriented)

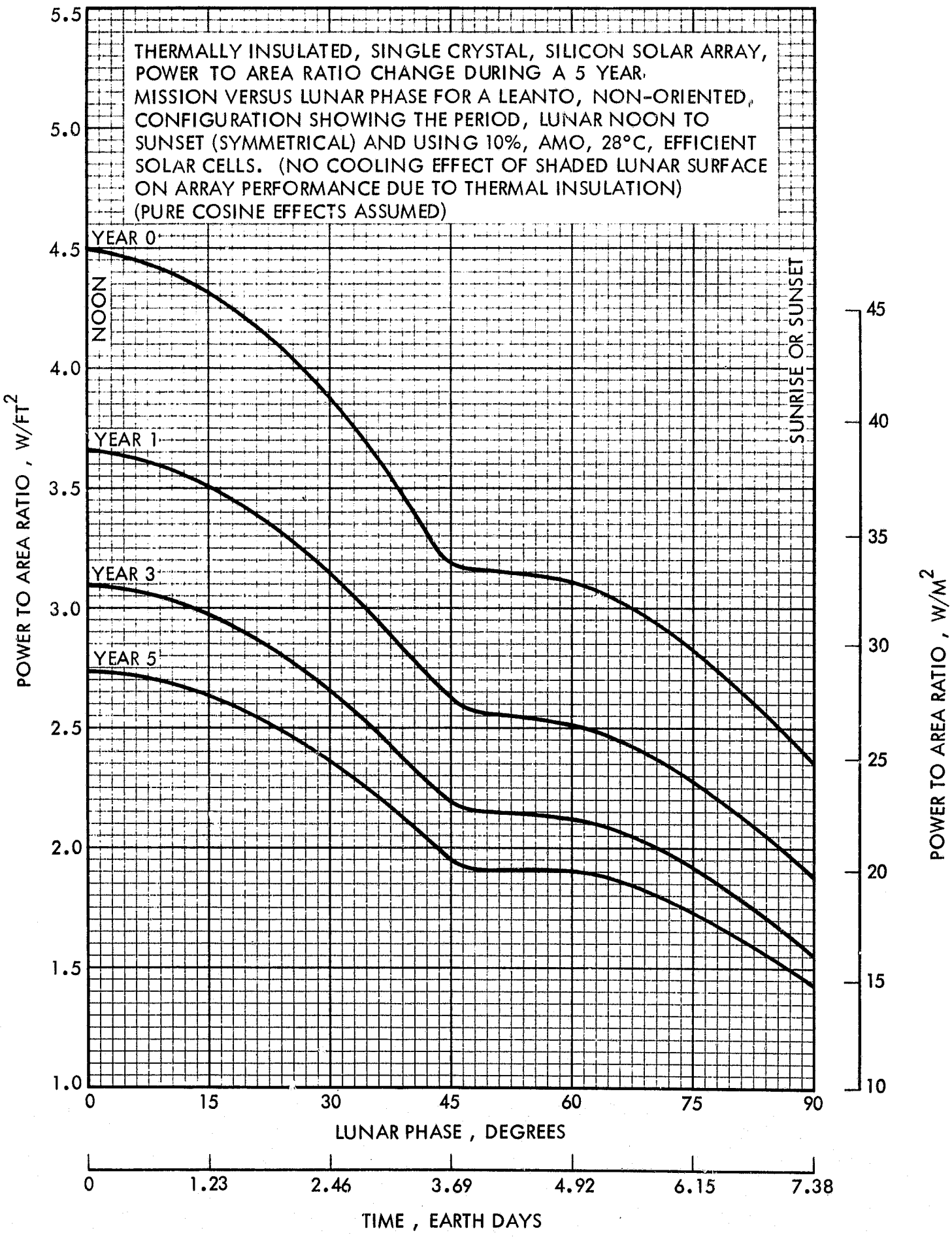

Figure 8.46 Power-To-Area Ratio for a Leanto Silicon Cell Solar Array Configuration (Thermally Insulated, Non-Oriented)

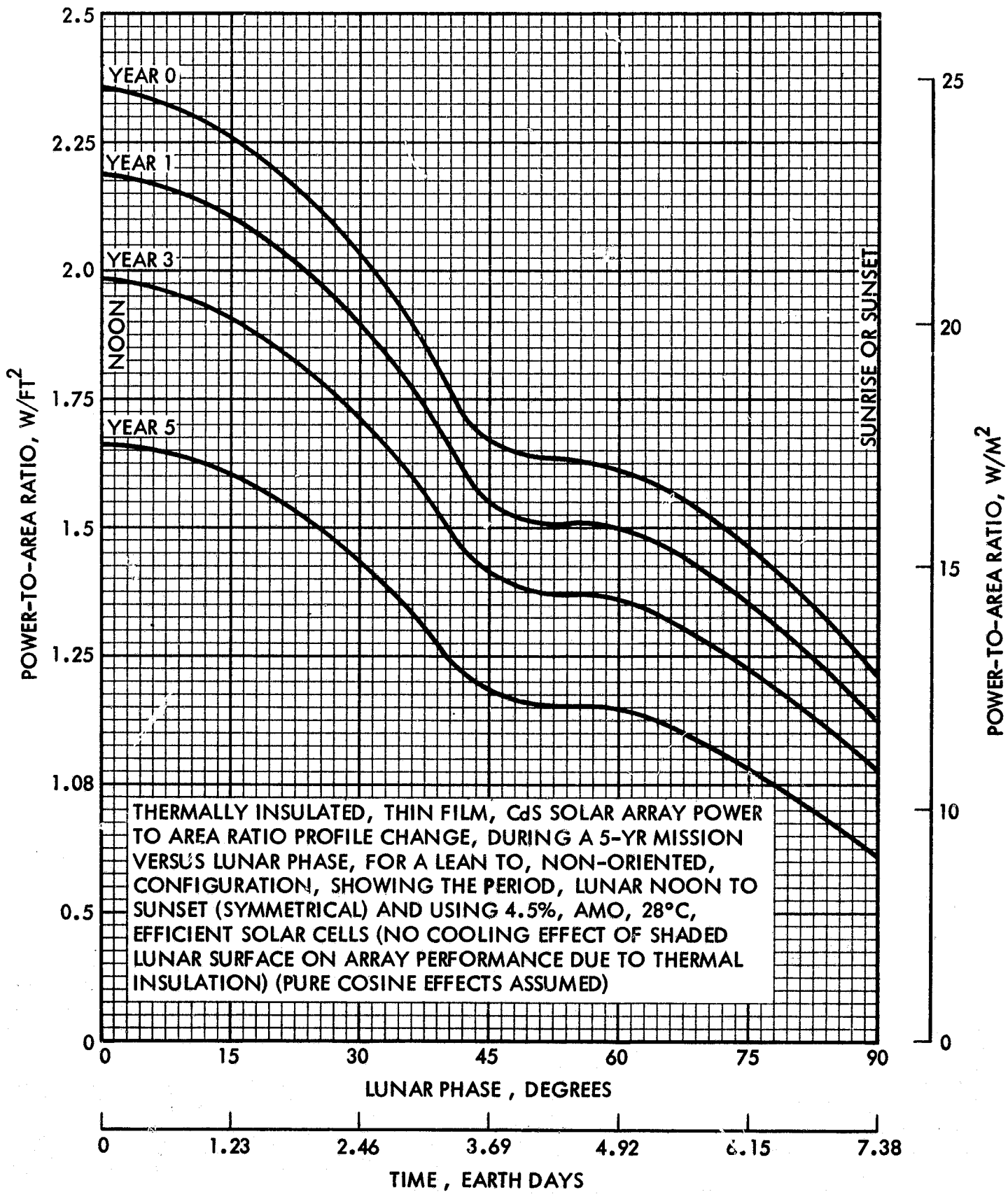

Figure 8.47 Power-To-Area Ratio for a Leanto CdS Thin Film Solar Array Configuration (Thermally Insulated, Non-Oriented)

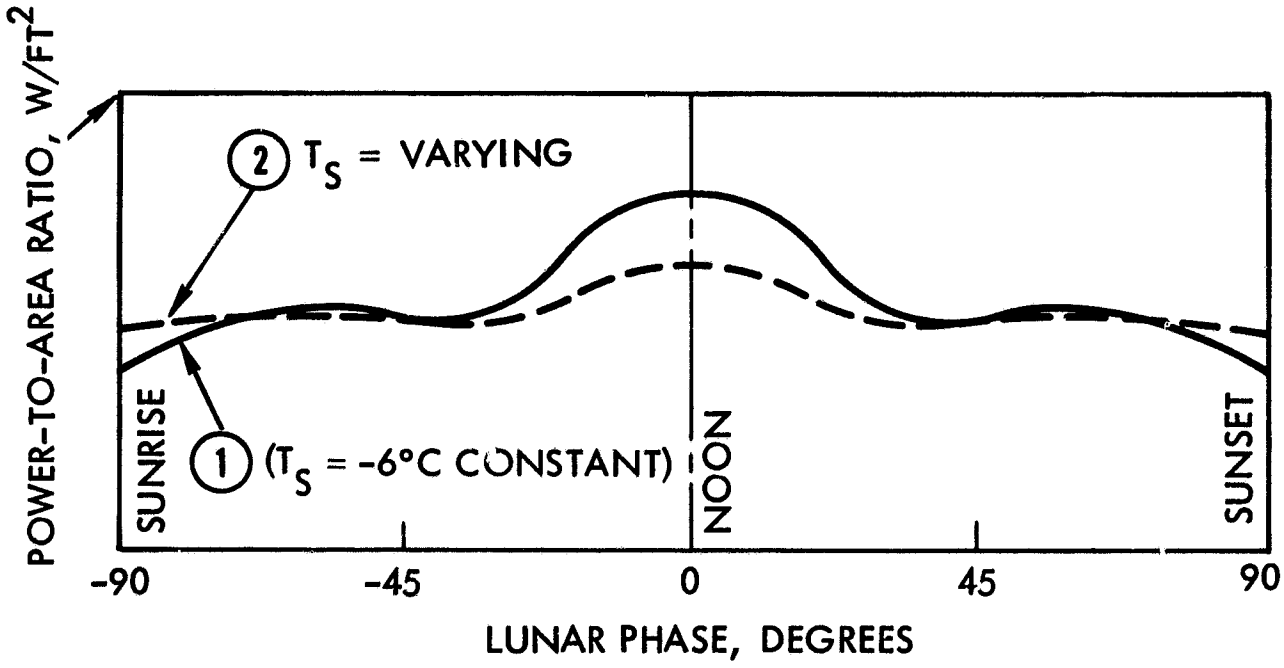

Figure 8.48 Comparison of Performance for Leanto Solar Array Configuration as a Function of Lunar Surface Temperature (Constant versus Varying)

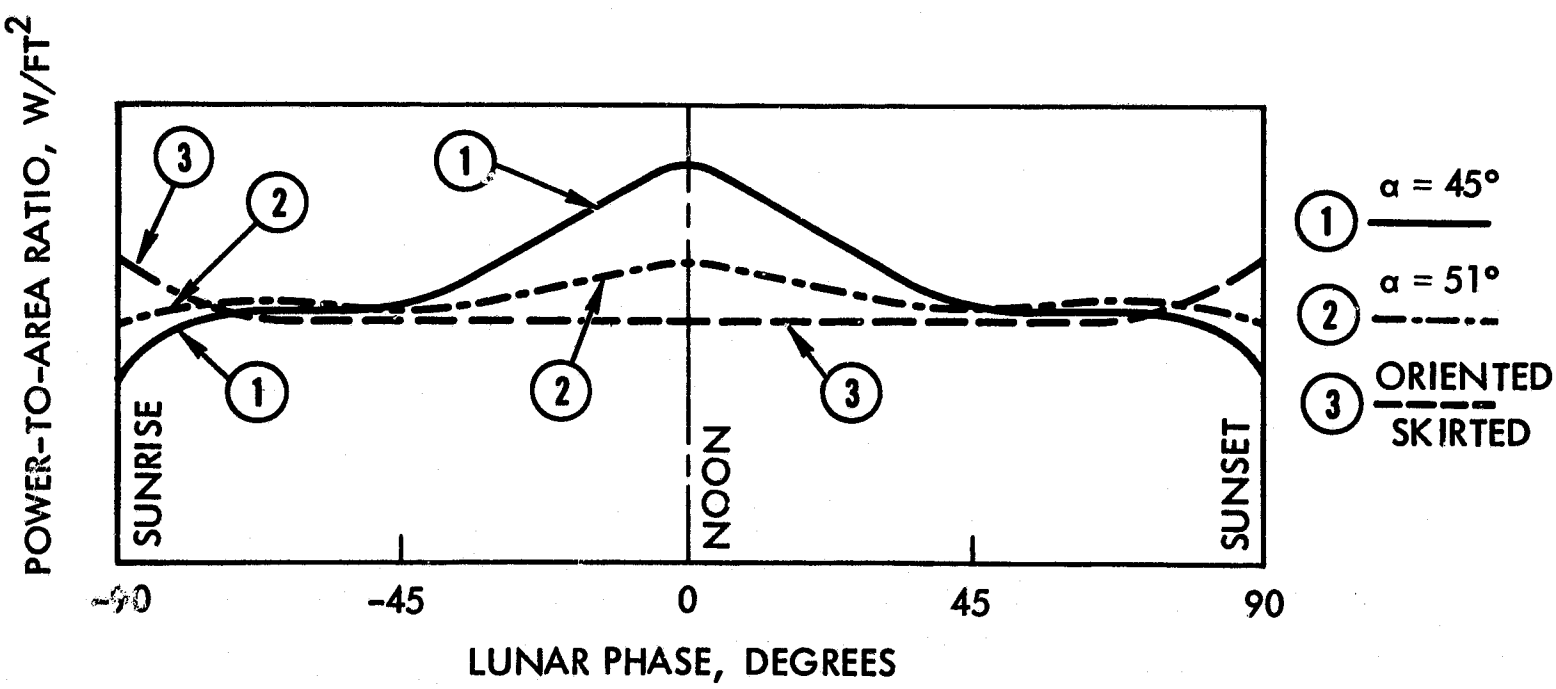

Figure 8.49 Comparison of Performance Between 45° and 51° Leanto Solar Array Configuration at Constant -6°C Shaded Lunar Surface Temperature

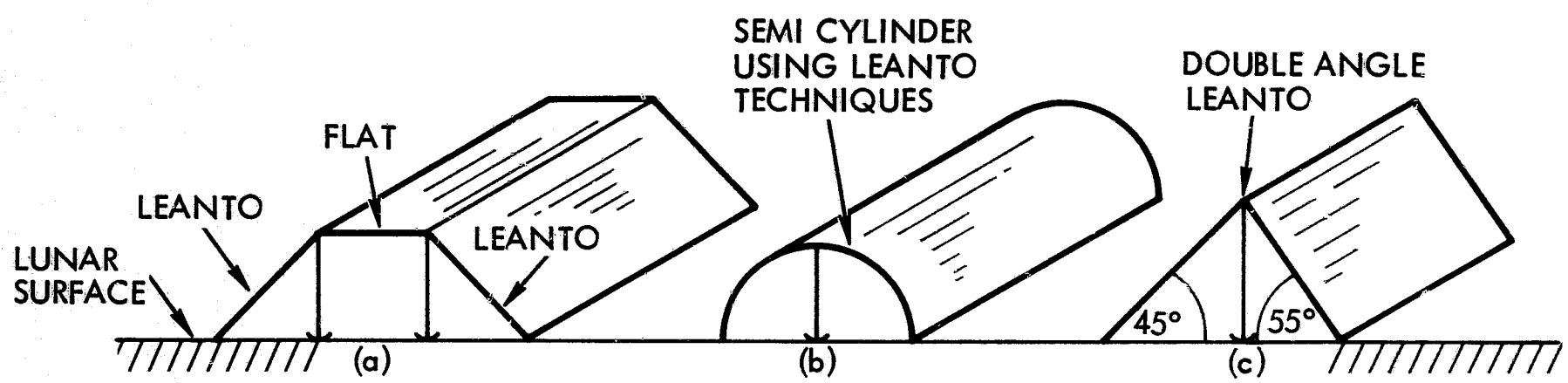

Figure 8.50 Various "Hybrid" Solar Array Configuration

9. SOLAR ARRAY CANDIDATE CONFIGURATIONS

The data generated in Sections 7.0 and 8.0 of this study was used to determine the candidate solar array area and weight requirements. The results were prepared in parametric form, so that the data could be applied to a broad range of load profiles and not be limited only to the one designated for the Program V mission. The output power profiles are based upon the assumptions and performance analysis presented in Section 8.0. Both single crystal silicon cells and CdS thin film performance was evaluated.

9.1 OUTPUT POWER PROFILE COMPARISONS

The output power profiles of each of the candidate array configurations are compared on an area, weight, and cost basis in Figures 9.1 through 9.12. These profiles assumed matched load conditions and operation at the optimum power regime of the array I-V characteristic curve. As previously discussed (Section 8.4.2), the actual "conditioned" power profile would be somewhat different from these depending on several factors. These include, but are not necessarily limited to, power conditioning characteristics, load matching requirements, equilibrium temperature variations, thermal gradients, and temperature transients. In addition, end-of-mission performance is depicted (one year), thus conservatively reflecting a lower power level than would be expected at the start of the mission. One case for a non-skirted, non-insulated oriented array was shown (Figures 9.1 to 9.3) to indicate the magnitude of performance degradation associated with permitting the back surface of the array to view the hot lunar surface. Some improvement could be achieved by insulating the back and mis-orientation but the resulting performance would still be lower than the oriented-skirted case.

Since the shaded lunar surface temperature was found to be an important parameter in arriving at array performance, the effect of this variable on the leanto array area, weight and cost was determined. This is shown in Figures 9.13 to 9.13 which indicate that total array area could be affected by as much as 15% (increase) if the assumed constant shaded lunar surface temperature was 55° higher. However,

this is not a realistic case since the leanto array is sized based upon the output power level at sunrise when the unshaded lunar surface temperature ranges from -173°C to -25°C during the first 12 hours of the lunar day and does not reach +50°C until 48 hours have elapsed (see Figure 9.11). Hence, as previously discussed in Section 8.3.2, and depicted on Figure 8.50, the major impact of an increased peak shaded lunar surface temperature at lunar noon would be to lower the output power level during this period only. This would tend to flatten the leanto array power output profile thus providing a closer match with the Program V load profile and imposing less of a power dissipation problem on the power conditioning system. The flat and oriented-skirted arrays, on the other hand are sized based upon the output power level at lunar noon. For these configurations, a 55°C increase in the peak noon shaded lunar surface temperature could result in an increase in array area requirements. However, even this potential increase could be overcome by use of the power profile shaping techniques described in Section 8.32, (hybrid arrays, mis-orientation).

9.2 CANDIDATE ARRAY CONSIDERATIONS

The parametric data displayed in Figures 9.1 to 9.12 depicts typical power output profiles for the various candidate array configurations. This included the flat, leanto, and oriented-skirted arrays. Both non-insulated and insulated case were shown and performance for single crystal silicon cells and CdS thin films were included. By matching these performance curves to the load profiles for the Program V mission (Figure 4.11), candidate array area and weight can be determined. The techniques for accomplishing this and the various mission alternatives that may be considered, are discussed in detail in Section 4.6.4.

Typical candidate arrays capable of meeting the lunar base requirements are shown in Figures 9.19 and 9.20. The weights listed on Figure 9.19 are for the solar array and support structure only and do not include power conditioning, cabling, or batteries if required. The total LEPEPS weights, together with costs are summarized in Table 4.9 of Section 4.6.4. The lightest solar array capable of meeting the Program V mission requirements was the oriented-skirted configuration (4110 lbs). The flat array was somewhat heavier (4980 lbs) and this

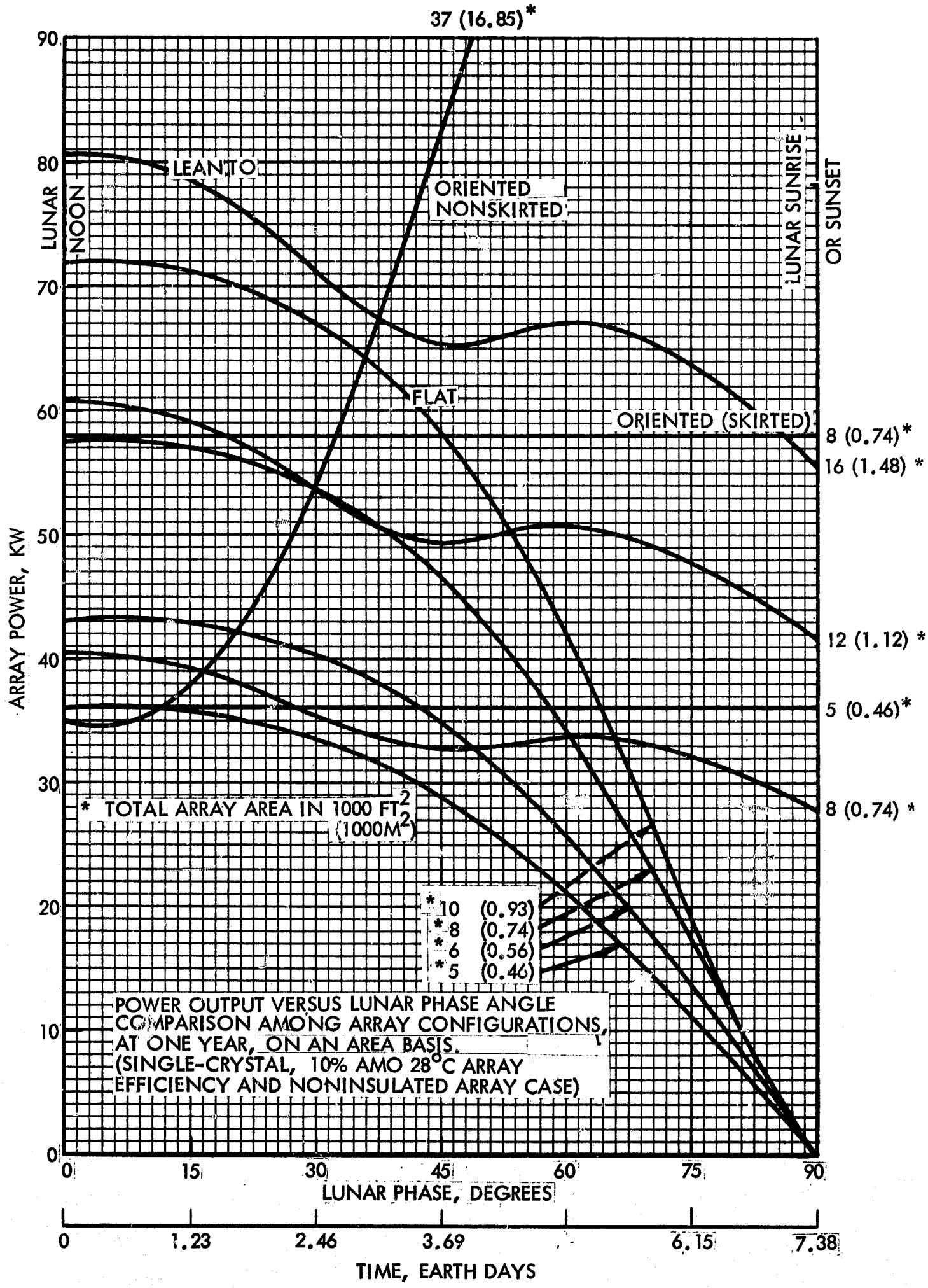

Figure 9.1 Silicon Cell Solar Array Gross Power Output Versus Lunar Phase for Constant Array Area (Non-Insulated)

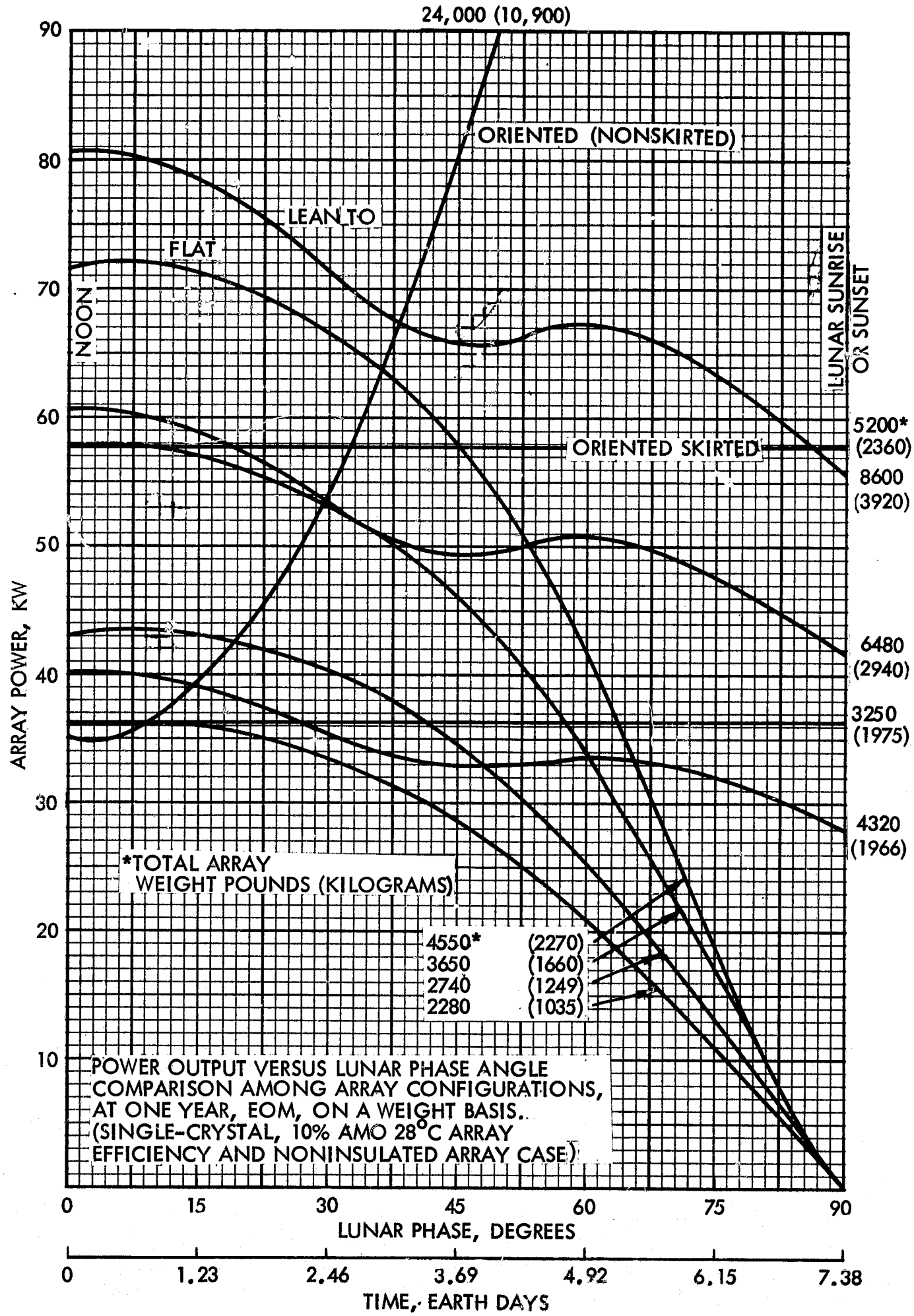

Figure 9.2 Silicon Cell Solar Array Gross Power Output Versus Lunar Phase for Constant Array Weight (Non-Insulated)

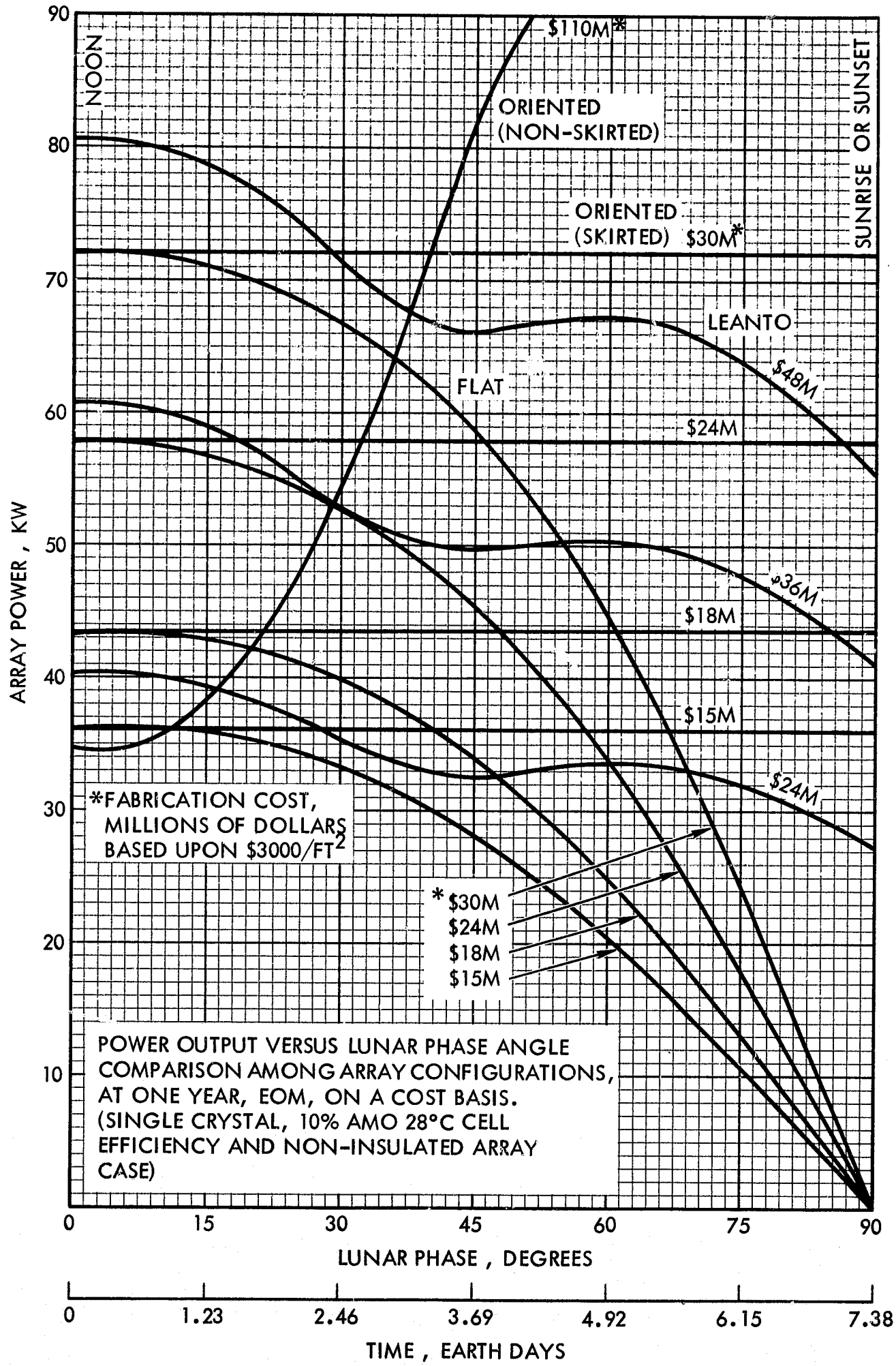

Figure 9.3 Silicon Cell Solar Array Gross Power Output Versus Lunar Phase for Constant Array Cost (Non-Insulated)

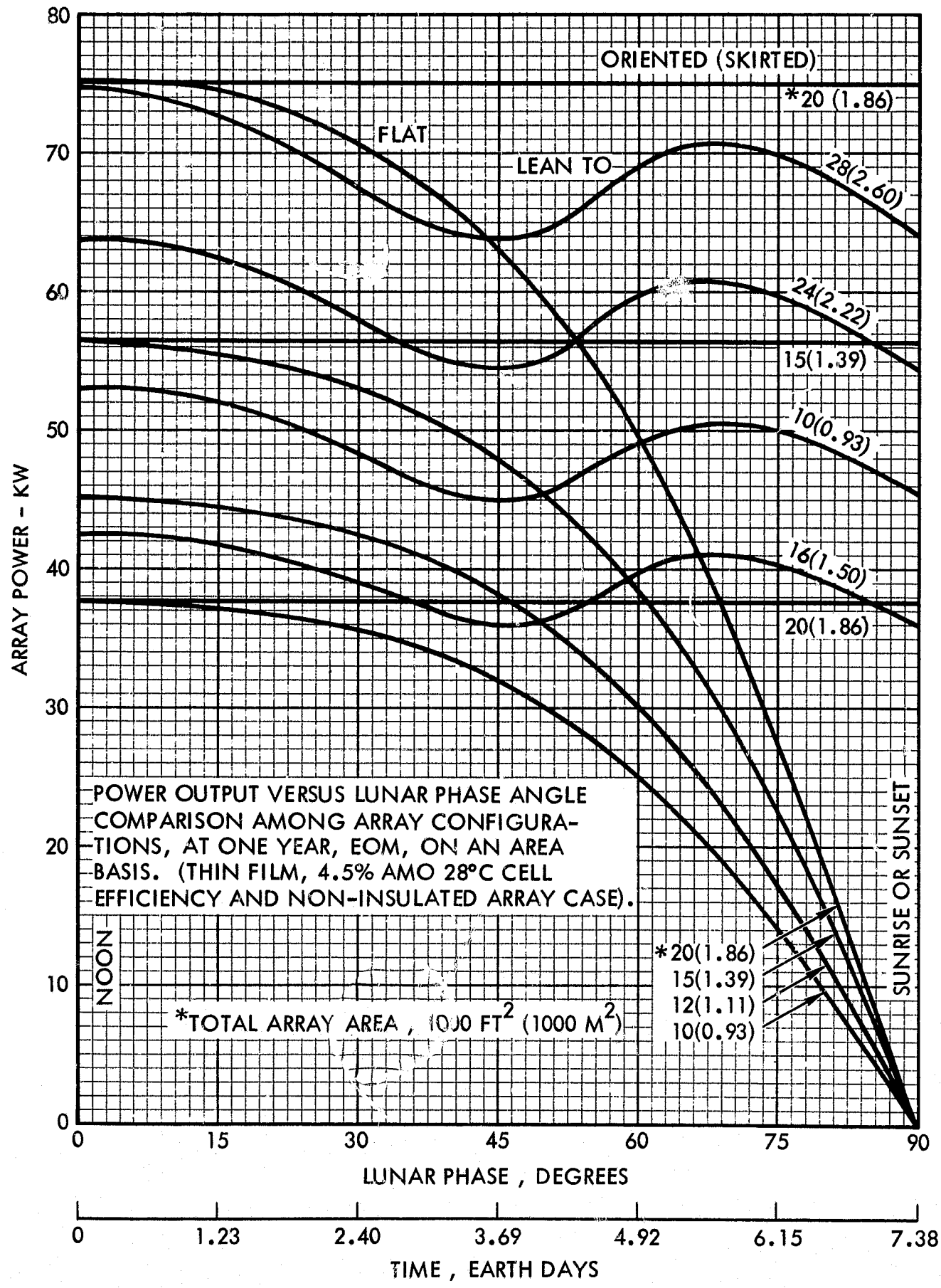

Figure 9.4 CdS Thin Film Solar Array Gross Power Output Versus Lunar Phase for Constant Array Area (Non-Insulated)

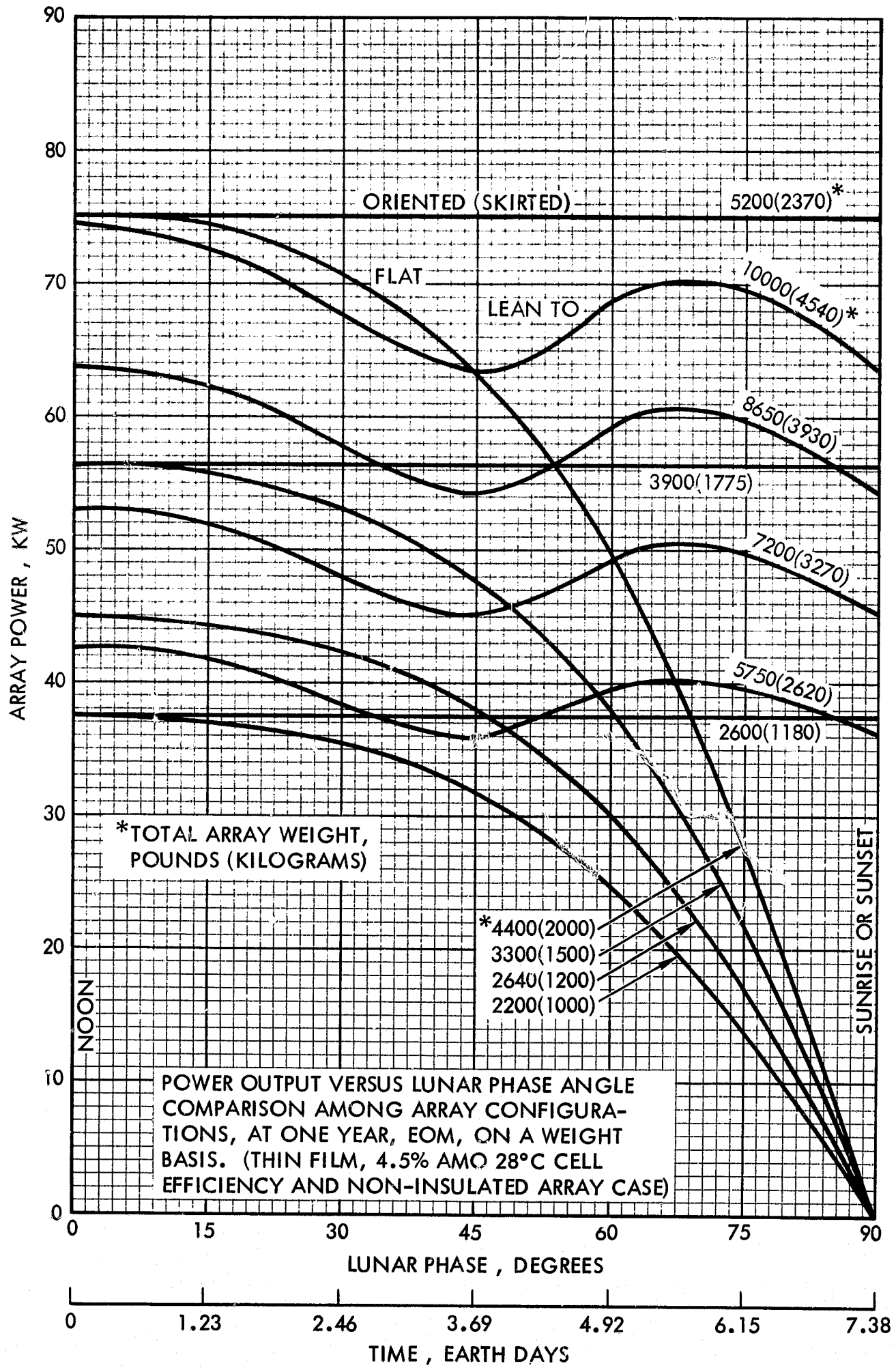

Figure 9.5 CdS Thin Film Solar Array Gross Power Output Versus Lunar Phase for Constant Array Weight (Non-Insulated)

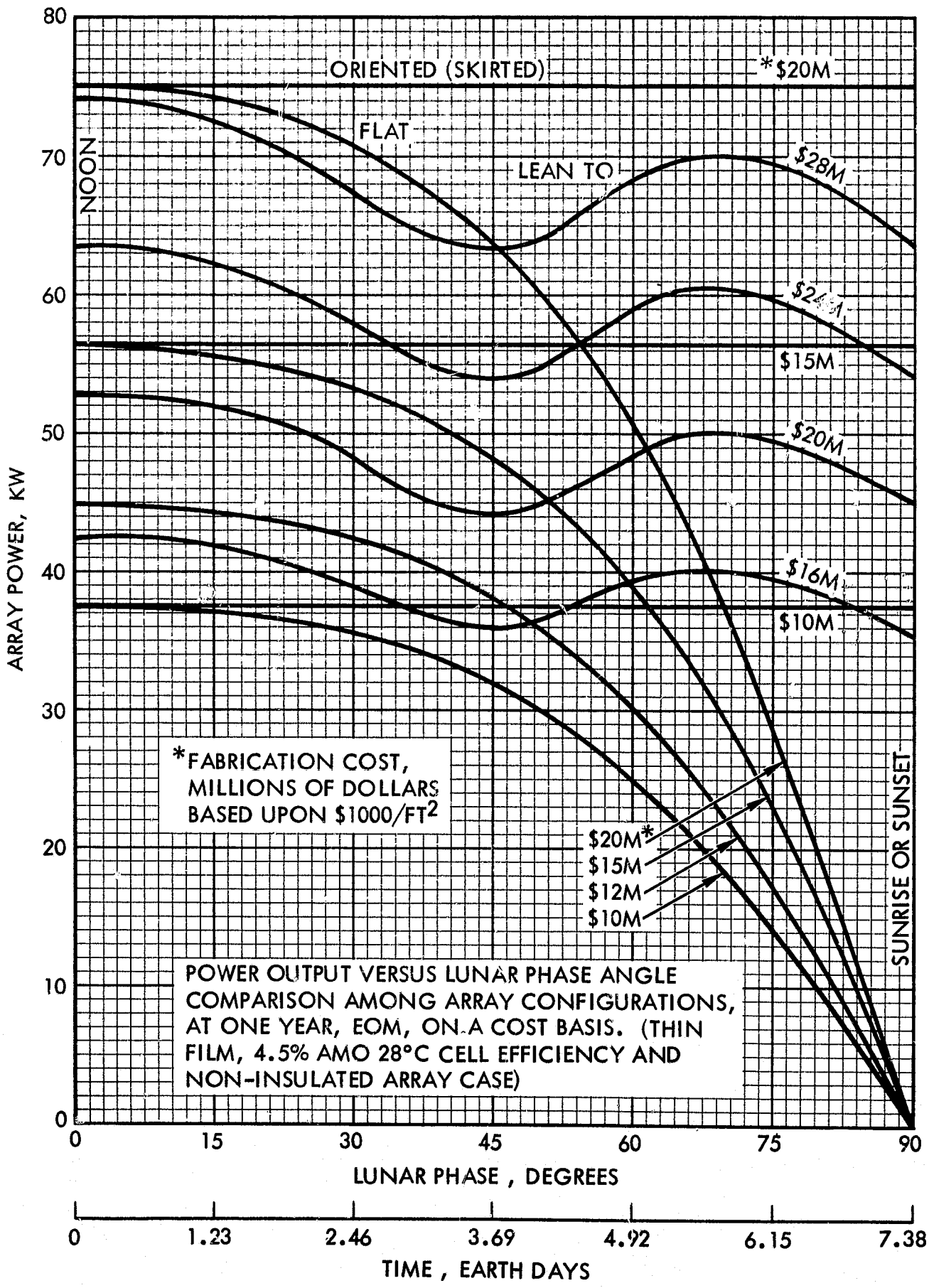

Figure 9.6 CdS Thin Film Solar Array Gross Power Output Versus Lunar Phase for Constant Array Cost (Non-Insulated)

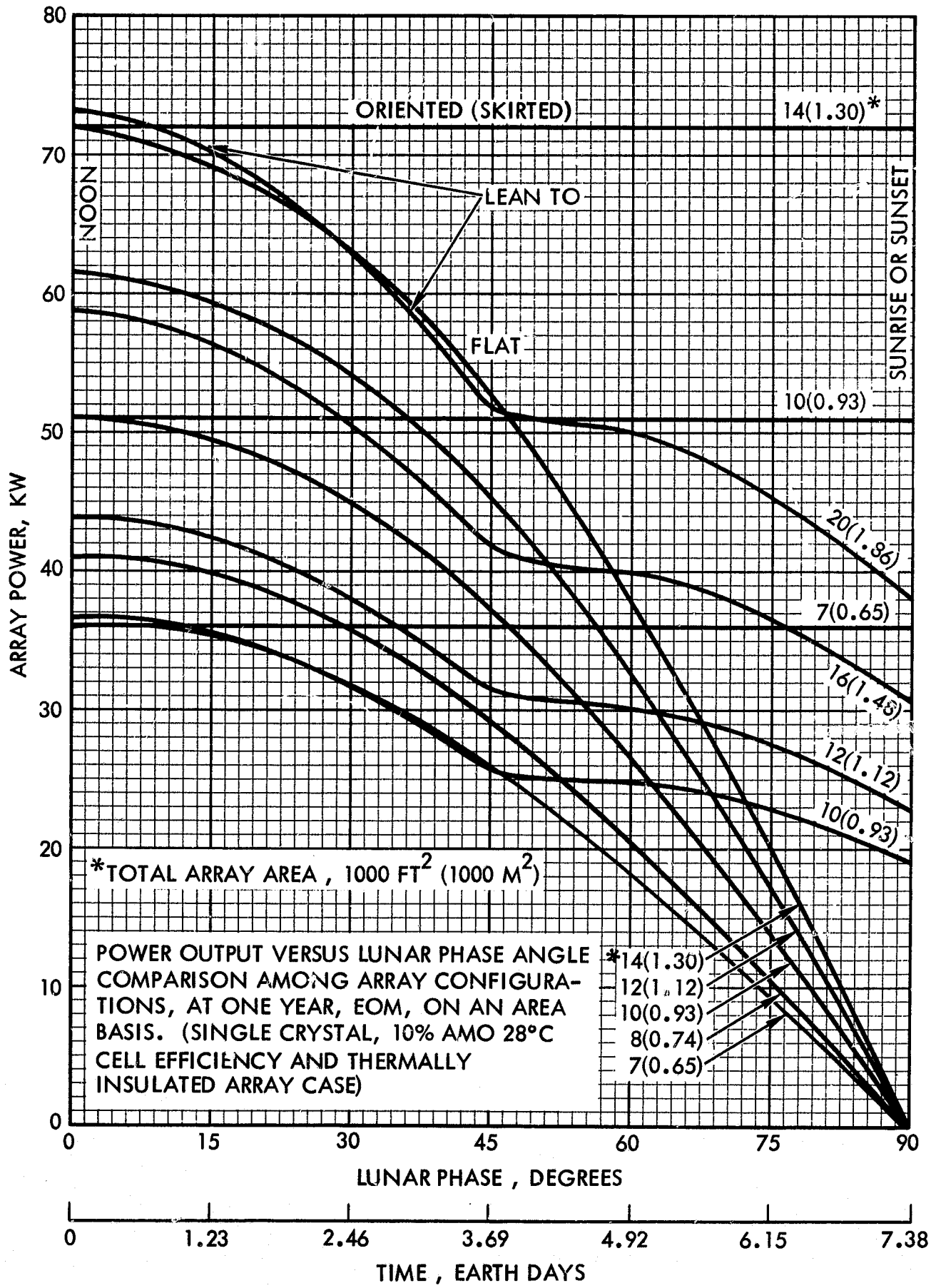

Figure 9.7 Silicon Cell Solar Array Gross Power Output Versus Lunar Phase for Constant Array Area (Insulated)

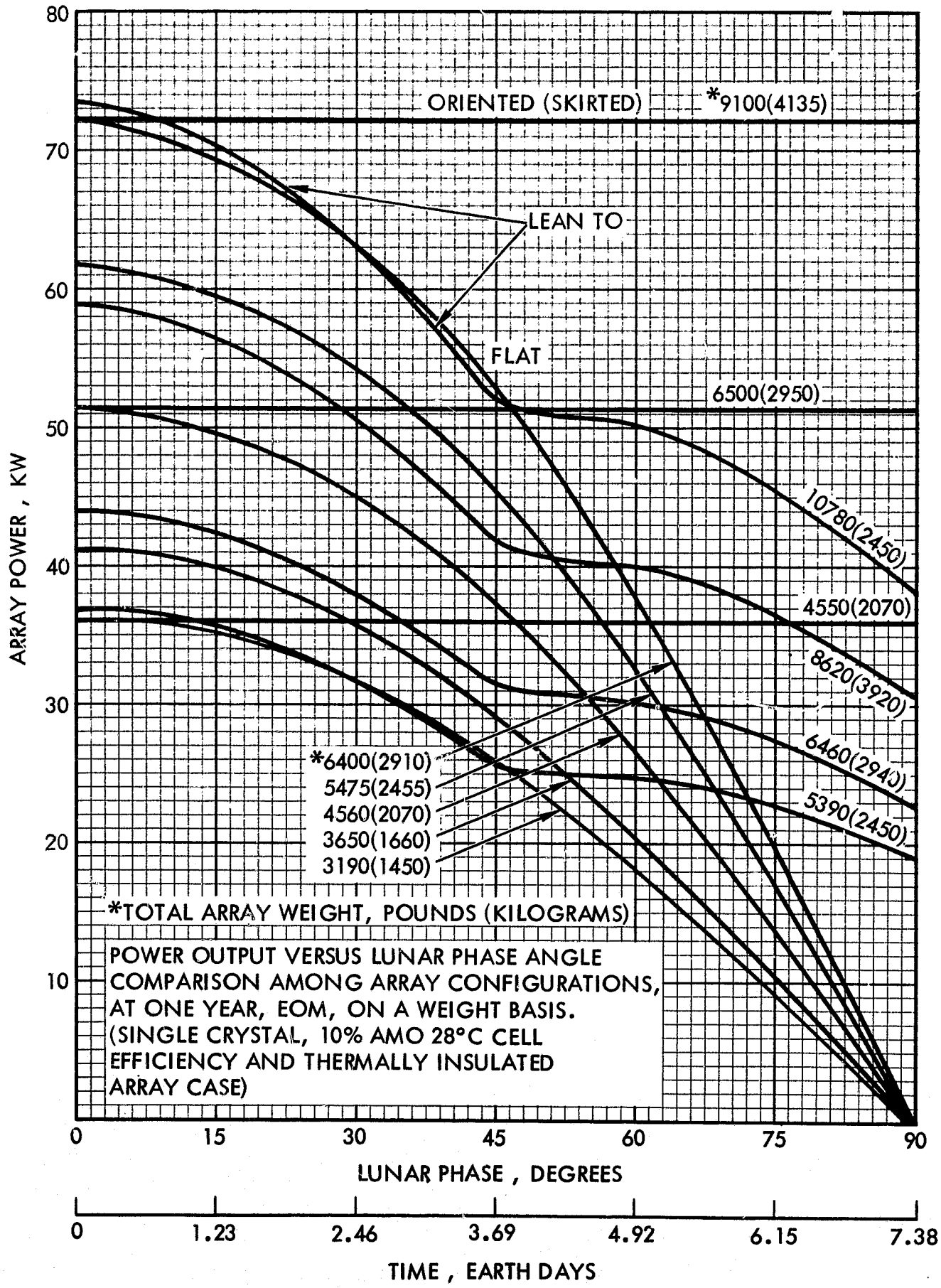

Figure 9.8 Silicon Cell Solar Array Gross Power Output Versus Lunar Phase for Constant Array Weight (Insulated)

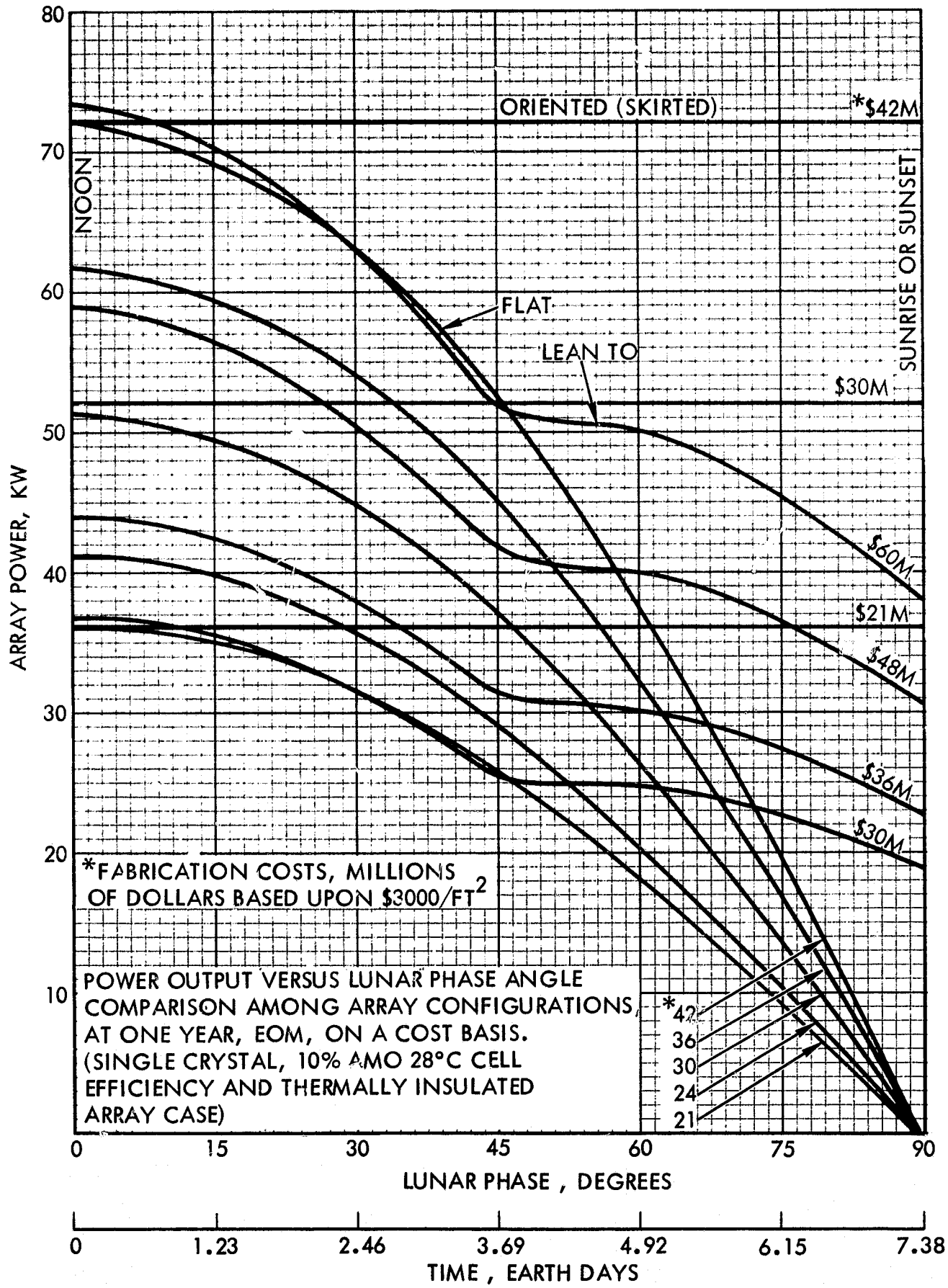

Figure 9.9 Silicon Cell Solar Array Gross Power Output Versus Lunar Phase for Constant Array Cost (Insulated)

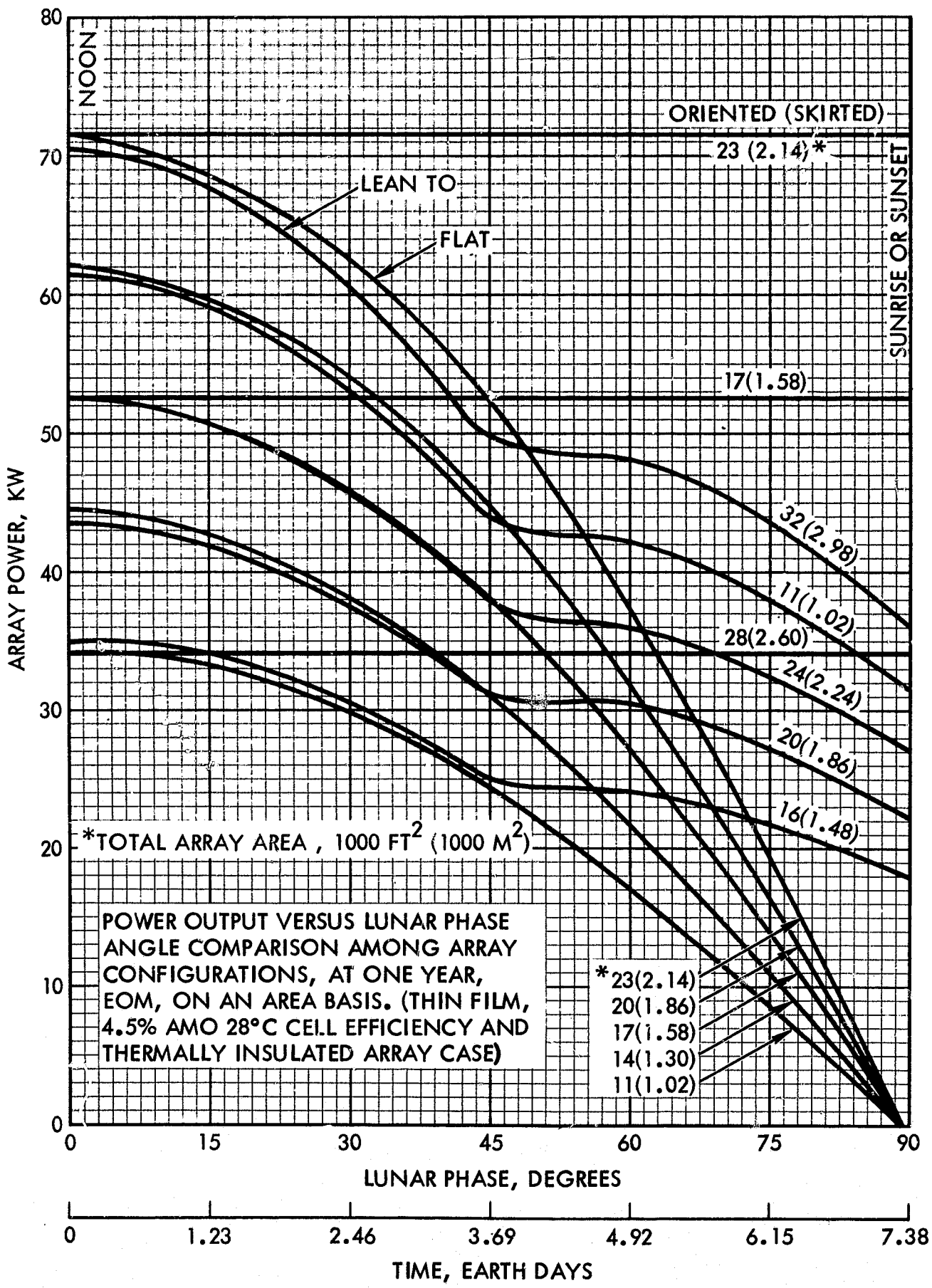

Figure 9.10 CdS Thin Film Solar Array Gross Power Output Versus Lunar Phase for Constant Array Area (Insulated)

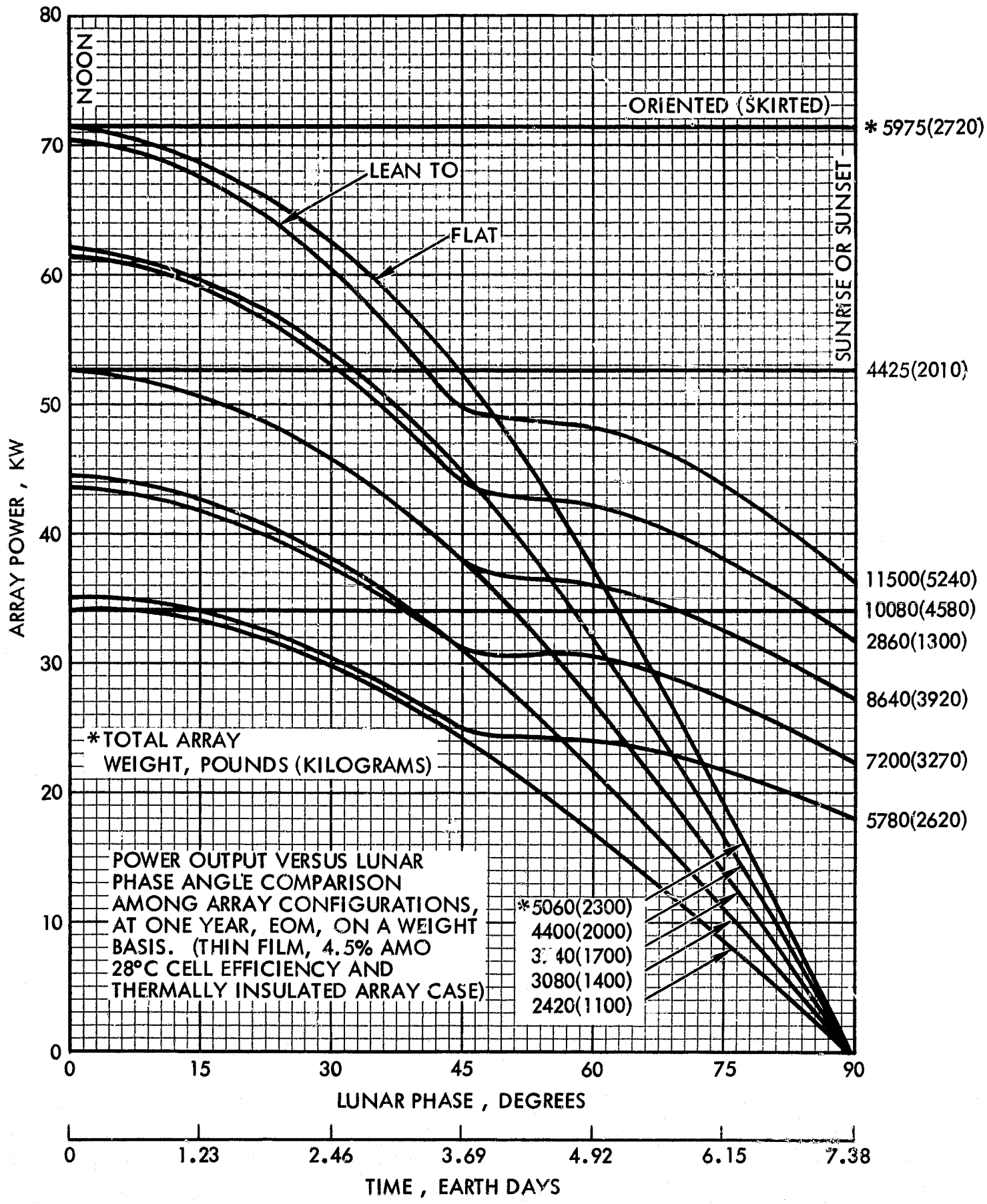

Figure 9.11 CdS Thin Film Solar Array Gross Power Output Versus Lunar Phase for Constant Array Weight (Insulated)

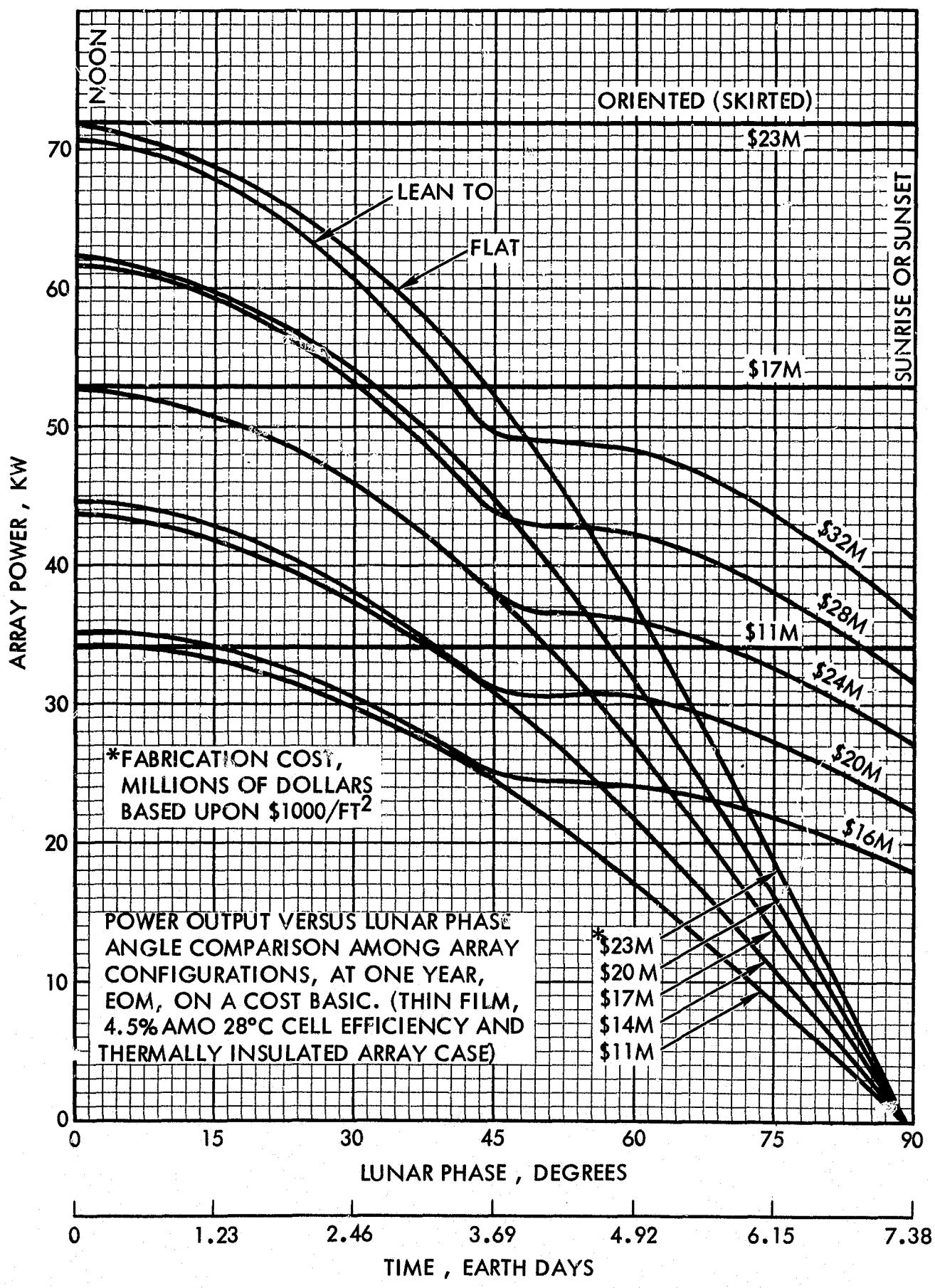

Figure 9.12 CdS Thin Film Solar Array Gross Power Output Versus Lunar Phase for Constant Array Cost (Insulated)

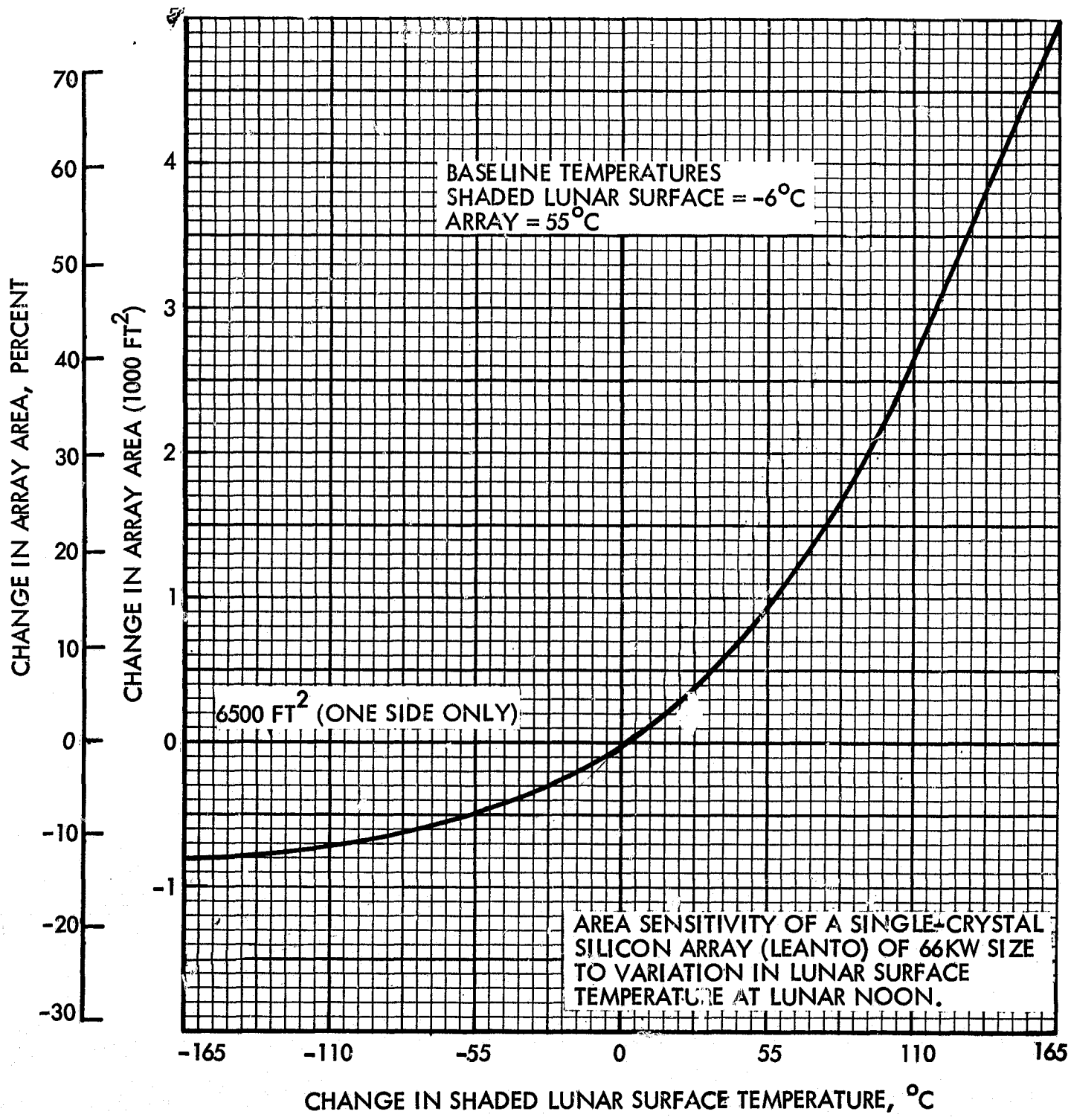

Figure 9.13 Silicon Cell Solar Array (Leanto) Area Sensitivity to Shaded Lunar Surface Temperature

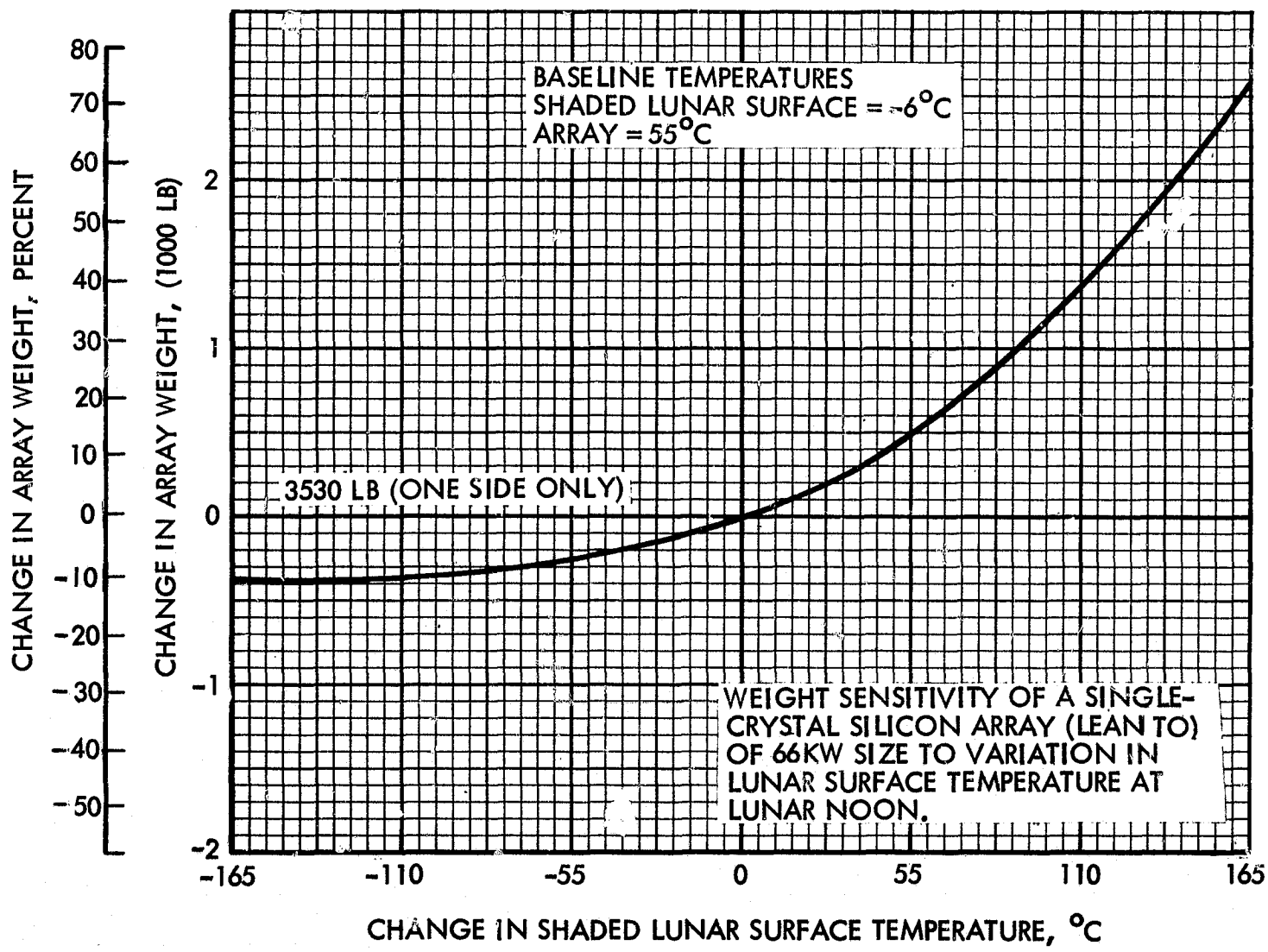

Figure 9.14 Silicon Cell Solar Array (Leanto) Weight Sensitivity to Shaded Lunar Surface Temperature

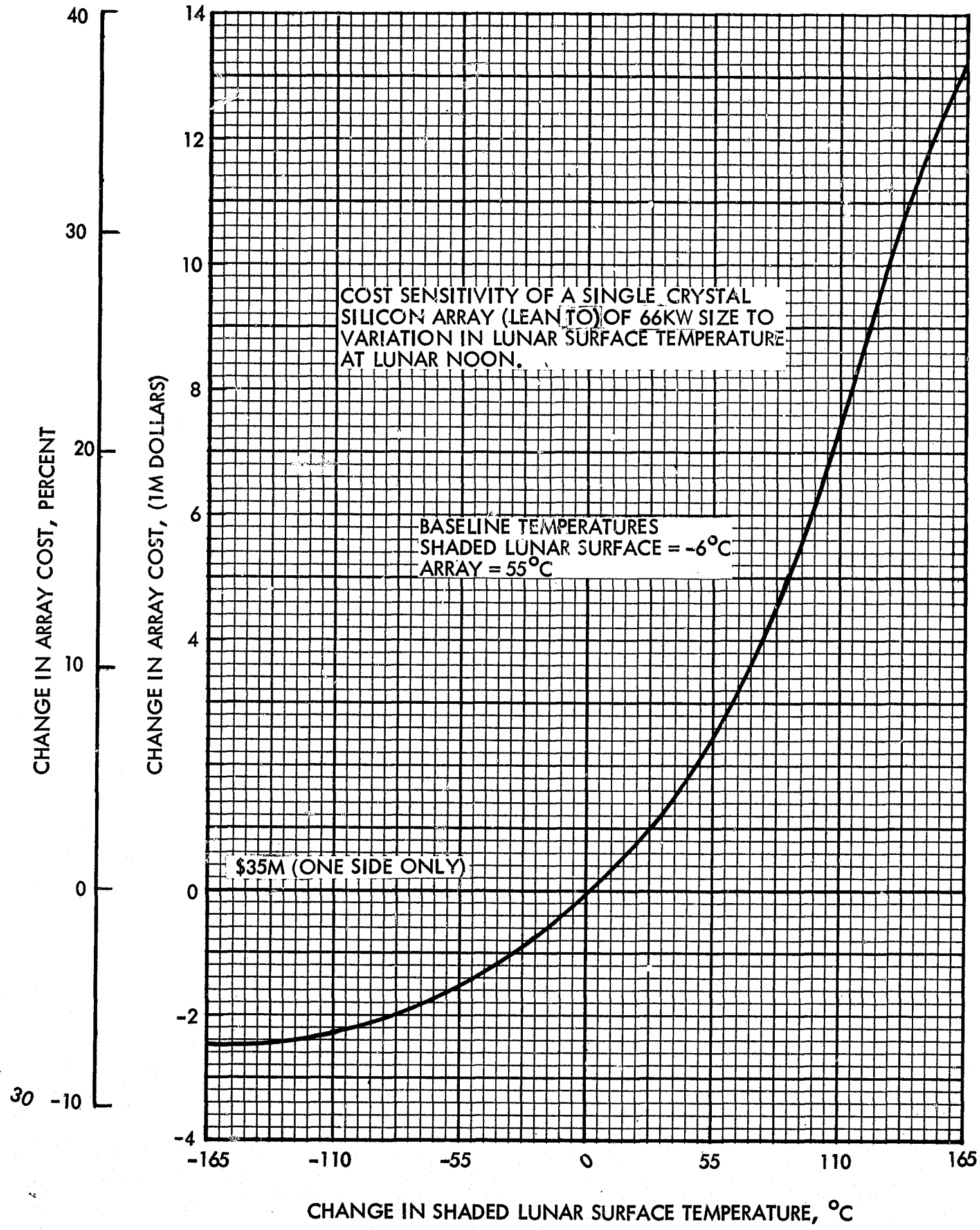

Figure 9.15 Silicon Cell Solar Array (Leanto) Cost Sensitivity to Shaded Lunar Surface Temperature

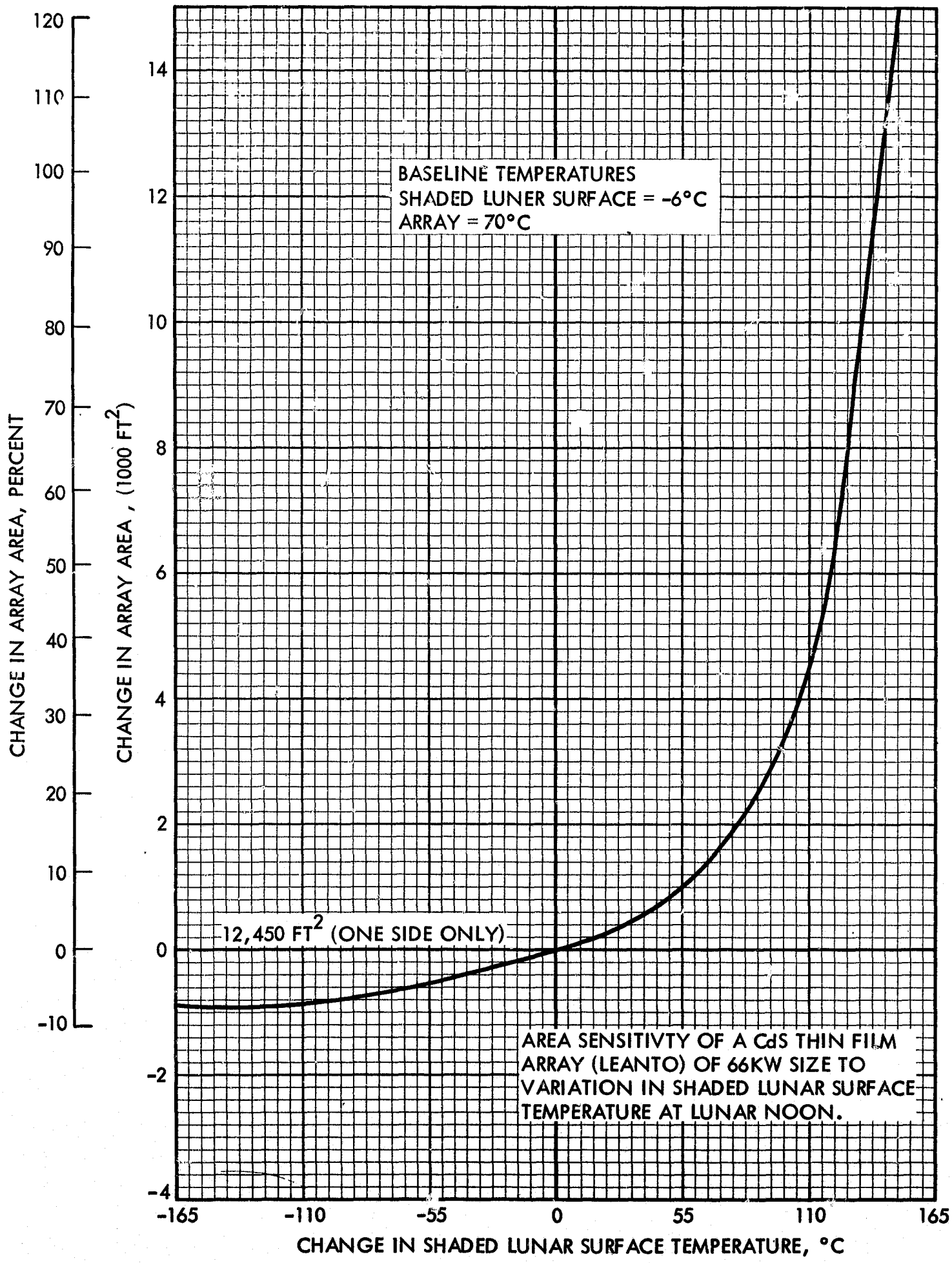

Figure 9.16 CdS Thin Film Solar Array (Leanto) Area Sensitivity to Shaded Lunar Surface Temperature

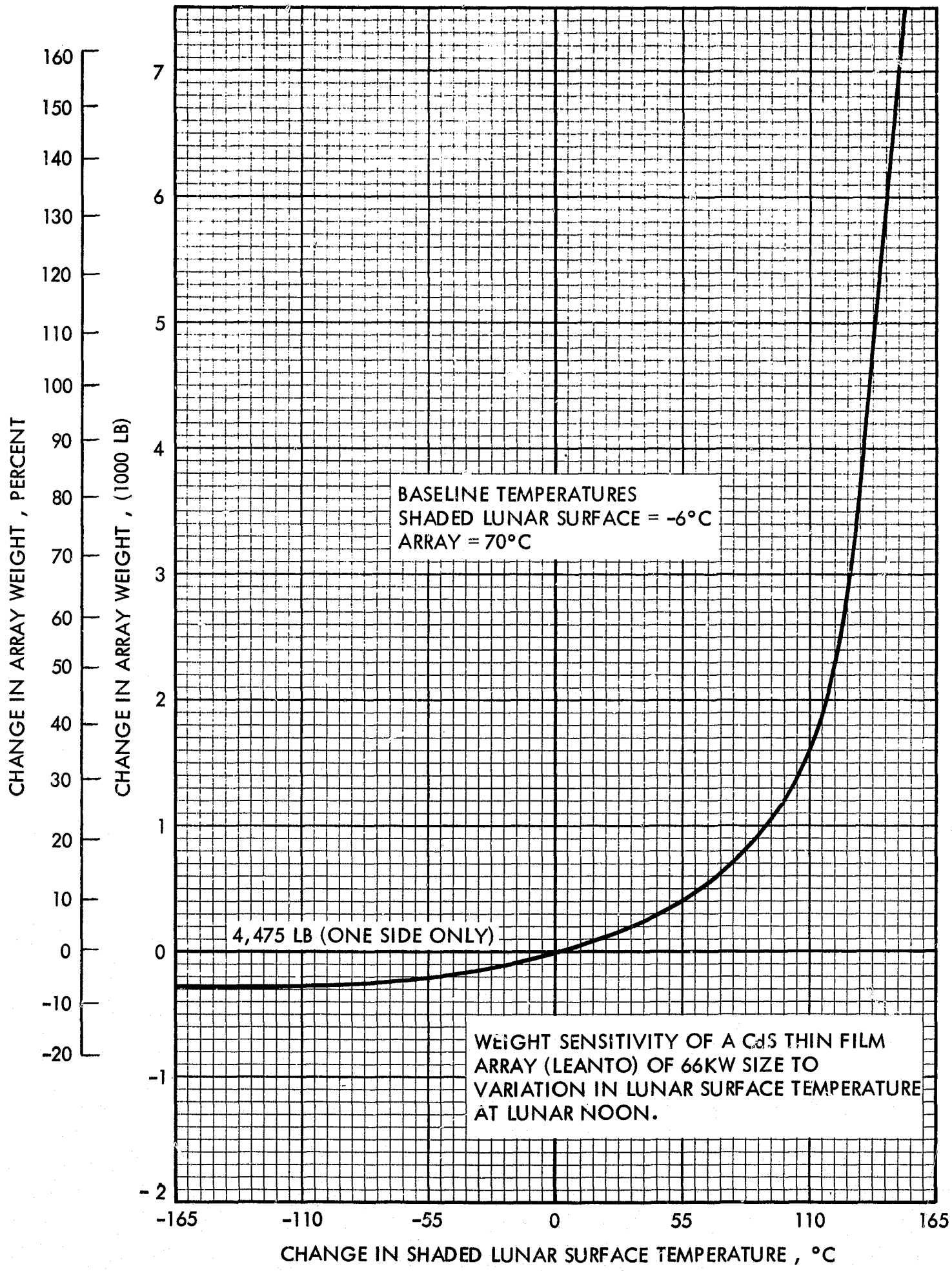

Figure 9.17 CdS Thin Film Solar Array (Leanto) Weight Sensitivity to Shaded Lunar Surface Temperature

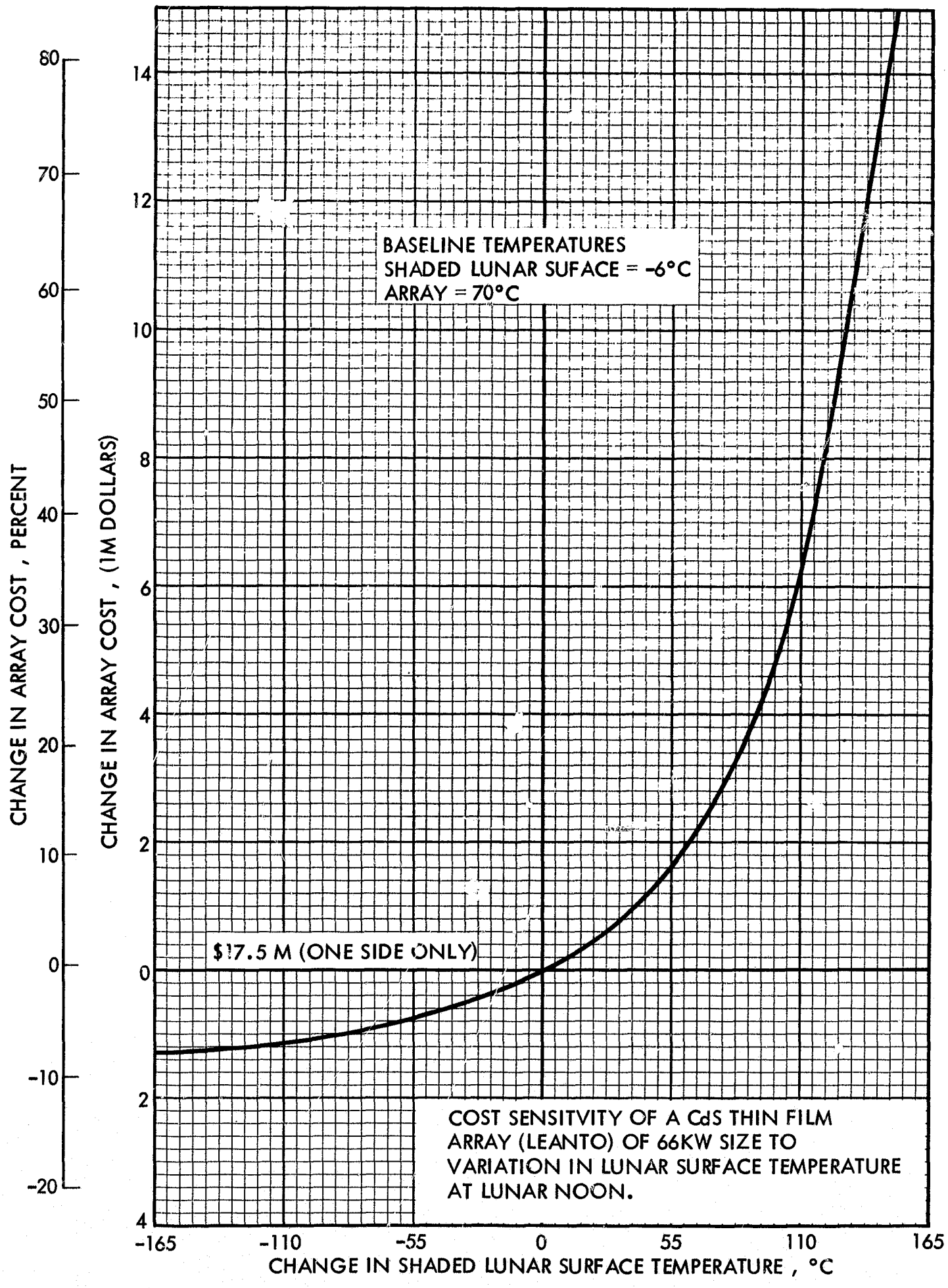

Figure 9.18 CdS Thin Film Solar Array (Leanto) Cost Sensitivity to Shaded Lunar Surface Temperature

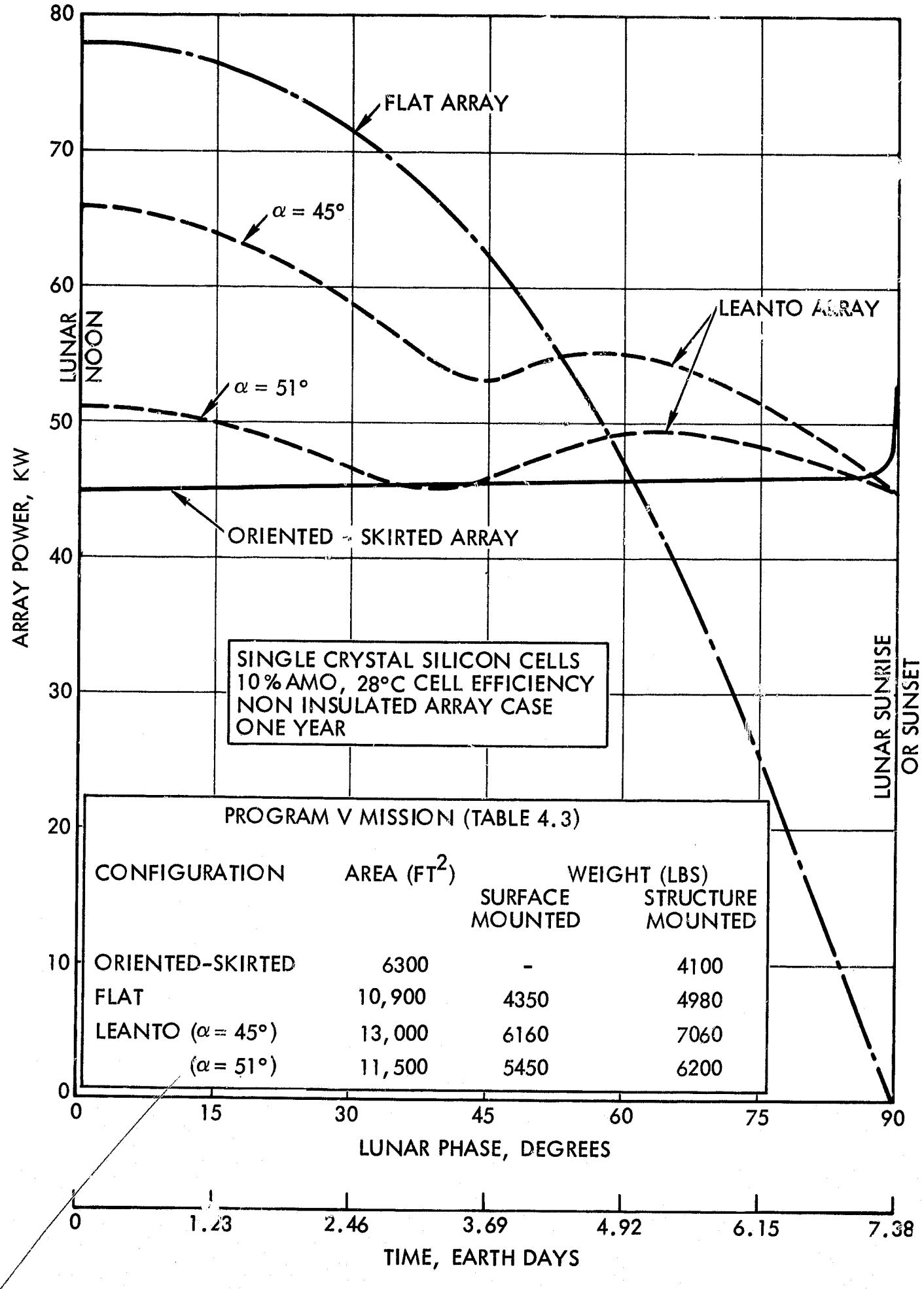

Figure 9.19 Comparison of Candidate Solar Arrays for Program V Mission

LEAN TO ARRAY
ON STRUCTURE OR (ON SURFACE)

$\alpha = 51°$	$\alpha = 45°$
A = 11,500 FT	A = 13,000 FT^2
W_A = 6200 (5450) LB	W_A = 7060 (6160) LB
W_{TOT} = 6650 (5900) LB	W_{TOT} = 7510 (6610) LB

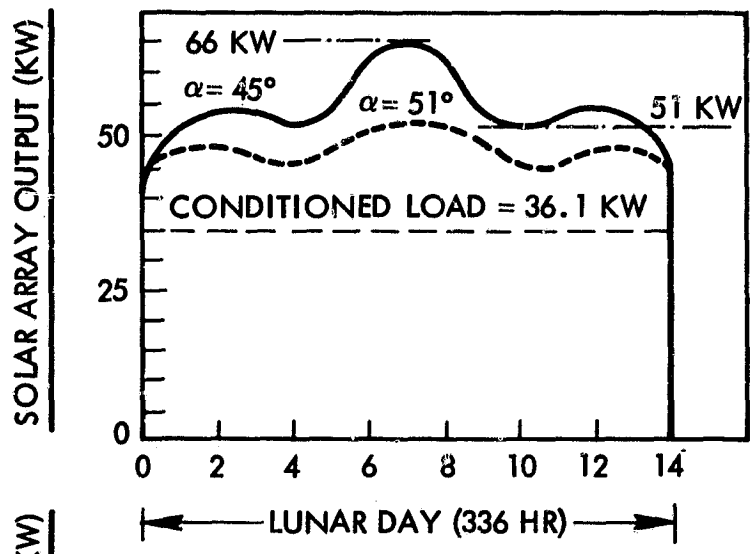

ORIENTED
ARRAY
(SKIRTED)
(ON STRUCTURE)

A = 6300 FT^2
W_A = 4110 LB
W_{TOT} = 4510 LB

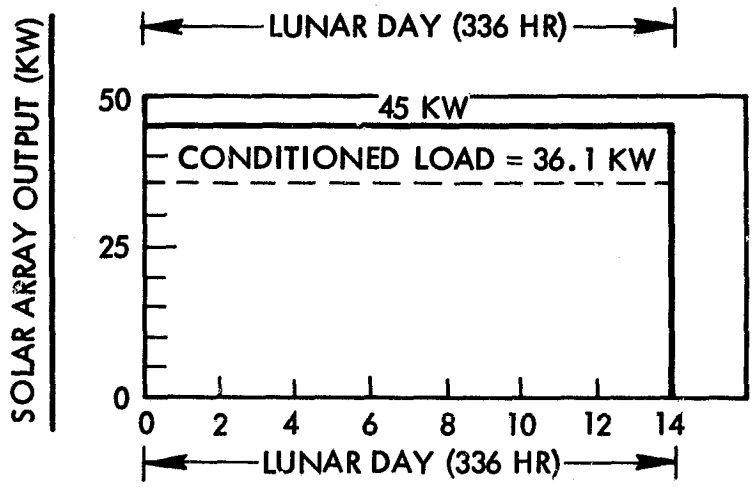

FLAT
ARRAY
(ON STRUCTURE)

A = 10,900 FT^2
W_A = 4980 LB
W_{TOT} = 6180 LB

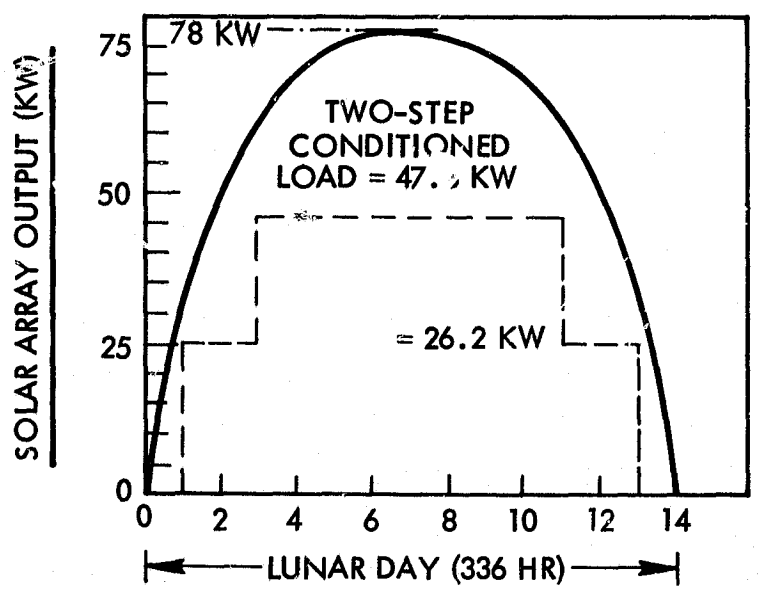

Figure 9.20 Candidate Solar Array Gross Output Power Profiles

weight did not include the required battery weight (600 lbs). The leanto array was the heaviest (5450 lbs for the 51° surface mounted case) but weighed less than the flat array including batteries.

The selection of an optimum candidate array is contingent upon many factors besides minimum weight. Of equal, if not greater importance are such additional criteria as cost, reliability, storage volume, and maintainability. Additional factors include the impact of the array configuration on the ERPS weight and cost, and the overall Program V mission costs. This would involve a highly complex mission analysis and tradeoff study. Some of these factors were discussed in Section 4, but a comprehensive assessment of the Program V mission requirements was beyond the scope of this study. Hence, the candidate array configurations shown in Figure 9.20 represent only a first approximation to arriving at an optimum solution. However, despite these limitations, it appears that if a non-articulated system was desired, a leanto configuration would provide the best choice. On the other hand, if the oriented-skirted configuration costs (non-recurring and recurring), storage volume, reliability, and maintainability can be made competitive with the leanto array, this concept would also have to be given serious consideration.

9.3 TOTAL AVAILABLE ENERGY COMPARISONS

The total available energy of a solar array on the lunar surface is reflected by,

$$E_{tot} = \int_{o}^{\pi} P_{o}\, dt \qquad (9.1)$$

This equation represents the area under the array performance curves depicted on Figures 9.1 to 9.12. This available energy is totally usable only in those unique cases where the power output profile and the load profile are identical. However, for mission planning purposes, it is quite often desirable to be able to estimate solar array area, weight, and cost as a function of total mission energy requirements. The parametric data on Figures 9.21 to 9.24 was prepared for this purpose. The data on Figure 9.21 for non-insulated, single crystal silicon cells also indicates that for a given total mission energy requirement, the oriented-skirted

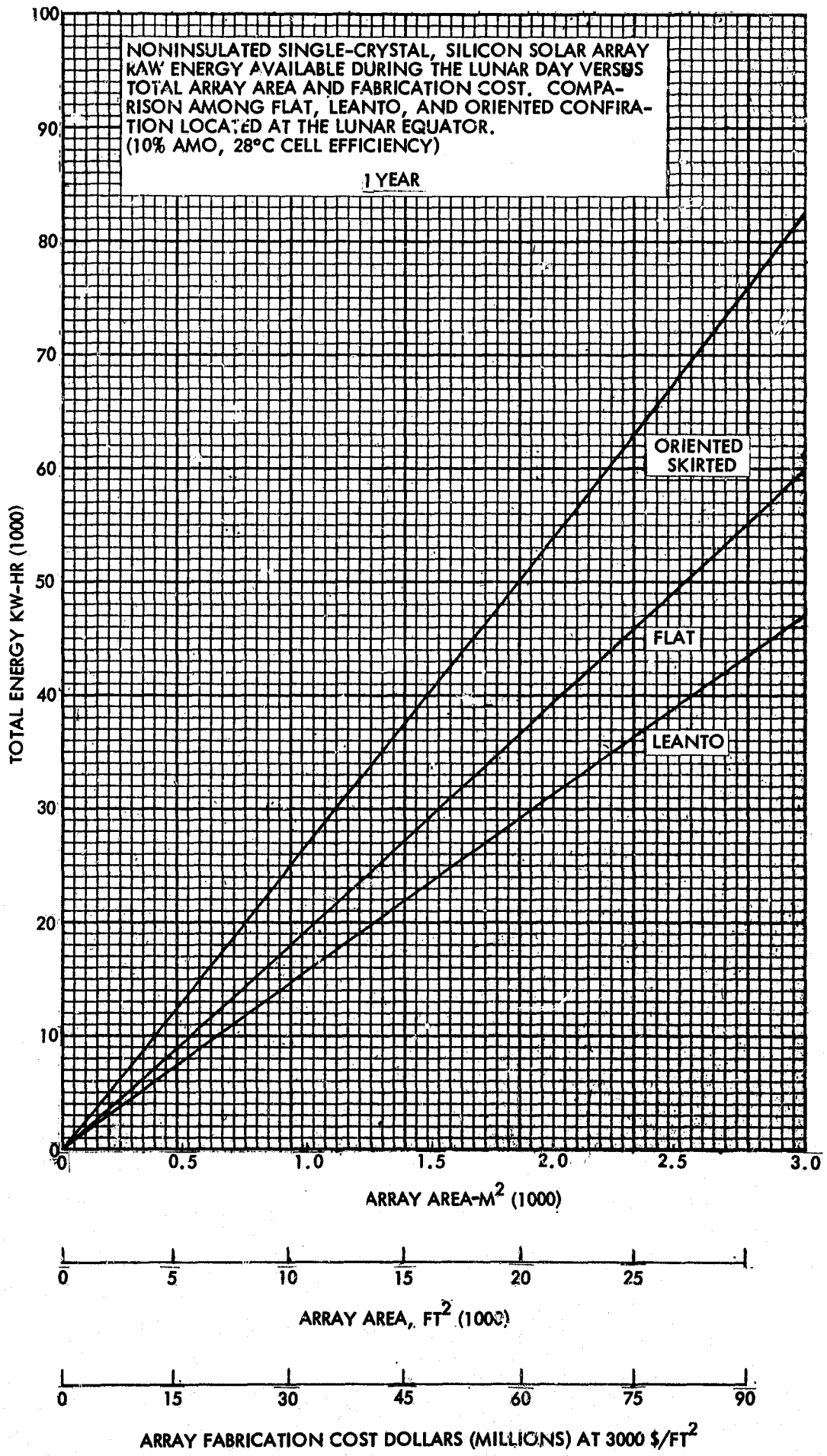

Figure 9.21 Total Silicon Cell Solar Array Energy Output Versus Array Area and Fabrication Cost

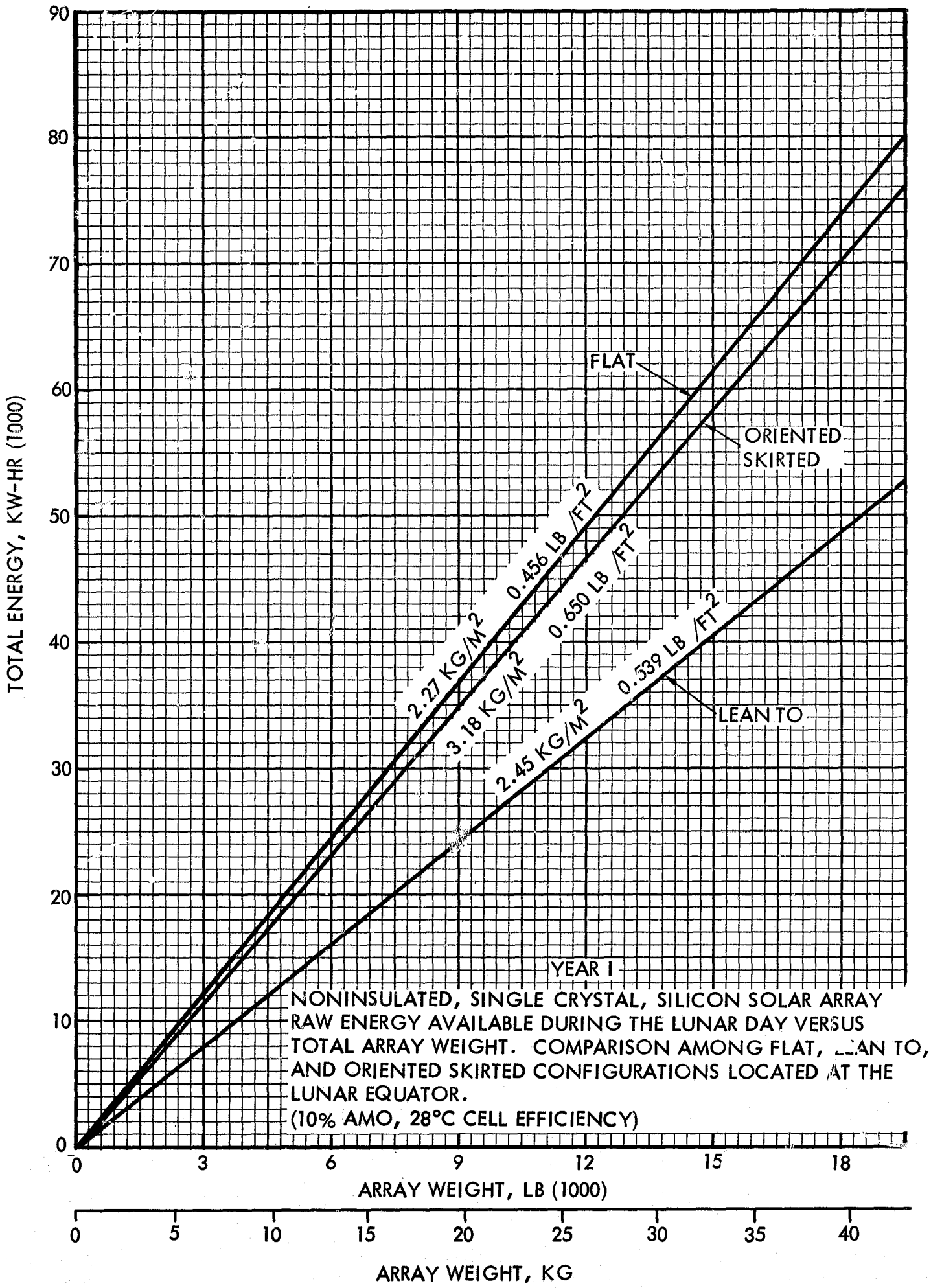

Figure 9.22 Total Silicon Cell Solar Array Energy Output Versus Array Weight

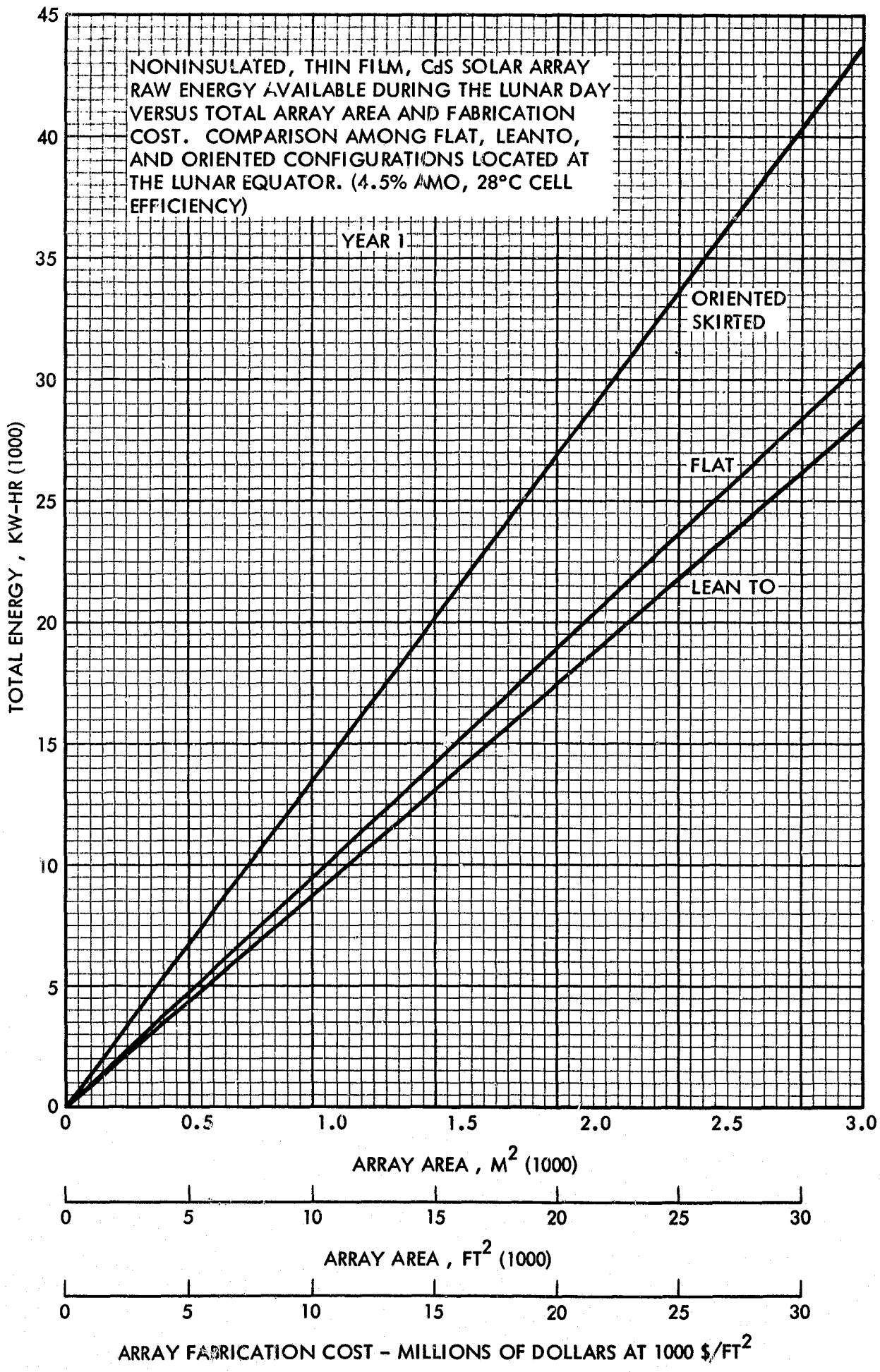

Figure 9.23 Total CdS Thin Film Solar Array Energy Output Versus Array Area and Fabrication Cost

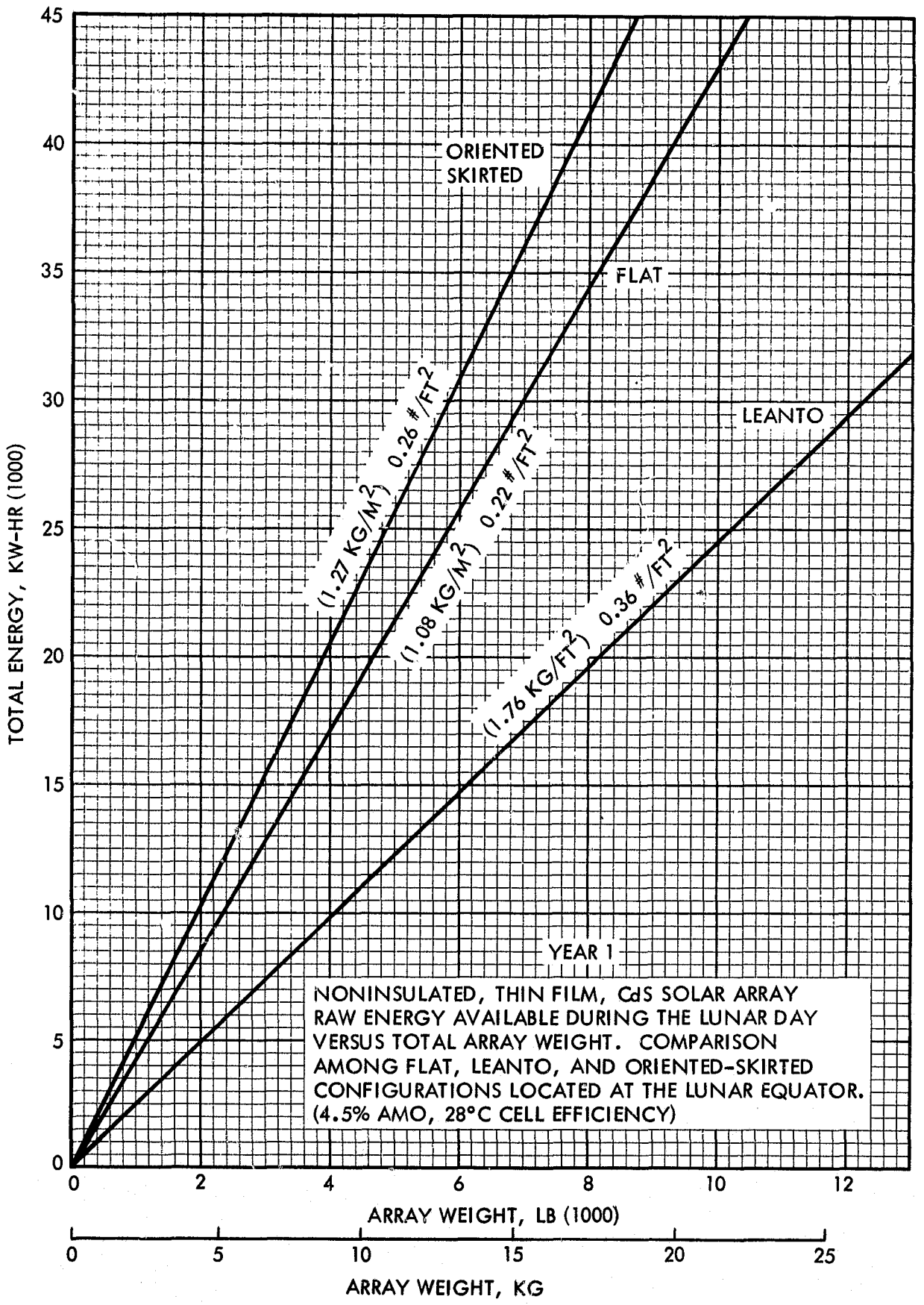

Figure 9.24 Total CdS Thin Film Solar Array Energy Output Versus Array Weight

array would require the least area. At an assumed constant unit cost (i.e., $3000/ft^2), it would also be the least costly. However, the costs associated with the development of automatic array orientation mechanisms or the operational costs associated with manual orientation would undoubtably negate this advantage. The flat array would be somewhat lighter than the oriented-skirted configuration (see Figure 9.22), but the weight saving would not be significant (less than 5%). Similar data is presented in Figures 9.23 and 9.24 for CdS thin film arrays. Finally, a comparison was made for a total energy output of 15, 500 kw-hrs which corresponds to the total unconditioned output energy required by the Program V mission for one lunar day (45 kw_e x 336 hrs = 15, 500 kw-hrs). The results are shown on Figure 9.25 for all three candidate configurations (flat, leanto, oriented-skirted).

An additional factor which could effect the total available energy from a solar array mounted on the lunar surface would be the surrounding terrain. For example, large boulders in the vicinity of the lunar base could appreciably reduce the available sunlight time. If the lunar base were located at the bottom of a large crater, the distance from and height of the crater lip above the lunar base could also effect the available sunlight time. The data presented in Figure 9.26 indicates the potential reduction in sunlight time as a function of obstacle height and distance. The impact of these shadowing effects should be taken into account by the solar array designer and mission planner during the implementation phase of any lunar surface exploration program.

9.4 RELIABILITY CONSIDERATIONS

The nominal size of the modular solar array which would be used to make up the larger candidate solar arrays for the Program V mission, was selected as 2.5 kw. The reasons for selecting this module size are discussed in Section 4.7. During this study, the relative reliability values for a 2.5 kw power level solar array, whose output voltage ranges from 50 to 1000 volts have been considered for both single crystal silicon and cadmium sulfide thin film celled arrays. The effect on array reliability of circuits with and without shunt diodes was also included. Array reliability predictions were based upon calculations using existing TRW Systems Group solar array reliability computer programs.

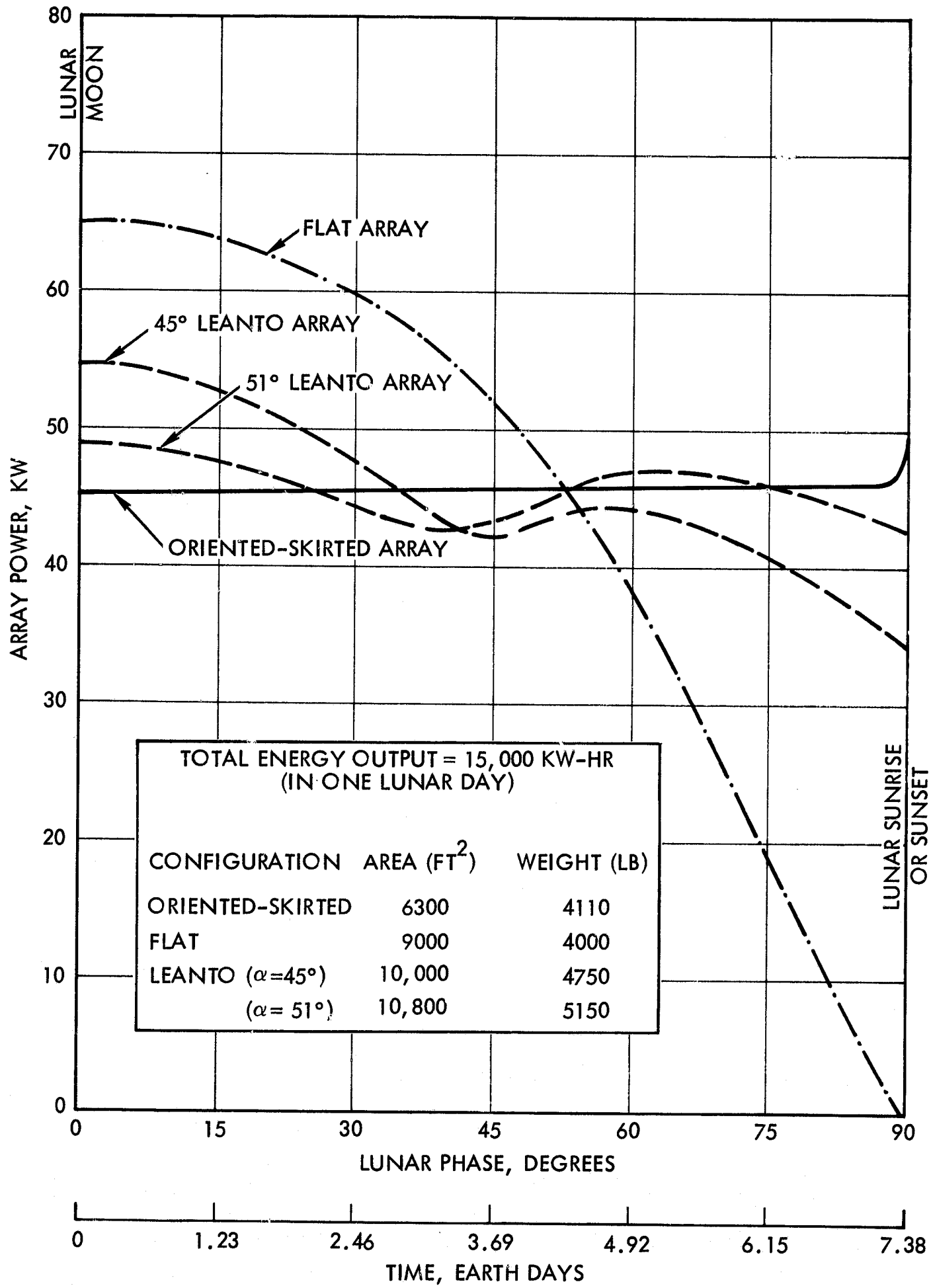

Figure 9.25 Comparison of Silicon Cell Solar Array Configurations for Constant Total Energy Output

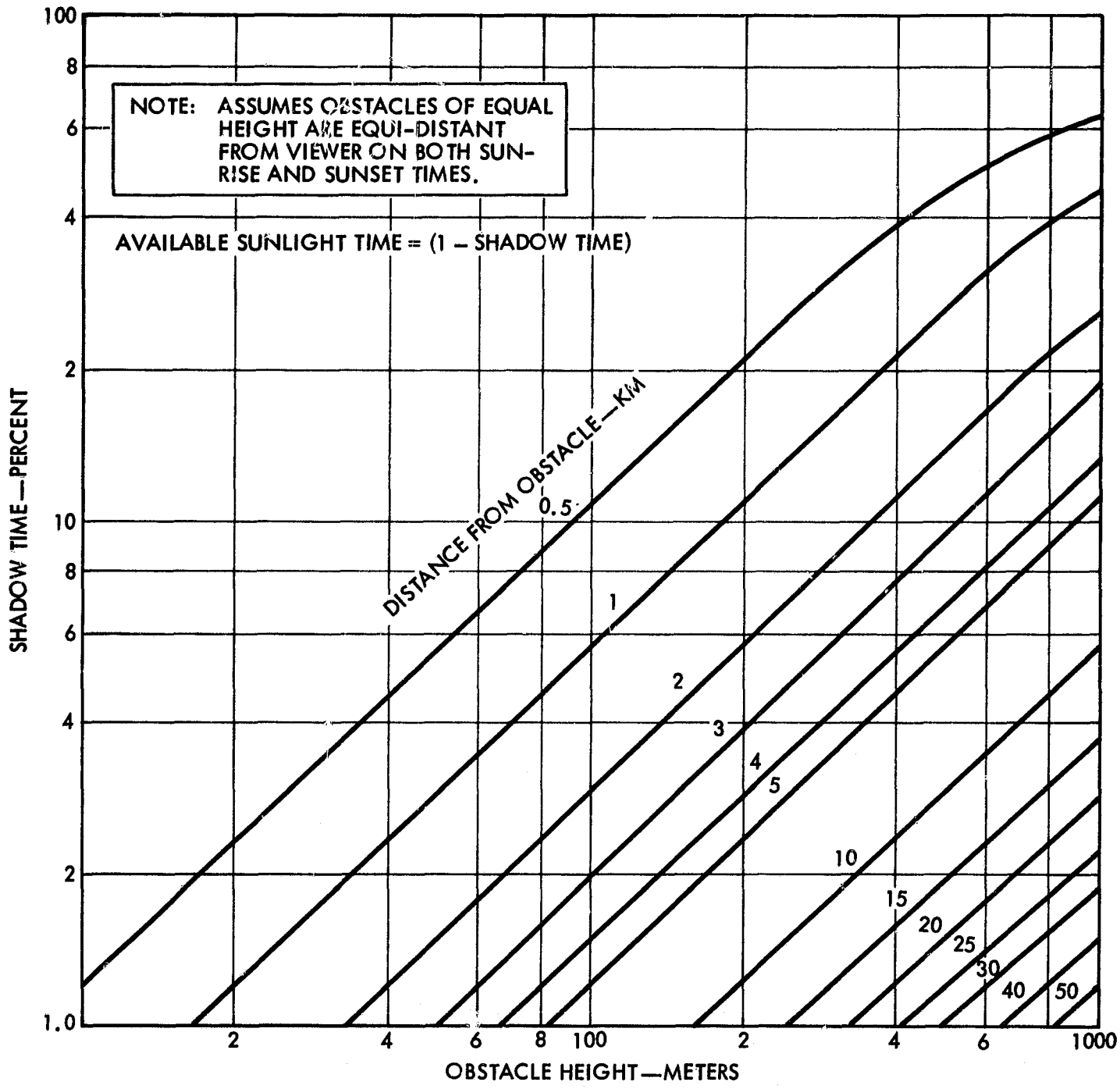

Figure 9.26 Shadow Time Versus Obstacle Height on Lunar Surface

Three array interconnection configurations were considered and are shown in Figure 9.27. The interconnection configurations are designated NP, for no parallel redundant interconnections; P, because of the use of redundant parallel interconnections with no shunt diodes; and PS, because of the addition of shunt diodes to configuration P. This analysis specifically assumed that the interconnections could be schematically represented as shown in Figure 9.27. The encircled connections are redundant, and thus, if any one opens (such that the cross-wire is disconnected but not the series wire), then no change in panel output occurs. Hence, the failure of the encircled interconnections was neglected in this analysis.

Configuration (NP) is known to have the lowest reliability value of the three cases and was eliminated from the analysis.

For configuration (P), it is a characteristic of the string that the power loss depends approximately on the largest number of failed cells in any one lattice. Figure 9.28 is a typical non-dimensionalized I-V curve for configuration (P), degraded by string (X), lattice (Y), and cell (Z), failures respectively. It can be seen that the event with the highest probability of occurrence is for 2 cells to fail in the Group 1 category (curve 1;1).

Examples of various possible I-V curves for Configuration (P) are shown in Figure 9.28. They consist of groups of curves corresponding to the following cases:

Group 0

No failure (curve 0)

Group 1

These correspond to a case with at least one parallel group of cells having one open-circuited cell and no other failures in the panel. They have been subdivided into eleven different curves because of the high probability of occurrence of this group. Only eleven curves need be considered because these are the only ones which each have a probability of occurrence equal to 0.00005 or greater. These eleven curves correspond to cases from exactly one parallel group of cells with one open-circuited cell (curve 1; 1), to exactly eleven parallel groups of cells with one open-circuited cell in each group (curve 1; 11).

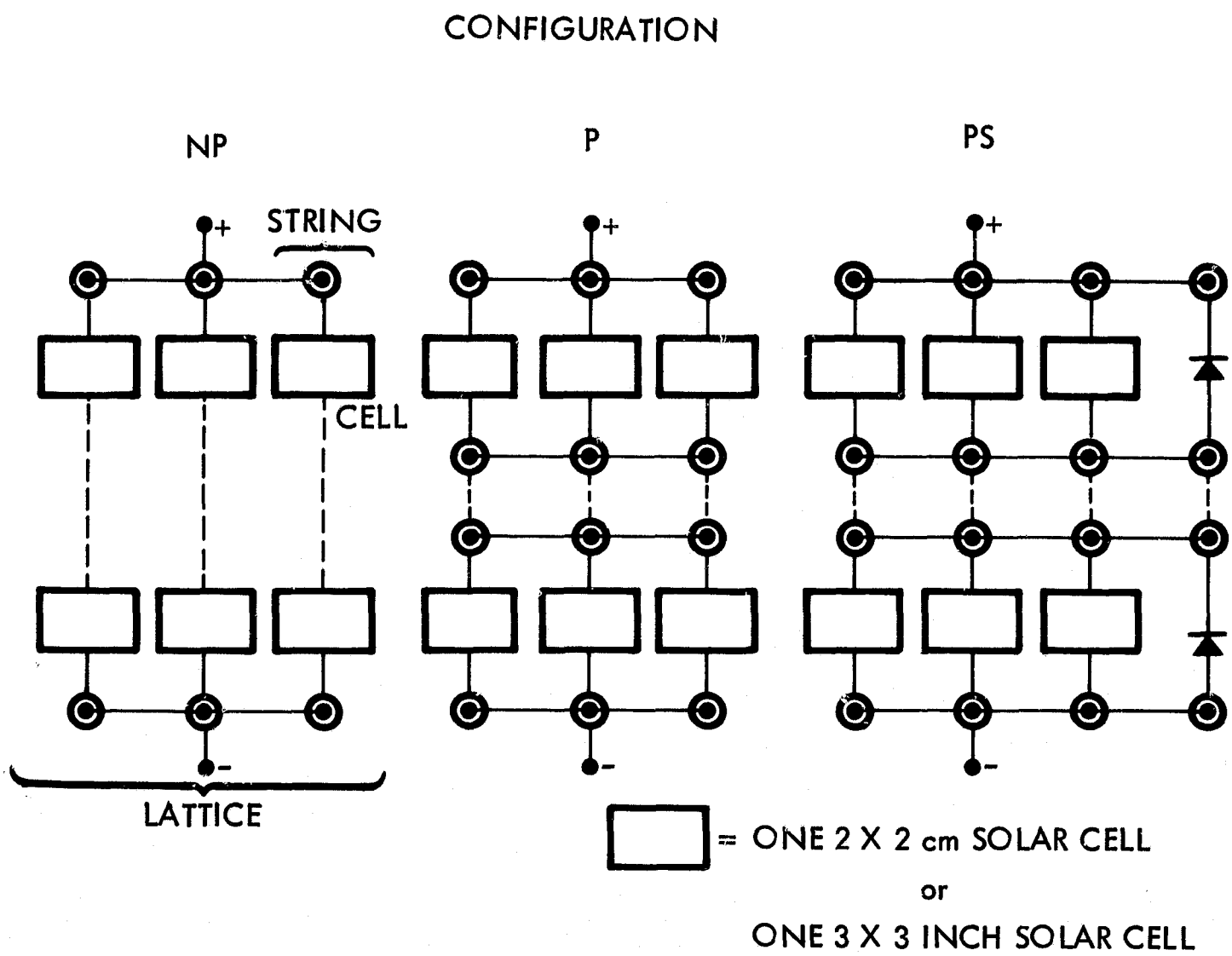

Figure 9.27 Various Alternative High Voltage Solar Panel Configurations

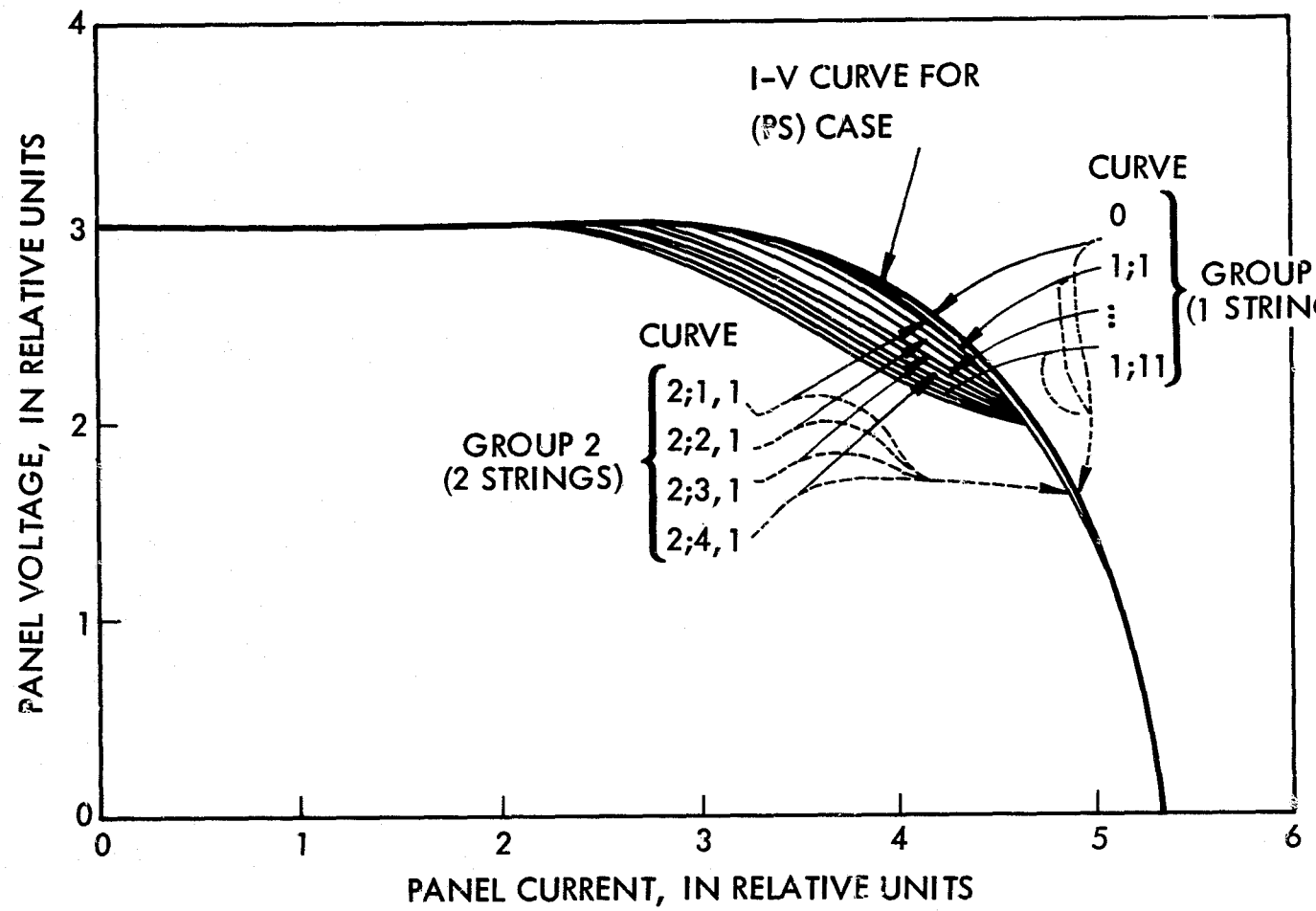

CURVE	PROBABILITY OF OCCURRENCE SYMBOL	VALUE	SUM
0	P_0	0.0607	0.0607
1;1	$P_{1;1}$	0.1702	
1;2	$P_{1;2}$	0.2382	
1;3	$P_{1;3}$	0.2225	
1;4	$P_{1;4}$	0.1557	
1;5	$P_{1;5}$	0.0872	
1;6	$P_{1;6}$	0.0407	0.9389
1;7	$P_{1;7}$	0.0163	
1;8	$P_{1;8}$	0.0057	
1;9	$P_{1;9}$	0.0018	
1;10	$P_{1;10}$	0.0005	
1;11	$P_{1;11}$	0.0001	
2;1,1	$P_{2;1,1}$	0.0001	
2;2,1	$P_{2;2,1}$	0.0001	
2;3,1	$P_{2;3,1}$	0.0001	0.0004
2;4,1	$P_{2;4,1}$	0.0001	
3	P_3	0.0000	
			1.0000

Figure 9.28 Typical Current-Voltage Curves and their Probability of Occurrence for Configuration "P" (without shunt diodes) and for Various Numbers of Open-circuited Cells per Array

Group 2

These correspond to a case with at least one parallel group of cells having two open-circuited cells and the remaining groups with less than two open cells. They have been subdivided into only four different curves because analysis indicated that only these groups had individual probabilities of occurrence of 0.00005 or greater. These curves correspond to four cases which each have exactly one parallel group of cells with two open-circuited cells, and which individually have from exactly one parallel group with one open-circuited cell (curve 2; 1, 1) to exactly four parallel groups with one open-circuited cell each (curve 2; 4, 1).

The panel I-V curves shown in Figure 9.28 provide favorable results (i.e., not much potential output power is lost) because of the assumption that solar cells in parallel with open-circuited cells will conduct heavily after an avalanche breakdown voltage of about 35 volts has been exceeded. If this breakdown voltage is actually lower, correspondingly less loss of panel output power will occur. Loss of panel voltage at currents less than 2 relative units for Group 1 and 1 relative unit for Group 2 are considered negligible for large numbers of cells per array.

The estimated probabilities of occurrence of the curves shown for configuration (P) are also tabulated in Figure 9.28. If the load line is a constant voltage at 4 relative voltage units, and if the definition of failure is that failure has occurred if output current falls below 2.5 relative current units, then the reliability of configuration (P) is as indicated in Table 9.1.

TABLE 9.1 RELIABILITY OF CONFIGURATION P

Configuration	Curves Providing Successful Operation	Probability of Occurrence	Reliability = Sum of Probabilities
P	0	.0607	0.6918
	1; 1	.1702	
	1; 2	.2382	
	1; 3	.2225	
	2; 1, 1	.0001	
	2; 2, 1	.0001	

The reliability parameters common to each configuration are:

t = hours

q = cell reliability = $e^{-\lambda t}$ = 0.99982482

r = number of series-connected cells

s = number of parallel-connected cells

For configuration (P),

$$P_0 = q^{rs} \tag{9.2}$$

$$P_{1;j} = \binom{r}{j}\left[\binom{s}{1}(1-q)q^{s-1}\right]^j\left[q^s + \binom{s}{1}(1-q)q^{s-1}\right]^{r-j} \tag{9.3}$$

When $P_{1;j}/\binom{r}{j}$ approaches 1, the foregoing can be treated as a binomial and approximated by the Poisson distribution R, so that,

$$\lambda = R = r\left[\binom{s}{j}(1-q)q^{s-1}\right] \tag{9.4}$$

and,

$$P_{1;j} \cong \frac{e^{-R}(R)^j}{j!} \tag{9.5}$$

The probability of exactly $(r - j_1 - j_2)$ rows with no cell failures, and of exactly j_1 rows with one cell failure, and of exactly j_2 rows with two cell failures is given by the following equation:

$$P_{2;j_1;j_2} = \frac{r!}{(r-j_1-j_2)!\,j_1!\,j_2!}\left[q^s\right]^{(r-j_1-j_2)}\left[\binom{s}{1}(1-q)q^{s-1}\right]^{j_1}\left[\binom{s}{2}(1-q)^2 a^{s-2}\right]^{j_2} \tag{9.6}$$

For configuration (PS), each cell failure results in the loss of only that cell's incremental power. Therefore, I-V curves, for configuration (PS) with a probability of occurrence of 0.9995, lie so close to the non-degraded curve, for the configuration (P), i.e.; zero failures in the panel, that they are assumed to be identical. The TRW Systems Group Reliability Program indicates that with shunt diodes across each of the lattices, all configurations considered result in an array reliability greater than 0.999999, for an allowable power loss of 0.12 %.

In this case, open shunt diodes have no electrical effect, and so can be neglected. On the other hand, each shorted shunt diode will subtract the voltage of one row of cells from the panel voltage. Of course, a large number of diodes will have to short in order to amount to an appreciable effect. The probability of exactly, x, out of, r, shunt diodes shorting, with the remaining (r-x) diodes either unfailed or open, is:

$$P_x = \binom{r}{x} P_{ds}{}^{x}(1 - P_{ds})^{r-x} \tag{9.7}$$

where

$$P_{ds} = \frac{\lambda_{ds}}{\lambda_d}(1 - e^{-\lambda_d t}) \tag{9.8}$$

and

$$\lambda_d = \lambda_{do} + \lambda_{ds} \tag{9.9}$$

For the case where at least one row has a failed cell, but no rows have more than one failed cell, which corresponds to the curves of Group 1 in Figure 9.28, properly functioning shunt diodes will move all these curves so close to Curve (0), as to be indistinguishable from it. However, an open shunt diode will cause some loss of output capability if it occurs in the same row as an open cell, i.e., the panel output characteristic would be essentially the same as Curve 1; 1 in Figure 9.28. The probability of an open failure of a diode is expressed by:

$$P_{do} = \frac{\lambda_{do}}{\lambda_d}(1-e^{-\lambda_d t}) = .00017515 \tag{9.10}$$

The probability of no open diode out of j diodes is $(1 - P_{do})^j$. Then the probability of exactly j rows with one open cell, no other open cells, and <u>no</u> open shunt diodes in the j rows with an open cell is :

$$P_{1;j;0} = P_{1;j}(1-P_{do})^j \qquad \text{where } j = 1, 2, \ldots, n \tag{9.11}$$

These values are tabulated in the middle column of Table9.2 below for j between 1 and 11:

TABLE 9.2 - VALUES FOR EQUATION (9.11)

j	$P_{1;j;0}$	$P_{1;j;1}$
1	0.17011	0.00003
2	0.23822	0.00008
3	0.22235	0.00012
4	0.15562	0.00011
5	0.08711	0.00008
6	0.04063	0.00004
7	0.01624	0.00002
8	0.00568	0.00001
9	0.00187	0.00000
10	0.00049	---
11	0.00013	---
Sum ≅	0.9384	0.0005

Similarly, the probabilities of exactly j rows with one open cell and one open shunt diode in the j rows with an open cell is determined by:

$$P_{1;j;1} = P_{1;j}\left[j\,P_{do}(1-P_{eo})^{j-1}\right] \text{ where } j = 1, 2, \ldots, n \qquad (9.12)$$

The calculations for this analysis were conservatively based on a lunar surface mission of three years (26, 280 hours) duration with the following assumptions:

(a) Failure rate (λ)

		Failures/10^9 Hours
λ = Cell Failure Rate (Open Circuits Only)	=	10
λ_{do} = Shunt Diode Open Circuit Failure Rate	=	30
λ_{ds} = Shunt Diode Short Circuit Failure Rate	=	70

(b) Open circuit failure rates for silicon and thin film cells were assumed to be identical. (This is felt to be a conservative assumption for thin films due to the nature of their design.)

(c) Both the silicon and thin film cells were assumed to always fail open. (Actual primary failure mode data on thin film cells is unavailable at this time.)

(d) The possibility of failure of the interconnections between parallel cells is neglected in this analysis.

(e) It is assumed that the probability of shunt diode failure resulting in significant array power loss is negligible.

(f) Array reliability was to be expressed in terms of allowable array power loss.

Figures 9.29 to 9.31 show the effect of array voltage on array reliability and allowable power loss at a given power level, based on the above assumptions. It is evident from these curves that array reliability is much improved when low voltage, high current arrays are used.

Comparison of silicon and thin film array reliability in Figures 9.29 and 9.30 indicates that array reliability for a given voltage configuration is higher for the array (silicon) with the greater number of cells, when percent allowable power loss is the basis of the comparison. This indicates that even though the expected number of cell failures is greater for silicon (14 cells for silicon vs 3.2 cells for thin film), the percentage of allowable array power loss per silicon cell failure results in higher

overall array reliability. This is only true as long as cell failure rates are identical for the two cell types and shunt diode protection is not used. This represents a worst case assumption for thin film cells due to the nature of their design.

With shunt diodes, the probabilities of occurrence of more than one row with both an open cell and an open shunt diode is considered negligible.

As for shorted diodes, when some rows have single open cells, the shorting of a diode in parallel with a row with an open cell would cause a negligible change in performance.

The last case considered was that corresponding to the case of more than one open cell per row. The occurrence of a panel with two open cells in the same row has a low probability of occurrence (0.0004) as noted on Figure 9.28. The probability of open diodes coinciding with rows with open cells then becomes negligible. Therefore, all rows with open cells are assumed to have properly functioning shunt diodes which causes the panel I-V curve to be essentially indistinguishable from the no failure case.

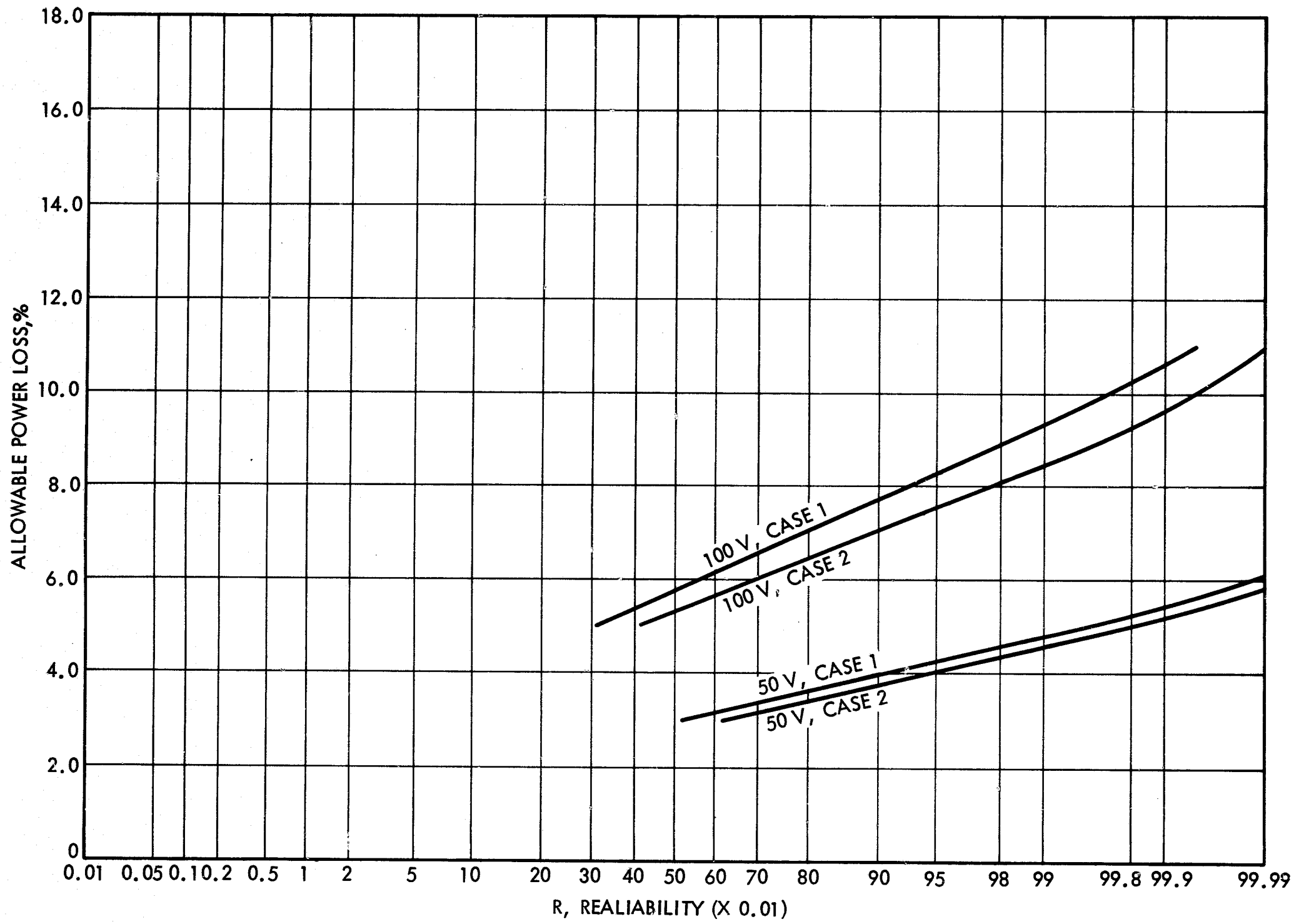

Figure 9.29 Allowable Power Loss Versus Reliability for 2.5 kw Silicon Cell Solar Array

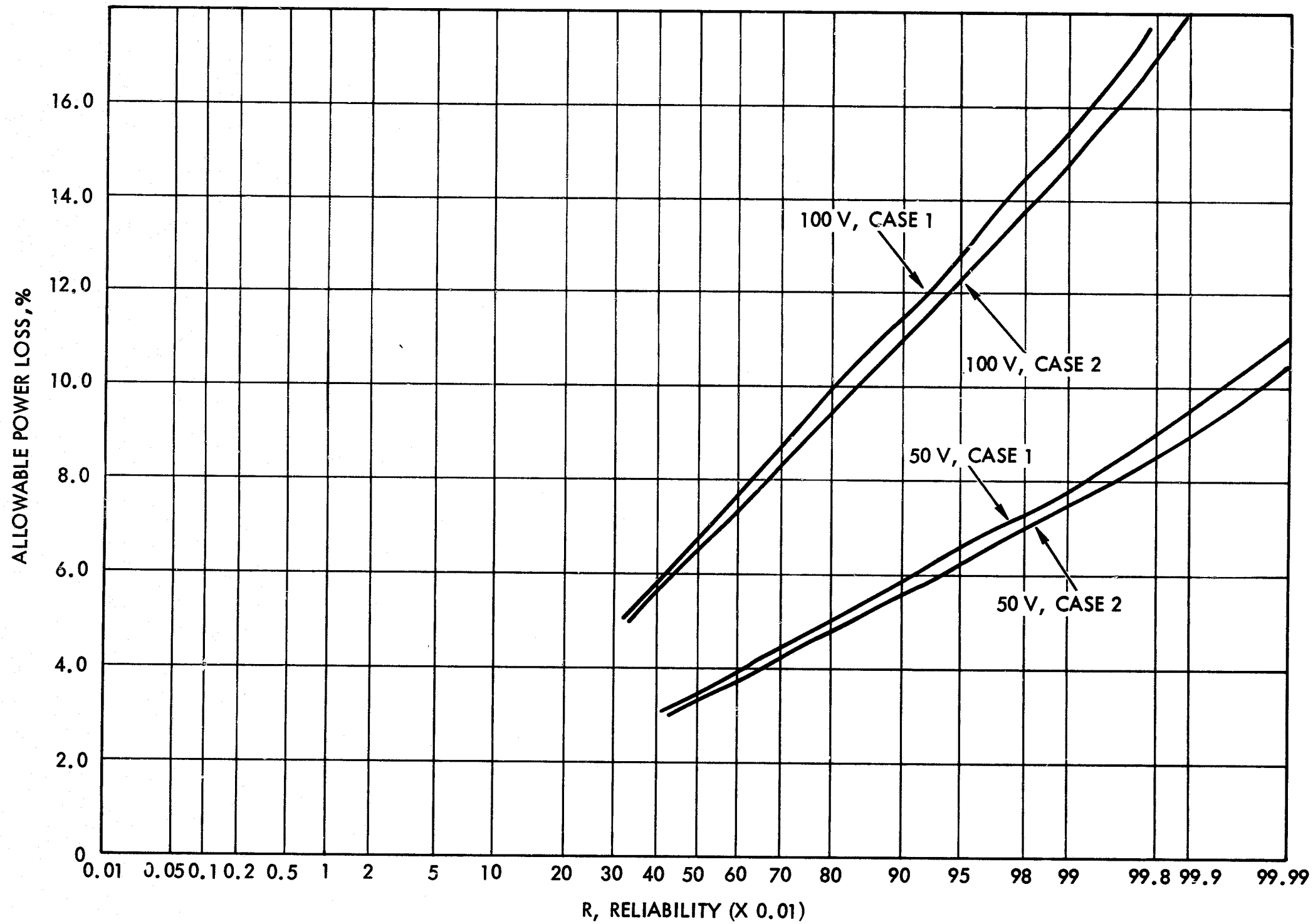

Figure 9.30 Allowable Power Loss Versus Reliability for 2.5 kw CdS Thin Film Solar Array

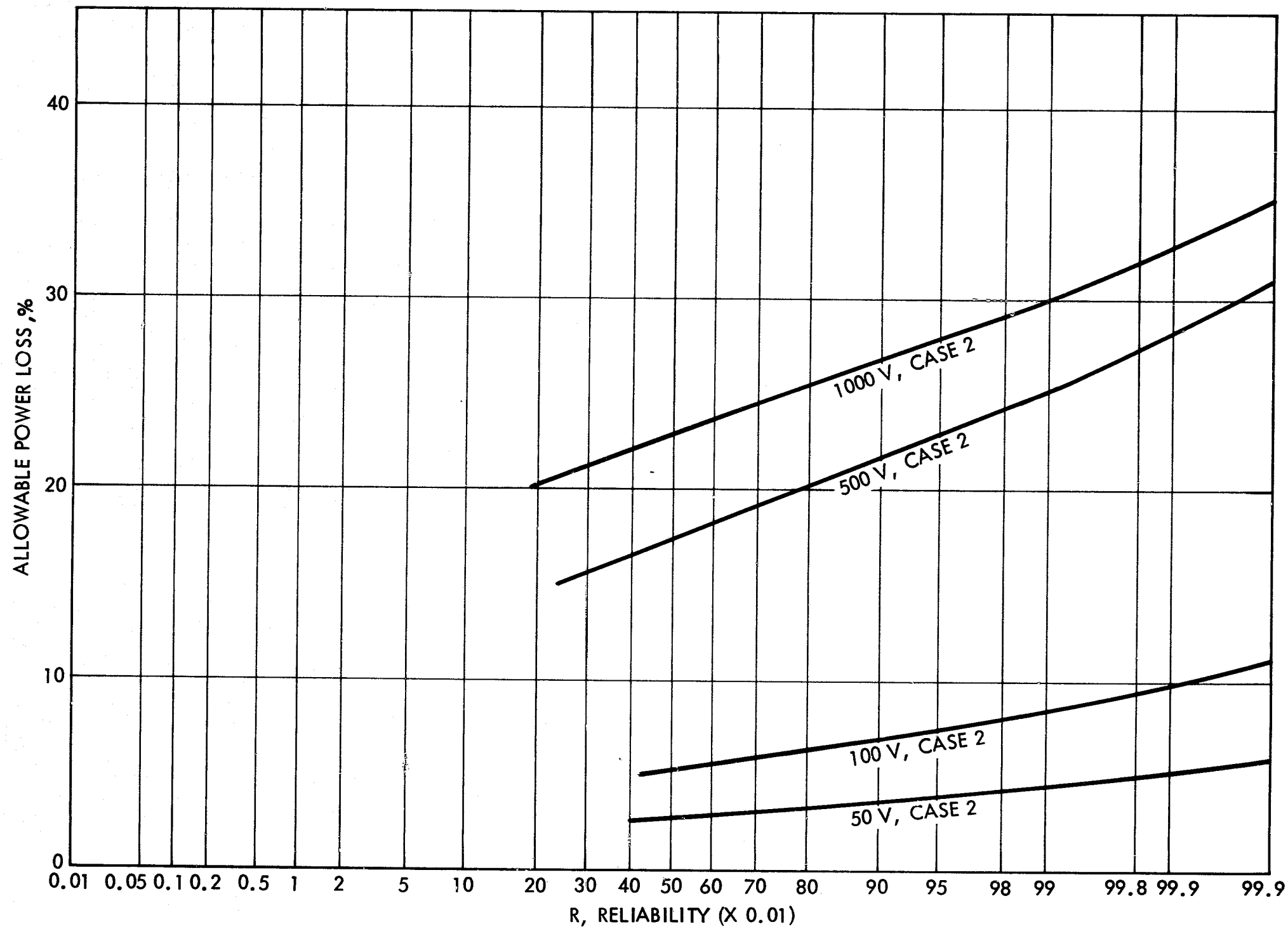

Figure 9.31 Allowable Power Loss Versus Reliability for 2.5 kw Silicon Cell Array for Various Voltages

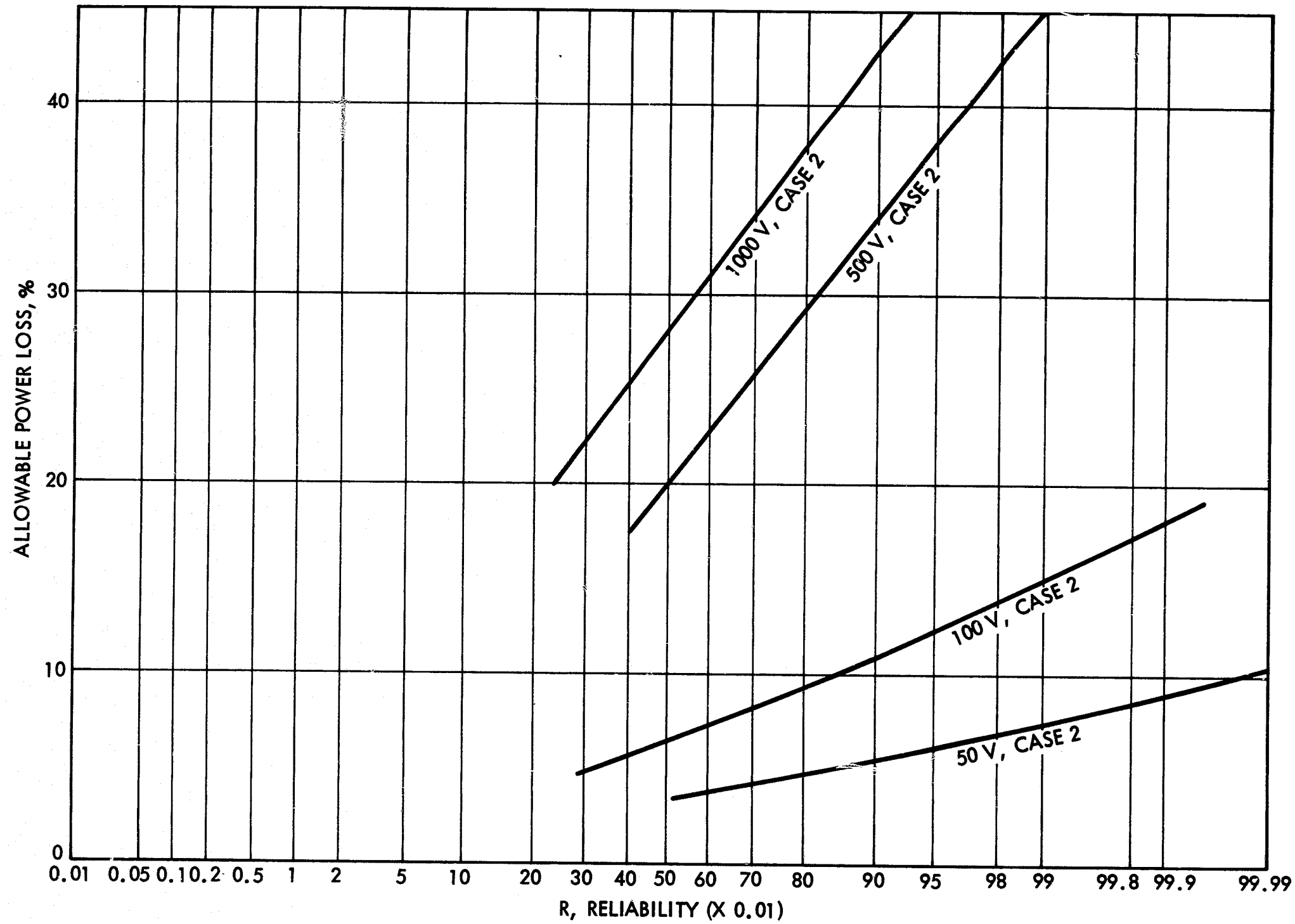

Figure 9.32 Allowable Power Loss Versus Reliability for 2.5 kw CdS Thin Film Solar Array for Various Voltages

10. POWER SYSTEM SYNTHESIS

10.1 ALTERNATE POWER SYSTEMS SURVEY

At the inception of this study, the initial objective was to conduct parametric analyses and tradeoff studies to permit selection of a Lunar Equipment Prime Electrical Power System (LEPEPS) and a Secondary Electrical Power System (SEPS). The LEPEPS was defined as the primary power source for the ERPS and also was required to furnish electrical power to the lunar base and energy depot establishment (shelter module and local extra-vehicular activities) following full deployment of all mission related equipment. The power profile and requirements for this system were previously described in Section 4. The SEPS was required to provide general purpose AC power for the ERPS Regulation and Control Subsystem and for the Telemetry Station System (TELSTATS), any other special power requirements from the initial launch phase to final system deployment (i.e., system start-up) and for unique conditions incurred by dormant or standby periods. However, during the early phases of this study, it was requested by NASA/MSFC that the assessment of the requirements for the SEPS be de-emphasized. As a result, the main activity in support of the SEPS during this study consisted of compiling the latest state-of-the-art performance data for various power conversion systems which conceivably could be utilized for implementation of a lunar surface exploration program in the 1972 to 1975 time period. The systems briefly considered during this study consisted of:

- primary batteries
- secondary batteries
- fuel cells
- nuclear static systems
- nuclear dynamic systems

A description of the performance capabilities of these various systems is provided in this section. An output power range of from 100 w to 35 kw_e was encompassed. Primary emphasis was placed on parameters such as energy density (lb/kw) and power to volume ratio (watt/cu. ft.), and estimated life (hours)consistent with lunar environmental conditions.

10.1.1 Primary Batteries

If total lunar surface mission energy requirements are modest (i.e., 10 to 600 kw-hours), primary batteries constitute a very simple, highly reliable approach to providing electrical power. Capable of operating both during the lunar day and lunar night, they permit maximum operational flexibility. However, currently achievable energy densities are in the range of only 10 to 20 percent of theoretical values. Hence, even for these comparatively low energy requirement missions, systems employing primary batteries are quite heavy.

Characteristics of the most commonly used primary batteries are shown in Table 10.1. The energy density range varies from 20 to 90 watt-hours/lb. and is highly dependent upon the rate of discharge. In addition, the useful operating temperature range of the battery is also fairly sensitive to this parameter. Progress in improving energy density has been extremely meager despite considerable research and development effort on the part of various government agencies and private industry. This is reflected in the estimates of projected future performance as given in Table 10.2. In fact, the prediction of achieving an energy density of 120 watt-hours/lb. for the magnesium-organic battery cell by 1975 is highly optimistic. Recent contracted government research for the development of high energy density batteries of at least 200 watt-hours/lb. has produced disappointing results. For the Program V lunar surface exploration mission defined for this study, primary battery energy densities projected to the early 1970's appear to be in the region of 80 watt-hours/lb. However, it should be noted that the energy densities quoted in Tables 10.1 and 10.2 are on a unit cell basis. For a complete battery system, the overall energy densities vary from 0.7 to 0.9 of these values depending upon packaging requirements. Based upon the current state-of-the-art of battery technology, it would appear that for emergency back-up power in the 100 to 500 watt range, a reserve type (electrolyte stored in separate compartment until ready for use) silver-zinc battery would be the most attractive candidate. These batteries could be manually or remotely activated.

Table 10.1

Primary Battery Cells

Type	Designation	Energy Density w-hrs/lb	Useful Operating Temperature Range °F
Non-Reserve[a]	Leclanche (Zn/MnO_2) (common dry cell)	20 - 60	+20 / +130
Non-Reserve	Magnesium dry cells		
	o MnO_2 depolarized	30 - 50	+40 / +130
	o Organic depolarized	60 - 90	+60 / +80
Non-Reserve	Mercury (Zn/HgO)	40 - 50	+35 / +160
Non-Reserve	Zinc-Silver Oxide	50 - 75	-20 / +140
Reserve[b]	Magnesium ("water activated")		
	o CuCl cathode	15 - 20	-20 / +90
	o AgCl cathode	20 - 30	-20 / +90
	Zinc-Silver Oxide	35 - 60	-40 / +60

*Depends on discharge rate and temperature

Ranges shown are limits corresponding to limits of 10 - 100 hour discharge period.
Lower temperature goes with lowest discharge rate (100 hours or more).

(a) Non-Reserve - Cells contain electrolyte

(b) Reserve - Electrolyte contained in separate compartment, activated manually or remote.

Table 10.2 Energy Density Projections for Primary Battery Cells (Reference 10.2)

Type	Cell Energy Density* (Watt-Hours/Pound)					
	(Non-Reserve) For 10-100 Hours Discharge			(Reserve) For One Hour Discharge		
	1964	1968	1975	1964	1968	1975
Leclanche	25	30	40			
Magnesium/MnO_2	35	40	50			
Magnesium/Organic	70	90	120			
Mercury	45	50	60			
Zinc-Silver	50	60	70			
Magnesium/CuCl				15	25	35
Magnesium/AgCl				20	30	40
Zinc-Silver				40	60	80

*Overall values for complete battery systems are 0.7 times tabulated values at 6 ampere-hour capacity and 0.9 times those values for a 50 ampere-hour system.

10.1.2 Secondary Batteries

Secondary batteries being rechargeable have broader applicability than primary batteries. For commercial and industrial applications, the lead-acid battery has by far the most widespread usage, despite its low energy per unit weight and limited cycle life. Low unit cost and ready availability are the key factors. More recently, newer types of secondary batteries are being utilized that are lighter, can be cycled many more times than lead-acid types, and can be sealed. Costs of these types are much greater than for a corresponding capacity in a lead-acid battery. Because of the cost, present applications are in the defense and space areas with commercial use limited to those applications where energy requirements are low, as in rechargeable flashlights, electric tooth brushes, hearing aids, transistor pocket radios, etc.

Three types of secondary batteries are currently in widest use. These are the nickel-cadmium, silver-cadmium and silver-zinc batteries which are named in the order of the most advanced state of development, largest area of application, and lowest energy density. Use of all three types can be expected to increase sharply over the next ten years as costs are reduced.

An important factor in the use of secondary batteries is the number of charge-discharge cycles the battery will take before failure. Figure 10.1 shows the projected energy density for the 3 kinds of battery cells listed above. These energy densities are based on a 100 percent depth of discharge. The charge efficiencies shown on this figure are based on power available at the battery terminals and does not include any losses associated with the charge control system. Figure 10.2 depicts the projected cycle life for these same three types of battery cells at 25 percent depth of discharge based on Earth orbital experience (100 minute orbit). Note that although the watt-hours per pound (delivered during any one discharge half-cycle) by the nickel-cadmium battery is considerably less than that for silver-zinc batteries, the longer cycle life of the former more than compensates for this factor on longer missions. The silver-zinc system is theoretically capable of a longer cycle life than is presently realized, but this technology gap has not been surmounted by current

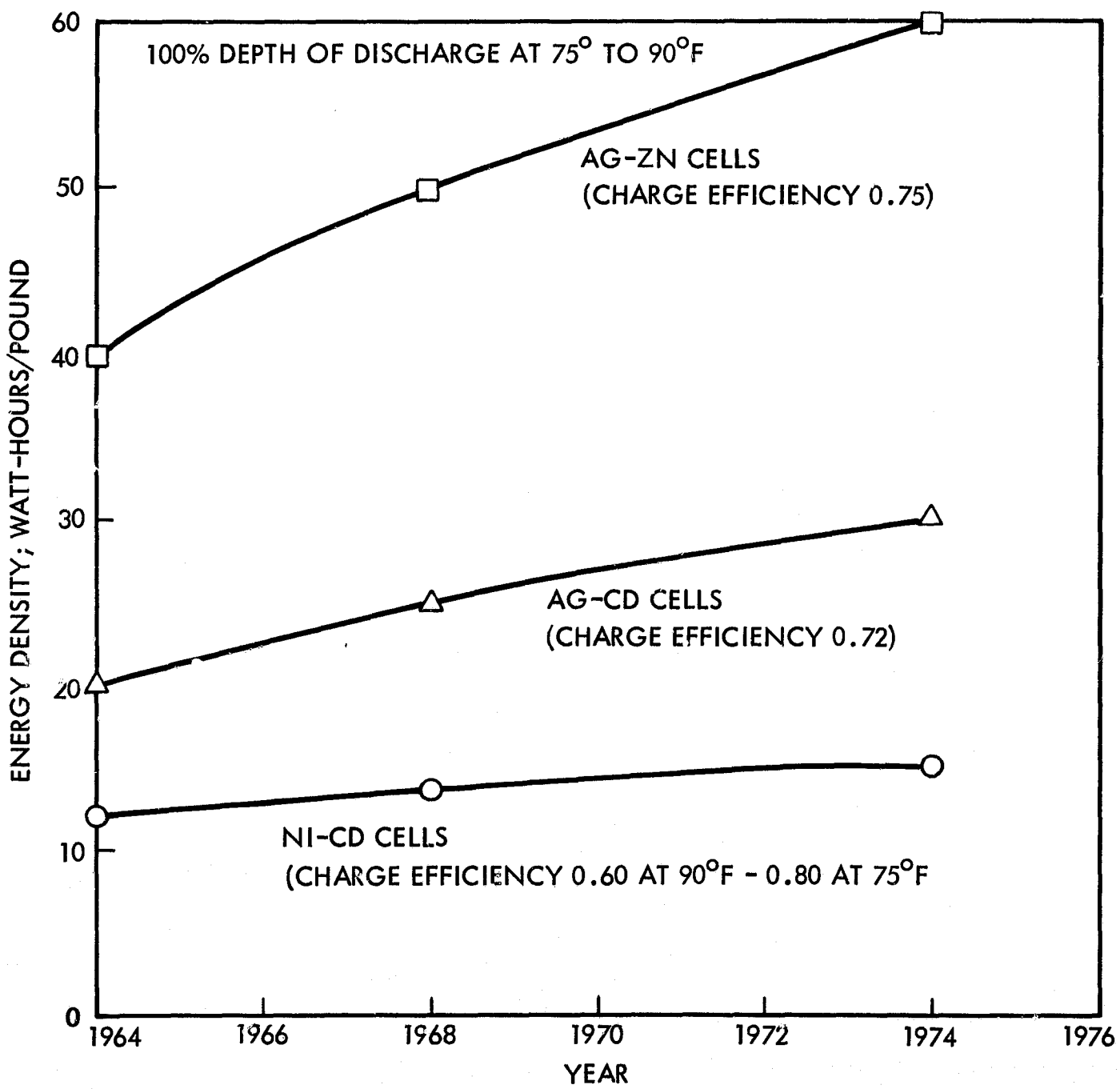

Figure 10.1 Projected Energy Density for Secondary Battery Cells (Reference 10.2)

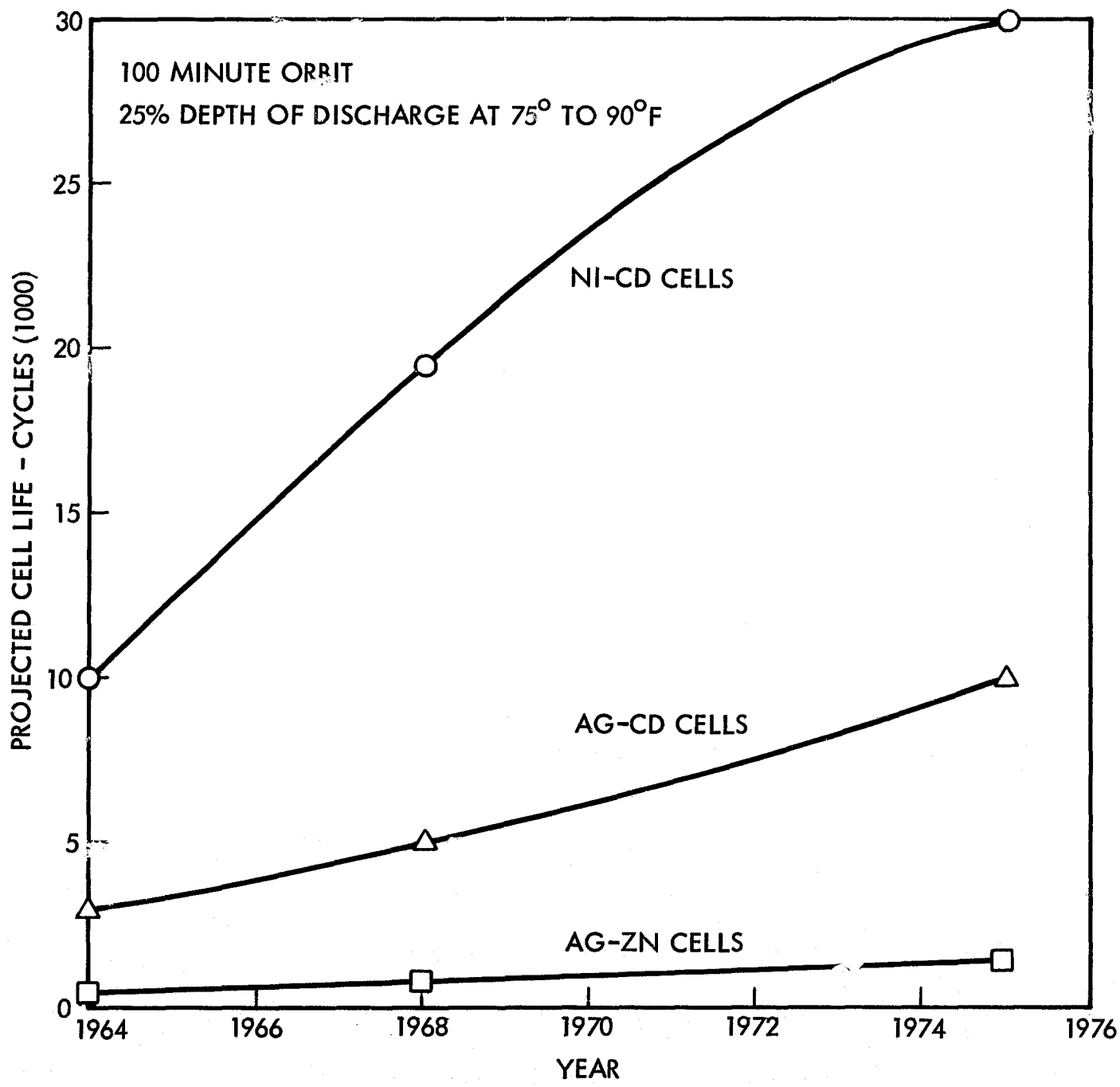

Figure 10.2 Projected Life for Secondary Battery Cells (Reference 10.2)

battery cell research and development work, despite intensive efforts by both government and industry.

As with primary batteries, most support for new developments in secondary batteries is provided by government sources. A large portion of this development effort is directed towards improvement of the three main types discussed. In addition, a small but concentrated effort is going on to investigate very high energy density secondary systems (over 100 w-hr/lb actual outputs). Current status of this work indicates that a major breakthrough would be necessary in order to seriously consider these advanced secondary batteries for the proposed lunar application. It is also very doubtful that sufficient reliability data will have been obtained by the early 1970's to permit their use on man-rated systems.

In summary, the maximum available energy densities for batteries that could be realized in the early 1970's from primary cells is 80 w-hr/lb and 60 w-hr/lb for secondary systems based on a 100 percent depth of discharge.

10.1.3 Fuel Cells

The fuel cell system converts chemical energy into electrical energy using techniques that avoid the thermodynamic limitations on efficiency imposed by the Carnot cycle. The principles involved have been known for over a century. However, because of economic considerations and other factors, the fuel cell had received limited development emphasis until the 1950's. In the 1950's, a resurgence of fuel cell research and development occurred, prompted primarily by the need for lightweight, auxiliary power in space systems. Because of the potential space application for the fuel cell, the major portion of development costs have been borne by government agencies. This effort has resulted in development of highly reliable and space proven hydrogen-oxygen fuel cells by three major companies (Pratt and Whitney, General Electric and Allis-Chalmers). Hydrogen-oxygen fuel cells were used on the Gemini program and are continuing to be used in the Apollo and Apollo Applications programs. The current work on this system is directed toward reduced specific reactant consumption (lb/kw-hr), increased energy density (w-hr/lb), further improvement in reliability, reduction of parasitic

power requirements (pumps, etc., for cooling and water removal), reduction of temperature difference between fuel cell and spacecraft radiator and increased cell life. Recent work has demonstrated the feasibility of electrolytically regenerative H_2-O_2 fuel cells. The current state-of-the-art indicates that an energy density of 15 w-hr/lb is achievable and 25 w-hr/lb is a possibility for the near future. Because of its present low energy density, the regenerative fuel cell does not appear to be practical for use on the Program V mission of this study. In addition, it is doubtful if sufficient reliability of the system can be demonstrated by the mid 1970's.

A considerable amount of current research and development work has been directed toward the hydrocarbon-air fuel cell, primarily because of the ready availability of inexpensive hydrocarbon fuels such as gasoline, kerosene, jet fuel and diesel fuel. To date, no reliable hydrocarbon-air system has been demonstrated. Even if a breakthrough did occur, lunar applications for hydrocarbon-air fuel cells would be impractical as the reconstitution of the hydrocarbon fuel would be impractical, if not impossible. This would mean logistic transportation of fuel for this system which, at $10,000/lb, would prove to be very costly.

In general, the current state-of-the-art of the H_2-O_2 fuel cell is in the range of 1 to 5 kw and a specific weight of from 50 to 75 lbs/kw. The efficiency varies between 50 and 60 percent. The specific fuel consumption is between 0.79 and 0.91 lbs/kw at rated power, and the cell life is in the range of 2000 to 2500 hours. Specific performance capabilities for three H_2-O_2 fuel cells are presented in Table 10.3. The data for the "present" Pratt and Whitney fuel cell applies to their PC3A-2 (Apollo) fuel cell. The "projected 1969" ratings are for the PC3A-4 (MOL) fuel cell. By the mid 1970's, it appears that extension of cell life to 4500 hours, reduction of parasitic power requirements to less than 4 percent, and the realization of 20 lbs/kw or less is possible. It should be pointed out that in order to achieve some of these improvements, tradeoffs with other parameters may have to be considered. For example, longer cell life may only be realized by an increase in the weight-to-power ratio or the net specific reactant consumption.

Table 10.3 Comparison of the State-of-the-Art of Fuel Cell Performance (References 10.3, 10.4, 10.12)

	General[b] Electric	Allis-Chalmers	Pratt & Whitney	
			Present (1967)	Projected (1969)
Gross Power (kw)	2[a]	2[a]	1.0-1.4	1.5-2.3
Type Cell	Ion Exchange	Alkaline	Alkaline	Alkaline
Specific Weight (lbs/kw)	20-70	80	200	137
Specific Volume (ft^3/kw)	0.3-2	2.7	9.3	4.5
Parasitic Power Requirements (%)	4 - 5	5	10.0	3.8
Efficiency (%)	50-60	50-60	67	73
Reactant Fuel Consumption (lbs/kw)	0.85-0.91	0.81-0.84	0.8	0.79
Life (hours)	2000	2500	1000	2000[c]
Operating Temperature (°F)	68-158	200	350-450	330-430
Weight (lbs)	40-140	161	246[d]	206[d]
Cost ($/kw)	62,500/ 125,000	not available	not available	not available

(a) These are "rated" power values

(b) The higher values represent current GE hardware; the lower values represent their advanced fuel cells which are currently under development.

(c) Have demonstrated 1000 hours to date (1967) for this advanced fuel cell.

(d) Weights based on being capable of withstanding 7 g's.

Figures 10.3, 10.4 and 10.5 present recent performance characteristic curves for the Allis-Chalmers fuel cell. Figure 10.3 shows the reactant consumption-power relationship; Figure 10.4 the waste heat-power relationship; and Figure 10.5, the voltage-power relationship. Figure 10.6 shows the effect of the parasitic power requirement on specific fuel consumption for various power levels for the General Electric fuel cells. Figure 10.7 shows the waste heat rejection for the present PC3A-2 (Apollo) and estimated heat rejection for the PCA3-5 (AAP) Pratt and Whitney fuel cells.

10.1.4 Nuclear Static Systems

Radioisotope thermoelectric generator (RTG) systems have been considered only for the dormant periods of the Program V mission to provide power to the base when in a standby condition. No detailed trade-off studies with other systems (i.e., primary and secondary batteries) were made during this study phase. However, during the next study phase it is recommended that a tradeoff study be conducted, when a better definition of secondary power requirements for emergency back-up, portable tools, instrumentation, telemetry, and any other base dormant period power is available. Table 10.4 and Figure 10.8 present some of the performance data and availability dates for some of these systems. Most of these systems are in the 50 to 500 watt range. A 20 kwe nuclear-static, thermal reactor/thermoelectric system (Reference 10.8) has been included because it is in the range of the ERPS power requirements. A preliminary review has indicated this system (including shielding) weighs approximately 26000 pounds (Reference 10.9) not including reactants and tankage for fuel cell-powered lunar surface vehicles. If the latter items are included, a total weight of 29000 lbs results. A comparison between this system and the solar array/fuel cell/ERPS is discussed in Section 4.6 of this report.

10.1.5 Nuclear Dynamic Systems

Although the scope of this study did not encompass a review of these systems, which are in general beyond the power range required for the emergency or dormant period of operation, they are included here for possible future reference. Performance data for the SNAP 2 and SNAP 8 using a thermal reactor and mercury Rankine cycle, are

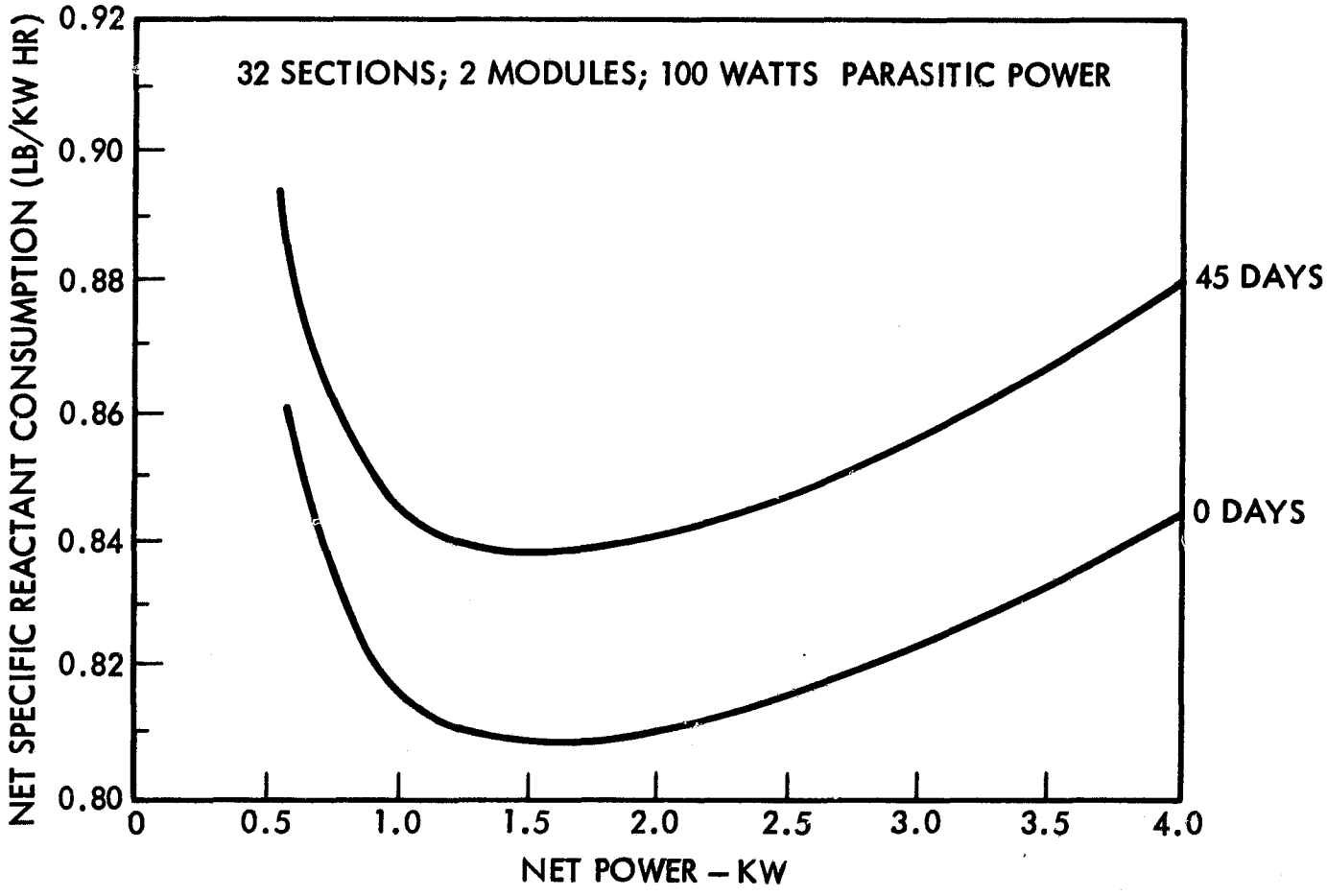

Figure 10.3 Two-Module Reactant Consumption Curves for AAP Earth Polar Orbital Mission

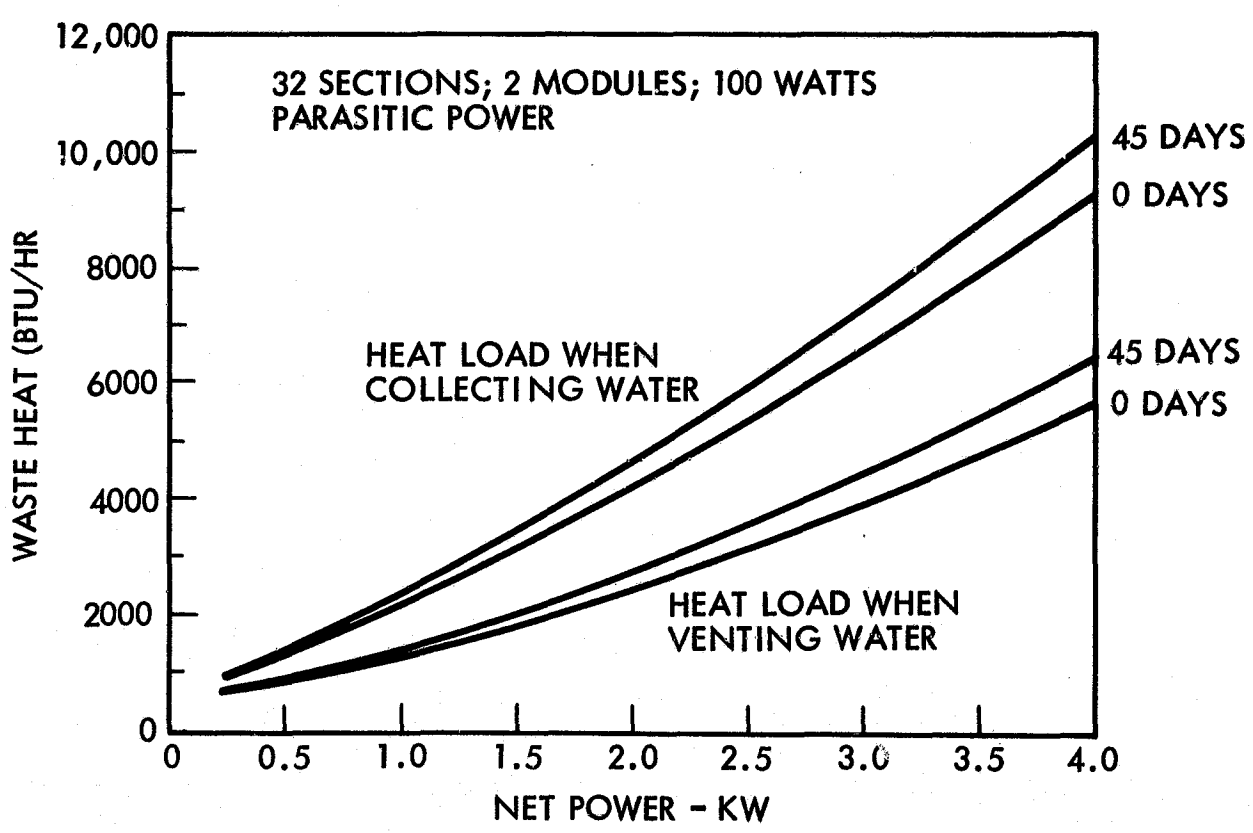

Figure 10.4 Two-Module Waste Heat Curves for AAP Earth Polar Orbital Mission (Reference 4)

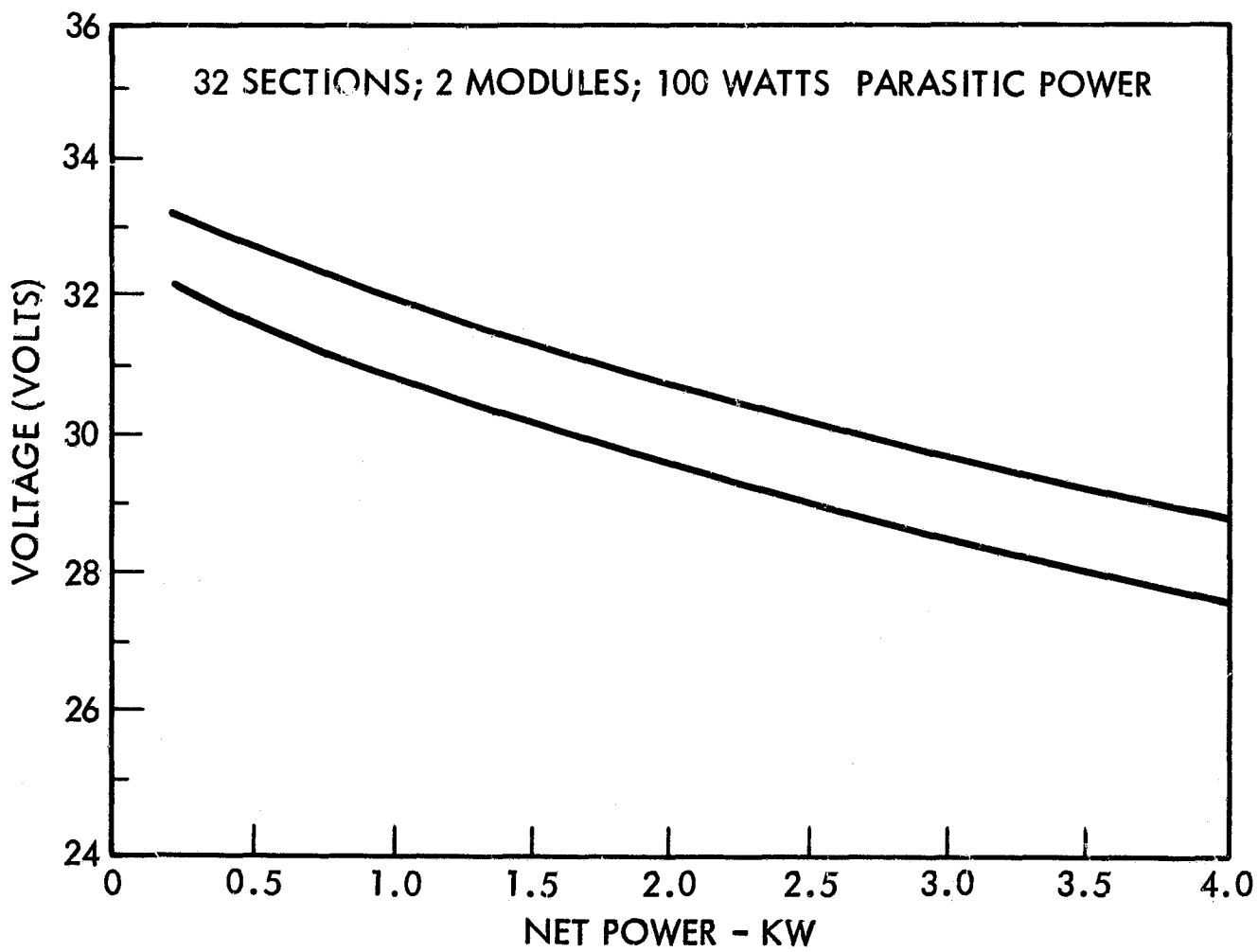

Figure 10.5 Two Module Voltage/Power Characteristics for AAP Earth Polar Orbital Mission (Reference 10.4)

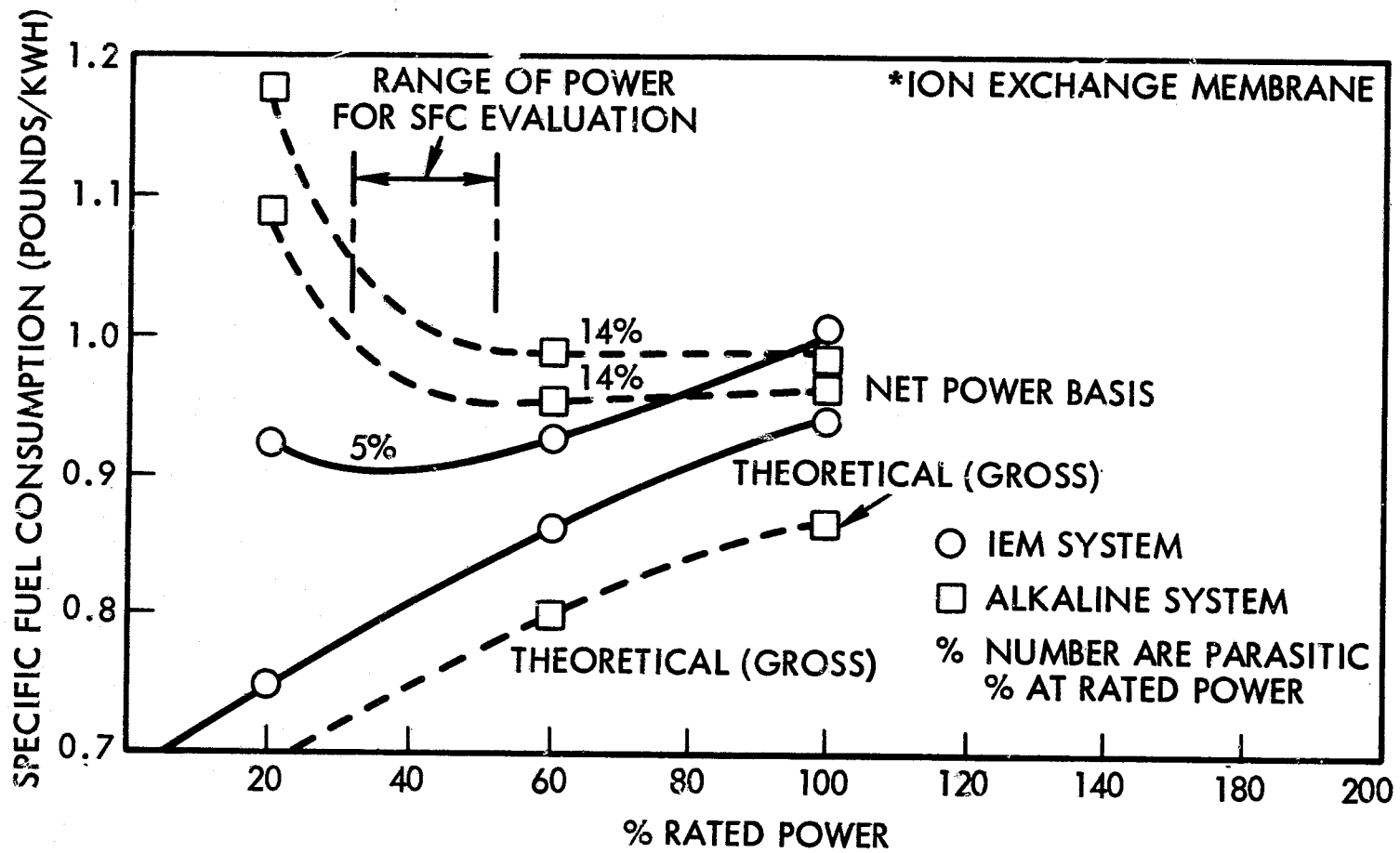

Figure 10.6 Fuel Cell Specific Fuel Consumption vs. % Rated Power (Reference 10.3)

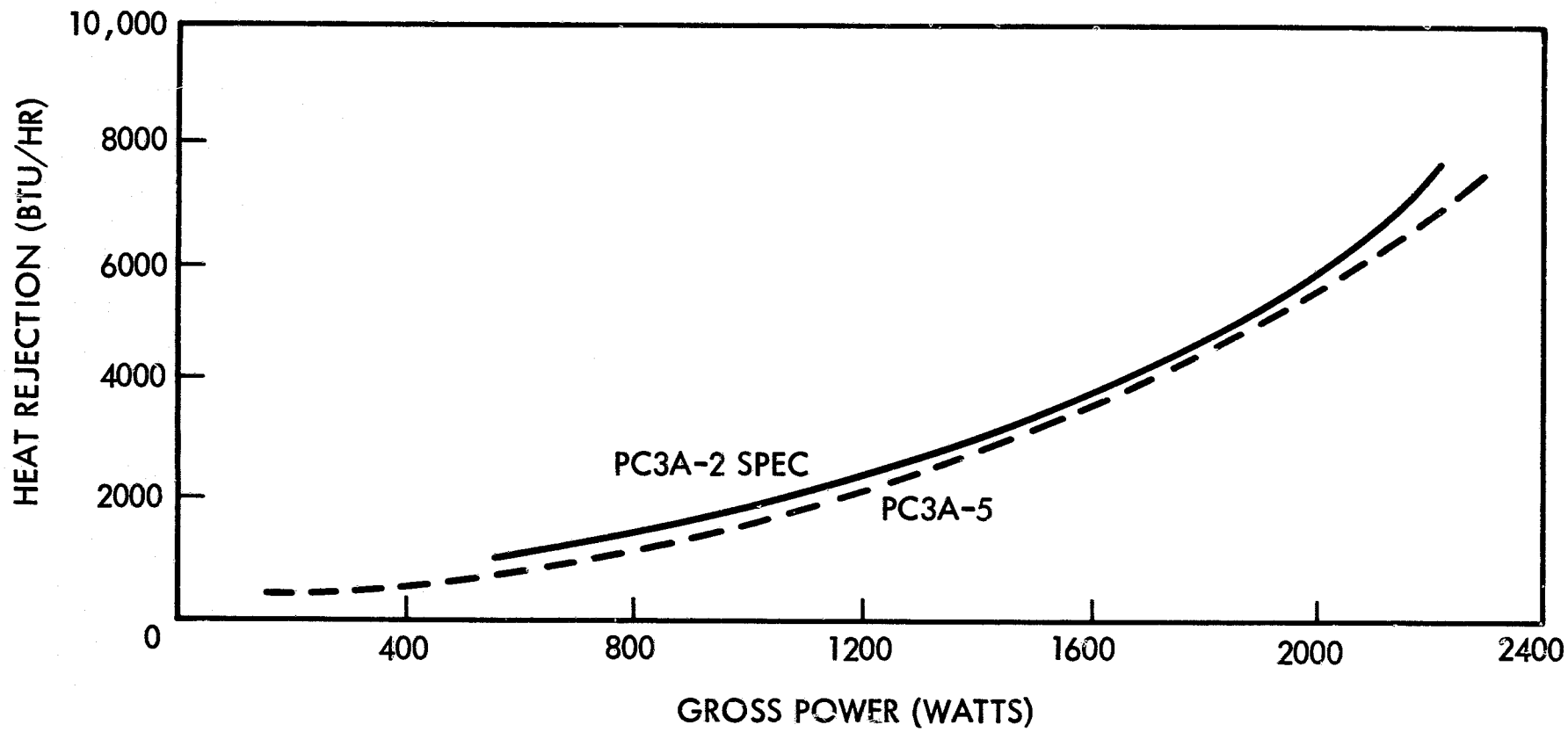

Figure 10.7 Estimated Heat Rejection to Radiator for P&W Fuel Cells (Reference 12.12)

Table 10.4 Comparison of RTG and Nuclear Reactor Thermoelectric Static Systems

	SNAP 10A	SNAP 27	SNAP 19	AI[a] Nuclear-Thermoelectric
Power (KWe)	0.5	0.073	0.05	20
Power (KW_t)	30	1.45	0.569	907
Life	1 year	1 year	1 year	1 year (est.)
Reactor	U-ZrH_x Thermal	Isotopic Thermal	Isotopic Thermal	U-ZrH_x Thermal
Power Conversion	Ge-Si Thermoelec.	Pb-Te Thermoelec.	Pb-Te Thermoelec.	Ge-Si Thermoelec.
Hot Junction Temperature, °F	930	1130	950	1272
Cold Junction Temperature, °F	615	525	400	1078
System Weight (lbs)	650[b]	42.7	60	26,000
Pounds/KWe	1300[c]	586	1200	1300
Availability	1967	1969	1969	1977
Reference	10.5	10.6	10.7	10.8

[a] Atomics International

[b] Unshielded Weight

[c] Based on unshielded weight

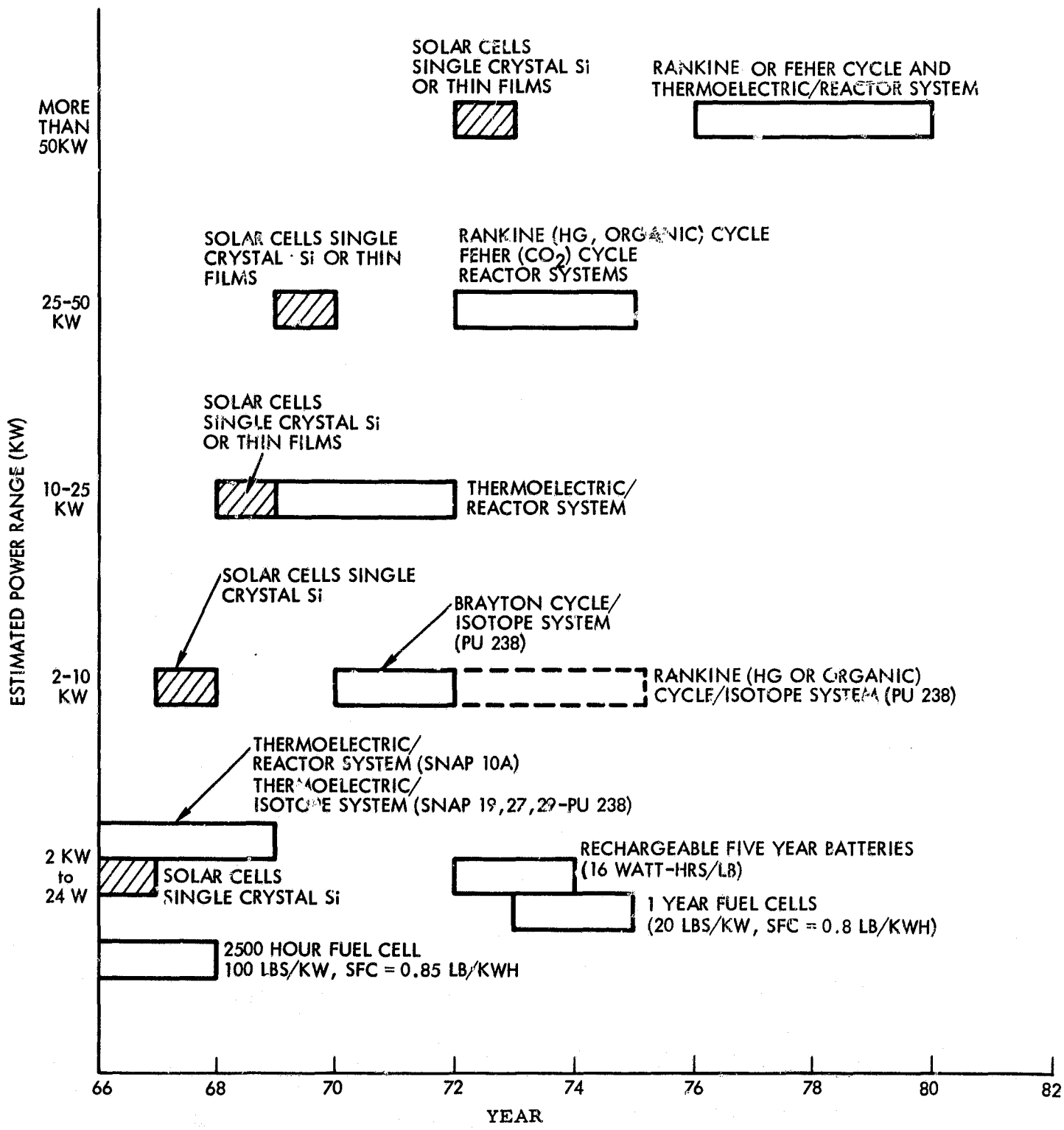

Figure 10.8 Estimated Date of Development Technology Completion (Reference 10.1)

presented in Table 10.5. Other systems including the Brayton, Organic and Feher cycles are shown in Figure 10.8. Figure 10.8 indicates that flight readiness of the isotope-powered Rankine (Hg or Organic) cycle systems will not occur earlier than 1975. While it is known that no major development effort is currently being funded for these systems, it is felt that if sufficient funding were provided, the 1975 availability date could be met. The Brayton, Organic-Rankine and Feher supercritical cycles, although having less technological development than the Hg Rankine cycle, have various distinct advantages over the Hg Rankine cycle and these systems should be evaluated during future studies. No tradeoff studies of the nuclear dynamic systems were made during this study phase.

10.2 REQUIREMENTS AND ASSUMPTIONS

10.2.1 General

The requirements which were used as a basis for defining the power system (LEPEPS) are discussed in Sections 4 and 5. The electrical requirements were established by Reference 4.2 and the environmental requirements were based upon the data presented in Section 5.

The electrical requirements as outlined in Reference 4.2 provided load profiles, voltage levels, and power conditioning criteria. However a considerable number of items required as inputs for full design consideration were omitted since this information was not available during this study phase. Wherever necessary judicious assumptions were made and identified. A more detailed assessment of these requirements can only be made after a comprehensive systems integration study has been conducted, since the Lunar Equipment Prime Electrical System (LEPEPS) has to interact with the ERPS, SEPS, and the shelter requirements. Hence, the definition of the LEPEPS and the related Design Requirements Document must be viewed as preliminary information during this study phase.

The form and flexibility of the load requirements (e.g., ERPS) can make a considerable difference to the power distribution method chosen, the overall efficiency, and other system characteristics. For example, if due to a choice of load input voltages the distribution efficiency were to fall from 80 percent to 60 percent, the solar array weight would have

Table 10.5 Comparison of Nuclear Reactor - Dynamic Systems (Reference 10.5)

	SNAP 2	SNAP 8
Power (KWe)	3	35
Power (KW_t)	50	600
Reactor	U-ZrH_x Thermal	U-ZrH_x Ther
Power Conversion	Hg Rankine	Hg Rankine
System Unshielded Weight (lbs)	1200	4575
Specific Weight (lbs/KWe)	400*	120-140*
Radiator Area (sq. ft.)	120	1400-1800
Availability	1975	1975

*Based on unshielded weights

to be increased more than 30 percent to provide the necessary power. This is only an illustration of the importance of choosing the optimum load voltages and other desired characteristics. The subject is treated extensively in a TRW Systems report on satellite power systems (Reference 10.13), which is applicable to this study.

10.2.2 Electrical Power Requirements

Table 10.6 lists the electrical power requirements used to arrive at the LEPEPS conceptual design.

Table 10.6 Load Electrical Power Requirements (Reference 4.2)

Item	Power, Kilowatts	Voltage & Regulation
Electrolysis	19.5 ± 0.5	195 ± 5 vdc
Liquefaction	12.2 ± 0.5	440 ± 20 vac, (400 ± 1 Hertz & 3 Ø)
Transfer and Circ. Pumps	1.4 ± 0.1	28 ± 2 vdc
Shelter*	3.0 ± 0.2	28 ± 2 vdc
Total	36.1 ± 1.3 kw	

*Added

It was assumed that the 3-phase ac power required for the liquefaction process is of the square wave form. It was also assumed that the solar array would provide the required power continuously during each manned lunar daytime period. During the lunar night the base power would be supplied by fuel cells. The power to be supplied during the unmanned lunar daytime period will be limited to the time period required to process the reduced quantity of reactants (see Discussion in Section 4.6). The baseline power profile to be used for the LEPEPS is shown in Figure 10.9a. Other permissible profiles considered are shown in Figures 10.9b and 10.9c. In all cases, 1150 kg of reactants was to be produced during each manned lunar day.

The power requirements correspond to Program V, which is a 3-man mission of one year duration, where the base is unattended for 6 months.

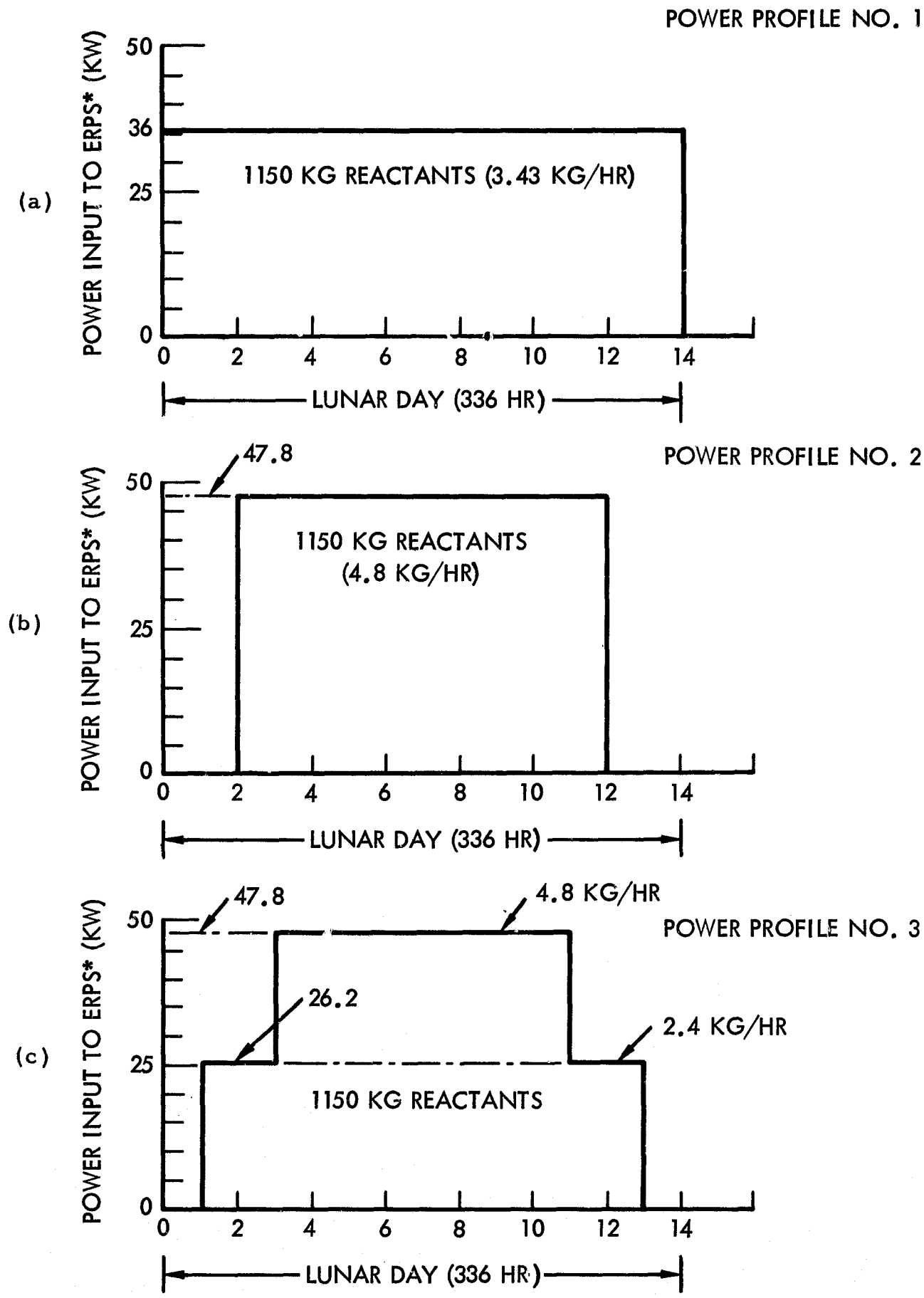

* INCLUDES APPROXIMATELY 3 KW AVERAGE FOR SHELTER POWER

Figure 10.9 ERPS Power Profiles

No allowance was made in the above requirements for instrumentation, telemetry, communications or emergency standby power. It was assumed that emergency power would be provided by high energy density Ag-Zn storage batteries, or fuel cells, as required.

It should also be noted that the Table 10.6 power requirements are as delivered to the loads. All distribution and conditioning losses have to be added before the minimum solar array power can be computed.

10.2.3 Environmental Requirements

It was decided during this study that no power conditioning and control equipment would be located in the ERPS module or the shelter based upon the conservative assumption that no space would be available. As a consequence, the effects of the lunar environment were applied to all elements of the power system and the impact on performance and weight assessed.

The applicable lunar environment is as given by data in Section 5. For the purpose of this study, the significant areas of concern were:

(a) Atmospheric pressure

(b) Solar thermal radiation inputs

(c) Lunar surface temperature and thermal radiation characteristics

(d) Particulate radiation

(e) Micrometeoroid bombardment

Table 10.7 lists the environment levels used and comments on some aspects of them. The lunar surface material was assumed to be thermally insulating and of low electrical conductivity.

10.2.4 Other Requirements

Additional factors which were also considered were:

(a) Handling size, shape and weight

(b) Design complexity (accessibility of controls)

(c) Surface (i.e., handling) temperature

(d) Monitoring of controls

(e) Ease of repair and replacement

(f) Safety

Various aspects of these basic requirements were reviewed in this study. However, a detailed evaluation of these factors and their impact on the final LEPEPS design were beyond the scope of this study.

Table 10.7 Lunar Environment

Item	Range or Value	Comments
Atmospheric Pressure	10^{-13} x Earth Standard Atmosphere	Voltage breakdown above 500 vdc. Allows use of small separation between high voltage conductors, simplifies connectors and insulation requirements. Units need not be fully enclosed.
Solar Thermal Radiation Input	Assumed as at 1.0 AU, 1396 W/M^2	Power system units have to be designed to reflect most of this input during operation.
Lunar Surface Temperature and thermal radiation	-133.5°C to +112°C Assume average albedo of 0.073	Power system units must be maintained in a much narrower temperature range during operation, e.g., -20°C to +55°C. Cable may be permitted greater temperature range.
Particulate Radiation	Electrons: $10^9/CM^2$ sec; Protons: $0.93 \times 10^9/CM^2$ sec } at 1-100 mev	No significant effects on normally, enclosed units. Possible deterioration of external insulation.
Micrometeoroid Bombardment	1 impact/M^2 sec for particles 2×10^{-7} mm diam. 10^{-16} impacts/M^2 for particles 3 cm diam.	No significant structural damage for normally enclosed units. Deterioration of exposed polished thermally emitting surfaces probable.

10.3 CANDIDATE SYSTEMS

10.3.1 Basic Functional Power System Configuration

Figure 10.10 shows the three generalized system concepts used. From these three basic concepts, the functional system configurations were evolved. The functional system configurations were then used as a basis for a specific system design selection.

In Figure 10.10, Concept No. 1 depicts an unregulated dc bus. The array voltage responds directly to the load, except for a possible voltage limiting function. The line regulation and power conditioning equipment supplies the regulated outputs for the various loads. The unregulated bus can also supply certain loads, such as heaters and switches directly. Concept No. 2 uses a regulator for the solar array to provide a regulated dc bus for distribution. An example of this would be in the use of the array regulator as a maximum power tracker for optimum power output utilization. Unregulated power conditioners convert and invert as required to provide the load outputs.

Concept No. 3 is much the same as Concept No. 2, except for use of a main inverter immediately after the array regulator producing a regulated ac bus. The power conditioning system would then transform, rectify, and convert as required for the load outputs.

The relative rigidity of the load voltage and regulation requirements led to a restricted number of configurations possible based on the three generalized system concepts shown in Figure 10.10. The resulting functional configurations are presented in Figures 10.11 and 10.12. In general, the method of approach followed that used in recent TRW Systems study conducted for JPL (Reference 10.14). Each configuration was evaluated in sufficient depth to permit a final selection but a detailed system trade-off and optimization was not conducted. The basis for the configuration choice was as follows:

10.3.2 Candidate Configuration Selection

10.3.2.1 Description of Candidate Configurations (Figures 10.11 & 10.12)

(a) Configuration 1a: In configuration 1a, the main bus voltage is completely unregulated. A shunt voltage limiter prevents array overvoltage from occurring. Each user of a regulated output has its own regulator. Where the load voltage differs

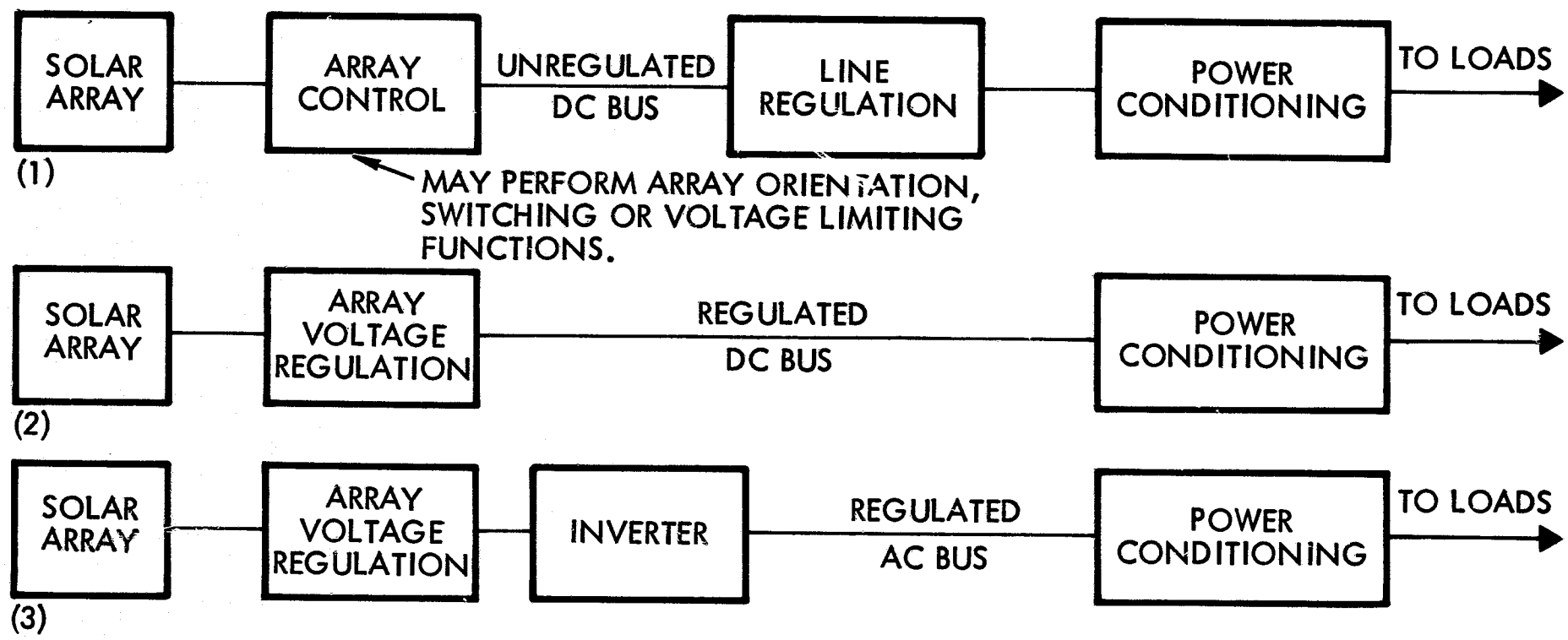

Figure 10.10 Generalized System Concepts

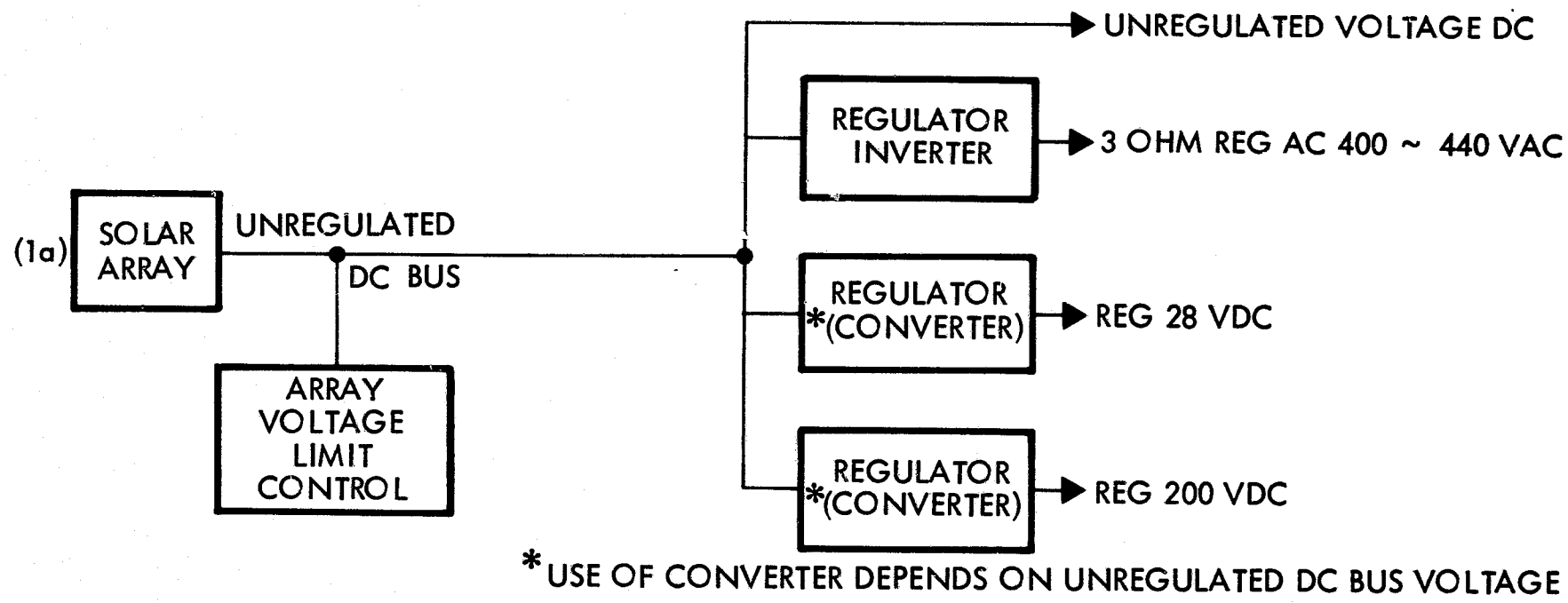

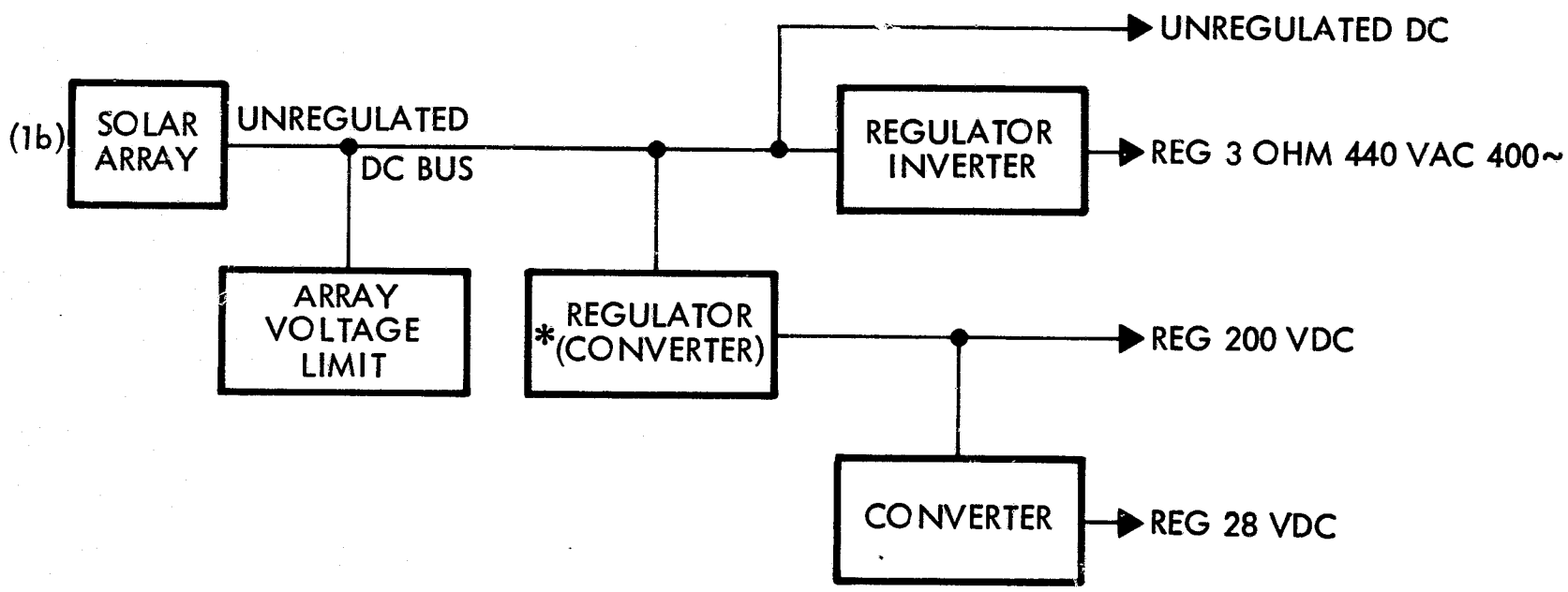

Figure 10.11 Power System, Unregulated Bus Configurations

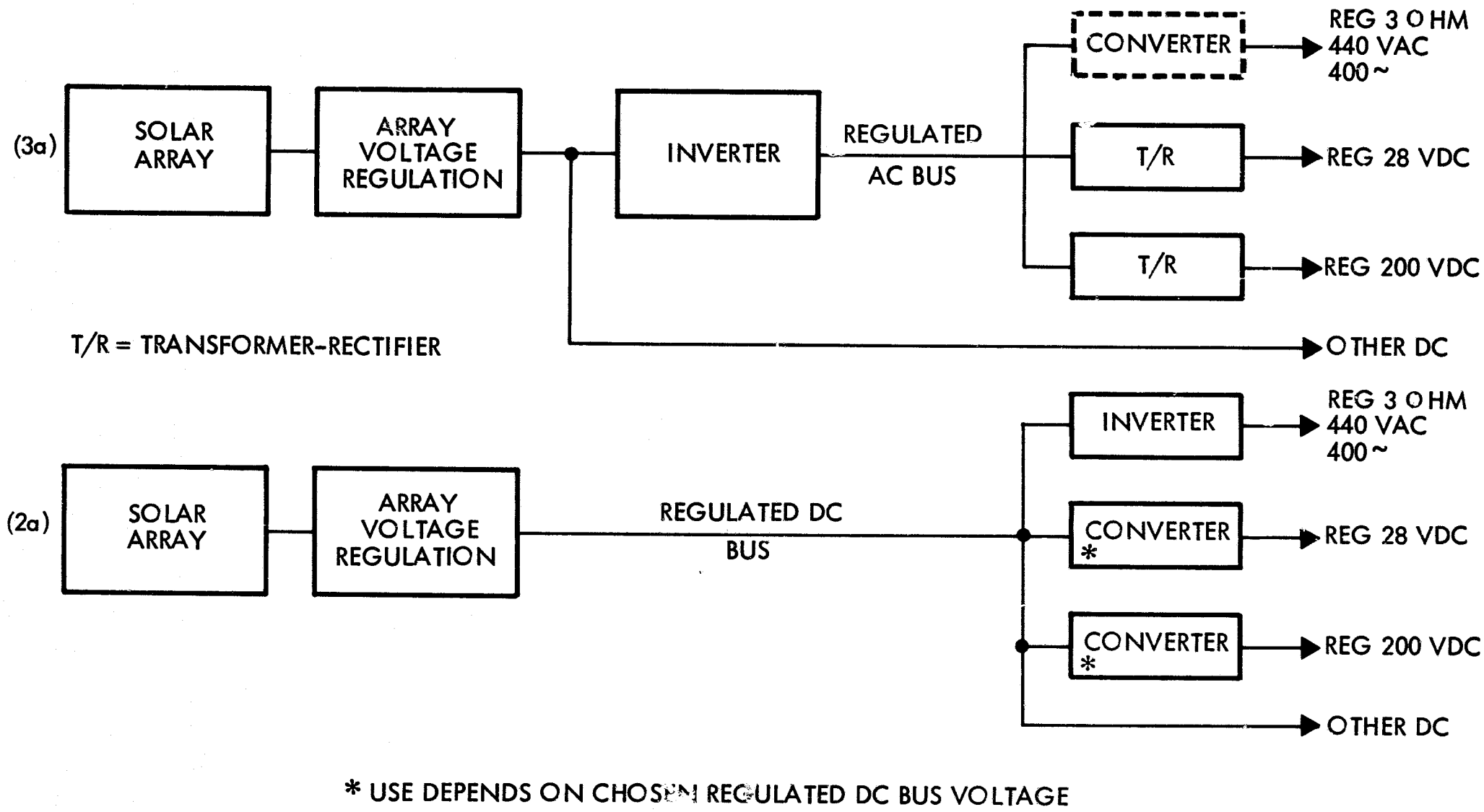

Figure 10.12 Functional Power System Configurations, Regulated Bus

greatly from the nominal bus voltage, a converter may also be required. Any unregulated load voltage requirements can come directly off the bus.

The scheme is flexible insofar as an unlimited number of regulator-converters can be added to the bus and the degree of regulation made to vary according to individual needs. However, a multiple number of regulators for a given total load power tends to decrease overall system distribution efficiency as compared with one or two regulator-converters.

(b) Configuration 1b: This configuration differs from 1a, in that a single regulator is used for the regulated dc loads. As noted earlier, this would tend to be more efficient than 1a, because the regulators used are fewer in number and relatively larger in power handling capacity.

For both configurations, 1a and 1b, the regulators used may be boost, buck, or even buck-boost types, depending on the nominal unregulated distribution bus voltage.

(c) Configuration 2a: This corresponds to system concept No. 2. In this configuration, the array voltage is regulated by a series regulator which can be fixed at any appropriate level.

For a varying load profile, particularly one which approximately followed the maximum array output capability, a maximum power tracker type of device would be in order. This concept is currently being developed at TRW Systems for applications where it is desired to maximize solar array utilization. For a fixed level of output power such as given by the reference load profile, the concept of a maximum power tracker is not applicable.

The main advantage of configuration 2a appears to be in the consolidating of all regulators into one with a probable gain in efficiency. Converters and inverters would be used where necessary for required output voltages.

(d) Configuration 3a: In configuration 3a, the solar array voltage is first regulated and then inverted so that the output is at some optimum ac voltage and frequency for distribution. The outputs are transformed and rectified as needed for user requirements. In this case, they would be transformed and rectified to produce 28 vdc and 200 vdc. Depending on the distribution frequency and voltage, a converter (ac) may or may not be used for the 440 vac load.

A basic advantage here is similar to configuration la, in that the distribution scheme is relatively flexible. It allows for the addition of an unlimited number of T/R's (Transformer-Rectifiers) or converters. The efficiency disadvantage accruing as a result of a large number of T/R's is also similar to that of la. Regulated high voltage ac has attraction for distribution of large amounts of power over relatively long distances. For the application considered in this study, the cable distances were expected to be relatively short, nullifying this particular advantage. Nevertheless, an ac distribution system has merit and should be considered in future applications.

10.3.2.2 Candidate LEPEPS Configuration

Configuration lb was chosen as representing a desirable design compromise between the performance extremes of configurations la and 2a. The ac distribution system was discarded because any advantages it might possess over a dc distribution were not readily apparent. Since the dc load requirements accounted for approximately two thirds of the load power, with 55 percent of the total at one voltage (195 vdc), a design selection was made in favor of the dc distribution system. It also appeared that a distribution voltage in the range of 200 to 300 vdc would result in a region where power conversion efficiency and hence system weight would remain very nearly optimal.

Configuration lb was therefore chosen and used as the basis for continuing study. In order to more fully examine and use this configuration for estimates of system weight, efficiency, etc., a discussion of relevant unit parametric data was felt to be in order. This area is covered in Section 10.4, which follows.

10.4 POWER CONDITIONING AND DISTRIBUTION DATA

10.4.1 Cabling

The system electrical power losses are made up of line (cable) losses and power conditioning regulation and conversion losses. Cabling losses and characteristics are now discussed. For the reference configuration shown in Figure 10.11 (configuration 1b), connecting cables consist of lines from each 2.5 kw array to a central connecting point, a main series bus to the main power conditioning, and any distribution lines such as from the main power conditioning to the shelter. The total line loss, P_{line}, is a function of line length, line resistance, line voltage, and total power transmitted. Or stated another way;

$$P_{line} = f(L, R, E, P_o) \qquad (10.1)$$

The line resistance, R, is a function of cross section and temperature as well as length.

It was decided to use No. 20 AWG copper stranded wire as a building block. A previous TRW study (Reference 10.15) concerned with lunar operations recommended the adoption of Kapton ("H" Film) as a wire insulation for the hard vacuum of the moon and temperature extremes that may be encountered on the Moon. The operating range used as a reference was -50°C to +150°C.

The resistance of No. 20 AWG wire is 10 ohms/1000 ft at a temperature of 25°C. The weight of the wire including insulation is 4.5 pounds per 1000 ft.

Before calculating line losses versus voltage, it was necessary first to establish a line voltage range. After some consideration of extremely high voltage ranges (e.g., >1000 vdc), it was decided arbitrarily to restrict the range to 500 vdc maximum. The question of high voltage breakdown at low gas pressures came up for examination. The breakdown voltage for air reaches a minimum in the vicinity of 2 or 3 mm Hg absolute pressure and then increases steadily with decreasing pressure. This is in accordance with the idea that the dielectric strength (volts/mil) of empty space is theoretically infinite. Since the lunar atmosphere was taken to be 10^{-13} times that of Earth at sea level, the breakdown voltage is expected to be above 500 vdc, in accordance with

Paschen's Law (Reference 10.16), which relates voltage breakdown to the gas pressure differential.

Bundles of 3 parallel No. 20 wires (3 positive and 3 return), 6 parallel and 12 parallel wires were postulated for comparison of IR drop and power loss. Figure 10.13 shows the voltage drop per 100 ft of line for 3, 6 and 12 wires at a line temperature, T, of $+25^{\circ}C$ and 2.5 kw transmitted power. It is apparent that 50 volts is an effective cutoff point for the 3 and 6 wire case, since the line voltage drop, ΔV, increases and becomes asymptotic near 50 vdc. For 12 parallel wires, it is somewhat better, but the voltage drop approaches 10 volts per 100 ft at 50 vdc. At 500 vdc and above, the curve is almost horizontal and the other asymptote is approached. The top cutoff point establishing the range is then 500 vdc.

When the power loss for 2.5 kw transmission is plotted versus line voltage, E, the hyperbolic nature of the curve is shown. Figure 10.14 shows the plot of

$$P_A = I^2 R_T = \left[\frac{2.5 \times 10^3}{E}\right]^2 R_T \qquad (10.2)$$

for paralleled No. 20 AWG wire.

The equation is of the form $Y = C X^{-2}$ which is an equilateral hyperbola having asymtotes at 50, 75 and 100 volts and P_A = 15, 10 and 3 watts, approximately. In order to make this information more useful, the power loss, P_A, was computed for 'N' arrays in parallel, for several wire combinations and for E = 50 to 500 volts.

The equation used was

$$P_{line,\ A} = \left[\frac{2.5 \times 10^3}{E}\right]^2 R_T \times L_A \times \frac{P_o}{2.5} \text{ watts} \qquad (10.3)$$

where

$P_{line,\ A}$	= Total power loss in parallel lines from array to collection point; watts
R_T	= Line resistance, Ohm/100 ft at $T = 25^{\circ}C$
L_A	= Line length = 100 ft
P_o	= Total array power required, kilowatts

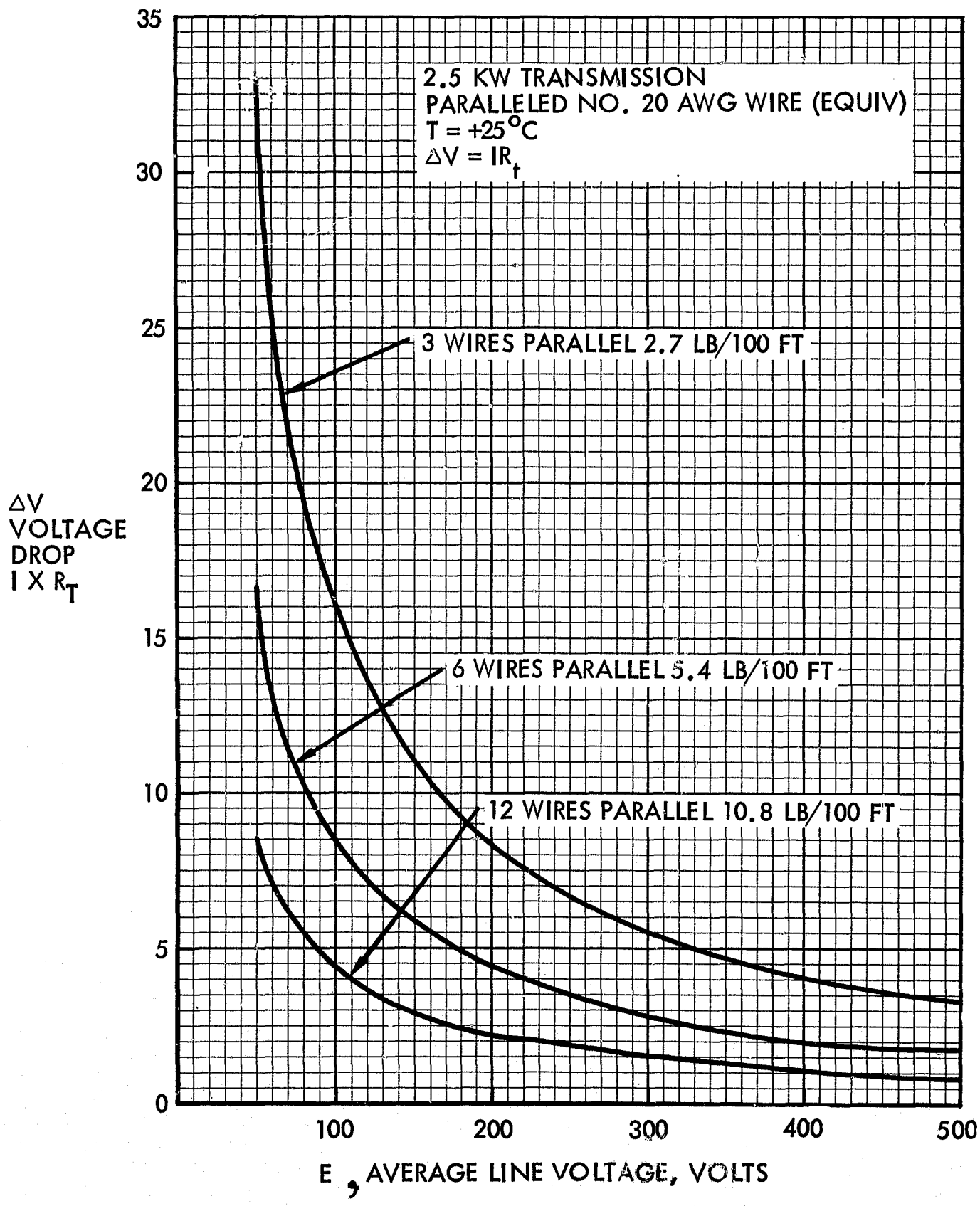

Figure 10.13 Average Voltage Drop per 100 ft Versus Average Line Voltage

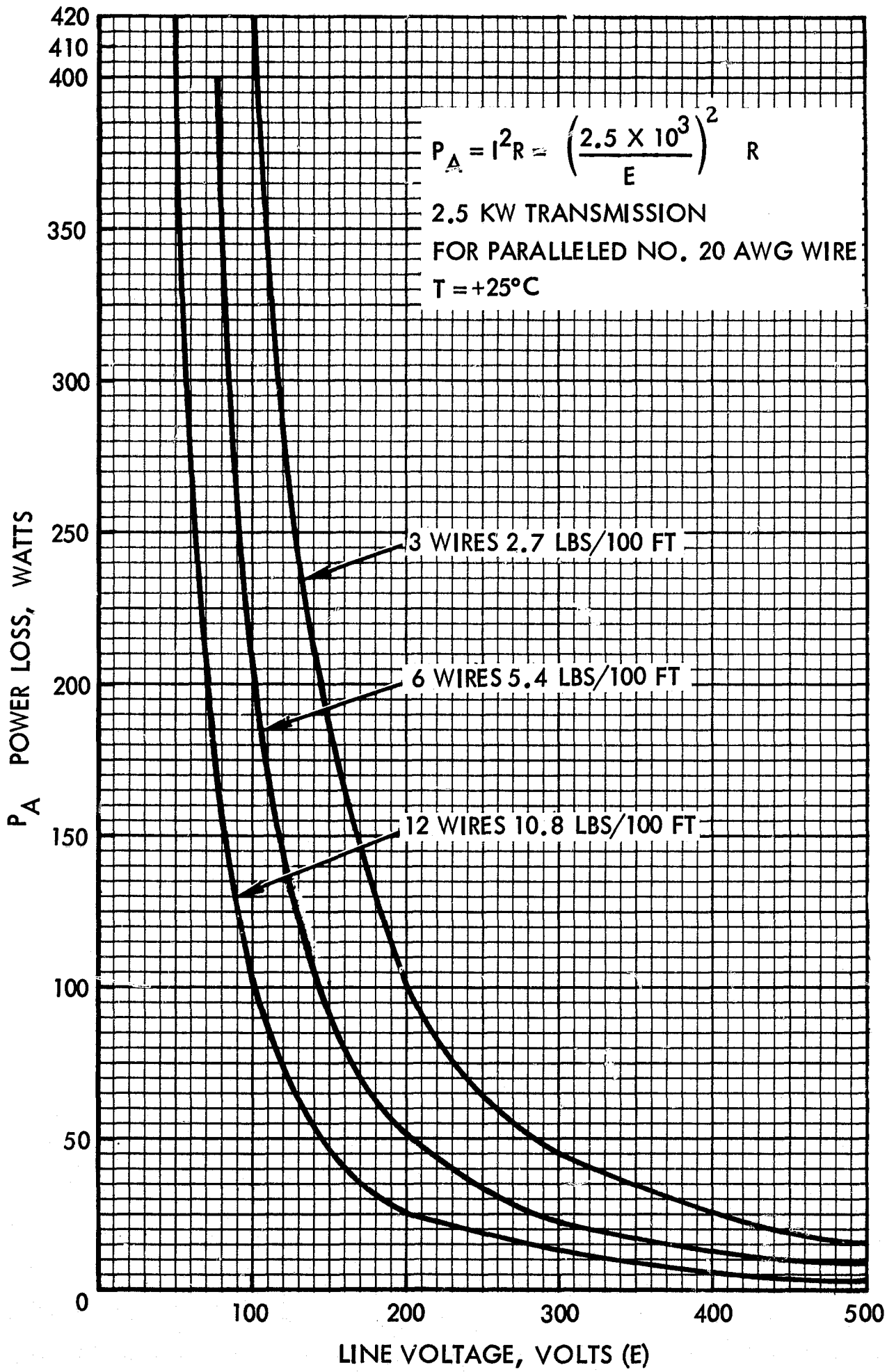

Figure 10.14 Power Loss per 100 ft Versus Line Voltage for Paralleled No. 20 AWG Wire

The results are shown in Figures 10.15, 10.16 and 10.17.

Power loss for the main connecting bus was similarly computed using data for No. 2 AWG copper wire as the reference. At a fixed weight of 20 pounds/100 ft and R_T = 0.016 ohms/100 ft, the power loss versus power transmitted was calculated for line voltages (E) from 50 vdc to 500 vdc. The result is shown in Figure 10.18.

Table 10.8 shows estimated total connector weights for various power levels. The connector weights are calculated by allowing 0.20 pound per connector for E = 100 vdc, 0.10 pound/connector for E = 200 to 500 vdc, and 0.40 pound/connector for E = 50 vdc. The total number of arrays used multiplied by the given weight per connector gives the total connector weight.

10.4.2 Voltage Regulators

The candidate configuration employs an unregulated bus. Therefore, for the regulated loads, line regulators are needed. These functions can be incorporated in the inverters or converters. However, they may also be treated separately or combined for higher efficiency and reliability.

The line regulator function can be buck, boost, or the buck-boost type, depending on the unregulated bus voltage range and the desired output voltage regulation. The boost and buck-boost regulators require pulse-width modulation techniques in order to provide a regulated output voltage higher than the input voltage. A bucking regulator could be either a pulse-width modulated or a dissipative type. However, because of the serious efficiency penalties in the system if the ratio of input to output voltage is large, dissipative regulators were not investigated further. An additional reason for rejecting dissipative regulators is the thermal requirement and resultant heat sink weight for use on the lunar surface.

Predicted efficiencies and weights for pulse-width modulated (PWM) boost and buck line regulators are shown in Figures 10.19 and 10.20. The graphs are a result of extrapolation of data for line regulators as found by previous TRW Systems study (Reference 10.14). Standby redundant configurations only are plotted. However, baseline weights would be about half that shown while efficiency would be slightly higher for the baseline regulators. Although weights for a buck-boost regulator are not plotted,

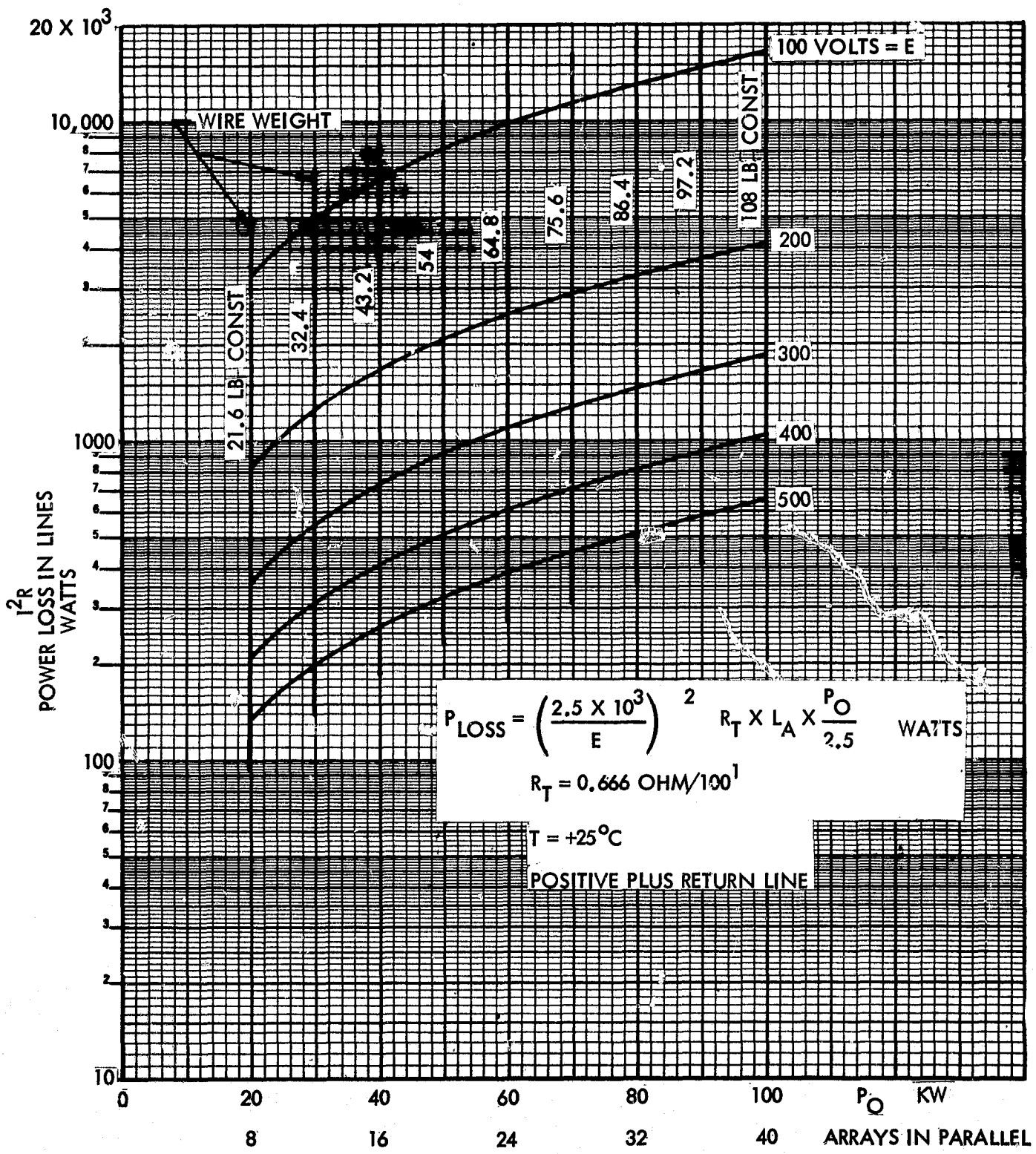

Figure 10.15 Parallel Arrays, Line Power Loss per 100 ft Distance for Insulated 3-Parallel Wire (No. 20 AWG)

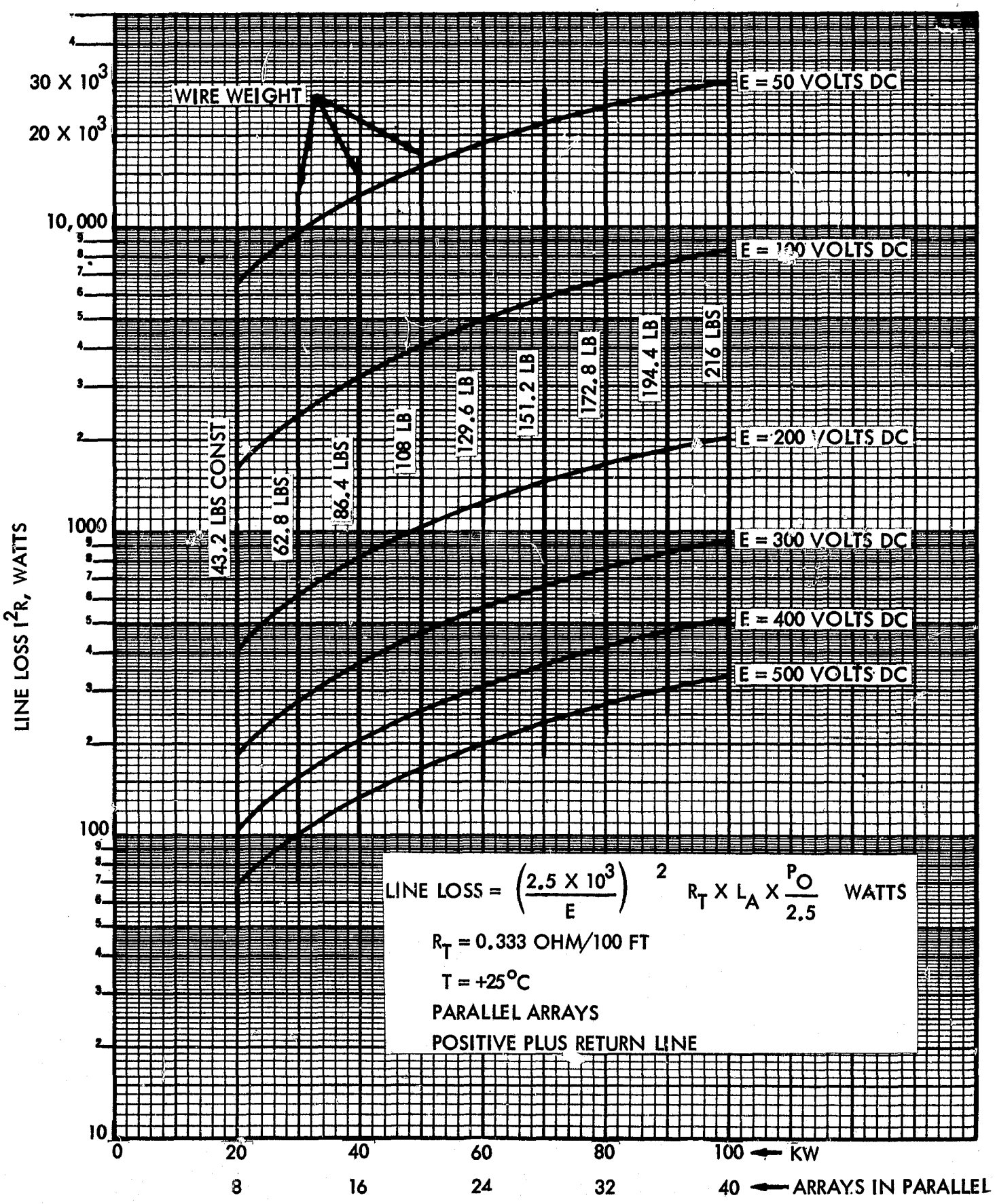

Figure 10.16 Line Power Loss per 100 ft Distance for Insulated 6-Parallel Wire (No. 20 AWG)

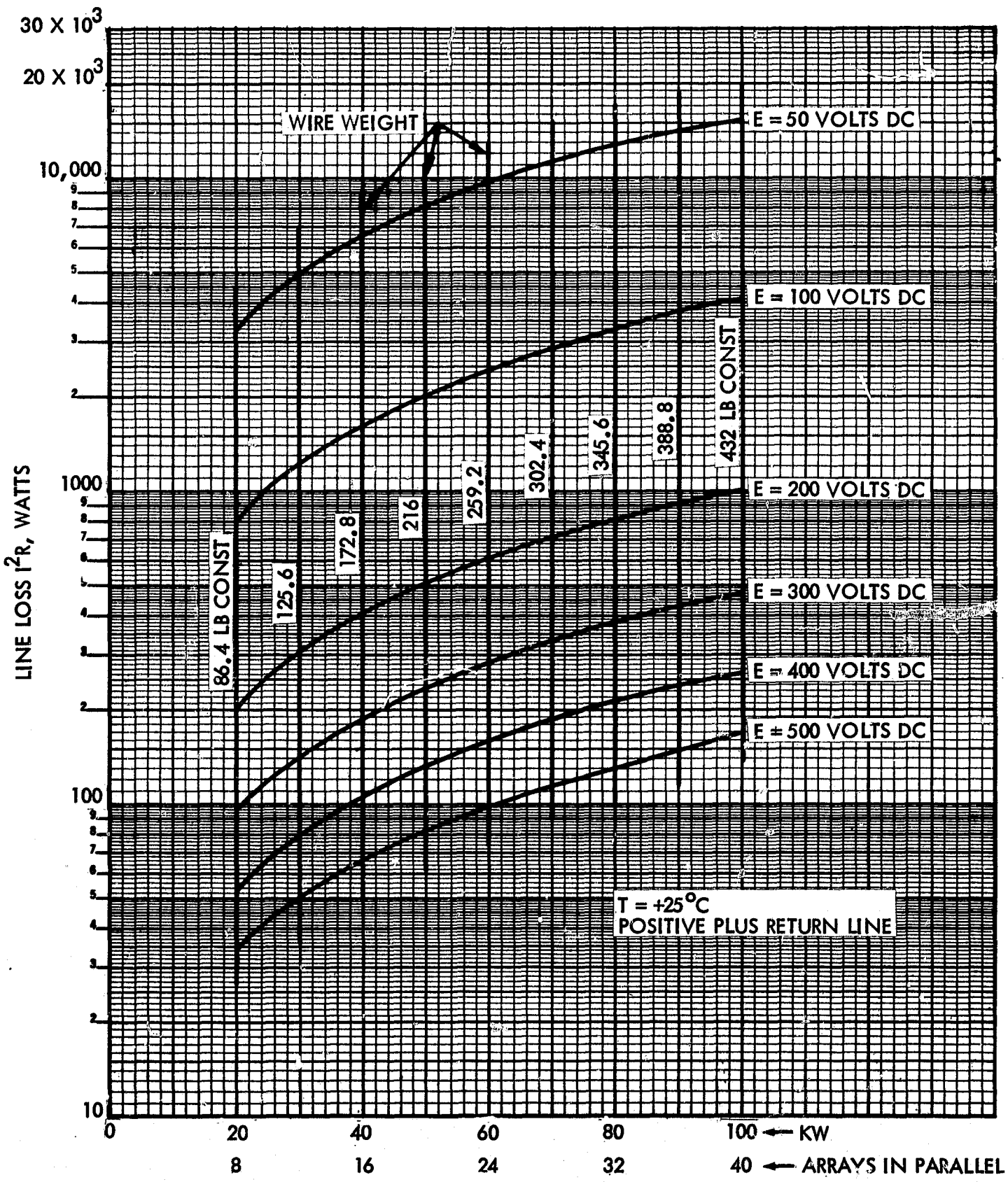

Figure 10.17 Line Power Loss Per 100 ft Distance for Insulated 12-Parallel Wire (No. 20 AWG)

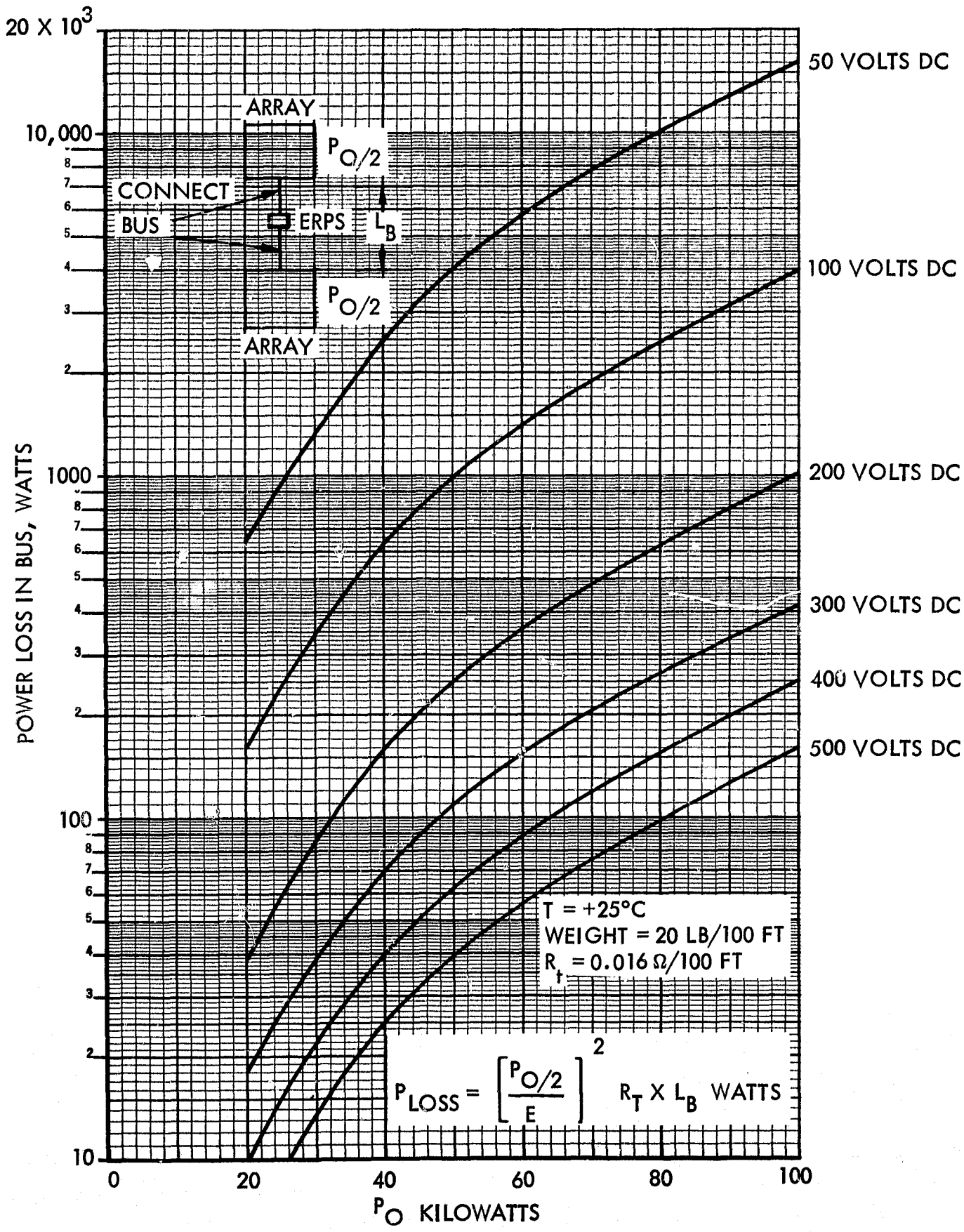

Figure 10.18 Power Loss for Connecting Bus Per 100 ft of length

Table 10.8 Estimated Total Connector Weights for Various Power Levels

Line Volts (dc)	Po, kw	20	40	50	60	80	100
50	Connector Weight, lb	6.4	12.8	16	19.2	25.6	32
100		3.2	6.4	8	9.6	12.8	16
200 to 500		1.6	3.2	4	4.8	6.4	8.0

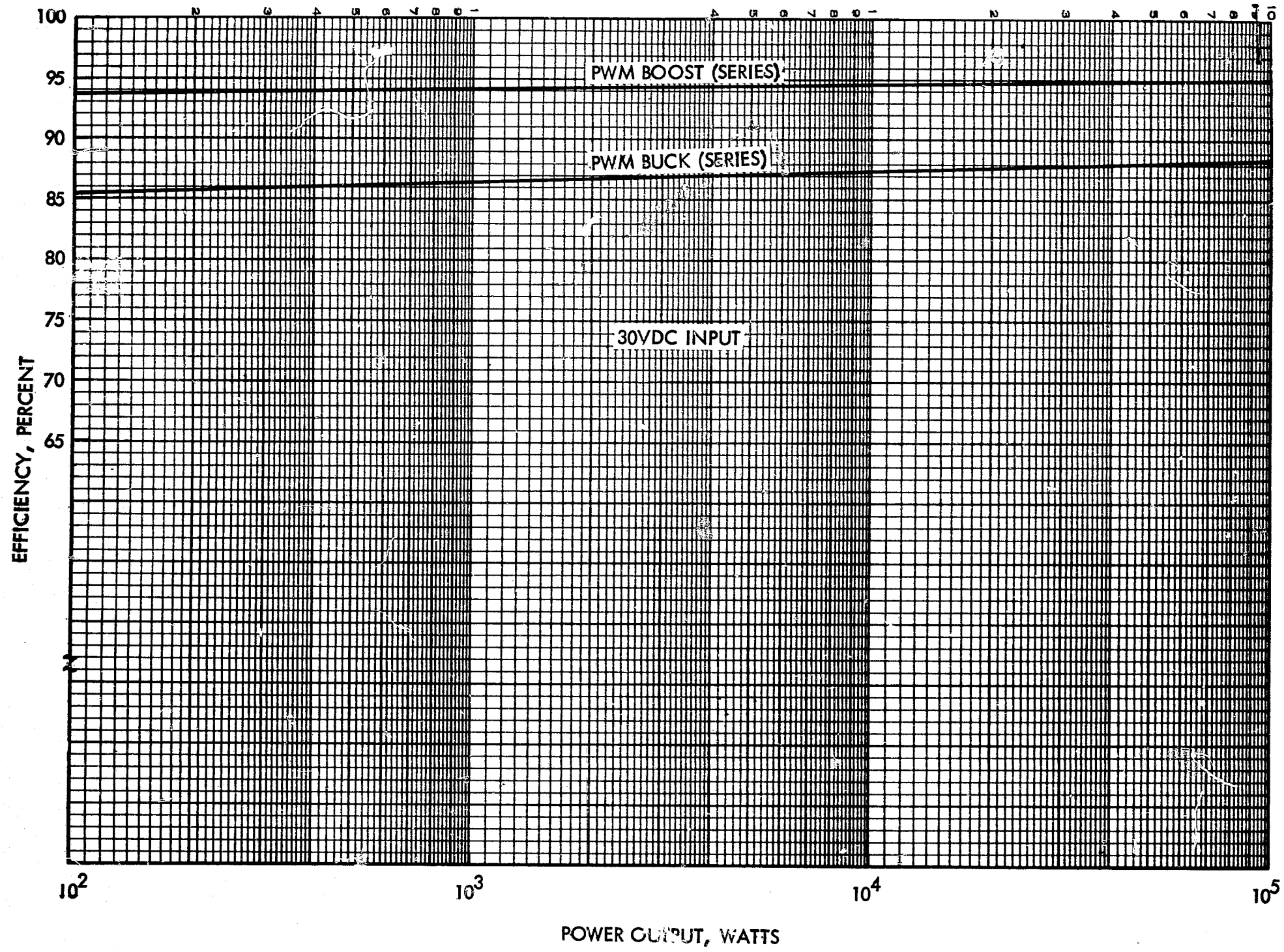

Figure 10.19 Line Regulator, Redundant Efficiency Versus Power Output

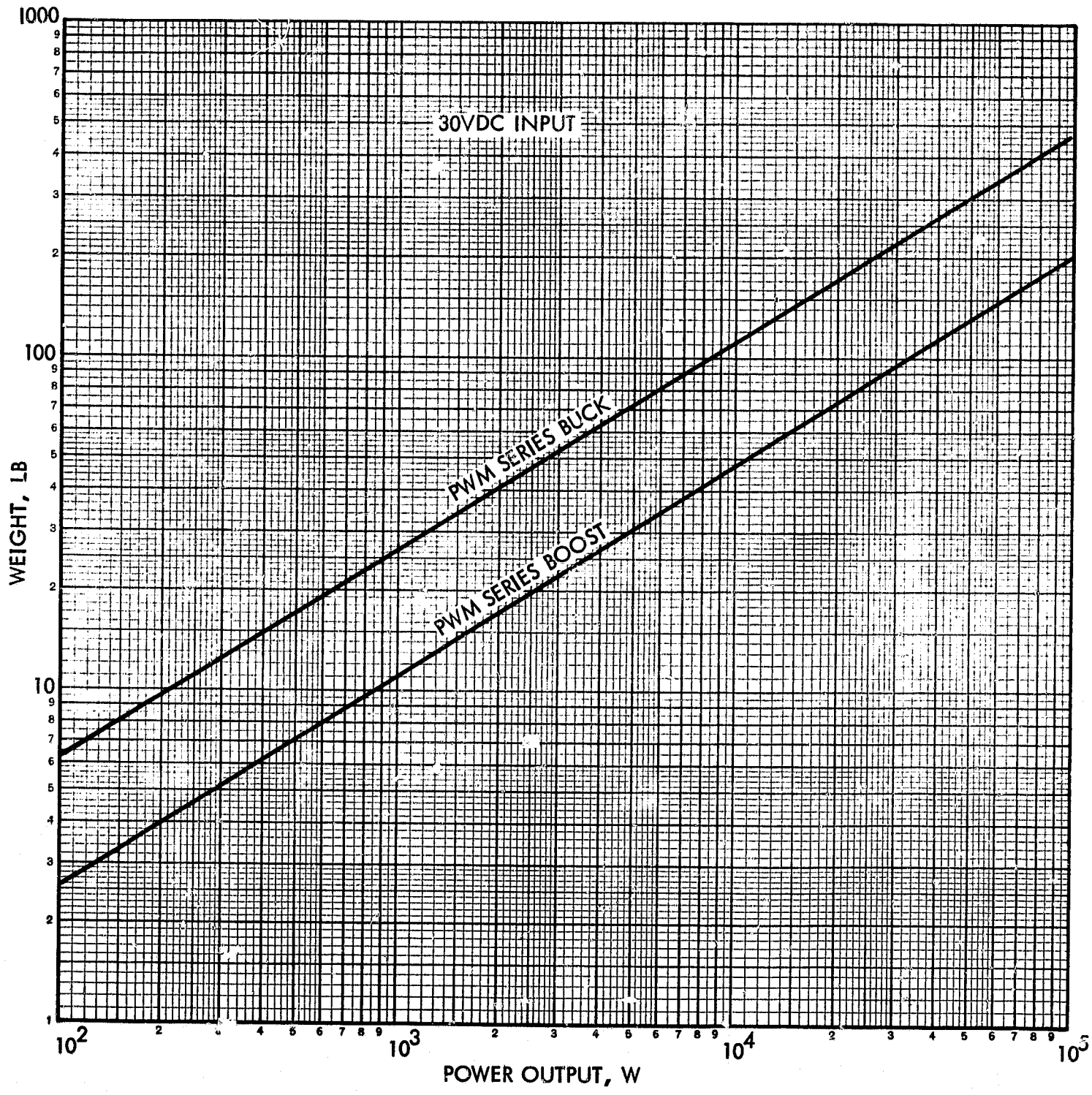

Figure 10.20 Line Regulator (Redundant) Weight Versus Power Output

they may be estimated as being 60 to 80 percent heavier than a bucking regulator. The efficiencies of a buck-boost may be taken as being the same as for a bucking regulator.

For both Figures 10.19 and 10.20, the data is given for an assumed 30 vdc input nominal. For assumptions of a different nominal input, the weight and efficiency should be modified by a correction factor which is given in Section 10.4.5. The plot of weight versus power for line regulators is assumed to follow an approximate form of,

$$W_T = C\,P^K \tag{10.4}$$

where W_T = Weight, pounds
C = Constant
P = Power Output, watts
K = Exponential Factor

The factor, K, varies with the frequency and the constant, C, used,

The values used were:

PWM Bucking Reg.; $W_T = 0.33\,P^{0.63}$

PWM Boost Reg.; $W_T = 0.13\,P^{0.64}$

The switching frequency of the regulator circuits is 6 KHz. It was found that this produces the maximum efficiency while minimizing the weight.

It is believed that the weight and efficiency predictions are relatively conservative.

10.4.3 DC to DC Converters

For line regulators, a voltage ratio, $\frac{Ein}{Eout}$ of 2 for a PWM bucking regulator or 0.5 for a PWM boost regulator, effectively marks the generally accepted limits of operation. Beyond these limits, operating efficiencies tend to fall off very rapidly. Consequently, for larger (or smaller for boost) ratios, converters are used whenever the efficiency tradeoff point is passed.

A block diagram of a typical unregulated dc-dc converter is illustrated in Figure 10.21. A square wave inverter (SWI) converter type was assumed. This is not necessarily the optimum type. However, it is a configuration whose characteristics are well known. Analysis of actual requirements might very well lead to the choice of another type of converter such as an Energy Storage Converter (ES) or a Push Pull (ES) type. These types are described fully in a previous TRW Systems study of satellite power systems conducted for NASA Goddard SFC (Reference 10.13) and also in a current TRW System study on Aerospace Power Conditioning (Reference 10.17). The theory and operation of these converters are discussed in these references.

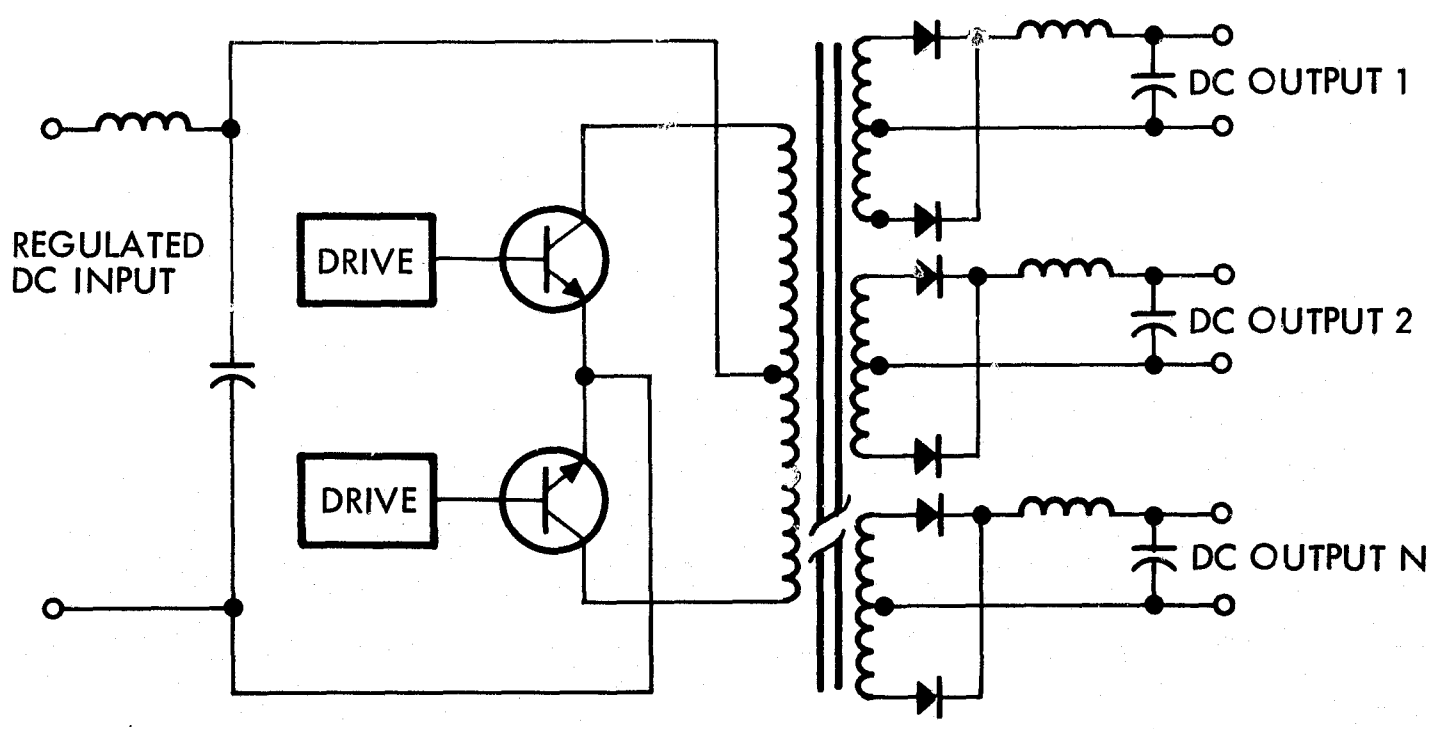

Figure 10.21 Block Diagram Unregulated DC-DC Converter

Figures 10.22 and 10.23 illustrate the estimated weight and conversion efficiency for redundant dc-dc converters. The figures include unregulated converters and pre-regulated converter combinations. As for the line regulators, the converter weights and efficiency are the result of extrapolations of previously calculated data. In general, the results are considered to be conservative. The data should be modified for other than the 30 vdc nominal input on which it was based.

10.4.4 DC-AC Inverters

Figures 10.24 and 10.25 show the weight and efficiency versus power output for 3 phase, 400 Hz, square wave inverters utilizing standby-redundant channels. The data is extrapolated and is based on 30 vdc nominal input. To provide for maximum utilization, combined forms of pre-regulator, converter and inverter are shown.

10.4.5 Correction Factors

Assuming fixed switching frequency (6 KHz), one of the larger remaining correction factors for weight and efficiency for regulators, converters and inverters, depends on the nominal input voltage. Figure 10.26 illustrates the correction factors for weight and efficiency. Whereas the efficiency is estimated to increase very little, the projected design weight is expected to be greatly affected by a significant change in the design nominal input voltage. The weight is expected to decrease steadily, reaching a minimum in the vicinity of 300 vdc input. Above this voltage an increase in output filter weights and other components is expected to cause an upturn. Since the above is intended to apply to high power (>1 Kw) level conditioning systems, where limited data exists, the predicted weights would have to be confirmed by future development tests.

Figure 10.27 shows the correction factor to be applied for power loss and voltage drop when the conductor cable temperature is varied above and below 25°C. The plot is based on the use of the formula for the resistance of standard annealed copper as a function of temperature, as given by the following relationship:

$$R_2 = R_1 \frac{234.5 + T_2}{234.5 + 25} \qquad (10.5)$$

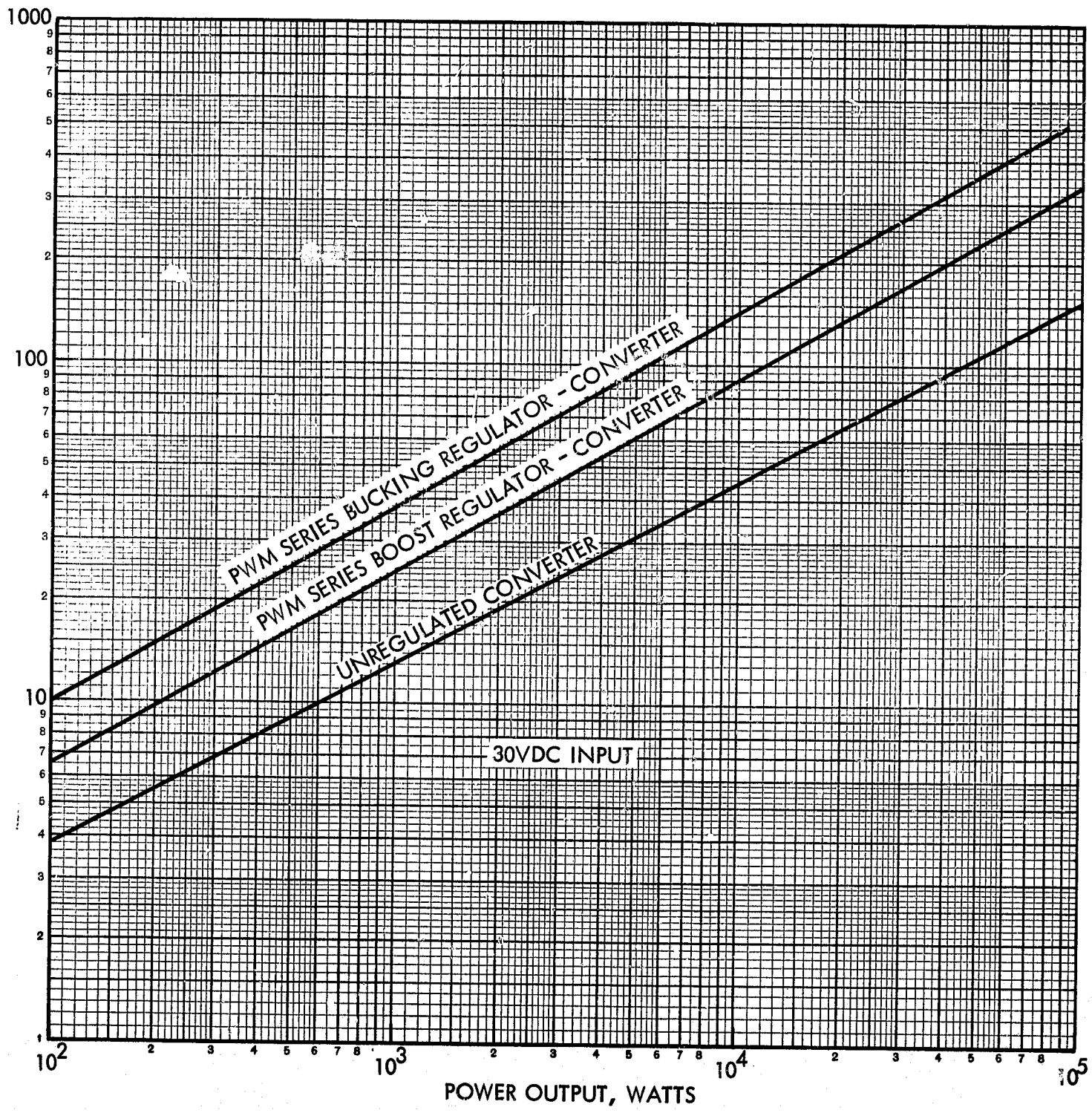

Figure 10.22 Converter (Redundant) Weight Versus Power Output

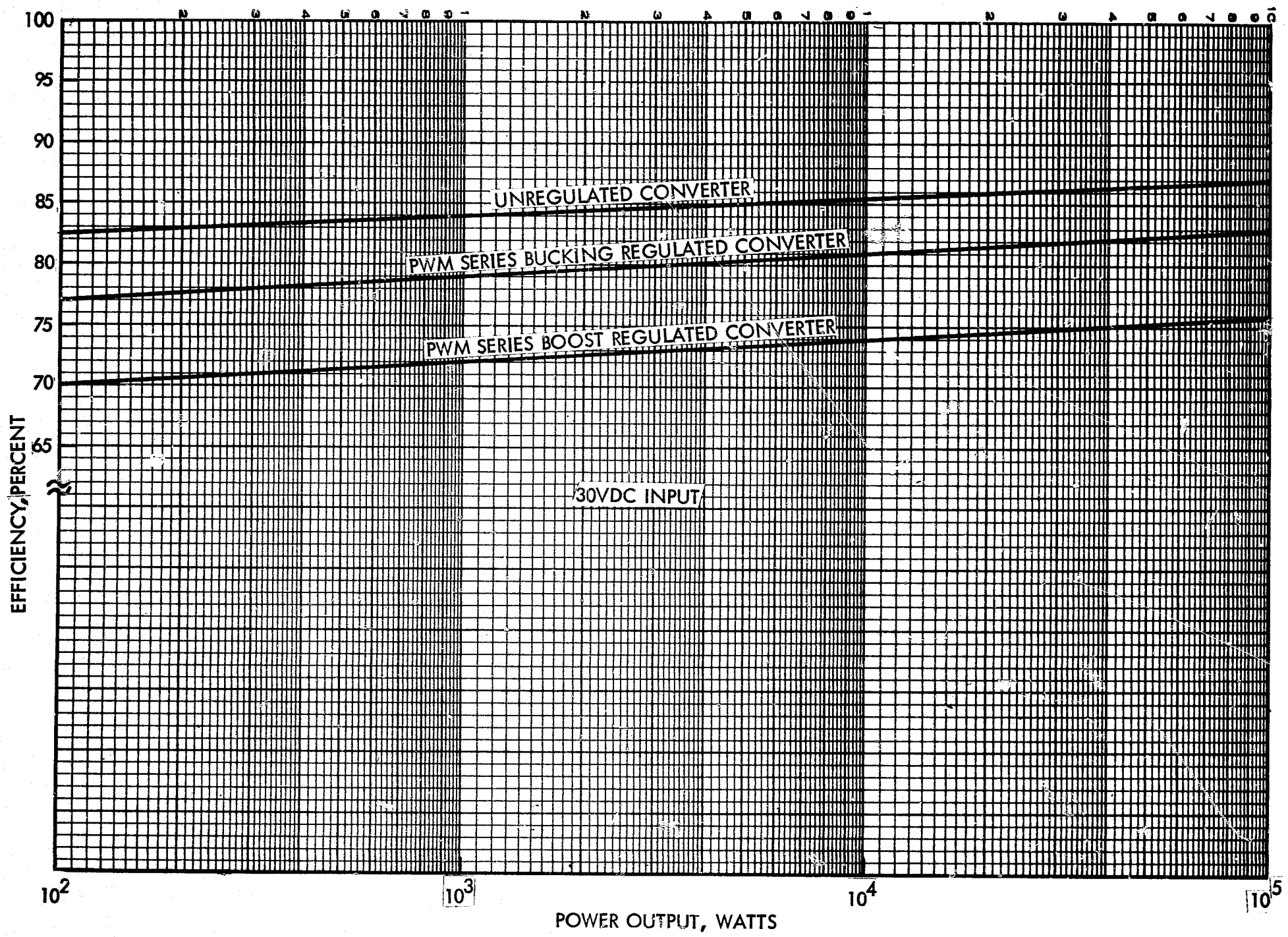

Figure 10.23 Converter, Redundant Efficiency Versus Power Output

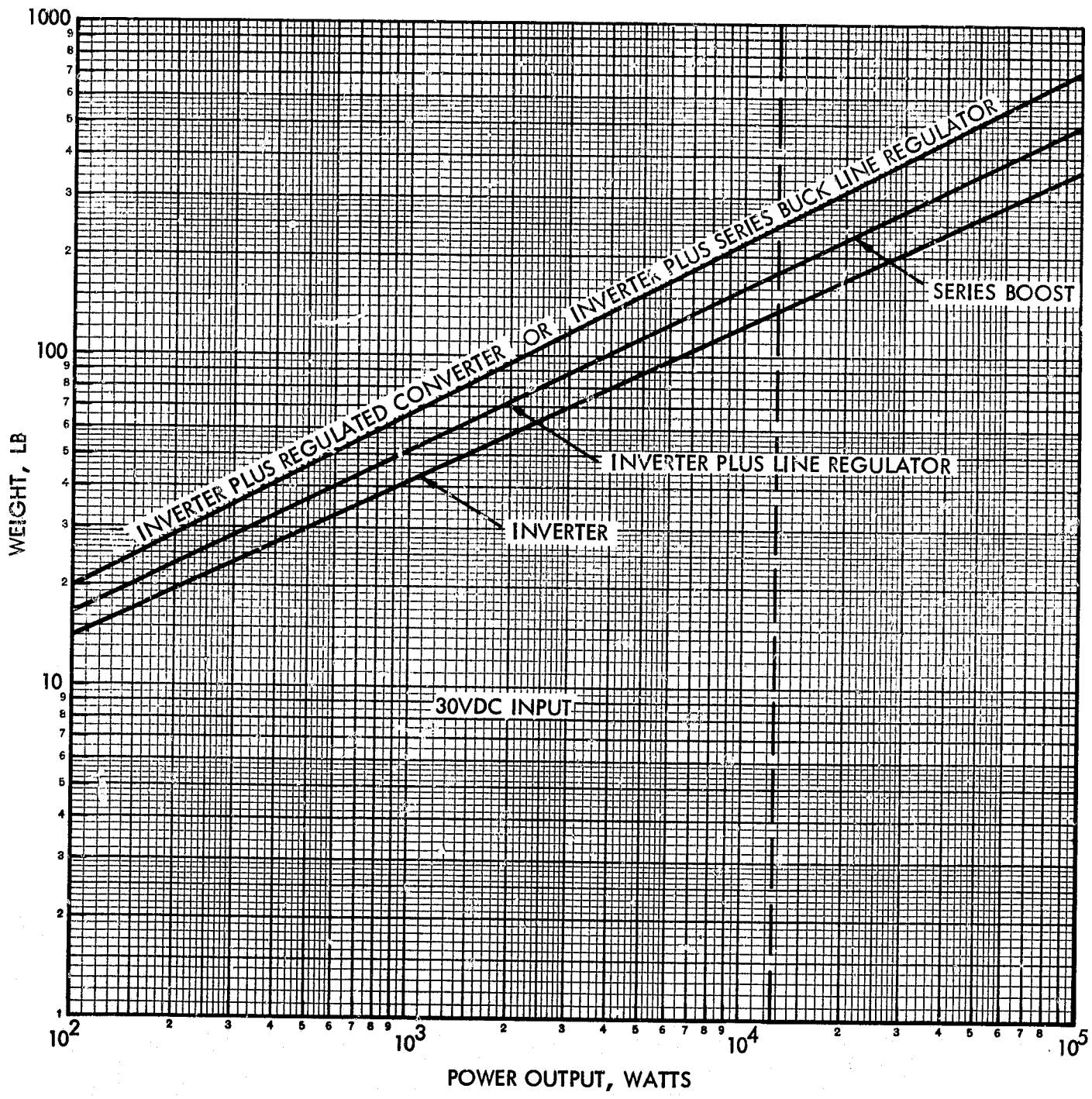

Figure 10.24 Regulator-Inverter (Redundant) Weight Versus Power Output

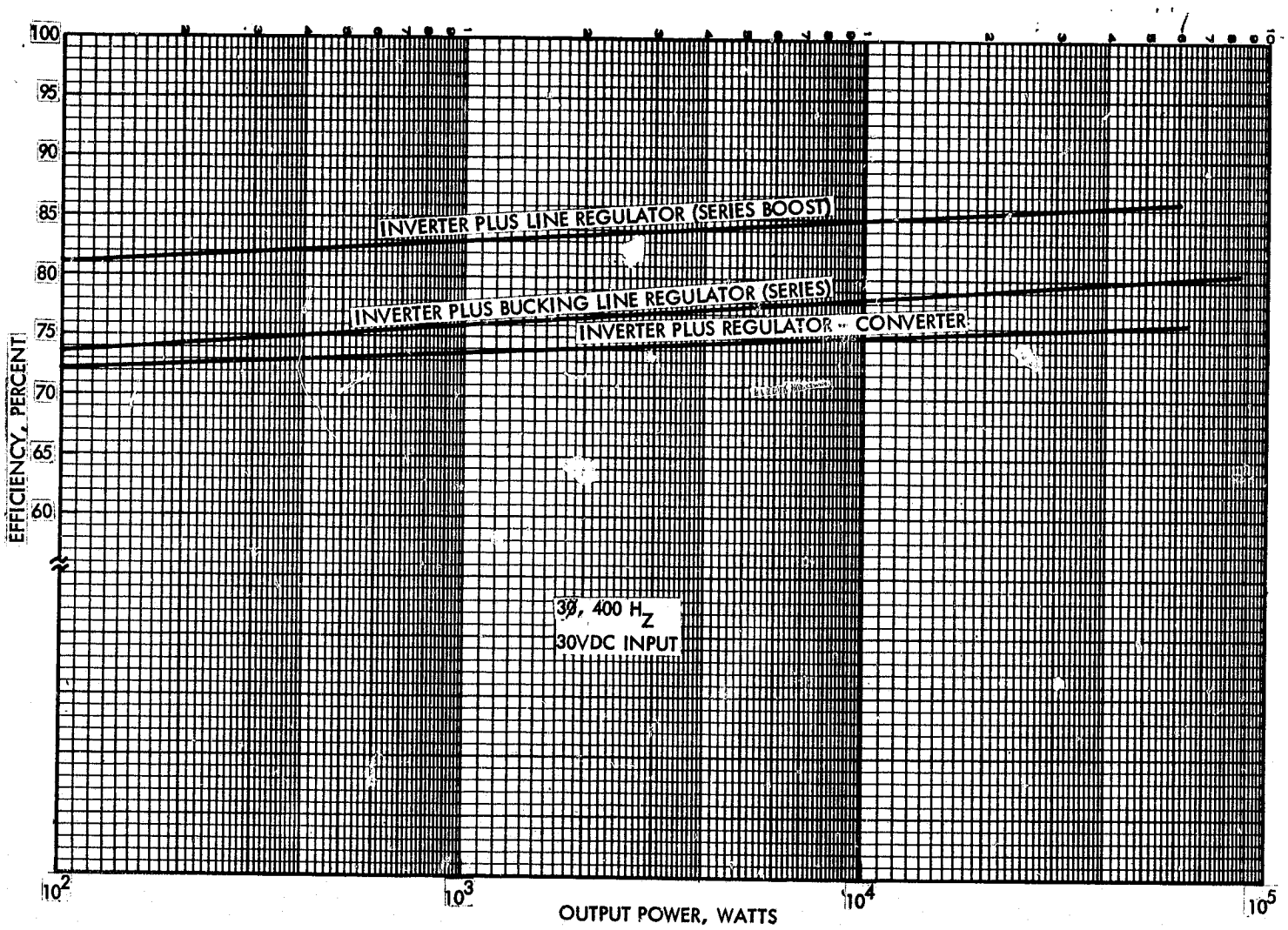

Figure 10.25 Load Power Conditioning Inverter (Redundant) Efficiency Versus Power Output

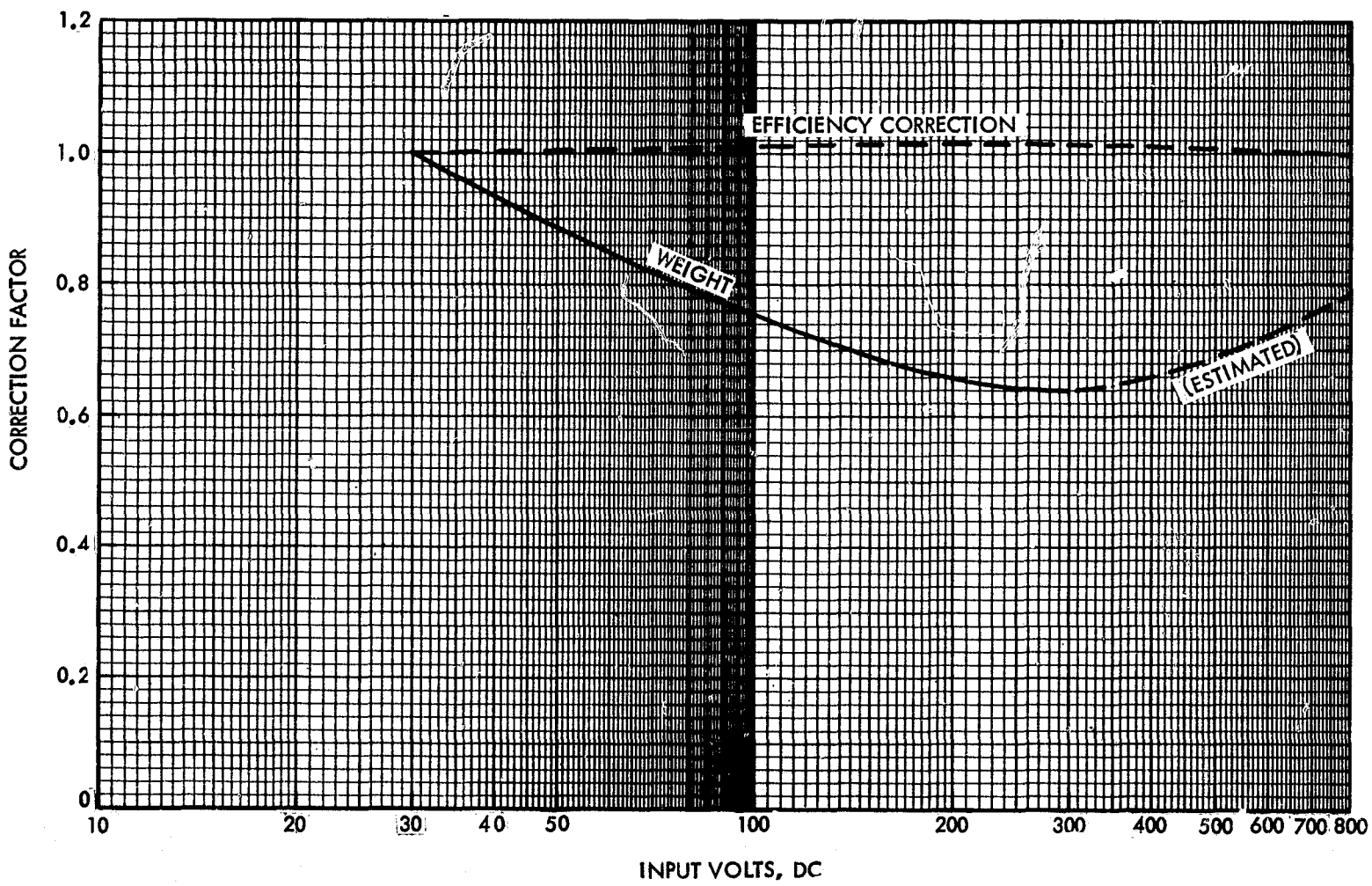

Figure 10.26 Weight and Efficiency Correction Factors for Converters, Regulator-Converters and Regulator-Inverter

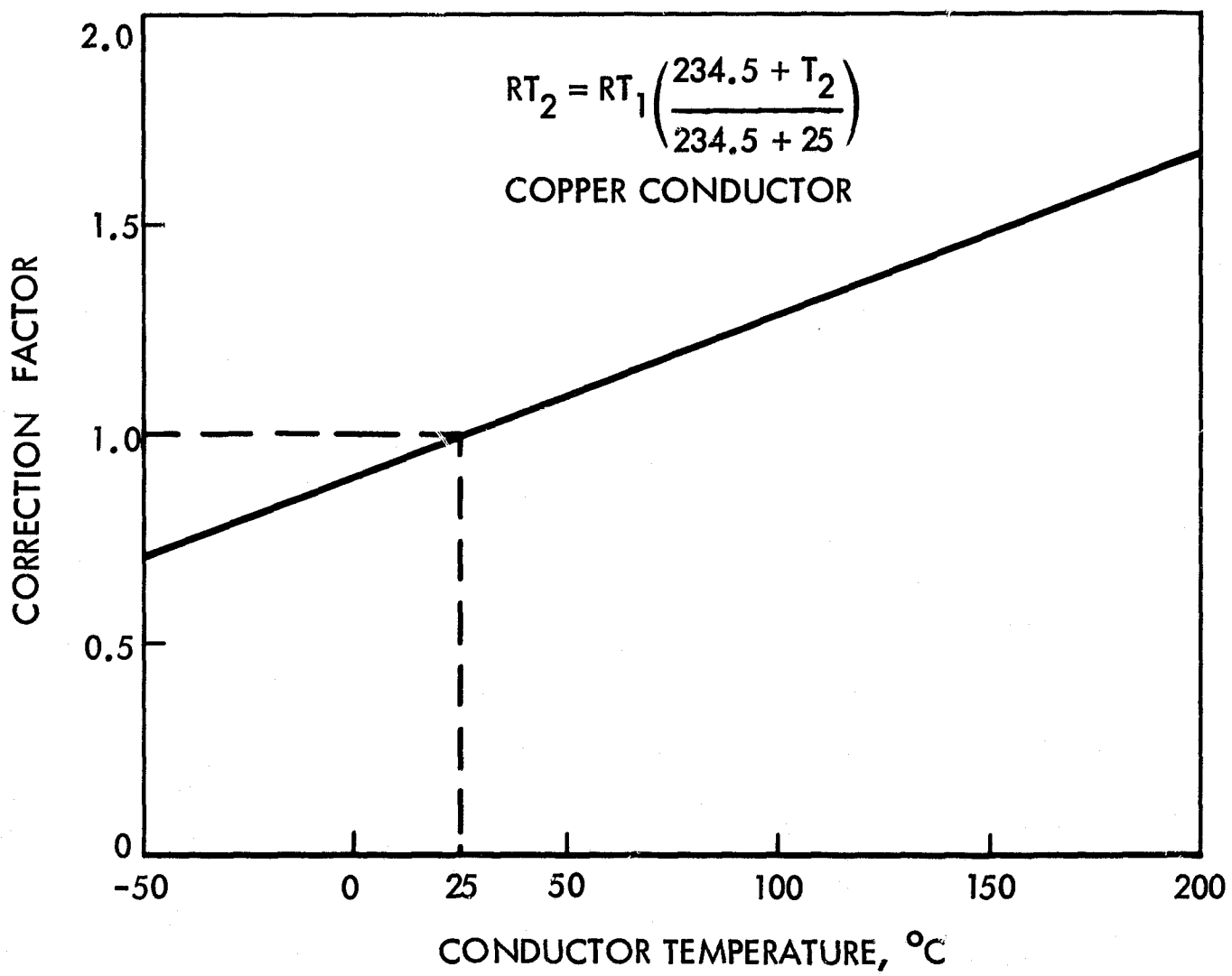

Figure 10.27 Correction Factor For Power Loss and Voltage Drop

where T_2 is the desired conductor temperature, in ^oC, and R_1 is the conductor resistance at a temperature of 25^oC, and R_2 is the conductor resistance at temperature T_2. Since both the power loss (I^2R) and voltage drop (IR) are directly proportional to the conductor resistance, the correction factor "F" formula becomes:

$$F = \frac{R_2}{R_1} = \frac{234.5 + T_2}{234.5 + 25} \qquad (10.6)$$

The correction factor applies to Figures 10.13 through 10.18 when the conductor temperature is other than 25^oC.

10.5 General System Considerations

10.5.1 Weight Tradeoffs

Figure 10.28 is an illustration of a possible layout for the candidate system, configuration 1b. For the configuration shown, the total system weight (W_{total}) comprises the weights of all power conditioning, distribution cabling and connectors, and the solar arrays. In a detail design, this would also have to include the weights of instrumentation, circuit protection thermal blocks, power switches, isolation components and possible manual type controls. Emergency operation requirements may also add to components and weight required using batteries, etc. It should be noted that the system weights given in this study were limited to the major LEPFPS components. For this analysis, these additional elements were not included but it is not anticipated that their inclusion would have any major impact on the results of this study.

The total system weight (W_{tot}), with the exclusions noted above, can be taken as;

$$W_{total} = Wt_{sa} + Wt_{cab} + Wt_{pc} \text{ , pounds} \qquad (10.7)$$

where,

Wt_{sa} = Weight of solar array
Wt_{cab} = Weight of cabling
Wt_{pc} = Weight of power conditioning

10.5.1.1 Solar Array

In general, the solar array weight is a function of various design considerations, fixed and variable, and the minimum output power re-

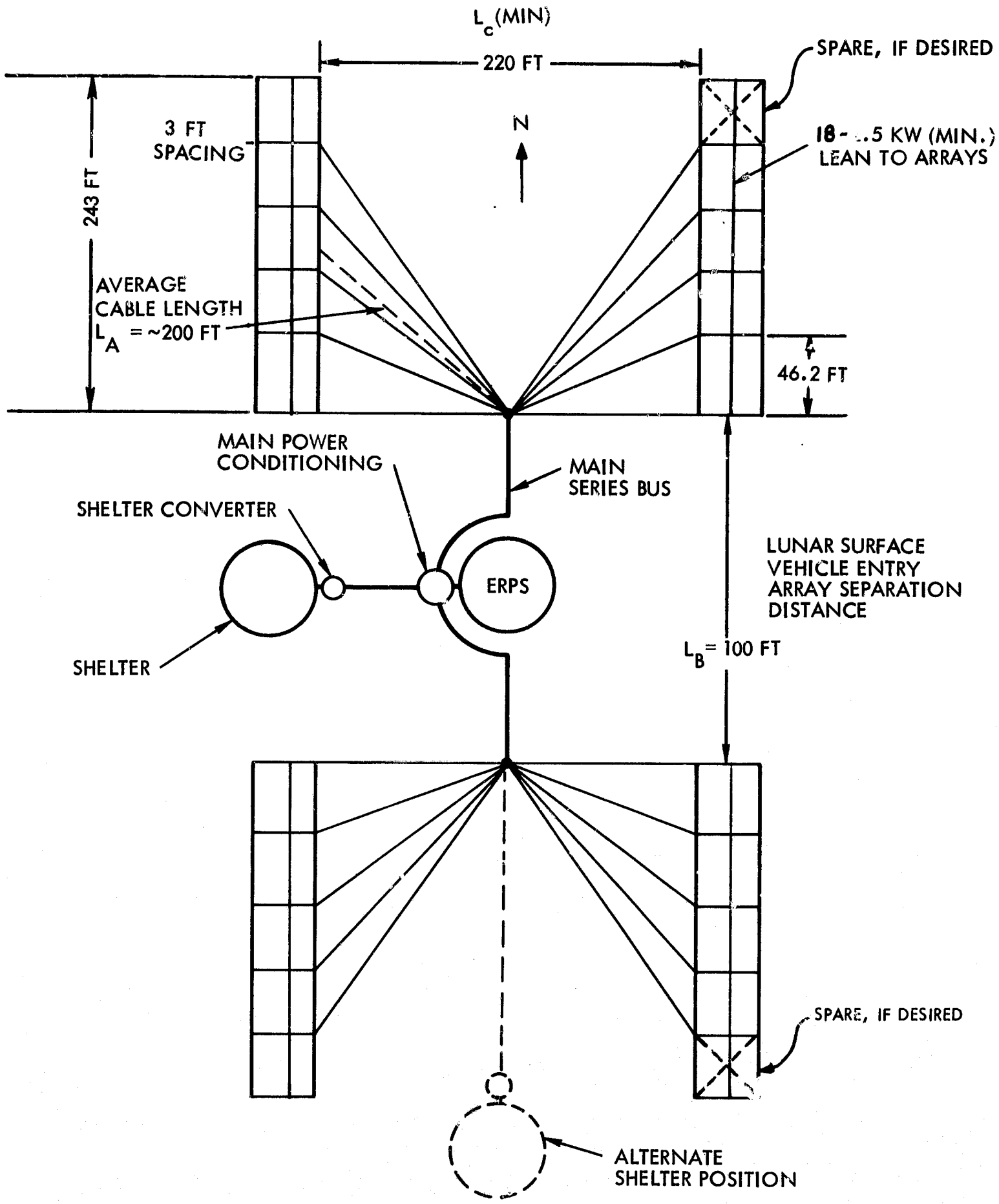

Figure 10.28 Schematic of Electric Power System for Lunar Base (45 KW-Minimum Gross Power)

quired. This may be expressed as:

$$Wt_{sa} = f(D, P_o') \qquad \text{(pounds)} \qquad (10.8)$$

where,

D = array design considerations and factors

P_o' = minimum output power required

At this point, f (D) may be regarded as a constant, A, for a given design and we are left with P_o'. P_o' in turn is a function of load power, P_o, and system distribution efficiency, η. This may be expressed as:

$$P_o' = f(P_o, \eta) = \frac{P_o}{\eta} \qquad (10.9)$$

Again P_o may be considered as fixed at, say, 36.1 Kw, the reference load. This leaves the system distribution efficiency, η, which consists of the conversion efficiency of the power conditioning system and the line losses. Thus,

$$\eta = \eta_{pc} \times \eta_{line} \qquad (10.10$$

Substituting in Equation 10.8, we determine the weight of the solar array, Wt_{sa} as,

$$Wt_{sa} = A \times \frac{P_o}{\eta_{pc} \times \eta_{line}} \qquad (10.11)$$

where,

A = Solar array design constant, pounds per kilowatt

P_o = Required load power, kilowatts

η_{pc} = Power conditioning conversion efficiency, percent

η_{line} = Line distribution efficiency, percent

If either the equivalent power conditioning efficiency or line distribution efficiency is lowered, the required array power, P_o', will be raised thus increasing the array weight. Obviously, a high system distribution efficiency is desired to minimize solar array weight.

10.5.1.2 Cable Weight

The cable weight (Wt_{cab}) is dependent on the cable sizes chosen and the total length employed. The cable size chosen is related to the line losses assumed as well as handling considerations, whereas the total length is related to the layout configuration employed and the total power to be transmitted. Figures 10.13 through 10.18 were employed in the choice of a particular line size.

In choosing a line size for a given length, the incremental increase in solar array weight resulting from line losses must be considered. For example, given P_o = 20 Kw, L_a (see Figure 10.27) = 100 ft, and E = 200 vdc, if a 21.6 pound line weight is chosen (see Figure 10.15), the estimated line losses are about 820 watts. If a 43.2 pound line weight is selected, the loss is halved to 410 watts (see Figure 10.16). In this case, 410 watts of array power has been traded for 21.6 pounds of increased cable weight. If the array specific weight is 100 lb/Kw or greater, the decrease in required array weight is at least 41 pounds. Therefore, the system weight tradeoff gain was at least 41-21 or 20 pounds. To the extent that the array specific weight or design constant, A, in equation 10.11 is greater than 100 lb/kw, the magnitude of the weight saving increases.

In general, it is true that for low line voltages (< 200 vdc), a small decrease in cable weight is usually more than offset by an increase in array weight. For any given length, power requirement, and line voltage, there is a line size which minimizes line losses so that

$$\uparrow \Delta \, Wt_{cab} = \downarrow \Delta \, Wt_{sa}$$

where, $\uparrow \Delta$ = increasing weight increments

$\downarrow \Delta$ = decreasing weight increments

This point is reached only after iteration for any given design. Because of the number of variables (e.g., length, resistivity, line voltage, power transmitted, temperature), it is not generally obvious as to which line size should be used for any given power level or configuration without extensive computations.

10.5.1.3 Power Conditioning Weight (Wt_{pc})

The power conditioning weight is a function of the power processed, the input and output voltages, and the number of outputs required. The foregoing assumes a constant range of acceptable temperatures, duty cycles, and redundancy. The predicted weights are shown in Figures 10.20, 10.22 and 10.24, for the types of power conditioning assumed for the candidate configuration.

The power processed, P_p, is not necessarily the same as P_o, the total load power, or P_o', the array output power. It depends on where the particular unit is placed in the configuration. In general, the power

processed, P_p, will equal the fraction of load power it has to deliver plus line losses between the load and the unit. To this it has to add its own losses. Or stated another way,

$$P_p = P_{load} + P_{line} + P_{internal} \tag{10.12}$$

Even if the conversion efficiency is high ($P_{int.}$ is low), the line losses may be high and greatly increase converter weight. However, from a preliminary examination it was concluded that an increase in converter weight would be negligible compared with the effects of converter inefficiency on solar array weight.

10.5.1.4 Summary of Weight Tradeoffs

Table 10.9 illustrates typical expected specific weights for power system elements. It should be noted that the array specific weight is by far the largest factor contributing to total LEPEPS weight, regardless of the array type. The influence of system distribution efficiency, η, is such that it should be possible to estimate total power system weight to within 20 percent of the detailed calculated value, by using equation 10.11, and a realistic value of the array design constant, A, when the total load power, P_o, and the system distribution efficiency, η, are known.

The obvious conclusion is that system distribution efficiency is a critical system weight tradeoff factor and should be maximized to produce a minimum weight design.

Table 10.9 Typical Specific Weights for Power System Elements

Item	Typical Specific Weight, Lb/Kw
Leanto Solar Array (Note 1)	157
Oriented Solar Array (Note 1)	92
Flat Solar Array (Note 1)	110
Cable, 6 Parallel Wire (No. 20 AWG)	≈2 lb/kw per 100'
Line Voltage Regulator (Note 2)	10
Line Regulator - Converter (Note 2)	15
Regulator - Inverter (Note 2)	20

Notes: 1. Using 45 kw minimum power output
2. Estimated at approximately 10 kw load

10.5.2 Cost Tradeoff

The cost of the power distribution system is small when compared to the total R&D cost of a solar array. Where the solar array may cost from $ 0.5 x 10^6 to $\$10^6$/kw, the cost of power conditioning for converters and regulators in the power range of 10 to 50 kw is estimated to be from $\$10^4$/kw for fabrication only to as high as $\$5 \times 10^4$/kw including development. The estimated fabrication cost of the cabling is relatively insignificant although development costs may be high.

The estimated development and fabrication costs for the solar arrays over-shadows the cost of all the other power system hardware and constitutes by far the greater (>80%) part of the system cost.

In the example of cable weight versus solar array weight tradeoff as given in paragraph 10.5.1.2, 410 watts of solar array power was saved and traded for 21 pounds of additional cable weight. Whereas the additional cable may cost a few hundred or even thousand dollars, the solar array cost saved is in the order of half a million dollars. This again underscores the importance of maximizing system efficiency to achieve minimum system cost.

The entire cost of power conditioning development may then be more than offset by an increase of a very few points in system efficiency. A development effort to produce a high efficiency system is obviously cost effective and should be given major emphasis in any program development planning.

10.5.3 Reliability

For this study, reliability is discussed only from the standpoint of providing guidelines for the LEPEPS. For power conditioning equipment, reliability usually increases as the following parameters change:

- Increases efficiency and redundancy
- Decreased operating temperature range, EMI requirements, ambient temperatures, number of outputs, parts count, and power dissipation level

For solar cell arrays, reliability usually improves as the following parameters change:

- Increased radiation protection
- Decreased temperature extremes

- Optimum series parallel cell interconnections is approached
- Open-cell circuit protection is incorporated

Whereas environmental extremes are imposed by the lunar surface system application, items such as parts count, efficiency, and redundancy are not. They are a function of design decisions made as a result of trading off weight, size, and cost against the highest reliability that is computed for a given arrangement. Such a tradeoff was beyond the scope of this study. However, the following general comments are applicable.

By selecting proper parts for this application and using appropriate quality control screening, and adequate thermal, mechanical, and electrical derating, the possibility of a failure can be virtually eliminated except for potential wearout failure modes. When redundancy techniques are properly implemented, the effect of unit wearout failure may be reduced to permit acceptable operation under forseeable conditions of operation. (See Section 9.4 for discussions of techniques for achieving solar array reliability.)

The presence of astronauts on the moon, who are available for system maintenance, is both a great advantage and a minor hazard. The advantage exists in that failed modules can be removed and repaired by the astronaut in the lunar shelter where even failed parts such as resistors or relays could be replaced. Such an advantage does not exist for present day unmanned spacecraft. The minor hazard is related to human fallibility. For example, if module replacement is improperly implemented, this could nullify or counter the presence of redundant channels due to short-circuits, reversal of polarity, etc. These factors indicate the necessity for establishing a design approach which would result in built-in reliability provisions. In view of the foregoing, the ground rules for the approach to Lunar Power System reliability should be formulated during the Program V implementation planning phase to insure a uniform approach for all mission oriented systems.

The method of utilizing parallel operating channels for all major power circuits was assumed for the purpose of defining a reference power system. Figure 10.29 illustrates a standby redundant configuration such as would be used for regulators. There are two parallel channels

depicted but only one is operating at a given time. The configuration requires circuitry to sense a failure in the main operating channel and also a switching element to transfer from the main channel to the standby channel.

The equation for probability of survival is,

$$P_s = 1 - (1-P_1 P_{sw})(1 - P_2 P_{sw}) \qquad (10.13)$$

where,

P_1, P_2 = reliability of each channel

P_{sw} = reliability of sensing and switching elements

The switching out of the failed channel and the energizing of the standby channel will produce an output transient during the switching interval. However, the use of line filters will act to suppress this effect. A probability of survival of 0.99 was assumed as the goal of the one year duration mission for each major system element. The choice of 0.99 was selected as an achieveable value and utilized in the absence of established ground rules or detailed tradeoff analyses during this phase of the study program.

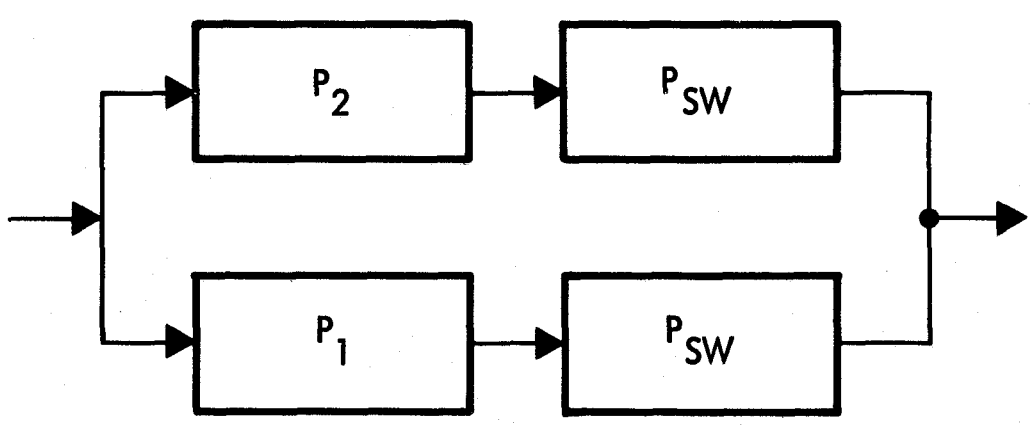

Figure 10.29 Standby Redundant System Reliability Model

10.5.4 Volume and Shape

The minimum volume of electronic equipment is usually determined by the quantity and type of components and parts to be packaged. The heat to be dissipated and also the mode of heat dissipation - whether by radiation or conduction, or both - greatly influences the shape as well as the volume of the equipment package.

After considering a sphere, cylinder and rectangular parallelpiped, the latter design was chosen for the candidate system design because it has the largest surface area per unit volume. It was also a convenient shape for packaging electronic components. Although the rectangular parallelepiped is the perferred shape for the reasons given above, final design proportions were not established during this conceptual study phase. If active thermal control such as circulating fluids are used, it might be desirable to maximize the mounting base area to provide for adequate cooling. On the other hand, dissipation of power by radiation would necessitate maximizing the radiating surface area. These considerations are discussed in section 10.5.5 on thermal control.

To provide a basis for volume estimates, an average equipment density of between 0.03 and 0.05 lb/cu. in. was used for the power levels indicated. In the absence of any definite thermal design specifications, a passive thermal control method using louvers and reflective paints to control radiated heat was assumed. Thus, for the candidate design, the mounting base area of each equipment package was not maximized but an approximate cube shape was assumed. This shape may have to be revised depending upon the results of a detailed thermal control analysis.

The shape of the solar cell panels are dictated by the type of array chosen and is discussed in sections 4.6, 4.7, and 4.8 of this report. The size and shape of electrical connectors and any items requiring handling by a suited astronaut on the lunar surface is governed largely by human factors considerations. Two of these factors are, typically, shape recognition and ease of manipulation (grasping).

The major considerations of thermal control, handling both on the Moon and on Earth, and maintenance requirements, are basic inputs for the design of the electrical power equipment. A change in the

emphasis in any one of these areas can greatly influence equipment volume and shape. It is essential that future studies give careful consideration to these factors.

10.5.5 Thermal Control

The baseplate temperature of power conditioning electronic components should be maintained in the range of -20°C to +55°C during lunar surface operation. Depending on the type of components in a given equipment box, it is very likely that the non-operating baseplate temperatures could be allowed to drop far below -20°C during the lunar night without incurring any damage. For example, storage temperatures of -65°C are acceptable for silicon rectifiers. However, the baseplate temperature would have to be brought well up into the operating range before the equipment could be used with safety. Damage to the components could be caused by application of power when at temperatures below the operating range. Hence, thermal pre-conditioning is essential before start-up of the LEPEPS.

It was previously assumed (paragraph 10.2.3) that all power conditioning and control units were located on the lunar surface and not in either the ERPS or shelter modules. When considering the options for thermal control, a number of alternatives become apparent. These are:

(a) Complete passive thermal control for each unit

(b) Complete active thermal control for each unit

(c) Combinations of active and passive thermal control

Furthermore, it is also possible to integrate the LEPEPS system with the ERPS or shelter thermal control systems. Use of the ERPS system could entail providing for a connection with a coolant fluid line. Where the distance between the power conditioning equipment and shelter is on the order of hundreds of feet, this may not prove to be desirable. However, if located in close proximity to the ERPS or shelter module, the integrated approach should be given serious consideration.

A previous TRW Systems study concerned with a Lunar Surface Electric Power Subsystem (Reference 10.15) concluded that a passive thermal control system consisting of surface mirrors, white paint surfaces, and louver assemblies such as used in Pioneer 6, would be effective. In addition, a sun shade concept to deal with possible migratory dust contamination of the mirrors, etc., was considered. The

The existence of migratory dust in appreciable quantities would be likely to degrade thermal control surfaces to some degree. Another concept which could be used either to supplement or replace louvers is the TRW Systems thermal switch. This consists of a small stainless steel bellows, the exterior of which is exposed to a sealed fluid reservoir mounted on a baseplate. The baseplate is fastened to the component mounting panel whose temperature is to be controlled. Fluid expansion caused by an increase in box temperature extends the bellows to close a low resistance thermal conduction path between the baseplate and the heat sink. Concepts such as the foregoing are recommended for consideration in detailed design studies of power conditioning elements for lunar surface applications. The thermal control of the solar panels would be passive and effected by the proper use of reflective surface coatings, skirting, and other techniques as discussed in section 8.2.

The thermal dissipation of the cables can be brought to the point where losses (see Figures 10.15, 10.16, 10.17, and 10.18) are approximately 1 watt per foot of length with 50 kw transmitted for the main power bus. This is the equivalent of approximately 15 watts per square foot of wire surface, or 16 mw/cm^2. However, the cable operating temperature can be allowed to go to +150°C, if necessary, although this would greatly increase the cable electrical resistance and its losses (see Figure 10.27). The desired cable temperature is +25°C or below. Thus, for thermal dissipation reasons in addition to personnel safety considerations, it would be desirable to support the cables above the lunar surface in a metal channel. The metal channel surface could be designed to control the cable thermal dissipation. The power conditioning elements could be passively controlled in a similar manner by proper design of the equipment enclosure.

Generally, it is impractical to design a thermal control system for each electric power system element without considering the needs of the shelter and ERPS and the possibilities for integration with their thermal control systems. An overall thermal control system analysis for the entire lunar base should be conducted to determine the most system effective approach.

10.5.6 Instrumentation

The requirements for power system instrumentation was beyond the scope of this study. Their selection is intimately related to the shelter and ERPS module requirements. Because of this, only preliminary list of instrumentation items for the electric power system was considered at this time.

Table 10.10, lists typical power system instrumentation requirements. A more detailed analysis is required to establish the total system needs, as well as the range and accuracy of the individual instruments.

Table 10.10 Instrumentation for Electric Power System

No.	System Element	Item Measured	Where Displayed
1	Solar Cell Panel	Temperature, Voltage and Current Output	Shelter, Earth
2	Main Series Bus at Array Cable Input Block	Temperature, Voltage and Current	Shelter, ERPS, Earth
3	Main Power Conditioning Box	Baseplate Temperatures, Input and Output Voltages Current and Frequency Status of Relay Switches	Shelter, ERPS, Earth
4	Shelter Converter	Baseplate Temperature, Input and Output Voltages and Current. Status of Relay Switches	Shelter, Earth
5	All Cables at Selected Points	Temperature and Voltage	Shelter, Earth

10.5.7 Fault Protection

It was assumed that fault protection as incorporated in the electric power system should be automatic. It would be designed to function long enough to allow an astronaut to repair or replace a damaged element. It could also be designed to permanently repair the fault. For the implementation of the standby series regulators and other power conditioning elements, attention must be paid to the inclusion of failure detection and switching circuits.

Standby redundance assumes the presence of an out-of-tolerance condition as a result of part failure. As a result it may prove necessary to sense the input and outputs of a given power conditioning element for an undervoltage or overvoltage condition.

In the event of a direct short circuit at the input terminals of a given element, a large overload can be imposed on elements supplying power to the failed element. For example, a short circuit in the transfer and circulation pump converter would impose an overload on the main dc branch series regulator. It is possible to protect against this occurrence by oversizing and derating. However, this tends to penalize element weight and efficiency. Therefore, current-limiting circuitry is preferred over element oversizing to protect against overloads. This would be done by using fuses.

The incorporation of short time delays is essential for the implementation of standby redundance channels. This is necessary to guard against the event of transient conditions. Design tradeoffs are necessary in the design of power conditioning using time delays in fault removal or standby redundant switching circuitry. In general, the aim should be to minimize the time delay to allow for speedy reaction to an element failure and switching to the standby channel.

If parallel non-switching circuits are used, they should be sufficiently derated to allow for a great increase in load in the event of a single circuit failure.

Recommendations for fault protection are dependent upon a detailed analysis of specific failure modes for all power system elements. The results of such an analysis would reveal areas where fault protection is required. Depending on the ground rules assumed for reliability and astronaut participation in equipment repair and replacement, detailed fault protection schemes can then be devised. The use of fuses, time delays, out of tolerance voltage and current sensors, and failure detection and switching circuits, was given as an example of the methods intended for consideration. A comprehensive failure modes and effects analysis must be conducted prior to the finalization of the LEPEPS design.

10.5.8 Emergency Operation

The definition of emergency operation used was that concerned with insuring operation of the life support power supply in the event of a system failure where power from the solar arrays to the shelter is cut off.

It is recommended that the major share of emergency power be furnished by fuel cells permanently connected to the shelter-regulated 28 vdc bus. To allow the fuel cells time to come up to full operating temperature, it is suggested that high power Silver-Zinc storage batteries be used and maintained in the fully charged condition. These batteries would provide power as soon as the voltage on the regulated 28 vdc shelter bus dropped to a certain level, say 26 vdc.

In order to charge and maintain the batteries in a charged condition, one approach would be to use a boost charger feeding off the 28 vdc bus. It would be necessary to use a boost type charger if the batteries were to discharge directly to the 28 vdc bus at a voltage no lower than 28 or 27 volts. Other similar techniques are also possible. The use of the battery/fuel cell emergency power system requires the incorporation of an undervoltage sensing and switching circuit for the shelter bus. When the life support system is not in use by the astronauts, i.e., during the lunar base dormant period, the emergency operation circuit could be deactivated.

10.5.9 Overall LEPEPS Criteria

The preceding discussions in Sections 10.5.1 through 10.5.8 have led to arriving at several conclusions regarding the LEPEPS. A summary of these findings are listed below.

(a) The system distribution efficiency, η, is of significant importance and should be maximized to achieve a minimum weight design.

(b) In view of the considerable impact on solar array cost, considerable development effort is warranted to produce a high efficiency distribution system.

(c) Ground rules for the approach to LEPEPS reliability should be formulated consistent with overall mission objectives and constraints.

(d) Criteria for thermal control and handling should be studied in greater depth, after more detailed mission ground rules have been formulated.

(e) Thermal control analyses should be performed for the overall lunar base on a fully integrated basis.

(f) A detailed study of fault protection should be performed only after a detailed failure modes and effects analysis has been performed on an overall electric power system (LEPEPS, SEPS, Telemetry, Instrumentation, Emergency Power, etc.).

(g) Emergency operation utilizing batteries and fuel cells to provide emergency power to the shelter 28 vdc bus should be studied in greater detail and its impact on astronaut survivability determined.

10.6 EXAMPLE OF SYSTEM SYNTHESIS

10.6.1 Solar Array Type Considerations

Figure 10.30 illustrates the three solar array types discussed in detail in Sections 4 and 8 of this report. The candidate array types considered were:

- Leanto
- Flat
- Oriented-skirted

The tradeoffs generally considered for these solar array configurations included output power characteristics, total area, weight, cost, complexity (reliability), ease of assembly and maintenance. For the purpose of depicting a system synthesis example, the key criteria for comparison was taken to be the output power characteristic. Figure 10.31 shows typical, albeit somewhat idealized, output power characteristics for the three array types. In calculating the minimum active solar array area required, a load power level of 36.1 kw (for Figures 10.31a and b only) and a system distribution efficiency of 80 percent was used. The dashed line depicts the approximate load profile while the heavy black line represents the maximum unconditioned power output into a matched load plotted against the time of lunar day.

Both the lean-to and the oriented array output power characteristics are compatible with the constant 36.1 kw load power profile

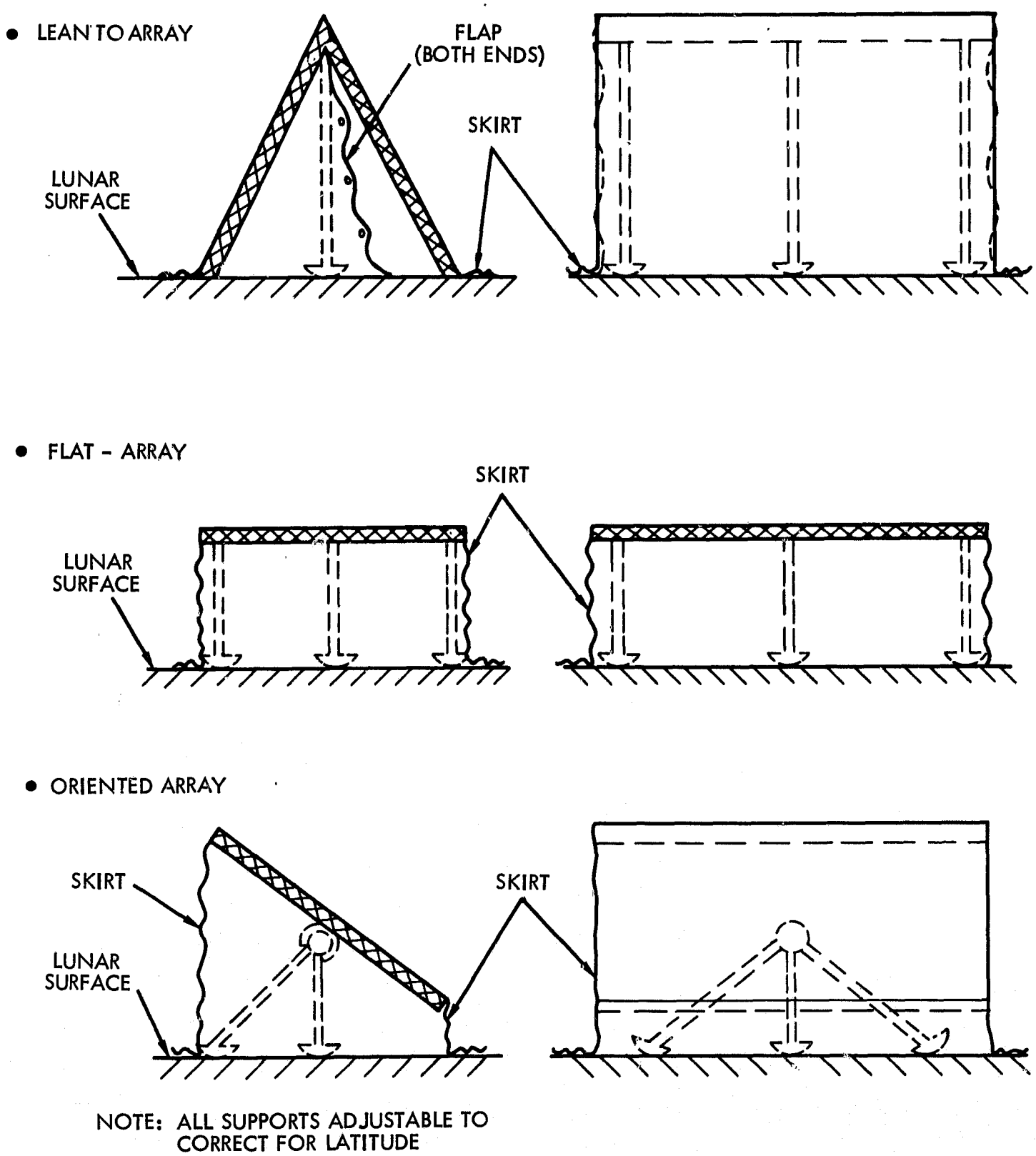

Figure 10.30 Candidate Solar Array Configurations

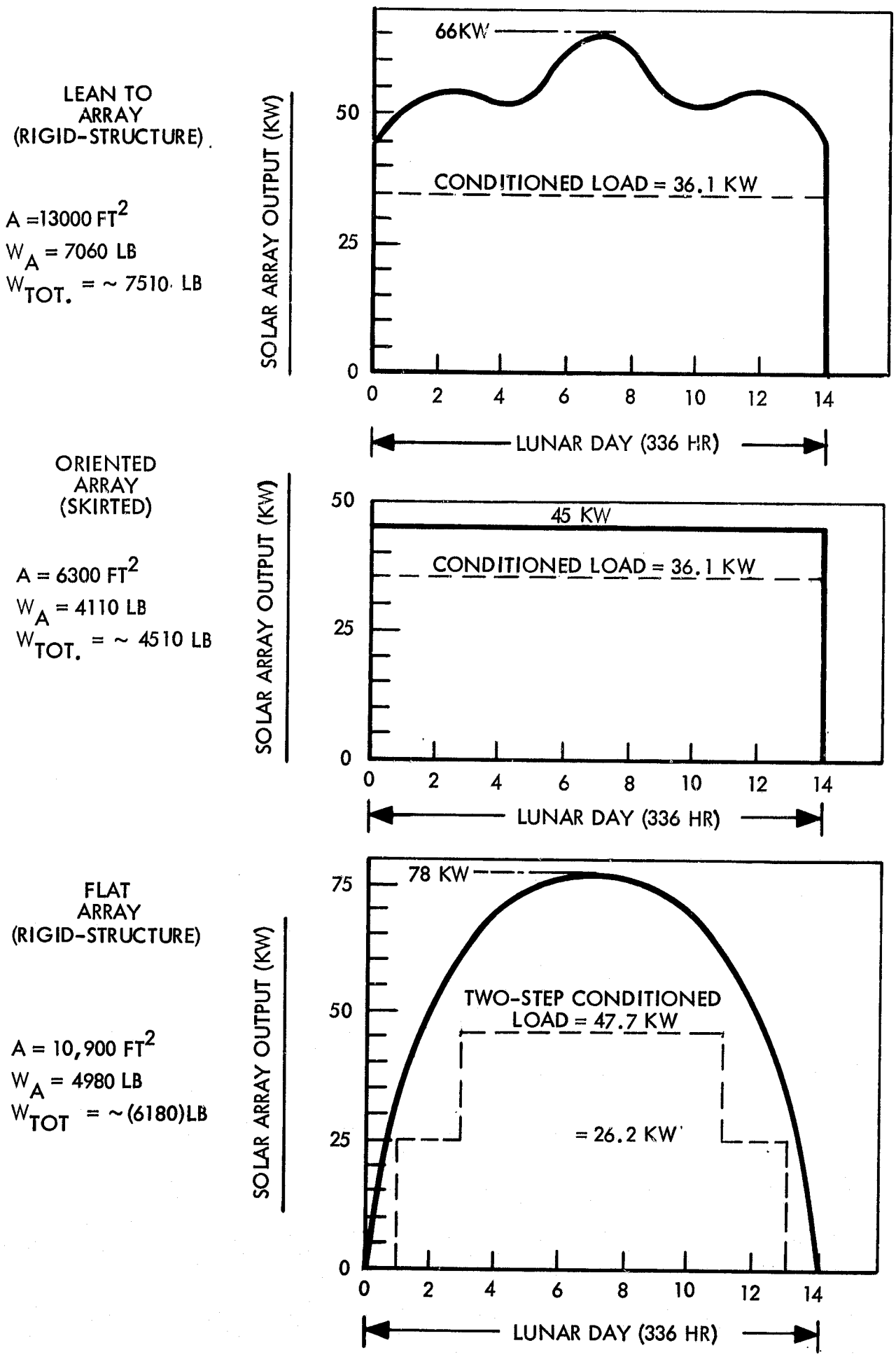

Figure 10.31 Candidate Solar Array Gross Output Power Profiles

assumed (see paragraph 10.2.2). The closest match is provided by the oriented array.

In the event a stepped load profile was chosen, a flat array could also be considered (see Figure 10.31c) since its sinusoidal output power characteristic provides a good match in this case.

To facilitate this discussion, the leanto array configuration was selected as the example to be used for system synthesis. This preliminary choice should not necessarily be interpreted as constituting the recommended selection for the Program V mission. A more detailed discussion of solar array selection is provided in Sections 4, 8, and 9. The limitations of this choice are obvious from an inspection of Figure 10.31a. This output power profile indicates that the full output of the solar array cannot be utilized and that the excess power generated over the required 45 kw (for an 80 percent efficiency) would have to be dissipated. Except at the terminators (lunar sunrise and sunset), the absence of a matched load will require that the maximum output power not be generated by the solar array. This excess power would have to be dissipated in the array voltage output controls and also in the array itself by an increase in the array equilibrium temperature.

The synthesis of a typical power system using the leanto solar array configuration is discussed in Section 10.6.2.

10.6.2 Synthesis of Configuration Using Leanto Solar Array

10.6.2.1 Synthesis Parameters and Method

Figure 10.32 is a block diagram of power system configuration 1b of Figure 10.11, modified to include a separate converter for the transfer and circulation pumps. The total load is taken from Table 10.6 and is 36.1 kw $\pm$ 1.3 kw. This was used as the baseline load profile, but the approach is equally applicable to other power levels. The variables considered were,

(1) Cable Lengths L_A and L_B (see Figure 10.28 for layout)

(2) Unregulated dc Bus Voltage of 50 vdc to 500 vdc

(3) Cable Temperature of -50°C to +200°C

(4) Load power: 10 to 70 kilowatts

For this example of system synthesis, variables (1), (3) and (4)

were fixed and variable (2), bus voltage was allowed to vary. The system constants selected were based upon a configuration that could meet the Program V mission requirements (see Figure 10.28) and are as follows:

(1) Cable Length L_A from array to connecting point = 200 ft

(2) Cable Length L_B, Series bus length = 100 ft

Cable Length L_C, Shelter line length = 300 ft

(3) Cable Temperature + 25°C

(4) Load Power 36.1 kw

The effect of variations in parameters (1), (3) and (4) on overall power system characteristics is treated in Section 10.6.3. Thus, with the baseline power system layout and electrical configuration identified, cable lengths and temperature levels selected, and a load power level assumed, it was now possible to calculate total system weight as a function of unregulated bus voltage.

The method used was to start with the load and work backward to determine the solar array output power requirements by calculating the power losses and element weights. The minimum required array power was then found by adding the load power to all of the system losses. This was done for every unregulated bus voltage increment over a range of 50 vdc to 500 vdc. Using equation 10.8 (paragraph 10.5.1) the weight of the solar array was then calculated. The weight of the total system at each unregulated bus voltage was found by adding the calculated cable and power conditioning system weights to the solar array weight.

10.6.2.2 Calculation of System Weight

The following is a summary of the results found when Figures 10.13 through 10.28 are used to calculate system weight.

A. Shelter Converter + Unregulated Converter

Output Power = 3.0 Kw

Input Voltage = 200 vdc (fixed)

Output Voltage = 28 vdc

Converter Weight (corrected) = 15 pounds

Converter Efficiency (corrected) = 0.86

Power Loss = 0.49 kw

Input Power Required = 3.49 kw

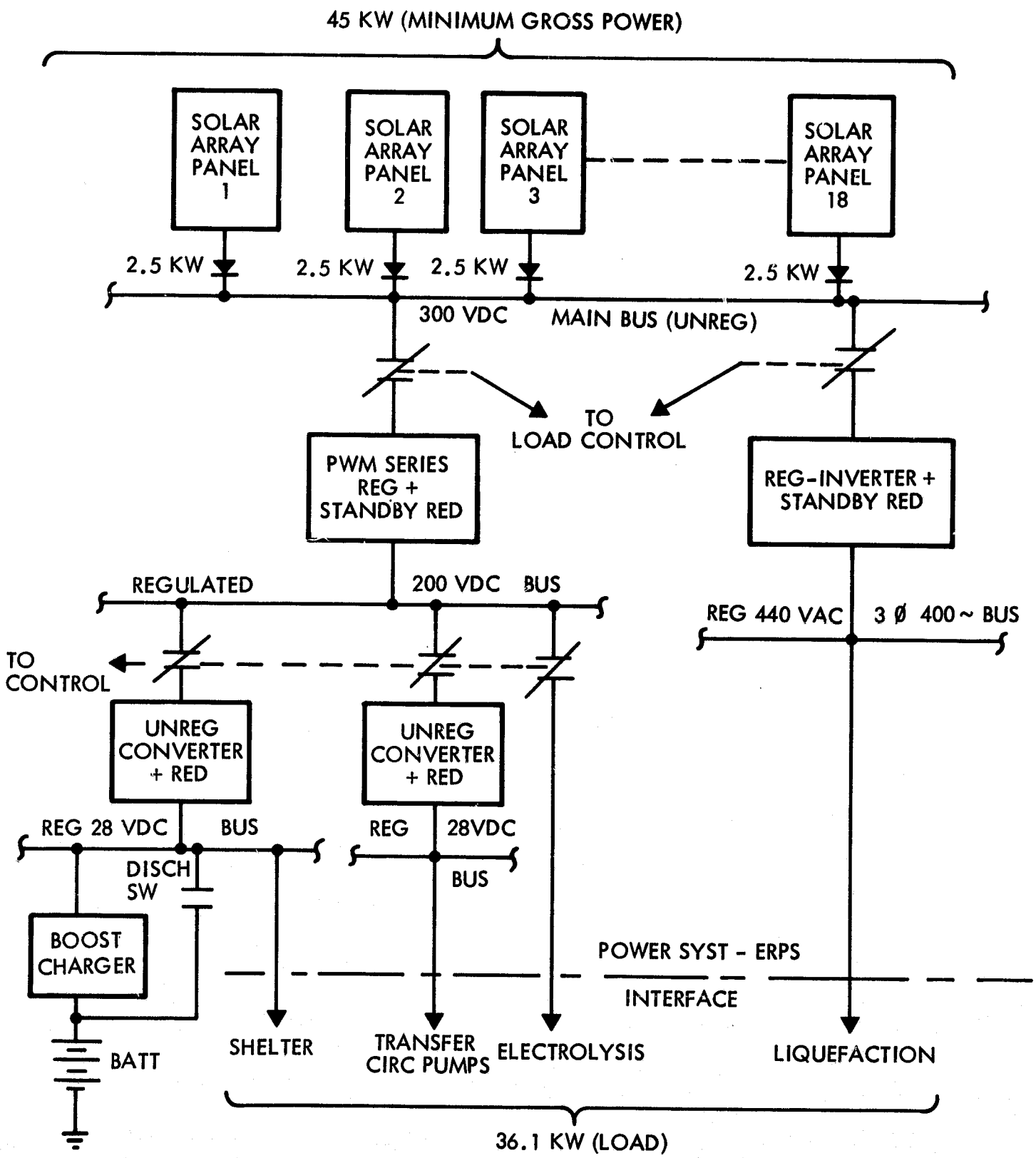

Figure 10.32 Block Diagram of Lunar Surface Power System (45 kw Leanto Configuration)

B. Shelter Line from Main PC to Unregulated Converter

Line Voltage = 200 vdc

Transmitted Power = 3.5 kw

Optimum wire weight at 300 ft = 32.4 pounds

Power Loss = 0.15 kw

C. Transfer and Circ. Pump Unregulated Converter

Output Power = 1.4 kw

Input Voltage = 200 vdc (fixed)

Output Voltage = 28 vdc

Converter Weight (corrected) = 9.8 pounds

Converter Efficiency (corrected) = 0.85

Power Loss = 0.25 kw

Input Power Required = 1.65 kw

D. PWM Series Regulator

Required Output Power = Shelter load + line loss + Pump load + Electrolysis

= 24.8 kw

Output Voltage = 200 vdc regulated

Using a baseline weight of 84 pounds (at 28 vdc) for a boost regulator and 200 pounds for a bucking regulator, and applying the correction factors of Figure 10.26, the weight and efficiency variations resulting from applying a variable unregulated nominal bus voltage are shown in Table 10.11

Table 10.11 Weight and Efficiency Versus Nominal Input Bus Voltage for PWM Series Regulator at 25 kw Output Power

Unregulated Bus Nominal Voltage (vdc)	Regulator Type	Calculated Weight (lbs)	Calculated Efficiency
50	Boost Reg. Conv.	135	0.80
100	Boost	64	0.95
200	Boost	55	0.95
200	Buck	130	0.88
300	Buck	128	0.88
400	Buck	132	0.88
500	Bucking Reg-Converter	165	0.75

The calculated regulator weight was plotted against array unregulated bus voltage (nominal) as one of the system weight components in Figure 10.33.

E. Regulator-Inverter

The required output power was 12.2 kw at 440 vac and 400 Hz in accordance with Table 10.6.

Table 10.12 shows the results of calculating inverter weight and efficiency for a fixed output power and variable input unregulated nominal bus voltage.

Table 10.12 Weight and Efficiency Versus Nominal Input Bus Voltage for Regulator-Inverter at 12.2 Kw Output

Unregulated Bus Nominal Voltage (vdc)	Type of Pre-Reg.	Calculated Weight (lbs)	Calculated Efficiency
50	Boost	210	0.75
100	Boost	132	0.86
200	Boost	114	0.86
200	Buck	162	0.78
300	Buck	160	0.78
400	Buck	165	0.78
500	Buck	175	0.75

The above weights are plotted as part of Figure 10.32.

F. Main Series Cable L_B

Length L_B = 100 ft

Table 10.13 shows the calculated power loss, for optimized line weights versus unregulated nominal bus voltage.

Table 10.13 Power Loss and Line Weight for Main Cable L_B

Unregulated Bus Nominal Voltage (vdc)		Total Power Transmitted, kw (excluding line loss)	Power Loss in line, (kw)	*Line Weight (lbs)
	50	47.8	0.74	100
Boost	100	40.8	0.32	40
	200	40.8	0.17	20
	200	44.3	0.23	20
Buck	300	44.3	0.10	20
	400	44.3	0.06	20
	500	50.9	0.04	20

*Optimized to produce minimum total of array weight increment plus line weight.

G. Cable L_A, Array to Main Bus Connector Block

The assumed average length L_A = 200 ft. As for L_B, a line weight was chosen which minimized the total of the array weight increments, Wt_{sa}, due to the line loss and the cable weight. The results of the calculations are given in Table 10.14.

Table 10.14 Array Cable L_A Weight vs. Unregulated Bus Nominal Voltage

Unregulated Bus Nominal Voltage (vdc)		Total Power Transmitted (kw)	Power Loss in line, (kw)	Total Optimized Line Weight (lb)
	50	48.5	8	864
Boost	100	41.1	3.3	344
	200	41.	1.7	172
	200	44.5	1.8	192
Buck	300	44.4	1.6	96
	400	44.4	0.9	96
	500	51.	0.3	200

The above line weight from Table 10.14 is combined with the line weight from Table 10.13 and plotted as a system component in Figure 10.33.

H. Required Array Power P_o' (Minimum Operating) and System Efficiency η

P_o' and η are arrived at by adding the total power transmitted to the line losses and comparing with the load requirement of 36.1 kw. Table 10.15 shows the calculated values.

Table 10.15 Required Array Power and System Efficiency vs. Unregulated Bus Nominal Voltage

Unregulated Bus Nominal Voltage (vdc)		Required Minimum Array Power, (kw)	Total System Efficiency, (%)
	50	56.5	64
Boost	100	44.4	81.3
	200	42.7	84.5
	200	46.3	78
Buck	300	46	79
	400	45.3	80
	500	51.3	70.5

Table 10.15 is also plotted in Figure 10.34. The results of Table 10.15 and Figure 10.34 apply for any of the solar array types considered during this study. Where the array specific weight (lb/kw) is less than that assumed for the leanto, a slightly different cable weight and power loss may result from an optimization procedure. However, for the purposes of this study, the difference was considered to be negligible and the same line weights were used for all the array types.

I. Array Weight

For the leanto solar array weight calculation, a value of 157 lb/kw pounds per kilowatt was used, based on 13,000 square feet of active area producing a minimum of 45 kw at a lunar phase angle of 90 degrees (sunrise). The calculated array weight increment was plotted in Figure 10.33. As can be seen, the array weight constitutes by far the greatest portion of the system weight. This solar array weight would differ with the various array types considered.

J. Total System Weight

The uppermost line in Figure 10.33 represents the sum of all the system components and therefore, the total system weight.

It should be noted that an allowance was made of from 400 to 500 pounds for "Array Controls", for boost regulation systems operating at 200 volts or below. This array control allowance was an estimate of the solar array weight increment plus the dissipative type controls which would be required for use with a nominal unregulated bus voltage of less than 200 vdc but higher than 100 vdc. These controls are required because a line boost regulator with an output of 200 vdc requires limiting the input to a maximum of 200 vdc. Although the use of a line bucking regulator also requires limiting the input voltage to some maximum value, the requirement is not as stringent and could be met by the use of Zener diodes set at approximately 50 volts above nominal. No weight allowance has been made for this since the precise requirements can only be determined for a detailed system design. However, for the power level under consideration this would amount to less than 100 pounds which is less than 2% of the total system weight. Figure 10.35 is another display of the results depicted in Figure 10.33, except that all power conditioning system component weights have been combined to better illustrate the impact on total system weight.

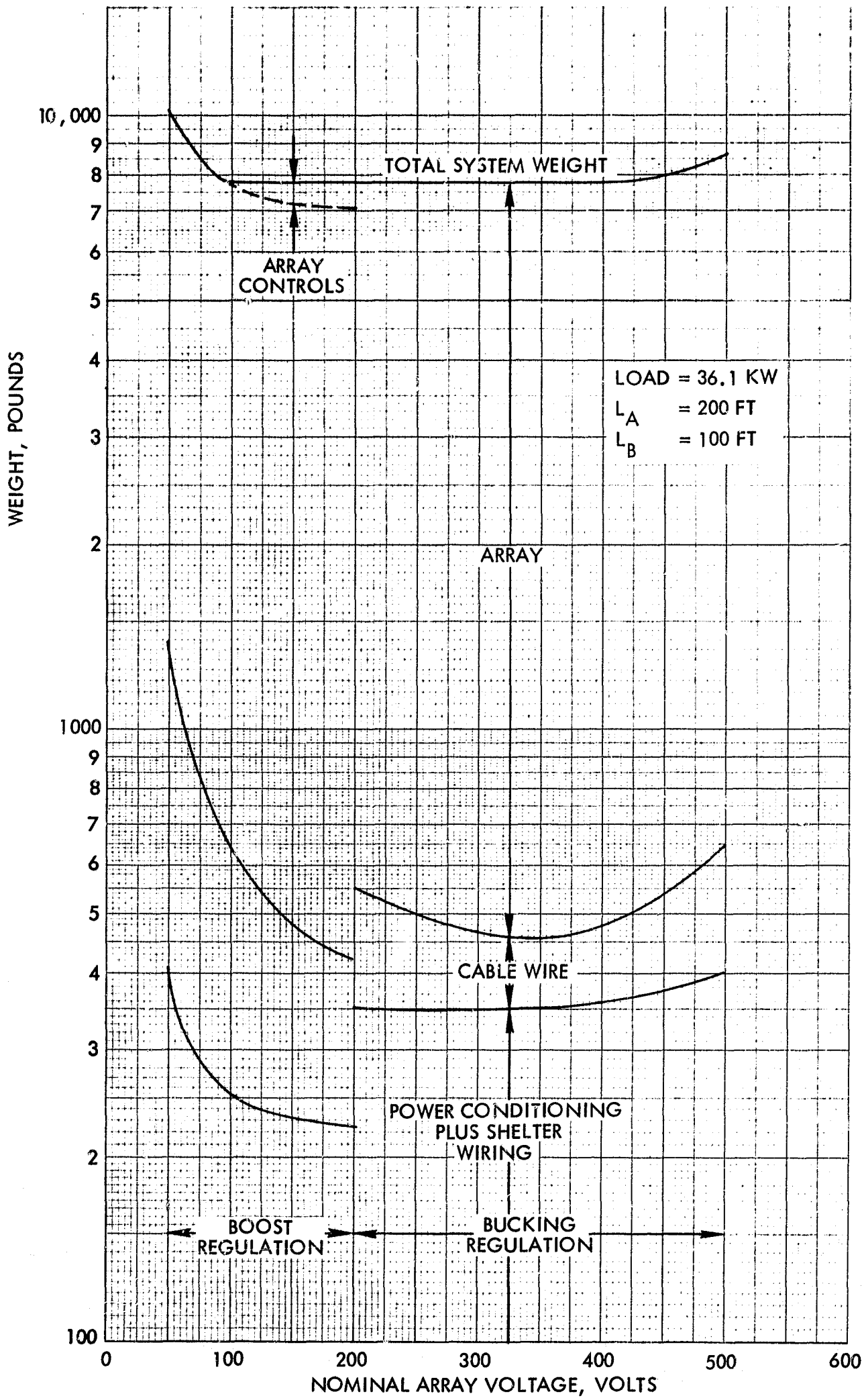

Figure 10.33 Breakdown of Leanto Lunar Power System Weight Versus Array Voltage (Power Conditioning Shred-Out)

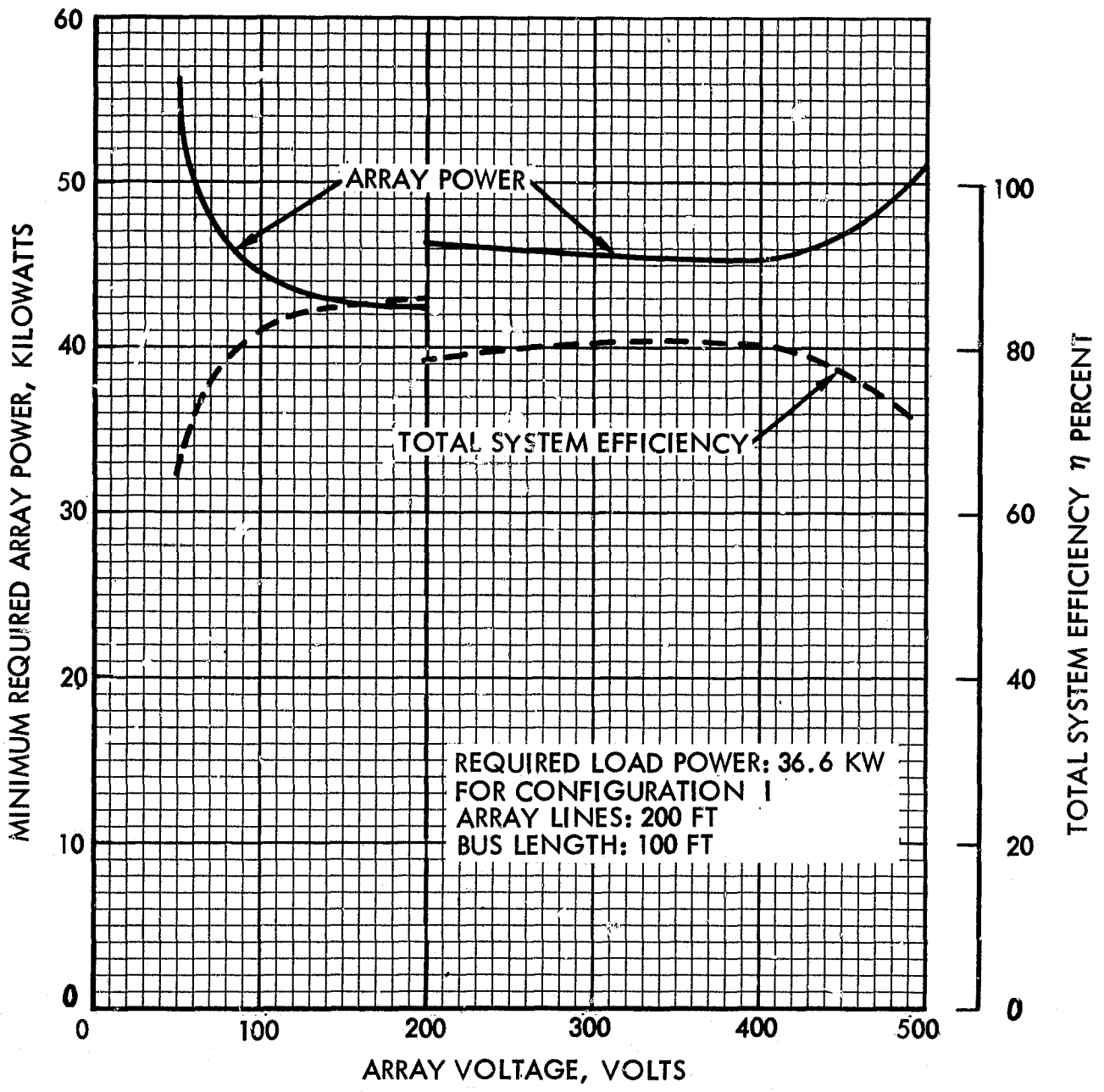

Figure 10.34 Required Array Power and System Efficiency Versus Array Voltage

In the range of 150 vdc to 450 vdc, the total system weight is very nearly constant and relatively insensitive to changes in the nominal unregulated bus voltage. It should be noted, however, that these results are applicable only for the previously selected values of cable length, temperature, and load. If any one of these fixed values is changed a considerable amount, the total system weight curve may not become nearly as flat in this region. It was found that increases in the values of these parameters all tended to increase the overall system weight, and shift the minimum system weight into the region of 300 to 400 vdc. Furthermore, it was determined that the required voltage input for the 3-phase inverter was approximately 255 vdc. Allowing for a line voltage drop of from 10 to 15 volts, a minimum unregulated bus voltage of 270 vdc at the array would be required. For these reasons, an unregulated bus voltage of from 270 vdc to 300 vdc was selected. However, because of the higher total system efficiency and correspondingly lower array power required in the 150 vdc to 200 vdc region (see Figure 10.34), a final selection should not be made until more detailed system tradeoffs are conducted.

10.6.3 Sensitivity to Changes in Parameters

The influence of variations in the system parameters line temperature, line length, and load power, was now examined. To simplify the use of the resulting curves in estimating their effect on total system weight, the sensitivity was determined for each case in terms of a non-dimensionalized total system weight ratio, and plotted to include lines of constant nominal unregulated array bus voltage.

Figures 10.36, 10.37 and 10.38 depict the sensitivity of system weight to changes in the indicated parameter. The following example is given to indicate how these sensitivity curves may be used for various systems.

Assuming that the average length of the array parallel lines, L_A, is actually 400 ft instead of the 200 ft used in the system synthesis, using Figure 10.38, a vertical line is drawn from L_A = 400 ft until it intersects all the constant array voltage lines. For an unregulated bus (array) voltage of 100 vdc, the predicted system weight ratio is approximately 1.12. This implies that the total system weight in Figure 10.33

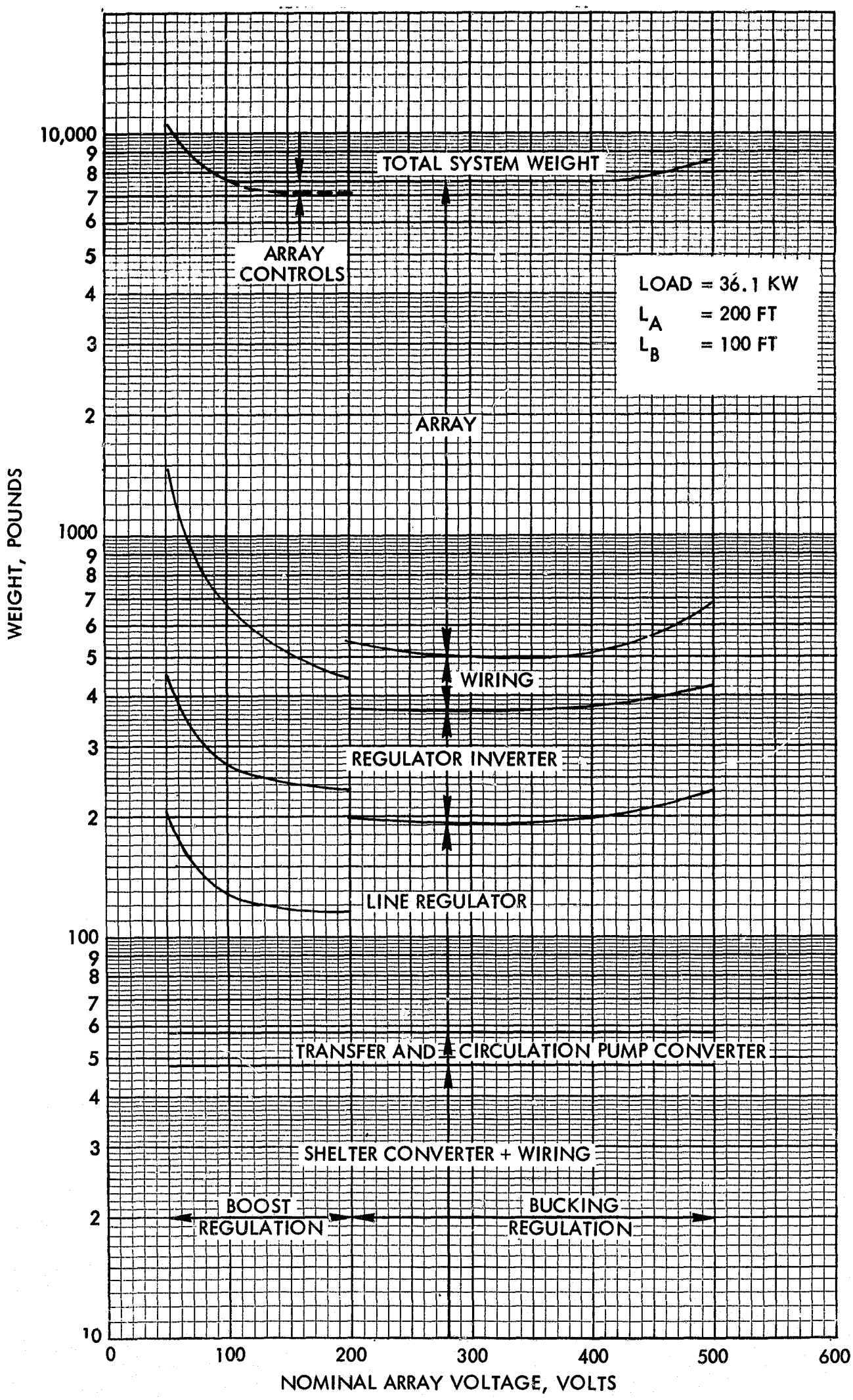

Figure 10.35 Breakdown of Leanto Lunar Power System Weight Versus Array Voltage

and Figure 10.35 of approximately 7,800 pounds at 100 vdc, should be multiplied by 1.12, which represents an increase of 12 percent. For 200 vdc, the system weight ratio is approximately 1.07 and an increase of 7 percent is indicated. The same approach can be used for all the sensitivity plots since they all apply to the system characteristics shown on Figures 10.32 and 10.34. Similar total system weight sensitivity curves could be made up for the flat and oriented-skirted arrays.

It should be noted that variations in these system design parameters have the least effect at 300 vdc and above. This illustrates the reason for selection of 300 vdc as the unregulated dc bus voltage for the candidate systems.

An increase in line temperature, T_L, from 25°C to +150°C, coupled with an increase in average length of array paralled lines from 200 ft to 400 ft, increases the total system weight by nearly 10 percent for a nominal array voltage of 200 vdc. This is equal to an increase of approximately 800 pounds, which would effectively nullify any apparent gain in using a boost line regulator at 150 to 200 vdc.

Another way of utilizing these sensitivity curves is to calculate the percent change in total system weight ratio per degree variation in cable temperature T_L, or per foot change of line lengths L_A and L_B. Figures 10.40 and 10.41 illustrate the results for variations in line lengths L_A and L_B. These curves are hyperbolic in character and approach a horizontal asymptote at approximately 400 vdc. This again indicates that, at least for reference system configuration and load, there is little to be gained in total system weight reduction by choosing an unregulated bus (array) voltage greater than 400 vdc. Similarly, these sensitivity plots only apply to the system synthesis example given in Figures 10.33 and 10.35. However, they may be applied to the other array configurations if the values taken from the curves are multiplied by the ratio of the total solar array weights (Wt_{sa}, leanto/ Wt_{sa}, flat or oriented). These extrapolations would be accurate to within approximately 2 percent for the total system weights shown on Figure 10.42.

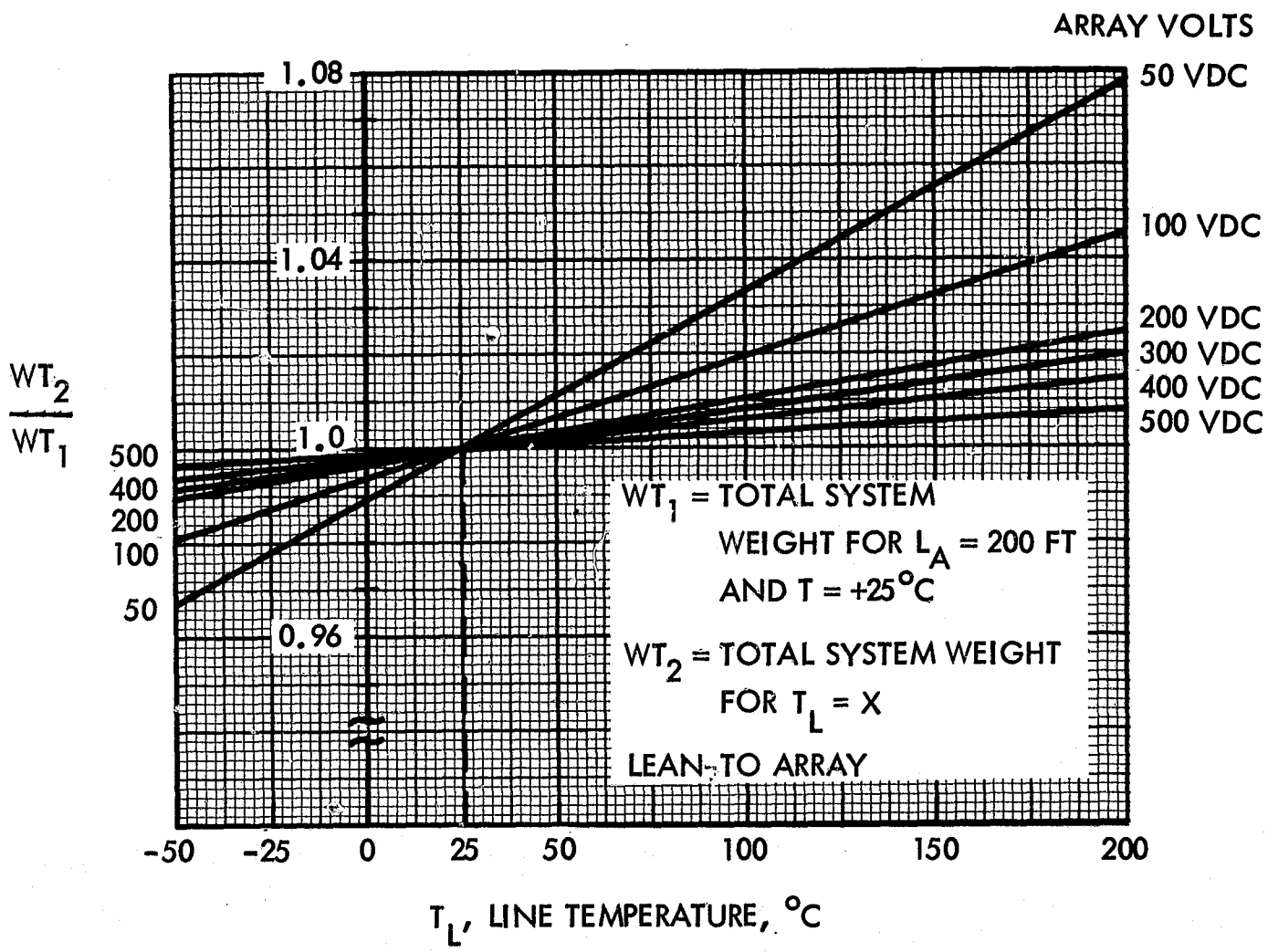

Figure 10.36 Total System Weight Ratio for Variable Line Temperature

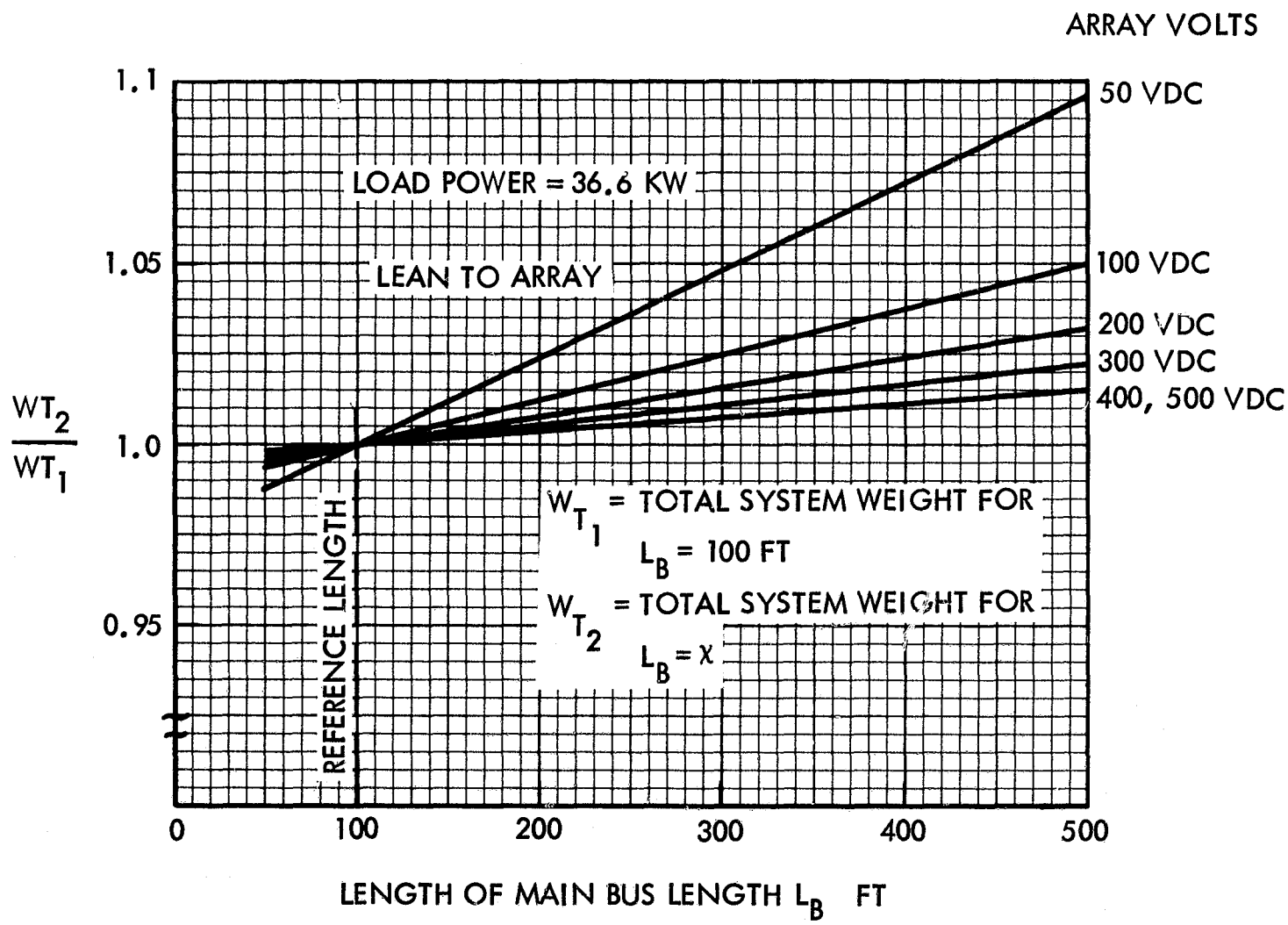

Figure 10.37 Total System Weight Ratio for Variable Main Bus Length

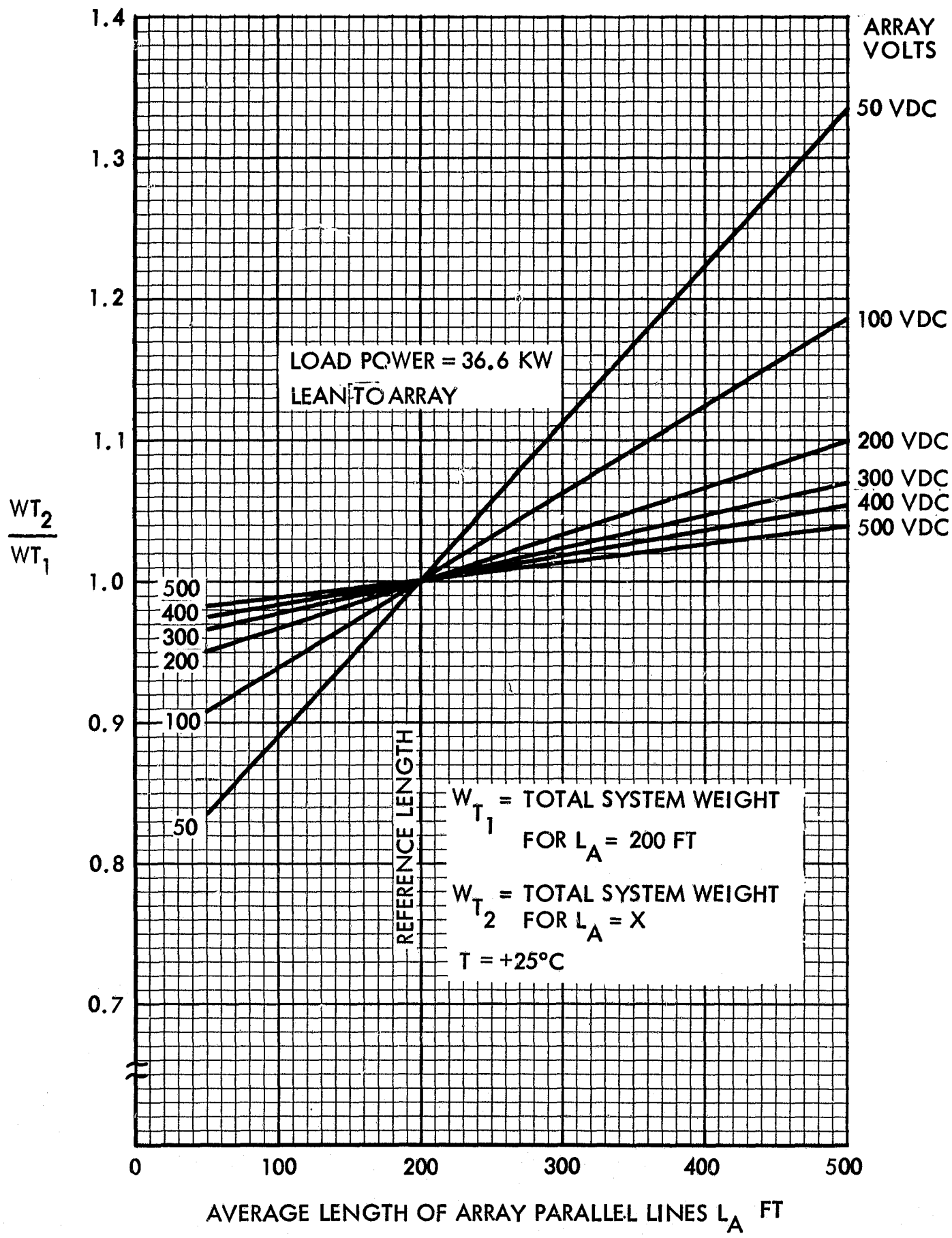

Figure 10.38 Total System Weight Ratios for Variable Line Length

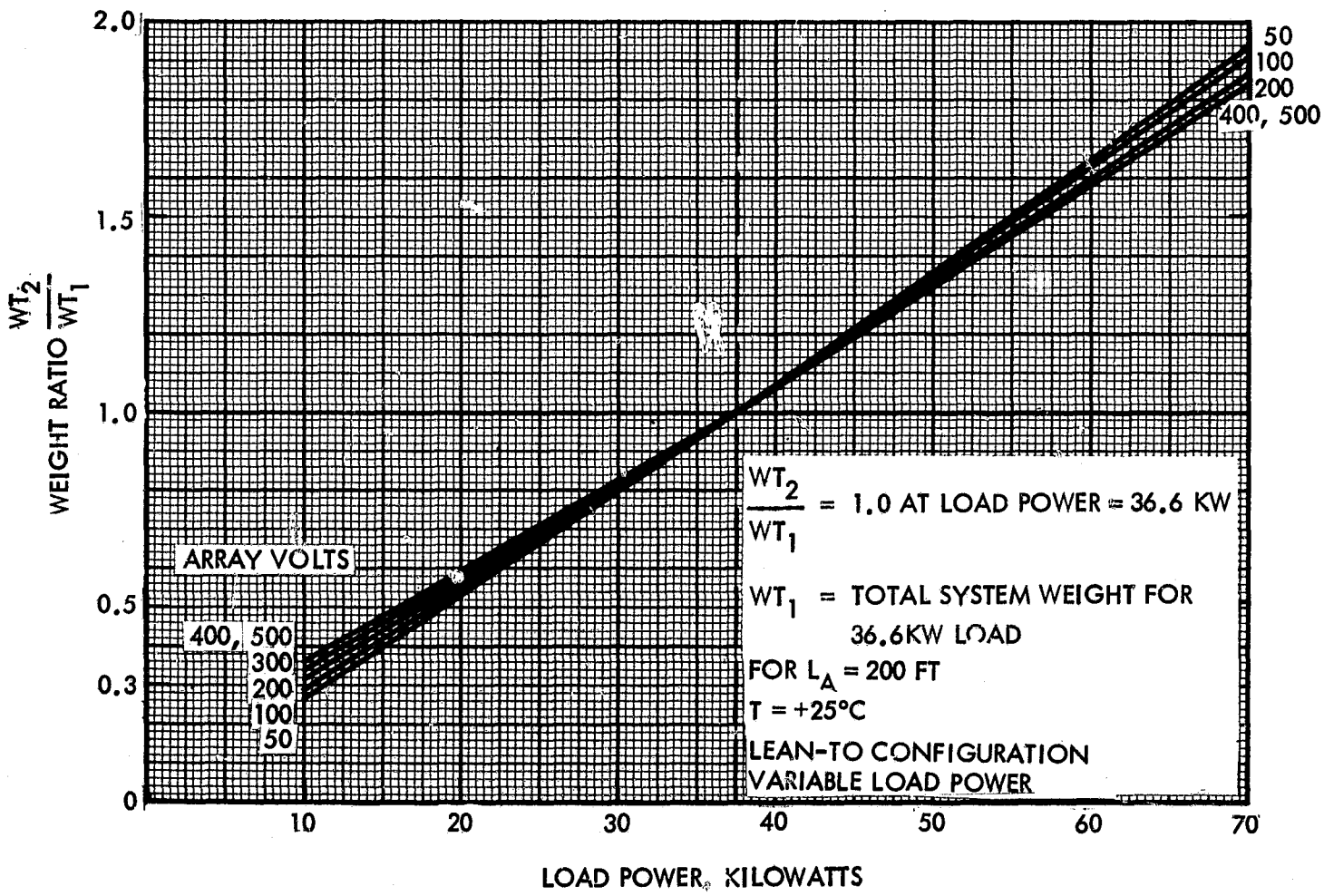

Figure 10.39 Total System Weight Ratio Versus Load Power

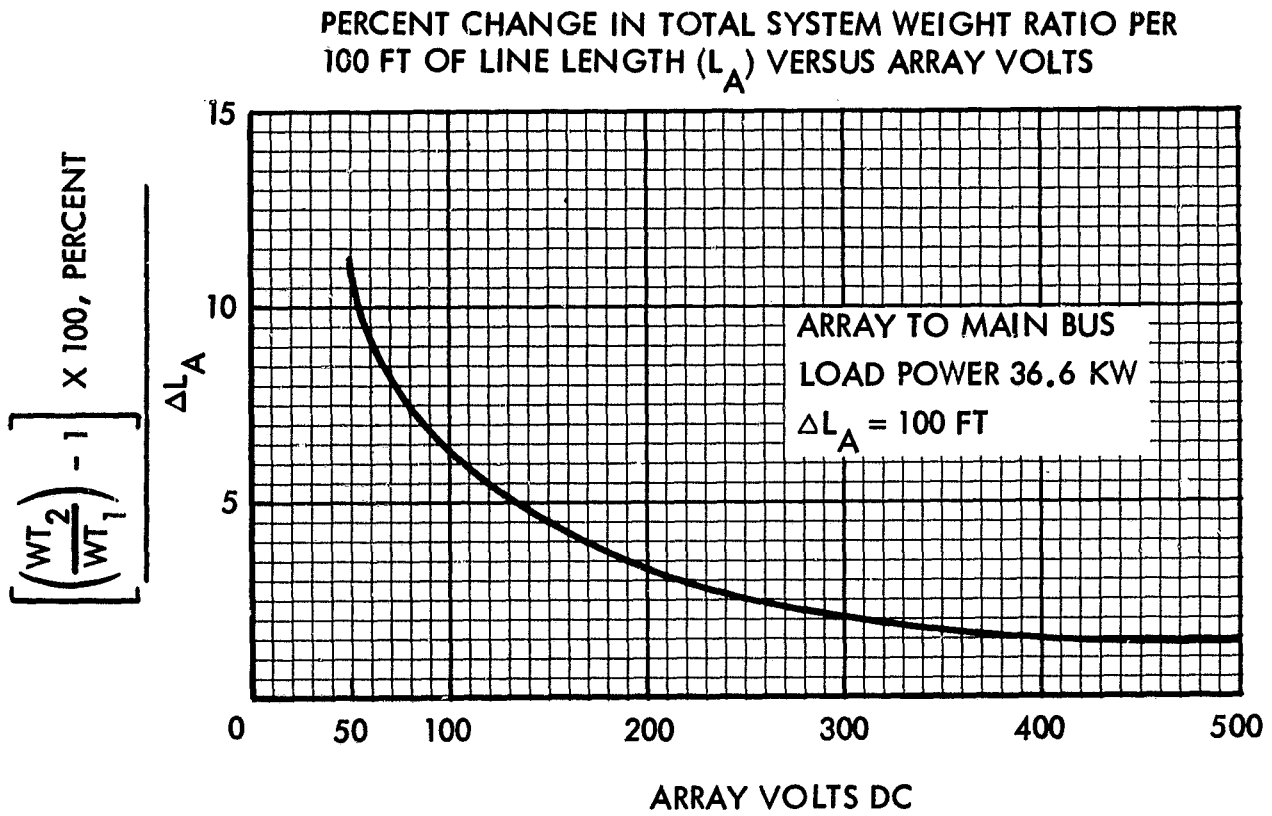

Figure 10.40 Percent Change in Total Power Systems Weight Ratio Versus Array Voltage (ΔL_A = 100 ft)

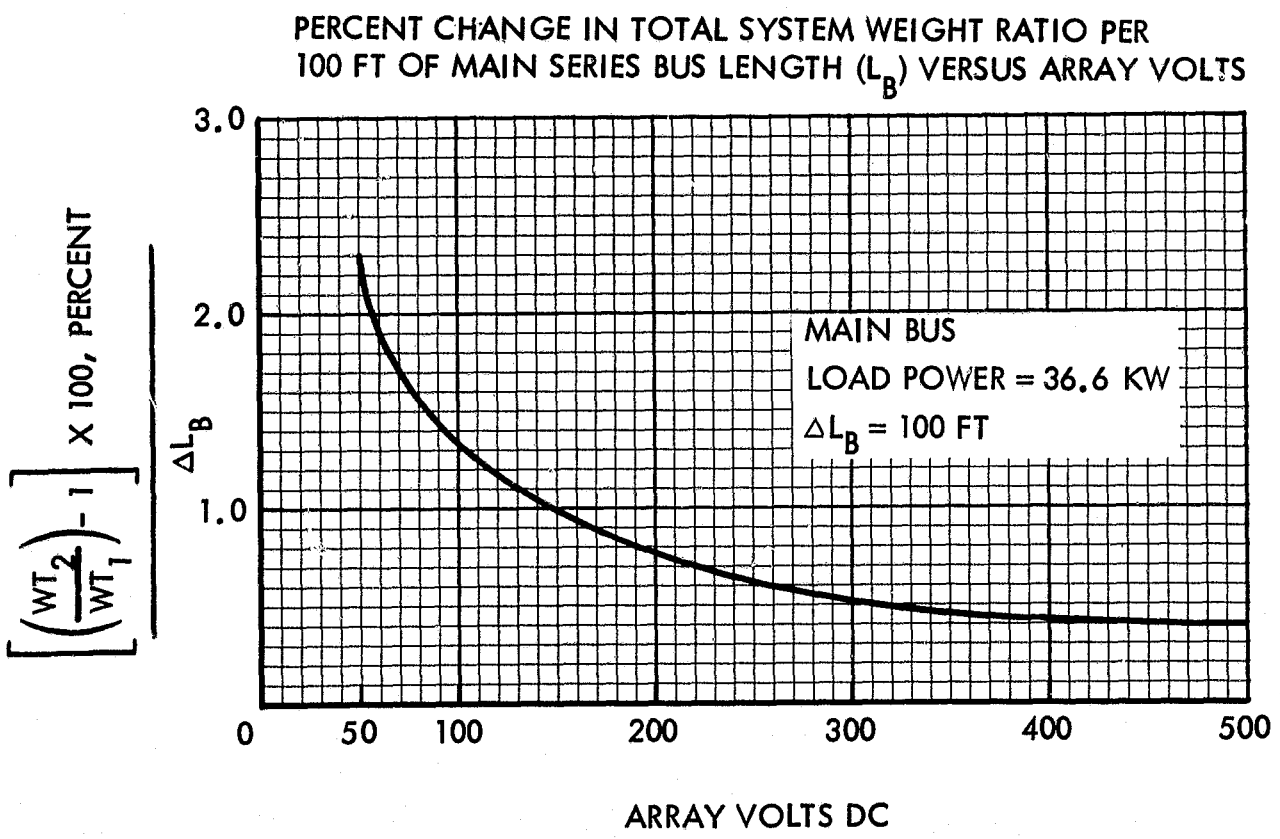

Figure 10.41 Percent Change in Total Power System Weight Ratio Versus Array Voltage (ΔL_B = 100 ft)

10.6.4 Effects of Changes in Choice of Solar Array Type

Using the results illustrated in Figures 10.33 and 10.35 it was possible to extrapolate similar values for the total system weight for the flat and oriented-skirted arrays. These results are shown on Figure 10.42. The oriented-skirted array requires much less active surface area than the 45° leanto-skirted configuration (see Section 9), and hence its total weight is considerably less. The flat-skirted array is more practical for use with the two step ERPS power profile (see Figure 10.31c). Batteries are needed to provide energy when the solar array output is less than the stepped level of power required. By use of a larger peak power level flat array (86 kw versus 78 kw) the batteries may be eliminated. However, the small saving in weight (less than 100 lbs.) is more than offset by the increase in array area and cost (see Figure 4.12 and Table 4.9).

A significant weight reduction can be achieved if the leanto array slope is changed from 45° to 51°. This system is still heavier than the oriented-skirted array (approximately 1400 lbs). However, the elimination of the requirement for orientation considerably enhances power system reliability and greatly reduces overall mission cost (see discussion in Section 4.6).

The output power characteristics of the oriented-skirted array and the 51° leanto array are very similar (see Figure 9.19). Hence, it is concluded that both configurations should be retained as candidate power systems for the Program V mission until more detailed thermal and system tradeoff analyses are conducted.

10.6.5 Rationale for Power Distribution System Selection

The basis for the approach to power distribution system selection, taken in Section 10.2, is described in Appendix F. The four configurations discussed in Appendix F constitute the baseline concepts considered before arriving at the candidate system.

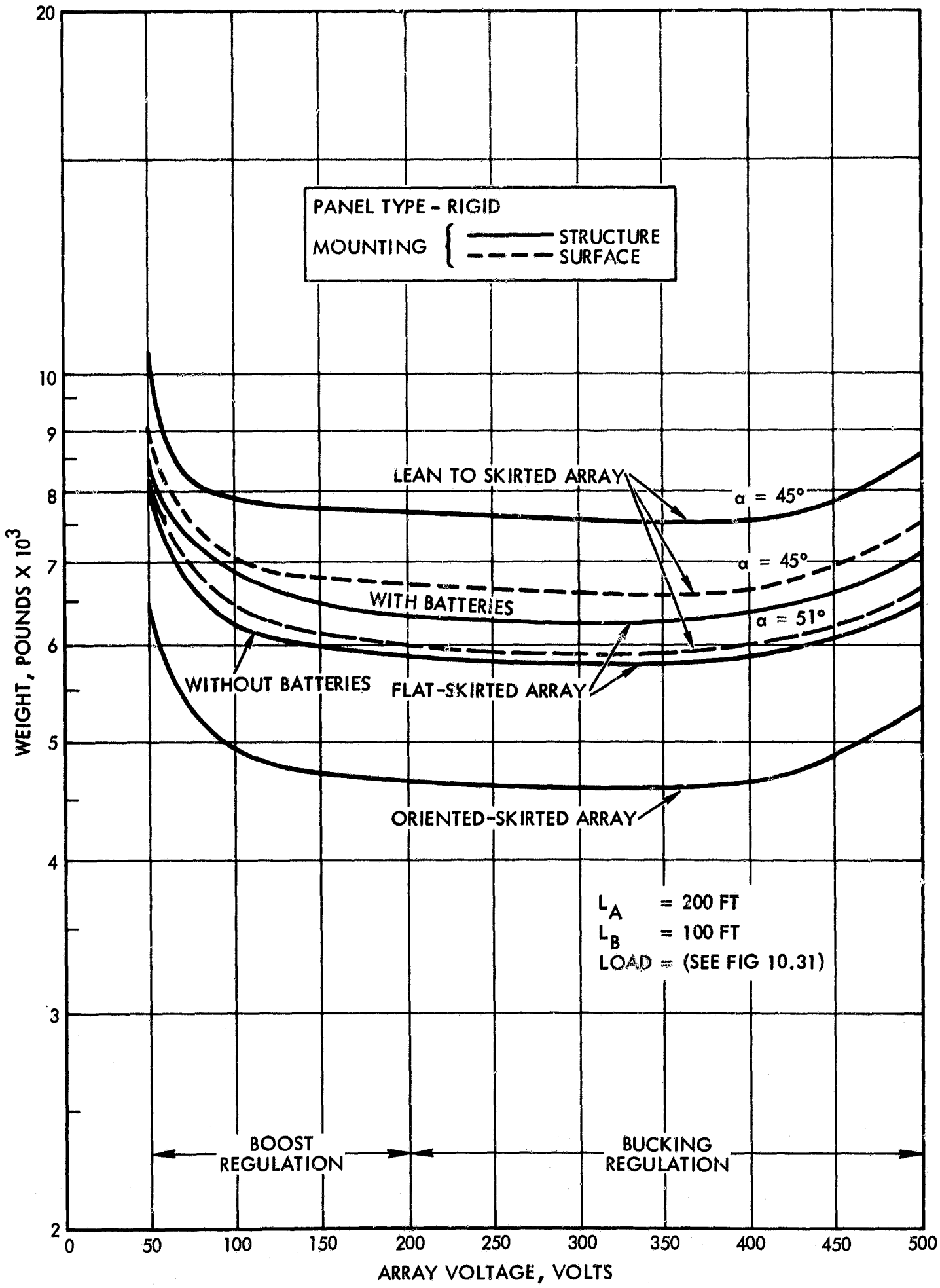

Figure 10.42 Comparison of Total Lunar Power System Weight for Various Array Configurations

11. PRELIMINARY DESIGN OF CANDIDATE POWER SYSTEM

11.1 DESIGN CONSIDERATIONS

One of the objectives of this study was to prepare a Design Requirements Document for a candidate lunar surface power system. The previous analyses and discussions included in this report have provided the parametric data and rationale for synthesizing an overall power system which included the solar array, power conditioning equipment, and the power distribution system. After a review of several solar array concepts, three candidate configurations emerged as being worthy of further consideration, namely; the flat, leanto and oriented-skirted types. In addition, it was determined that an unregulated dc bus voltage of 300 vdc represented the best region to operate the system. Finally, based on a layout of the lunar base, it was established that average power distribution cable lengths of 200 feet and a main bus length of 100 feet would be utilized.

It has been established during this study that the determination of an optimum solar array configuration would require considerable additional analyses in both the mission planning and system integration areas. However, since the preferred power profile (see Reference 4.2) for the Program V mission was the single step case at the 36.1 kw level, it was possible to eliminate the flat array on this basis. The choice between the leanto and oriented-skirted arrays was not as clear cut. If minimum system weight was to be used as a criteria, it is obvious that the oriented-skirted array should be selected. However, if maximum mission cost effectiveness and potentially higher reliability are desired, it is evident from the summary data of Table 4.9, that the 51° leanto would be superior. Since both systems were well below the maximum allowable weight of approximately 10600 pounds (5300 kg), this was no longer a deciding factor. In view of the foregoing considerations, it was decided to base the Design Requirements Document on the leanto solar array configuration. Should future mission criteria require that the flat or oriented-skirted array be utilized, the data and requirements outlined in the Design Requirements Document are sufficiently flexible to permit use of this specification with a minimum number of changes required.

11.2 DESIGN REQUIREMENTS DOCUMENT - LEANTO ARRAY CONFIGURATION

A Design Requirements Document (DRD) was prepared using the leanto solar array as the candidate configuration. It has been included as Appendix B of this report. For the most part this document was based upon the requirements as outlined in Table 10.6 and Reference 4.2.

This document provides the design requirements for a Lunar Surface Power System (LSPS) to be used in conjunction with the Program V mission. The mission requirements have been outlined in Section 4. of this report. However, despite these requirements and the information provided in Reference 4.2, there is still considerable data lacking with respect to the characteristics of the various electrical loads. Typical of these are:

- Load start-up limits
- Power factor
- Duty cycle
- Transients
- Output ripple, peak to peak
- Overloads
- Electromagnetic characteristics

Additional factors not established during the time period of this study include reliability levels, thermal control interfaces, and lunar base start-up and shut-down operation procedures. Operation and maintenance of the LSPS during the six-month, unmanned dormancy period also requires further definitization.

Wherever possible, assumptions have been made and they are reflected in the DRD with the added notation, "To Be Confirmed", (TBC). These values were based upon TRW Systems experience with this type of electrical system or component. In those cases where this was not possible, the DRD has designated these requirements as, "To Be Supplied" (TBS).

A detailed discussion of the Program Development Plan for the implementation of the LEPEPS only is outlined in Section 12. A similar plan will be required for the SEPS when the requirements for this system are determined. It is anticipated that during the Phase 3 portion of this program, the DRD would be finalized in accordance with the latest mission requirements.

12. PROGRAM DEVELOPMENT PLAN

12.1 PROGRAM CONSIDERATIONS

The foregoing study has served to investigate a wide variety of concepts and modes of operation to arrive at a candidate configuration for a Lunar Surface Power System (LSPS). The LSPS would consist of both a primary and secondary electric power system (LEPEPS and SEPS) as previously defined in Section 4. These systems are required to support the operations of a lunar based energy depot which is to be utilized in support of the Program V mission. The objectives of this mission are to conduct extensive scientific experiments in conjunction with exploration of the lunar surface. A three man, one-year mission is envisioned. It would consist of two ninety (90) day manned exploration periods with a dormant, unmanned, one hundred and eighty (180) day period interspersed between them. The requirements for this mission are discussed in Section 4 and References 4.2 and 4.3.

The primary function of the energy depot would be to supply reactants (H_2 and O_2) to the fuel cell powered lunar roving vehicles and shelter module (night-time operation). The LSPS would provide electric power to implement a water electrolysis and reactant liquefaction and storage operation which would regenerate these reactants for reuse in an electrolytic reactant production system (ERPS) such as is currently under investigation (References 4.2 and 4.3). The LSPS would also provide electrical power for operation of the shelter module during the lunar day and for scientific experiments being conducted in the vicinity of the lunar base. Finally, during the unmanned, so-called, dormant period, the LSPS would provide power for base instrumentation and telemetry requirements as well as for the ERPS which would be operating at a reduced duty cycle or production rate.

12.2 PROGRAM IMPLEMENTATION DEFINITION

In keeping with NASA policy, the Lunar Surface Power System development program would be carried out by a sequency of implementation phases. Each phase is defined to correspond to a specifically approved activity to be undertaken only after review and analysis of preceding work. Thus each phase represents a focused effort with definable end objectives. Initiation of a phase, therefore, represents a specific limited agency commitment, both internally and externally.

A fundamental concept pertinent to such phased implementation is participation by management in the review and decision-making activities before proceeding from one phase to the next. This executive review would be the responsibility of a Lunar Energy Depot Program Director, supported by a LSPS Project Office, as the representatives of NASA general management.

The general definitions for the implementation phases associated with the Lunar Surface Power System are given below:

- <u>Phase A - Advanced Studies</u>
  Phase A corresponds to the analysis of a proposed agency objective or mission in terms of alternative approaches or concepts. It includes the research and technology development required to support such analysis and to assist in determining whether the proposed technical objective or mission is feasible and achievable.

- <u>Phase B - Project/System Definition</u>
  Phase B includes detailed study, analysis and preliminary design directed toward the selection of a single systems approach from among the alternate approaches resulting from Phase A.

- <u>Phase C - Design Implementation</u>
  Phase C includes the detailed definition of the final system concept, including the system design and the breadboarding of critical components and subsystems, as necessary to pro-

vide reasonable assurance that the technical milestone schedules and resource estimates for the next phase can be met, and that definitive contracts can be negotiated for Phase D.

- Phase D - Development and Operations
  Phase D includes final hardware design and development, fabrication, assembly and test, and operations.

Throughout each phase, emphasis is placed on identifying those aspects of the proposed project that require the development of technology beyond the current state of the art, and the specific manner in which this technology is to be developed is defined.

12.3 PROJECT SEQUENCE AND BASELINES

In support of the phased implementation approach, formal baselines would be established in sequence as illustrated in Figure 12.1 to allow review and control by various levels of project management. A generic project is discussed below along with the related sequence of project activities.

12.3.1 Program Requirements Baseline

A program level requirements framework is needed as a basis for the Phase A advanced studies. This is provided by a Preliminary Program General Specification. The related project control point is designated as the Program Requirements Baseline. It should be established prior to or early in Phase A by the Cognizant Program Office in NASA Headquarters or delegated to the responsible NASA center.

12.3.2 Project Initiation and Planning

Based upon the results of the Phase A study, a project proposal should be generated by the program office and submitted to NASA general management. The initiation of the project is authorized when a project approval document (PAD) is issued. The PAD establishes the scope of the project and assigns project and system management responsibility. The detailed planning for the project is then accomplished by the project office and documented as a Project Development Plan (PDP). When approved by the program director, the PDP becomes the primary operating document for project implementation.

FOLDOUT FRAME

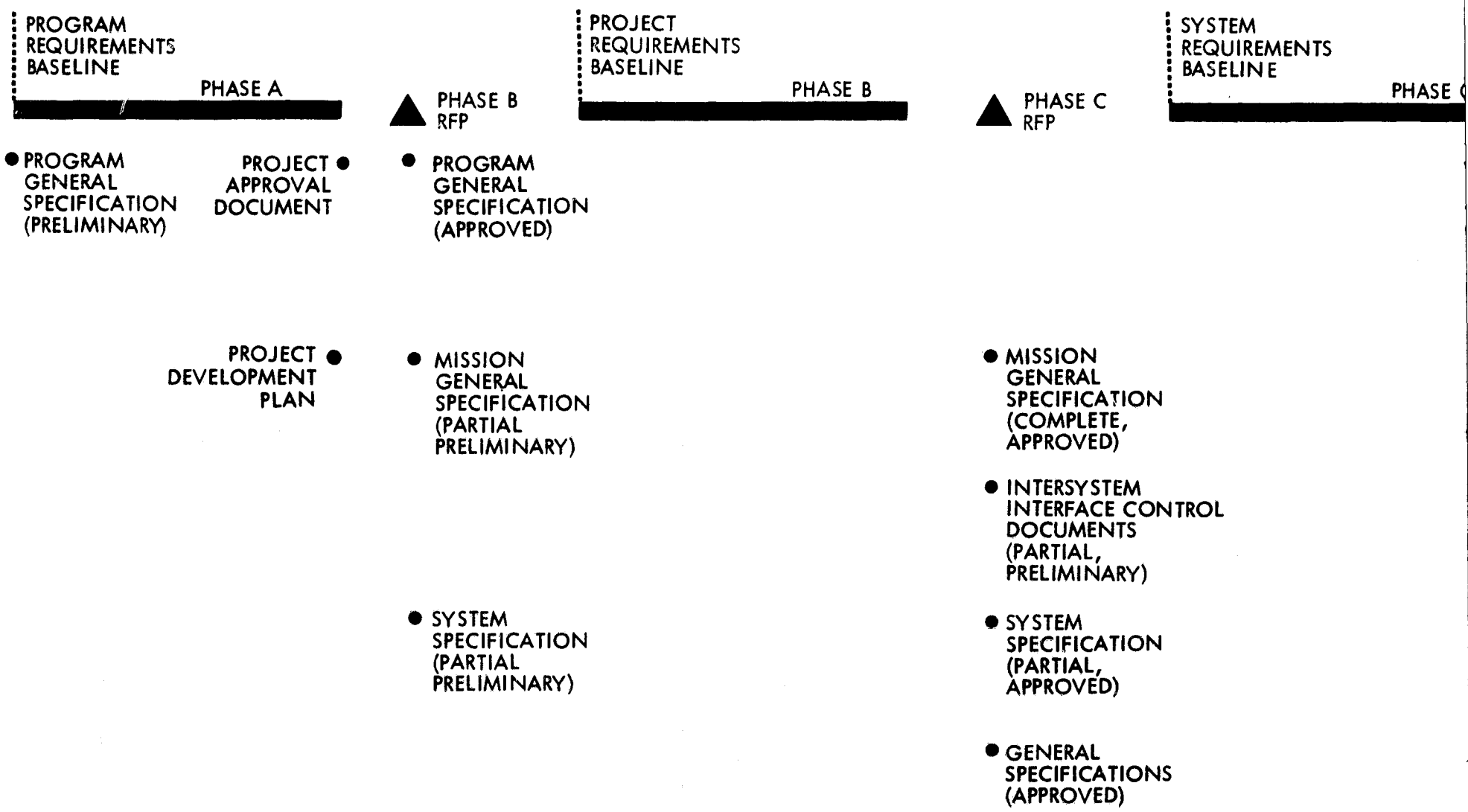

Figure 12.1 Project Sequence and Baselines

FOLDOUT FRAME

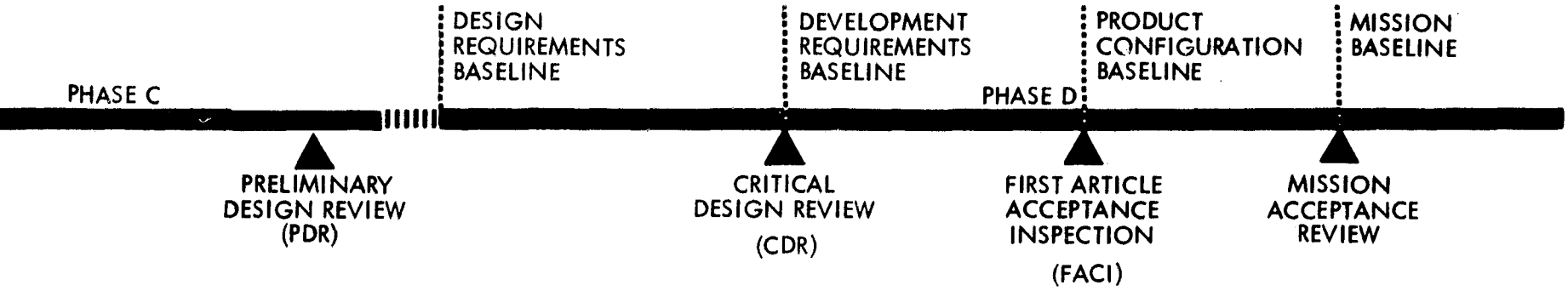

- INTERSYSTEM INTERFACE CONTROL DOCUMENTS (COMPLETE, APPROVED)
- SYSTEM SPECIFICATION (COMPLETE, APPROVED)
- CEI PART I SPECIFICATIONS (PARTIAL, APPROVED)
- CEI INTERFACE CONTROL DOCUMENTS (PARTIAL, APPROVED)
- CRITICAL COMPONENT LIST (APPROVED)
- LONG LEAD-TIME CRITICAL ITEMS REQUIREMENTS (COMPLETE, APPROVED)

- CEI PART 1 SPECIFICATIONS (COMPLETE, APPROVED)
- CEI INTERFACE CONTROL DOCUMENTS (COMPLETE, APPROVED)
- CRITICAL COMPONENTS SPECIFICATIONS (APPROVED)
- MANUFACTURING DRAWINGS AND DATA (APPROVED)

- CEI PART II SPECIFICATIONS (APPROVED)

- AS MODIFIED CONFIGURATION AND ASSOCIATED DATA VERIFIED

12.3.3 Project Requirements Baseline

The next major step in project implementation is the Phase B project definition. The related technical requirements base to govern the Phase B work is usually provided by the following documents, which correspond to the project requirements baseline:

- Program General Specification (approved): The preliminary version of this document utilized as the basis for the Phase A studies is updated to incorporate results of the intervening work and is issued under the approval of the program director. It defines the overall performance and design requirements for the project.
- Mission General Specification (partial, preliminary): This document defines overall performance and design requirements associated with the mission. It includes requirements at the system level and for intersystem interfaces. Requirements peculiar to each launch opportunity are provided either within the main text or by means of individual addenda as convenient.
- System Specification (partial, preliminary): This document corresponds to the top-level requirements document for a particular system area. It defines the associated functional system as an entity, establishes system performance requirements, defines directly or by reference the interfaces with other functional systems, identifies the breakdown of the system into functional areas along with related performance requirements, establishes system standards, and delineates system testing requirements.

These three documents are issued as part of the Phase B RFP. The project requirements baseline for a system or major system element is than formally established when these documents are made applicable by a Phase B contract.

12.3.4 System Requirements Baseline

As a result of Phase B, a particular project approach is selected for the associated system to serve as a basis for Phase C. The related configuration data corresponds to the system requirements baseline. This data is embodied in the following documents.

- Program General Specification (updated, approved)
- Mission General Specification (complete, approved)
- Intersystem Interface Control Documents (partial, preliminary): These define and control the various intersystem interfaces when established in the appropriate specifications. They consist of schematic diagrams, functional block diagrams, data sheets, and drawings which define the interfaces in detail.
- System Specification (partial, approved): The preliminary version used as the basis for Phase B is updated as the result of the intervening project definition work. Those portions which define technical requirements for Phase C are complete.

The above requirements documents for the system requirements baseline are issued as part of the Phase C RFP, and the related work definition is documented as part of the contractor's Phase C proposal. The system requirements baseline is then formally established by the Phase C contract.

As indicated above, the system specification and the intersystem interface control documents are only partially completed when the system requirements baseline is established. However, those portions which define technical requirements documents come under project configuration control at the beginning of Phase C.

12.3.5 Design Requirements Baseline

To realize the Phase C objective, a detailed definition of the system must be determined and a definitive Phase D proposal must be generated. The technical data base needed for this corresponds to the design requirements baseline for a particular system. This data is embodied in the

following documents, which supplement or update the system requirements baseline data.

- Intersystem Interface Control Documents (complete, approved)
- System Specification (complete, approved)
- Part I CEI Specifications, Performance, and Design Requirements (partial, approved): This part of the CEI specification defines requirements peculiar to the design, development, test and qualification of the contract end item.
- CEI Interface Control Documents (partial, approved)
- Critical Components List (complete, approved): Certain comments of a CEI may require individual specification and qualification. These are designated as critical components and are listed in Part I of the associated CEI specification. A combined list of such components is generated for the complete system.
- Long Lead-Time Critical Items Requirements (complete, approved): Certain components of a CEI (i.e., isotope inventory for the SEPS RTG and for supporting facilities) may require early procurement. Hence, approval prior to or at the beginning of Phase D may be required.

The technical basis for the design requirements baseline is defined as the result of a Preliminary Design Review (PDR). A PDR is conducted for each CEI and constitutes a formal technical review of the basic approach for its design. PDR's are completed for each CEI during Phase C when the basic design approach has been identified, and the requisite preliminary design documentation has been prepared.

The required results from the PDR are as follows:

(a) The compatibility of the selected design approach with Part I of the detailed specification for the CEI will be established.

(b) The compatibility of the CEI with other system equipment/facilities will be established by review of predesign drawings, schematic diagrams, layout drawings, envelope drawings,

in-board profiles, review of performance characteristics for functional compatibility, etc.

(c) The integrity of the selected design approach will be established by review of analyses, breadboard models, mockups, circuit logic diagrams, packaging techniques, etc. This is done by the contractor as the basis for selection of the design approach presented.

(d) The parts of the design to be subjected to detailed engineering analysis will be identified.

(e) The producibility of the selected design will be extablished by review of the requirements for special tools and facilities to manufacture the CEI in the quantities required.

Phase C must also develop a detailed definition of the Phase D development and operations phase. This is documented as a Phase D proposal. The design requirements baseline is then formally established when this proposed work statement and the related configuration documentation are made applicable by a definitive Phase D contract.

12.3.6 Development Requirements Baseline

On the basis of the design requirements baseline, Phase D proceeds with detailed design and production planning. The next contractual baseline milestone corresponds to the formal identification and approval of specific engineering documentation which defines the design of the CEI. This will be released for manufacturing the end item in the operational configuration and for qualification testing. This stage is designated as the development requirements baseline and is established for each CEI by a Critical Design Review (CDR). The corresponding system baseline is established when development requirements baselines have been attained for all CEI's of the system. The Critical Design Review is a formal technical review of the design of a contract end item. The CDR occurs when the detailed design is essentially complete, to formally establish the design as the basis for technical support data, etc. Prior to the CDR, the exact interface relationship of the CEI to other system (or inventory) equipment/facilities will be

established, and will appear in approved interface control documents which fix the interfaces for the CEI.

The required results from the CDR are as follows:

(a) The compatibility of the CEI, as designed, with Part I of the detailed specification for the CEI will be established.

(b) The system compatibility of the completed design will be established by comparison of the interface control documentation with the engineering drawings for the CEI. The interface documentation will, if appropriate, reflect agreement of contractors that are developing interfacing items of equipment/facilities.

(c) The integrity of the design will be established by review of analytical and test data.

As a result of the CDR, all interface control documents are completed and approved. The Part I critical components specifications are also complete. The complete set of manufacturing drawings and associated data are released and put under configuration control, with all subsequent Class I changes referred to the cognizant system management office.

12.3.7 Product Configuration Baseline

After approval of the design and release for manufacture of the operational configuration, Phase D continues with production, type approval (qualification) test, subsystem integration, and system assembly and test. The next contractual baseline milestone corresponds to formal inspection of a first operational unit. This stage is designated as the product configuration baseline and is established for each CEI by a First Article Configuration Inspection (FACI). The corresponding system baseline is established when product configuration baselines have been attained for all CEI's of the system. When a CEI such as the Lunar Surface Power System is composed of many CEI's, it may be appropriate to conduct only one FACI for the integrated system.

The FACI is a formal technical review conducted by the cognizant system management office to audit and approve product configuration and acceptance test requirements constituting Part II of the CEI specification, including the associated manufacturing documentation referenced in the specification. This involves three aspects:

(a) Audit of qualification test results to verify that the design embodied by the hardware undergoing qualification testing satisfies the requirements of the Part I CEI specification.

(b) Audit of the applicable configuration data and production process to verify that the first operational hardware item is identical to the qualified hardware, and so satisfies the specified requirements by identity.

(c) Audit of the acceptance process to verify that it will ensure all subsequent accepted hardware to be identical to the first operational unit.

That is, during the FACI, an audit is accomplished by establishing the exact relationship between the configuration of the CEI identified for follow-on manufacturing (the operational unit under inspection) and the configuration of the CEI qualified. The FACI also establishes the exact relationship of the CEI as described by released engineering documentation to the CEI as manufactured and assembled. Also, the FACI establishes the validity of the acceptance testing of the CEI by direct comparison of the acceptance test methods and test data with the specified performance of the CEI.

Part II of the CEI detailed specification, once audited and accepted at the FACI, serves as the basic documentation for configuration management of the CEI for the remainder of Phase D. All changes to the CEI, after FACI, will be implemented only to reflect approved changes to Part II of the CEI specification. A major engineering change (new type-model-series) or an indication that the configuration being produced does not accurately reflect released engineering may require repeating the complete FACI.

12.3.8 Mission Baseline

After the FACI, the Part II CEI specification will be complete and approved and the exact relationship between the "as-built" and "as-designed" configuration will have been established. The acceptance testing will have been validated by direct comparison of specified performance with acceptance test methods and test data. This then establishes the basis for acceptance and delivery of follow-on operational articles. Any approved changes to the configuration after the FACI will be incorporated in the configurational documentation and in the affected hardware and software so as to produce the completely current "as-modified" configuration.

To ensure that all approved changes have been incorporated for the mission, a mission acceptance review is conducted when the item is committed for the mission, to verify that the as-modified configuration corresponds to the final approved configuration for the mission. This then establishes the mission baseline for the item. The mission baseline for the system is achieved when all of its elements have achieved their individual mission baselines.

12.4 PROGRAM PLAN

The current study activities associated with the Lunar Surface Power System constitute a partial fulfillment of the Phase A program requirements as defined in Section 12.2. One of the initial objectives was to formulate parametric data and establish the conceptual design and requirements for the LEPEPS. Similar data must still be generated for the SEPS. These power systems (LEPEPS and SEPS) are to be based upon the latest state-of-the-art technology consistent with achieving a technology readiness status by the end of 1972. They must be adequate to meet the Program V mission requirements as outlined in Section 4. In addition, by utilizing a modular concept and employing commonality principles as outlined in this report, these systems can also provide a multi-mission capability.

12.4.1 Major Milestones

The program implementation phase definitions provided in Section 12.2 are the generalized versions provided by the NASA document NPC500-1. Because the current emphasis is on technology development, it appears desirable to modify these phases so as to better define the major milestones for the LEPEPS development program. Table 12.1 lists the revised categories as they are applied to this development plan and identifies the corresponding NPC500-1 phases.

Table 12.1 Major Milestones for Lunar Surface Power System Development

Phase No. (LSPS Program)	Phase (NPC500-1)	Phase Category
1	A	Parametric Data and Concept Definition
2	A	Sub-System Development and Optimization
3	B	Concept Verification/Test and Research
4	C	Final System Definition and Prototype Development
5	D	Flight System Design/Fabrication/Qualification

The Program Plan has been limited to identifying only the development requirements for the LEPEPS (solar array, power conditioning, power distribution, controls). A similar plan for the SEPS has been deferred until a Phase 1 study is carried out and the preliminary design requirements identified for this system.

The overall Program Plan for the LEPEPS is shown on Figure 12.2. The current study which culminates in the issuing of this Final Report constitutes the major Phase 1 effort. Supplementary thermal model analyses will be conducted to support the Phase 2 detail design of an engineering test model of a solar array panel. The major emphasis in Phase 2 will be to conduct an experimental test program to identify the technology requirements associated with the design of a solar

array for operation on the lunar surface. Compatibility of the materials and design features of the candidate solar array with the launch vehicle and lunar surface environment will be demonstrated.

It has been assumed that concurrent with the Phase 2 activities, additional program planning studies would be conducted to better define the Program V mission requirements. This could include a further assessment of ERPS system requirements as well as total mission energy requirements. Based upon this premise, Phase 3 activities would be initiated in mid 1969 to conduct detail design studies and additional experimental test model evaluations (where required) for a specific mission-oriented LEPEPS system. This phase would result in the selection of a specific solar array power system to meet the latest mission objectives established by NASA and any associated AAP contractor. Preliminary system design requirements would be established and important interfaces with the lunar energy depot and ERPS would be identified. The interface problem has been simplified to some extent during this current Phase 1 study, by the decision to use multiple, standard, 2.5 kw (nominal) solar array panels to provide the gross power requirements. Operational problems associated with power system transportation, handling, deployment and orientation (if employed) would be assessed. Preliminary designs of the recommended versions of all the subsystems that make up the LEPEPS would be prepared. Phase 3 activities would be completed by January 1970 and a LEPEPS system definition report would be delivered to NASA at this time.

The Phase 4 final system definition and prototype development would be initiated in February 1969 based upon NASA's review and approval of the Phase 3 report. The work during this phase would include preparation of the final LEPEPS design. Where required, breadboards and/or analog simulators would be built and utilized to confirm the adequacy of the selected final design. Emphasis would be on ferreting out performance problems associated with critical components or establishing the environmental compatibility of the materials selected.

The preparation of a complete set of management plans for use in Phase 5 is another important program goal that must be achieved during Phase 4. Typical of these plans and related data are the following:

- Design Plan
- Make-or-Buy Plan
- Manufacturing Plan
- Test Plan
- Quality Assurance and Reliability Plan
- Failure Mode and Effects Analysis Plan
- PERT-Cost and Schedules
- Interface Control Plan
- Configuration Management Plan
- Project Control and Data Management Plan
- Mission Operations Evaluation Plan
- Electromagnetic Compatibility Control Plan
- Value Engineering Plan
- Development and Prelaunch Operations Plan
- CEI Identification List
- Critical Components List

The Phase 4 activities will culminate in a Preliminary Design Review (PDR) in July 1970.

Upon approval of the Phase 4 effort by NASA, work on Phase 5, Flight System Development, would be initiated in August 1970. The detail design of the final LEPEPS and design would be completed in February 1971, and a Critical Design Review (CDR) would be conducted in March 1971. After obtaining approval from NASA of these designs, Engineering Test Models (ETM) and Proof Test Models (PTM) of the prototype system would be fabricated. Development and qualification testing would be initiated. It is estimated that a fully qualified LEPEPS would be available by April 1971. Production of the "flight" articles would be started a few months prior to completion of qualification. The First Article Configuration Inspection (FACI) would take place in September 1972. Upon completion of Acceptance Testing at the LEPEPS

FOLDOUT FRAME

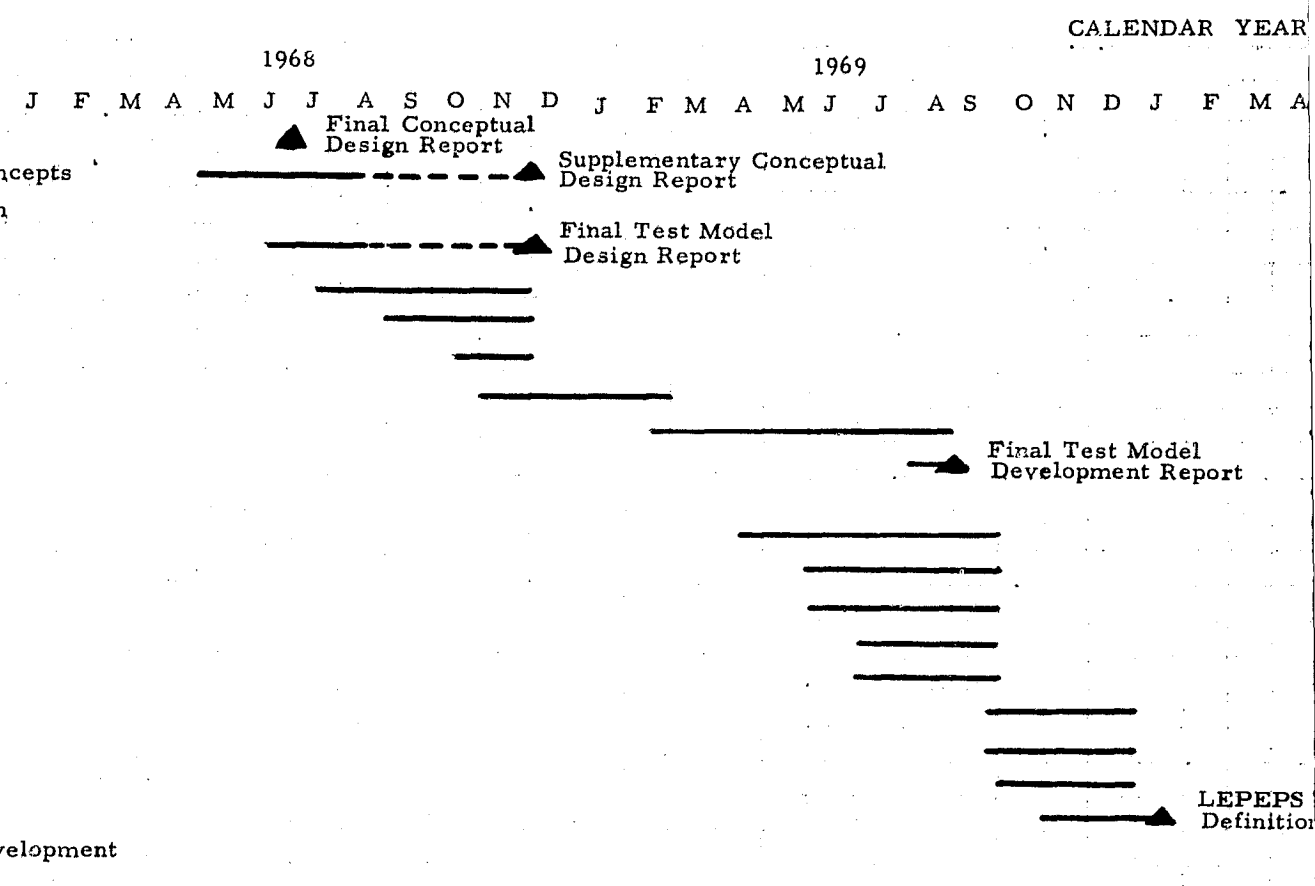

MAJOR MILESTONES

Phase 1 - Parametric Data & Concept Definition
- o Thermal Models - Candidate Solar Array Concepts

Phase 2 - Sub-system Development & Optimization
- o Solar Array & Substrate Design Rqmts.
- o Detail Design of Engr. Test Model
- o Detail Design of Test Fixture
- o Detailed Test Plan
- o Fabrication of ETM and Test Fixture
- o Experimental Test Program
- o Solar Array Panel Development Report

Phase 3 - Concept Verification/Test & Research
- o Solar Array & Structure Design
- o Power Conditioning System Design
- o Power Distribution System Design
- o Stowage & Deployment Design
- o LEPEPS Control System Design
- o LEPEPS/ERPS Interface Spec. (Prelim.)
- o LEPEPS/Logistics Interface Spec. (Prelim)
- o Prelim. Design of LEPEPS
- o LEPEPS Specification (partial; preliminary)

Phase 4 - Final System Definition & Prototype Development
- o Subsystem Specification
- o Critical Component Breadboards
- o LEPEPS Specification (partial, approved)
- o Management Plans (time-phased)
- o Preliminary Design Review

Phase 5 - Flight System Design/Fabri./Qualif.
- o Detail Design of LEPEPS
- o LEPEPS Specification (complete, approved)
- o Intersystem Interface Control Doc. (complete, approved)
- o CEI Part I Spec. & Interface Control Doc. (partial, approved)
- o Critical Components & Long Lead Critical Items Rqmts (complete, approved)
- o Critical Design Review
- o ETM & PTM Fabrication
- o Development/Qualification Testing
- o Production of Flight Articles
- o Assembly and Checkout
- o Acceptance/Integration Testing

FOLDOUT FRAME

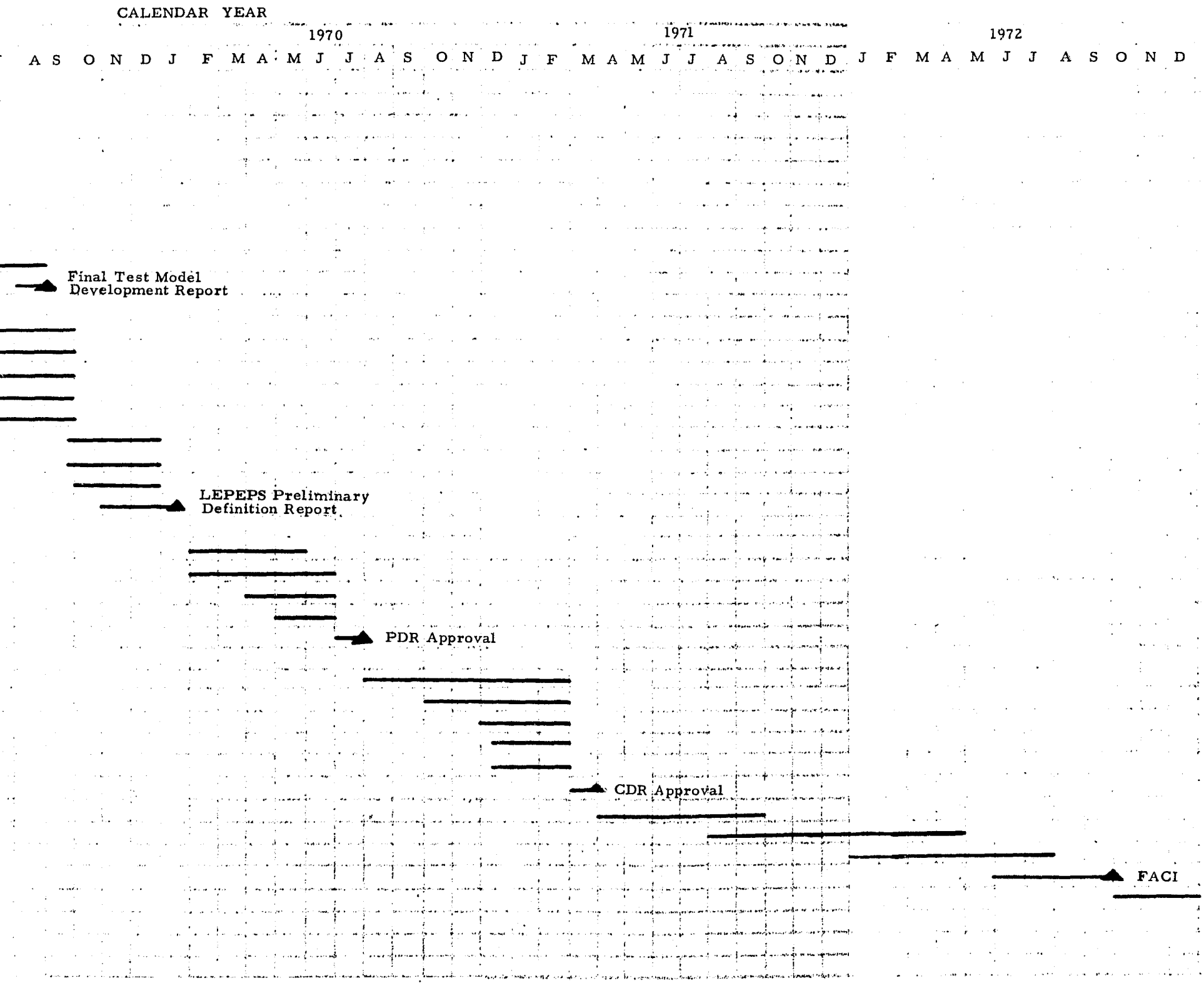

Figure 12.2 Lunar Exploration Primary Electric Power System (LEPEPS) Program Development Plan

contractor's facility, the system will be shipped to the AAP Payload Integration Center at NASA/MSFC for integration with the Saturn V launch vehicle. Final checkout will occur at the Vertical Assembly Building (VAB) and the Complex 39 launch pad at NASA/KSC. During the various mission operations phases (launch, Earth orbit, cis-lunar injection and transfer, lunar orbit, lunar descent, LEPEPS transportation and deployment, and ERPS start-up and activation), the LEPEPS contractor will provide support to the AAP Payload Integration Contractor, and the various organizations (NASA/MSC, NASA/KSC, JPL/TDAS, etc.) charged with the responsibility for implementation of the lunar energy depot.

REFERENCES

1.1 "Study to Establish Criteria for a Solar Cell Array for Use as a Primary Power Source for a Lunar-Based Water Electrolysis System - Technical Plan"; TRW Systems Report No. 7440-62, 15 August 1967. (NASA/MSFC Contract No. NAS8-21189)

1.2 "Lunar Surface Power System Study - Monthly Progress Report No. 3"; TRW Systems Report No. 7440-93, 15 November 1967.

1.3 "Study and Design Optimization of a Water Electrolysis System - Technical Plan"; Chrysler Corporation - Space Division, Technical Report HEG-R59-67, 5 August 1967.

4.1 "Study to Establish Criteria for a Solar Cell Array for Use as a Primary Power Source for a Lunar-Based Water Electrolysis System"; NASA/MSFC RFP No. DCN-1-7-40-79268, 4 May 1967.

4.2 "First Quarterly Technical Progress Report on the Study and Design Optimization of a Water Electrolysis System"; Chrysler Space Division Report HEG-R93-67, 10 October 1967 (NASA/MSFC Contract No. NAS8-21190).

4.3 "Second Quarterly Technical Progress Report on the Study and Design Optimization of a Water Electrolysis System"; Chrysler Space Division Report HGS-R10-68; January 1968.

4.4 "Study of Mission Modes and System Analysis for Lunar Exploration - Final Report - Recommended Lunar Exploration Plan"; LMSC Technical Report, Vol. III; No. A847942; 30 April 1967.

4.5 "Reactor and Shield Subsystems for MORL and Lunar Base Power Plants"; J. D. Gylfe; Proceedings of IECEC at Miami Beach, Fla.; August 13-17, 1967.

4.6 "Cryogenic Engineering"; R. B. Scott; Van Nostrand Co., 1959.

4.7 "The Challenge of Alternate Approaches to the Achievement of Lunar Exploration and Exploitation" by David Paul, III, SAE Preprint No. 650833, 4 October 1965.

4.8 "Testing of Lunar Surface Vehicles Under Simulated Lunar Gravity Conditions" by H. Schoefer, SAE Preprint 660144, 10 January 1966.

4.9 "Water Extraction in the Lunar Environment "; A. E. Wechsler, P. E. Glaser, and J. W. Salisbury; paper presented at 2nd Annual Meeting of the Working Group on Extraterrestrial Resources; Holloman AFB; October, 1963.

4.10 "Work and Thermal Loads on Men Working in Space Suits" ; H. P. Roth, Chrysler Space Division Report No. REL-HFG-65-1 (NASA Document N66-17395), New Orleans, La., 16 August 1968.

5.1 R. E. Smith, et al., "Space Environment Criteria Guidelines for use in Space Vehicle Development, 1967 Revisions ", (NASA TMX 53521 Vol. 4) dated 2-1-67.

5.2 S. C. Charters, et al., "High Speed Impact on Metal Projectiles in Targets of Various Materials ", Proceedings of 3rd Symposium on Hypervelocity Impact, Arnold Research Foundation, October 1959.

5.3 W. R. Webber, "Solar Flare Proton Data ", Nucleonics, August 1961.

5.4 "Geology of Lunar Base ", NAA Report No. SID61-358, Space and Information Division, Space Science Laboratory, dated 5-4-62.

5.5 "Surveyor I Scientific Evaluation and Analysis Team Reports ", Jet Propulsion Laboratories, June 1966.

5.6 LMSC Final Report A847942, "Study of Mission Modes and Systems Analysis for Lunar Exploration (MIMOSA)" NAS 820262, April 30, 1967

6.1 "Approved Materials and Processes List for Surveyor ", Hughes Aircraft Print 291002, 27 October 1965.

6.2 "List of Materials Processes used on LEM, AEA and DEDA Projects ", TRW Drawing M227709, 23 May 1966.

6.3 "List of Materials and Processes Approved for use on DSSO Programs". TRW Drawing M234395.

6.4 Private communication with R. G. Downing, 15 August 1967.

6.5 "Spacecraft Materials Guidebook", Jet Propulsion Laboratories, Revision 4, 1966.

6.6 M. J. Mirtich, et al., "The Performance of N/P Silicon and CdS Solar Cells as Affected by Simulated Micrometeoroid Exposure", NASA/Lewis, 3-67.

6.7 Interim Design Report, EdS 7027-1DR, "Development of Lightweight Rigid Solar Panel", 18 May 1966, NAS7-428.

7.1 "Performance of Very Thin Silicon Solar Cells", E. Ralph, 6th Photovoltaic Specialists Conference, March 1967.

7.2 "Status of the Clevite CdS Thin Film Solar Cell", F. Shirland, 6th Photovoltaic Specialists Conference, March 1967.

7.3 "Report on Cadmium Telluride Thin Film Solar Array Technology", F. Blake, et al, 6th Photovoltaic Specialists Conference, March 1967.

7.4 "Performance of N/P Silicon and CdS Solar Cells as Affected by Simulated Micrometeroids Exposure", M. Mirtich, et al, 6th Photovoltaic Specialists Conference, March 1967.

7.5 "Final Report for Design and Fabrication of a Deployable Large Area Solar Cell Array Supporting Structure", JPL 951107, Report No. 20869-3, April 1967.

7.6 "Preliminary Missions and Systems Analysis", J. Kendrick, TRW Systems Interim Report, September 1967.

7.7 Interim Report I, "Lunar Environment and Materials Survey for Lunar-Based Photovoltaic Solar Arrays", R. Boring, NAS8-21189, September 1967.

7.8 Personal Communication with R. K. Yasui of JPL on December 23, 1967 regarding Boeing V-Ridge Concentrator Solar Array Performance.

7.9 "Phase I Report on the Development of Deployable Solar Arrays", Contract NAS 5-3987, A. C. Maier and B. Lake, Report No. 64B119, Ryan Aeronautical Co., 15 October 1964.

7.10 "Fabrication Feasibility Study of a 30 Watt/Pound Roll-up Solar Array", W. G. King, Fairchild Hiller Corporation Space and Electronics Systems Division, Germantown, Maryland, Report No. 652-00101-Q4, 15 October 1967.

7.11 Proposal for the Study of a Multi-Mission Solar Electric Propulsion Spacecraft, Proposal No. 9451.000, TRW Systems, Redondo Beach, California, 22 May 1967.

7.12 "Cadmium-Sulfide Solar Cells in a Deployable Array Composed of Rigid Frames", L. Lyle McMahand and Henry Oman, The Boeing Company.

7.13 "Advances in Energy Conversion Engineering", Papers presented at 1967 Intersociety Energy Conversion Engineering Conference, The American Society of Mechanical Engineers, August 13-17, 1967.

7.14 "Development of Lightweight Rigid Solar Panels", Contract NAS 7-428, W. Mentrey, Electro-Optical Systems, Inc., Pasadena, Calif., 18 May 1966.

7.15 "Flexible Integrated Solar Cell Array", K. A. Ray, W. D. Brown, W. T. Manion, Hughes Aircraft Company/Space Systems Division, March 1966, Project 8173, Task 81730-007, Contract No. AF 33(615)-2750.

7.16 "Flexible Integrated Solar Cell Array", 2nd Quarterly Report, K. A. Ray, W. D. Brown, W. T. Manion, Hughes Aircraft Company/Space Systems Division, December 1965, Project 8173, Task 81730-007.

7.17 "Flexible Integrated Solar Cell Array", 1st Quarterly Report, K. A. Ray, W. D. Brown, W. T. Manion, Hughes Aircraft Company/Space Systems Division, September 1965, Contract No. AF 33(615)-2750.

7.18 "Report on Cadmium Telluride Thin Film Solar Array Technology", F. A. Blake, GE Spacecraft Department, K. L. Hanson, GE Spacecraft Department, L. D. Massie, AF AeroPropulsion Lab., 27 March 1967.

7.19 "Feasibility Study 30 Watt per Pound Roll-up Solar Array", Quarterly Technical Report No. 1, K. L. Hanson, GE Spacecraft Department, 15 October 1967, Contract JPL 951970.

7.20 "Large Area Solar Array", Contract JPL 951653, The Boeing Company, Aerospace Group, October 1967.

7.21 "Comparative Analysis of Solar Thermionic and Photovoltaic System", The Staff Spacecraft Power Programs, Electro-Optical System, Inc., 21 October 1965, JPL Contract 951066, EOS Report No. 6937-Final.

7.22 "Design and Evaluation Study of Deployable Solar Array for Spinning Satellites", NASA Contract NAS 5-3989, Hughes Aircraft Company/Space Systems Division, October 1964

7.23 "Final Report for the Positive Deployable Solar Array Development Program", Contract No. NAS 5-3988, Goddard Space Flight Center, Greenbelt, Maryland, SSD 52.4, July 1 - September 30, 1964.

7.24 "Final Report for Fabrication Feasibility Study of a 20 Watt per Pound Solar Cell Array", Contract JPL 951132, W. Ratcheson, The Boeing Company, Code Ident. No. 81205.

10.1 "Power Systems"; Space/Aeronautics R&D Issue, 1967

10.2 "Stored Energy Section", Power Sources Division, TRW

10.3 "New Generation Fuel Cell Power Systems for Space Applications", General Electric, Paper presented at 1965 IEEE Meeting, Houston, Texas.

10.4 "Description and Theory of Operation, 2kw Fuel Cell Module for Aerospace Applications", Allis Chalmers Technical Brochure, dated January 1967.

10.5 "Space Power Systems State of the Art", George Szego, Institute for Defense Analysis, Washington, D.C., AIAA Paper No. 64-525

10.6 "SNAP 27 Power Supply System", General Electric Document No. 6300-146A.

10.7 "SNAP 19 Phase II Final Summary Report", MND-3169-83, August 1965 AEC Contract AT(30-1)-3169.

10.8 Data from Presentation at TRW by Don Gylfe of Atomics International.

10.9 Preliminary Analysis of 20 kwe Lunar Based Solar Cell/Fuel Cell Power System with Fuel Cell Reactant Regeneration.

10.10 Task 2.1 (Energy Depot Requirement Survey) Study to Establish Criteria for a Solar Cell Array for Use as a Primary Power Source for a Lunar-Based Water Electrolysis System.

10.11 Working Papers, "Baseline Electrolytic Power System", Information Chrysler Corporation

10.12 "Fuel Cell Briefing", L. M. Handley, October 1967, Pratt and Whitney Aircraft.

10.13 "Study and Analysis of Satellite Power Systems Configurations for Maximum Utilization of Power", TRW Final Technical Report No. 04898-6001-R000, dated 1 September 1967, by J. Leisenring. Prepared for NASA Goddard SFC, Contract No. NAS

10.14 "Power System Configuration Study and Reliability Analysis", TRW Final Report No. 07171-6001-R000, dated 18 September 1967, by W. G. Binckley. Prepared for JPL, sponsored by NASA under Contract No. 951574.

10.15 "ALSEP Apollo Lunar Surface Experiment Package", Phase 1 Report, TRW Report No. 5491-6009-R0000, dated 17 February 1966. Prepared for NASA Manned Spacecraft Center under Contract No. NAS9-5183.

10.16 Paschen, F., Annalen der Physik Und Chemie, Vol. 37 pp 69-96 (1889).

10.17 "Analysis of Aerospace Power Conditioning Component Limitations", Second Quarterly Letter, Contract NAS7-546, 1 October 1967 through 30 December 1967 for NASA Chief, Solar and Chemical Power Systems, Washington D.C., by B. F. Farber, TRW Systems.

BIBLIOGRAPHY

1. Life Support for Lunar Exploration, G. M. Freedman; LMSC, AAS Paper No. 67-323 (EN-3)-1.
2. Surface Transportation Systems for Lunar Operations, S. Romano; GMC, SAE Paper No. 650838; NASE &M Meeting, Los Angeles, California; October 4-8, 1965.
3. Locomotion Energy Requirements for Lunar Surface Vehicles, F. Pavlics; GMC, SAE Paper No. 660149; Auto. Engrg. Conf.; Detroit, Michigan; January 10-14, 1966.
4. Space Environment Criteria Guidelines for use in Space Vehicle Development, NASA Technical Memorandum X-53521, February 1, 1967.
5. Preliminary Requirements Document of Electrolytic Reactants Production System for Lunar Surface Power Systems - Appendix B of PR-DCN 1-7-40-79268.
6. Space Power Systems Advanced Technology Conference; NASA SP-131; LeRC, Cleveland, Ohio, August 23-24, 1966.
7. The Supercritical Thermodynamic Power Cycle, E. G. Feher; McD-Astropower Division; 2nd Intersociety Energy Conversion Engineering Conference, Miami Beach, Florida; August 13-17, 1967.
8. SNAP-27 Power Supply System; GE-M &SD Document No. 6300-146A.
9. Isotope Power Systems for Lunar Roving Vehicles and Small Shelters, W. C. Schmil, J. F. Burgard, I. E. Randall; NAA-AI, pgs. 380-396; IECE Conference, Los Angeles, California; September 26-28, 1966.
10. Small Thermoelectric Generators for Long Unattended Operation, R. A. Lockwood; NAA-AI, pgs. 397-403; IECE Conference, Los Angeles, California; September 26-28, 1966.
11. Solar Cells Today, P. Rappaport, RCA Laboratories, New Jersey; pgs. 404-408; IECE Conference, Los Angeles, California; September 26-28, 1966.
12. Discussion of Power Systems for Solar Probes - Solar Photovoltaic Concepts, S. Gross; Boeing Company; pgs. 24-32; IECE Conference, Los Angeles, California; September 26-28, 1966.

13. Discussion of Solar Power Systems for Solar Probes - Thermoelectrics and Thermionics, P. J. Brosens; TEECO, Massachusetts; IECE Conference, Los Angeles, California, September 26-28, 1966.
14. Drift Field Solar Cells on Silicon Web, K. S. Tarneja, R. K. Riel, J. M. Hicks, R. V. Babcock; Westinghouse, Penn.; pgs. 50-59; IECE Conference, Los Angeles, California; September 26-28, 1966.
15. Comparative Studies of an Electrical Power Generator for a Mars Probe/Lander, M. Koslover; Avco Corporation, Mass.; pgs. 60-83; IECE Conference, Los Angeles, California; September 26-28, 1966.
16. Review of Solar Concentration Technology, A. R. Heath, Jr.; E. L. Hoffman, NASA/LRC; pgs. 231-237; IECE Conference, Los Angeles, California; September 26-28, 1966.
17. A 50-Watt Portable Generator Employing a Solar - Powered Stirling Engine; D. A. Trayser, J. A. Eibling; Battelle Memorial Institute, Ohio; pgs. 238-244; IECE Conference, Los Angeles, California; September 26-28, 1966.
18. A High Energy Density Zinc/Oxygen Battery System, S. M. Chodosh, E. G. Katsordis, M. G. Rosansky; Ceesona-Moos Laboratories; pgs. 266-270; IECE Conference, Los Angeles, California; September 26-28, 1966.
20. A Review of Batteries and Fuel Cells for Space Power Systems, R. C. Shair, S. R. Lerner, P. A. Joyner, G. E. Evans; pgs. 833-838; Journal of Spacecraft and Rockets, Vol. 4, No. 7; July 1967.
21. Photovoltaic Power, P. Rappaport; RCA, New Jersey; pgs. 838-841; Journal of Spacecraft and Rockets; Vol. 4, No. 7; July 1967.
22. Study to Establish Criteria for a Solar Cell Array for use as a Primary Power for a Lunar Based Water Electrolysis System - PR-DCN 1-7-40-79268, Exhibits A and B.
23. Lunar Exploration and Survival, J. Green, DARL Res. Communication No. 8, Paper No. 4038, June 1966; 131 pp.
24. Human Factors and Environmental Control/Life Support Systems Study Program; Lunar Exploration Systems for Apollo; NASA-CR-60909; December 16, 1964; NASA N65-17603, (CFSTI $4.00), 142 pp.

25. Location of a Lunar Base, J. W. Salisbury and C. F. Campen, Jr.; GRD Res. Notes No. 70; October 1961; AFCRL-870, DDC AD 273 816; 44 pp.

26. Exploitation of Lunar Water Resources, M. V. Vasilik, Master's Thesis; August 1964; DDC AD 610 226; NASA N65-20442; 83 pp.

27. Lunar Excavation Techniques in Rock, J. J. O'Kobrick, Master's Thesis; August 1964; DDC AD 610 225, NASA N65-21130; 125 pp.

28. A Lunar Power Plant, R. H. Armstrong, et al.; Report No. ANL-6261; December 1960; 137 pp.; Abstracted in Trans. Am. Nucl. Soc., V. 3, No. 2; December 1960; pp. 383-384.

29. Lunar Drill Study Program, A. V. Dundzila and J. A. Campbell; Report No. ARF 8208-6; January 1961; DDC AD 258 618: 211 pp.

30. Astronauts May Mine the Moon for its Oxygen, Chem. Eng., V. 72, No. 14; June 5, 1965; pp. 62-64.

31. Development of a Lunar Base, J. Brit. Interplanet Soc., V. 13, No. 3; May 1954; pp. 166-169; also in Man and the Moon, ed. by R. S. Richardson, N.Y., World Publ. Co., 1961; pp. 130-133.

32. Land Locomotion on the Surface of Planets, Paper presented at ARS Space Flight Report to the Nation, New York, N.Y., 9-15 October 1961: ARS Paper No. 2015-61: 48 pp.; also in ARS J., V. 32, No. 11; November 1962: pp. 1651-1659.

33. Mechanics of Locomotion and Lunar Surface Vehicle Concepts; Paper Presented at SAE Automotive Eng. Congress and Exposition, Detroit, Michigan; 14-18 January 1963, SAE Paper No. 632K, 19 pp.

34. Thermal Aspects of Long-Term Storage of Propellants on the Lunar Surface; Paper Presented at ARS 17th Annual Meeting and Space Flight Exposition, Los Angeles, California; 13-18 November 1962; ARS Paper No. 2690-62; NASA N63-11273; 37 pp.

35. Lunar Manufacturing, B. B. Carr; Paper Presented at ARS 17th Ann. Meeting and Space Flight Exposition, Los Angeles, California; 13-18 November 1962; ARS Paper No. 2689-62; 6 pp; also published as Recovery of Water or Oxygen by Reduction of Lunar Rock; AIAA J., V. 1, No. 4; April 1963; pp. 921-924.

36. A System Design Technique Applied to Extraterrestrial Surface Vehicles, H. J. Cornille; pp. 137-142; in AIAA/AAS Stepping Stones to Mars Meeting (Baltimore, Md., 28-30 March 1966); N.Y., AIAA, 1966; 577 pp.

37. Comparative Costs of Nondestructive Methods of Transporting Material to a Lunar Base, R. A. Cornog; pp. 691-705; in Advances in the Astronautical Sciences Vol. 6 (Proc. of the 6th Ann. AAS Meeting, New York, 18-21 January 1960); N.Y., Macmillan, 1961; 898 pp.

38. Lunar Basing, J. DeNike; pp. 265-278; in Advances in the Astronautical Sciences, Vol. 10 (Proc. AAS Symp. on Manned Lunar Flight, Denver, Colo., December 29, 1961), ed. by G. W. Morgenthaler and H. Jacobs, No. Hollywood, Calif.; Western Periodicals Co., 1963; 302 pp.

39. Lunar Basing, J. DeNike and S. Zahn; Aerospace Eng., V. 21, No. 10; October 1962; pp. 8-14.

40. Lunar Constructions, G. Dileonardo; ARS J., V. 32, No. 6; June 1962; pp. 973-975.

41. Crew Safety and Survival Aspects of the Lunar Landing Mission, H. M. Drake; pp. 195-215; NASA N62-12866; in Proceedings of the National Meeting on Manned Space Flight (Held in St. Louis, Mo., 30 April - 2 May 1962), N.Y., IAS, 1962; 318 pp.

42. Problems of Lunar and Planetary Exploration, J. L. Friend; Proc. Lunar and Planet. Exploration Colloq., V. 3, No. 1 (NAA Publ. No. 513W11), May 15, 1962; pp. 69-79.

43. Lunar Exploration Vehicles and Equipment, J. E. Froelich and A. B. Hazard; pp. 279-302; in Advances in the Astronautical Sciences Vol. 10 (Proc. AAS Symp. on Manned Lunar Flight, Denver, Colo., December 29, 1961), ed. by G. W. Morgenthaler and H. Jacobs, No. Hollywood, Calif., Western Periodicals Co.; 1963; 302 pp.

44. Life Support Systems for the Lunar Base, J. G. Gaume; Paper Presented at ARS Semi Ann. Meet., Los Angeles, Calif., 9-12 May 1960, ARS Paper No. 1227-60; 11 pp.

45. Electrically-Propelled Cargo Vehicle for Sustained Lunar Supply Operations, J. W. Larson, et al; NASA-CR-67807; June 28, 1965; NASA N66-10612; 235 pp.

46. Life Support System for Stay Time Extension Module (STEM), F. R. Gross; Report No. SP-3778; January 20, 1965; NASA N66-21850; 58 pp.

47. Man-System Locomotion and Display Criteria for Extraterrestrial Vehicles, NASA-CR-71757, December 1965, NASA N66-22226, 67 pp.

48. Vehicle-Soil Dynamics on the Moon, J. D. Halajian; Paper Presented at SAE Automotive Eng. Cong. and Exposition, Detroit, Michigan; 14-18 January 1963; SAE Paper No. 632B; 8 pp.

49. Apollo Logistics Support Systems Molab Studies: Lunar Shelter/ Rover Conceptual Design and Evaluation, E. C. San Juan; NASA-CR-61049; November 1964; NASA N65-24015; 108 pp.

50. Operational Considerations for a Lunar Surface Fixed Shelter with a Small Roving Vehicle, H. J. Heglin; pp. 27-35; in AIAA Fourth Manned Space Flight Meeting (Held in St. Louis, Mo., 11-13 October 1965), N.Y., AIAA, 1965; 343 pp.

51. Lunar Surface Vehicles, L. L. Hofstein and A. W. Cacciola; Paper Presented at ARS 15th Ann. Meeting, Washington, D.C.; 5-8 December 1960; ARS Paper No. 1124-60, 13 pp.; also in Astronautics, V. 6, No. 2, February 1961, pp. 36-38, 52, 54.

52. Planning and Development of Lunar Bases, R. W. Johnson; pp. 285-300; in AIAA/NASA Third Manned Space Flight Meeting (Houston, Texas, 4-6 November 1964), New York, AIAA, 1964.

53. A Comprehensive Analytical Basis for Long-Range Planning Decisions in Future Manned Space and Lunar-Base Programs, D. P. Joy and F. D. Schnebly; Paper Presented at ARS 17th Ann. Meet. and Space Flight Exposition, L.A., Calif., 13-18 November 1962; ARS Paper No. 2714-62; 56 pp.

54. Characterization of Lunar Surfaces and Concepts of Manned Lunar Roving Vehicles, L. Lawrence, Jr. and P. W. Letti; Paper Presented at SAE Automotive Eng. Cong. and Exposition, Detroit, Michigan, 14-18 January 1963; SAE Paper No. 632L, 19 pp.

55. Vehicles for Lunar Exploration, M. Lee; Sci. J., V. 2, No. 8, August 1966; pp. 51-56.

56. Lunar Missions and Exploration, C. T. Leondes and R. W. Vance; New Yrok, Wiley, 1964; 669 pp.

57. Solar Turbo Power Plant Design, D. B. MacKay and E. L. Leventhal; Trans. ASME, Ser. A., J. Eng. Power, V. 82, No. 4; October 1960; pp. 315-324.

58. A Systematic Approach to Shelter Design for Lunar Exploration, F. W. McRae and G. L. Mitcham; Paper Presented at SAE National Aeronautic and Space Engineering and Manufacturing Meeting, Los Angeles, Calif.; 4-8 October 1965; SAE Paper No. 650834; 14 pp.

59. Design Study for Lunar Exploration Hand Tools, D. S. Crouch; NASA-CR-65271, December 1965; NASA N66-20991; 207 pp.

60. Lunar Rock Coring Device Design Study, D. S. Crouch; NASA-CR-65188; October 1965; NASA N66-15364, 197 pp.

61. Next Generation Lunar Transports, J. O. Matzenauer; Paper Presented at SAE Advanced Launch Vehicles and Propulsion Systems Conference, Huntsville, Ala.; 14-16 June 1966; SAE Paper No. 66043, 9 pp.

62. Selection of Power Systems for Lunar Roving Vehicles, J. R. May; Paper Presented at ARS Space Power Systems Conference, Santa Monica, Calif.; 25-28 September 1962, ARS Paper No. 2523-62; 18 pp.

63. A Manned Lunar Surface Vehicle Concept, E. A. Naumann; Paper Presented at AIAA/AFLC/ASD Support for Manned Flight Conference, Dayton, Ohio; 21-23 April 1965; AIAA Paper No. 65-250; 28 pp.

64. Preliminary Locomotion Analysis of Lunar Surface Vehicles, W. B. Sponsler, Report No. NSL 62-164; August 1962; 29 pp.

65. Apollo Logistics Support Systems Molab Studies: Task Report on Molab Concept Evaluation Methods, D. Ross; NASA-CR-61021, 1964; NASA N65-12022; 8 June - 21 August 1964, 47 pp.

66. The Challenge of Alternate Approaches to the Achievement of Lunar Exploration and Exploitation, D. Paul; Paper Presented at SAE National Aeronautic and Space Engineering and Manufacturing Meeting, Los Angeles, Calif.; 4-8 October 1965; SAE Paper No. 650833; 8 pp.

67. Environmental Control Development and Lunar Base Support Systems, Proc. Lunar and Planet. Explorations Colloq., V. 3, No. 3 (NAA Publ. No. 513W13), November 1963; pp. 119-126

68. The Ecological Complex in Extraterrestrial Bases, S. H. Dole; Paper No. P-3009, November 1964; DDC AD 608 840; 7 pp.

69. Water Recovery in Lunar Environment, R. N. Rickles; Space/Aeronautics, V. 41, No. 3, March 1964; pp. 103, 105.

70. The Manufacture of Propellants for the Support of Advanced Lunar Bases, S. D. Rosenberg; Paper Presented at SAE National Aeronautic and Space Engineering and Manufacturing Meeting, L.A., Calif.; 4-8 October 1965; SAE Paper No. 650835; 16 pp.

71. Technologies for Lunar Base Support, J. W. Salisbury; Proc. and Planet. Exploration Collog., V. 3, No. 3, (NAA Publ. No. 513W13); November 63; pp. 31-37.

72. The Implications of Water as a Lunar Resource, J. W. Salisbury; Proc. Lunar and Planet. Exploration Colloq., V. 3, No. 3 (NAA Publ. No. 513W13), November 1963; pp. 39-53.

73. Economic Implications of Extracting Propellants from the Moon, R. J. Salkeld; J. Spacecraft and Rockets, V. 3, No. 2, February 1966; pp. 254-261

74. Propellant Production on the Moon, H. M. Segal; Space/Aeronautics; V. 40, No. 4; September 1963, pp. 92-94.

75. The Manned Lunar Base, G. A. Smith; Proc. Lunar and Planet. Exploration Colloq., V. 3, No. 3, (NAA Publ. No. 513W13); November 1963; pp. 3-9.

76. A Study of the Feasibility of Using Nuclear Versus Solar Power in Water Extraction from Rocks, J. Green; Report No. SID 64-1430; 31 July 1964; AFCRL 64-733; DDC AD 608 225, 252 pp.

77. Techniques for Lunar Water Exploration, J. K. Westhusing and C. Crowe; Final Report; September 30, 1964; AFCRL 64-814; DDC AD 608 957, NASA N65-15284; 408 pp.

78. The Lunar Base: A Bibliography, L. R. Magnolia and A. K. Kunlap; Report No. 9990-6450-KU-000, August 1963, DDC AD 413 433, NASA N63-22777; 92 pp.

79. Scientific Exploration of the Moon Using a Roving Vehicle, O. L. Tiffany and E. M. Zaitzeff; Paper Presented at SAE Automotive Engineering Congress, Detroit, Michigan; 10-14 January 1966; SAE Paper No. 660145; 8 pp.

80. Advanced Life Support Systems for the Lunar Base, B. E. Welch; Proc. Lunar and Planet. Exploration Colloq., V. 3, No. 3 (NAA Publ. No. 513W13); November 1963; pp. 101-109.

81. Westinghouse Lunar Powerplants Study, Av. Wk. Space Technol., V. 79, No. 9, August 26, 1963, p. 63.

82. Lunar Mobile Laboratory: Design Characteristics, R. E. Wong and L. Galan; Paper Presented at SAE Automotive Eng. Congress, Detroit, Michigan; 10-14 January 1966; SAE Paper No. 60146; 11 pp.

83. Visual Display Simulation of Lunar Landing Under Remote Control by a Human Operator; H. F. Meissinger, F. J. Belsky; Space Rendezvous, Rescue and Recovery Symposium; EAFB, California; September 10-12, 1963 (TRW Report No. 9352.2-27 of 14 April 1965).

84. Human Performance Capabilities in Spacecraft Control; Leland G. Summers; HFS and AAS Symposium, San Fernando Valley State College, Northridge, California; April 14-15, 1965 (TRW Report 9350.6-63 of 25 August 1963).

85. Lunar Power Systems, F. Schulman and A. H. Smith; AIAA Paper No. 67-902; AIAA Fourth Annual Meeting and Technical Display, Anaheim, California, 23-27 October, 1967.

86. Solar Cell Array for Lunar Surface Operations, A. E. Mann; Sixth Photovoltaics Specialists Conference, Vol. II; Cocoa Beach, Florida; 28-30 March 1967.

APPENDIX A

USE OF SOLAR ARRAY TO CONSERVE LUNAR SURFACE VEHICLE REACTANTS

USE OF SOLAR ARRAY TO CONSERVE LUNAR SURFACE VEHICLE REACTANT

The performance of lunar surface vehicles (LSV) can be enhanced by mounting solar cells on the top and sides of the vehicle. Solar energy received by these cells is converted into electrical energy similar to the output of the fuel cells which normally provide the energy needs of the LSV.

The effectiveness of solar cells mounted above the LSV depends primarily upon the phase angle of the Sun with respect to the array and the temperature of the array. The same performance characteristics as discussed in Section 8 with regard to the LEPEPS solar array apply to the LSV installation. For example, the flat array generates little power at sunrise and sunset due to the small phase angle. Just as the leanto was found to improve the sunrise/sunset characteristics, mounting solar cells on the sides of the LSV tends to make the power profile more nearly constant throughout the day. And just as the use of edge skirts was found to have an important effect on the power output of the primary array, likewise the suppression of view angles of the hot lunar surface would be beneficial to the LSV array.

Provision for a solar array over the manned compartment would shade the LSV and reduce the environmental control and life support (ECS/LS) power requirements. Likewise, the presence of a temperature conditioned body beneath the solar array blocks its view of the hot lunar surface and improves the power output. For simplicity in the following analysis, the solar array power output was assumed to remain constant at an average value of 4 w/ft^2 throughout the lunar day as discussed in Section 4.4.3. This is believed to be a conservative assumption, but should be confirmed at a later date by more detailed analysis. The many interactions between the solar array design, temperatures and LSV operational factors should be considered.

Effective use of a solar array to augment the fuel cells will depend upon the power demand profile of the vehicle. During stationary periods, excess power supplied by the array will be unused unless secondary batteries are provided to store the excess energy, above that which may be required to satisfy the continuous environmental control and life support power requirements.

In the following analysis three lunar surface vehicles were considered (Figure 4-4 of Section 4).

Table A.1 Lunar Surface Vehicle Performance Characteristics

Vehicle	Max. Power (kw), P_{max}	Total Energy Required (kw hr), P_{tot}	Mission Duration (hr), T_M	Average Power (kw) P_{avg}	ECS LS Power (kw), P_L
LRRV	9	4000	2020	1.98	0.42
MOLAB	5	525	336	1.56	0.39
LSSM	3	5	6	0.83	--

The MOLAB vehicle will be used as an example in developing the following performance equations and curves, since this is the vehicle being considered for the Program V mission.

Figure A-1 shows the percent of total vehicle power supplied by the solar array versus elapsed time for several different duty cycles. In the first case (Figure A-1a), the vehicle continually absorbs energy from the solar array at some average power level (P_{avg}), over the entire mission duration. The second case (Figure A-1b) utilizes batteries to store energy when the actual power demand, P_{min}, is lower than the value, P_{sa}, supplied by the solar array. In the third case, a "worst-possible" duty cycle (max. power, then min. power, Figure A-1c and 1d) has been assumed without the use of batteries for storage, in which case a portion of the solar energy is wasted when the vehicle is stationary.

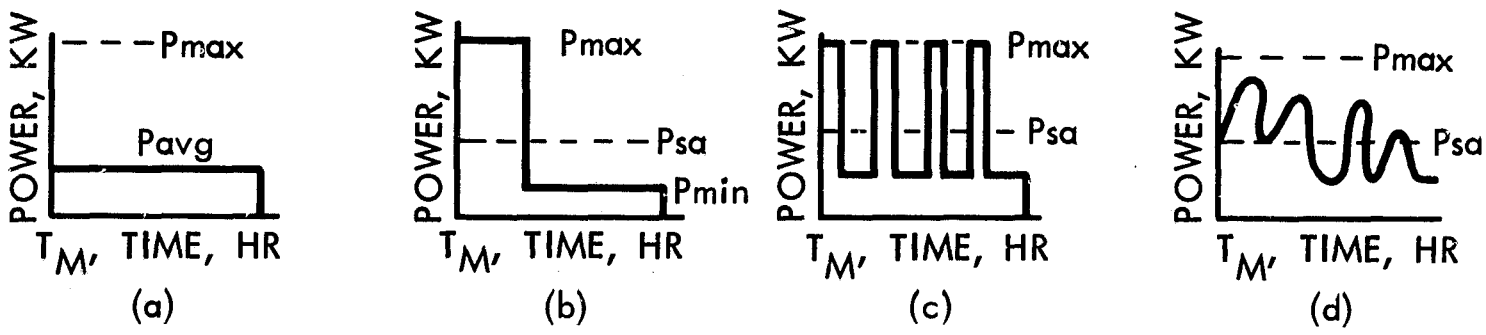

Figure A.1 Typical Power Profiles for LSV

The percent power, η_p, for Case A-1a (steady power output) in terms of solar array area, A, (producing an average of 4 w/ft^2 = 0.004 kw/ft^2. See Section 4.4.3) is,

$$\eta_p = \frac{\text{power produced}}{\text{avg. power needed}} = \frac{0.004A}{1.56} = 0.00256A \qquad (A.1)$$

The equation for Case A-1b (two levels of power, with battery storage) is,

$$\eta_p = \frac{\text{power utilized}}{\text{avg. power needed}} =$$

$$= \frac{\begin{bmatrix}\text{energy utilized}\\ \text{during max.}\\ \text{power demand}\\ \text{periods}\end{bmatrix} + \begin{bmatrix}\text{life support}\\ \text{energy}\\ \text{demands}\\ \text{during}\\ \text{stationary}\\ \text{periods}\end{bmatrix} + \left[\begin{pmatrix}\text{battery}\\ \text{efficiency}\end{pmatrix}\begin{pmatrix}\text{power}\\ \text{pro-}\\ \text{duced}\end{pmatrix} - \begin{pmatrix}\text{life}\\ \text{support}\\ \text{power}\end{pmatrix}\begin{pmatrix}\text{length of}\\ \text{min. pwr.}\\ \text{period}\end{pmatrix}\right]}{\text{Total energy required}}$$

$$= \frac{(86)(0.004A) + (250)(0.39) + (0.6)(0.004A - 0.39)(250)}{525} \qquad (A.2)$$

where, length of max. energy demand = 86 hours

length of min. energy demand = 250 hours

power from solar array = 0.004A kw (i.e., 4w/ft^2)

life support power = 0.39 kw

battery recharge efficiency η_c = 0.6

total energy required, 525 kw-hrs

It should be noted that with an array area smaller than 98 ft^2 (0.39 kw at 4w/ft^2) all the power produced is absorbed by the life-support system. Excess power produced by larger areas during intermittent stationary periods could be stored in secondary batteries. However, the batteries may not be able to utilize all the power that they absorb due to the recharge efficiency η_c.

For Case A-1c or 1d (two levels of power, no battery storage) the conditions are

$$\eta_p = \frac{\text{power produced}}{\text{avg. power needed}} = \frac{0.004A}{1.56}; \quad A \leq 98 \text{ ft}^2 \qquad \text{(A. 3)}$$

$$= \frac{(86)(0.004A) + (0.39)(250)}{1.56}; \quad A > 98 \text{ ft}^2$$

With an array smaller than 98 ft^2 all the power produced will be absorbed by the known steady-state demands of the life-support system. For larger arrays, a max/min. power cycle is assumed in which for a period of 86 hours, up to 5 kw may be absorbed and used from the array, and for a period of 250 hours only the life support demand (0. 39 kw) is used. Any excess power from the solar array would be dumped.

System Weight. The battery weight required to store excess solar energy varies directly as the length of time, T_s, the period when the vehicle is stationary. Normal stopping times for MOLAB would be expected to fall in the range of 1 to 10 hours. System weight, W, is related to solar array area (at W_a = 0. 5 lbs/ft^2) and amount of energy to be stored in the batteries (at W_b = 30 lb/kw hr), as shown in Figure A-2 and expressed by the relationship,

$$W\,(\text{lb}) = W_a A + W_b (P_s - P_L) T_s = 0.5A = (30)(0.004A - 0.39)T_s \qquad \text{(A. 4)}$$

where P_s is the solar power generated (0. 004A kw) and P_L is the life support power level (0. 39 kw).

The percent saving in LSV propellant is equal to the percent energy from Equation A. 2,

$$\eta_p (525) = 0.004A\,(336 - T_s) + 0.39\,T_s + 0.6\,(0.004A - 0.39)T_s \qquad \text{(A. 5)}$$

Solving for A and substituting in Equation A. 4 gives

$$W = \frac{(525\,\eta_p) - (0.156\,T_s)}{1.34 - (0.0016\,T_s)}\,(0.5 + 0.12\,T_s) - 11.7\,T_s \qquad \text{(A. 6)}$$

The system weight is shown in Figure A-3 as a function of stationary time, T_s, and percent energy saved by solar array.

The weight of fuel and tankage saved is ΔW_{ft}, and is expressed by the equation,

$$\Delta W_{ft} = (525\ \eta_p)\ (0.91)\ (1 + 0.3) = 620\ \eta_p \qquad (A.7)$$

System weight is shown in Figure A-4 as a function of ΔW_{ft} and stationary time. The break-even line is indicated, along which the total system weight is equal, with and without the solar array.

Figure A-5 is a plot of percent of total energy supplied by the solar array/battery system versus the stationary period for various system weights. This is obtained by solving Equation (A.6) for (η_p), so that,

$$\eta_p = \eta_{TE} = \frac{(1.34 - 0.0016\ T_s)\ (W) + 15.8\ T_s}{262 + 63\ T_s} \qquad (A.8)$$

NOMENCLATURE

A = area of solar array, (ft^2)

P_{max} = maximum power available, (kw)

$P_L = P_{min}$ = minimum power (for ECS/LS), (kw)

$P_s = P_{sa}$ = solar array power, (kw)

T_s = stationary time of vehicle, (hrs.)

T_M = mission duration, (hrs.)

W_a = weight/unit area of solar array, (lbs)

W_b = battery weight/unit energy, (lbs)

W = system weight (solar array plus batteries), (lbs)

W_{ft} = weight of fuel and tankage, (lbs)

η_c = recharge efficiency for batteries, (%)

η_p = percent power, (%)

η_{TE} = percent total energy, (%)

η_{sa} = percent average power from solar array, (%)

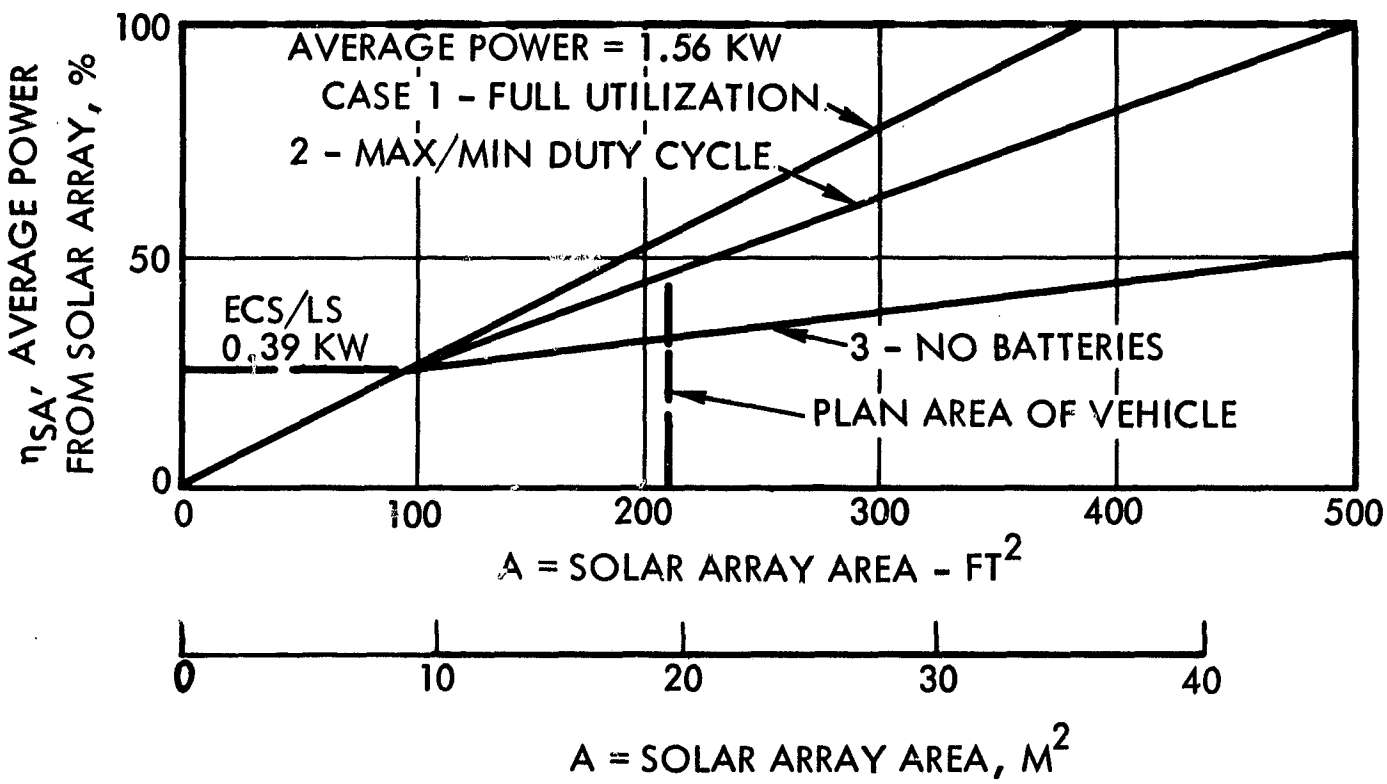

Figure A.2 Percent Power from Solar Array vs. Area (MOLAB)

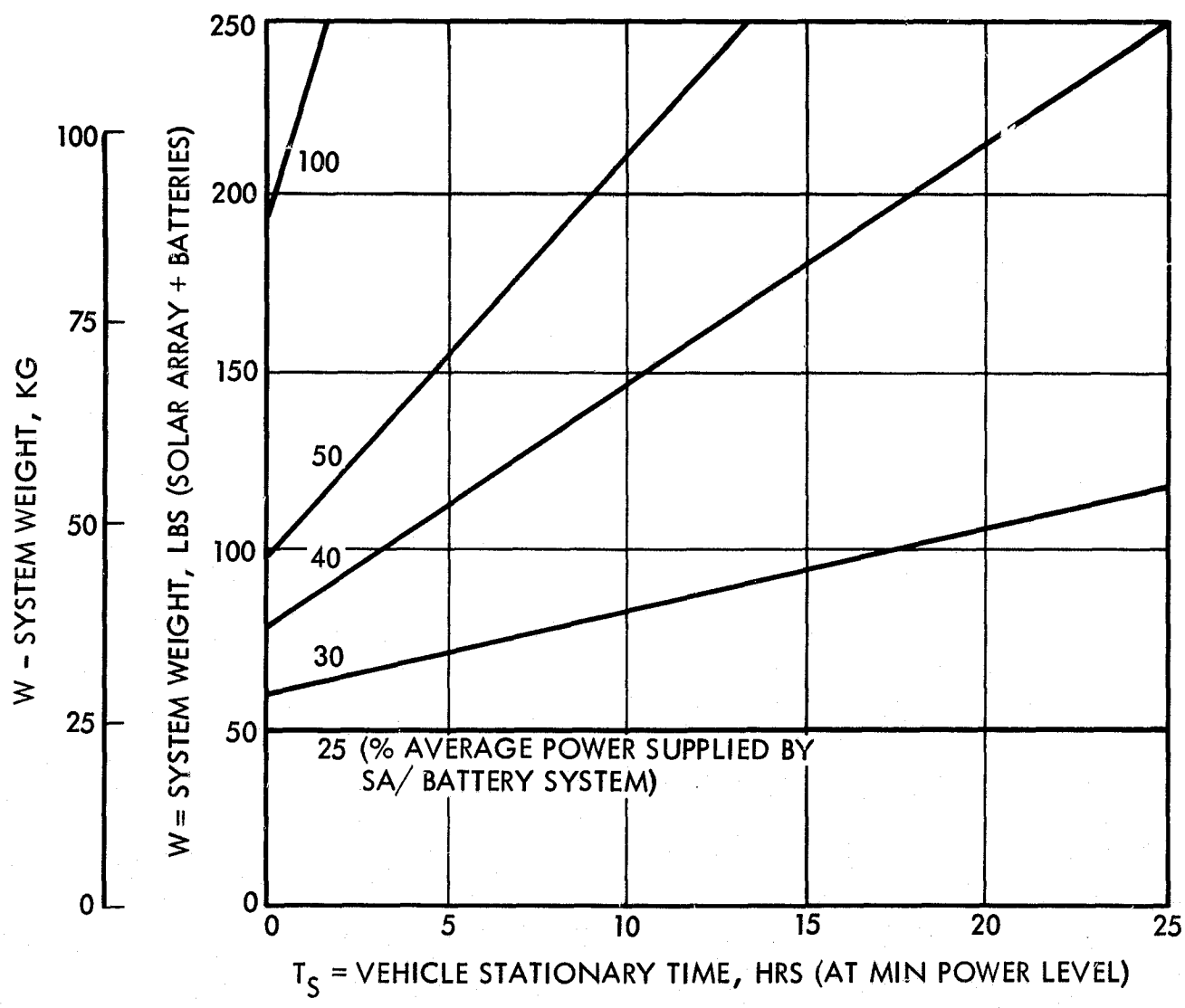

Figure A.3 System Weight vs. Stationary Time (MOLAB)

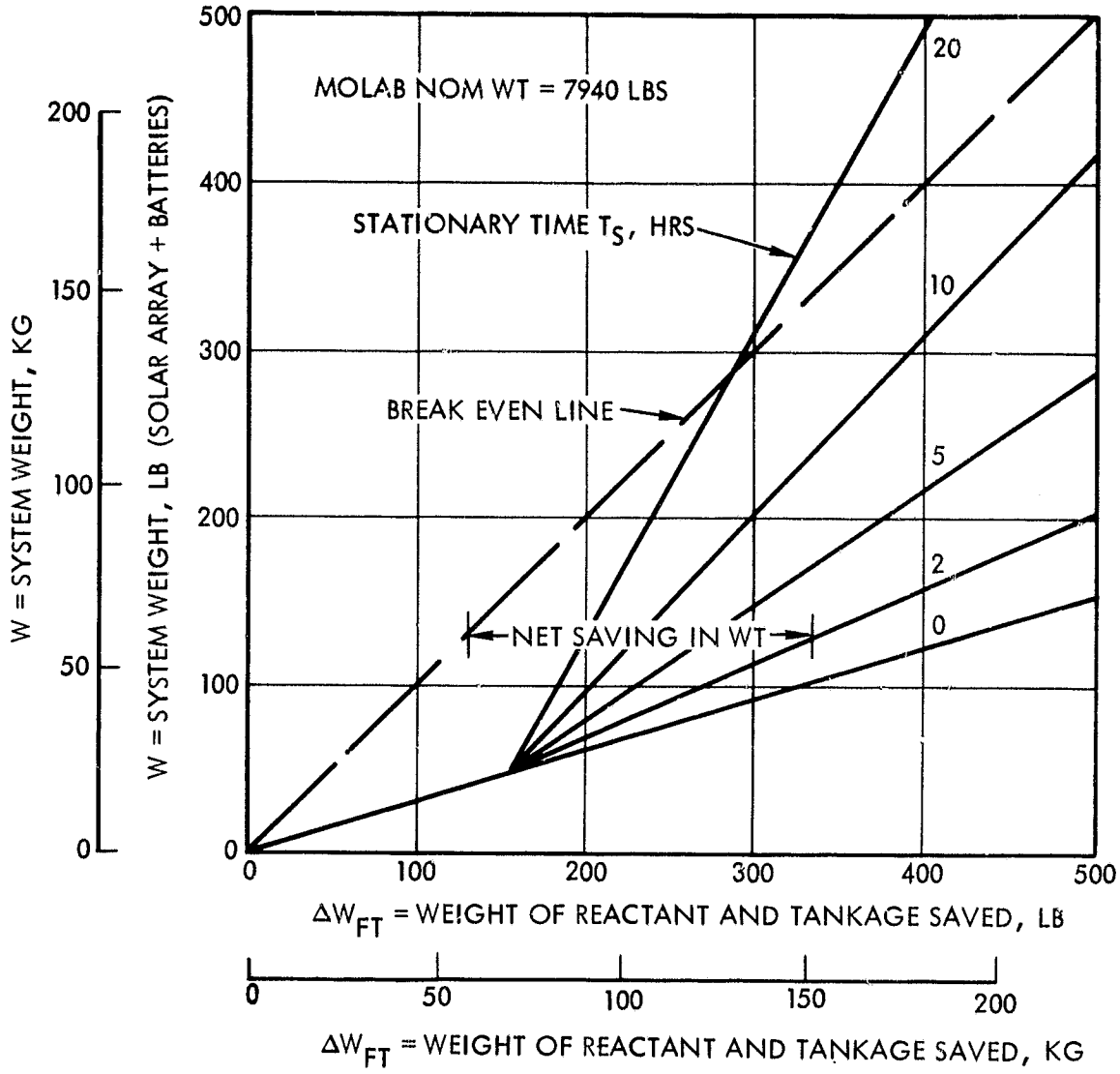

Figure A.4 System Weight vs. Reactant Saved

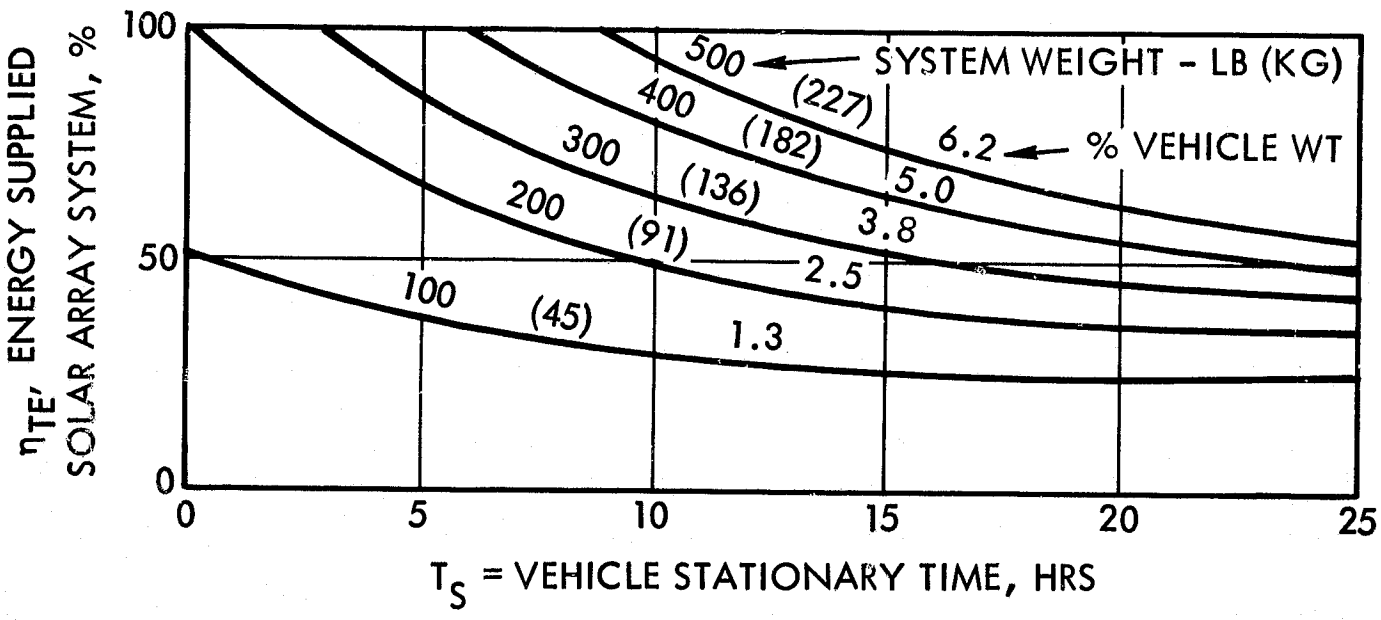

Figure A.5 Percent Energy vs. Stationary Time (MOLAB)

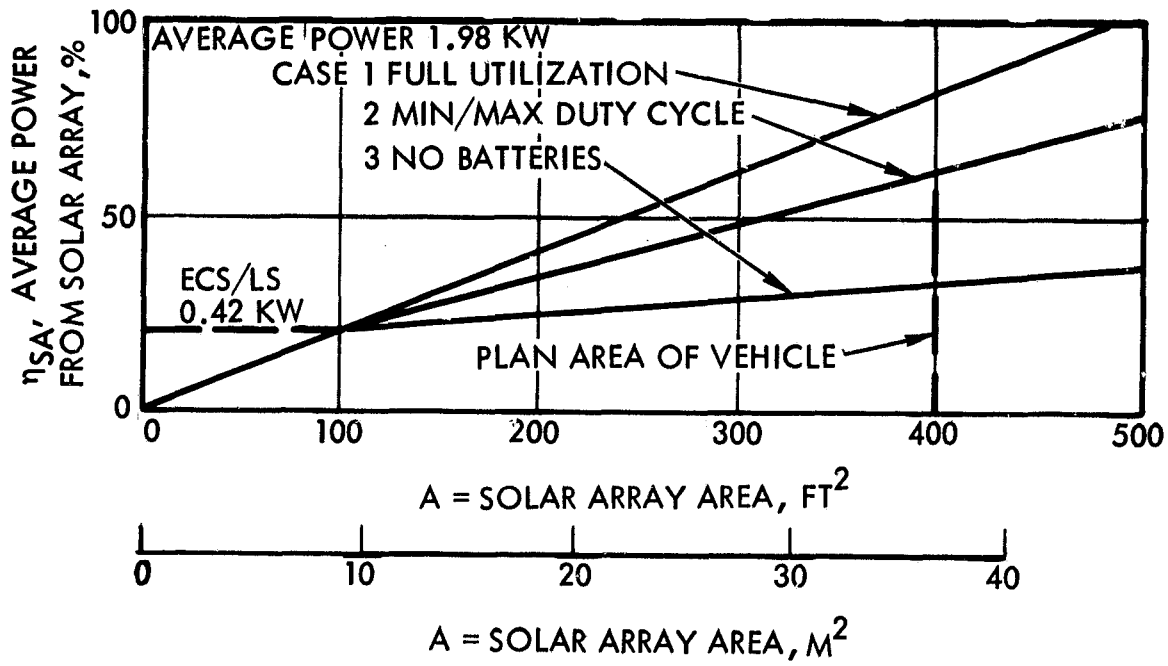

Figure A.6 Percent Power from Solar Array vs. Area (Long Range Reconnaisance Vehicle)

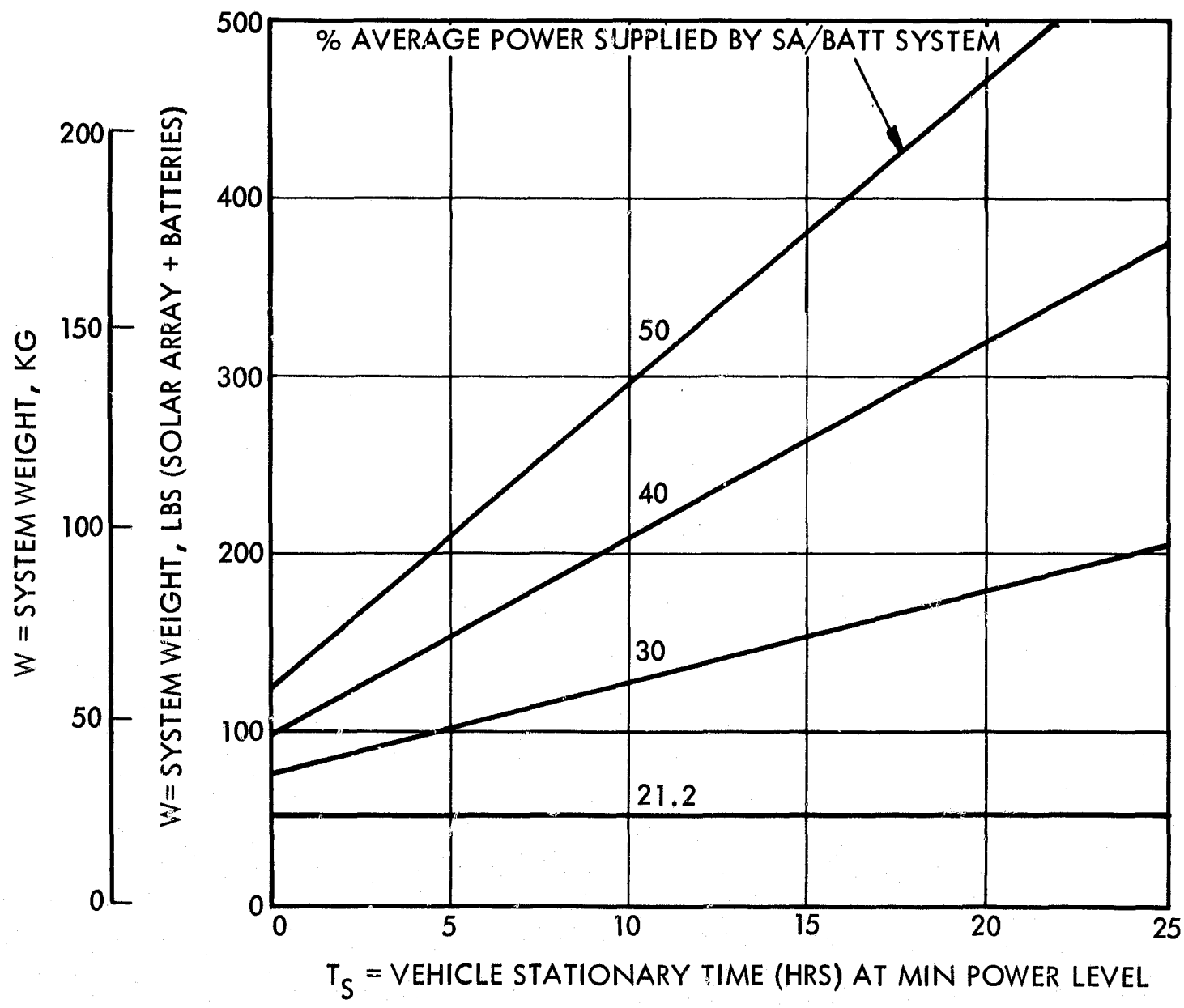

Figure A.7 System Weight vs. Stationary Time (Long Range Reconnaisance Vehicle)

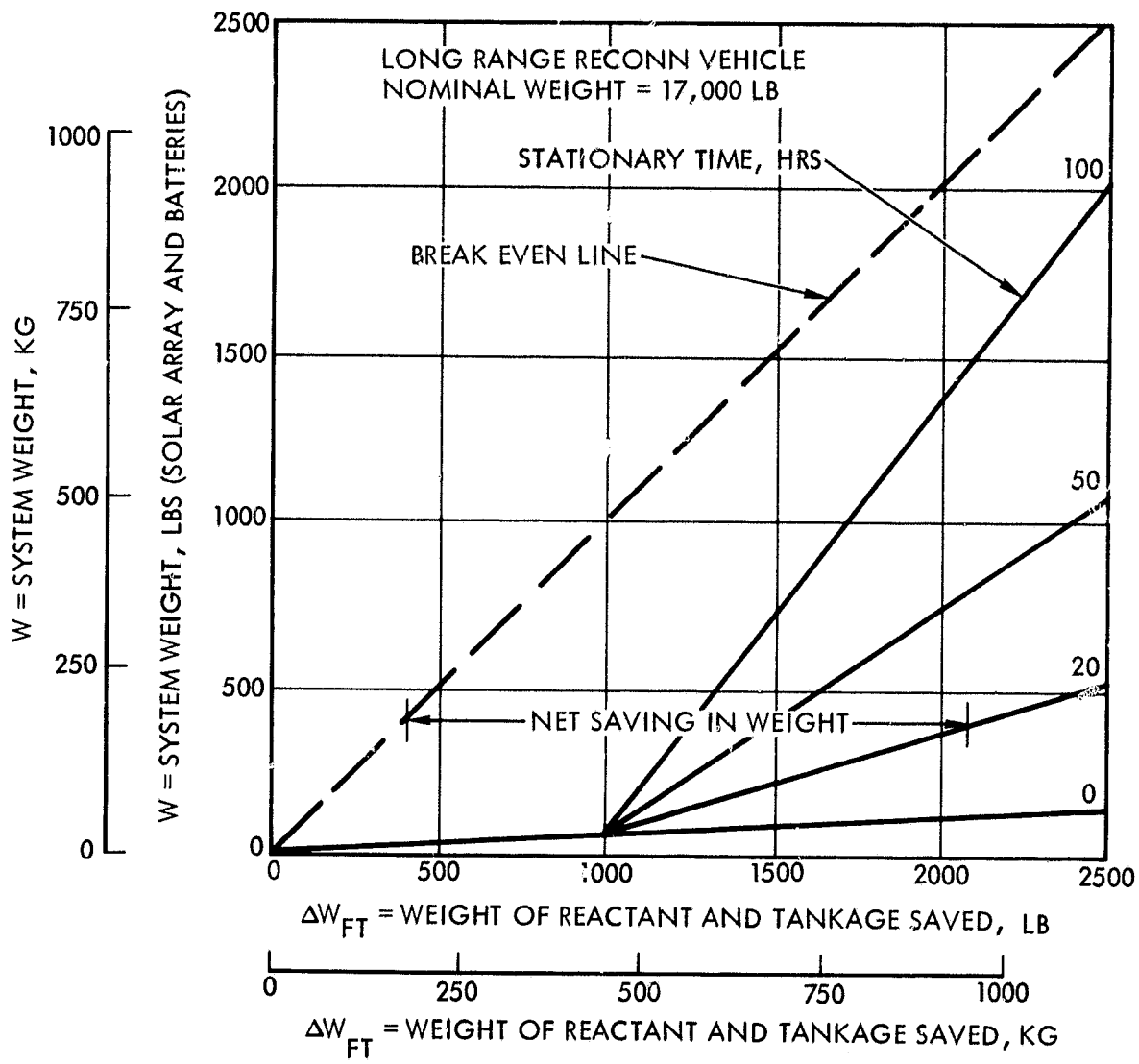

Figure A.8 System Weight vs. Reactant Saved

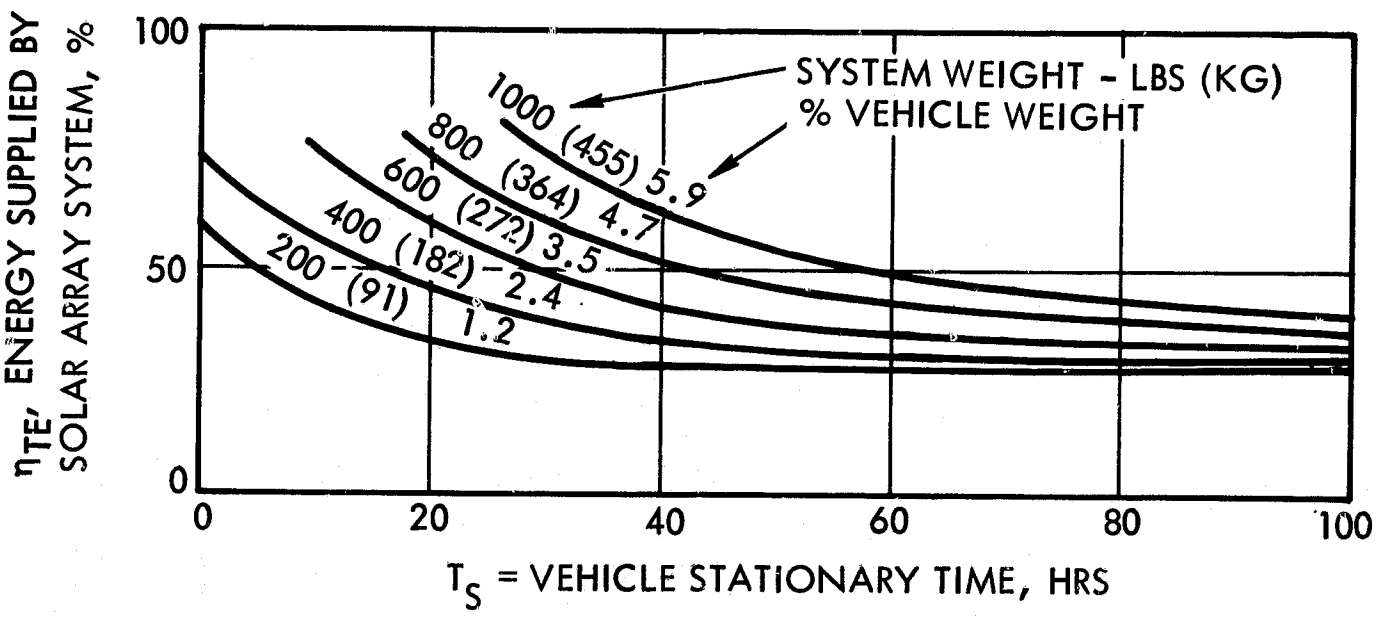

Figure A.9 Percent Energy vs. Stationary Time (Long Range Reconnaisance Vehicle)

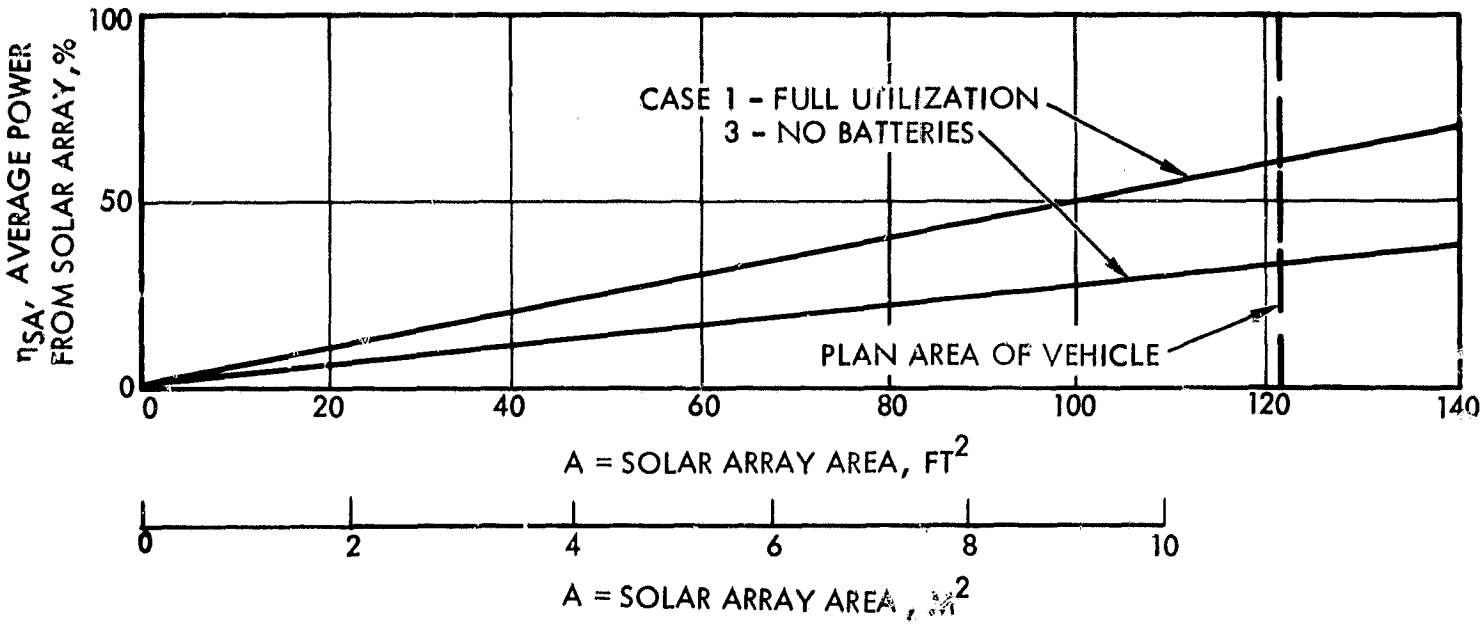

Figure A.10 Percent Power from Solar Array vs Area (LSSM)

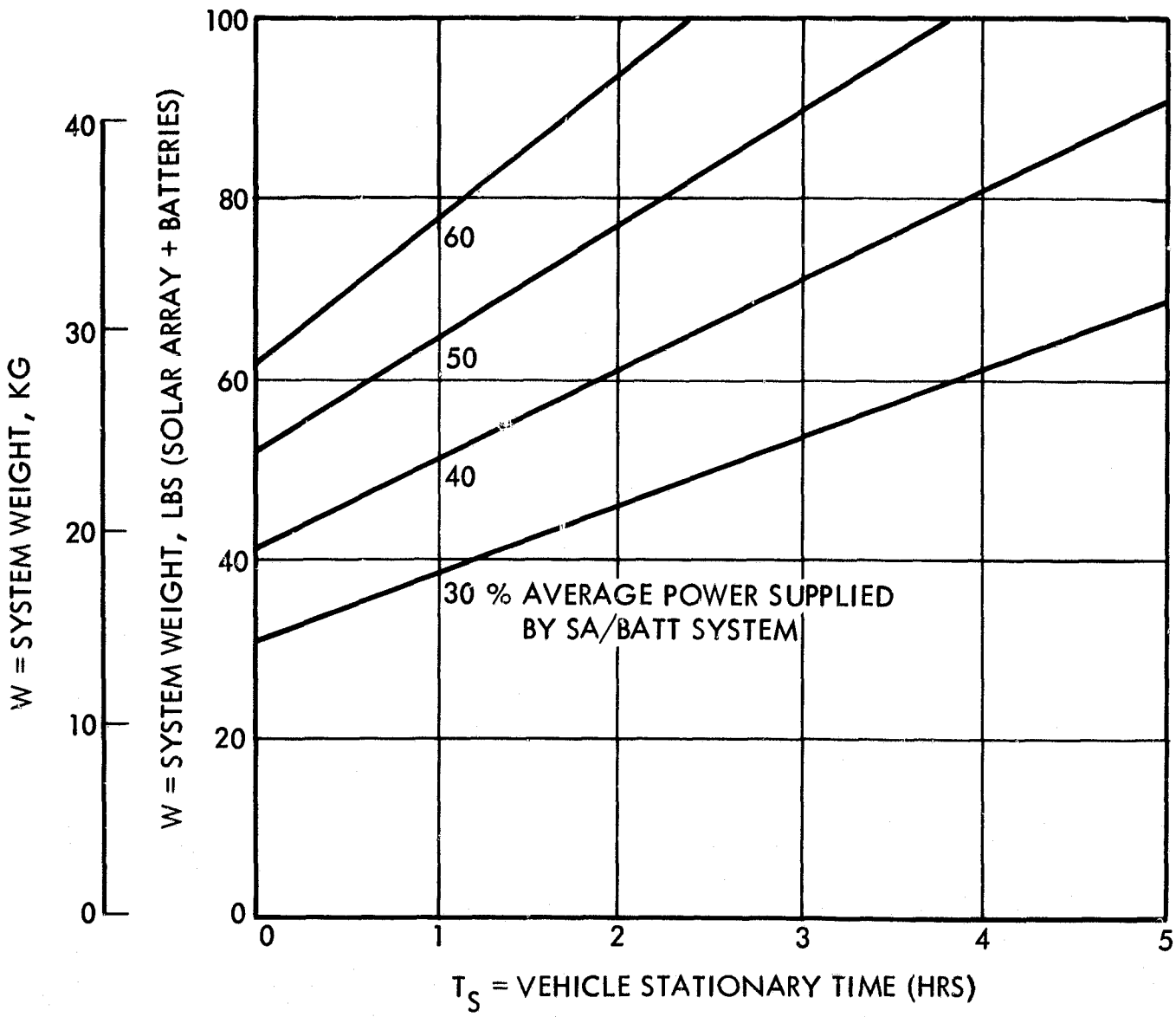

Figure A.11 System Weight vs. Stationary Time (LSSM)

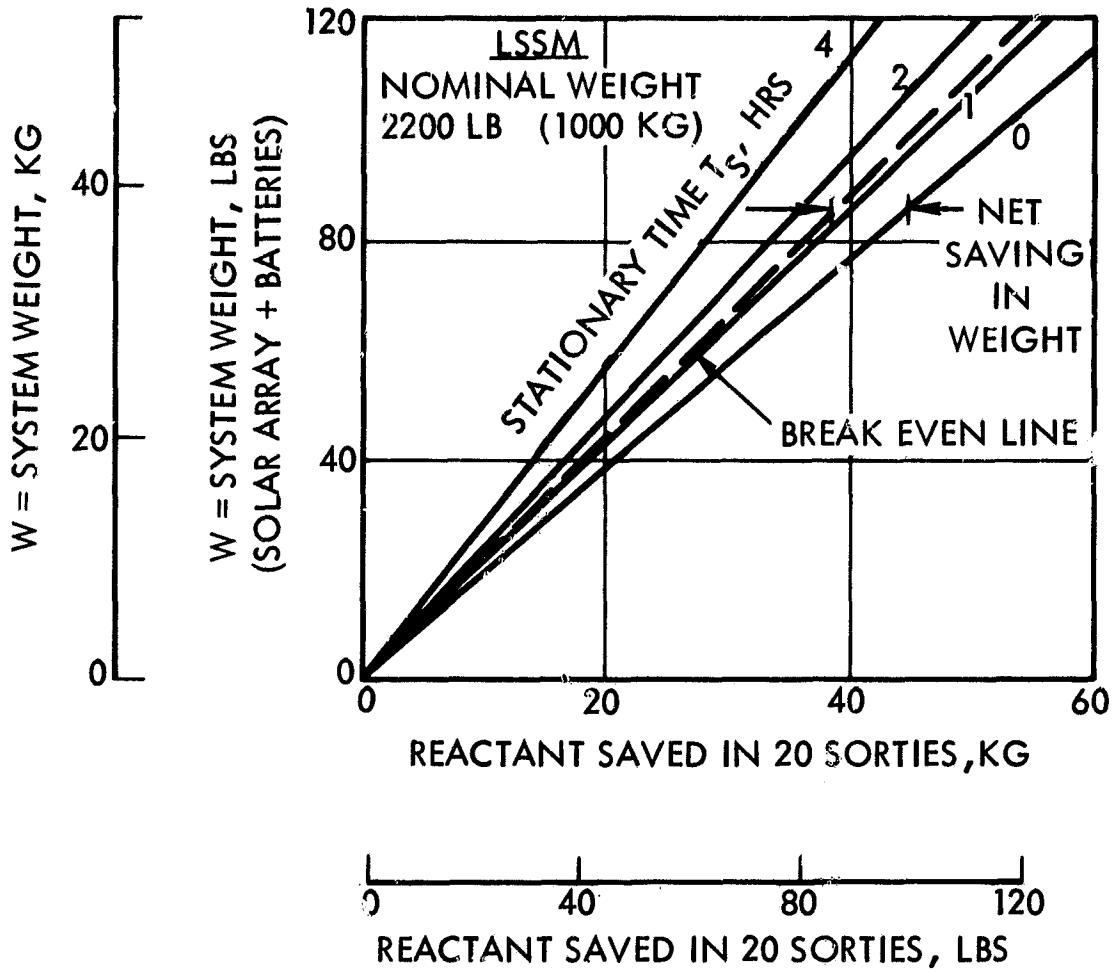

Figure A.12 System Weight vs. Reactant Saved

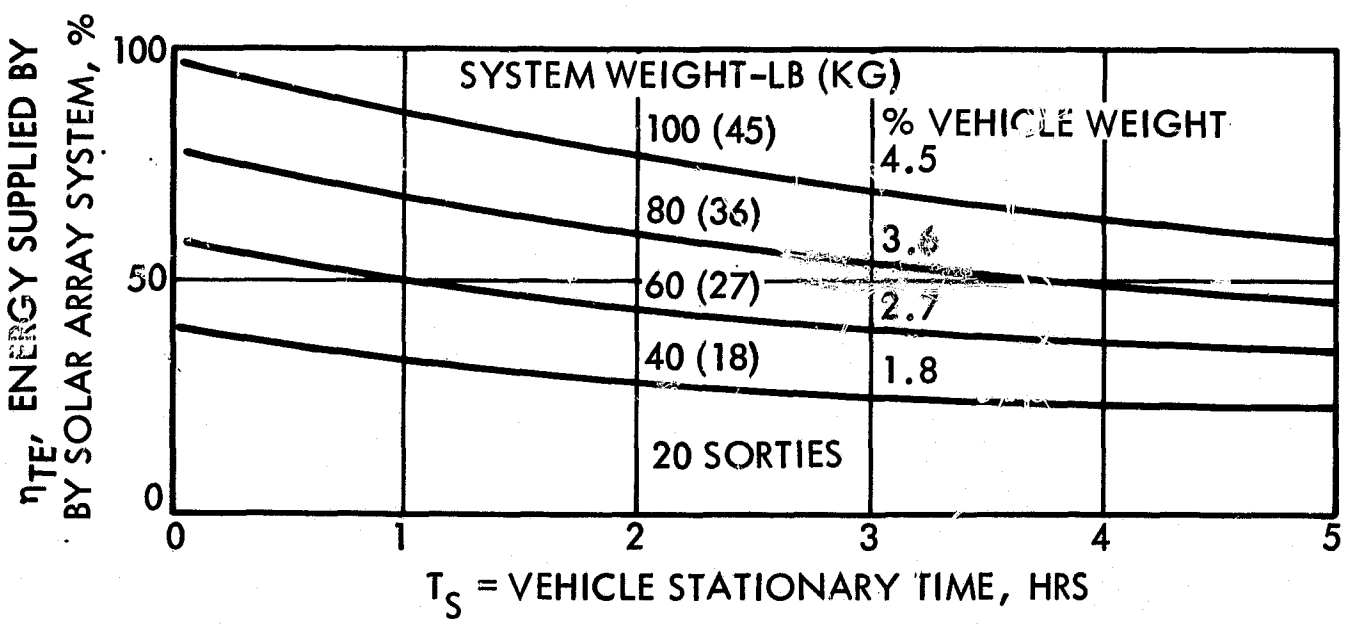

Figure A.13 Percent Energy vs. Stationary Time (LSSM)

APPENDIX B

DESIGN REQUIREMENTS DOCUMENT

FOR

A LUNAR SURFACE POWER SYSTEM

1. SCOPE

1.1 GENERAL

This document establishes, on a preliminary basis, the requirements for a Lunar Surface Power System (LSPS). The LSPS will be used to provide electric power in support of a lunar based Electrolytic Reactants Production System (ERPS). In addition the LSPS will furnish electric power to sustain base operations during periods of darkness and dormancy. The LSPS consists of the Lunar Exploration Primary Electric Power System (LEPEPS) and the Secondary Electric Power System (SEPS). This document is limited to identifying the requirements or for the LEPEPS.

1.2 LIMITATIONS

The electric power system described conforms to a selected baseline mission of three men on the lunar surface for two 90 day periods interspersed with a 180 day unmanned dormant period. The power requirements to the users (ERPS and Shelter) are in conformance with the preliminary Program V mission as noted by Reference 2.1.

The power distribution and control system tentatively selected, is one of several considered during a study to establish criteria for a solar cell array for use as a primary power source on the lunar surface (References 2.2 and 2.4).

In those cases where data was not available in Reference 2.1, assumptions have been made. They are reflected in this DRD with the added notation, "To Be Confirmed", (TBC). These values were based upon TRW Systems experience with this type of electrical system or component. In those cases where this was not possible, the DRD has designated these requirements as "To Be Supplied", (TBS).

2. REFERENCE DOCUMENTS

2.1 "Study and Design Optimization of a Water Electrolysis System (Preliminary Working Papers)", Space Division of Chrysler Corporation, Huntsville Operations, Contract NAS8-21190, 19 September, 1967.

2.2 "Study to Establish Criteria for a Solar Cell Array for use as a Primary Power Source for a Lunar Based Water Electrolysis System, Technical Plan", TRW Document 7440-62, 15 August 1967.

2.3 TRW Report 5491-6009-R0000, Phase I Report ALSEP Appollo Lunar Surface Experiment Package, 17 February 1966. Prepared under Contract NAS9-5183 for Manned Spacecraft Center, NASA.

2.4 TRW Report 09681-6002-R000; "Study to Establish Criteria for a Solar Cell Array for Use as a Primary Power Source for a Lunar-Based Water Electrolysis System - Phase I Final Technical Report"; Contract NAS8-21189, NASA/MSFC; 30 June 1968.

2.5 TRW Report 3310.2-50, Preliminary Missions and Systems Analysis for Study of a Solar Cell Array for Use as a Primary Power Source for a Lunar-Based Water Electrolysis, Task 2, Contract NAS8-21189 for NASA/MSFC, September 15, 1967.

2.6 TRW Report 07171-6001-R000, Power System Configuration Study and Reliability Analysis, Final Report, Contract 951574 for JPL, September 18, 1967.

3. SYSTEM DESCRIPTION AND OPERATION

3.1 DESCRIPTION

The primary electric power system (LEPEPS) will consist of the following elements:

a) Solar Arrays
b) Load Power Conditioning
c) Monitoring and Operation Controls

d) Standby Power Storage and Associated Controls

e) Connecting Cabling and Harnesses

A block diagram showing the relationship of all the above subassemblies is given in Figure B.1. A tentative layout of all the equipment using judiciously selected separation distances is shown in Figure B.2.

3.2 OPERATION REQUIREMENTS

3.2.1 Active

During the lunar day the photovoltaic solar arrays will provide electric power at 300 volts dc to the main unregulated bus. Here the power will be distributed between the ac and dc loads. At the ac branch the input voltage from the solar array will be regulated prior to inversion. This regulated output will then be inverted to provide a 3 phase square wave output at 400 Hz and 400 vac. The output provides power to the ERPS liquefaction system.

At the dc branch a line bucking PWM series regulator will receive the unregulated 300 vdc array voltage and provide an output of 195 $\pm$ 5 vdc to the regulated +200 vdc bus. From the regulated +200 vdc bus three output power lines will be provided. One line will go directly to the ERPS electrolysis system. Another line will go to the Shelter where the +200 vdc regulated input is to be converted to +28 vdc for shelter use. The remaining line will go to the transfer and circulating pumps after first being converted to 28 vdc. Lines for monitoring and manual remote control of switching will go from the power conditioning equipment to the Shelter. Automatic switching control will also be provided.

Emergency standby power will be connected to the Shelter regulated +28 vdc bus only as shown in Figure B.1. Power during the lunar night will be provided on a non-emergency basis by fuel cells.

3.2.2 Dormant Operation

When in the dormant, unmanned mode for periods as long as six months, the LEPEPS will provide 2 kw of power during the lunar day for maintenance of base equipment. During the lunar night, maintenance power will be provided by the SEPS and fuel cells which are not included as part of this DRD.

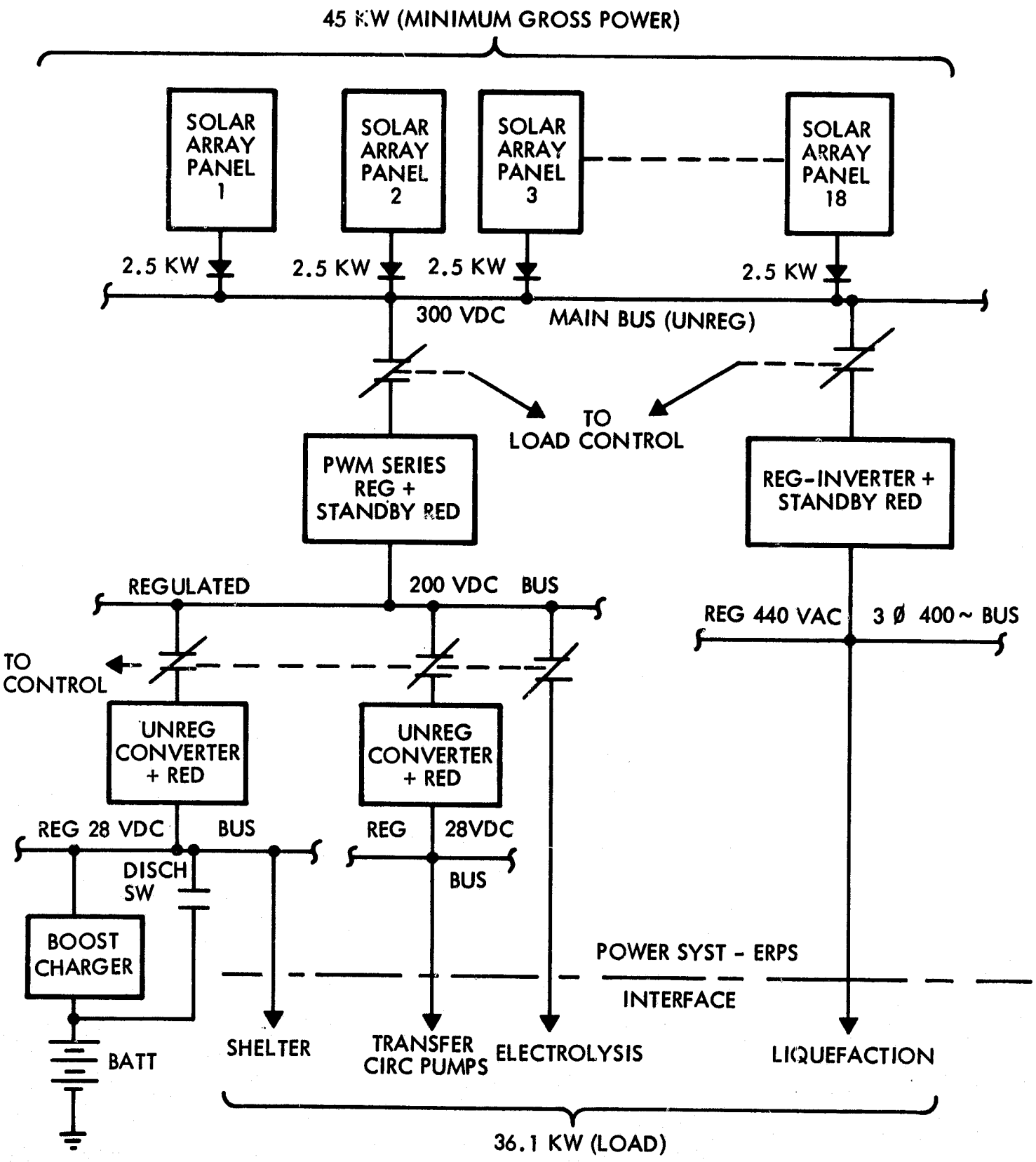

Figure B.1 Block Diagram of Lunar Surface Power System (45 kw Leanto Configuration)

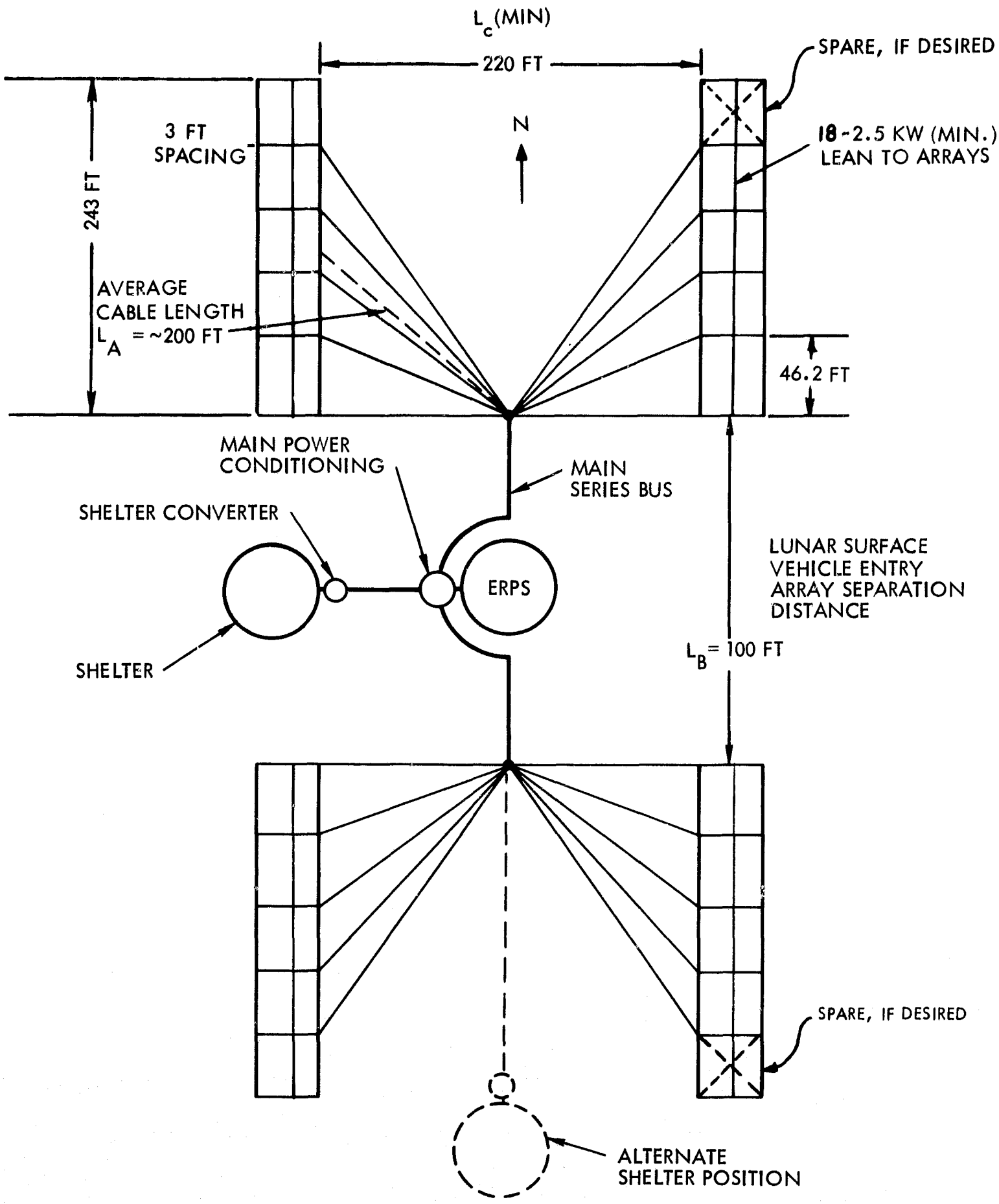

Figure B.2 Schematic of Electric Power System for Lunar Base (45 kw-Minimum Gross Power)

4. SYSTEM REQUIREMENTS

4.1 GENERAL

The LEPEPS will be designed and constructed to satisfy all the requirements noted herein.

4.2 TESTS

The completed LEPEPS produced in accordance with this design requirements document will be tested as noted in Section 7 of this document.

4.3 POWER LEVELS AND OUTPUTS

4.3.1 Load Power

Load Power will be provided as noted in Table B.1.

Table B.1 Load Power Requirements

Load	Power, kw	Voltage	Regulation
Electrolysis	19.5 ± 0.5	195 vdc	± 5 vdc
Liquefaction	12.2 ± 0.5	440 vac 400 Hertz, 3ϕ	±20 volts rms ± 1 Hertz
Transfer and Circulation Pumps	1.4 ± 0.1	28 vdc	± 2 vdc
Shelter	3.0 ± 0.2	28 vdc	± 2 vdc

4.3.2 Solar Array Power

The minimum unconditioned operating power to be provided by the solar array will be 45 kilowatts at a nominal array voltage of 300 vdc to allow for an overall distribution system efficiency of 80 percent plus a 3 percent contingency factor. Each solar array panel will be designed to produce a minimum of 2.5 kw at 300 vdc and nineteen solar array panels are to be connected in parallel as shown in Figure B.1. Solar array voltage will be designed so as to produce no more than 375 volts

(TBC) under open circuit conditions of operating temperature and insolation.

4.4 UNIT DESIGN CHARACTERISTICS

4.4.1 Solar Arrays

The photovoltaic conversion material will consist of 8 mil thick, single crystal silicon cells plus 0.006 in. thick glass covers for protection. Each solar array will be designed to conform to the following limits for Lunar Surface operation. Solar arrays will be of the 'lean to' type (Reference 2.4).

4.4.1.1 Power to area ratio performance (minimum) at end of mission (EOM) will be consistent with the values listed below:

W/ft^2	W/M^2	Life
10.2	110	Yr 0
8.2	88.2	Yr 1
6.95	74.7	Yr 3
6.25	67.2	Yr 5

4.4.1.2 Weight, Volume and Area Limitations

a) Weight A solar array panel will weigh 370 Earth pounds (maximum).

b) Area The active surface area of a unit array will be 685 sq. ft. nominal.

c) Volume The volume occupied by an array panel (packed) will not exceed 80 cubic ft.

4.4.1.3 Array Operating Temperatures

The array will be designed so as to stay within an operating range of -173°C to +100°C during the lunar day. The array structure will be capable of undergoing this temperature change at the rate depicted in Figure B.3 without any resulting mechanical deterioration or degradation of the electrical power output.

4.4.2 Load Power Conditioning

4.4.2.1 PWM Series Regulator - DC Branch

The PWM series regulator will be of the bucking type. It will be designed to be standby redundant and have an estimated reliability of 0.99 after 1 year of operation. Characteristics of the PWM regulator will be in accordance with the limits stated in paragraph 4.4.2.1.1 and 4.4.2.1.2.

4.4.2.1.1 Regulator Electrical Characteristics

Outputs:	Single, +195 ± 5 vdc
Rated Maximum Output Power:	30 kilowatts
Input Voltage Range:	(+250 vdc to TBS)
Regulator Efficiency:	0.88
Output Ripple, Peak to peak:	± 0.5 volt (TBC)
Transients:	± 5% (TBC)

4.4.2.1.2 Regulator Weight, Volume and Shape Limits

a) Weight: The regulator weight will be 130 pounds max.

b) Volume: The regulator volume will be 1.5 ft^3 max.

c) Shape: The preferred design shape is rectangular

4.4.2.2 Regulator - Inverter, AC Branch

The regulator-inverter will consist of a regulator section and an inverter section connected in series with the output of the regulator. The regulator will be of the bucking type. Both sections will be designed to be standby redundant and have an estimated reliability of 0.99 after 1 year of operation. Characteristics of the regulator-inverter will be in accordance with the limits stated in paragraphs 4.4.2.2.1 and 4.4.2.2.2.

4.4.2.2.1 Regulator-Inverter Electrical Characteristics

Outputs:	Single at 440 vac ± 20 vac
Rated Maximum Output Power:	15 kilowatts
Input Voltage Range:	(+250 vdc to
Load Type:	Inductive
Inverter Output:	3 Ø square wave at 400 ± 1 Hz
Reg-Inverter Overall Inversion Efficiency at Rated Power:	0.78
Output Ripple, Peak to peak:	± 0.25% RMS (TBC)

Transients:	± 5% (TBC)
Duty Cycle:	(TBS)
Power Factor:	0.15 (TBC)
Load Start-up Limits	+50% overload (TBC)

4.4.2.2.2 Regulator-Inverter Weight, Volume and Shape

a) Maximum Weight:	160 pounds
b) Maximum Volume:	1.9 ft^3
c) Shape:	Preferred design is a rectangular shape

4.4.2.3 Unregulated Converter- Shelter

The Shelter unregulated converter will accept a regulated input of +195 ± 5 vdc and convert it to an output of 28 ± 2 vdc. Inputs and Outputs will be filtered. The converter will be designed to be standby redundant and have an estimated reliability of 0.99 after 1 year of operation. Characteristics of the Shelter unregulated converter shall be in accordance with the limits stated in paragraphs 4.4.2.3.1 and 4.4.2.3.2.

4.4.2.3.1 Converter Electrical Characteristics

Outputs:	Single at 28 ± 2 vdc
Rated Max. Output Power:	4 Kilowatts
Input Voltage Range:	+190 vdc to +200 vdc
Converter Efficiency:	0.86
Ripple, Peak to peak:	100 mv
Transients:	± 5% (TBC)
Load Start up Limits:	+ 50% overload (TBC)
Load Type:	Resistive

4.4.2.3.2 Converter Weight, Volume and Shape

a) Maximum Weight:	15 pounds
b) Maximum Volume:	0.25 ft^3
c) Shape:	Rectangular

4.4.2.4 Unregulated Converter - Transfer and Circulating Pumps

The transfer and circulating pump converter will accept a regulated input of +195 ± 5 vdc and convert it to an output of 28 ± 2 vdc. Inputs and outputs will be filtered. Provision will be made for possible high start up load power requirements to be determined in the design phase. The transfer and circulating pump electrical converter will have a standby redundant channel and have an estimated reliability of 0.99 after

1 year of operation. General characteristics of the converter are to be in accordance with the limits stated in paragraphs 4.4.2.4.1 and 4.4.2.4.2.

4.4.2.4.1 Converter Electrical Characteristics

Outputs:	Multiple at 28 ± 2 vdc
Rated Max. Output Power:	2 Kilowatts
Input Voltage Range:	+190 vdc to +200 vdc
Converter Efficiency:	0.85
Ripple, Peak to peak:	100 mv
Transients:	± 5% (TBC), ± 50% input for 10 ms max.
Load Start up Limits:	+ 50% overload (TBC)
Load Type:	Inductive

4.4.2.4.2 Converter Weight, Volume and Shape

a) Maximum Weight:	10 pounds
b) Maximum Volume:	0.2 ft^3
c) Shape:	Rectangular

4.4.2.5 Power Conditioning Operating Temperatures

Heat sink operating temperatures of all power conditioning are to be kept in the range of -20°C to +55°C. This will be achieved by utilizing a method of thermal control consisting of louvers and emissive coatings. If active thermal control methods are found to be necessary, as a result of detailed design study, the maximum limits on weight and volume may be increased accordingly.

4.4.3 Monitoring and Operation Controls

Provision will be made for the monitoring and operation by remote control switching of all units of the power system. Such monitoring will be located at the Shelter or other designated place. The objective in general is to provide for automatic monitoring and correction of faults when they occur. The presence of humans on the lunar surface and the ready accessibility of power conditioning elements and controls, leads to a requirement for manual controls in order to maximize protection. Items to be monitored are as follows in Table B.2.

Table B.2 Monitoring of Power System

Item	Component	Notes
Temperature	All Units	--
Input Voltage	All Power Conditioning	--
Output Voltage	All Units	--
Input and Output Current	All Units	--
Solar Input (Insolation)	Solar Array	Sample only
Switch Positions	All Power Conditioning	Main Standby
Switch Positions	Array Main Bus to Load	--
Frequency Output	Reg-Inverter	--
Unit Pressure	Any Sealed Units	Leak or Over-Pressure Detection
Other		

4.4.3.1 Controls - Manual

Provision will be made for the remote switching of any operating unit by a control located at the Shelter. Mandatory manual controls will consist of at least the following:

a) Main Power Switch: This switch which will normally be automatic in operation is to be capable of being activated remotely. Its function is to disconnect the loads from the main unregulated bus when the array output voltage is outside limits to be specified later.

b) Standby Switching: Where a standby (redundant) section of a given power control unit does not switch to operation automatically, provision must be made for manually activated switching.

c) Connect/Disconnect Switching: Provision is made for connecting and disconnect of the following:

1. Individual Solar Array Units from main bus.
2. Loads from all regulated output buses.
3. Fuel Cells, or other lunar night and emergency power, from regulated 28 vdc bus. (This area is to be covered in a later study).
4. Other (TBS)

d) Reliability: All manual and automatic controls will be designed to provide the maximum reliability (Minimum TBS) commensurate with weight and size limitations.

4.4.3.2 Controls - Automatic

Automatic switching logic will be provided for all items noted in paragraph 4.4.3.1. All automatic switching will incorporate a manual remote override.

4.4.4 Standby Power Storage and Associated Controls

A standby power storage utilizing nickel cadmium or other type secondary batteries will be connected to the Shelter regulated 28 vdc bus. This power storage will provide emergency power as required in the event of an interruption in power from the solar array and until the regular fuel cell standby power can be brought up to full output.

The battery power storage will not normally be used for lunar night operation except for emergencies. Controls for charging and discharging the batteries will be provided together with monitoring.

The minimum battery rated output capacity after 1 year operation will be (TBS) ampere-hours at 28 vdc nominal. Other characteristics are to be as follows:

Max. battery weight:	TBS
Max. battery volume:	TBS
Operating temperature range:	$50^{o}F$ to $100^{o}F$
Normal charge rate:	16 hour (TBC) plus trickle
Max. charge voltage:	33 volts (TBC)
Charge egulator type:	TBS

4.4.5 Connecting Cabling and Harnesses

4.4.5.1 General:

All cabling and harnesses will use stranded copper wire insulated by H-Film (see Reference 2.3). All array panels are to use a cable for negative return.

4.4.5.2 Protection

The main power bus lines will be protected by a cage or other shield and raised off the lunar surface if so determined by further study.

4.4.5.3 Connectors

The connectors used shall be of a type approved by a human factors analysis of lunar surface applications (see Reference 2.3).

4.4.5.4 Array to Main Series Bus Connector Power Cables

Average length:	200 ft
Average voltage drop:	10 vdc
Number of cable lines:	19 plus, 19 minus
Total max. cable weight:	100 pounds
Total max. losses:	1.5 kilowatts at 167 amps
Operating temperature range:	-50°C to +150°C
Power capacity rated:	50 kw at 300 vdc nominal

4.4.5.5 Main Series Power Bus

Length:	100 ft
Voltage drop max:	2.5 volts
Maximum weight:	20 pounds
Maximum power loss:	100 watts at 167 amps
Operating temp. range:	-50°C to +150°C
Rated power capacity:	50 kw at 300 vdc nominal

4.4.5.6 Power Line from 200 vdc Bus to Shelter

Maximum length:	300 ft
Maximum losses:	150 watts at 20 amps
Maximum weight at 300 ft:	32 pounds
Operating temperature range:	-50°C to +150°C
Rated power capacity:	4 kw at 200 vdc nominal

4.4.5.7 Monitoring and Control Cabling

4.4.6 Fault Protection

All circuitry must be designed to incorporate protection against the occurrence of an overvoltage or overcurrent. A means of failure detection is to be provided and provision made for automatic or manual switching in of compensating standby circuits. Load undervoltage protection is also to be considered and incorporated in the LEPEPS if the results of further study so indicate.

4.4.7 Maintenance

Each array panel will be designed for ease of maintenance on the lunar surface. Construction will be preferably of a modular form employing the maximum of interchangeability.

4.4.8 Assembly, Handling and Ancillary Components

Each unit will be designed for ease of assembly and handling on the lunar surface. The units will further be provided with sufficient ancillary handling devices so as to facilitate handling both on the lunar surface and on the Earth.

4.4.9 Materials, Structural and Electrical

This section of the DRD is concerned with parts, processes, and lists of preferred parts and materials. It will be supplied after further study.

5. INTERFACES

5.1 OPERATIONAL

These interfaces comprise the electrical and physical interaction with the users of the LEPEPS and the lunar environment, except for a general statement of power profiles and lunar environment, details of the interfaces are outside the scope of the study (Reference 2.4) on which this DRD is based. The major electrical interfaces are listed:

a) Electrical

1. ERPS
2. Lunar Shelter
3. Lunar Night Operation Power Storage
4. Unmanned (Dormant) Power Control

Power profiles for the ERPS and lunar shelter are illustratedin Figures B.4a and B.4b. Examples of items which may connect across a given interface are as follows: Power cables, instrumentation leads, control and sensor leads, communication-direct and telemetry.

b) Physical

1. Lunar Surface Environment (see para. 6)
2. Connectors, electrical and fluid to ERPS, lunar shelter and etc.

c) Electromagnetic

Possible interference with communications is to be minimized by shielding and design (per MIL-I-6181D and MIL-E-6051C).

5.2 LAUNCH PHASE

a) Mechanical: Saturn V Shroud

b) Electrical: Saturn V GSE/ACE

c) Other: (TBS)

5.3 STORAGE

5.3.1 Lunar Surface: (TBS)

5.3.2 Earth Storage: (TBS)

6. ENVIRONMENTS

6.1 GENERAL

Lunar Environments are assumed to be as noted in Reference 2.4 for the Lunar Model.

6.2 PRESSURE AND DENSITY OF LUNAR ATMOSPHERE

Based on data in Reference 2.4 the atmospheric pressure and density is assumed to be 10^{-13} that of Earth at sea level.

6.3 TEMPERATURE OF LUNAR SURFACE

The lunar surface temperature variation is as shown in Figure B.3.

6.4 SOLAR RADIATION

The value of the solar constant at 1.0 AU is to be used for the lunar surface and is 1396 W/M^2. The solar spectrum is considered to follow that of Johnson for AMO and 1 AU as described in Reference 2.4.

6.5 MICROMETEOROIDS

From 1 impact/m^2 sec for particles 10^{-7} m diam to 10^{-16} impacts/m^2 sec for 3 cm diam particles.

6.6 PARTICULATE RADIATION (In accordance with Reference 2.4)

6.7 TRANSPORTATION VIBRATION

6.7.1 Lunar: (TBS)

6.7.2 Earth: (TBS)

6.8 HANDLING SHOCK

6.8.1 Lunar: (TBS)

6.8.2 Earth: (TBS)

6.9 LAUNCH ENVIRONMENTS

6.9.1 Vibration, Acceleration and Shock as per Saturn V (TBS)

6.9.2 Temperature: (TBS)

7. TESTING

7.1 GENERAL

All array panels are to be tested under conditions exceeding in severity those expected in operation.

7.2 SYSTEM ASSEMBLY

Assembly of the system will be performed under conditions of simulated lunar gravity. All tools and other instrumentation will be as intended for lunar surface use (Reference 2.4).

7.3 COMBINED TEMPERATURE AND PRESSURE

All power conditioning and control units, cabling, harnesses, connecting blocks, etc. comprising the LEPEPS, with the exception of the solar array shall be temperature cycled under conditions of lunar vacuum.

A description and number of the cycles as applicable to each is to be supplied later (TBS).

7.4 THERMAL CONTROL

All array panels comprising the LEPEPS will be tested for operation at 1.0 AU solar insolation, a pressure of 10^{-13} atmospheres (Earth) and simulated lunar surface view conditions sufficient to determine the satisfactory operation of the thermal control design.

7.5 CABLING (TBS)

Tests other than thermal are to be specified at a later date.

7.6 SOLAR ARRAY TESTING (TBS)

7.7 HANDLING SHOCK AND VIBRATION (TBS)

All units shall be tested for satisfactory operation after subjection to handling shock and vibration at the maximum levels as called out, paragraphs 6.7, 6.8 and 6.9.

7.8 OTHER TESTS (TBS)

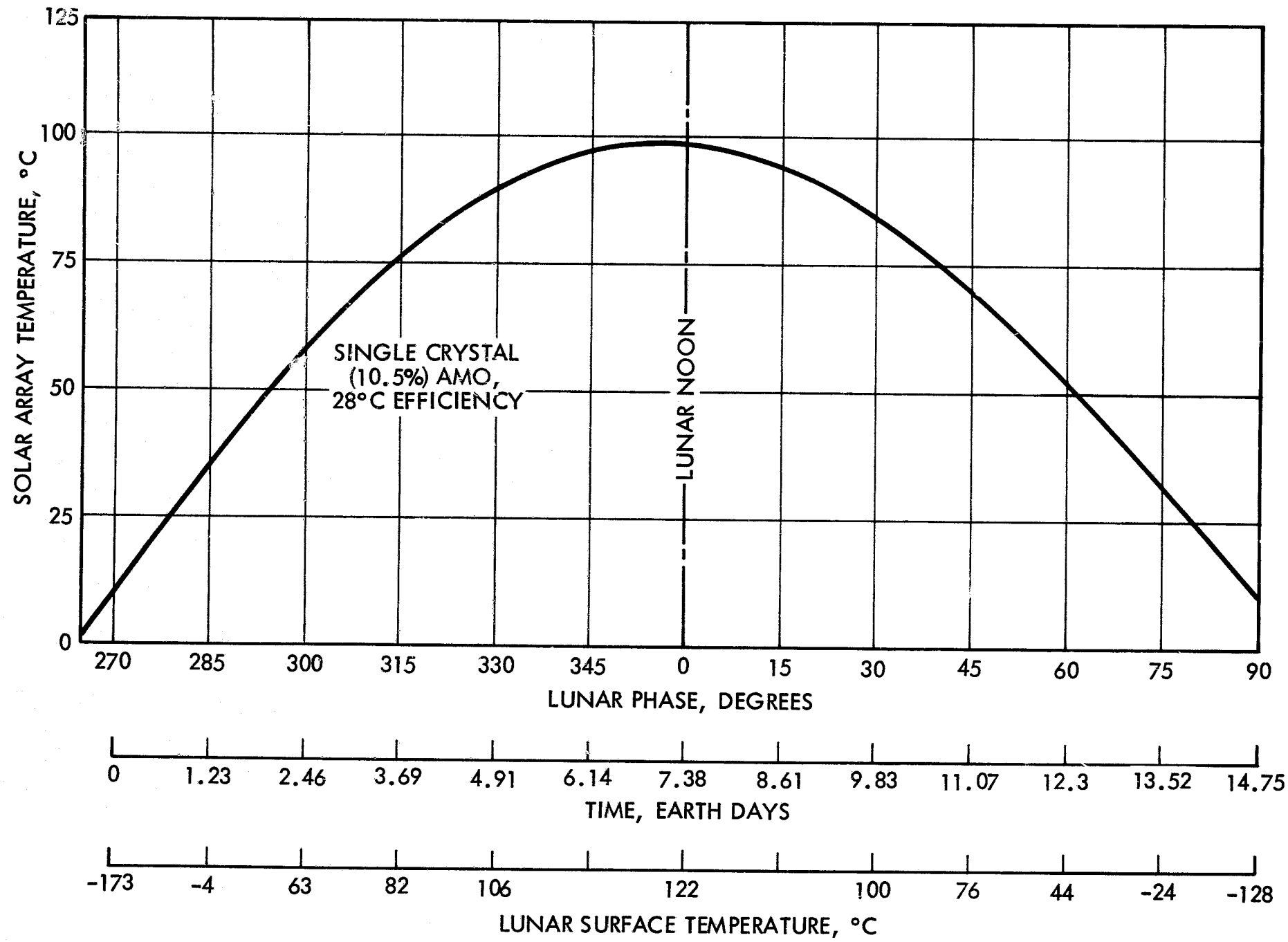

Figure B-3 Typical Maximum Solar Array Temperature Variation

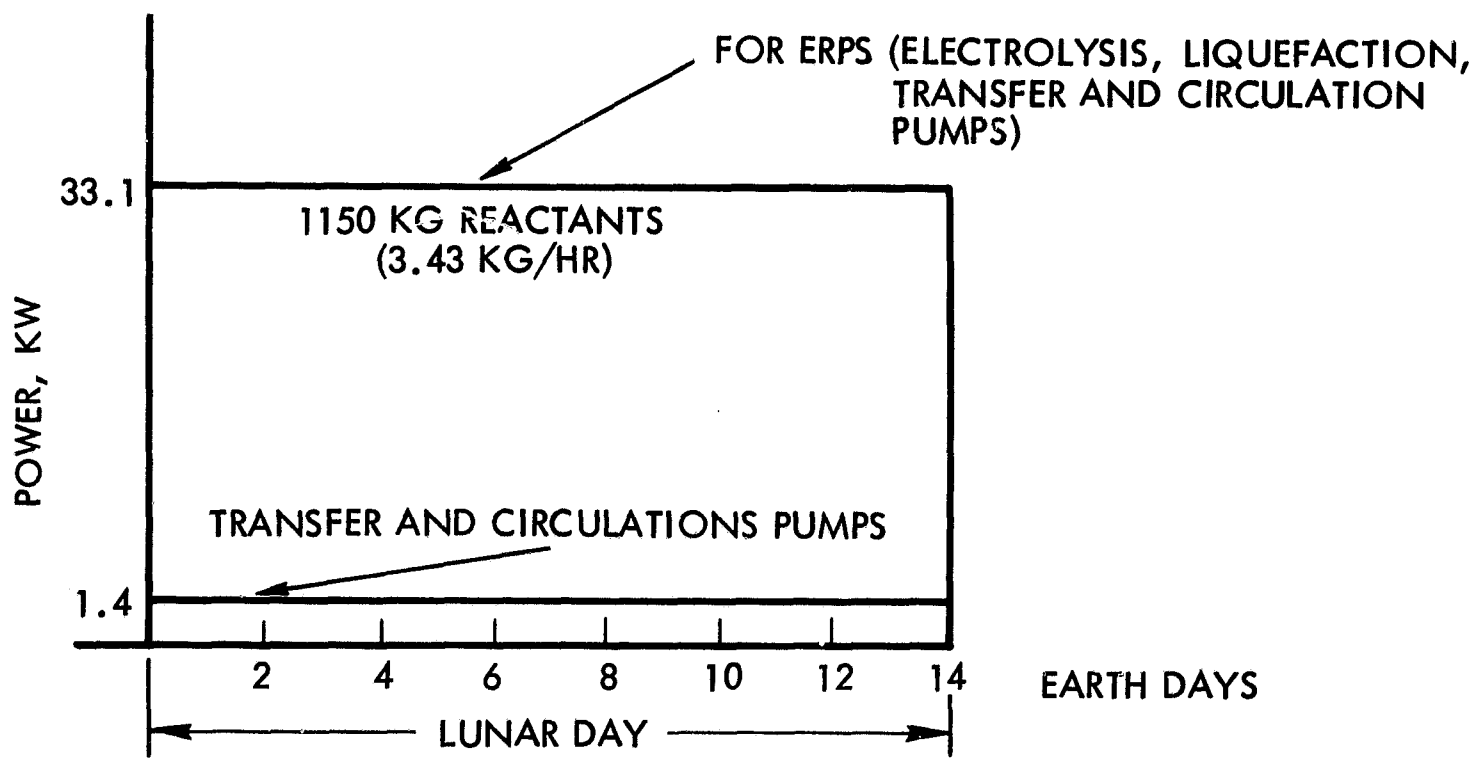

(A) POWER PROFILE FOR ERPS

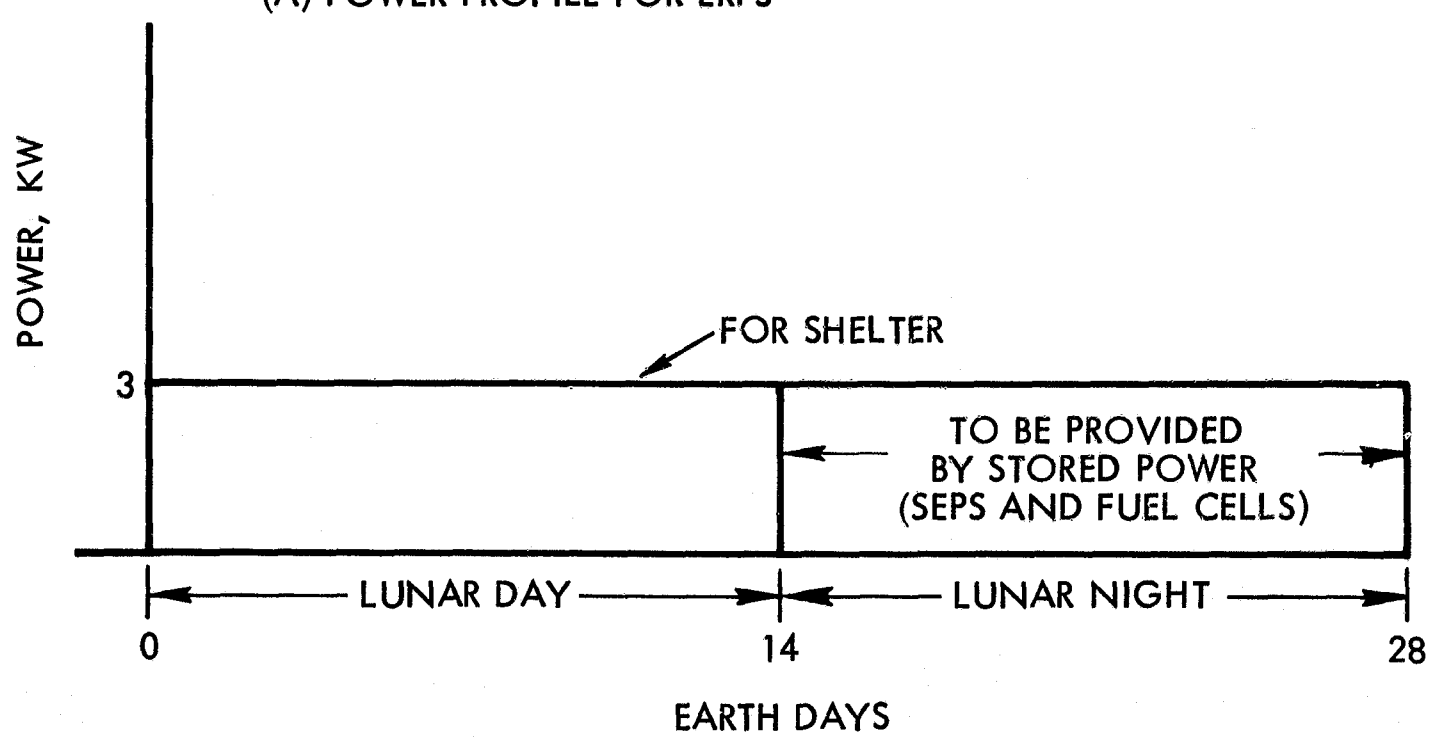

(B) POWER PROFILE FOR SHELTER

Figure B.4 Program V Power Profiles

APPENDIX C

RESIZING OF BOEING LIGHTWEIGHT SOLAR ARRAY CONCEPT TO MEET THE LEPEPS STANDARD MODULE REQUIREMENTS

RESIZING OF BOEING LIGHTWEIGHT SOLAR ARRAY CONCEPT TO MEET THE LEPEPS STANDARD MODULE REQUIREMENTS

Appendix C depicts the analyses used for resizing the Boeing lightweight solar array concept. The configuration has been sized to be compatible with the requirements for the standard 3.3 ft x 8.0 ft module recommended during this study for the LEPEPS.

CRITERIA FOR RESIZING RIGID PANELS

Assume stowed panels will be adequately restrained against launch/boost loads,

Resize Panel Structure to:

1) 39 in. width x 96. length
2) Limit stress to 75% yield when carried flat by 4 corners in a 1.0 "G" field.
3) Size open bays that cannot be easily supported during launch/boost to $F_N > 10$ cps
4) Assume 0.75 in. maximum beam depth

BOEING CONCEPT

Data:

1) A 24. x 24. in. substrate panel exhibits F_N = 36. cps
2) Substrate and Cells = 26. ft^2 = 11.2 lb
   Allow 1.8 lb for struct. calcs. 1.8
   Wt. for calculations: 13.0 lb
3) Substrate pretension: 12. lb/in.

Assumptions:

1) Double "U" sheet beryllium beams, thickness as req.,
2) Panel divided into 4 bays, 24. x 39. in. (see F_N calculation)
3) Let combined tensile loads be additive.

Configuration:

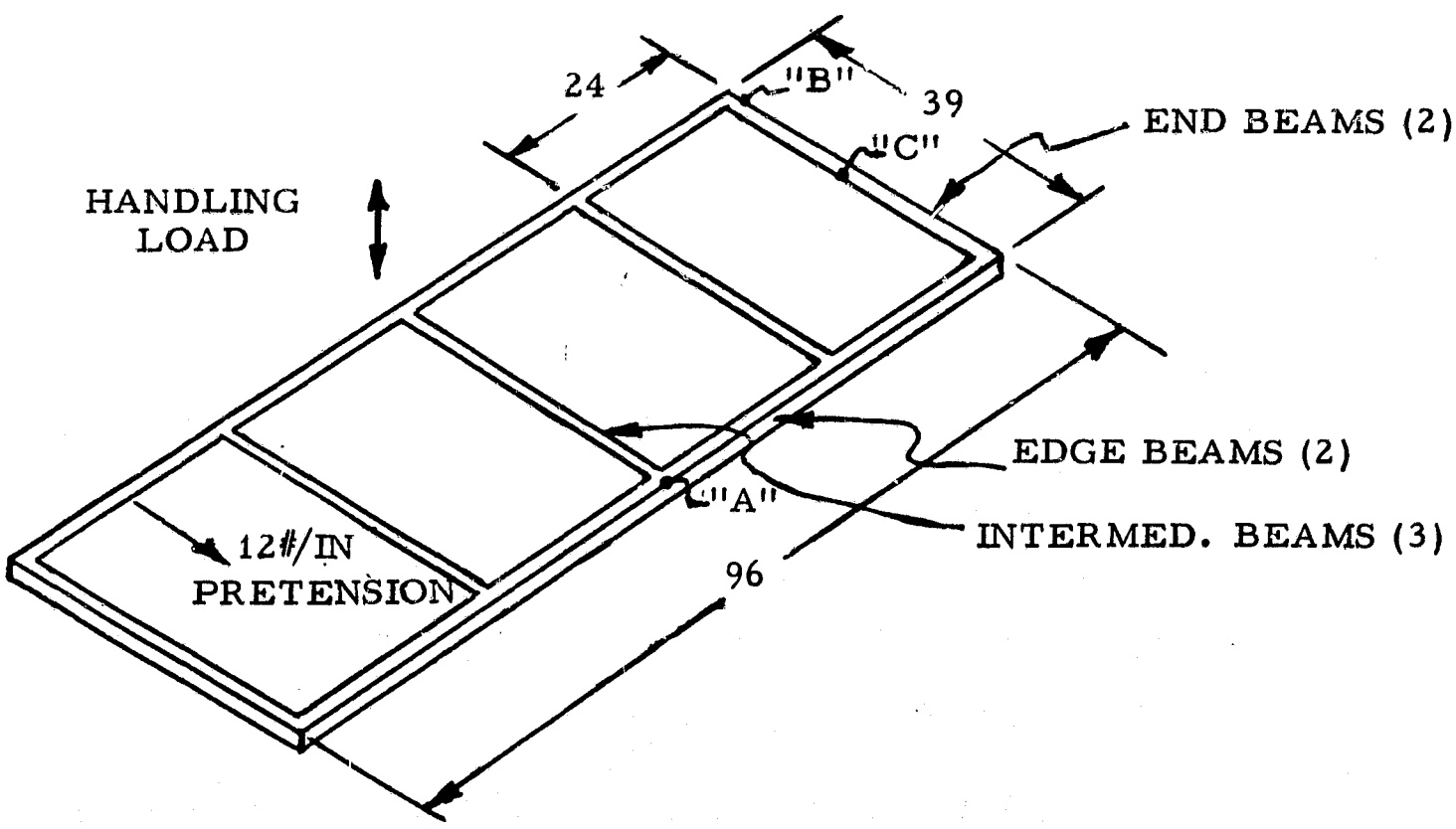

F_N Calculation:

Check the Boeing Configuration, 24 x 24 in. sections, $F_N = 36$ cps for applicability of the membrane vibration formula:

$$F_N = \frac{\alpha}{2\pi}\sqrt{\frac{9\,S}{A\,q}}$$

$$F_N = \frac{4.44}{6.28}\sqrt{\frac{(386.)(12.)}{(24.^2)(2.95)(10^{-3})}}$$

$$F_N = 37.\ \text{cps}$$

Where:

α = 4.44 (for square)

S = 12 lb/in.

A = $24.^2$

q = $\frac{0.424}{144} = 295(10^{-3})$ lb/in.^{2}

g = 386. in/sec^2

This checks fairly close, indicating the applicability of the formula, calculate the F_N of a 24. x 39. section,

$$F_N = \frac{4.62}{6.28}\sqrt{\frac{(386.)(12)}{(24.)(39.)(2.95)(10^{-3})}}$$

$$F_N = 30.4\ \text{cps}\ \ (\text{OK})$$

Where:

α = 4.62 (3:2 rect.)

S = 12. lb/in.

A = 24. x 39.

Analysis of Beams:

1) Total stress is combination of substrate pretension (in-plane bending) and handling stress (out-of-plane bending).

2) Matl: Beryllium sheet, F_{ty} = 55000. PSI

   F_{allow} = (0.75) (55000.) = 41200

3) Major load is pretension, therefore configure beams with double metal thicknesses to resist in-plane bending.

4) Ignore torsion stress due to substrate pretension eccentricity.

Edge Beams:

Point "A" (Critical)

Pretension

12 lb/in. = w

(W = wl)

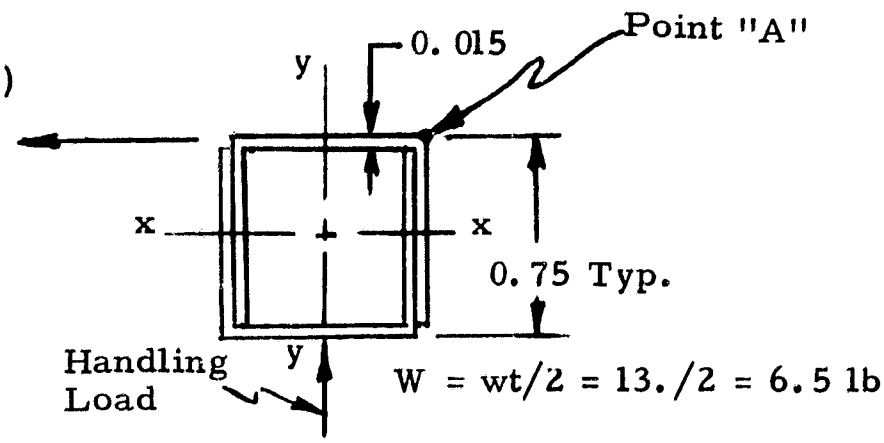

Pretension Stress: (Beam-fixed ends - unif. load)

$$F_b = \frac{My}{I_{yy}}$$

$$F_b = \frac{(5.76)(10^2)(3.75)(10^{-1})}{(6.7)(10^{-3})}$$

$$F_b = 3.22\,(10^4) = 32200.\ \text{psi}$$

Where:

$$M = \frac{Wl}{12}$$

$$M = \frac{(12)(24^2)}{12} = 576.\ \text{in. lb.}$$

$$Y = 0.75/2 = 0.375\ \text{in.}$$

$$I_{yy} = \frac{BH^3}{12} - \frac{bh^3}{12}$$

$$I_{yy} = \frac{(0.75)(0.75^3)}{12} - \frac{(0.72)(0.69^3)}{12}$$

$$I_{yy} = 0.0264 - 0.0197$$

$$I_{yy} = 0.0067\ \text{in.}^4$$

Handling stress: (Pin ends - unif. load)

$$F_b = \frac{My}{I_{xx}}$$

$$F_b = \frac{(7.8)(10)(3.75)(10^{-1})}{(5.)(10^{-3})}$$

$$F_b = 5.85\,(10^3) = 5850.\ \text{psi}$$

Total Stress:

$$F_b = 32200. + 5850. = \underline{\underline{38050.\ \text{psi}}}$$

Margin:

$$\text{M.S.} = \left(\frac{F_{allow}}{F_{actual}} - 1\right)100$$

$$\text{M.S.} = \left(\frac{41200.}{38050.} - 1\right)100 = +\ 8.\%$$

Where:

$$M = \frac{Wl}{8}$$

$$M = \frac{(6.5)(96.)}{8} = 78.\ \text{in. lb.}$$

$$Y = 0.75/2 = 0.375\ \text{in.}$$

$$I_{xx} = \frac{BH^3}{12} - \frac{bh^3}{12}$$

$$I_{xx} = 0.0264 - \frac{(0.69)(0.72^3)}{12}$$

$$I_{xx} = 0.0264 - 0.0214$$

$$I_{xx} = 0.0050\ \text{in.}^4$$

Weight of edge beams: (Total 2)

$$\text{Wt.} = (\text{Area})(\text{length})(0.066\ \text{lb/in}^3)$$

$$\text{Wt.} = (6.)(0.75)(0.015)(2.)(96.)(0.066) = 0.855\ \text{lb}$$

End Beams:

Point "B" Critical)

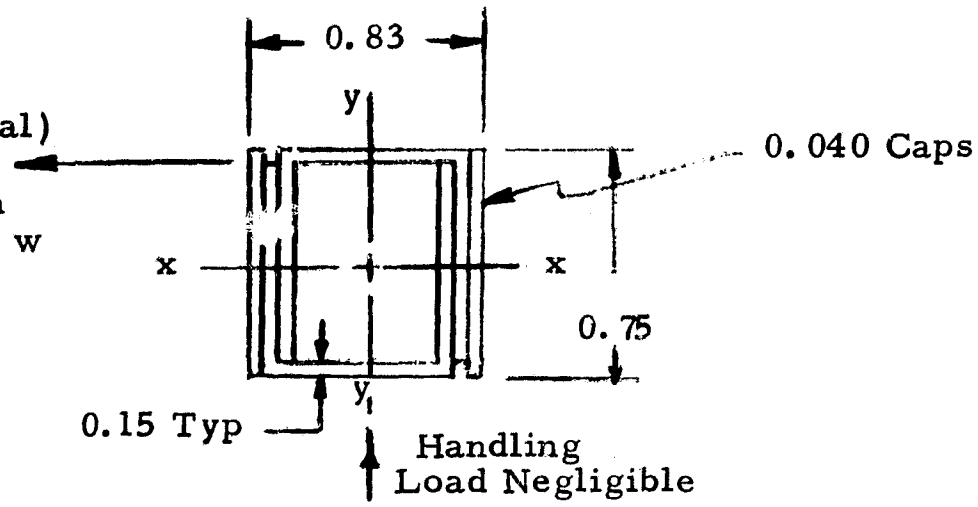

Pretension stress (fixed end beam - unif. load)

$$F_b = \frac{My}{I_{yy}}$$

$$F_b = \frac{(1.52)(10^3)(4.15)(10^{-1})}{(1.6)(10^{-2})} \quad (10^4)$$

$$F_b = 3.95\ (10^4) = \underline{\underline{39500.\ psi}}$$

(Margin = +5%)

Where:

$$M = \frac{Wl}{12}$$

$$M = \frac{(12)(39^2)}{12}$$

$$M = 1520.\ \text{in-lb}$$

$$Y = \frac{0.83}{2} = 0.415\ \text{in.}$$

$$I_{yy} = \frac{BH^3}{12} - \frac{bh^3}{12}$$

$$I_{yy} = \frac{(0.75)(0.83^3)}{12} - \frac{(0.72)(0.69^3)}{12}$$

$$I_{yy} = 0.0357 - 0.0197$$

$$I_{yy} = 0.016\ \text{in.}^4$$

Point "C" (Midbeam)

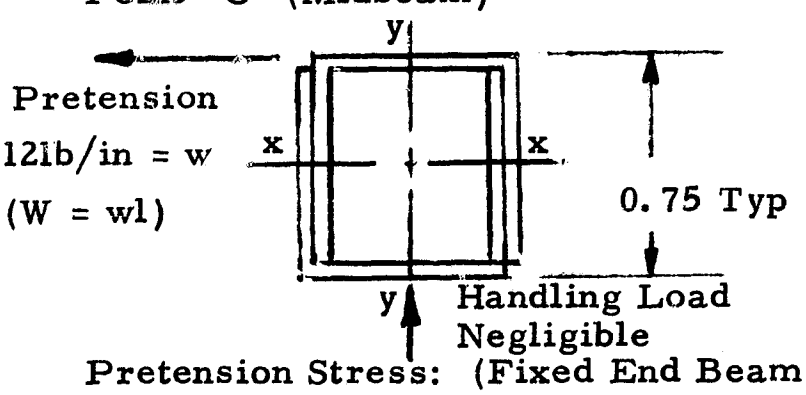

Pretension Stress: (Fixed End Beam-un.ld.)

$$F_b = \frac{My}{I_{yy}}$$

$$F_b = \frac{(7.6)(10^2)(3.75)(10^{-1})}{(6.7)(10^{-3})} \quad (10^4)$$

$$F_b = 4.25\ (10^4) = \underline{\underline{42500.\ psi}}$$

(Margin = -2.% OK)

Where:

$$M = \frac{Wl^2}{24}$$

$$M = \frac{(12)(39^2)}{(24)}$$

$$M = 760\ \text{in-lb}$$

$$Y = 0.375$$

$$I_{yy} = 0.0067$$

Point "B" requires 0.040 in. thick caps, Point "C" requires only the basic beam. Therefore, the caps may taper out to the end beam center as shown below. The caps should also taper out on the edge beams to the same length

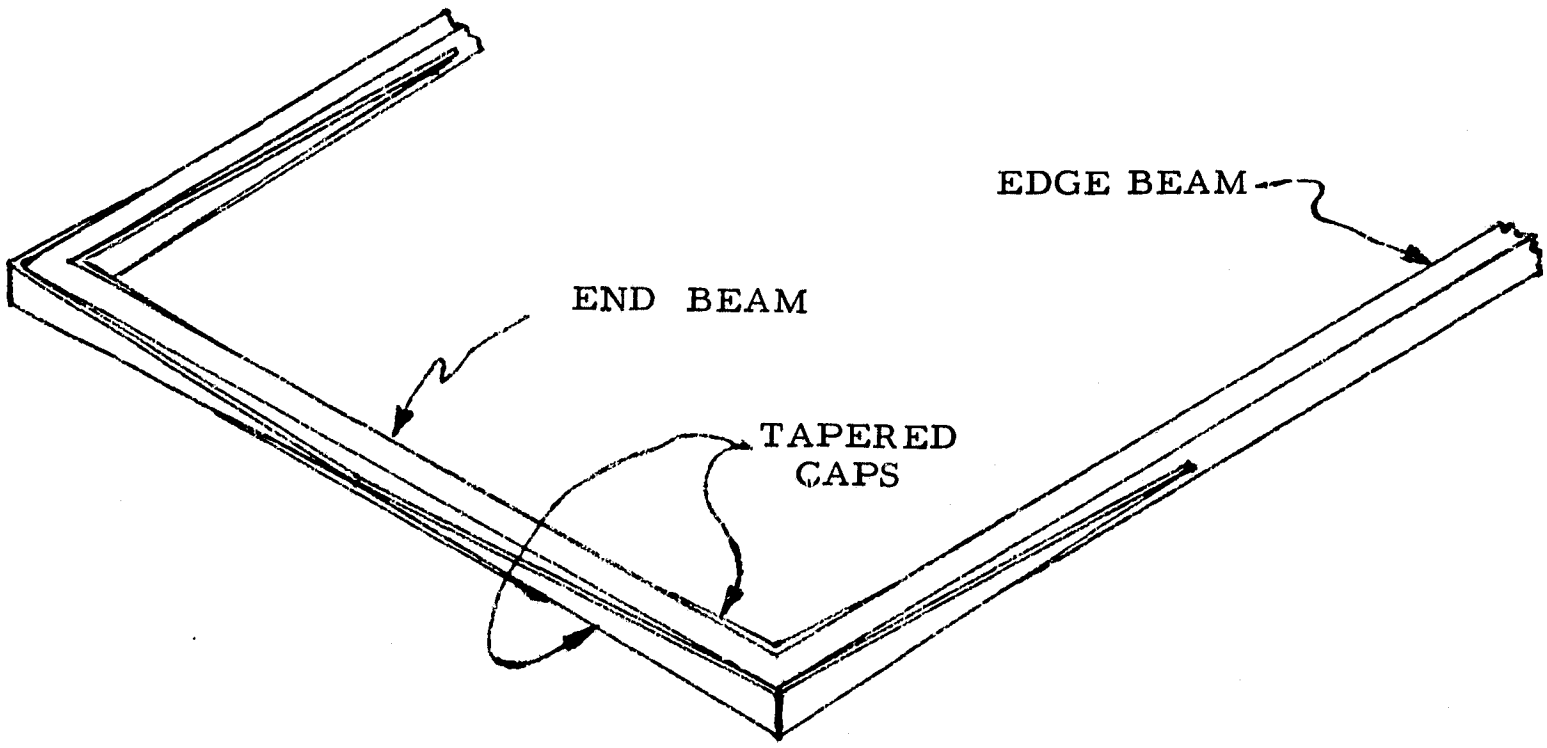

End Beam Wts: (2)

$$Wt. = (2.)(6.)(0.75)(0.015)(39.)(0.066) = 0.348 \text{ lb}$$

Tapered Cap wts: (8)

$$Wt. = (8.)\left(\frac{39}{2}\right)(0.75)(0.04)(0.066) = 0.309 \text{ lb}$$

Intermediate Beams: (3)

Pretension loads are equalized, Analyse for out-of-plane bending due to handling loads

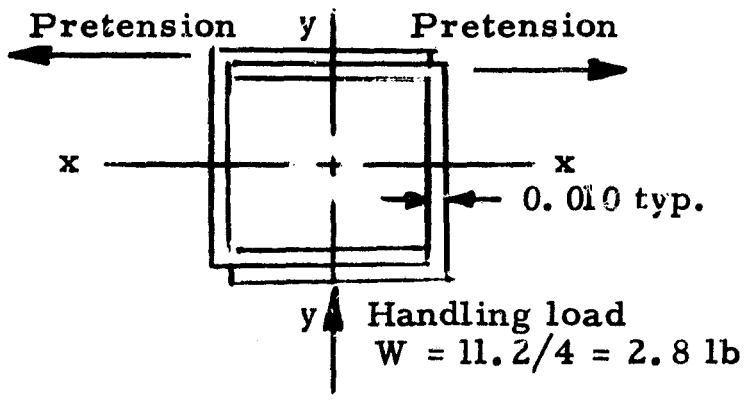

Handling stress (pin end beam - unif. load)

$$F_b = \frac{MY}{Ixx}$$

$$F_b = \frac{(1.36)(10^1)(3.75)(10^{-1})}{(4.6)(10^{-3})} \quad (10^3)$$

$$F_b = 1.11\ (10^3) = \underline{\underline{1110.\ psi}}\ \text{(low)}$$

Weight: (3 beams)

$$Wt = (3.)(6.)(0.75)(0.010)(39)(0.066) = 0.348\ lb$$

Where:

$$M = \frac{Wl}{8}$$

$$M = \frac{92.8)(39.)}{8}$$

$$M = 13.6\ in\text{-}lb$$

$$Y = 0.375$$

$$I_{xx} = \frac{BH^3}{12} - \frac{bh^3}{12}$$

$$I_{xx} = \frac{(0.75)(0.75^3)}{12} - \frac{(0.73)(0.71^3)}{12}$$

$$I_{xx} = 0.0046\ in^4$$

Total Panel Weight:

Substrate and Cells:	11.200	
Edge Beams:	0.855	
End Beams:	0.348	
Tapered Caps:	0.309	1.87 lb(Structure)
Inter. Beams:	0.348	
Misc. Shear Clips:	0.010	
Total/Panel	13.070 lb	

APPENDIX D

ANALYSIS OF TRW SYSTEMS STRUCTURAL CONCEPTS

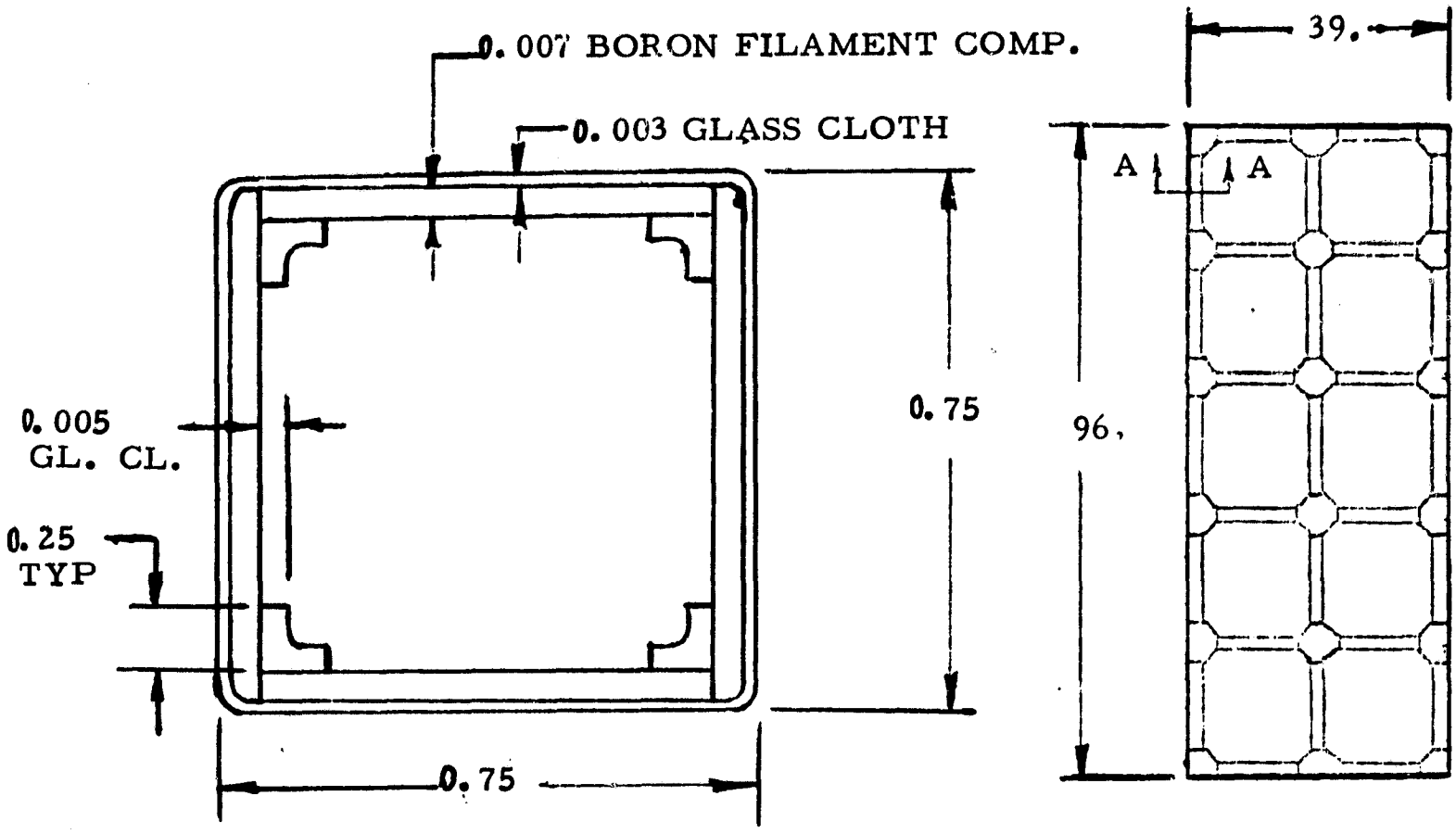

Sec. A-A

Concept D.1 - Boron Tube

Wt. per running ft.
glass cloth = (0.747)(4)(12)(0.003)(0.06) = 0.00644

Wt. per running ft.
boron filament composite = (0.737)(4)(12)(0.007)(0.0525) = 0.01297

Total = 0.01941 lb/ft

Wt. per running ft.
glass covered angles = (0.5)(12)(4)(0.005)(0.006) = 0.00720

Total = 0.02661 lb/ft

Total running ft. = $\frac{(96)(3)}{12} + \frac{(39-2.25)}{12}(6)$ = 42 ft 4 1/2 in.

Total frame wt. = 42 ft 4 1/2 in. x 0.02661 lb/ft = 1.125 lb

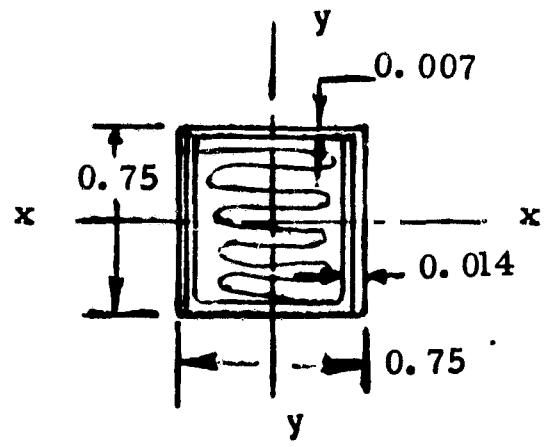

Concept D. 2 - Boron - Honeycomb Beam

$$I_{x-x} = \frac{BH^3}{12} - \frac{bh^3}{12} \; ; = 0.0264 - (0.722)(0.736)^3$$

$$= 0.0264 - 0.0240 = 0.0024$$

$$I_{y-y} = 0.0264 - \frac{(0.736)(0.722)^3}{12} = 0.0264 - 0.0231 = 0.0033$$

$$F_{b_{yy}} = \frac{My}{I_{yy}} = \frac{(5.76 \times 10^2)(3.75 \times 10^{-1})}{0.0033} = 65,400 \text{ lb/in}^2$$

$$F_{b_{xx}} = \frac{Mx}{I_{xx}} = \frac{(7.8)(3.75)10^3}{24} = 12,200 \text{ lb/in}^2$$

$$F_{allow} = 0.75 \times 110,000 = 82,500 \text{ lb/in}^2$$

Total Stress:

$$F_b = 65,400 + 12,200 = \underline{\underline{77,600 \text{ lb/in}^2}}$$

Margin

$$M.S. = \left(\frac{F_{allow}}{F_{actual}} - 1\right) 100 = \left(\frac{82,500}{77,600} - 1\right) 100 = \underline{\underline{6.2\%}}$$

Weights

$$V = (96 \times 4) + (39 \times 10) \quad (0.75)(0.014) = 8.14; \; 8.14 + 4.07 = \underline{\underline{12.2 \text{ in}^3}}$$

$$V = (774)(0.75)(0.007) = 4.07$$

Weight = (12.21)(0.0525) = 0.641 lb (Boron Composite Material)

Weight = $\frac{206}{1728} \times 8.1 \text{ lb/ft}^3 = 0.965$ lb (Honeycomb)

APPENDIX E

PROPERTIES OF CANDIDATE SOLAR ARRAY MATERIALS

PROPERTIES OF CANDIDATE SOLAR ARRAY MATERIALS

A survey was made of various materials that could be considered for the candidate solar array substrates. The results are presented in this appendix. Their applicability is discussed in Section 7 of this report.

1. Density and Modules of Elasticity

In a comparison of densities with other aerospace materials, only alloyed magnesium and aluminum approach the low density of beryllium. Titanium, structural and high allow steels, and high temperature alloys range from two and one-half to five times the density of beryllium. In addition, beryllium is the lightest available metal that will not vaporize appreciably in the vacuum of space.

While alloyed magnesium and aluminum compare favorably with beryllium on a density basis, these materials have tension moduli significantly below that of beryllium. At room temperature, the modulus of beryllium is higher than that of the more widely used structural metals - and this relationship persists up to the temperatures at which beryllium loses useful strength. This high elastic modulus makes practical the design of lightweight rigid components.

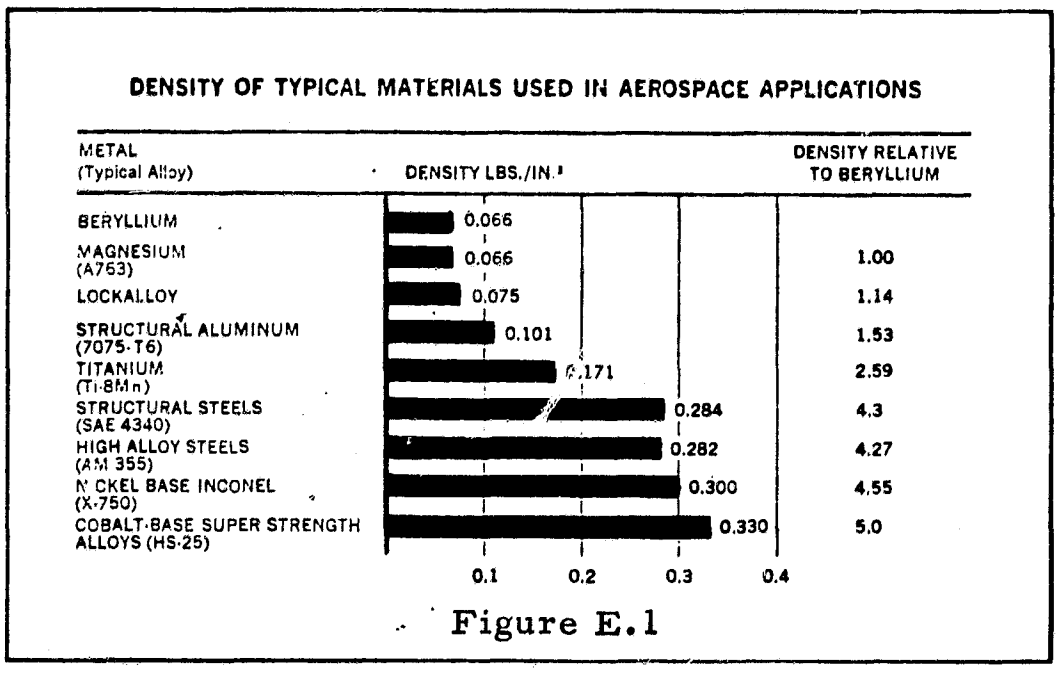

Figure E.1

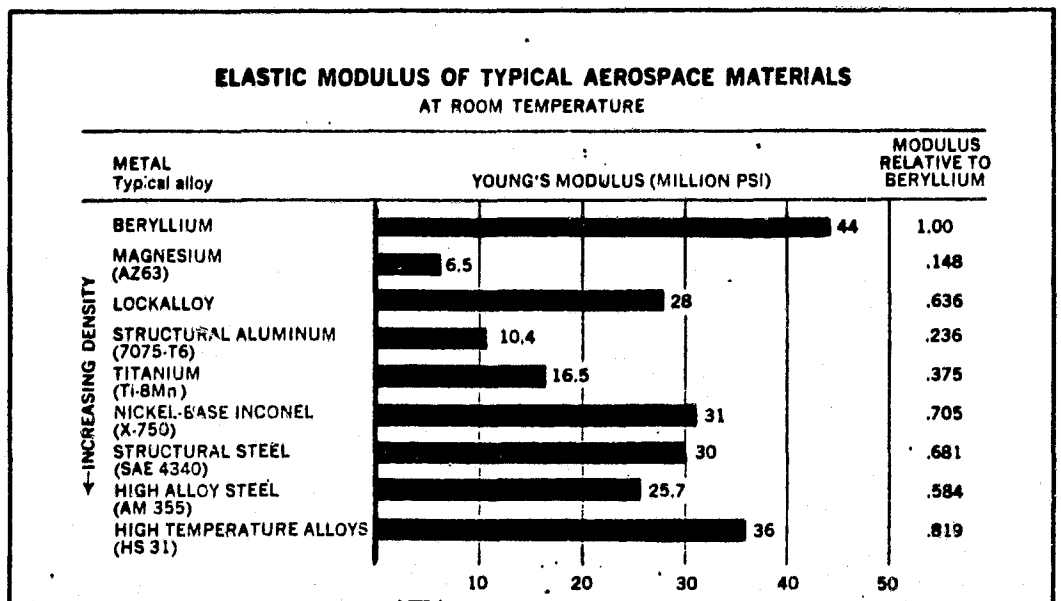

Figure E.2

2. Strength-to-Density Ratio

On a strength-to-density basis, beryllium is competitive with the more commonly used metals: magnesium, titanium, aluminum, steels, and high temperature alloys at room temperature. And it is superior to the other light metals at elevated temperatures, retaining its strength up to about 1100°F

In the use of most high strength materials, the need for rigidity usually results in an overweight section of higher than necessary strength. The high elastic modulus and low density of beryllium thereby enable the engineer to design lightweight structural members to minimum thickness. In a purely buckling application, a beryllium column will be lower in weight than a column made of any other metal of equal length and load carrying ability.

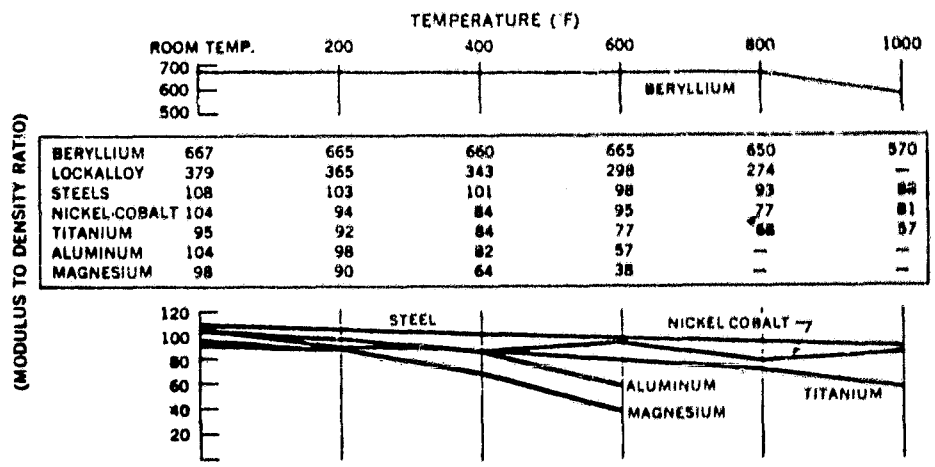

	ROOM TEMP.	200	400	600	800	1000
BERYLLIUM	667	665	660	665	650	570
LOCKALLOY	379	365	343	298	274	—
STEELS	108	103	101	98	93	[illegible]
NICKEL-COBALT	104	94	84	95	77	81
TITANIUM	95	92	84	77	68	57
ALUMINUM	104	98	82	57	—	—
MAGNESIUM	98	90	64	38	—	—

Figure E.3

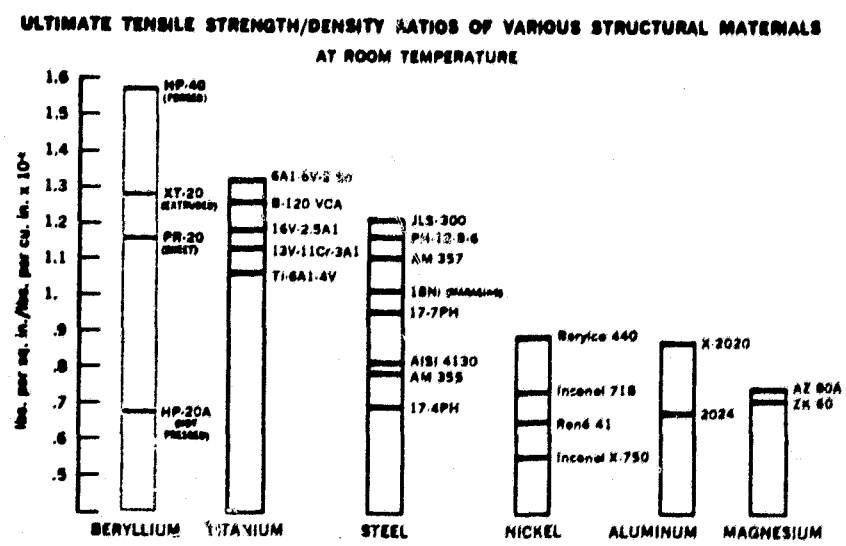

Figure E.4

2. Strength-to-Density Ratio (Continued)

Figure E. 8 illustrates the computed weight of monocoque cylinders of beryllium and several other materials loaded in buckling. The cylinders are equal in outside diameter and length with varying wall thicknesses so that each will carry buckling loads of the same magnitude. The weight of each cylinder is relatively proportional to the density of the metal, divided by the square root of the elastic modulus.

A similar illustration can be offered to show the advantages offered by beryllium in bending. In Figure E. 9, a cantilever beam is considered where the length and thickness are restricted and the beam is designed to limiting elastic deflections.

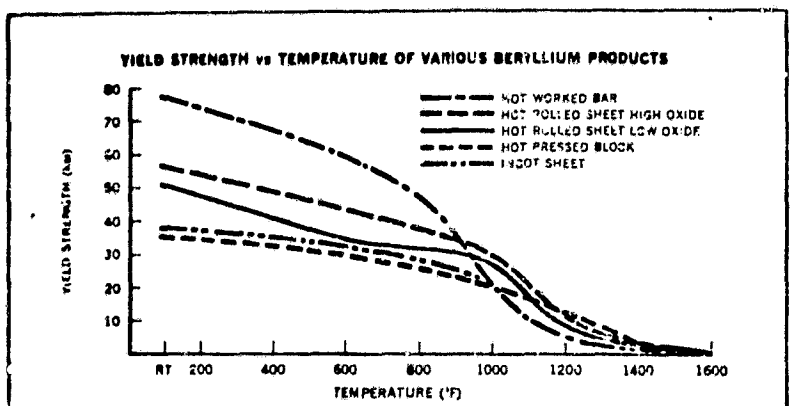

Figure E. 5

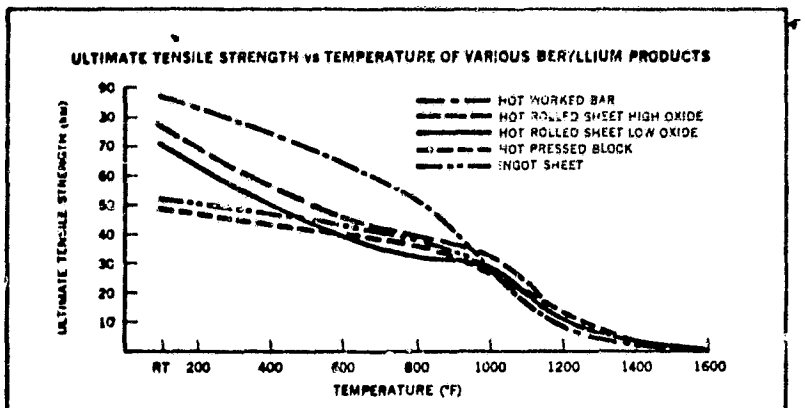

Figure E. 6

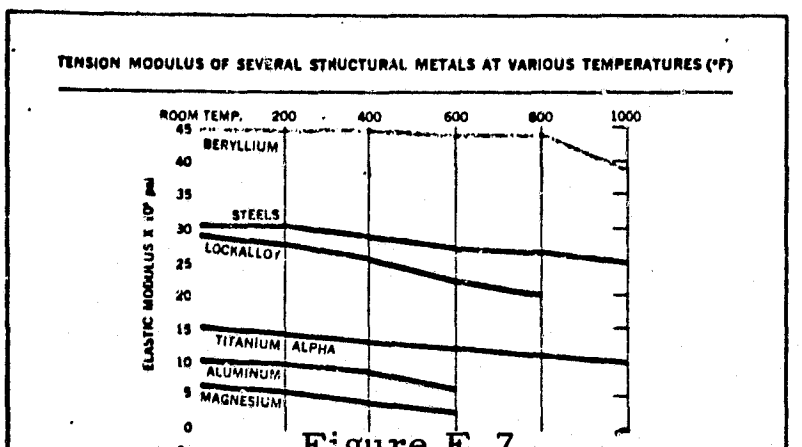

Figure E. 7

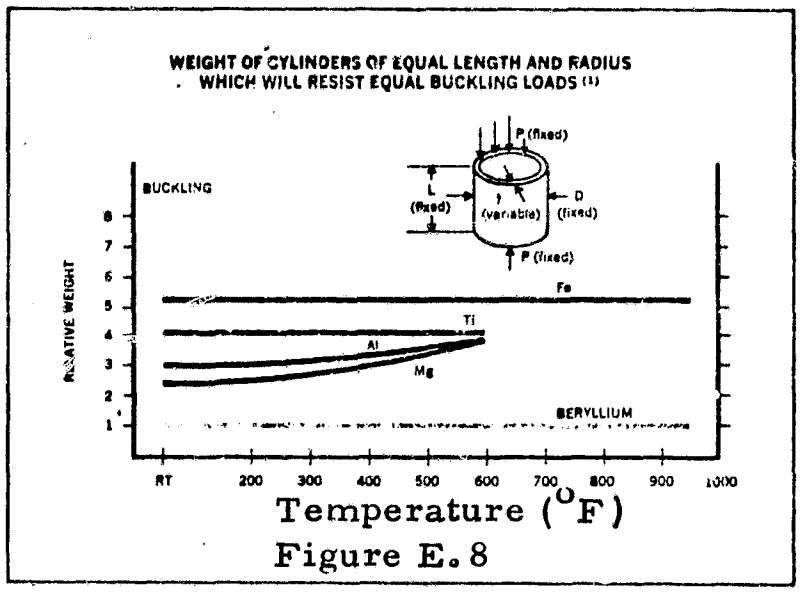

Figure E. 8

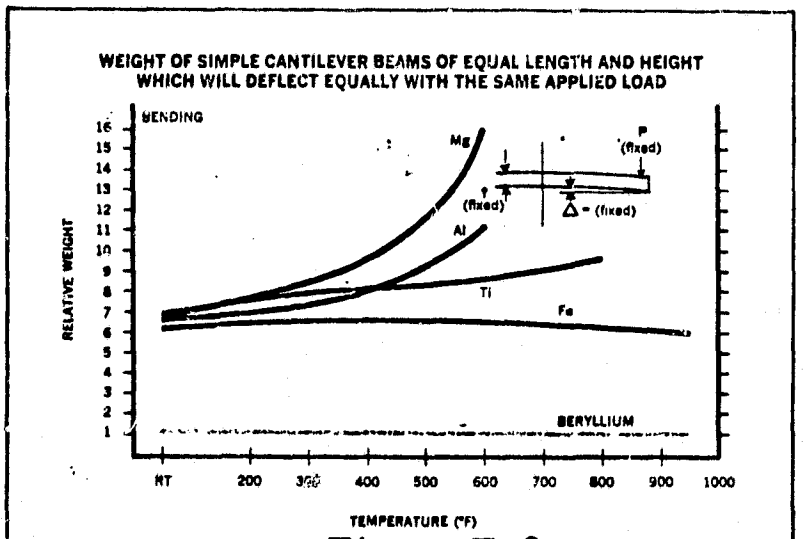

Figure E. 9

3. Specific Heat

Many of the first applications for beryllium in reentry vehicles resulted from the inability of other materials to withstand the extreme temperatures and to absorb the heat developed during the limited duration of reentry. The high specific heat of beryllium allows its use as a structure in areas where stronger and more refractory materials would be heated to temperatures well in excess of their service ranges. Figure E.10 illustrates the specific heat of beryllium compared with several structural alloys.

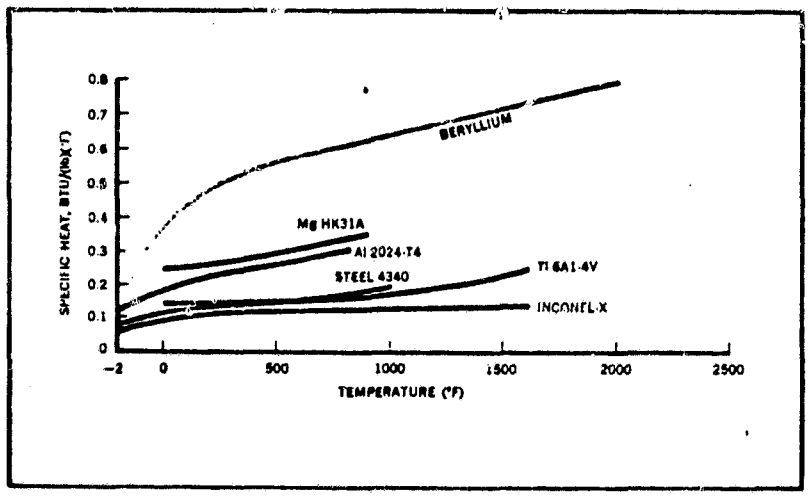

Figure E.10

4. Thermal Expansion

Figure E.11 shows that the coefficient of expansion of beryllium approximates that of stainless steel and nickel and cobalt alloys. This compatibility of expansion eliminates many of the design problems arising from the high expansion of other light metals.

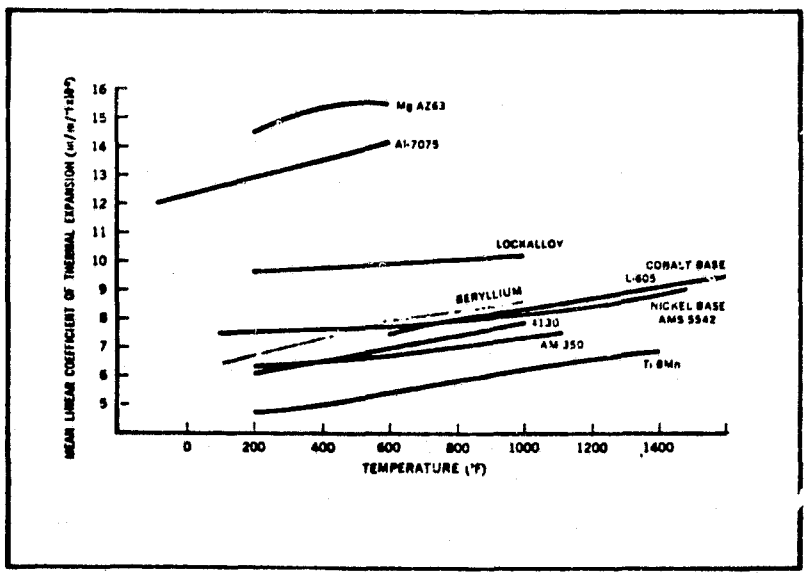

Figure E.11

5. Thermal Conductivity

The thermal conductivity of various metals is shown in Figure E.12. Of the commonly used aerospace materials, only aluminum exceeds beryllium in thermal conductivity. Where heating of a structure is involved, high thermal conductivity helps to eliminate thermal gradients and protects the part against warpage and buildup of surface heat. Its advantage in heat sink applications is apparent.

The combination of beryllium's unique thermal properties contributes greatly to the metal's excellent dimensional stability - even under difficult service conditions.

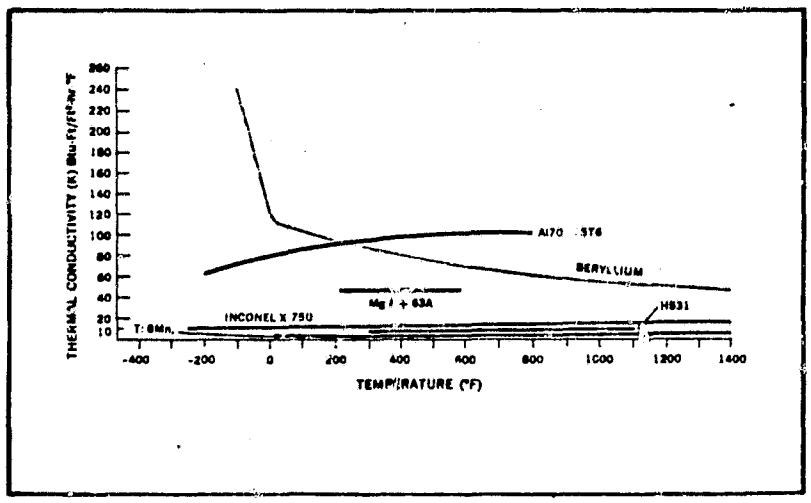

Figure E.12

APPENDIX F

ELECTRIC POWER SYSTEM ANALYSIS

APPENDIX F

ELECTRIC POWER SYSTEM ANALYSIS

1. INTRODUCTION

Four distribution configurations for the primary electric power system are discussed. The units comprising these configurations are also described in some detail. The technical rationale presented was used as the basis for a tentative selection of a reference power system in Section 10.2 of this study.

2. DISCUSSION

Four configurations were considered. These are:

1) Full AC Distribution
2) Full DC Distribution
3) AC-DC Distribution (large AC section)
4) AC-DC Distribution (large DC section)

Figures F-1 through F-4 illustrate these configurations. Before discussing each configuration, it will be noted that each contain units common to at least one other configuration. These are:

a) Solar Array voltage control or limiter
b) Inverter(s)
c) Pulse Width Modulated (PWM) Series Regulators
d) Transformer Rectifier Units (T/R)
e) Converters, regulated or unregulated

A discussion on each is given as being helpful to understanding the comments on the configurations as a whole.

2.1 SYSTEM UNITS

2.1.1 Array Voltage Limiters

Voltage limiters used for solar array control may be either shunt or series types. Each of these may be either of the switching (pulse width modulated) type or of the dissipative type. In general, the dissipative voltage limiter is less complex and has better response than its pulse-

width modulated counterpart. On the other hand, the dissipative regulator may penalize the system design in that its potentially large heat dissipation may introduce serious thermal control problems in the system. In addition, the dissipative type, if used in the series configuration, introduces a serious inefficiency in the power system. Series dissipative voltage limiters used as solar array controls were not considered further because high-efficiency is a paramount need. Dissipative shunt regulators have found extensive application in a variety of spacecraft. The simplest application of this approach is the use of zener diodes to limit the solar array output voltage directly. A more accurate voltage limit can be achieved by sensing output voltage and controlling an active shunt element. This element in turn may be of either a dissipative or switching type. If connected in shunt with the entire solar array, the dissipative type must handle the maximum difference in power between the solar array capability at its voltage limit and the load demand. For the large power system under consideration in this study, this approach might be inappropriate because of the thermal control problems that would result and the large additional heat sink weight required.

Although a variety of designs have been considered for switching shunt regulators to eliminate thermal control problems, none has been developed thus far. In applying the dissipative shunt limiters to spacecraft systems, several methods have been developed to minimize their heat dissipation, and to minimize the effects of the dissipation on the spacecraft thermal control system. These methods consist chiefly of shunting only a portion of the series-connected solar cells in an array and controlling only a portion of the parallel-connected solar cells where possible to minimize the maximum dissipation of the shunt element.

Pulse width modulated series regulators may be divided into two categories for voltage-limiting applications. In the first category, the voltage limiter senses output voltage and adjusts the duty cycle of the series-switching element to maintain the desired output limit. With this approach, if the output voltage is less than the voltage limit, as in the case of the unregulated bus system configurations, the series switching element is driven into saturation and the limiter has the characteristic of a small constant voltage drop between the solar array and the

main bus. The second category of this basic approach is that of a series-voltage limiter controlled to provide maximum solar array power tracking capability. Properly designed, this approach permits nearly full utilization of the solar array maximum power capability despite its variations in magnitude and voltage as a function of solar intensity and array temperature.

A major advantage of the pulse width modulated series regulators is the fact that this mode of operation causes excess solar array power capability to be rejected at the solar array rather than converting this power into heat within the regulator. Figures F.5 and F.6 illustrate the application of the two methods.

2.1.2 Inverters and Transformer Rectifiers (T/Rs)

Figure F.7 is a block diagram of a pulse width modulated inverter with a transformer rectifier (T/R) shown added on. The T/R (or T/Rs) may be separated from the inverter by quite a long length of line if necessary. Any inverter can be changed to a converter by adding an appropriate T/R and filtering each output. By driving the inverter with a pulse width modulated square wave, a quasi square wave output is derived. The driven inverter has some particular advantages:

1. Because of drive deadtime, current spikes are not usually generated.
2. The rms value of the output can be made to vary by varying the PWM duty cycle (on-to-off time ratio).

This system can be used to provide regulated AC outputs. Inverter efficiency can be quite high, in the order of 95 percent or above, depending on operating load. For maximum reliability, a standby inverter would have to be included. This would lower the operating efficiency slightly.

2.1.3 Pulse Width Modulated (PWM) Series Regulators

PWM regulators utilize power transistors in a switching mode with a controlled duty cycle to achieve the voltage regulation. They generally offer higher efficiencies than do dissipative regulators, although this is obtained at the cost of a loss in frequency response and output impedance.

For relatively steady loads this tradeoff is minimal in effect. Maximum efficiency is approached as the difference between input and output voltages becomes smaller. The input and output voltages of power regulators are designed to be nearly equal under worst operating conditions and normally do not reach a ratio as high as 2:1 at other times. The following paragraphs discuss some characteristics of the bucking, boost, and buck-boost pulse width modulating regulators.

A bucking regulator is used where the input voltage is always higher than the output voltage. The basic block diagram for this type of regulator is shown in Figure F.8. The output voltage is related to the input voltage by the ratio t_{on}/T, where t_{on} is the ON time of the switch and T is the total drive period. Figure F.9 shows typical series losses for a range of output currents under saturated conditions when losses are a function of output current only.

As the ratio of input-to-output voltage ratio increases, the losses increase primarily as a result of greater switching losses. For maximum efficiency, the best switching frequency according to a recently conducted TRW Study (Reference 10.13) appears to be in the range of 3KHz to 6KHz.

A boost regulator is used where the input voltage is always less than the output voltage. Figure F.10 is a block diagram of a constant-frequency boost regulator of the pulse width modulated type. This case is the inverse of the bucking regulator. The ratio of output to input voltage is T to t_{off}, with T the total drive period and t_{off} the OFF time of the shunt switching element. Maximum efficiency of a boost regulator only occurs when the input voltage is slightly higher than the output voltage (not a normal operating mode for this type of regulator). The shunt element is open in this case, with all losses confined to the series elements. This condition can occur when the power available from the solar array is maximum (i.e., low temperature in sunlight). As for the bucking regulator the efficiency is greater as the input/output ratio approaches unity.

A buck-boost regulator is used where output voltage is related to input voltage by the ratio t_{on}/t_{off} which are respectively the ON and OFF times of the switch. When a 50 percent duty cycle for the switch occurs the input and output voltages are equal. When t_{on} is greater than t_{off}, the circuit boost the voltage and inversely the circuit bucks the voltage when t_{on} is less than t_{off}.

Figure F.11 illustrates the basic block diagram of the circuit. When in the boosting mode, the saturated switch and series choke losses are dominant; while in the bucking mode, the switching losses predominate. Compared to either buck or boost regulators, the buck-boost type has a lower efficiency.

2.1.4 Converters-Regulated and Unregulated

Figure F.7 may also be considered as a block diagram for a converter and is but one of the converter types possible. Some of these are:

Regulated Squarewave Converter (RSWI)
Pulse Width Converter (PWI)
Energy Storage Converter (ES)
Push-Pull Energy Storage Converter (Push-Pull ES)

Each of these have advantages and disadvantages which are beyond the scope of this discussion. The PWI is discussed only as an example and the reader is referred to other TRW Systems study work (i.e. Reference 10.13) for a full discussion.

As shown by Figure F.7, the PWI circuit combines inversion and regulation functions in the pulse width inverter stage. Switching reference frequency (f) is determined by a separate oscillator transistor. Duty cycle of the inverter switch is controlled by an error amplifier to maintain a constant average rectified output voltage, independent of input voltage and load variations. In an unregulated DC-DC converter the input is regulated DC and the inverter switch duty cycle depends only on output load variations.

An advantage of the PWI is that regulation and inversion functions are combined in a single element. A disadvantage is that separate output circuits (integrating) are needed for each output as opposed to the squarewave for the RSWI converter. For high-power maximum efficiency operation, a push-pull energy storage converter is a likely candidate. As for the series regulators the maximum efficiency switching frequency appears to be between 3 KHz and 6 KHz. In practice, however, because of the greatly increased power requirements for lunar surface application and the resulting extrapolation of existing low powered equipment data, the final optimum switching frequency chosen is conjectural and must be based on further study.

2.1.5 Comments on System Units

Figure F.12 shows unit efficiency versus percent of full rated output. It will be noted that the T/R units and Inverter remain at a high level of efficiency, even when the loads drop below 10 percent of full rated output. The PWM regulator is almost as good above about 5 percent of full output, while a converter deteriorates in efficiency falling off sharply below 20 or 30 percent of full load. These characteristics may have relevance for thermal control if loads are expected to fluctuate sharply.

Unit operating efficiency is also improved somewhat as input voltage increases above 30 vdc. The precise voltage input level at which maximum efficiency of operation is realized is not known for each unit, but is expected to be in the region of 300 to 400 vdc based on past studies. However, as for the optimum switching frequency, extrapolation of voltage data for low powered equipment to high powered applications may lead to considerable error. Thus, conclusions on the optimum voltage operation for power conditioning units is best left to a future study.

2.2 ELECTRIC POWER SYSTEM CONFIGURATIONS

2.2.1 Configuration 1, Full AC Distribution

This is illustrated in F.1. The system consists of an array voltage control or limiter, an inverter, an ac distribution bus, and load power conditioning. The load power conditioning consists of a 3 ϕ, 400 Hz vac converter regulator and two transformer-rectifier units for the 28 and 200 vdc loads. Line regulation is provided on the output of the T/Rs. This allows each load to have separate regulation tolerance. An alternative is to regulate the inverter output instead of each load separately. However, this approach might not allow the proper regulation for each load. It would probably be the most efficient to have a combined inverter-regulator if load voltage requirements permitted. Apparent system advantages and disadvantages are now listed.

ADVANTAGES

- o Flexibility

  Easy to add or subtract T/Rs for different load requirements.

- o Power Transmission

  Possible to transmit high power levels over relatively long distances incurring low losses and relatively low cable weight.

- o Efficiency

  Efficiency of the basic units, inverters and T/Rs is relatively insensitive to large load fluctuations.

DISADVANTAGES

- o Efficiency

  Decreased by increased number of regulators required.

- o Radiated Interference

  Increased by large lengths of cable at high frequencies.

- o Frequency Complexity

  Possible complexity if the inverter frequency differs from the 3 ϕ 400 Hz converter for liquification.

The advantages are not overwhelming, but neither do the disadvantages rule out the ac system application. Rather it is a matter for further study when load requirements are better defined.

2.2.2 Configuration 2 - Full DC Distribution

This configuration is shown in Figure F.2. There are several options here. The solar array modules may be all connected in parallel as for Configuration 1, or separated into completely independent groups. Using independent groups allows the use of different array bus voltages for each group in question. Since the load voltages are 28 vdc, 200 vdc and 440 vac, the use of three array voltages may result in a greater overall efficiency.

The array voltage limiter is not shown in Configuration 2, although it would have to be used. The types used vary depending on whether independent sections or one fully paralleled solar array is used. For example, assuming independent sections, two solar array modules may be used for the 28 vdc loads. If these are constant loads and matched to the array near peak output, a dissipative limiter such as zener diodes could be used. The 200 volt bus section could possibly use the same method. On the other hand, if large fluctuations occurred in the liquifaction or electrolysis loads, a partial shunt regulator for array voltage limiting would be indicated to reduce thermal dissipation problems.

Apparent system advantages and disadvantages are listed as follows:

ADVANTAGES

- Efficiency

  Separate solar array module sections for each major load bus resulting in best possible matching to load voltages and high efficiency.

- Simplicity

  Few major power conditioning units. Separate array voltage control unit may not be required.

DISADVANTAGES:

- o Flexibility

  Relatively inflexible for major load changes. Requires adding or switching array modules for each independent section.

- o Reliability

  If different solar array module voltages are used for each section, interchangeability is lost. Requires increased total array area or module number for acceptable reliability.

- o Power Losses on Long Lines

  Power losses on long lines are increased when power is distributed at low voltages.

In general, while the system concept looks attractive for an application where the load requirements are well-known and fixed, the system inflexibility influences strongly against its choice.

2.2.3 Configurations 3 and 4 - AC-DC Distribution

As illustrated in Figure F.3, Configuration 3 may be regarded as a 'mirror image' of Configuration 4 shown in Figure F.4. In Configuration 3, the major load distribution branch is the ac branch, whereas for Configuration 4, the dc branch predominates. In this case, approximately forty-five percent of the load has the advantages and disadvantages of Configuration 1, the full ac distribution. The array voltage control is shown in series as for PWM application, but it may be shunted or combined with the inverter.

In comparing Configuration 3 with Configuration 4, it can be seen that where a separate unregulated converter is needed for the regulated 28 vdc bus on Configuration 4, the same function is performed in Configuration 3 by a T/R.

Whereas, the electrolysis load of 19.5 kw has a separate PWM regulator all for itself on Configuration 3 which may be shut down in the event of regulator failure, this is not the case for Configuration 4.

A total failure of the PWM series regulator on Configuration 4 would require emergency operation power for the shelter. By comparison, the same emergency power would be required in the event of an inverter failure on Configuration 3. Thus, on the reliability question, the matter is not open and shut, and the choice to be made is not obvious.

At this point, it is not possible to say which basic system is the most efficient. Because Configuration 4 presents the possibility of using only one regulator for approximately two thirds of the total load, it may very well be the most efficient.

Since the distribution cable lengths are relatively short and voltages can be made quite high, dc power line losses should be equivalent to or less than ac line losses. On Configuration 4, an additional inverter in line with the 3 ϕ 400 Hz converter is unnecessary and removes possible ac frequency matching problems.

On balance, therefore, it appears that a system similar to Configuration 4 would be the best choice for the system application as now defined in Reference 4.2.

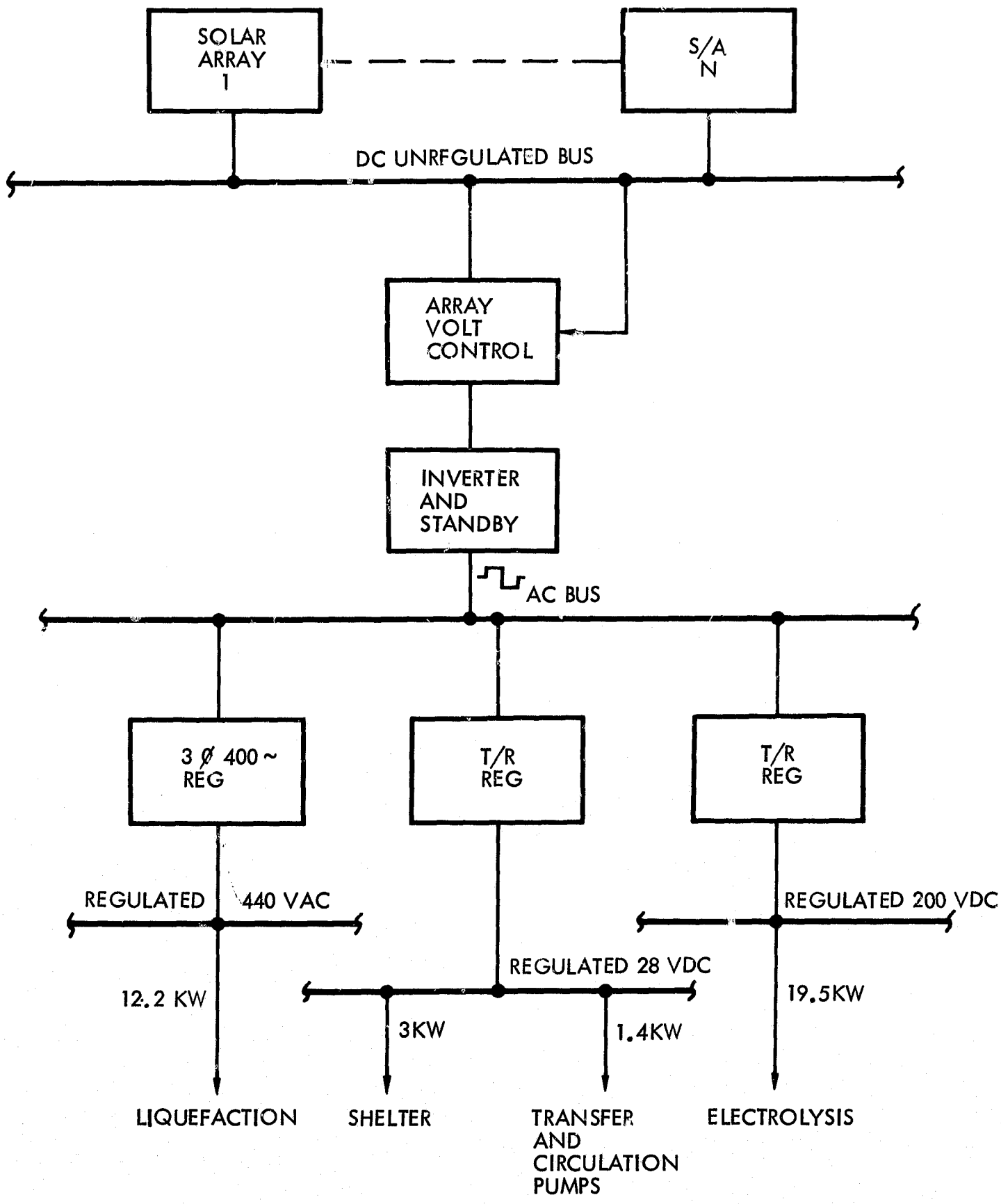

Figure F.1 Lunar Surface Power System (Configuration 1) (Full AC Distribution)

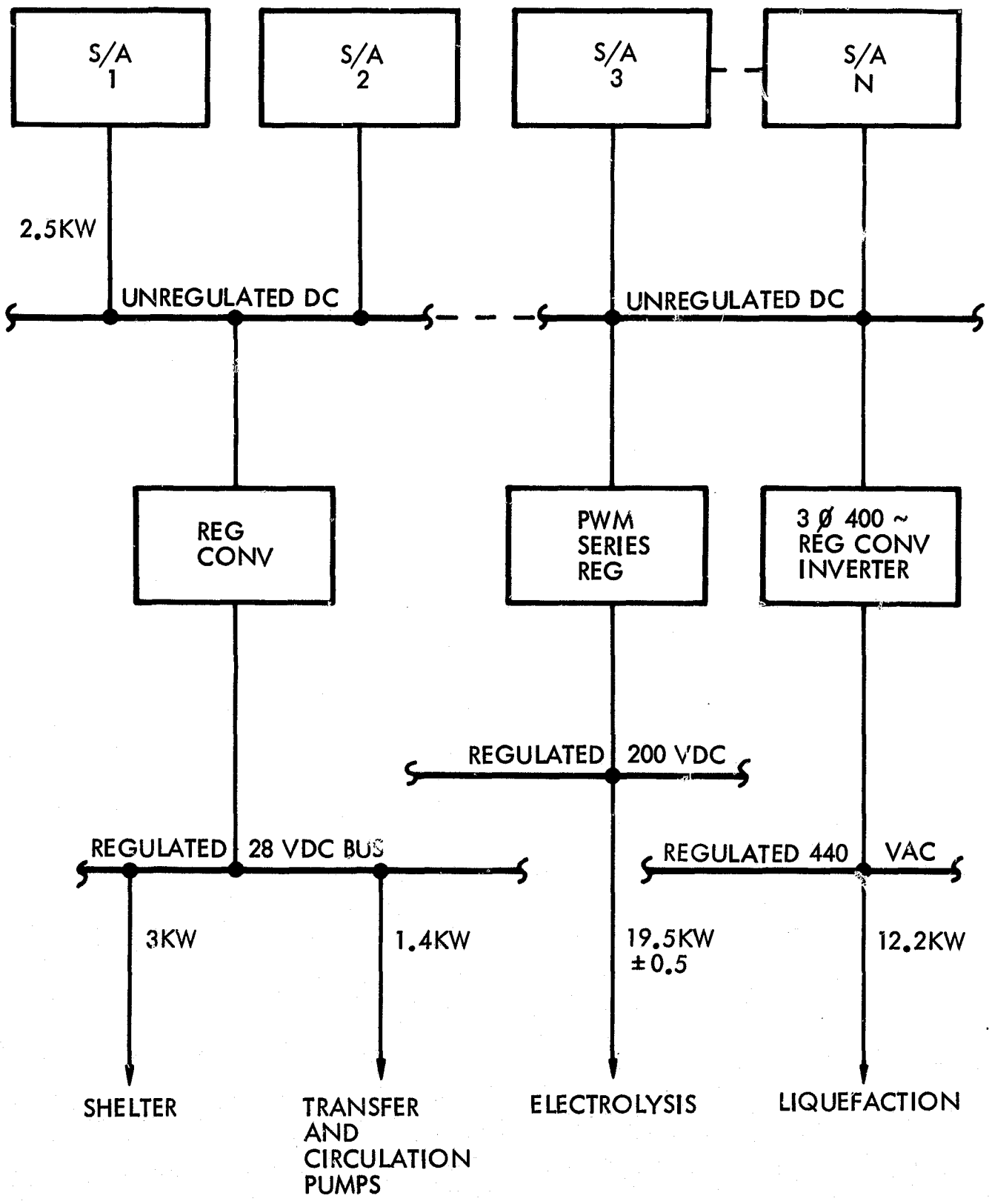

Figure F.2 Lunar Surface Power System (Configuration 2) (Full DC Distribution)

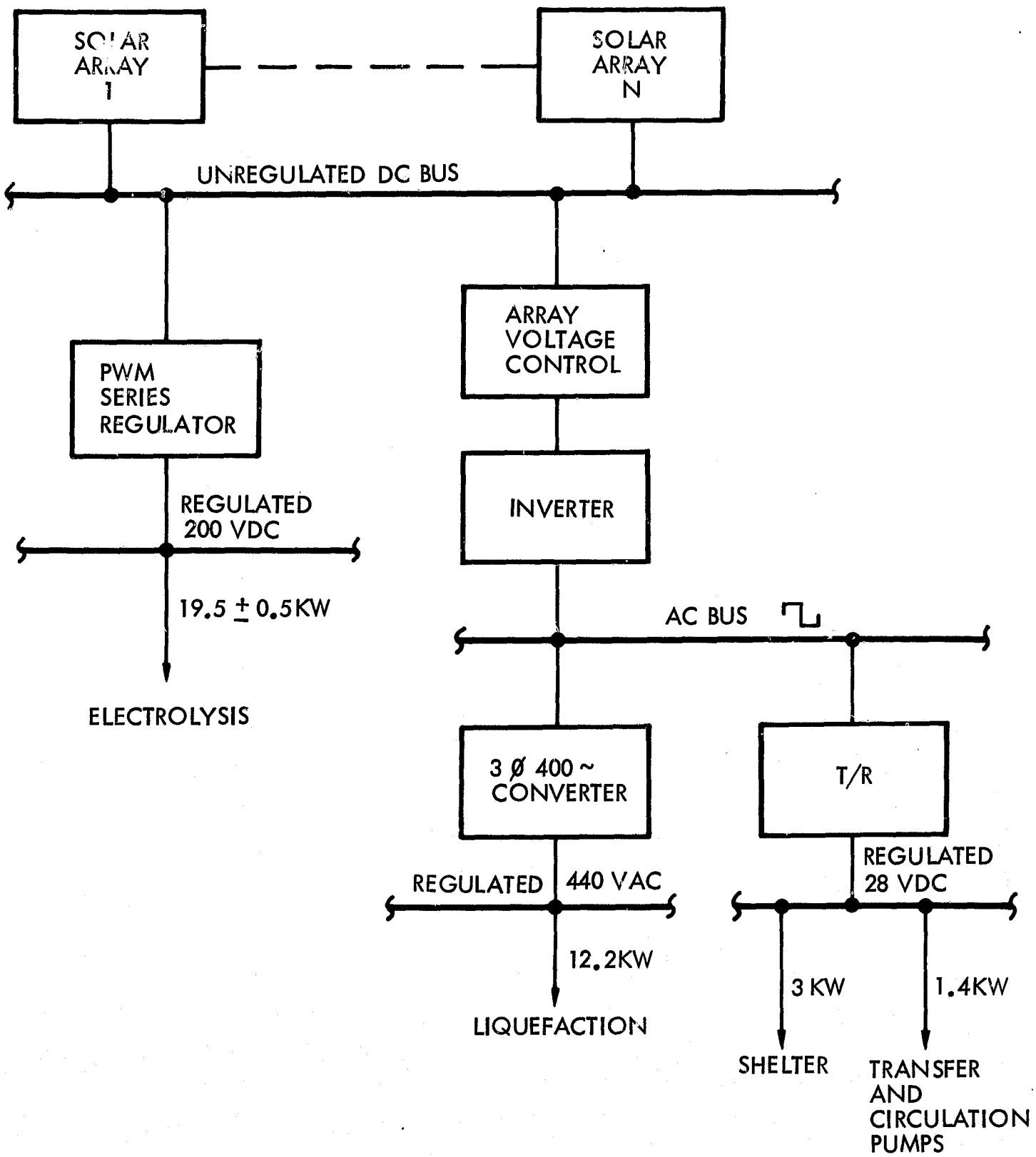

Figure F.3 Lunar Surface Power System (Configuration 3) (AC-DC Distribution)

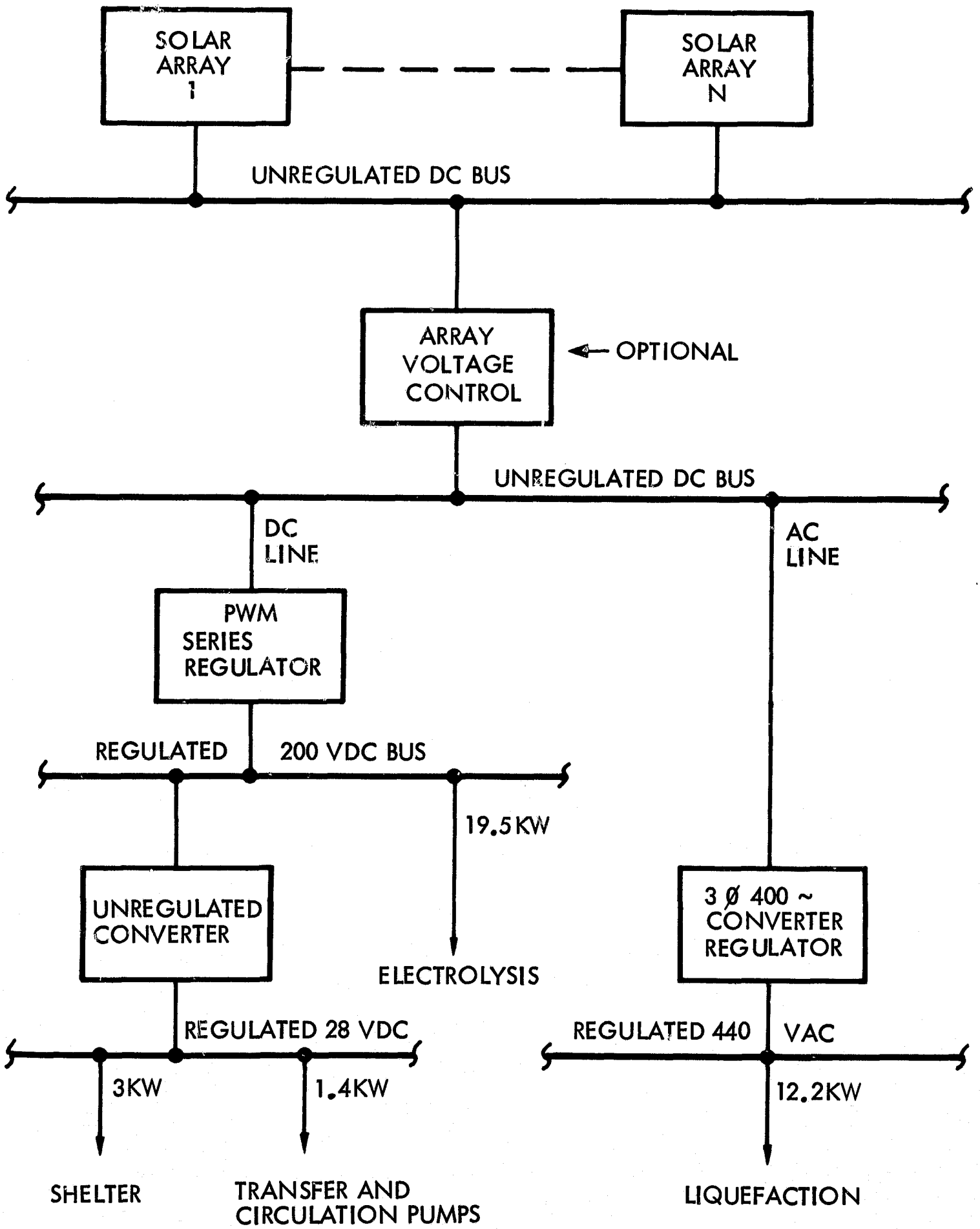

Figure F.4 Lunar Surface Power System (Configuration 4) (AC-DC Distribution)

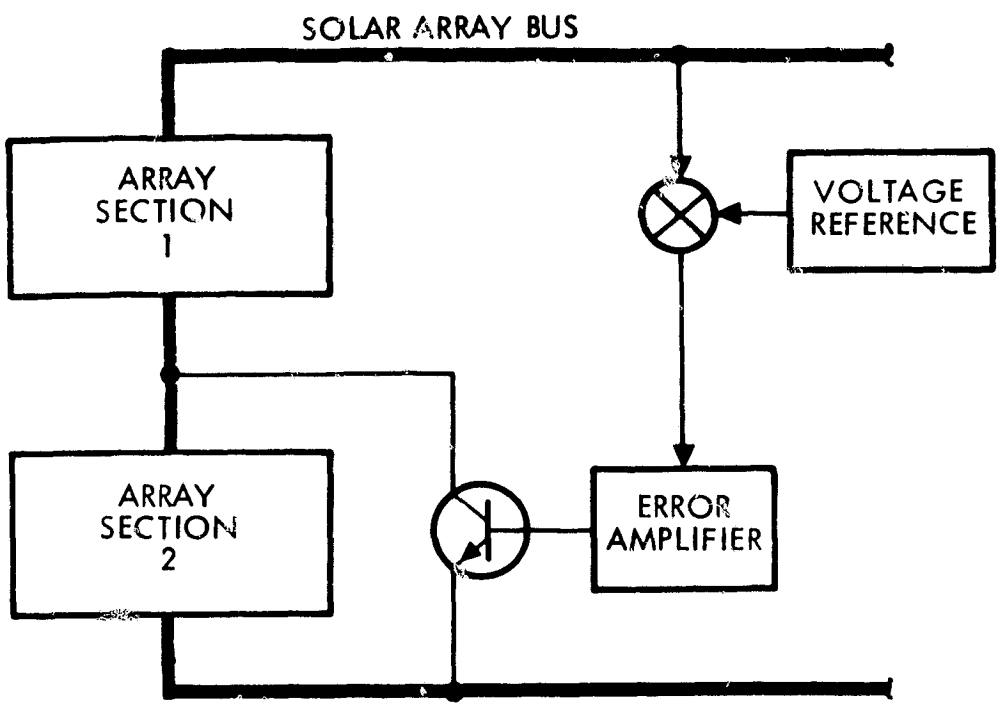

Figure F.5 Partial Shunt Solar Array Voltage Limiter

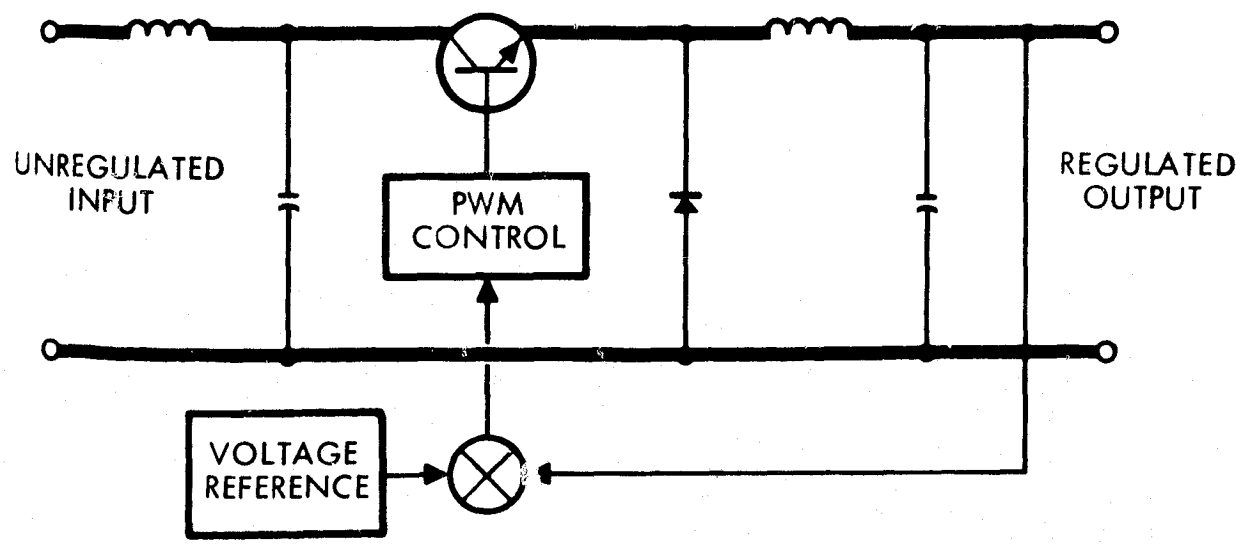

Figure F.6 PWM Bucking Solar Array Voltage Limiter or Line Regulator

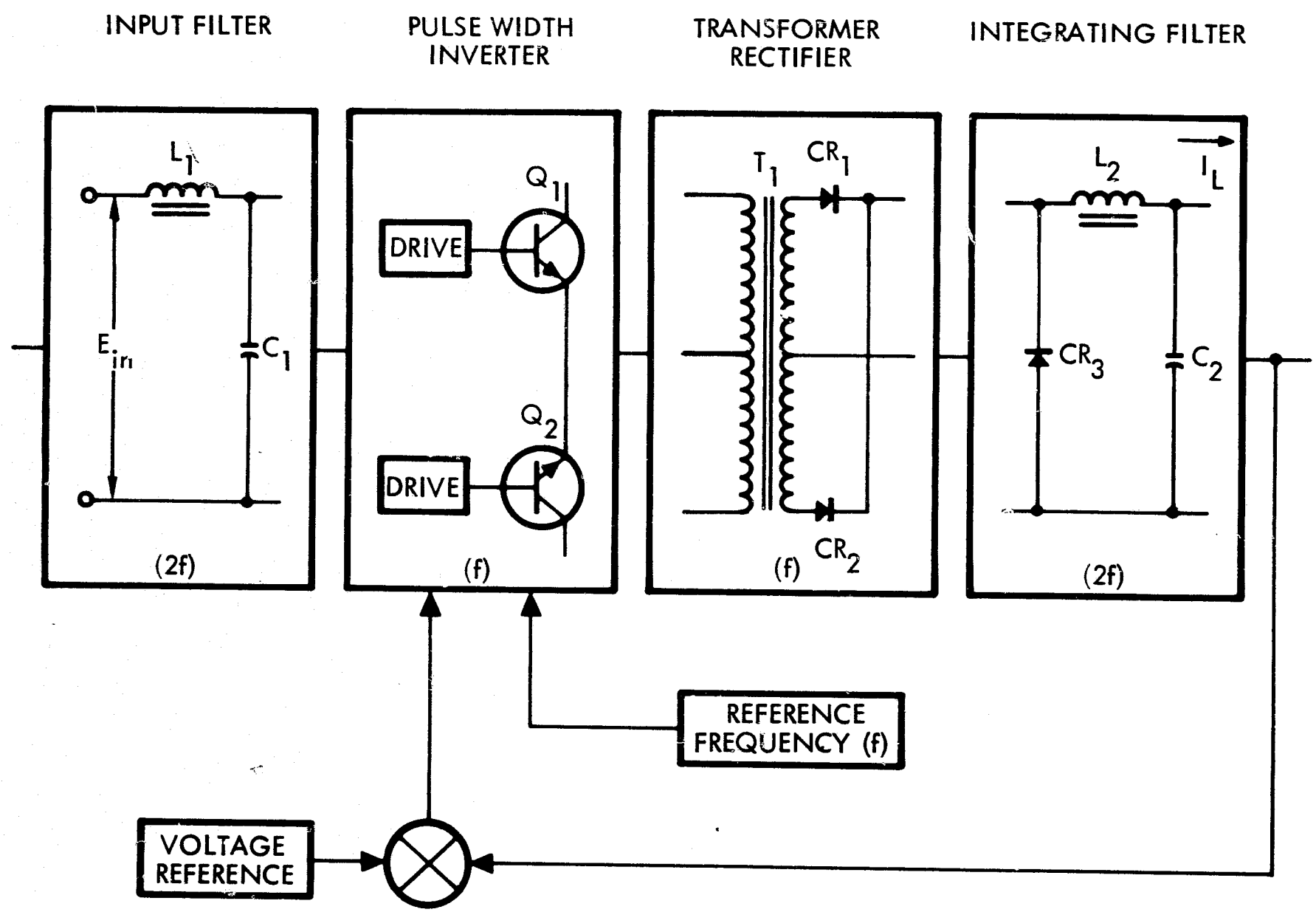

Figure F.7 Block Diagram, PWI Converter

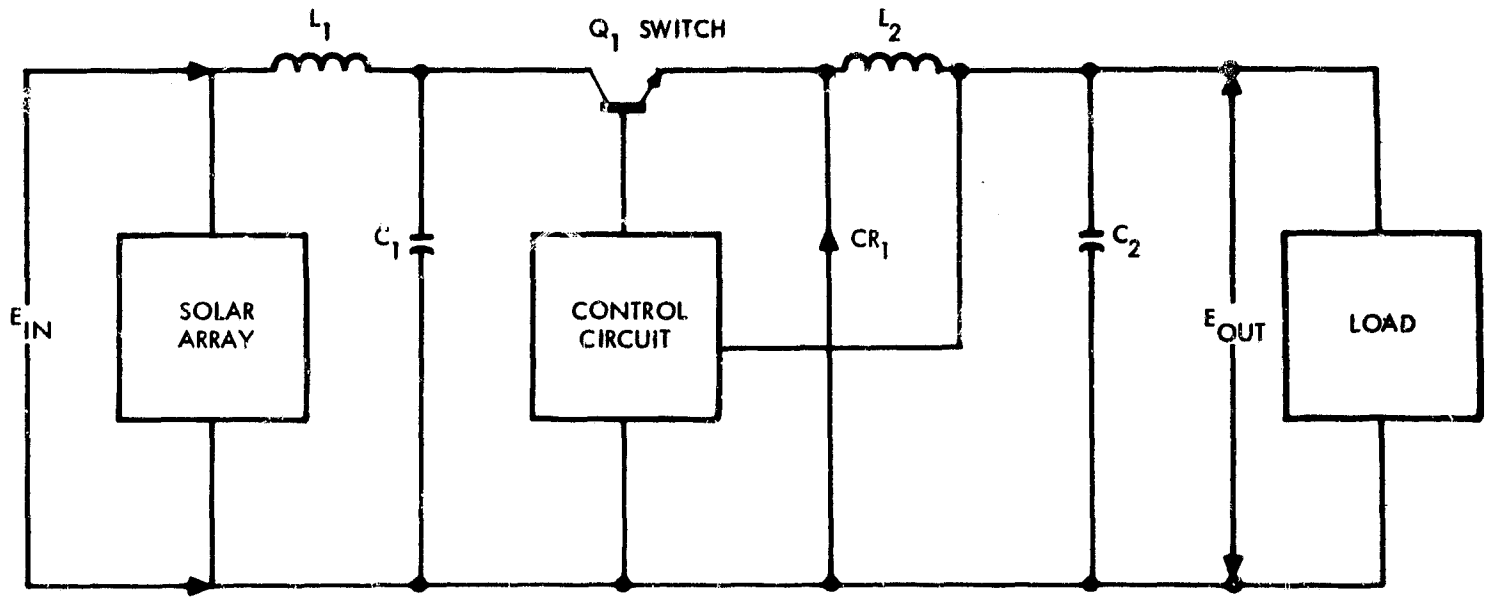

Figure F.8 Pulse Width Modulated Bucking Regulator Block Diagram

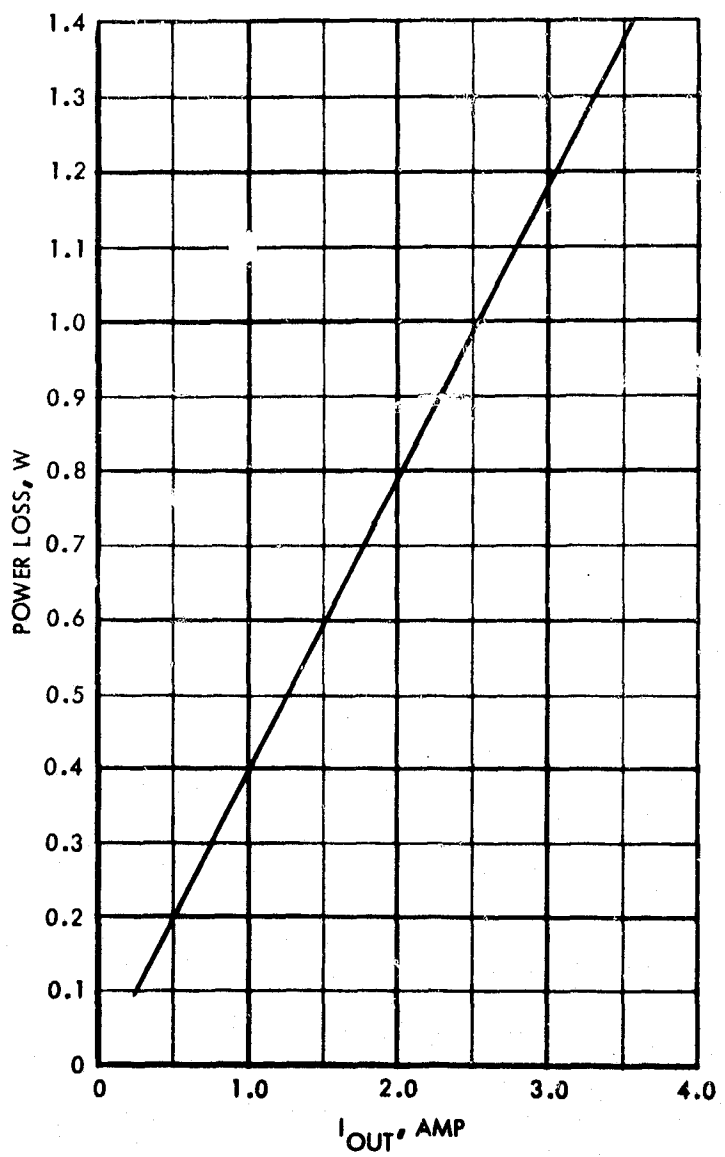

Figure F.9 Pulse Width Bucking Regulator, Saturated Conditions

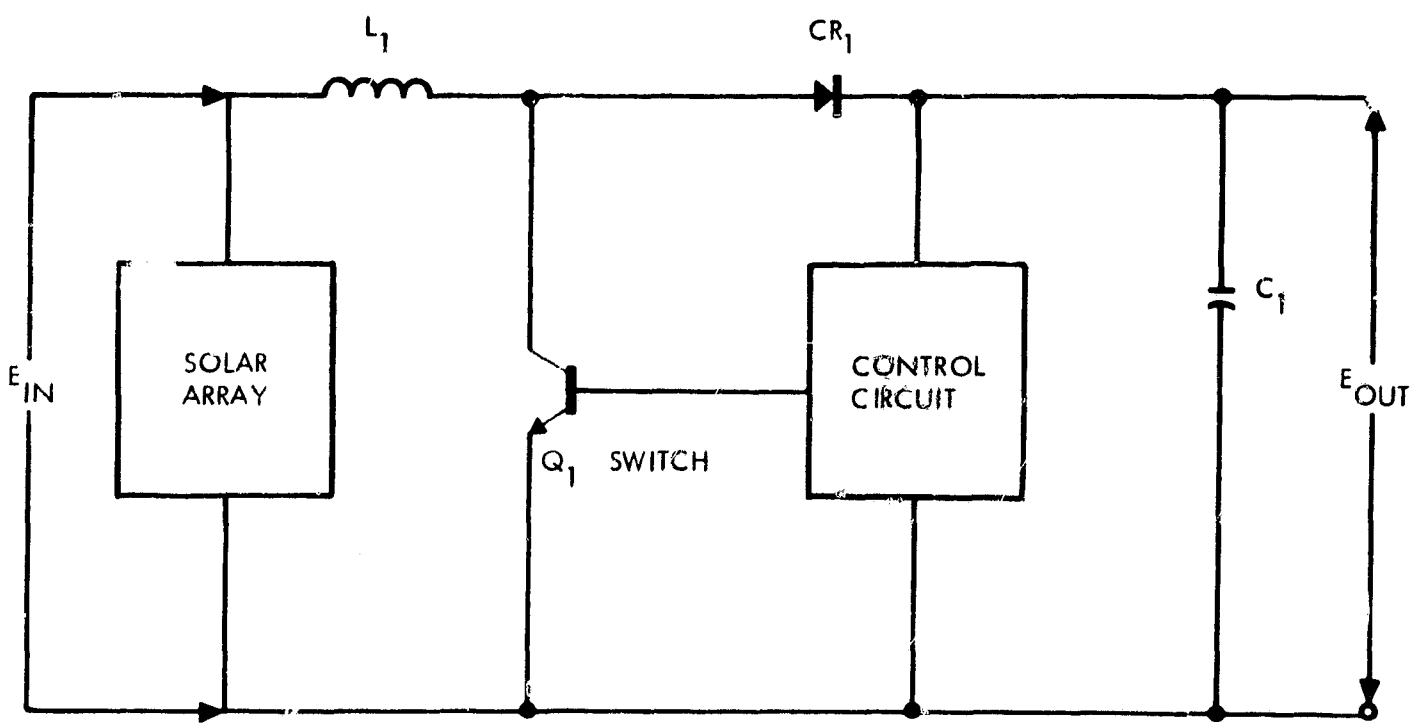

Figure F.10 Pulse Width Modulated Boost Regulator Block Diagram

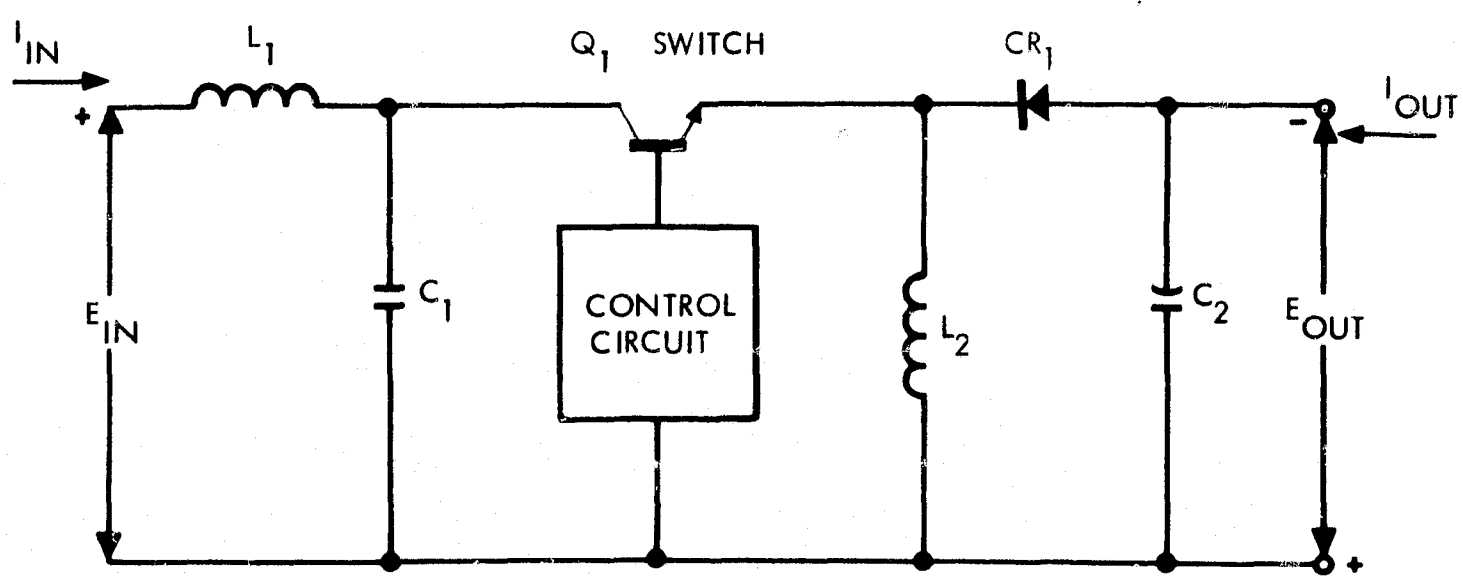

Figure F.11 Pulse Width Modulated Buck-Boost Regulator Block Diagram

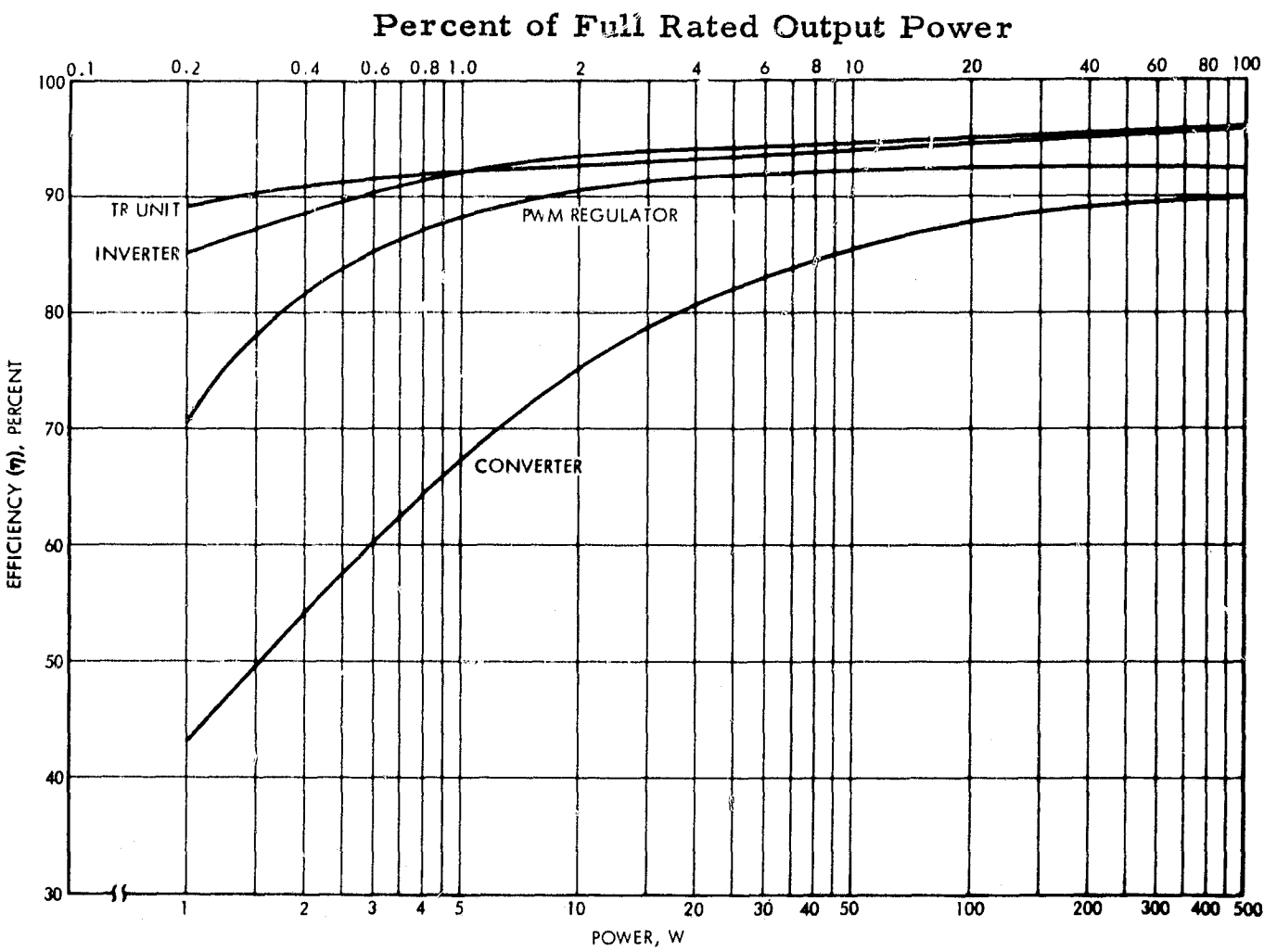

Figure F.12 Maximum Efficiency as a Function of Power Output

APPENDIX G

SOLAR ARRAY WEIGHT AND POWER LEVEL CALCULATION CHARTS

SOLAR ARRAY WEIGHT AND POWER LEVEL CALCULATIONS

It is often convenient to estimate solar array power level, area, and weight for various specific densities or specific powers. The parametric data depicted in Figures G.1, G.2, and G.3 was prepared for this purpose during this study.

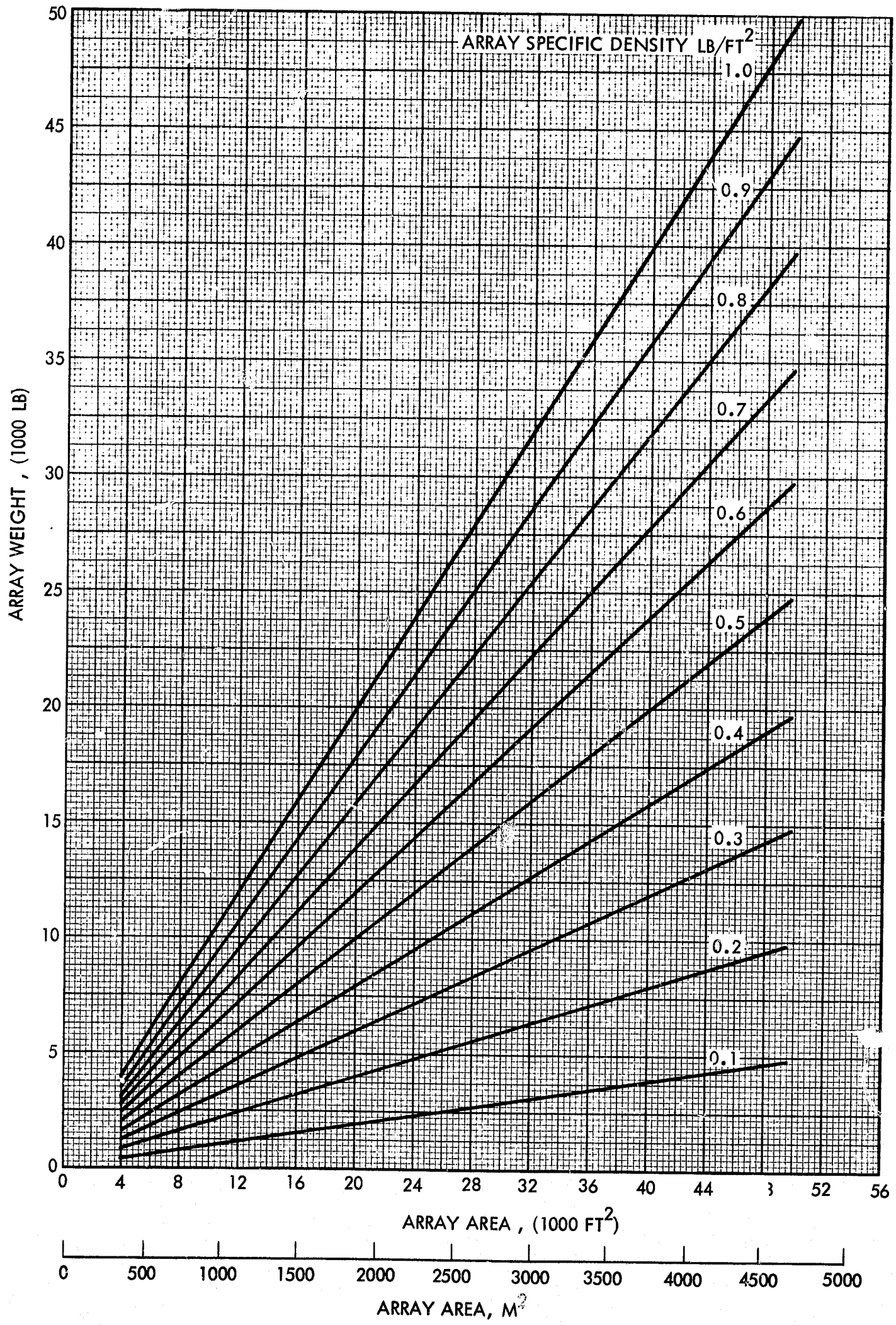

Figure G.1 Solar Array Weight Versus Array Area as a Function of Array Specific Density

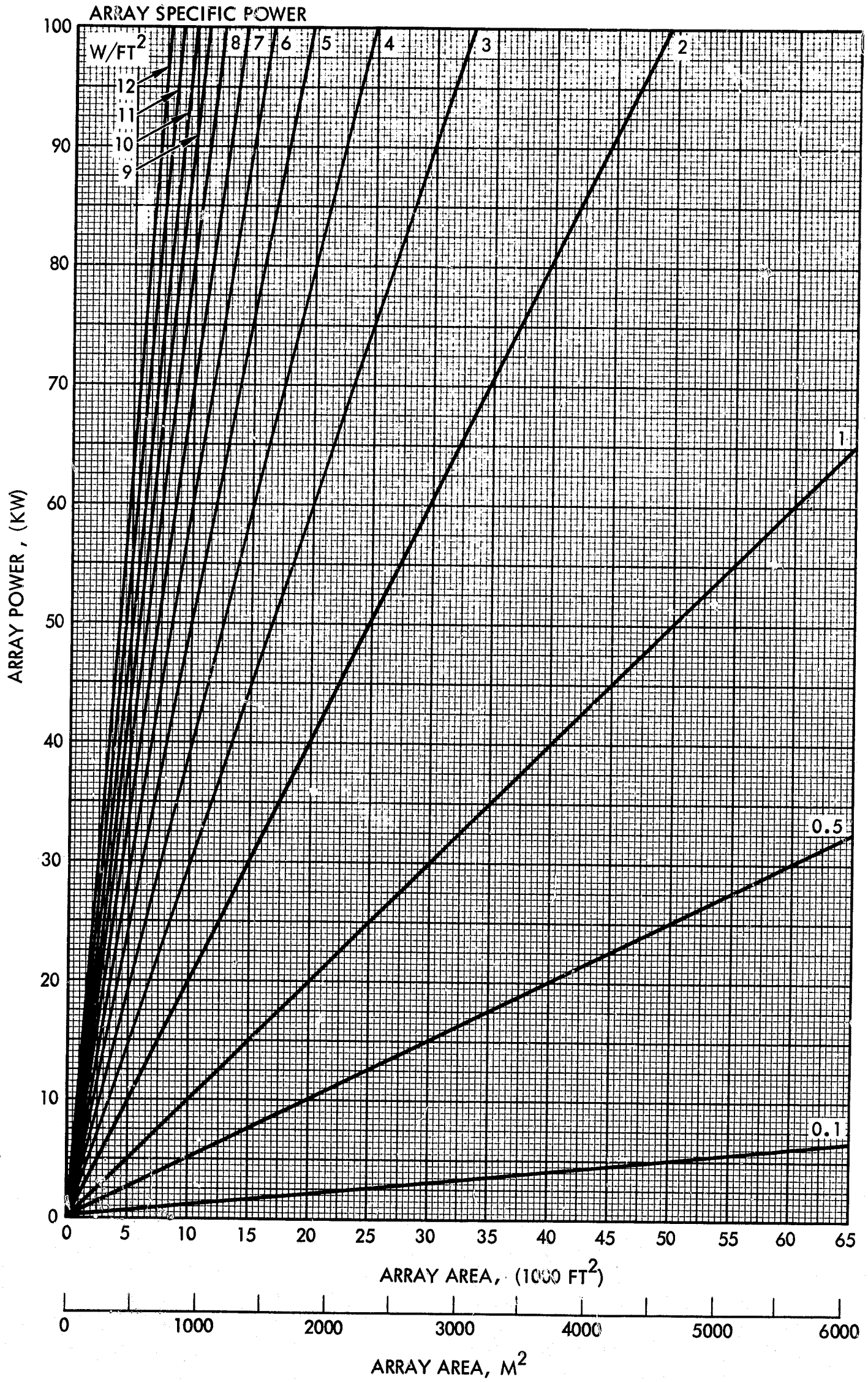

Figure G.2 Solar Array Power Versus Array Area as a Function of Array Specific Power

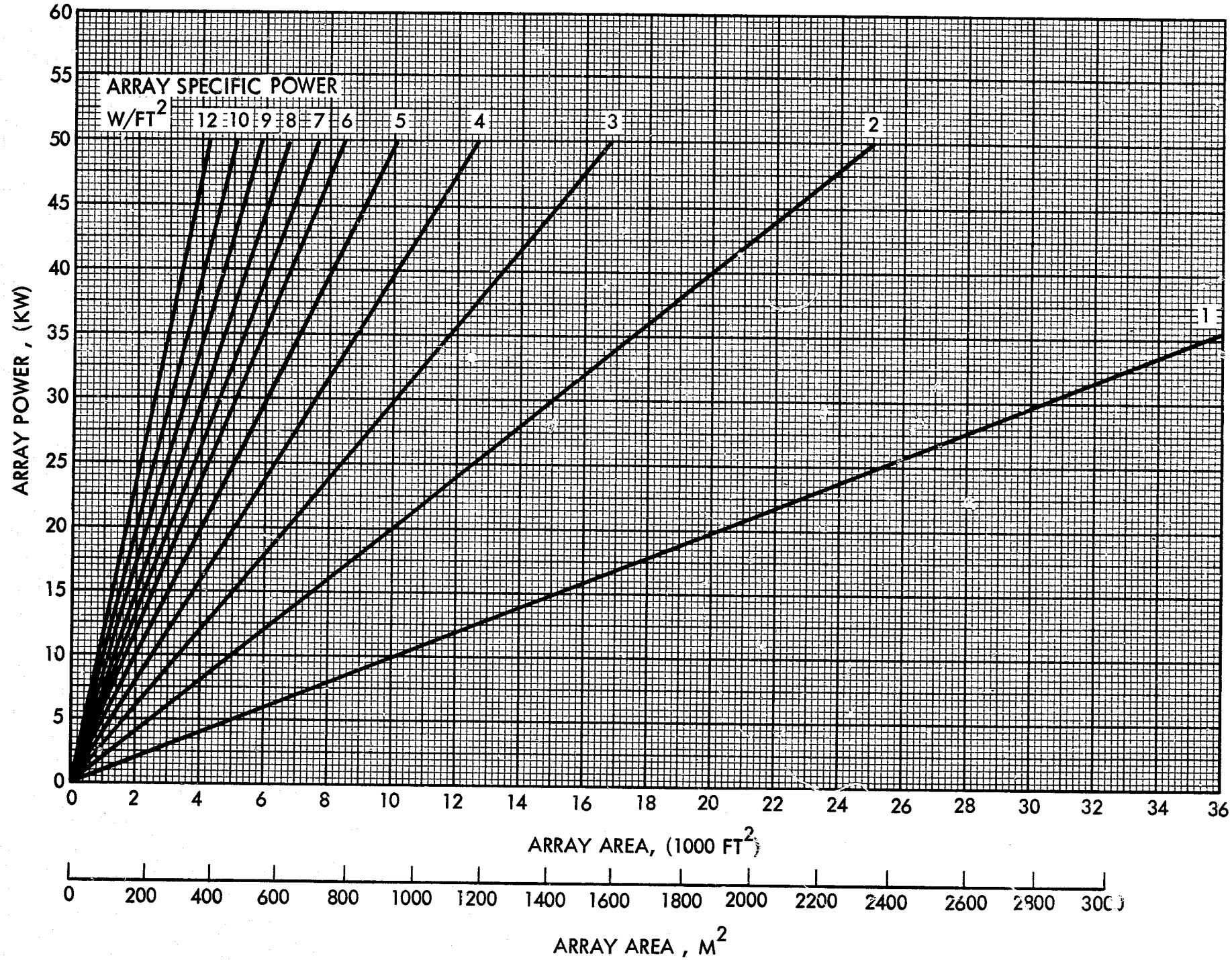

Figure G.3 Solar Array Power Versus Array Area as a Function of Array Specific Power